STARS

2015

Assessing Biofiltration Pretreatment for Ultrafiltration Membrane Processes

Andrea Cumming
University of Central Florida

ASSESSING BIOFILTRATION PRETREATMENT FOR ULTRAFILTRATION
MEMBRANE PROCESSES

by

ANDREA CUMMING NETCHER
B.S. University of Central Florida, 2010
M.S. University of Central Florida, 2012

A dissertation submitted in partial fulfillment of the requirements
for the degree of Doctor of Philosophy
in the Department of Civil, Environmental, and Construction Engineering
in the College of Engineering and Computer Science
at the University of Central Florida
Orlando, Florida

Spring Term
2015

Major Professor: Steven J. Duranceau

ABSTRACT

An engineered biological filtration (biofiltration) process treating a nutrient-enriched, low-alkalinity, organic-laden surface water downstream of conventional coagulation-clarification and upstream of an ultrafiltration (UF) membrane process was assessed for its treatment effectiveness. The impact of biofiltration pretreatment on UF membrane performance was evaluated holistically by investigating the native source water chemistry and extending the analysis into the drinking water distribution system. The biofiltration process was also compared in treatment performance to two alternative pretreatment technologies, including magnetic ion exchange (MIEX®) and granular activated carbon (GAC) adsorption.

The MIEX®, GAC adsorption, and biologically active carbon (BAC) filtration pretreatments were integrated with conventional pretreatment then compared at the pilot-scale. Comparisons were based on collecting data regarding operational requirements, dissolved organic carbon (DOC) reduction, regulated disinfection byproduct (DBP) formation, and improvement on the downstream UF membrane operating performance. UF performance, as measured by the temperature corrected specific flux or mass transfer coefficient (MTC), was determined by calculating the percent MTC improvement relative to the existing conventional-UF process that served as the control. The pretreatment alternatives were further evaluated based on cost and non-cost considerations.

Compared to the MIEX® and GAC pretreatment alternatives, which achieved effective DOC removal (40 and 40 percent, respectively) and MTC improvement (14 and 30 percent, respectively), the BAC pretreatment achieved the lowest overall DOC removal (5 percent) and

MTC improvement (4.5 percent). While MIEX® relies on anion exchange and GAC relies on adsorption to target DOC removal, biofiltration uses microorganisms attached on the filter media to remove biodegradable DOC.

Two mathematical models that establish an empirical relationship between the MTC improvement and the dimensionless alkalinity to substrate (ALK/DOC) ratio were developed. By combining the biofiltration results from the present research with findings of previous studies, an empirical relationship between the MTC improvement versus the ALK/DOC ratio was modeled using non-linear regression in Minitab®. For surface water sources, UF MTC improvement can be simulated as a quadratic or Gaussian distribution function of the gram C/gram C dimensionless ALK/DOC ratio. According to the newly developed empirical models, biofiltration performance is optimized when the alkalinity to substrate ratio is between 10 and 14. For the first time a model has thus been developed that allows for a predictive means to optimize the operation of biofiltration as a pretreatment prior to UF membrane processes treating surface water.

I dedicate this dissertation to my brilliant and loving mother, Lety Nieves. Without her shining

example and endless support, I would not be able to reach these heights and continue to reach

higher and higher.

ACKNOWLEDGMENTS

TABLE OF CONTENTS

LIST OF FIGURES

LIST OF TABLES

LIST OF ABBREVIATIONS

ACH	aluminum chlorohydrate coagulant
alum	aluminum sulfate coagulant
ANOVA	statistical analysis of variance
AOC	assimilable organic carbon
ATP	adenosine triphosphate
BAC	biologically activate carbon
BAF	biological aerated filter
BDOC	biodegradable dissolved organic carbon
BGAC	biologically granular activated carbon
biofiltration	biological filtration
CEB	chemically enhanced backwash
CEI	chromatic elemental imaging
CF/RO	cartridge filter/reverse osmosis
CFUs/mL	colony-forming units per milliliter
CIP	clean in place
CMF	continuous membrane filtration
County	County of Maui Department of Water Supply
cP	centipoise
CU	color units
DBP	disinfection by-product
DBPR	Disinfection Byproducts Rule

DO	dissolved oxygen
DOC	dissolved organic carbon
DOM	dissolved organic matter
EBCT	empty bed contact time
EDS	energy dispersive spectroscopy
EDX	energy dispersive x-ray spectroscopy
EEM	excitation-emission matrix fluorescence spectroscopy
EPA	Environmental Protection Agency
EPS	extracellular polymetric substances
flux	membrane water production
FTIR	Fourier Transform infrared spectroscopy
g	grams
g/L	grams per liter
GAC	granular activated carbon
gal/ft^2-d	gallons per square feet-day
gal/ft^2-d-psi	gallons per square feet-day-psi
gpm	gallons per minute
gpm/ft^2	gallons per minute per square feet
GPS	global positioning system
HAA$_5$	haloacetic acids
HDPE	high density polyethylene
HLR	hydraulic loading rate

HPC	heterotrophic plate counts
HR	high rate
kg/m-s	kilograms per meter-second
L	liter
L/m^2-h	liters per square meter-hour
L/m^2-h-bar	liters per square meter-hour-bar
L/min	liters per minute
lb-s/ft^2	pound-seconds per square feet
LC-OCD	liquid chromatography with organic carbon detection
MCLs	maximum contaminant levels
MF	microfiltration membrane filtration
MG	million gallon
mg/L	milligrams per liter
mg/L as CaCO$_3$	milligrams per liter as calcium carbonate
MGD	million gallons per day
MIEX$^{®}$	anion exchange
MIEX$^{®}$-ACH	coagulation-clarification pilot unit process
min	minute
mS/cm	millisiemens per centimeter
MW	molecular weight
μg/L	micrograms per liter
μm	micrometer

Na	not available
NF	nanofiltration membrane filtration
NOM	natural organic matter
NS	not specified
ntu	nephelometric turbidity units
PAC	Project Advisory Committee
PAC	powdered activated carbon
PACl	polyaluminum chloride coagulant
PAS	polyaluminum sulfate coagulant
PES	polyetherfulfone
psi	pounds per square inch
PVC	polyvinyl chloride pipe
PVDF	polyvinylidene fluoride
raw	Olinda raw water
RLUs	relative light units
S/A	sand/anthracite
SEM	scanning electron microscopy
SUVA	Specific ultraviloet absorbance at 254 nanometers wavelength
TC	tailored collaboration
TCTMP	temperature corrected transmembrane pressure
TDS	total dissolved solids
TFE	tetrafluoroethylene lined caps

TMP	transmembrane pressure
TOC	total organic carbon
TSS	total suspended solids
TTHM	total trihalomethanes
UCF	University of Central Florida
UF	ultrafiltration membrane filtration
UV 254	ultraviolet absorbance at 254 nanometers wavelength
WRF	Water Research Foundation
WTP	water treatment plant
x-ACH	coagulated-flocculated-settled water, where x is control or technology used
x-UF	plant ultrafiltration membrane filtrate, where x is control of technology used
°C	degrees Celcius

CHAPTER 1. INTRODUCTION

In surface water treatment, low pressure ultrafiltration (UF) membranes are widely used because of their ability to remove pathogens and supply safe drinking water. Although UF membranes provide an effective barrier against pathogens, the efficiency of UF processes is limited by membrane fouling and poor disinfection byproduct (DBP) precursor removal (Alspach et al., 2005; 2008). Improving the productivity of UF membranes can be accomplished by incorporating pretreatment processes. Of the identified pretreatment technologies, biological filtration (biofiltration) has attracted the most recent attention from researchers (Gao et al., 2011). Researchers have found that biofiltration pretreatment can enhance UF processes by producing biologically stable water (Wend et al., 2003; Basu & Huck, 2004; Halle et al., 2009; Huang et al., 2011; Wei et al., 2011; Peldszus et al., 2012). While these bench and pilot scale research findings indicate that the use of biofiltration pretreatment for UF processes is effective, further investigation on the pilot-scale is necessary to:

- Examine the biological filter (biofilter) performance for other types of surface waters, particularly low alkalinity sources,
- Understand the impacts of integrating biofiltration within conventional pretreatment (coagulation, flocculation, and sedimentation) and UF membrane processes, and
- Develop practical models that can predict biofilter performance.

To contribute to the knowledge base with regards to biofiltration pretreatment, a biofiltration process treating low alkalinity, organic acid-laden surface water downstream of conventional pretreatment and upstream of a UF membrane process was assessed. The performance of

biofiltration pretreatment was compared to other advanced pretreatment technologies, including magnetic ion exchange (MIEX®) and granular activated carbon (GAC) adsorption. Furthermore, results from previous biofiltration studies were incorporated to develop an empirical model for predicting biofilter performance.

Background and Objectives

In August of 2012, the County of Maui Department of Water Supply (County) partnered with the Water Research Foundation (WRF) and the University of Central Florida (UCF) to investigate biological pretreatment of a low alkalinity, organic acid-laden surface water treated at the Olinda Water Treatment Plant (WTP) located in proximity of Makawao, Maui, HI. The Olinda WTP employs a conventional-UF process and faces treatment challenges related to elevated DBP formation and UF membrane fouling. The water quality and operational challenges are due in part to the difficulties of coagulating low alkalinity, acidic pH, organic-laden surface water.

To address Olinda's unique water treatment challenges, the County, WRF, and UCF entered into a tailored collaboration (TC) to evaluate advanced pretreatment technologies, including MIEX®, GAC adsorption, and biologically active carbon (BAC) filtration, ahead of a UF membrane process. These pretreatment options were selected for evaluation because of their ability to remove dissolved natural organic matter (NOM) that contribute to DBP formation and UF membrane fouling (Miltner et al., 1992; Boyer & Singer, 2005; Gao et al., 2011; Badawy et al., 2012).

The pretreatment alternatives were assessed according to a holistic technical approach that examined the water quality from the watershed supply to the finished water distribution system.

The Olinda WTP's coagulation and UF processes were investigated to serve as the research control for assessing the MIEX®, GAC, and BAC pretreatment options. In addition, results from the present BAC evaluation and from other biofiltration studies were assessed to develop a new mathematical model for predicting biofiltration performance.

Overall, the research focused on four primary objectives:

- Objective 1 – Examine Watershed Quality

- Objective 2 – Confirm Existing Conventional-UF Process Operations

- Objective 3 – Evaluate the UF Pretreatment Alternatives

- Objective 4 – Investigate a New Model Approach for Predicting Biofiltration Performance

The objectives were accomplished through the completion of several research tasks. Table 1-1 presents the research implementation schedule for each of the following research tasks.

- Task 1 – Surface Overland Flow Water Quality Analysis

- Task 2 – Conventional-UF Process Water Quality and Operational Monitoring

- Task 3 – Coagulation Jar Testing Evaluation

- Task 4 – MIEX® Pretreatment Pilot Testing

- Task 5 – GAC Pretreatment Pilot Testing

- Task 6 – BAC Pretreatment Evaluation

- Task 7 – MIEX®, GAC, and BAC Pretreatment Evaluation

- Task 8 – Empirical Model Development for Biofiltration Performance

The findings of each task are presented and discussed herein. One or more of the identified pretreatment alternatives could provide the County with newer approaches that improve the quality and economics of water treatment. Furthermore, the research was conducted to provide the water community with additional information on the treatment effectiveness, method of implementation, and operational guidance of UF pretreatment alternatives not commonly used in existing UF treatment strategies, particularly biofiltration.

Table 1–1 Research Task Implementation Schedule

Task	Date
1	November 15, 2012; January 31, 2013; April 30, 2013; August 6, 2013; October 22, 2013; and May 12, 2014
2	September 4, 2012 through February 3, 2013; and April 27, 2013 through December 31, 2013
3	September 19, 2012; April 23, 2013; April 24, 2013; and May 17, 2014 through June 1, 2014
4	September 4, 2012 through February 3, 2013
5	April 27, 2013 through July 5, 2013
6	August 10, 2013 through December 31, 2013
7	January 1, 2014 through September 1, 2014
8	October 1, 2014 through February 15, 2015

The Upcountry Water Supply

The County provides drinking water to the majority of Maui's population from a combination of groundwater and surface water resources. The County's Upcountry water system is one of the larger drinking water communities on the island, where treated surface water is distributed to Upcountry Maui customers through the Upper Kula, Lower Kula, and Makawao interconnected

water systems. The water distribution systems are configured to allow water transfers between the three networks during times of drought. The three distribution systems are segregated due to differences in system elevation, and each system contains within its service area its own water treatment plant (WTP):

- The Olinda WTP is comprised of an integrated conventional-UF process that supplies the upper elevation properties via the Upper Kula distribution system;

- The Pi'iholo WTP is a conventional direct filtration surface water treatment facility that provides water to customers through the Lower Kula distribution system; and,

- The Kamole WTP is an integrated direct coagulation and UF process that, along with several groundwater wells, supplies the lower elevation customers through the Makawao distribution system.

An overview schematic of the Upcountry water system is depicted in Figure 1-1. A summary description of the Upcountry water supply and treatment systems is presented in Table 1-2. The Upcountry surface water supply originates from the native rainforest located in the East Maui watershed and is generally characterized by relatively low hardness, low alkalinity, and acidic pH. The source water's organic levels, measured as total organic carbon (TOC), vary from 1 to 20 mg/L depending on the system elevation of each plant.
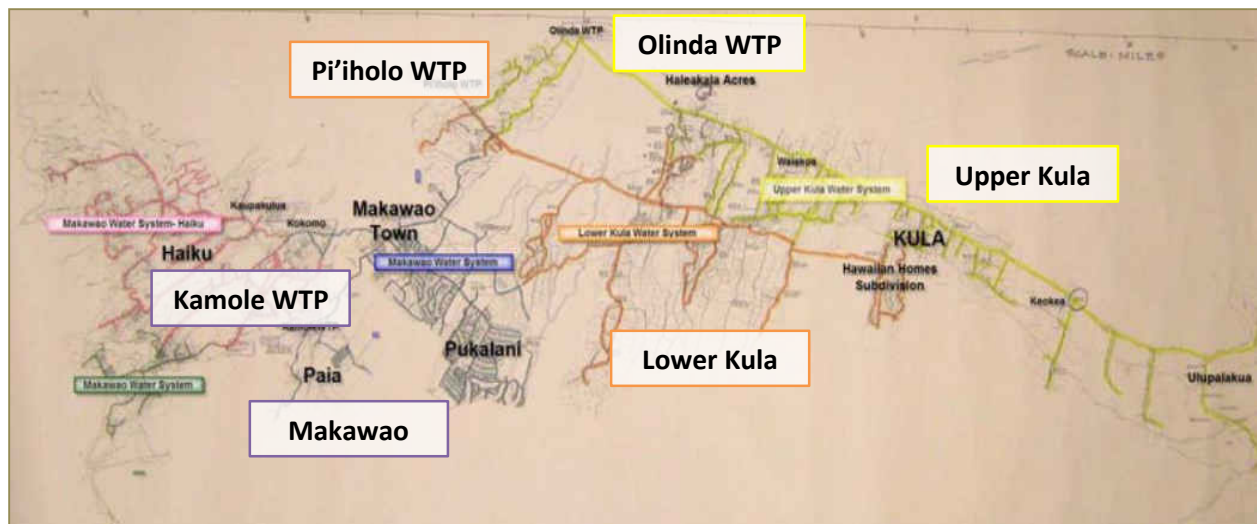
Figure 1–1 Upcountry Water System Schematic
Source: Adapted from Davis et al., 2008

The Upcountry treatment plants employ similar multi-barrier treatment schemes, consisting of destabilization and removal of turbidity and NOM by coagulation and granular or membrane filtration, chemical disinfection, and corrosion control. Unlike the Kamole and Pi'iholo WTPs, the Olinda WTP treats the highest TOC source water for which conventional-UF treatment is insufficient to control DBP formation with free chlorine disinfection. In order to control regulated DBP levels in the Upper Kula system, the Olinda WTP relies on pre-formed chloramines for primary and secondary disinfection. Because the chloramine residual is incompatible with the free chlorine residual of the Lower Kula and Makawao systems, the Upper Kula system is intentionally kept isolated (Farley et al. 2012).

Table 1–2 Upcountry Water Supply and Treatment Systems Summary

Parameter	Makawao			Lower Kula	Upper Kula
Water Source(s)	Kaupakalua, Haiku, and Pookela Wells	Hamakuapoko Well	Wailoa Ditch	Pi'iholo Reservoir	Waikamoi and Kahakapao Reservoirs
Type	Ground	Ground	Surface	Surface	Surface
Treatment Plant	---	Kamole WTP	Kamole WTP	Pi'iholo WTP	Olinda WTP
Treatment Process	---	GAC	Coagulation-Ultrafiltration, Low TOC	Direct filtration, Moderate TOC	Conventional-Ultrafiltration, High TOC
Primary Disinfection	Chlorine	Chlorine	Chlorine	Chlorine	Chloramines
Secondary Disinfection	Chlorine	Chlorine	Chlorine	Chlorine	Chloramines
Corrosion Control	---	---	Soda Ash	Soda Ash	Lime

Keeping the Upper Kula system isolated is challenging during times of drought because the higher elevation communities cannot be supplemented by the lower systems. Additionally, the County must issue mandatory water usage restrictions. To complicate matters, the Upper Kula system must implement a rigorous distribution system flushing schedule to prevent nitrification episodes, common to chloraminated systems (Zhang et al., 2009). Frequent flushing of the system leads to the loss of valuable treated water. In addition to the distribution management challenges, the County has been encountering operational limitations at Olinda WTP related to UF membrane fouling. The suspected high organic and possibly biological fouling nature of the Olinda WTP source water necessitates frequent UF membrane backwashes and chemical cleans in place (CIPs). Frequent backwashes and CIPs decrease water productivity and increase chemical waste streams.

Upgrading the Olinda UF process to include additional pretreatment may serve the dual purpose of lowering UF membrane fouling and DBP precursors. Addressing Olinda's membrane fouling

and DBP formation concerns would present the County with the options of increasing water production at the Olinda WTP and converting the Upper Kula disinfection residual to free chlorine. The conversion of the Upper Kula disinfection residual to free chlorine would permit unrestricted water transfers among the three Upcountry network distribution systems.

The Olinda WTP Facility Layout

The Olinda WTP treats water originating from the highest reaches (above 4,000 feet) of the Waikamoi rainforest in the East Maui watershed. The source water is collected by an overland flow capture method consisting of a 1.1 mile-long flume that conveys water to a dam-reservoir system for storage prior to transport to the Olinda plant site. Before April 2013, the rectangular flume consisted of redwood originally constructed in the 1930s and rebuilt in 1974. However, due to water losses of up to 40 percent, construction began in April 2013 for the replacement of the 40-year-old redwood flume with a new aluminum flume of the same dimensions (14 by 27 inches) and flow capacity (1.1 MGD).

The flume collects surface run-off water and stream water from the Haipua'ena and Puanokamoa streams through a series of intakes. The water collected in the flume is combined with Waikamoi stream water and conveyed to two 15 million gallon Waikamoi reservoirs. The water is then stored in two 50 million gallon Kahakapao reservoirs before traveling to the Olinda plant. The TOC of the raw water going into the plant ranges from 4 to 19 mg/L; however, a profile of the water quality as it travels to the plant has yet to be conducted. Understanding the water quality of the source water as it is conveyed through the watershed was believed to serve as a means to identify additional watershed management strategies for improving the downstream treatment processes.

The Olinda WTP operates as a coagulation, flocculation, sedimentation and UF surface water plant. A process schematic of the Olinda WTP is presented in Figure 1-2. Following pre-sedimentation in the Kahakapao reservoirs, raw water is injected with aluminum chlorohydrate (ACH) coagulant, mixed, and flocculated in two slow mix basins. ACH, a prehydrolyzed metal salt coagulant, is manufactured to exert a low demand on the raw water alkalinity (Letterman & Yiacoumi, 2011). Therefore, the Olinda WTP uses ACH in place of more common metal salts, such aluminum sulfate, that are known to cause a significant drop in pH for low alkalinity waters (Budd et al., 2004).

The coagulation and flocculation treatment steps serve to remove color and the suspended and colloidal solids that coalesce into larger particles and settle out in an 8.5 million gallon sedimentation basin. The clarified water is then pumped through a UF membrane process that removes most of the remaining fine particulates. Ammonia and chlorine are added to form chloramines that serve to disinfect the water. Food grade lime is added for pH adjustment and stabilization prior to storage in the clearwell. Finished water from the clearwell supplies the Upper Kula distribution system. UF backwash, containing diluted hypochlorite and citric acid chemicals, is directed to backwash lagoons to be recycled back into the treatment process. The average production rate of the Olinda WTP is approximately 2 MGD; and the peak processing capacity is about 2.7 MGD.
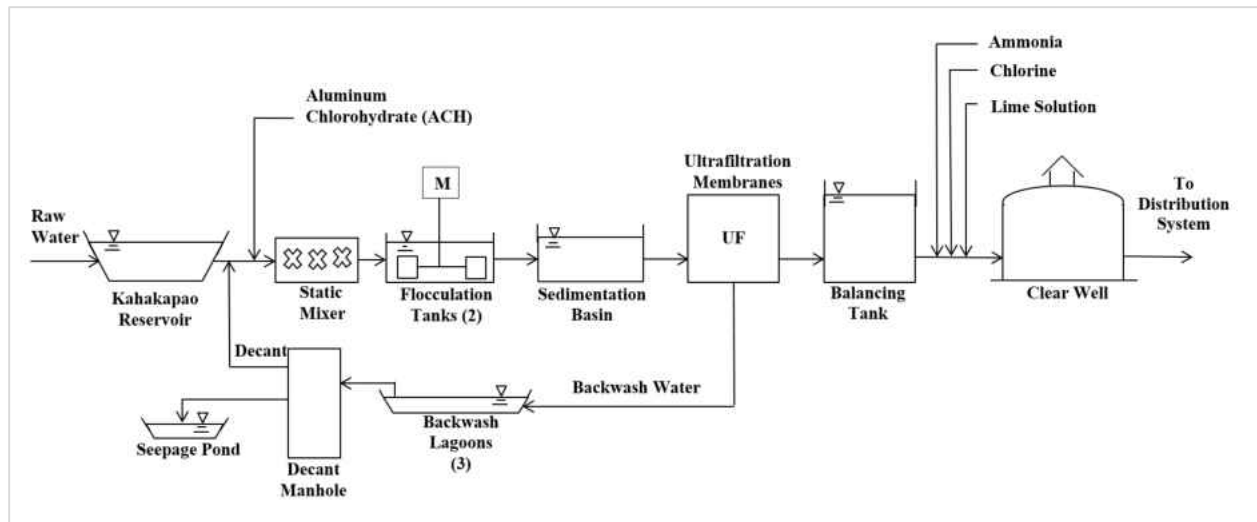
Figure 1–2 Olinda WTP Schematic

Prior to 2007 the Olinda plant relied on microfiltration (MF) membranes with nominal pore size of 0.1 μm; however, in early 2007 the plant was upgraded to UF membranes having a nominal pore size of 0.01 μm (Alspach et al., 2008). The UF process utilizes pressurized outside to inside MEMCOR® L10V polyvinylidene fluoride (PVDF) hollow fiber membranes to achieve up to 6 log removal of *Giardia* and *Cryptosporidium*. The UF membranes are operated at a targeted constant flux of about 23.6 gal/ft^2-day. To prevent particulate and organic foulant materials from accumulating on the membrane surface, the membranes are backwashed via water and air scour every 20 minutes and cleaned with sodium hypochlorite daily. The citric acid CIP frequency was designed for about every 18 days based on a maximum transmembrane pressure (TMP) of 10 psi. However, due to the high fouling nature of the source water, the UF membranes are often cleaned with citric acid approximately every 72 hours. The relatively high cleaning frequency hampers treatment productivity and increases the production of citric acid and sodium hypochlorite chemical waste.

The Olinda WTP produces finished water with low alkalinity, turbidity, solids, total hardness (calcium and magnesium), and an average TOC of 2.3 mg/L (see Table 1-3). Although the average TOC concentration may be classified as moderate, the organic matter remaining in the Olinda filtered water is highly reactive and produces large amounts of regulated DBPs with free chlorine. Therefore, the plant uses monochloramine for disinfection to control the levels of regulated DBP formation. According to the United States Environmental Protection Agency's (USEPA's) 2008 Optimization Study, the use of monochloramine disinfection at the Olinda plant is effective in achieving the County's DBP goals (Davis et al., 2008). The County established treatment goals for maintaining annual average and peak DBP concentrations at or below 50 and 80 percent of the regulatory limit. USEPA's 2006 Stage 2 Disinfectants and Disinfection Byproducts Rule (DBPR) sets maximum contaminant levels (MCLs) at 0.080 mg/L for total trihalomethanes (TTHMs) – chloroform, bromodichloromethane, dibromochloromethane, and bromoform; and 0.060 mg/L for haloacetic acids (HAA$_5$) – chloroacetic acid, dichloroacetic acid, trichloroacetic acid, bromoacetic acid, and dibromoacetic acid (USEPA, 2006).

Table 1–3 Olinda WTP Finished Water Quality

Parameter	Minimum	Average	Maximum
pH Target	8.5	8.8	9.0
TOC	0.5	2.3	4.6
Alkalinity (mg/L as CaCO$_3$)	2	5.4	26
Turbidity (ntu)	0.01	0.07	0.85
Total dissolved solids (mg/L)	12	24	41
Calcium (mg/L)	1.1	2.5	5.6
Magnesium (mg/L)	0.3	0.4	1.1

CHAPTER 2. LITERATURE REVIEW

Overview of Ultrafiltration Membrane Processes

In surface water treatment, UF membranes provide a physical barrier to protect consumers from exposure to microbial pathogens by achieving less than 0.1 ntu filtered water turbidity and greater than 4 log removal of *Giardia lamblia* and *Cryptosporidium*. Biological and particulate contaminants greater than the membrane pore size (typically ranging from 0.005 to 0.1 µm) are captured on the membrane surface by the pressure driven sieving process. While UF processes consistently remove particulate matter, UF membrane filtration alone does not remove dissolved contaminants, specifically NOM (Duranceau & Taylor, 2011). Dissolved NOM reacts with chemical oxidants during disinfection to form regulated DBPs (Reckhow & Singer, 2011).

In addition to poor DBP precursor removal, UF membranes face operational challenges with membrane fouling caused by the accumulation of particulate, colloidal, organic, or biological matter. The buildup of these "foulants" on the membrane surface increases the operating TMP required to maintain constant water production (flux). Hence, to keep constant flux at low TMPs, foulants must be removed by performing membrane backwashes and chemical cleanings (Gao et al., 2011). Frequent backwashes and cleans increase the cost of treatment and limit the amount of water that can be supplied to consumers. Consequently, enhancing the UF process requires the removal of NOM and other foulants prior to UF membrane filtration (Duranceau & Taylor, 2011).

Ultrafiltration Membrane Concepts

The UF membrane process is commonly configured as a hollow-fiber membrane module, through which flow passes from inside to outside or outside to inside of the hollow-fiber. The "straw-like" fibers are typically manufactured from polyvinylidene fluoride (PVDF), polyetherfulfone (PES), polysulfone, polypropylene, and cellulose triacetate. The UF membranes are designed as either dead-end or cross-flow filters. Like conventional filters, dead-end UF membranes filter the entire feed water stream. Cross-flow UF membranes treat a portion of the feed water stream, and the remaining unfiltered water is recycled back into the process (Duranceau & Taylor, 2011).

The UF membrane process is operated at a constant flux rate (J), which is expressed in Equation 2-1 as the filtered water (filtrate) flow rate (Q) per unit membrane area (A) (Alspach et al., 2005). The flux may be modeled according to the resistance in series in model (Equation 2-1), in which flux is directly proportional to the TMP (Equation 2-2) and inversely proportional to the water viscosity and the total membrane resistance. As the filtering resistance increases due to the accumulation of foulants, the TMP required to keep constant flux increases. The UF membrane performance is evaluated by normalizing the flux response to the TMP driving force using the specific flux (Equation 2-3). Since the specific flux is temperature dependent, Equation 2-4 is utilized to allow the comparison of specific fluxes at varying feed water temperatures by adjusting to a standard temperature. Together, the TMP and temperature corrected specific flux are used to monitor membrane performance, for which more pronounced TMP rise and specific flux decline signal membrane fouling (Alspach et al., 2005).

$$J = \frac{Q}{A} = \frac{\Delta P}{\mu(R_m + R_t)} \qquad\qquad (2\text{-}1)$$

$$\Delta P = P_{Feed} - P_{Filtrate} \qquad (2\text{-}2)$$

$$J_{SP} = \frac{J}{\Delta P} \qquad (2\text{-}3)$$

$$J_{SP,20^oC} = J_{SP} \times \frac{1.777 - 0.052T + 6.25 \times 10^{-4}T^2}{\mu_{T_{20^oC}}} \qquad (2\text{-}4)$$

Where:

J = Membrane flux (L/m^2-h or gal/ft^2-d)

ΔP = Transmembrane pressure (TMP; bar or psi)

μ = Water absolute viscosity (kg/m-s or lb-s/ft^2)

R_m and R_t = Membrane and total fouling resistance coefficients (1/m or 1/ft)

P_{Feed} and $P_{Filtrate}$ = Feed and filtered water pressure (bar or psi)

J_{SP} = Specific flux (L/m^2-h-bar or gal/ft^2-d-psi)

$J_{SP,20^oC}$ = Specific flux at 20 ^{o}C

T = Measured temperature (^{o}C)

$\mu_{T_{20^oC}}$ = Absolute viscosity at 20 ^{o}C (1.002 cP or 10^{-3} kg/m-s)

Ultrafiltration Membrane Fouling

In their review, Gao and colleagues (2011) attributed UF membrane fouling to four principal fouling agents: particle, colloidal, organic, and microbial or biological matter. Particulate and colloidal fouling occurs when the membrane pore spaces are blocked. In organic fouling, organic matter deposits or adsorbs onto the membrane surface. Biological fouling results from the attachment and growth of bacteria on the membrane surface. Although particulate fouling is for

14

the most part understood, the specific interactions and mechanisms of organic and biological fouling remain unclear (Gao et al., 2011). In order to better identify and understand these fouling mechanisms, researchers have been developing and implementing innovative technology and methods, including size exclusion chromatography, liquid chromatography with organic carbon detection (LC-OCD), confocal laser scanning microscopy, scanning electron microscopy, fluorescence excitation-emission matrix spectroscopy (EEMs), and adenosine triphosphate (ATP) monitoring (Jiang et al., 2010; Peiris et al., 2010; Huber et al., 2011; Sun et al., 2011; Nguyen et al, 2012).

Membrane fouling is controlled operationally by employing membrane backwashes and chemical cleans (Alspach et al., 2005). Membranes are backwashed for a short duration in 30 to 60 minute intervals with air and water streams. Foulants not removed by backwashing accumulate on the membrane surface and cause an increase in TMP during constant flux production. To maintain a stable operating flux at low TMPs, a clean in place (CIP) is performed using acid, caustic, or hypochlorite chemicals. The acid cleaning removes inorganic foulants by soaking membranes in citric acid. The high pH cleaning removes organic and biological matter by contacting the membrane fibers with sodium hydroxide or sodium hypochlorite, depending on the membrane material compatibility. Frequent membrane backwashes and CIPs interrupt water production and decrease the membrane recovery, which is the percentage ratio of the volume of treated water available for distribution to the total volume of water used for distribution, backwashing, and cleaning (Alspach et al., 2005). In addition, more frequent chemical cleans generates larger volumes of cleaning chemicals. The presence of citric acid in recycled membrane backwash water has been shown to hamper the coagulation efficiency (Boyd et al., 2012). Because of the limited

productivity and disruption of coagulation efficiency, advanced pretreatment is necessary to reduce membrane fouling. As a result, membrane researchers aim to evaluate membrane pretreatment alternatives that enhance UF membrane performance (Huang et al., 2009).

Ultrafiltration Membrane Pretreatment

Integrating pretreatment technologies ahead of membranes serve to remove the foulants and improve membrane performance. Some presently identified UF pretreatment options include coagulation-clarification (conventional), adsorption (GAC and PAC), MIEX®, pre-oxidation (ozone), and biofiltration (Huang et al., 2009; Gao et al., 2011). Of these technologies, biofiltration along with MIEX® and GAC require additional research to establish the effects on UF treatment and production efficiency, particularly under low alkalinity conditions and in conjunction with conventional treatment (Huang et al., 2009; Gao et al., 2011; Huck et al., 2011).

Many whom have studied the integration of conventional pretreatment ahead of UF membrane filtration (Liang & Singer, 2003; Chen et al., 2007; Matilainen et al., 2010; Xiao et al., 2010) have shown this approach to be an effective strategy for reducing the DBP formation and membrane fouling of many surface water sources. However, for surface waters rich in DBP precursors, the chemical destabilization and removal of NOM by coagulation and clarification pretreatment may not be sufficient to control DBP formation with free chlorine disinfection (Lovins et al., 2003). Furthermore, coagulation and clarification pretreatment mainly remove the larger hydrophobic NOM fraction and allow for the passage of smaller and hydrophilic NOM that have been shown to contribute to membrane fouling (MWH, 2005; Lozier et al., 2008; Huang et al., 2009). To fill in the treatment gaps of conventional pretreatment, recent research efforts are focusing on the

investigation of advanced pretreatment technologies, including MIEX®, adsorption, and most recently biofiltration (Gao et al., 2011).

<u>MIEX® High Rate System</u>

MIEX® was developed by Orica Watercare, Inc. to remove dissolved NOM by exchanging with a chloride (or bicarbonate) ion on the magnetized resin surface. The magnetized iron oxide component allows the resin to be applied in a high rate (HR) fluidized bed process, in which water flows up through the contactor and is mixed with resin (Boyer & Singer, 2005; 2006; Singer et al., 2009). The success of MIEX® as a NOM removal technology prompted researchers to investigate MIEX® as an alternative pretreatment for UF membranes (Boyer & Singer, 2005; Gao et al., 2011).

In a pilot study that examined MIEX® ahead of coagulation, settling, and UF membranes, Xu and researchers (2011) concluded that MIEX® reduced membrane pore blocking and cake resistance fouling by removing hydrophobic and hydrophilic NOM, mostly in the 3,000 to 100,000 dalton molecular weight (MW) range. In a similar bench-scale study, Liu and colleagues (2011) recognized the possibility for MIEX® to have wide application in UF pretreatment because MIEX® removed large MW organics, including polysaccharides and proteins that contribute to specific membrane flux decline. Other researchers attributed small to negligible improvements in membrane performance to moderate reductions in high MW hydrophilic and neutral organics or resin carry over (Humbert et al., 2007; Huang et al. 2012). Based on the conflicting findings, it is evident that additional research is needed to examine the effect of MIEX® on UF operation.

Activated Carbon Adsorption

Adsorption via powdered activated carbon (PAC) and granular activated carbon (GAC) processes is used to remove target dissolved contaminants, including taste and odor compounds, synthetic organic chemicals, color forming organics, and DBP precursors. The adsorption process operates via chemical reactions or physical attractions on the carbon's active surface sites. The extent of adsorption mainly depends upon the strength of the affinity of the activated carbon for the dissolved species. This relationship is quantified by adsorption isotherm models, which describe the amount of dissolved species (i.e. organics) that can be adsorbed onto the activated carbon at equilibrium. A commonly utilized isotherm model is the Freundlich isotherm, which is described by the mathematical expression presented in Equation 2-5 (MWH, 2005).

$$q = KC^{1/n} \tag{2-5}$$

Where:

q = Loading (mg dissolved organics/g GAC)

K = Freundlich adsorption capacity parameter $(mg/g)(L/mg)^{1/n}$

1/n = Freundlich adsorption intensity parameter (dimensionless)

C = Concentration of dissolved organics (mg/L)

The isotherm relationship is typically developed through laboratory experiments and is necessary for determining important design and operational parameters. The design parameters for GAC in the fixed-bed mode include the empty bed contact time (EBCT), carbon usage rate, and carbon bed life. These parameters, for which mathematical equations are presented in Equations 2-6

through 2-10, aid in determining the necessary mass of GAC, contactor size, and GAC replacement

frequency (MWH, 2005).

$$EBCT = \frac{V}{Q} \qquad (2\text{-}6)$$

$$CUR = \frac{C_{inf}}{K(C_{inf})^{1/n}} \qquad (2\text{-}7)$$

$$M_{GAC} = EBCT \times Q \times \rho_F \qquad (2\text{-}8)$$

$$V_{treated} = \frac{GAC_{Mass}}{CUR} \qquad (2\text{-}9)$$

$$Bed\ Life = \frac{V_{treated}}{Q} \qquad (2\text{-}10)$$

Where:

EBCT = Empty bed contact time (min)

Q = Flow rate to GAC contactor (L/min)

V = Volume of GAC in contactor (L)

CUR = Carbon usage rate (g/L)

C_{inf} = Influent concentration of dissolved organics (g/L)

M_{GAC} = Mass of GAC at selected EBCT (g)

ρ_F = Density of GAC media (g/L)

$V_{treated}$ = Volume of water treated (L)

Depending on the GAC's contactor size and replacement requirements, GAC applied in a fixed-

bed mode can be costly. PAC offers a lower cost method of application (MWH, 2005). Because

of the cost benefit, researchers have focused on investigating PAC adsorption as a UF enhancement option (Gao et al., 2011). However, recent studies reveal that PAC adsorption may have variable impacts on both DBP control and UF membrane fouling depending on the PAC and membrane specifications (Kristiana et al., 2011; Stoquart et al., 2012; Boyd, 2013).

The uncertainly of PAC as an effective treatment alternative emphasizes the need to consider GAC as a viable option for improving the operation of UF processes. In a pilot-scale study, Tsujimo and associates (1998) determined that fixed-bed GAC pretreatment prevented irreversible fouling and allowed for stable UF process operation. The success of GAC pretreatment is most likely due to the removal of dissolved NOM as Huang and researchers (2007) have showed that NOM contributes directly to organic fouling. Although the results show promise for GAC as an effective pretreatment strategy, additional research is necessary to validate the impacts of water quality improvements on the production efficiency of UF membranes.

Overview of Biofiltration

Biofiltration provides a novel cost-effective treatment option for removing biodegradable NOM, ammonia, nitrate, iron, manganese, and taste and odor caused by geosmin and methylisoborneol (MIB) (Bouwer & Crowe, 1988; Urfer et al., 1997; Moll & Summers 1999; Brown & Lauderdale, 2006; Simpson, 2008; Zhu et al., 2010; Summers et al., 2011; Tekerlekopoulou et al., 2013). Researchers have demonstrated that by removing biodegradable nutrients, biofilters can produce biologically stable water with lower DBP formation potential (Rittmann & Snoeyink, 1984; Bouwer & Crowe, 1988; Miltner et al., 1992; Miltner et al., 1995; Persson et al., 2006). Recently,

the application of biofiltration has expanded to include UF membrane pretreatment. A summary of the results from previous biofiltration research is presented in Table 2-1.

Biofiltration Concepts

Biofiltration applications consists of operating granular media filters to promote the attachment and growth of a biofilm. Biofilms can support a wide variety of microbial groups, but generally form in the same sequential manner: deposition and adsorption of organic molecules to form a "conditioning film", adsorption of microorganisms on the film, secretion of extracellular polymeric substances (EPS) to fortify the film, and growth of microorganisms.

The microbial communities present within the biofilms serve to remove biodegradable contaminants from water by contaminant diffusion into the biofilm and biological degradation (Zhu et al., 2010). To enhance biological degradation of target contaminants within biofilters, many researchers have investigated the impacts of water characteristics and filter operations (Urfer et al., 1997; Niquette et al., 1998; Huck et al., 2000; Liu et al., 2001; Summers et al., 2011; Lauderdale et al., 2012; 2014).

Table 2–1 Literature Summary of Biofiltration Research in Water Treatment

Filter Type	Scale	Water Source	Raw Water Quality					Performance % Removal		Down-stream Process	Reference Source
			pH	Temp. (°C)	Alk. (mg/L CaCO₃)	Hardness (mg/L CaCO₃)	Nutrient Addition (Yes/No)	Turb.	Organics		
Mixed Media (Anthracite/ Sand/ Garnet)							N	NA	AOC: 75.3% TOC: 26%	NS	
Dual Media (GAC/Sand)	Pilot	Surface water (reservoir)	6.3-7.6	3.5-31	20.9-31	43.5-64.5	N	NA	AOC: 86.4% TOC: 51%	NS	LeChevallier et al., 1992
Mono-media (GAC)							N	NA	AOC: 86% TOC: 56%	NS	
Sand	Bench	Coagulated and ozonated surface water	NA	22.5	33 (Adj.)	NA	Y	NA	TOC: 16-33%		Hozalski et al., 1995
		Coagulated and ozonated groundwater	8	22.5	260	NA	Y	NA	TOC: 13-18%	NS	
		Coagulated and ozonated synthetic water (with soluble extracellular materials)	7.9	22.5	76	NA	Y	NA	TOC: 30-33%		
Sand	Pilot	Surface water	7.9	5-6	250	158	N	70%	DOC: 7.7%	UF	Lipp et al., 1998
BAC (1st stage dual, 2nd stage mono, and direct dual)	Pilot/ full scale	Surface water	5-8.2	1-25	NA	NA	N	NA	BDOC: 22-50%	NS	Laurent et al., 1999

Filter Type	Scale	Water Source	Raw Water Quality					Performance % Removal		Down-stream Process	Reference Source
			pH	Temp. (ºC)	Alk. (mg/L CaCO$_3$)	Hardness (mg/L CaCO$_3$)	Nutrient Addition (Yes/No)	Turb.	Organics		
GAC								33-50%	DOC: 21-31%		
Anthracite	Pilot	Ozonated groundwater	8.2	22	165	NA	N	33-50%	DOC: 3-28%	NS	Rittmann et al., 2002
Sand								33-50%	DOC: 5-24%		
BAC	Bench	Dechlorinated Tap Water with the addition of humic/fulvic acids	NA	22	NA	NA	Y	NA	TOC: 22.5%	Mem-brane process	Wend et al., 2003
Iron-oxide coated sand			NA	22	NA	NA		NA	TOC: 19%		
Dual Media (Anthracite/ Sand)	Bench	Synthetic feedwater	NA	NA	300-350	325-350	Y	NA	TOC: 24-30%	UF	Basu & Huck, 2004
Dual Media (Anthracite/ Sand)	Bench	Synthetic feedwater (with TOC composed of 65% humic acid and 35% readily biodegradable components)	NA	NA	300-350	325-350	N	NA	TOC: 50%	UF	Basu & Huck, 2005
Activated Clay, Aeiolite	Full-scale	Water reclamation effluent (pre-chlorination)	6-7	25-30	NA	NA	N	NA	DOC: 35-45% AOC: 42-48%	CF/RO	Hu et al., 2005
GAC	Bench	Biologically Treated Sewage Effluent	6.8-7.5	NA	NA	NA	N	NA	DOC: 65%	UF & NF	Shon et al., 2005
GAC	Pilot	Groundwater	NA	NA	NA	NA	N	NA	TOC: 65% BDOC: 93%	NS	Brown & Lauderdale, 2006

Filter Type	Scale	Water Source	Raw Water Quality					Performance % Removal		Down-stream Process	Reference Source
			pH	Temp. (°C)	Alk. (mg/L CaCO₃)	Hardness (mg/L CaCO₃)	Nutrient Addition (Yes/No)	Turb.	Organics		
Dual Media (Anthracite/ Sand)	Bench	Synthetic feed water (tap water spiked with humic acid, easily biodegradable organics, nitrogen, and phosphorus)	NA	NA	NA	283	Y	NA	TOC: 48% DOC: 36%	UF & NF	Mosqueda-Jimenez & Huck, 2006
GAC						NA	N	NA	DOC: 12% BDOC: 34% AOC: 22%		
Expanded Clay (fine)	Pilot	Surface Water	6.9-7.3	1.5-20.2	23-32	NA	N	NA	DOC: 5% BDOC: 30% AOC: 35%	Mem-brane process	Persson et al., 2006
Expanded Clay (coarse)						NA	N	NA	DOC: 3% BDOC: 28% AOC: 41%		
Dual Media (Anthracite/ Sand)	Bench	Surface water impacted by WW effluent, urban, industrial, and agriculture runoff	7.95 – 8.40	0-23	160 -250	200 - 350	N	75 - 80%	DOC: 11% TOC: 22-32%	UF	Halle et al., 2009
Dual Media (Anthracite/ Sand)	Bench	Synthetic tap water (dechlorinated with humic acid addition)	7.2-7.6	20	300-350	325-350	Y	NA	DOC: 64-95% TOC: 73-96%	NF	Mosqueda-Jimenez & Huck, 2009
Sand	Pilot	Domestic wastewater (secondary effluent)	7.2	19.3	NA	NA	N	76-86%	DOC: 10-13% UV254: 3-5%	UF	Zheng et al., 2009a
Sand	Bench	Domestic wastewater (secondary effluent)	6.9-7.2	NA	NA	NA	N	NA	Biopolymers: 62%	UF	Zheng et al., 2009b
PAC	Bench	Water Treatment Plant (Post-Ozonated)	6.67	10.3	31	NA	N	NA	DOC: 5-16% BDOD: 30-45%	NS	Markarian et al., 2010

24

Filter Type	Scale	Water Source	Raw Water Quality					Performance % Removal		Down-stream Process	Reference Source
			pH	Temp. (°C)	Alk. (mg/L CaCO$_3$)	Hardness (mg/L CaCO$_3$)	Nutrient Addition (Yes/No)	Turb.	Organics		
Sand	Bench	Surface water affected by industrial, sewage, and agricultural pollution.	6.7-8.6	5-27	NA	NA	N	NA	BDOC: 55-73% UV254: 32-46%	NS	Tang et al., 2010
Sand	Pilot	Domestic wastewater (secondary effluent)	7.2	13-26	NA	NA	N	80%	DOC: 10% Biopolymers: 48%	UF	Zheng et al., 2010
BAF	Bench	River Water	NA	20	NA	NA	N	77%	TOC: 51% UV254: 37%	UF	Huang et al., 2011
Dual Media (Anthracite/ Sand)	Pilot	Surface water impacted by agricultural, industrial and municipal runoff	7.95-8.4	0-23	160-250	200-350	N	72%	NA	UF	Hucket al., 2011
GAC	Pilot	Ozonated surface water	7.79	7.05	260	NA	N	NA	DOC: 22%	UF	Velten et al., 2011
Aerated Pebble bed	Pilot / Bench	Synthetic feedwater (tapwater with 1:30 domestic sewage and 0.5 mg/L humic acid)	8	20	NA	NA	Y	>90%	TOC: 83% DOC: 55% UV254: 44% AOC: 85% BDOC: 92%	UF	Wei et al., 2011*
BAC	Bench / Pilot	Ozonated surface water impacted by agricultural runoff	6.95	22	NA	NA	N	50%	DOC: 25% UV254: 10%	UF	Geismar et al., 2012
Dual Media (Anthracite/ Sand)	Pilot	Surface water	7.6-8.8	0.7-25.3	147-289	178-355	N	55-96%	DOC: <15% TOC: <20%	UF	Peldszus et al., 2012

Filter Type	Scale	Water Source	Raw Water Quality					Performance % Removal		Down-stream Process	Reference Source
			pH	Temp. (ºC)	Alk. (mg/L CaCO₃)	Hardness (mg/L CaCO₃)	Nutrient Addition (Yes/No)	Turb.	Organics		
Sand	Pilot	Biologically active, aerated, surficial groundwater	7.7	27.5	166	471	N	25%	TOC: 15%	UF	Tharamapalan, 2012; Duranceau & Tharamapalan, 2013
GAC (10.8 min EBCT)	Bench	Seawater	8.03	25	NA	NA	N	60%	DOC: 60% AOC: 98%	RO	Naidu et al., 2013
GAC (7.2 min EBCT)								60%	DOC: 65% AOC: 97%		
GAC (5.4 min EBCT)								60%	DOC: 58% AOC: 97%		
Dual Media (Sand/GAC)	Pilot	Pre-ozonated, coagulated, softened, and settled river water	7.1	NA	112	136	Y	99%	DOC: 36%	Disinfec-tion and corro-sion control	Lauderdale et al., 2014
Dual Media (Sand/ Anthracite)								99%	DOC: 9.8%		
Dual Media (Sand/GAC)	Pilot	Coagulated, settled, and ozonated surface water	7.5	NA	100	240	Y	99%	DOC: 21.5%	Disinfec-tion	Lauderdale et al., 2014
Dual Media (Sand/ Anthracite)								99%	DOC: 5.6%		
GAC	Full / Pilot	Ozonated and non-ozonated surface water	7.61	7.9	89	NA	N	59%	TOC: 3% DOC: 3%	UF	Wang, 2014

*Reference was published in Bioinformatics and Biomedical Engineering, (iCBBE) 2011 5th International Conference on May 12, 2011; the Institute of Electrical and Electronics Engineers (IEEE) released a notice of retraction after the conclusion of the research presented herein (IEEE, 2015).
NS = not specified; NA = not available; DOC = dissolved organic carbon; TOC = total organic carbon; BDOC = biodegradable dissolved organic carbon; AOC = assimilable organic carbon; BAF = biological aerated filter; GAC= granular activated carbon; PAC = powder activated carbon; BAC = biological activated carbon; BAF = biological aerated filter; CF = cartridge filter; RO = reverse osmosis; NF = nanofiltration

The major water quality parameters that have been shown to affect the performance of biofilters include temperature, pH, organic carbon, alkalinity, and nutrients – nitrogen and phosphorus (Huck et al., 2000; Chaudhary et al., 2003; Lauderdale et al., 2014). While difficult to control, colder water temperatures may have detrimental impacts on the overall removal of biodegradable contaminants, particularly NOM (Hozalski et al., 1999; Emelko et al., 2006). Additionally, microorganism generally thrive in near neutral pH (6.5 to 8) environments (Metcalf & Eddy, 2003). The level of substrate, which can be represented by dissolved organic carbon (DOC), is known to directly impact biofiltration performance (Chaudhary et al., 2003; Huck & Sozanski, 2008; Velten et al., 2011). Using a first-order empirical model, Huck and researchers (1992; 1994) demonstrated that the biodegradable organic matter (BOM) removal was directly proportional to the BOM concentration in the biofilter feed water.

Although some researchers note the importance of alkalinity in biological processes, few studies have examined the effect of alkalinity on biofiltration performance (Hozalski et al., 1995; Metcalf & Eddy, 2003; Ren et al., 2010). Alkalinity is the measure of a water supply's ability to neutralize acids (Sawyer et al., 2003). Hence, alkalinity directly influences the chemistry of the aquatic environment (Jensen, 2003). Waters rich in alkalinity also tend to be rich in total hardness, which is generally considered as the sum of calcium and magnesium hardness (Sawyer et al., 2003; Zhu et al., 2010). These major cations are known to play a vital role in the development and maintenance of biofilms by helping bind negatively charged EPS together to form the biofilm matrix (Lion et al., 1988; van Loosdrecht et al., 1989; Geesey et al., 1999; Lattner et al., 2003; Song & Leff, 2006). Novak and researchers (1998) have demonstrated the importance of calcium and magnesium for effective flocculation of activated sludge. Additionally, Ren and coworkers

(2010) have demonstrated the importance of quantifying the net alkalinity consumption in membrane bioreactor systems. However, little to no research has been conducted on the direct influence of alkalinity or inorganic carbon on the performance of biofilters, particularly as pretreatment to UF membranes.

Instead, researchers have focused on altering the feed water characteristics through pH adjustment, nutrient addition with nitrogen or phosphorus source, and pre-oxidation with ozone or peroxide (Hozalski et al., 1995; Graham, 1999; Wend et al., 2003; Basu & Huck, 2004; Lauderdale et al., 2011; 2012; 2014). Implementing these strategies to enhance the treatment and operating efficiency of biofilters is recently known as "engineered biofiltration" (Lauderdale et al., 2011; 2012; 2014).

Of the "engineered biofiltration" strategies, supplementing the nutrient availability in the feed water is generally the most common. When augmenting the nutrient availability, researchers typically make adjustments based on the carbon to nitrogen to phosphorus (C:N:P) molar ratio. According to LeChevallier and researchers (1991), a C:N:P ratio of 100:10:1 is sufficient to support microbiological activity. Based on the earlier work of LeChevallier et al. (1991), Huck, Lauderdale, and other researchers have targeted a C:N:P molar ratio of at least 100:10:1 to promote adequate bio-growth and removal of biodegradable contaminants (Basu & Huck, 2004; Mosqueda-Jimenez & Huck, 2006; Lauderdale et al., 2014).

In addition to supplementing nutrients, Lauderdale and researchers (2014) have implemented pH adjustment as a strategy to maintain a neutral pH range (6.5 to 8). The researchers also applied peroxide as a pre-oxidant to reduce the head loss across the biofilter (Lauderdale et al., 2014).

Other researchers have successfully applied ozone as a pre-oxidant (ozonation) to increase the fraction of biodegradable NOM and improve the overall DOC removal and corresponding DBP formation (Miltner et al., 1992; Hozalski et al., 1999; Moll & Summers, 1999; Velten et al., 2011). While pre-oxidation strategies offer additional benefits, pre-oxidation systems, particularly ozonation, represent an additional capital and operating cost for utilities. The added costs are a significant consideration for utilities that face high electrical rates, as for the County of Maui (Reiling et al., 2009; Lekven, 2011).

The performance of biofiltration is also influenced by filter design and operating parameters, including the EBCT, hydraulic loading rate (HLR), backwashing protocol, and granular media type (Urfer et al., 1997; Niquette et al., 1998; Huck et al., 2000; Liu et al., 2001; Emelko et al., 2006). Biofilters are typically designed and operated in a down-flow configuration. The EBCT, defined previously in Equation 2-6, is a chief operating parameter. In an earlier study, Hozalski and researchers (1992) showed that increasing the EBCT increased the organic carbon removal efficiency of biofiltration. While Huck and colleagues support these previous findings, their research demonstrated that increasing the EBCT beyond 15 minutes tends to produce diminishing returns on the level of DOC removal (Huck et al., 2000; Huck & Sozanski, 2008).

Increasing the EBCT can be accomplished by increasing the filter depth and is related to the HLR according to Equation 2-11. The HLR describes the water filtration velocity across the depth of the biofilter. Traditionally, biofilters have been operated at slow filtration rates (HLR = 0.5 to 2 gpm/ft^2) (Reckhow & Singer, 2011). Recently, research efforts have focused on operating filters at more rapid filtration rates (2 to 6 gpm/ft^2) to reduce footprint requirements while maintaining DOC removals (Huck & Sozanski, 2008; Halle et al., 2009; Peldszus et al., 2012; Velten et al.,

2011; Geismar et al., 2012; Naidu et al., 2013). Although applying more rapid filtration rates reduces the biofilter contactor size, slower filtration rates are known to effectively promote the attachment and growth of the biofilm on the media (Huck et al., 2000; Shon et al., 2005; Zheng et al., 2009a; Mosqueda-Jimenez & Huck, 2009; Zheng et al., 2010).

$$\text{HLR} = \frac{Q}{A} = \frac{D}{EBCT} \tag{2-11}$$

Where:

Q = Flow rate (gpm)

A = Filter area (ft^2)

D = Filter depth (ft)

While the purpose of biofiltration is to achieve good biofilm development on the media, backwashing is necessary to avoid high pressure drops caused by deposited particles and excess bio-growth (biofouling) (Simpson, 2008; Zhu et al., 2010). Backwashing strategies include bed fluidization, collapse pulsing, and air scour with negligible to 50% bed expansions (Rittmann & Snoeyink, 1984; Niquette et al., 1998; Huck et al., 2000; Persson et al., 2006; Peldszus et al., 2012). Researchers have demonstrated that backwashing with or without air scour is not detrimental to maintaining the necessary biofilm on the media (Amirtharajah et al., 1991; Huck et al., 2000; Chaudhary et al., 2003; Huck & Sozanski, 2008). Additionally, chlorine in the backwash water does not appear to impair full-scale systems, but may be detrimental to bench or pilot scale systems which have not established a robust biofilm community (Miltner et al., 1995; Liu et al., 2001; Huck & Sozanski, 2008). To reduce the usage of treated water for backwashing and increase the water recovery, it is desirable to extend the filtration time between backwashes also known as filter run

time. In an earlier study, Goldgrabe and colleagues (1993) reported biofilter run times between 92 to 224 hours. A more recent study conducted by Lauderdale and colleagues (2014) operated the biofilters at about 24-hour filter run times.

Biofilters typically employ sand, anthracite, or GAC media. While some researchers have demonstrated that sand and anthracite biofilters achieve similar biodegradable DOC removal rates as BAC filters, BAC tends to achieve more favorable DOC removals under colder or less favorable conditions (Huck et al., 2000; Liu, et al., 2001; Emelko et al., 2006). In GAC filtration, the DOC removal mechanism goes through three major stages: adsorption, adsorption/biodegradation, and biodegradation. In the first stage, DOC is primarily removed by adsorption onto the active carbon sites. In the second stage, the active carbon sites are nearly spent and biofilms begin develop. In the final stage, the active carbon sites are exhausted and DOC removal is primarily attributed to biodegradation. As the treatment mechanism shifts from adsorption to biological, DOC removal has been observed to be highest during adsorption and decrease to a lower steady-state removal during biodegradation (Simpson, 2008; Zhang et al., 2010). Nevertheless, the biodegradation mechanism serves to biologically stabilize the feed water and has been shown to provide effective pretreatment to UF membrane processes (Halle et al., 2009; Peldszus et al., 2012).

Biofiltration as Pretreatment to Ultrafiltration Membrane Processes

Because of the recognized benefits of biofiltration, its application in drinking water treatment has recently expanded to include pretreatment for UF membrane processes. The study conducted by Wend and colleagues (2003) on the direct biofiltration of a synthetic organic acid surface water before low pressure membranes helped fuel the interest in applying biofiltration pretreatment for UF membrane processes in drinking water. Wend et al.'s (2003) research demonstrated that biofiltration reduced membrane fouling by reducing the feed water's bacterial cell count. Following Wend et al.'s (2003) research efforts, Huck and colleagues conducted bench and pilot scale studies on the direct biofiltration of synthetic and natural surface waters ahead of UF membranes. Huck's research group found that biofiltration reduced the membranes' operating TMP rise by significantly removing turbidity, organics, and biopolymers from the feed water (Basu & Huck, 2004; 2005; Mosqueda-Jimenez & Huck, 2006; 2009; Halle et al., 2009; Huck et al., 2011; Peldszus et al., 2012; Wang, 2014).

Similar studies performed by Persson et al. (2006), Huang et al. (2011), and Velten et al. (2011) support the ability of biofilters to alleviate UF membrane fouling by reducing the feed water's turbidity, organics, and biological activity levels. However, the researchers did not present a comparison of the improvement in UF operating parameters – TMP or specific flux (Persson et al., 2006; Huang et al., 2011; Velten et al., 2011). Biofiltration pretreatment has also been shown to be effective for other water sources, including surficial groundwater (impacted by surface water) and biologically treated wastewater (Shon et al., 2005; Zheng et al., 2009a; 2009b; 2010; Duranceau & Tharamapalan, 2013). Although previous research shows promise for the successful

implementation of biofiltration pretreatment, limited research has been conducted on low alkalinity, organic acid-laden surface water supplies.

The research matrix, illustrated in Figure 2-1, organizes the research that has been conducted on biofiltration pretreatment for low pressure membranes with respect to low, moderate, and high alkalinity and dissolved organic carbon (DOC) ranges. It is clear from the research matrix that the majority of the research has focused on high alkalinity water supplies. Little to no research is available regarding biofiltration of low alkalinity water sources.

In addition, few studies have investigated the integration of biofiltration within a conventional-UF process. The research conducted by Lipp and colleagues (1998) suggested that integrating coagulation, sand filtration, and UF enhances the overall turbidity removal. Wei and researchers (2011) reported favorable results when integrating biofiltration ahead of a coagulation and UF process, but the research was conducted for only a six-day period. Therefore, clear insights into pretreatment impacts of biofiltration within conventional-UF processes remains lacking. Since conventional processes are common to surface water treatment, water professionals and utilities would benefit from a better understanding of the role of biofiltration within conventional-UF systems.
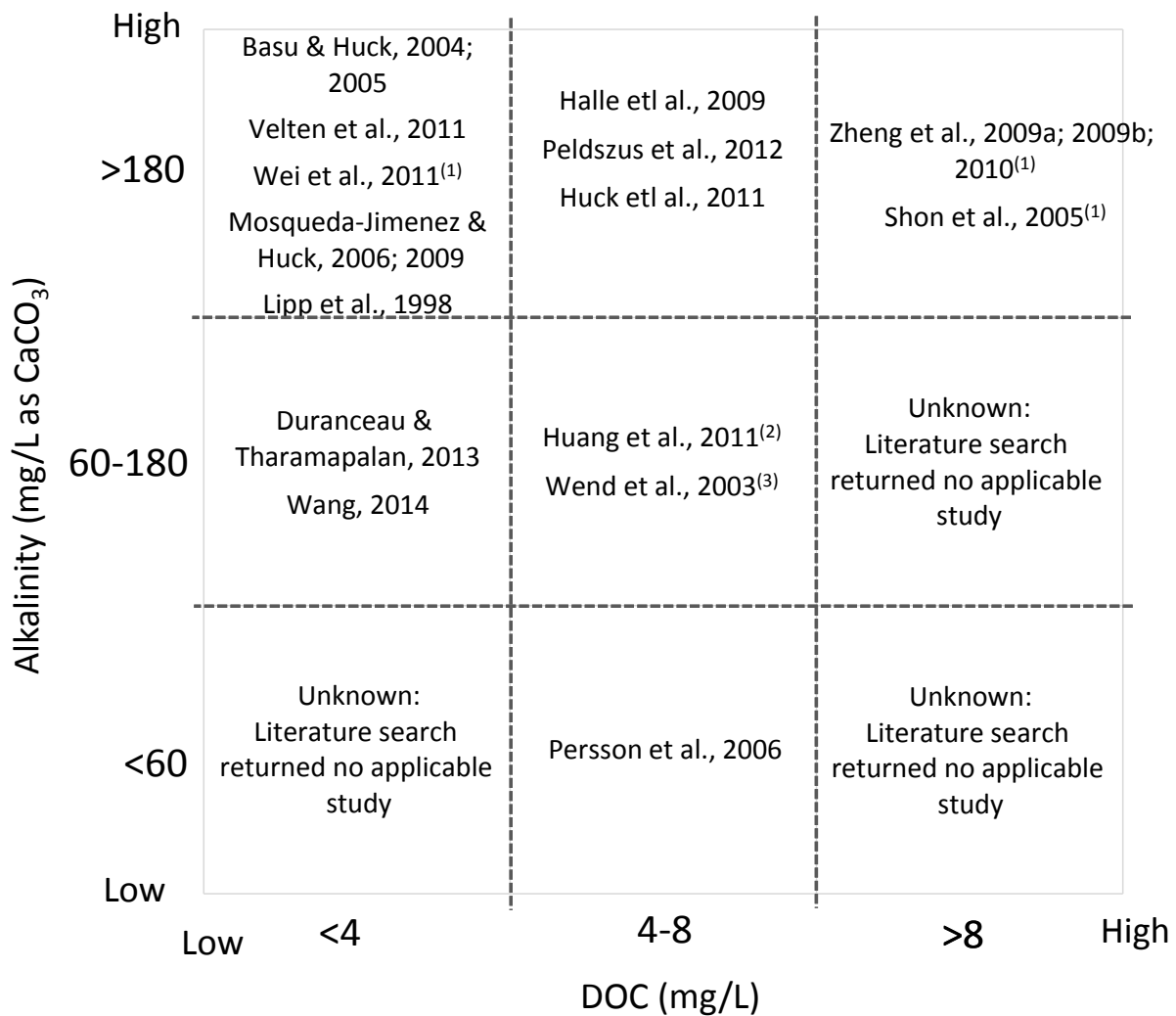
Figure 2–1 Biofiltration Pretreatment Literature Summary Matrix

(1) Alkalinity assumed to be approximately 200 mg/L as $CaCO_3$ based on typical characteristics of domestic wastewater (Metcalf & Eddy, 2003)
(2) Alkalinity range retrieved from previous study conducted by Cai et al., 2003
(3) Alkalinity range retrieved from the City of Bozeman's WTP Water Quality Report (2009)

Modeling Biofiltration Performance

According to Huck and Sozanski (2008), modeling methods fall under three major categories: operation, design, and research. Each approach offers varying degrees of complexity and comprehensiveness. Operation-geared models are more simple and easily understood, while research models are generally more complex and comprehensive. Design models typically fall in the middle range between operation and research models (Huck & Sozanski, 2008). Of the models applied to biofiltration performance, the majority are research-type models that offer little use for practical application by water purveyors and professionals.

The steady-state biofilm model developed by Rittmann and McCarty (1980) is considered to be the most accepted and is often utilized as a model framework for other models (Urfer et al., 1997; Chaudhary et al., 2003; Metcalf & Eddy, 2003; Huck & Sozanski, 2008). The model incorporates Monod kinetics and Fick's second law to develop equations that relate the substrate concentration (target contaminant) to kinetic constants, diffusivity constants, and biofilm properties. The model framework is described by three major equations, included in Equations 2-12 through 2-14 in dimensionless units (Rittmann & McCarty, 1980).

$$S_b^* = S_s^* + J^* L^* / D^* \qquad (2\text{-}12)$$

$$S_{min}^* = b/(Yk - b) \qquad (2\text{-}13)$$

$$L_f^* = \frac{1 + S_{min}^* J^*}{S_{min}^*} = J^* k \, Y / b \qquad (2\text{-}14)$$

Where:

$$S_b^* = S_b/K_s \tag{2-15}$$

$$S_s^* = S_s/K_s \tag{2-16}$$

$$S_{min}^* = S_{min}/K_s \tag{2-17}$$

$$J^* = J\tau/K_s D_f \tag{2-18}$$

$$L_f^* = L_f/\tau \tag{2-19}$$

$$L^* = L/\tau \tag{2-20}$$

$$D^* = D/D_f \tag{2-21}$$

$$\tau = \left[K_s D_f/kX_f\right]^{1/2} \tag{2-22}$$

S_b = Bulk liquid substrate concentration (mass of substrate/volume)

S_s = Substrate concentration at interface (mass of substrate/volume)

S_{min} = Minimum substrate concentration that supports biofilm (mass of substrate/volume)

D = Free liquid diffusivity (area/time)

D_f = Biofilm diffusivity (area/time)

K_s = Half rate constant from Monod equation (mass of substrate/volume)

k = Maximum specific rate of substrate utilization (1/time)

Y = Yield coefficient (biomass/mass of substrate)

b = Overall biofilm decay coefficient (1/time)

X_f = Biofilm density (biomass/volume)

L_f = Biofilm thickness (length)

L = Effective diffusion layer thickness (length)

Following the establishment of the model framework, Saez and Rittmann (1988; 1992) and Rittman and McCarty (2001) developed "pseudo-analytical solutions" based on fitting algebraic equations to numerical solutions of the steady-state biofilm model equations. An analytical solution was developed by Zhang and Huck (1996), who assumed a plug flow reactor (biofilter) configuration to solve for the depth of the filter (X), which is presented in Equation 2-23.

$$X = \frac{v\tau}{\alpha D_f} \int_{S_{sx}^*}^{S_{so}^*} \frac{dS_S^*}{J^*} + \frac{vL}{\alpha D} \ln \frac{J_o^*}{J_x^*} \qquad (2\text{-}23)$$

Where:

$$S_{so}^* = S_{so}/K_s \qquad (2\text{-}24)$$

$$S_{sx}^* = S_{xo}/K_s \qquad (2\text{-}25)$$

v = Hydraulic loading rate (length/time)

α = Specific surface area (biofilm surface area/volume of bioreactor, 1/length)

x = Longitudinal distance along column (length)

J_o = Flux of substrate into biofilm at inlet of column (mass of substrate/area-time)

J_x = Flux of substrate at outlet of column (mass of substrate/area-time)

S_{so} = Substrate concentration on biofilm at inlet of column (mass of substrate/volume)

S_{sx} = Substrate concentration on biofilm outlet of column (mass of substrate/volume)

Huck and his research team built upon their analytical solution (Equation 2-23) and developed the concept of dimensionless contact time or X*. In their model, presented in Equation 2-26, the dimensionless EBCT is related to the actual EBCT, reactor specific surface area, biodegradable organic matter (BOM) diffusivity in the biofilm, biofilm density, and biodegradation kinetic parameters (Zhang & Huck, 1996; Huck & Sozanski, 2008).

$$X^* = \vartheta \frac{\alpha D_f}{\tau} \int_{S_{sx}^*}^{S_{so}^*} \frac{dS_s^*}{J^*} + \frac{L^*}{D^*} ln \frac{J_o^*}{J_X^*} \tag{2-26}$$

Where:

$$\vartheta = X/v = EBCT \tag{2-27}$$

The dimensionless contact time model, which is further simplified in Equation 2-28, has been shown to effectively describe the percent removal of substrate by biofilters under varying conditions (Huck & Sozanski, 2008).

$$X^* = \vartheta \alpha D_f^{1/2} \left(k X_f / K_s\right)^{1/2} \tag{2-28}$$

While the concept of dimensionless contact time provides a predictive tool for estimating the substrate removal of biofilters, Huck and Sozanski (2008) recognize that further model development is needed to apply the X^* concept to biofiltration as pretreatment to UF membranes. Furthermore, the dimensionless contact time approach still requires the quantification of kinetic constants and biofilm density, which entails controlled experimental and laboratory conditions. Therefore, there remains a need for the development of a simple, practically-oriented model for predicting the performance of biofiltration pretreatment ahead of UF membrane processes.

CHAPTER 3. METHODS AND MATERIALS

The research project approach embraced a holistic methodology, where water quality was examined from source to distribution system. The Waikamoi watershed quality was profiled to understand the chemistry of the water as it travels to the Olinda WTP. The need for additional pretreatment was then confirmed by monitoring the operation and water quality of the existing treatment process and verifying coagulation operations with jar testing experiments. Pilot-scale evaluations of MIEX®, GAC, and BAC as UF pretreatment alternatives were also conducted by utilizing the existing conventional and UF pilot system as the control. The control UF pilot was compared to the full-scale UF process to illustrate that the pilot was representative of the full-scale. Furthermore, the pretreatment options were assessed based on improvements to the quality and production efficiency of the finished water that is supplied to consumers. A graphical representation of the research project structure is provided in Figure 3-1.

Surface Overland Flow Water Quality Analysis
- Water quality monitoring througout Waikamoi watershed

Confirmation of Existing Conventional-UF Process
- Water quality & operational monitoring
- Jar testing
- Pilot vs full scale UF comparison

MIEX®, GAC, and BAC Pretreatment Evaluation
- Water quality & operational monitoring
- Pilot pretreatment-UF vs control-UF comparison

Figure 3–1 Research Project Structure

Surface Overland Flow Water Quality Analysis

The native watershed was characterized by investigating the native source water chemistry and extending the analysis from the flume into the drinking water distribution system. This complex transport is believed to impact the water chemistry; hence, characterizing the watershed quality is expected to aid the County in making watershed management decisions that enhance the downstream UF treatment processes. Furthermore, understanding the source water variability can better equip treatment plant operators to make process adjustments, such as coagulant dosing, as a response to changes in the raw water quality.

To account for seasonal variability and weather impacts, six watershed sampling and testing events were conducted on November 15, 2012, January 31, 2013, April 30, 2013, August 6, 2013, October 22, 2013, and May 12, 2014. Samples were collected at various flume intakes and outlet structures, the Waikamoi reservoirs, two caisson pipelines that feed the Kahakapao reservoirs, and the Kahakapao reservoirs. Specific sampling locations varied depending on the physical accessibility and water availability during the sampling event. The sampling locations with approximate GPS coordinates are listed in Table 3-1. Pictures of the sampling locations are illustrated in Figures D-1 through D-8 of Appendix D.

Table 3–1: Waikamoi Watershed Sampling Locations

Location	GPS Coordinate	Description	Date Sampled	
Kahakakapao Reservoir 1 & 2	20^0 48' 15" N 156^0 15' 54" W	50 million storage (MG) reservoirs	Nov '12 Jan '13 Apr '13	Aug '13 Oct '13 May '14
1st Caisson Pipeline	20^0 48' 32" N 156^0 15' 5" W	Conveys water to Kahakapao reservoirs	Nov '12 Jan '13 Apr '13	Aug '13 Oct '13 May '14
2nd Caisson Pipeline	20^0 48' 38" N 156^0 14' 42" W	Conveys water to Kahakapao reservoirs	Nov '12 Jan '13 Apr '13	Aug '13 Oct '13 May '14
Waikamoi Reservoirs	20^0 48' 38" N 156^0 13' 58" W	15 MG storage reservoirs when Kahakapao reservoirs are full	Nov '12 Jan '13 Apr '13	Aug '13 Oct '13 May '14
Flume Outlet[1]	20^0 48' 34" N 156^0 13' 50" W	Collects water from surface run off and streams	Nov '12 Jan '13 Aug '13	Oct '13 May '14
Blue Pipeline	20^0 48' 34" N 156^0 13' 50" W	Conveys water from highest elevation and combines with flume outlet	Nov '12 Jan '13 Aug '13	Oct '13 May '14
White Pipeline	20^0 48' 34" N 156^0 13' 50" W	Additional pipe intake that runs parallel to flume and combines with flume outlet	Apr '13 May '14	
Flume Intake 2	20^0 48' 36" N 156^0 13' 20.5" W	Middle of flume intake	Nov '12 Jan '13	Apr '13 May '14
Flume Intake 1	20^0 48' 37.8" N 156^0 12' 51.5" W	Beginning of flume intake	Nov '12 Jan '13	Apr '13
Combined Flume Outlet	20^0 48' 34" N 156^0 13' 50" W	Concrete outfall structure at flume end	Apr '13 Aug '13	Oct '13 May '14

(1) Flume outlet was original wooden structure during Nov 2012, Jan 2013, and April 2013 sampling; temporary PVC pipeline structure during Aug 2013 sampling; and new aluminum structure during Oct 2013 and May 2014 sampling.

For each sampling location, the inorganic, organic, and biological water quality was determined according to the Standard Methods (APHA, AWWA & WEF, 2005). The inorganic parameters included pH, temperature, turbidity, alkalinity, dissolved oxygen (DO), total suspended solids (TSS), total dissolved solids (TDS), iron (Fe), manganese (Mn), calcium (Ca), magnesium (Mg), silica (Si), aluminum (Al), chloride (Cl^-), sulfate (SO_4^{2-}), and bromide (Br^-). The organic water quality was assessed by measuring the color, ultraviolet absorbance at 254 nanometer (nm) wavelength (UV 254), dissolved organic carbon (DOC), and specific UV absorbance (SUVA). SUVA is the ratio of UV 254 to DOC [(UV254×100)/DOC] and was utilized to define the hydrophobicity of NOM. Generally, higher SUVA values (greater than 4) correspond to hydrophobic NOM and lower SUVA values signal hydrophilic NOM (Lozier et al., 2008). Preliminary raw water TOC and DOC results demonstrated that the TOC was mainly composed of DOC (see Table D-1 and Figure D-9 of Appendix D). Therefore, water quality testing included DOC measurements rather than TOC to effectively allocate project resources.

Biological water quality is typically measured by culture-based heterotrophic plate counts (HPCs). The standard HPC methods require a laboratory equipped with an autoclave and microbiological fume hood, and incubation times ranging from 48 to 168 hours. To allow for more expedient biological detection in a remote island location, an alternative method was used to determine the biological activity. The microbial content was determined by measuring the relative adenosine tri-phosphate (ATP) content of the water with a 3M™ Clean-Trace™ NG Luminometer (St. Paul, MN). Although ATP measurements are commonly used in the medical and food industries to monitor contamination and maintain quality control, ATP is not typically implemented in drinking water monitoring. However, because ATP is an activated energy carrier present in microorganism,

drinking water researchers and purveyors have recently recognized the beneficial use of ATP as a tool to monitor biological activity (Hammes et al., 2010; Evans et al., 2013). In addition to the ATP found within viable cells, Hammes and researchers (2010) have shown that significant amounts of extracellular ATP may also be present in natural waters. Therefore, both free (extracellular) ATP and total (extracellular plus viable cells) ATP were measured according to manufacturer instructions using 3M Clean-Trace^{TM} Water-Free ATP and Water-Plus Total ATP testing kits (see Table D-2 of Appendix D).

The water quality sampling and testing protocol is summarized in Table 3-2. The average water quality data was organized by sampling location and seasonal or weather condition. The compiled results were evaluated to detect water quality trends or patterns that may be useful in identifying alternative source water management strategies.

Table 3–2: Waikamoi Watershed Sampling and Testing Protocol

Water Quality Parameters[1]	Sampling and Testing Protocol
pH, Temperature, Turbidity, DO, Free and Total ATP[2]	Duplicate water samples were collected in 500 milliliter (mL) high density polyethylene (HDPE) bottles and analyzed at time of collection.
Alkalinity, Color[3], UV 254, DOC, SUVA	Samples were collected in one L opaque HDPE bottles (duplicated about 1 every 5) and analyzed at the Olinda WTP laboratory.
TSS, TDS, Fe, Mn, Ca, Mg, Si, Al, Cl^-, SO_4^{2-}, Br^-	Samples were collected in one L opaque HDPE bottles (duplicated about 1 every 5) and shipped on ice to UCF laboratories for analysis.

(1) Water quality was analyzed according to standard methods (Table A-1 of Appendix A).
(2) The ATP was measured by following manufacturer instructions (Table D-2 of Appendix D).
(3) The true color was measured for samples filtered through a 0.45 µm membrane filter.

Free and Total Adenosine Triphosphate Analysis

In the 3M method, ATP (either freely available or extracted from bacterial cells) reacts with a luciferin-luciferase reagent, derived from fireflies. The reaction between ATP and the reagent complex produces a light emission that is measured using the luminometer and recorded as relative light units (RLUs). The RLU measurements were converted to ATP concentrations (10^{-12} g/mL or pg/mL) by developing free and total ATP calibration curves. Calibration curves were constructed by measuring the free and total RLUs of duplicate samples with known ATP concentrations (pg/mL) and plotting the average RLU measurements versus known ATP concentrations. The ATP standards, summarized in Table 3-3, were prepared by diluting a 100 mM standard solution of adenosine 5'-triphosphate (specifications provided in Table C-1 of Appendix C) in NERL^{TM} high purity water. The free and total calibration curve data in Table 3-3 was used to establish the mathematical relationship between RLUs and ATP concentration (pg/mL). The free and total ATP calibration curves and laboratory quality control analysis are presented in Appendix B.

Table 3–3: Free and Total ATP Calibration Curve Data

Std.	Standard Concentration (pg ATP/mL)	Average Standard Concentration (RLUs)	
		Free ATP	Total ATP
0	0	20	20
1	0.5	16	15
3	10	82	82
4	50	343	315
5	100	693	627
6	300	2123	1811
7	500	2218	2941
8	1000	4910	5749
9	2500	15155	14305
10	5000	31434	31434

Confirm Existing Conventional-UF Process Operations

The existing conventional-UF process served as the treatment baseline for evaluating the pretreatment alternatives. To compare the impact of pretreatment on the pilot-scale, the full-sale UF process was simulated using a UF pilot skid that filtered plant-settled water as in the full-scale process. A conceptual schematic of the unit operations for the full-scale system and simulated control-UF pilot is presented in Figure 3-2. The control-UF pilot skid was operated throughout the study to assess the effect of pretreatment on UF operating and water quality performance. Water quality and operational parameters for the full and pilot scale processes along with jar testing experiments were evaluated to:

- Assess the coagulation operation effectiveness

- Confirm the need for additional pretreatment

- Illustrate the representativeness of the pilot-scale to the full-scale system
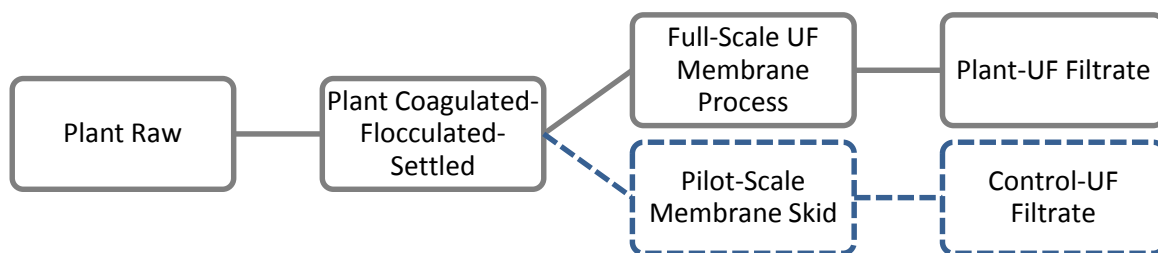
Figure 3–2 Full and Pilot Scale UF Process Schematic

Evaluation of Coagulation Process Performance

Particulate and organic removal efficiencies of the full-scale coagulation process were evaluated by performing jar testing experiments. A jar testing machine, shown in Figure 3-3, was used to coagulate, flocculate, and settle Olinda raw water at varying ACH coagulant doses and pH ranges.

The ACH coagulant information is summarized in Table C-1 of Appendix C. Other coagulation optimization strategies include using an alternative coagulant or employing coagulant aids. Alternative metal salt coagulants, including alum and ferric chloride, were not evaluated because these traditional coagulants consume significant amounts of alkalinity. Hence, switching to either aluminum or ferric chloride would require the addition of carbonate or hydroxide alkalinity and increase the cost of water production (Budd et al., 2004). The additional chemical cost is not expected to be offset by improved coagulation performance as Yan and colleagues (2007; 2008) have demonstrated that prehydrolyzed metal salt coagulants, such as ACH, achieve similar DOC removals compared to traditional metal salt coagulants. The addition of coagulant aids, such as cationic polymers, has been shown to enhance DOC removal; however, polymer coagulants can aggravate fouling of low pressure membranes (Wang et al., 2011). Thus, the evaluation of cationic polymer aids was not included in the jar testing experiments.

Figure 3–3 Jar Testing Machine

The experimental protocol for the jar testing is presented in Table 3-4. The jar tester's operating sequence was determined by performing preliminary jar tests. The preliminary jar tests were accomplished by varying the ACH coagulant dose, mixing speeds, and detention times to approximate possible full-scale regimes. Based on the preliminary results, the jar testing sequence was set to three cycles: 300 rpm for 15 seconds (short duration rapid mix), 15 rpm for 25 minutes (slow mix), and 0 rpm for 45 minutes (sedimentation). Additional jar tests were performed to examine the effect of ACH coagulant dose and pH on settled water turbidity, color, UV 254, DOC, and SUVA. Turbidity and organic removals were calculated and plotted on contour plots as functions of ACH dose and pH using Minitab® 17 software (Minitab, 2010). The contour plots were utilized to determine whether the full-scale plant was operating within optimal coagulation operating ranges.

Table 3–4 Jar Testing Protocol

Jar Test	Sequence	Operation	Water Quality[1]
Preliminary Run 1 (September 19, 2012)	200 rpm, 15 sec 10 rpm, 10 min 0 rpm, 1 hr 25 min	14 to 24 ppm$_v$ ACH No pH Adjustment	Turbidity
Preliminary Run 2 (April 23, 2013)	160 rpm, 45 sec 35 rpm, 10 min 25 rpm, 10 min 0 rpm, 30 min	14 to 18 ppm$_v$ ACH No pH Adjustment	pH, Temperature, Alkalinity, Turbidity, Color, UV 254, DOC, and SUVA
Preliminary Run 3 (April 24, 2013)	200 rpm, 10 sec 160 rpm, 35 sec 25 rpm, 20 min 0 rpm, 60 min	14 to 18 ppm$_v$ ACH No pH Adjustment	pH, Temperature, Alkalinity, Turbidity, Color, and UV 254
Experimental Runs 1 - 8 (May 17, 2014 through June 1, 2014)	300 rpm, 15 sec 15 rpm, 25 min 0 rpm, 45 min	11 to 30 ppm$_v$ ACH 5.4 to 8.7 pH units	Turbidity, Color, UV 254, DOC, and SUVA

(1) Water quality was analyzed according to standard methods (Table A-1 of Appendix A)

Water Quality Monitoring

Water quality was monitored throughout the Olinda WTP and control-UF pilot from September 2012 to February 2013 (MIEX® testing) and from April 2013 to December 2013 (GAC and BAC testing). The sampling duration allowed for the observation of seasonal impacts on water quality. Water quality was measured for raw water (raw), plant coagulated-flocculated-settled water (plant-ACH), plant UF filtrate (plant-UF), and control-UF pilot filtrate (control-UF). Temperature, pH, turbidity, alkalinity, color, UV 254, and DOC parameters were measured daily. Solids, hardness, metals, and anions concentrations were measured approximately twice per month. A summary of the water sampling and testing evaluation is presented in Table 3-5.

Table 3–5 Existing Conventional-UF System Water Quality Monitoring

Water Sampling Location	Water Quality Parameter[1]	Target Testing Frequency	Analyst	Statistical Analysis
Raw Plant-ACH Plant-UF Control-UF	Temperature pH Turbidity Alkalinity Color UV 254 DOC SUVA TSS TDS Hardness (Ca, Mg) Metals (Si, Mn, Fe, Al) Anions (Cl$^-$, SO$_4^{2-}$, Br$^-$)	Daily Daily Daily Daily Daily Daily Daily Daily Bi-weekly Bi-weekly Bi-weekly Bi-weekly Bi-weekly	County County County County County County County County UCF UCF UCF UCF UCF	Descriptive statistics (average, standard deviation & confidence interval); Hypothesis testing
Raw Plant-ACH	EEMs	One data set	UCF	
Plant-UF Control-UF	DBP formation potential: Cl$_2$ and TTHMs after 6, 24, 48, 96, and 168 hours HAA$_5$ after 96 hours	Twice quarterly	UCF	Hypothesis testing; Comparison to MCLs

(1) Water quality was analyzed according to standard methods (Table A-1 of Appendix A)

In addition to utilizing UV 254, DOC, and SUVA to determine the quantity and expected hydrophobicity of the dissolved organic matter (DOM) in the Olinda water, the DOM was further characterized by performing excitation-emission matrix fluorescence spectroscopy (EEMs) analysis. For the EEMs analysis, a jar testing machine at the 300, 15, and 0 rpm set-points and plant-applied ACH dose was utilized to coagulate, flocculate, and settle a portion of Olinda raw water collected on July 11, 2014. The Olinda settled and remaining raw water samples were filtered through a 0.45 µm membrane filter to exclude particulate and large colloidal matter from the samples. For each filtered sample, a quartz fluorescence cuvette and RF-1501 Shimadzu spectrofluorophotometer were used to expose the sample to an excitation light and measure the resultant fluorescence emitted from the sample (Shimadzu Corporation, 1994). Excitation wavelength inputs were varied every 5 nanometers (nm) from 220 to 400 nm. At each excitation wavelength, the fluorescence emission output was manually recorded from 300 to 570 nm in 5 nm increments. The three-dimensional data was plotted as an excitation-emission matrix (EEM) contour plot in Minitab®.

The EEM diagrams for the Olinda raw and coagulated-settled water were compared against theoretical EEM characterization templates to determine the major DOM fractions. Researchers in the area of EEMs have generalized the interpretation of EEM diagrams by delineating regions, where fluoresce intensity peaks specify different fractions of DOM (Chen et al., 2003; Hudson et al., 2007; Bridgeman et al., 2011). As shown in the EEM example template (Figure 3-4), the major DOM fractions include hydrophobic fulvic and humic acids (regions III and IV) originating from plant matter, and aromatic proteins that may originate from free (region I and II) or biologically-bound (mainly region II) amino acids (Bridgeman et al., 2011).

49
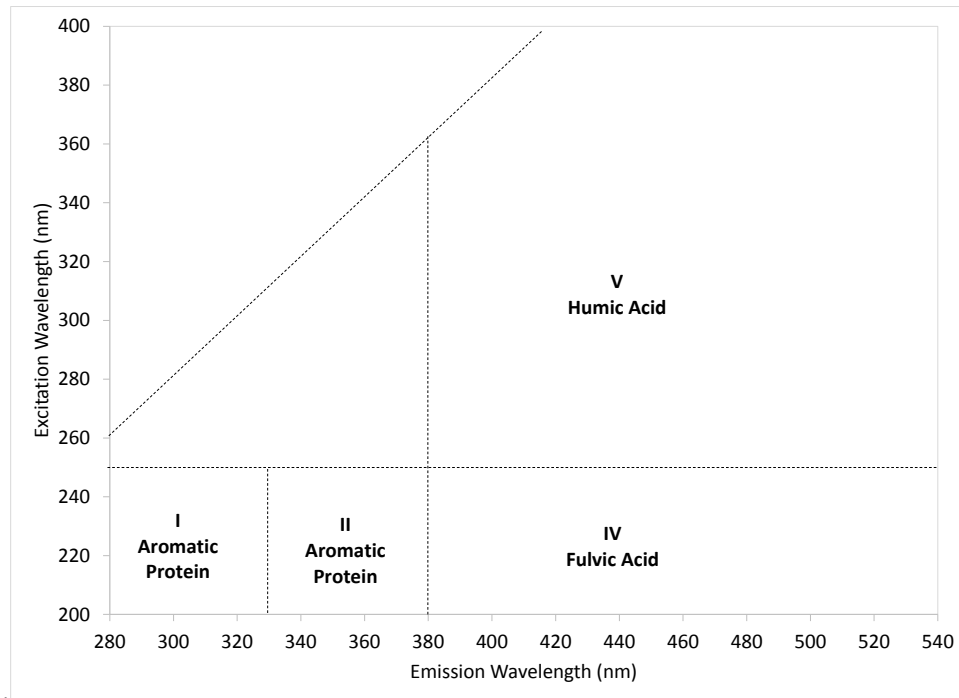
Figure 3–4 Template for EEM Characterization of DOM
Source: Adapted from Chen et al., 2003.

The EEMs analysis was performed after the conclusion of the pretreatment pilot testing because the spectrofluorophotometer equipment was not available prior to 2014. However, characterizing the DOM of the raw and settled waters will provide a qualitative understanding of the nature of the organics that contribute to DBP formation and UF membrane fouling at the Olinda WTP.

Plant-UF and control-UF filtrate DBP formation potential was determined to simulate the level of chlorinated DBPs anticipated to form within the distribution system. DBP formation was simulated by pH adjusting the filtrate samples to 8.8 pH units using food grade lime, then dosing with sufficient sodium hypochlorite (2.5 to 4 mg/L) to maintain a 0.2 mg/L chlorine residual after seven days of contact time. The specifications for the lime and sodium hypochlorite dosing solutions are provided in Table C-1 of Appendix C. The dosed samples were incubated at ambient temperatures

(12 to 25 $^{\circ}$C) in borosilicate glass amber bottles with TFE lined caps. Chlorine residual and TTHM content were measured after 6, 24, 48, 96, and 168 hours of incubation. Although the standard method (2005) defines ultimate DBP formation as seven days of incubation time, the longest detention time in the Upper Kula system is about four days. Therefore, the HAA_5 concentration was measured after a 96 hour contact time. From September 2012 to April 2013, HAA_5 concentrations were analyzed according to Standard Method 6251B. Starting May 2013, HAA_5 concentrations were measured using both Standard Method 6251B and EPA Method 552.3. On average, the EPA 552.3 method yielded higher percent recoveries for a known concentration of HAA_5. Therefore, EPA 552.3 HAA_5 results were used in the DBP formation potential evaluations.

Pilot and full scale water quality data was organized into time-series graphs to reveal seasonal trends and irregularities. In addition to identifying seasonal impacts, particulate and organic removal efficiencies were evaluated to establish the treatment benchmark. Finished water DBP formation potential results were compared to regulatory MCLs to demonstrate the need for additional DBP precursor removal treatment. Furthermore, UF feed water quality, specifically turbidity, iron, manganese, aluminum, UV 254, DOC, and SUVA, was evaluated to identify possible UF membrane foulants that may be removed by alternative pretreatments.

Hypothesis tests, including paired t-tests and analysis of variance (ANOVA), were employed to determine whether the pilot and full scale filtrate water quality averages were significantly different. In the paired t-tests, the average of paired differences (i.e. average of pH_1 minus pH_2) was compared to the null hypothesis, which assumed that the average of differences was zero. If the calculated t-statistic was less than the t-critical at 95 percent confidence, then it was confirmed that there was no significant difference between the averages. In the ANOVA testing, the variation

between treatments was compared to the variation within treatments. If the calculated F-statistic was less than the F-critical at 95 percent confidence, then the variation between and within treatments was similar and the averages were considered to be the same (Mac Berthouex & Brown, 2002). Demonstrating likeness between the pilot and full scale UF process with respect to water quality was necessary to prove that the control-UF pilot effectively simulated the full-scale UF membrane process.

Ultrafiltration Process Confirmation

Evoqua Water Technologies (San Diego, CA) provided two MEMCOR® SM 1 AUTO membrane pilot skids, shown in Figure 3-5. The UF pilot skid was used to simulate the Olinda UF membrane process. The technical specifications of the UF pilot as compared to the full-scale UF system are summarized in Table 3-6. The UF pilot was operated within the confines of its technical specifications and was limited to an average operating flux of 19.2 gal/ft^2-day. Because the average UF pilot flux was lower than the full-scale UF operating flux of 23.6 gal/ft^2-day, it was not possible to directly establish similitude between the full-scale and pilot scale membrane TMP and specific flux. However, both the full and pilot scale UF membranes were manufactured by Evoqua with the same PVDF membrane material characteristics and operating schemes. Between September 2012 and December 2013, full and pilot scale UF operational data (feed water temperature and flow rate, TMP, and backwashing and CIP frequencies) was collected. The operational monitoring matrix is outlined in Table 3-7. Pilot and full scale membrane TMP, temperature corrected specific flux, cleaning frequency, and percent recovery were compiled and assessed.

Table 3–6 Olinda Full and Pilot Scale Technical Specifications

Item	Olinda WTF's UF Membrane	Evoqua UF Membrane Pilot
UF Membrane module details	MEMCOR® L10V; Polyvinylidene fluoride (PVDF) hollow fiber; 0.04 μm Nominal pore size; 6 Log removal of *Giardia* and *Cryptosporidium*	MEMCOR® S10V; Polyvinylidene fluoride (PVDF) hollow fiber; 0.04 μm Nominal pore size
Membrane age	Greater than 5 years	Virgin
Membrane area per module	252 ft^2; 9600 membranes per module	300.3 ft^2
Membrane modules per rack	112	1
Number of racks	3	1
Total membrane area	84,672 ft^2	300.3 ft^2
"Filter" mode operation	Pressurized outside to inside filtration	Pressurized outside to inside filtration
Average design production capacity	2 MGD	5760 gpd (4 gpm)
Peak design production capacity	2.7 MGD	6087 gpd (4.23 gpm)
D.O.H. max approved flow and flux rate	5.08 MGD; 60 gal/ft^2-day	-
Target water flux rate	Average Design (2 MGD): 23.6 gal/ft^2-day; 4.41 gpm per module Peak Design (2.7 MGD): 31.9 gal/ft^2-day; 5.95 gpm per module	Average Design: 19.2 gal/ft^2-day Peak Design: 20.3 gal/ft^2-day
Backwash mode	Water/Air backwashing. Backwashing is based on run time, volume produced, or rise in TMP	Automatically initiated and controlled, using low pressure air scour and feed flush
Backwash frequency	Approximately every 20 minutes	Approximately every 20 minutes
Chemically enhanced backwash (CEB)/maintenance frequency	No chemical backwash practiced	No chemical backwash
Backwashing chemical types and concentrations	N/A	N/A
Clean in place (CIP) operation and frequency	Based on TMP rise and resistance TMP pre-CIP: >10; TMP post-CIP: 2.10 Resistance pre and post CIP: 1.10 and 1.00 Approximately 72 hours (Note: The design CIP frequency was 18 days)	Based on TMP rise TMP pre-CIP: 29 psi; TMP post-CIP: 10-20 psi
Clean in place chemical types and concentrations	Citric acid and 15% sodium hypochlorite	Citric acid (about 300 g) and 15% sodium hypochlorite (about 100-150 mL)
Membrane integrity monitoring	Online turbidity meters	Turbidity measurements
Residuals handling	Backwash water and CIP wastewater is discharged to the settling lagoons, which is decanted back to the WTP raw water supply	Backwash water and CIP wastewater is discharged to waste

D.O.H. = Department of Health (State of Hawaii)

Figure 3–5 MEMCOR® SM 1 AUTO Pilot Skid

Table 3–7 UF Process Operational Monitoring Matrix

Process	Parameter	Protocol[1]
Pilot-Scale	✓ Water temperature (ºC); flow rate (gpm); feed pressure (psi); and filtrate pressure (psi) ✓ Backwashing frequency (20 minute default) ✓ CIP frequency	✓ Water temperature was measured and recorded at least three times daily. ✓ Flow rate, feed pressure, and filtrate pressure readings were manually recorded from online flow meters and pressure gages at least three times daily. ✓ The membrane pilot employed automatic backwashes at programmable time intervals. ✓ Sodium hypochlorite followed by citric acid CIPs were performed when TMP exceeded 22 psi (three quarters of the maximum housing pressure)
Olinda Full-Scale	✓ Water temperature (ºC); flow rate (gpm); TMP (psi) ✓ Backwashing frequency ✓ CIP frequency	✓ Water temperature, flow rate, and TMP data was compiled for each full-scale skid (CMF 1, 2, and 3). ✓ Process employed automatic backwashes every 20 minutes. ✓ Sodium hypochlorite and citric acid CIP maintenance activities were recorded.

(1) The specifications for the CIP chemicals are included in Table C-1 of Appendix C.

Ultrafiltration Pretreatment Assessment

Pilot testing was conducted to determine whether integrating MIEX®, GAC adsorption, or BAC filtration within a conventional-UF process would enhance the treatment and production efficiency of the UF membrane filtration. Since one of the UF pilot skids served as the dedicated research control, MIEX®, GAC, and BAC pretreatment alternatives were sequentially pilot tested. From September 2012 to February 2013, MIEX® pretreatment was evaluated by collecting and analyzing pilot-scale water quality and operational data. At the end of the MIEX® phase, the control-UF and pretreatment-UF membrane modules were sent to Evoqua for autopsy analysis. Replacement membranes (supplied by Evoqua) were inserted into the UF pilot skids for the subsequent GAC and BAC evaluation phase. Between April 2013 and December 2013, the impact of GAC media filtration in the adsorption, transition, and biological (BAC) mode was assessed by monitoring and comparing water quality and operational parameters. At the conclusion of the BAC evaluation phase, the control-UF and pretreatment-UF membrane modules were shipped to Avista Technologies (San Marcos, CA) for autopsy analysis.

The effect of MIEX®, GAC adsorption, and BAC filtration pretreatment on UF performance was evaluated by comparing the operational requirement, organic removal, DBP formation potential, and UF membrane TMP, specific flux, percent recovery, and autopsy results to the research control. The pretreatment alternatives were further evaluated with respect to relative advantages and disadvantages, economic non-cost considerations, and conceptual opinions of probable construction and operating costs. Additionally, the BAC pretreatment pilot results along with findings from similar biofiltration pretreatment studies were evaluated to develop a predictive mathematical model using the method of curve fitting with non-linear regression in Minitab®.

MIEX® Pretreatment Pilot Testing

The MIEX® system was evaluated as a pretreatment alternative ahead of the coagulation-clarification and UF membrane processes. This arrangement, shown in Figure 3-6, was selected because applying the MIEX® system before coagulation has been shown to reduce coagulant dosage requirements and enhance the turbidity and organic removal of a downstream coagulation process. Although alternatively placing the MIEX® system after coagulation could possibly reduce the MIEX® treatment capacity, researchers suggest that MIEX® pretreatment prior to coagulation provides effective cost and treatment benefits (Singer & Bilyk, 2002; Boyer & Singer, 2006; Xu et al., 2013).

Pre-sedimentation → MIEX® System → Coagulation-Flocculation-Sedimentation → UF Membrane
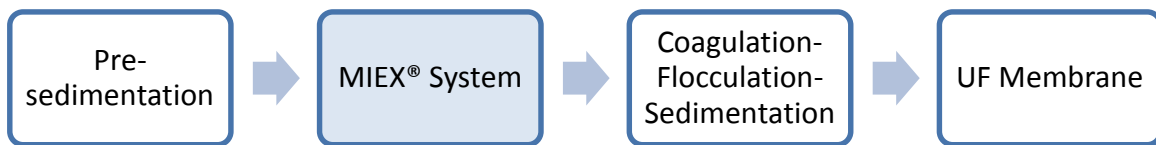
Figure 3–6 MIEX® Pretreatment Process Schematic

Pilot Equipment

The MIEX®, coagulation-clarification, and UF membrane treatments were simulated using piloting equipment, shown in Figure 3-7. Orica Watercare Inc. (Englewood, CO) supplied the 10 gallon per minute (gpm) MIEX® high rate pilot system (Figure 3-7a). The general MIEX® design specifications are summarized in Table 3-8. The MIEX® system treated raw water by contacting the water and resin in the up-flow fluidized bed contactor to promote the exchange of negatively charged DOC with chloride ions on the resin surface. Tube settlers within the contactor were used to promote adequate separation of the water and resin as the water moved up through the contactor.
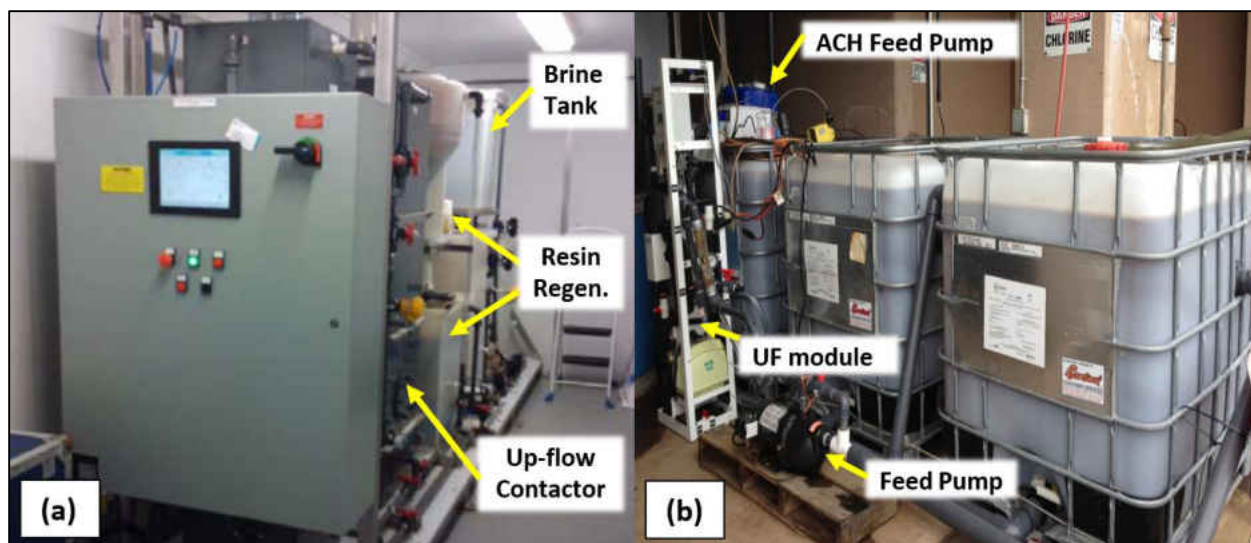
Figure 3–7 MIEX® High Rate (a) and Coagulation-Clarification (b) Pilots

Table 3–8 MIEX® Technical Design Summary

Parameter	Value
Maximum flow capacity	10 gpm
Resin contactor concentration	200 - 250 mL/L
Resin use	2.0 L/MG
Contact time	4 - 8 minutes
Resin regeneration rate	1 gal/1000 gal treated
Regenerant	Sodium Chloride (350 lb/MG)
Salt brine residual production	400 gal/MG

To inhibit biological growth on the resin and tube settlers, a small dose of sodium hypochlorite (less than 0.5 mg/L Cl_2) was added to the raw inlet. Additionally, spent resin was recycled back into the process through an automated regeneration sequence. The MIEX® system's regeneration sequence comprised of five fill and drain cycles that served to re-substitute chloride ions on the resin exchange sites (Ostrowski, 2011). The substitution process generated a concentrated brine stream, rich in salt and organics (Singer et al., 2009). The brine stream is typically disposed directly to the sanitary sewer and treated at the wastewater treatment facility (City of St Cloud, 2011; Palm

57

Beach County, 2014). However, since the Olinda WTP does not have access to a wastewater collection system, the brine solution was trucked to the wastewater treatment facility for disposal.

Following MIEX® treatment, the water was conveyed by a two-inch diameter PVC pipeline and injected with ACH coagulant. The ACH coagulant was flash mixed inside the pipe as it traveled about 18 inches before flowing into three 250 gallon ($42 \times 36 \times 38$ inch) carboys arranged in series. The three carboys in series functioned as the flocculation and sedimentation basins. The basins were connected by four-inch PVC pipe segments with 90 degree elbows to prevent short-circuiting. The settled water from the third carboy supplied the feed water to the MEMCOR® UF pilot module.

The County with the assistance of Orica staff constructed the coagulation-clarification pilot, which is displayed in Figure 3-7b. A comparison of the full-scale to pilot-scale coagulation is presented in Table 3-9. The pilot ACH dose was lower than the full-scale plant as a result of the expected reduction in coagulant demand by MIEX® pretreatment. The average full and pilot scale flocculation detention times were comparable; however, the full-scale settling rate was an order of magnitude lower than the pilot-scale. Reproducing the full-scale loading rate would have required installation of 17 carboys, which was not possible given site space constraints. Therefore, the pilot settling rate was more representative of typical industry standards (0.5 gpm/ft^2) (MWH, 2005).

Table 3–9 Coagulation, Flocculation, and Sedimentation Operating Conditions

Parameter	Olinda WTP Full-Scale	Pilot-Scale	
Process Flow	2 MGD	8 gpm	6 gpm
Coagulation	ACH is flash mixed in a 8 inch cement-lined ductile iron pipe	ACH flash mixing in a 2 inch PVC pipe	
ACH dose	Varies seasonally 15 to 35 mg/L	11.8 to 39 mg/L	5.9 and 11.8 mg/L
Flocculation Detention Time	25 minutes	25.8 minutes	38.7 minutes
Loading Rate	0.035 gpm/ft^2	0.43 gpm/ft^2	0.29 gpm/ft^2

Pilot Operation

The MIEX® pretreatment process and control-UF pilots were operated intermittently from September 4, 2012 to February 3, 2013. To determine the pretreatment operational requirements and impacts on UF operation, operational parameters for the MIEX® system, coagulation-clarification, MIEX®-UF, and control-UF pilots were collected and recorded. The MIEX® operational parameters included flow rate, contactor top and bottom resin concentration, and regeneration maintenance set-points. The operating parameters recorded for the coagulation pilot were flow rate and ACH dose. As outlined in Table 3-7, The MIEX®-UF and control-UF pilot operation was monitored by recording feed water temperature, flow rate, TMP, and backwash and CIP frequencies. Furthermore, pilot process observations and maintenance activities were recorded in operator logs. Throughout the MIEX® piloting phase, process changes to the MIEX®, coagulation, and UF pilots were implemented in an effort to maintain adequate treatment across the unit operations. A summary of the target operational conditions and specifications implemented throughout the MIEX® pretreatment evaluation is presented in Table 3-10.

Table 3–10 MIEX® Pilot Testing Operational Conditions

Testing Period	MIEX® & Coagulation Operation[1]	UF Pilot Operation[1]
September 4, 2012 to October 13, 2012	✓ Flow capacity: 8 gpm ✓ Contact time: 4-8 minutes ✓ Top and bottom resin concentration: 0 and 20-35% ✓ Regeneration tank resin concentration: 50% ✓ Resin volume regenerated: 25% ✓ Regeneration resin dosed: 2.1% ✓ Brine conductivity: 150 mS/cm ✓ Bags of salt added: 1.5/wk ✓ LMI pump ACH dose: 0.3-1 mL/min	✓ Target feed flow: 4 gpm ✓ Max feed flow: 4.23 gpm ✓ Water flux: 19.2 to 20.3 gal/ft^2-day ✓ Filtrate pressure: 6-8 psi ✓ Backwash frequency: 20 min
October 14, 2012 to October 26, 2012	✓ Same as previous	✓ Water flux: 19.2 to 20.3 gal/ft^2-day ✓ Filtrate pressure: 6-8 psi ✓ Backwash frequency: 10 min
October 27, 2012 to November 5, 2012	✓ Flow capacity: 6 gpm	✓ Water flux: 19.2 to 20.3 gal/ft^2-day ✓ Filtrate pressure: 6-8 psi ✓ Backwash frequency: 10 min
November 6, 2012 to November 21, 2012	✓ Flow capacity: 6 gpm	✓ Water flux: 19.2 to 20.3 gal/ft^2-day ✓ Filtrate pressure: 0 psi ✓ Backwash frequency: 10 min
November 22, 2012 to February 3, 2013	✓ Flow capacity: 6 gpm ✓ Cole Parmer Masterflex Digital pump ACH dose: 0.1-0.2 mL/min	✓ Water flux: 19.2 to 20.3 gal/ft^2-day ✓ Filtrate pressure: 0 psi ✓ Backwash frequency: 10 min

(1) If operational parameter is not specified, parameter is the same as in previous testing period.

At pilot start-up, the MIEX® pilot plant treated an average 8 gpm flow rate, which was then dosed with ACH coagulant at a rate of 0.3 to 1.0 mL/min using a positive displacement LMI pump prior to UF membrane filtration. Like the full-scale UF process, the UF pilots were automatically backwash every 20 minutes with air scour and water rinse. In addition, the UF pilots were operated with about 6 to 8 psi of back pressure to simulate the pressure head in the full-scale filtrate holding tank.

On October 14, 2012, ten minute backwash frequencies were implemented for the MIEX®-UF and control-UF pilots to increase the membrane filter runs between CIPs. Although a ten minute backwashing frequency is below the industry standard (Alspach et al., 2005), it was necessary to increase the frequency to avoid the build-up of coagulation flocs that were carried over from the coagulation pilot. To promote adequate settling of the flocs, the flow rate of the MIEX® pilot was reduced to 6 gpm (lowest operating range) on October 27, 2012. In addition, the UF filtrate back pressure was reduced to atmospheric on November 6, 2012 to lower the feed pressure required to operate the UF pilot at the constant flux rate of 19.2 gal/ft^2-day.

Floc carry-over continued to be observed from the coagulation pilot onto the UF membrane despite efforts to improve coagulation settling. It was determined that the floc carry over was caused in part by pin floc formation, which indicated that the LMI pump was oversized for ACH dosing of MIEX® treated water. Therefore, on November 22, 2012, the LMI pump was replaced with a Cole Parmer Masterflex Digital peristaltic pump (Vernon Hills, IL) that was capable of feeding ACH at a rate between 0.1 and 0.2 mL/min. Larger, more discrete flocs were observed after the pump change-out occurred. Although complete settling of the floc was not achieved, an improvement in UF operation was documented. At the conclusion of the MIEX® testing, the control-UF and

MIEX®-UF membrane modules were sent to Evoqua for autopsy analysis. In the autopsy analysis, Evoqua physically inspected the exterior and interior of the membrane modules and performed scanning electron microscopy (SEM) and energy dispersive x-ray spectroscopy (EDX) analyses to identify foulants present on the membrane fiber surfaces.

<u>Additional Limitations</u>

Several operational challenges impacted the treatment and operating efficiency of the MIEX®, coagulation, and UF pilots that required modification to the methods used in support of the research. It was determined that the MIEX® manufacturer Orica Watercare, Inc. used paint-lined drums to store and transport the MIEX® resin to the Olinda WTP project site. Paint chips fragmented from the inner lining of the containers mixed with the resin that was used to operate the MIEX® pilot. The presence of paint chips in the resin clogged the contactor and regeneration equipment, disrupted the resin regeneration cycle, and caused resin loss. In order to resolve the complications initiated by the paint chips, the paint chips were manually strained from the resin. Additionally, several MIEX® alarms were triggered by irregularities with the software control settings related to the regeneration cycles. Other issues included: malfunction of regeneration conductivity probes; loss of internal air pressure with accompanying pump failure; and power outages.

In addition to shutdowns caused by technical difficulties, the pilot units operated intermittently from November 7, 2012 to the beginning of February 2013 in order to accommodate drought conditions and full-scale membrane repair and replacement activities at the Olinda WTP. The intermittent pilot shutdowns made it difficult to maintain steady-state operation of the pretreatment

and control pilot plants. However, from November 22, 2012 to December 14, 2012, the unit operations were operated in unison to establish the pretreatment impact on UF performance.

Water Quality

To examine the impact of MIEX® pretreatment on water quality, organic and inorganic water quality parameters were measured across the pilot unit processes: MIEX®, coagulation-clarification (MIEX®-ACH), MIEX®-UF, and control-UF pilots. A summary of water quality monitoring locations, parameters, and frequencies are provided in Table 3-11.

Table 3–11 MIEX® Testing Phase Water Quality Monitoring

Water Sampling Location	Water Quality Parameter[1]	Target Testing Frequency	Analyst	Statistical Analysis
Raw	Temperature	Daily	County	Descriptive statistics (average, standard deviation & confidence interval); Hypothesis testing
MIEX®	pH	Daily	County	
MIEX®-ACH	Turbidity	Daily	County	
MIEX®-UF	Alkalinity	Daily	County	
Plant-ACH	Color	Daily	County	
Control-UF	UV 254	Daily	County	
	DOC	Daily	County	
	SUVA	Daily	County	
	TSS	Bi-weekly	UCF	
	TDS	Bi-weekly	UCF	
	Hardness (Ca, Mg)	Bi-weekly	UCF	
	Metals (Si, Mn, Fe, Al)	Bi-weekly	UCF	
	Anions (Cl^-, SO_4^{2-}, Br^-)	Bi-weekly	UCF	
MIEX®-UF Control-UF	DBP formation potential: Cl_2 and TTHMs after 6, 24, 48, 96, and 168 hours HAA$_5$ after 96 hours	Two experimental sets in Dec. 2012 & Jan. 2013	UCF	Comparison to MCLs

(1) Water quality was analyzed according to standard methods (Table A-1 of Appendix A)

To determine whether MIEX® pretreatment effectively improved the quality of finished water distributed to customers, MIEX®-UF and control-UF filtrate DBP formation potential was evaluated on December 7, 2012 and January 28, 2013. For each DBP experiment, full-scale post treatment was simulated by pH adjusting the control-UF and MIEX®-UF filtrates close to 8.8 pH units with food grade lime prior to chlorine disinfection with 4 mg/L of sodium hypochlorite. After disinfection, DBP samples were incubated at the on-site ambient temperature, which was subject to diurnal variation. After approximately 6, 24, 48, 96, and 168 hours of contact time, the chlorine residual and TTHM concentration were measured. Of the selected contact times, the 96 hour (or four day) sample represented the estimated longest detention time in the distribution system. Consequently, the HAA_5 formation potential was measured at the four day contact time. The water quality and DBP formation potential results were analyzed using descriptive statistics and hypothesis testing (paired t-test and ANOVA).

Adsorption and Biological GAC Pretreatment Pilot Testing

To compare the performance of GAC media in the adsorption and biological modes, the impact of integrating GAC after coagulation-clarification and before UF membrane filtration was evaluated. The sequence of the unit operations, displayed in Figure 3-8, was selected to reduce turbidity loading and high MW organic compounds loading to the GAC filtration system. Reducing the turbidity and high MW organic loading serves to extend the GAC filtration runs between backwashes and promote the adsorption and biodegradation of medium to low MW organics (MWH, 2005; Basu & Huck, 2004; Huck & Sozanski, 2008; Velten et al., 2011).

Pre-sedimentation → Coagulation-Flocculation-Sedimentation → GAC or BAC Filtration → UF Membrane
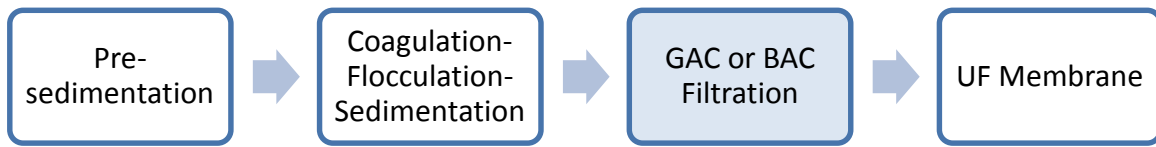
Figure 3–8 GAC and BAC Pretreatment Process Schematic

Pilot Equipment

GAC media filtration was pilot tested in the adsorption, transition, and biological operating modes, as pretreatment after coagulation-clarification, and ahead of UF membrane filtration. Ka'anapali Coffee Farms (Lahaina, HI) supplied a down-flow Stark fiberglass filtration vessel for the GAC adsorption and BAC filtration pilot testing. The pilot equipment was set up with a dedicated pump and piping system to convey plant settled water to the MEMCOR® control-UF pilot and Stark filtration vessel. The dedicated pump and piping system allowed for the continuous operation of the control-UF and pretreatment-UF pilots during times of full-scale plant shut-downs. In anticipation of full-scale plant shut-downs, the County operations staff produced excess settled water to continuously supply the GAC/BAC and UF pilots.

The Stark vessel was installed with an underdrain, holding tank, and pumping system to supply the GAC media filtered water to the second MEMCOR® UF pilot. The GAC/BAC and UF pilot layout is illustrated in Figure 3-9. The interior of the filter vessel was filled with 16 inches of Evoqua's UltraCarb® 1240 GAC over 3 inches of pea gravel that served to cover the lateral underdrain system and provide support for GAC media (see Figure 3-10). The underdrain system consisted of six perforated lateral PVC pipes (about 1.5 inches in diameter) that served to collect the GAC filtered water. The filtered water was combined in a perpendicular center pipe (approximately 3 inches in diameter) and pumped to the downstream UF process. The Stark

65

filtration vessel was operated with about six to eight inches of water headspace to allow for fluidized bed backwash of the GAC media. The media filtration design parameters are outlined in Table 3-12.
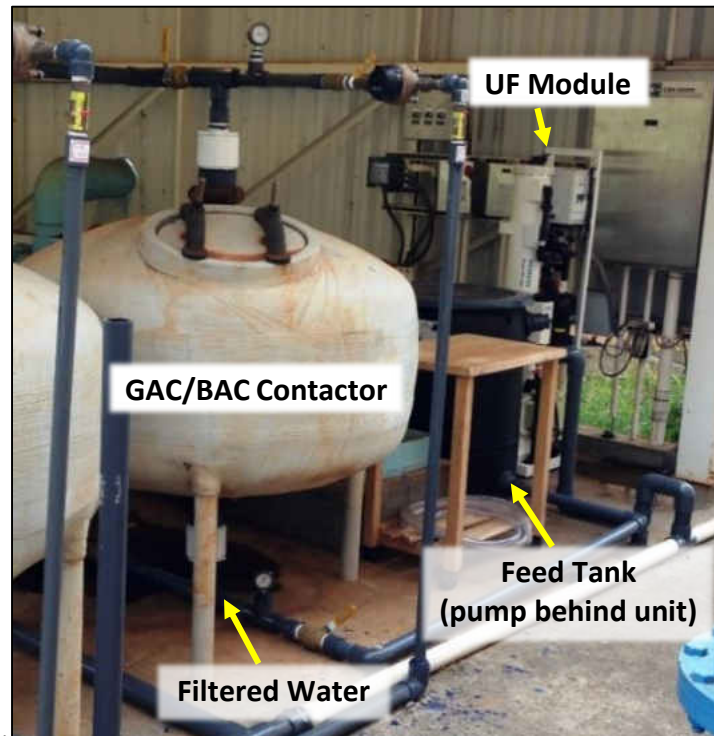
Figure 3–9 Stark Fiberglass Filtration Vessel and MEMCOR® UF Pilots
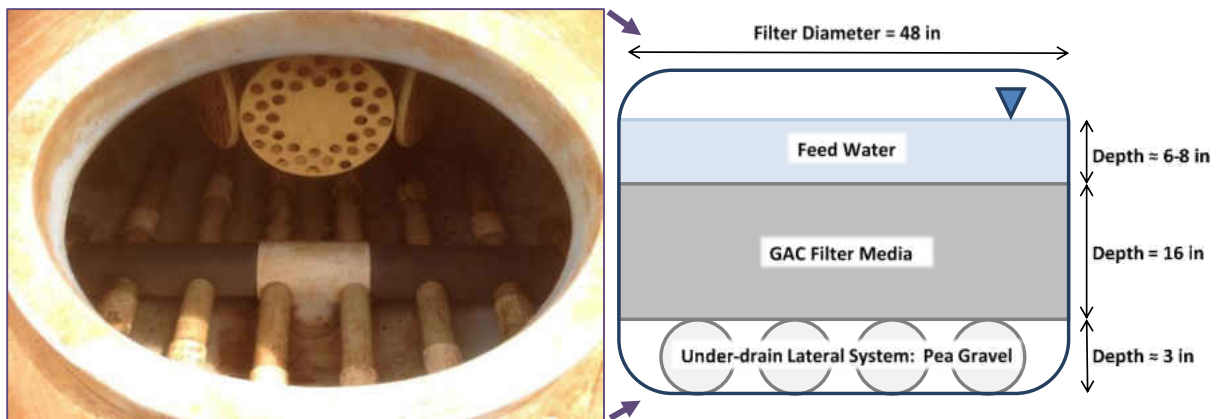
Figure 3–10 Stark Filtration Vessel Interior and Design Schematic

Table 3–12 Granular Activated Carbon Filter Design Specifications

Design Specification	Value
Media Identification	UltraCarb® 1240
Carbon Type	Bituminous Coal
Media Mesh Size	12 x 40 US mesh
Media Effective Size	0.65 mm
Media Uniformity Coefficient	1.9
Media Apparent density	495 g/L
Filter Diameter	48 in
Filter Cross Sectional Area	12.57 ft^2
Pea gravel depth	About 3 in
Media Depth	16 in
Media Volume	16.76 ft^3

Pilot Operation

From April 27, 2013 to December 31, 2013, the operational performance of the GAC media filtration pretreatment was monitored as it progressed from adsorption to biological mode (GAC and BAC mode, respectively). The technical summary of the operational conditions for the GAC and BAC pilot testing is listed in Table 3-13. The media filter was operated in down-flow filtration mode at a target EBCT between 10 and 15 minutes, which was selected to balance the trade-off between providing sufficient contact time for organic adsorption or biodegradation and capital construction costs. Based on the pilot filter dimensions, a 15 minute EBCT corresponded to a flow rate of about 8.5 gpm and HLR of 0.7 gpm/ft^2. Although the design HLR fell below the rapid filtration range (2 to 6 gpm/ft^2) employed in similar biofiltration studies (Halle et al., 2009; Peldszus et al., 2012), slower filtration rates promote the attachment and growth of biomass on the media (Huck et al., 2000).

Table 3–13 GAC and BAC Pilot Testing Operational Conditions

Testing Period	GAC-BAC Pilot Operation[1]	UF Pilot Operation[1]
GAC Adsorption (April 27, 2013 to July 20, 2013)	✓ Carbon mode: Adsorption ✓ Target flow rate: 12.5 gpm ✓ EBCT: 10 minutes ✓ HLR: 1.0 gpm/ft^2 ✓ Backwash mode: Fluidized bed ✓ Backwash flow: 25 gpm ✓ Backwash duration: 30 minutes	✓ Target flow rate: 4 gpm ✓ Target water flux: 19.2 gal/ft^2-day ✓ Filtrate pressure: 0 psi ✓ Backwash frequency: 20 min
BAC Transition (July 21, 2013 to August 9, 2013)	✓ Carbon mode: Transition (GAC adsorption capacity exhausted) ✓ C:N:P Ratio: 100:12:0.2	✓ Same as previous
BAC Filtration (August 10, 2013 to November 2, 2013)	✓ Carbon mode: Biological ✓ Initiated mono-potassium phosphate (KH_2PO_4) addition (0.5 mg/L as PO_4^{3-}) ✓ C:N:P Ratio: 100:10:1.7	✓ Same as previous
BAC Filtration (November 3, 2013 to December 31, 2013)	✓ Carbon mode: Biological ✓ Initiated pH adjustment with sodium hydroxide (between 6 and 8 pH units) ✓ C:N:P Ratio: 100:9:1.9	✓ Same as previous

(1) If operational parameter is not specified, parameter is the same as in previous testing period.

To prevent the excess accumulation of particulate matter and biomass, fluidized bed backwashes were performed at 25 gpm for 30 minutes. During the GAC adsorption evaluation phase, backwashes were performed when the pressure drop across the filter exceeded approximately 5 psi. The 5 psi pressure drop was selected because of the ability to operate the GAC at relatively long filter runs that were greater than 220 hours. As the GAC developed a biofilm and entered into the BAC mode, the backwashes were performed when the pressure drop exceeded about 10 psi, which corresponded to filter run times between 24 and 380 hours.

Additional operational parameters that were monitored daily included the media filter pilot throughput (total gallons treated), feed and outlet pressure (psi), and backwashing frequency. To assess the impact of GAC and BAC pretreatment on UF performance, the pretreatment-UF and control-UF pilot skids were operated at a target flux rate of 20.3 gal/ft^2-day, no back pressure, and 20 minute backwash frequency. The feed temperature, flow rate, TMP, and CIP maintenance activities were documented for the UF pilot skids as described in Table 3-7. Furthermore, shut-downs and maintenance activities for the GAC/BAC pretreatment and UF membrane pilots were documented in operator logs. At the conclusion of the GAC and BAC pilot testing, the pretreatment-UF and control-UF membrane modules were shipped to Avista technologies for a third-party membrane autopsy analysis. Upon receipt by Avista, the modules were physically inspected prior to a visual stereoscope analysis of the fibers and foulant analysis using loss on ignition. Additional testing included a test for the presence of carbonates, presence of microbiological organisms, Fourier transform infrared spectroscopy (FTIR), energy dispersive X-ray (EDX), SEM, and chromatic elemental imaging (CEI) testing. CEI allows the identification of individual elements in the foulant by analyzing the X-ray patterns emitted when an electron beam is passed across the surface (Avista, 2015).

Media Filtration Modes

At pilot start-up, the GAC media was operated in adsorption mode allowing for the removal of dissolved organics onto the active carbon sites. After about 12 weeks of operation, the active GAC adsorption sites were exhausted and the GAC media entered into the transition stage. In the transition mode, bacteria began to colonize and form biofilms on the GAC media surface. During

the transition phase, the C:N:P ratio was about 100:12:0.2, which signaled a phosphorus deficiency. In an effort to overcome the phosphorus limitation and enhance biological activity, an engineered biofiltration strategy was employed, where the feed water was supplemented with orthophosphate. About 0.5 mg/L of orthophosphate nutrient was added to the BAC feed water starting August 10, 2013, which marked the beginning of engineered biofiltration operation mode. The chemical specifications for the orthophosphate solution is provided in Table C-1 of Appendix C. With the orthophosphate supplementation, the C:N:P ratio was adjusted to 100:10:1.7 which satisfies the 100:10:1 minimum ratio recommended by Lauderdale and colleagues (2014).

Due to drought conditions experienced from September 7, 2013 to December 4, 2013, the full-scale plant was operationally limited to two to five hours a day. During this intermittent full-scale operation, the UF-control, BAC, and pretreatment-UF pilot plants were operated continuously by feeding excess settled water produced by the full-scale plant. In October 2013, a drop in the BAC feed water pH to below 5 units was observed. Acidic pH values may inhibit bacterial activity. Therefore, beginning November 3, 2013, pH adjustment with sodium hydroxide was implemented to raise the pH of the BAC feed water to a near neutral range (between 6 and 8 pH units). The BAC pilot was operated with orthophosphate addition and pH adjustment until the end of pilot testing on December 31, 2013.

<u>Water Quality</u>

Water quality was measured across the pretreatment and control unit operations to quantify the impact of GAC media filtration (adsorption, transition, and biological) on UF membrane performance with respect to operation and finished water quality. A summary of the water quality monitoring locations, parameters, and frequencies is included in Table 3-14.

Table 3–14 GAC/BAC Testing Water Quality Monitoring

Water Sampling Location	Water Quality Parameter[1]	Target Testing Frequency	Analyst	Statistical Analysis
Raw	Temperature	Daily	County	Descriptive
Plant-ACH	pH	Daily	County	statistics
GAC/BAC	Turbidity	Daily	County	(average,
Pretreatment-UF	Alkalinity	Daily	County	standard
Control-UF	Color	Daily	County	deviation &
	UV 254	Daily	County	confidence
	DOC	Daily	County	interval);
	SUVA	Daily	County	Hypothesis
	TSS	Bi-weekly	UCF	testing
	TDS	Bi-weekly	UCF	
	Hardness (Ca, Mg)	Bi-weekly	UCF	
	Metals (Si, Mn, Fe, Al)	Bi-weekly	UCF	
	Anions (Cl^-, SO_4^{2-}, Br^-)	Bi-weekly	UCF	
Plant-ACH	Free and Total ATP	Bi-weekly	County	Descriptive
GAC/BAC	HPC	Bi-weekly	County	statistics;
	Dissolved Oxygen	Daily	County	Hypothesis
	Phosphate	Bi-weekly	County/UCF	testing
	Nitrate	Bi-weekly	UCF	
Pretreatment-UF Control-UF	DBP formation potential: Cl_2 and TTHMs after 6, 24, 48, 96, and 168 hours HAA$_5$ after 96 hours[2]	Four experimental sets in April, Aug., Oct. & Dec. 2013	UCF	Comparison to MCLs

(1) Water quality was analyzed according to standard methods (Table A-1 of Appendix A).
(2) HAA$_5$s were measured according to EPA Method 552.3.

As in the MIEX® phase, inorganic and organic water quality was characterized according to pH, temperature, turbidity, alkalinity, solids, hardness, anions, metals, color, UV 254, DOC, and SUVA. In addition, the biological activity of the plant-ACH feed water and activated carbon filtered water was examined using biological monitoring tools, including nutrient availability (phosphate and nitrate), signs of bacterial respiration (dissolved oxygen), free ATP (extracellular), cellular ATP (total minus free), and HPC. The free and total ATP measurements were compared to traditional HPC (CFUs/mL) values to determine whether a relationship could be discerned. The proportion of extracellular ATP to total ATP (free/total ATP) was used as a surrogate for the fraction of inert ATP, such as biopolymers, that may contribute to membrane fouling. Also, the relative amount of viable cells was determined by subtracting the free ATP from the total ATP. The ATP activity on the GAC media was not examined because collecting GAC samples would have required the shut-down of the biofilter pilot. Velten and colleagues (2011) agree that in many cases sampling biomass from biofilters may not be feasible. Additionally, the researchers asserted that analyzing the DOC and suspended microbial activity across biofilters serves as adequate monitoring tools for assessing biofilter performance (Velten et al., 2011).

To investigate the effect of GAC media filtration on finished water quality, the DBP formation potential was determined during the each phase of GAC filtration: adsorption mode at pilot start-up (April 28, 2013); the transition mode (August 5, 2013); biological mode with orthophosphate addition (October 21, 2013), and biological mode with orthophosphate addition and pH adjustment (December 9, 2013). The water quality results were analyzed using descriptive statistics and hypothesis testing.

CHAPTER 4. RESULTS AND DISCUSSION

Surface Overland Flow Water Quality Analysis

The Waikamoi watershed serves as the Olinda WTP's water supply and is intermittently unavailable for use during drought. The headwaters of Waikamoi stream originate in the Haleakala National Park where vegetation is predominately native shrub lands with sparse alien grasses. In the intermediate slopes of the hydrologic unit, the Waikamoi stream flows through native communities of Ohia forests and Uluhe shrub lands that lie within the Waikamoi Preserve and Koolau Forest Reserve. Historical water quality records as provided by the State of Hawaii (2009) for the Waikamoi watershed are limited to temperature, turbidity, dissolved oxygen, total dissolved solids and nutrients; however, these data (when collected) are obtained downstream along the Waikamoi ditch at lower elevations than the supply that feeds the Olinda WTP.

In an effort to obtain a more complete characterization of the Waikamoi watershed, inorganic, organic, and biological water quality parameters were collected throughout the native watershed as the water flows from the flume to the Olinda WTP. The Waikamoi watershed sampling and testing events were conducted on November 15, 2012, January 31, 2013, April 30, 2013, August 6, 2013, October 22, 2013, and May 12, 2014. Of the sampling events, dry weather was observed in April 30, 2013, August 6, 2013, and October 22, 2013, while rainy weather was observed on November 15, 2012, January 31, 2013, and May 12, 2014. The sampling locations with corresponding GPS coordinates are depicted on a Google satellite map in Figure 4-1.
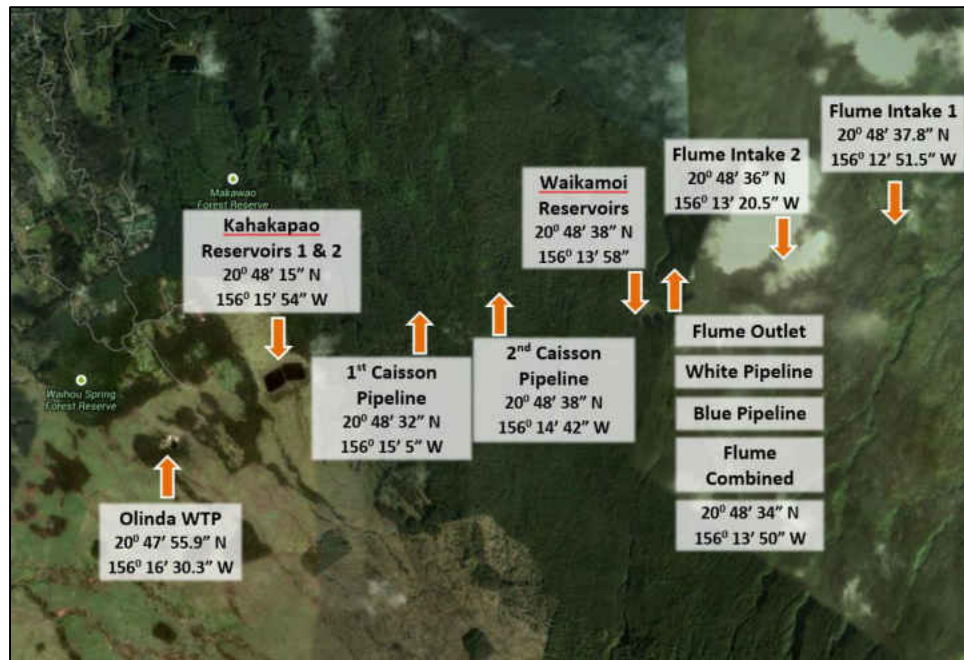
Figure 4–1 Waikamoi Watershed Sampling Locations

Water samples were collected at several locations:

1. Kahakapao 50 MG reservoirs 1 and 2

2. Waikamoi 15 MG reservoirs

3. First (1st) and second (2nd) caisson pipelines

4. Combined flume outlet

5. White pipeline

6. Flume outlet

7. Flume intakes 1 and 2

8. Blue pipeline

The blue pipeline intake collects water from the highest elevation reaches of the Waikamoi stream.

The flume intakes 1 and 2 represent sampling locations at the end (Haipua'ena stream) and middle

(combined overland runoff) of the rectangular flume. The flume outlet represents the combined flow of captured runoff, Haipua'ena stream, and Puanokamoa stream waters. The white pipeline, which runs parallel to the rectangular flume, collects water from the Puanokamoa stream. The water collected in the blue pipeline, white pipeline, and flume is mixed at the combined flume outlet structure. The combined flume water and additional Waikamoi stream water is diverted to the Waikamoi reservoirs. Downstream of the Waikamoi reservoirs, the 1st and 2nd caisson pipelines transport collected water to the Kahakapao reservoirs, which store and pre-settle the source water prior to treatment at the Olinda WTP. The impact of watershed elevation and weather condition on pH, turbidity, DOC, extracellular (free) ATP, cellular (total minus free) ATP, and free/total ATP fraction is illustrated by the dry versus rainy column graphs, shown in Figures 4-2 through 4-7. The dry versus rainy column graphs for the temperature, DO, alkalinity, color, UV 254, SUVA, and metals are presented in Figures D-10 through D-21 of Appendix D.
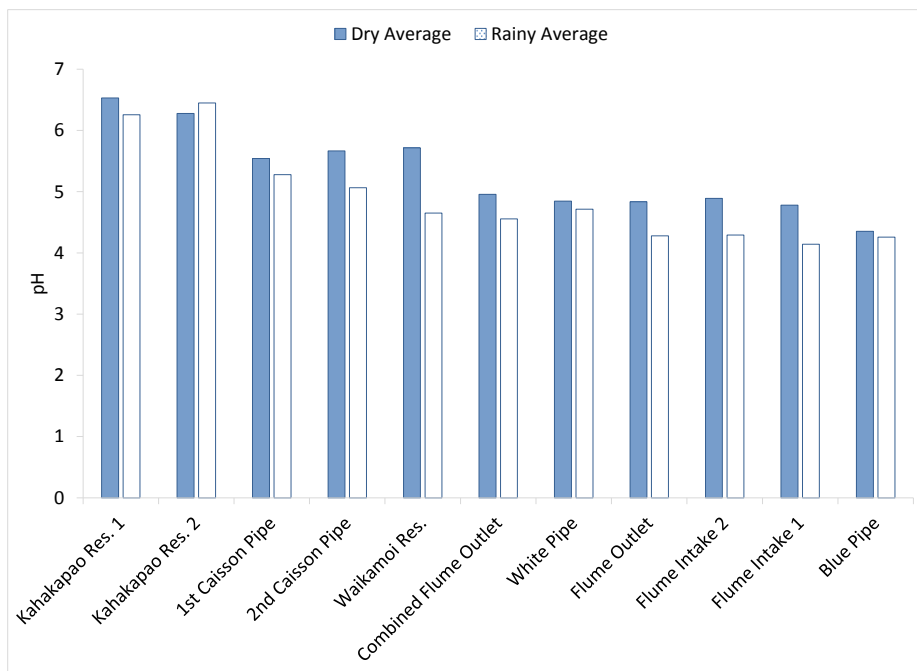
Figure 4–2 Dry vs Rainy pH
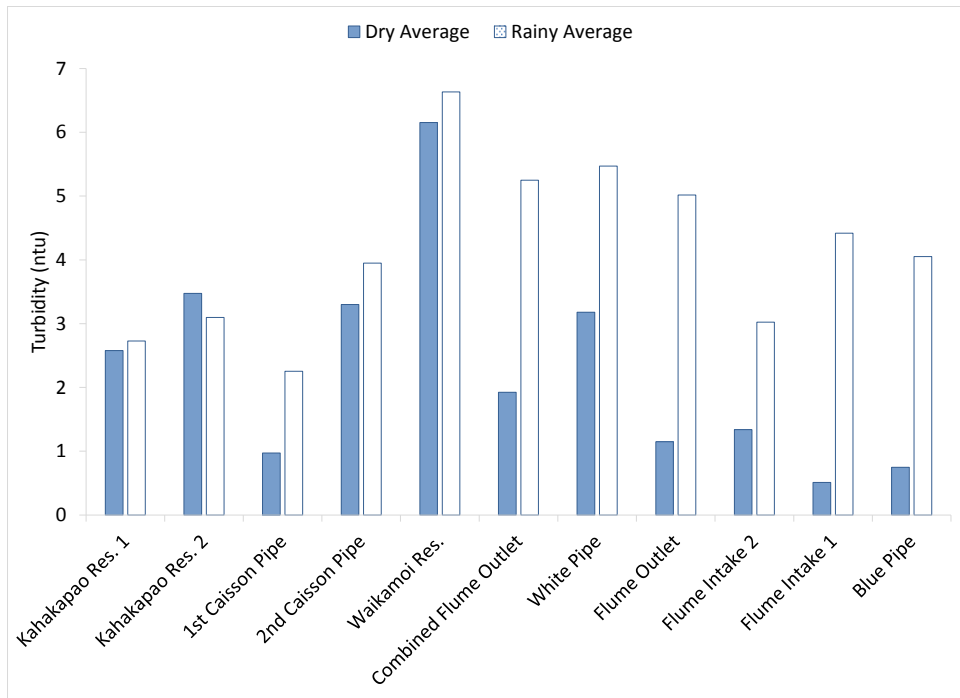
Figure 4–3 Dry vs Rainy Turbidity
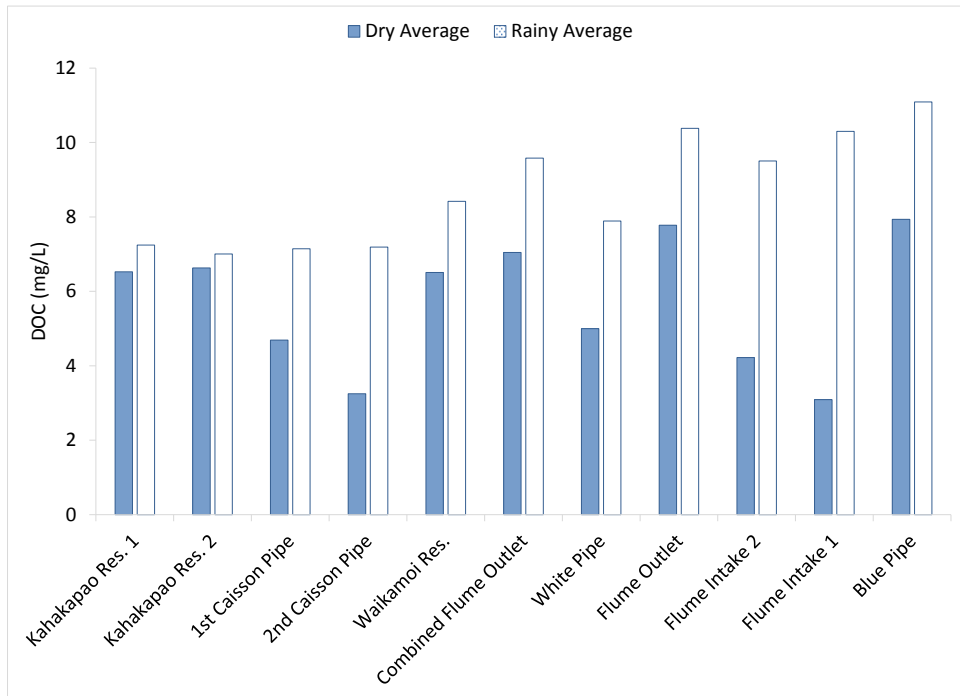
Figure 4–4 Dry vs Rainy DOC
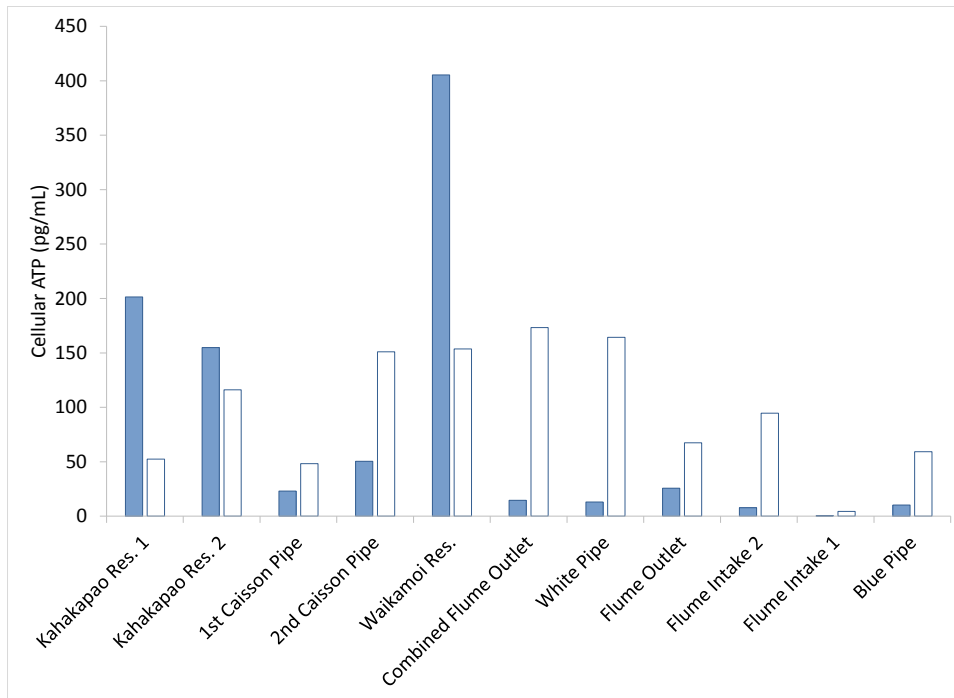
Figure 4–5 Dry vs Rainy Cellular ATP
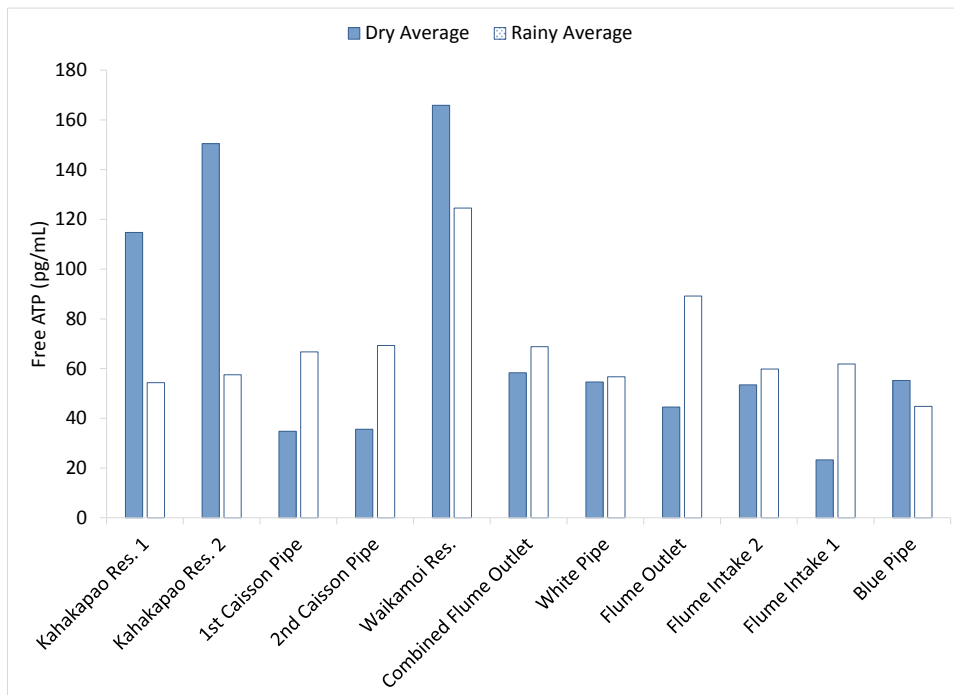
Figure 4–6 Dry vs Rainy Extracellular ATP
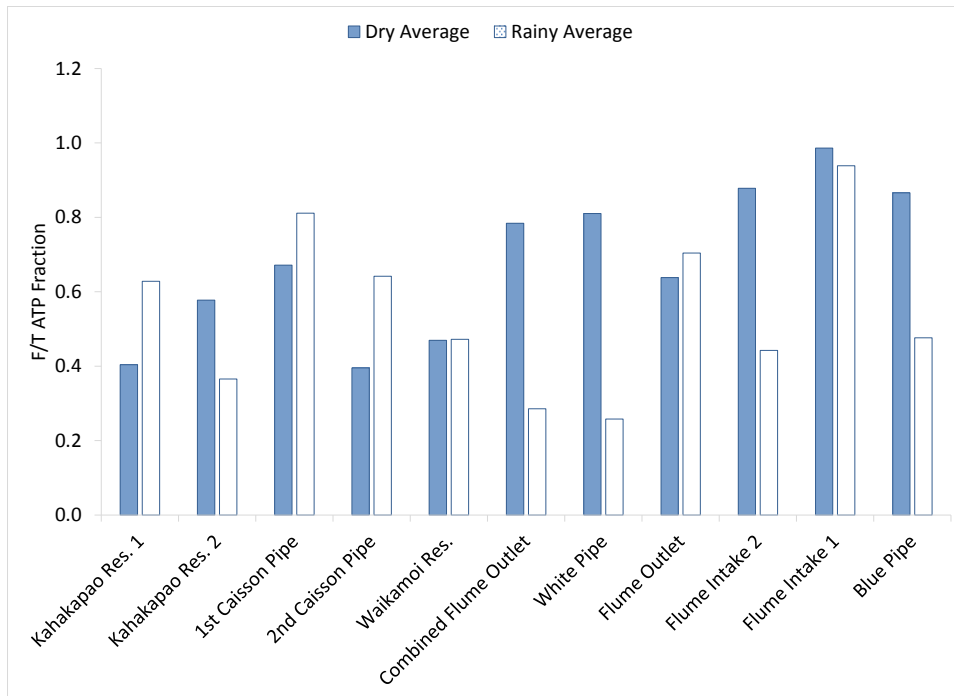
Figure 4–7 Dry vs Rainy F/T ATP Fraction

Overall, the major water quality trends indicate that the highest watershed locations contained elevated DOC levels of up to about 12.3 mg/L and low pH of 4 units, and the reservoirs contained the higher biological ATP levels reaching about 900 pg/mL. According to the dry versus rainy turbidity averages, the turbidity levels increased during rainy weather conditions by up to 4 ntu at the headwaters; however, pre-settling in the Kahakapao reservoirs attenuated the turbidity spikes. Similar to the turbidity, the organic content as measured by DOC, color, and UV 254 was higher during rainy conditions. The Kahakapao reservoirs attenuated a portion of the organic loading to the Olinda WTP; however, the rainy average DOC levels remained about 10 percent higher than the dry average DOC. Utilizing the DOC and UV 254 measurements, the character of the organic carbon was determined by calculating the SUVA values throughout the watershed. For the watershed sampling locations, the relatively high SUVA values ranging from about 3 to 6 L/mg-

78

m indicate that the Waikamoi surface water is rich in hydrophobic humic and fulvic organic acids originating from the native rainforest vegetation (Lozier et al., 2008).

As shown in Figures 4-5 and 4-6, the extracellular and cellular ATP levels were higher during the rainy conditions for the flowing sampling locations, but lower during the dry conditions for the reservoirs. The higher ATP counts during the rainy conditions in the overland flow capture locations are likely due to the higher water flows uptaking more inert and viable ATPs. The higher ATP counts during the dry conditions in the reservoirs is attributed to lower water levels, which allows for more interaction between the water and the expected biologically active sediment layer within the reservoirs. When evaluating the free/total ATP fraction (see Figure 4-7), it is apparent that lower fractions were present in the Waikamoi reservoirs. The lower free/total ATP fraction signals a higher quantity of viable cells relative to the total ATP. The higher biological activity in the Waikamoi reservoirs likely resulted from the relatively deep sediment layer within the reservoirs during sampling. The higher ATP provided the County sufficient evidence to fund the cleanout and rehabilitation of both Waikamoi reservoirs, scheduled for implementation prior to this body of work being completed. The relining and rehabilitation of the two Waikamoi reservoirs was completed at the time of this document being published.

In addition to the observed increase in the biological activity of the water supply, the concentration of metals, including iron, manganese, aluminum, and calcium, were found to increase across the reservoir storage (see Figures D-16 through D-19 of Appendix D). It is expected that iron, manganese, and aluminum originated from the metals naturally present in the volcanic soil (Garrett, 2000). However, it is likely that the additional calcium originated from the reservoir's concrete material. The increase in calcium with corresponding increase in alkalinity (Figure D-12)

across the Waikamoi and Kahakapao reservoirs implies that the organic acid source water is dissolving the calcium from the concrete structures (Zivica & Bajza, 2000).

Based on the water quality observations, the following watershed management strategies were identified.

- The County should consider placing high elevation source intakes temporarily offline during the elevated DOC seasons (rainy conditions) to help dampen the organic load to the Olinda WTP.

- The treatment operating staff can anticipate the use of higher ACH coagulant doses during and after rain events due to higher organic and turbidity levels in the source water.

- The biological activity and leaching of metals may be reduced by implementing a sediment cleaning schedule for the Waikamoi and Kahakapao reservoirs.

- The County should consider providing a protective coating or lining for the Kahakapao reservoirs to prevent leaching of the concrete, which could lead to structural failure.

- The County should continue to monitor water quality within and throughout the Waikamoi watershed conveyance system that provides raw water to the Olinda WTP.

Confirm Existing Conventional-UF Process Operations

The purpose of confirming the existing conventional-UF process operations was to: (1) validate the full-scale coagulation efficiency, (2) demonstrate the need for additional pretreatment, and (3) show representativeness between the full and pilot scale UF processes. The research objectives

were accomplished by conducting jar testing experiments, and monitoring the water quality and operational performance of the full-scale Olinda WTP and pilot control-UF processes.

Evaluation of Coagulation Process Performance

Jar testing experiments were conducted on the Olinda raw water at varying ACH coagulant doses and pH ranges to confirm current performance of the Olinda WTP's coagulation operation. The coagulation performance was evaluated according to particulate and organic removal efficiencies as measured by turbidity, color, UV 254, DOC, and SUVA. The experimental data for the preliminary and experimental jar tests are compiled in Table E-1 of Appendix E. The three-dimensional contour plots of turbidity, color, UV 254, DOC, and SUVA removals versus ACH coagulant dose and pH are shown in Figures 4-8 through 4-12.
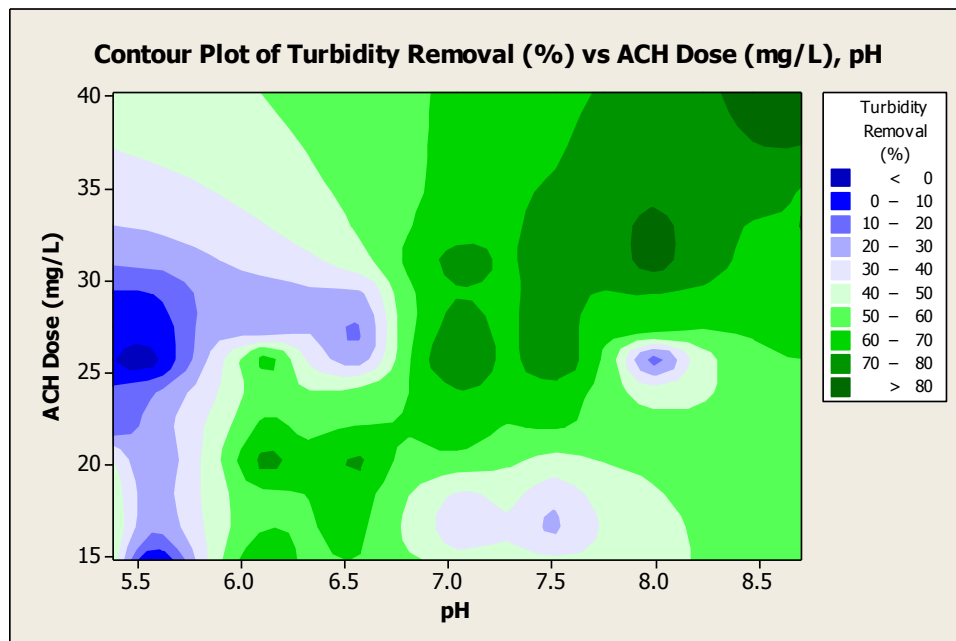
Figure 4–8 Turbidity Removal
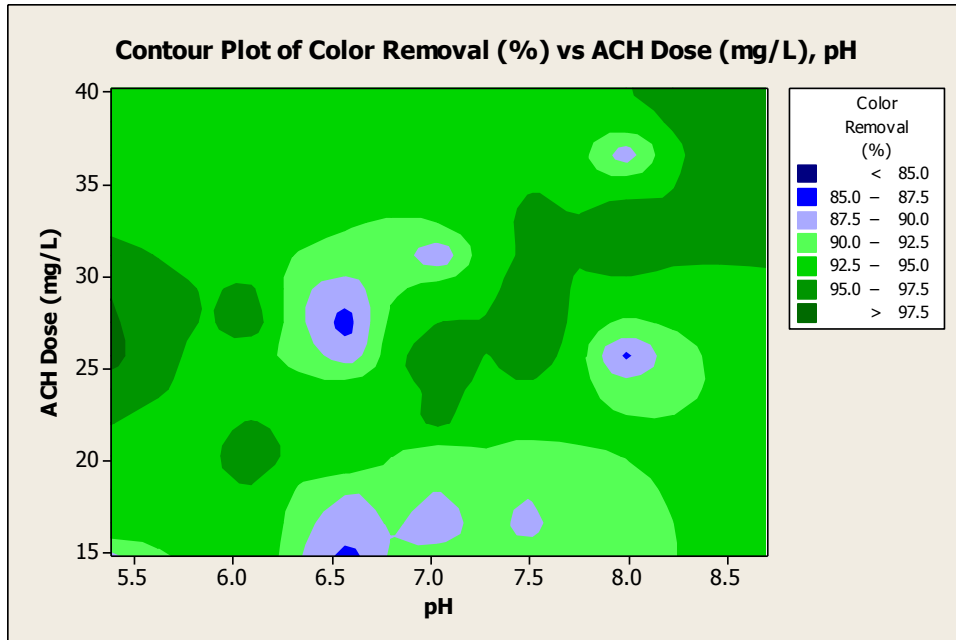
Figure 4–9 Color Removal
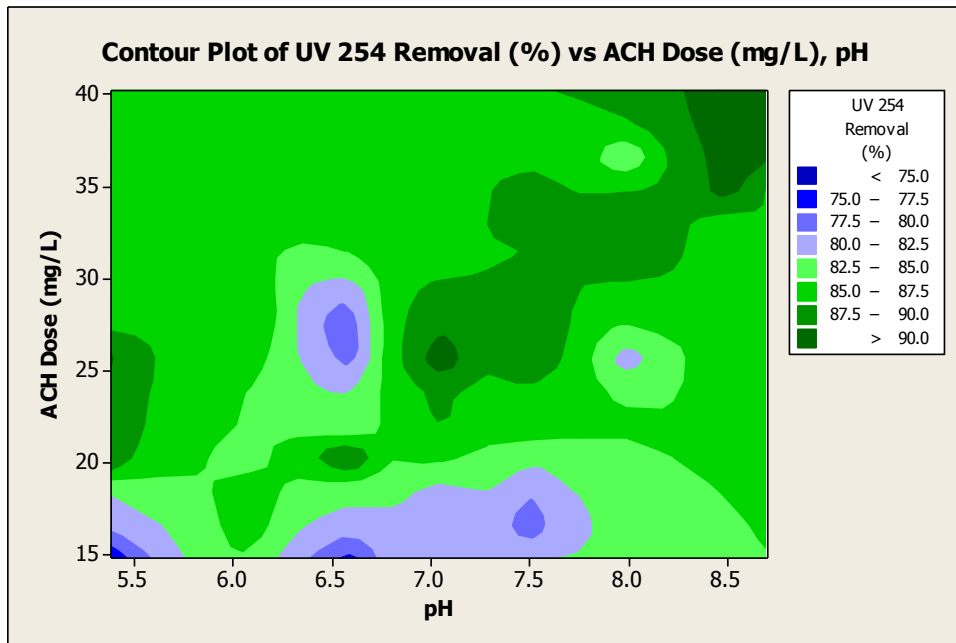
Figure 4–10 UV 254 Reduction
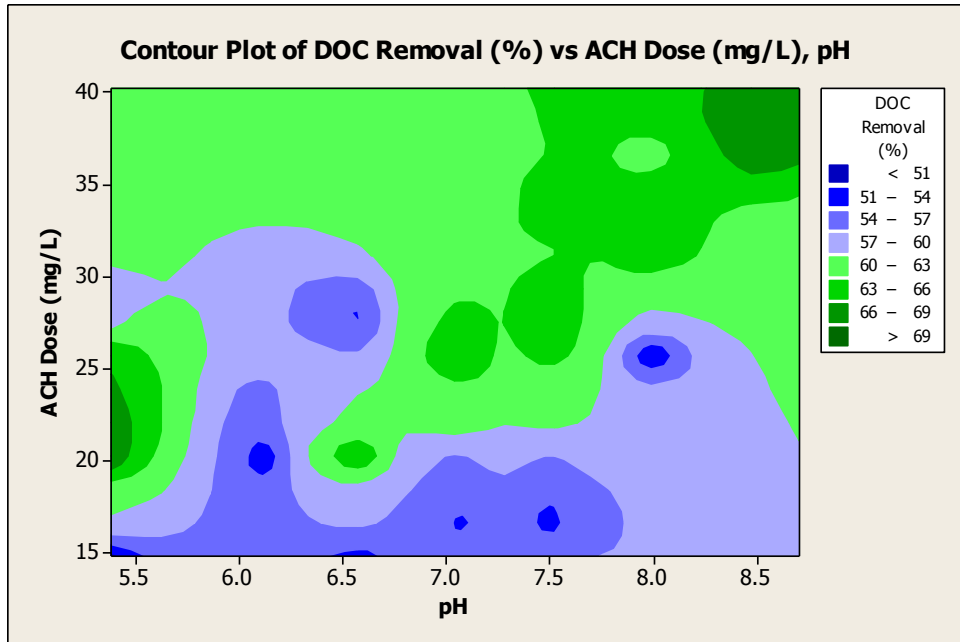
Figure 4–11 DOC Removal
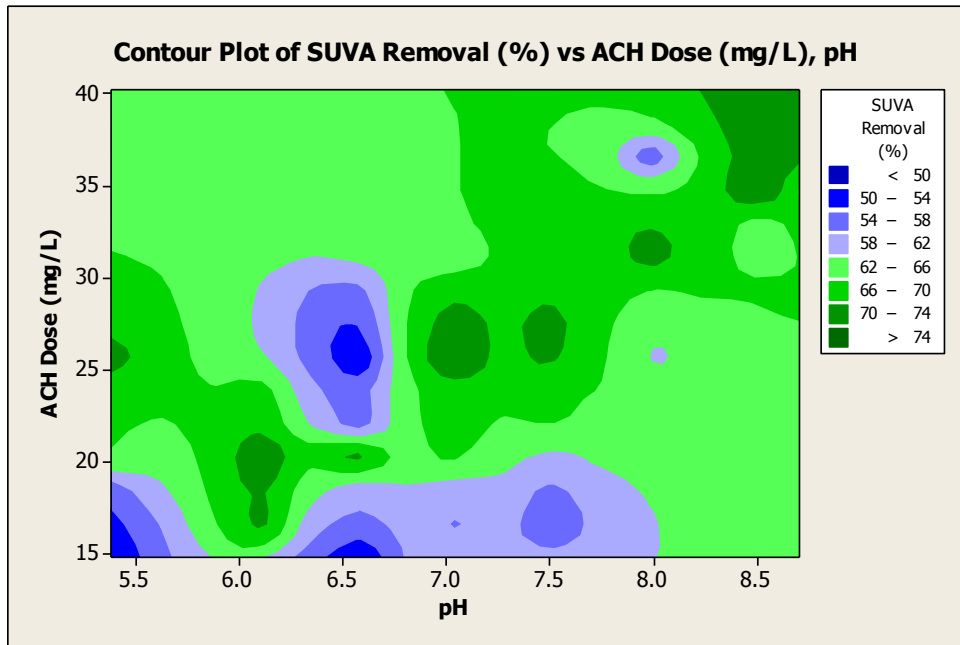
Figure 4–12 SUVA Reduction

The full-scale coagulation operated at ACH coagulant doses between 20 and 33.5 mg/L and pH levels between 5.5 and 6.5 units. Under these conditions, the turbidity, color, UV 254, DOC, and SUVA removals were greater than 20, 92, 82, 50, and 65 percent. The lower turbidity removals were mainly observed in the lower pH range, which fell below the pH (6.7 units) of minimum solubility for ACH (Pernitsky & Edzwald, 2003). Below the pH of minimum solubility the coagulant hydrolysis products promote more charge neutralization rather than the sweep floc enmeshment. The sweep floc mode of operation was observed at higher coagulant dose and pH ranges and achieved more effective turbidity removal.

Although turbidity removal was depressed at a lower pH range, the DOC removal reached 70 percent. The efficient removal of DOC at lower pH results from charge neutralization and organic-complex formation mechanisms (Budd et al., 2004; MWH, 2005; Yan et al., 2007; Yu et al., 2007). The trade-off between organic and turbidity removal under depressed versus elevated pH ranges has been demonstrated in the work of other researchers (Budd et al., 2004; Matilainen et al., 2010). However, review of the turbidity and DOC contour plots reveals that a balance was achieved around 6 pH units. A pH of 6 coincides with the average pH of the raw water. At the average raw water pH level, turbidity removal was greater than 70 percent and DOC removal was greater than 50 percent.

Achieving a DOC removal greater than 50 percent agrees with the findings of other coagulation studies that investigated the optimization of DOC removal for high SUVA (greater than 4) water sources (Archer & Singer, 2006; Matilainen et al., 2010). Furthermore, the jar testing results revealed that coagulation achieved a higher UV 254 removal (82 percent) as compared to the DOC removal (50 percent). The greater reduction in UV 254 measurements implies that as expected the

coagulation process removed a higher percentage of the aromatic carbon fraction. The effective removal of aromatic, hydrophobic-type organic carbon is further supported by the decrease in the SUVA values from greater than 4 L/mg-m before coagulation to less than 2.3 L/mg-m after coagulation. After coagulation, the change in SUVA values suggests that the organic fraction shifted from large hydrophobic compounds to more neutral or hydrophilic organics (Archer & Singer, 2006; Matilainen et al., 2010).

The jar testing results, specifically turbidity and organic removal, were further analyzed by determining the average removals at optimum ACH coagulant doses. The optimum coagulant dose was selected based on the dose that achieved the highest organic and turbidity removals at the lowest chemical usage rate. In cases where the highest organic and turbidity removals were not aligned, optimizing organic removal took precedence. An example of dose selection is illustrated in Figure 4-13. The turbidity and organic removals from the optimum coagulant doses were averaged and compared to the full-scale coagulation removals to determine whether the Olinda WTP is achieving efficient treatment. The Olinda full-scale turbidity and organic water quality results are summarized in Table E-2 of Appendix E. The treatment efficiency comparison between the bench-scale jar tests and full-scale coagulation is presented in Figure 4-14. As compared to the full-scale system, the turbidity and organic removals from the jar testing experiments differed by at most 20 percent. Thus, the Olinda WTP's coagulation process was determined to be operating within the optimum particulate and organic removal ranges for the jar testing conditions tested.
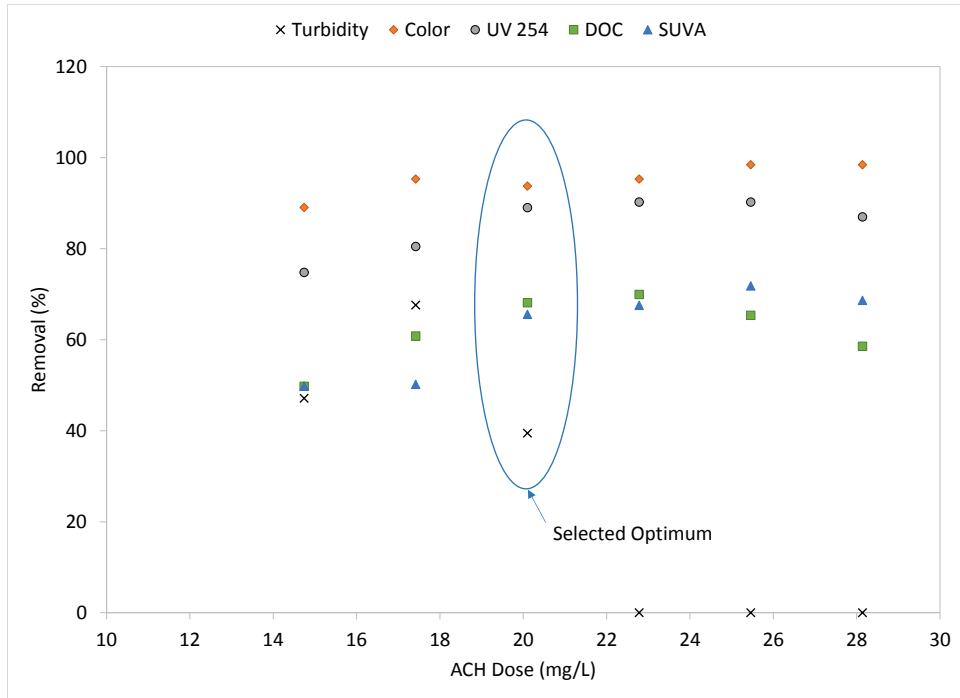
Figure 4–13 Selection of Optimum ACH Coagulant Dose
Note: Experimental jar test was conducted on May 17, 2014.
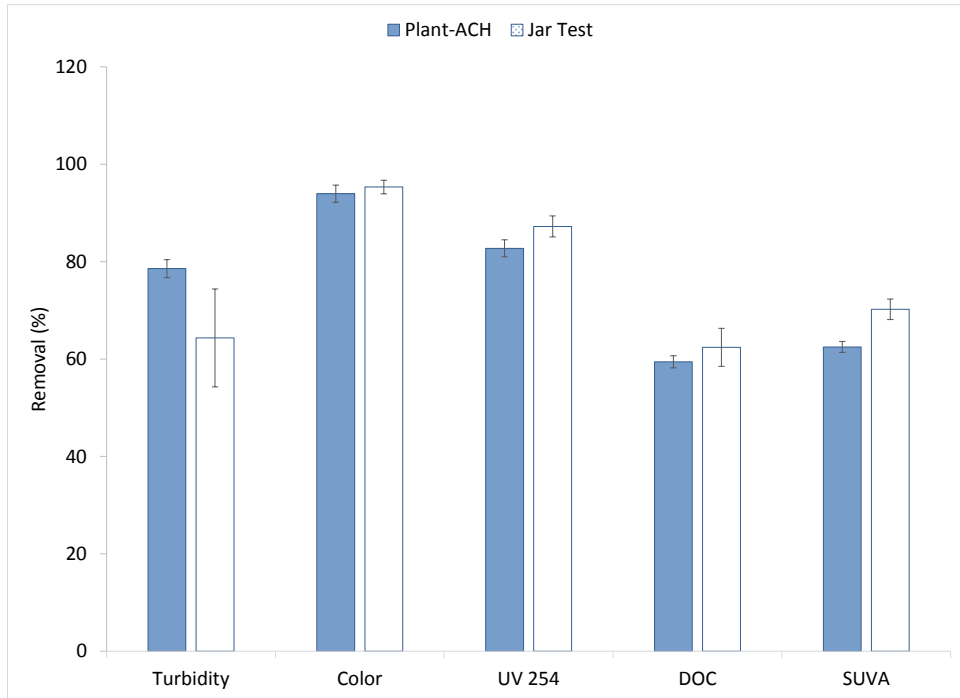
Figure 4–14 Bench to Full Scale Comparison of Particulate and Organic Removal

In an effort to identify coagulation optimization strategies, the jar testing experiments included varying the coagulant dose and adjusting the raw water pH. The use of alternative coagulants or cationic polymer aids were not investigated. Alternative coagulants (alum and ferric chloride) were not tested because these traditional coagulants consume significant levels of alkalinity during coagulation (Budd et al., 2004). Additionally, cationic polymers may worsen membrane fouling (Wang et al., 2011). Considering these limitations, the County can opt to target the identified optimum DOC removal range between 50 and 70 percent by varying the ACH dose and adding caustic or lime to raise the pH near 6 pH units. Even with DOC removals between 50 and 70 percent, it is expected that additional organic removal treatment is necessary to achieve DOC removals greater than 70 percent for efficient DBP control with free chlorine disinfection.

Water Quality Analysis

Water quality was monitored across the full and pilot scale UF processes to identify seasonal water quality trends, compare full-scale and pilot-scale UF treatment performance, and confirm the need for additional pretreatment. Minimum, maximum, and average water quality results for the raw, plant-ACH, plant-UF, and control-UF water samples are presented in Table E-2 of Appendix E. A summary of the average pH, temperature, turbidity, color, UV 254, DOC, SUVA, iron, and aluminum is included in Table 4-1. The accompanying time-series graphs are illustrated in Figures E-1 through E-8 of Appendix E. The raw water temperature gradually increased from about 15 °C in the winter to 22 °C in the summer. The average raw water pH was 5.9 pH and ranged from 4.6 to 7.3 units. Coagulation slightly decreased the pH of the water to 5.7 pH units. Because of the low filtrate water pH of 5.7, the County adds food-grade lime for pH stabilization and corrosion control.

Table 4–1 Olinda WTP Average Water Quality

Water Quality	Raw	Plant-ACH	Plant-UF	Control-UF
pH	5.9	5.7	5.7	5.6
Temp. ($^{\circ}$C)	18.7	19.1	19.3	19.4
Turb. (ntu)	3.2	0.74	0.06	0.05
Fe (mg/L)	0.612	0.053	0.012	0.010
Al (mg/L)	0.256	0.042	0.008	0.007
Color (CU)	70	3	2	2
UV254 (1/cm)	0.309	0.047	0.043	0.043
DOC (mg/L)	6.8	2.7	2.3	2.3
SUVA (L/g-m)	4.6	1.7	1.9	1.9

During continuous operation of the Olinda WTP, coagulation of the relatively low-turbidity, low-alkalinity, organic-laden raw water reduced the turbidity, color, and DOC to typically less than 0.5 ntu, 5 CU, and 3.5 mg/L C. From November 2012 to February 2013 and September to December 2013, the Olinda plant was operated intermittently due to full-scale maintenance activities and seasonal drought conditions. During the intermittent operation, the raw and settled water turbidities experienced spike levels of up to 12 and 2.8 ntu, respectively. The spike in raw water turbidity likely resulted from the accumulation and re-suspension of solids in the raw water intake during subsequent plant shut-downs and start-ups. The elevated settled water turbidity levels signals that the unsteady-state operation of the coagulation process caused a destabilization and suspension of the settling basin's flocculant sludge layer. In turn, the carry-over of small or pin floc aggregates was observed in the plant settled water. The carry-over of suspended matter directly contributes to UF fouling. Therefore, poor control over the settled water turbidity is expected to negatively impact UF operation, particularly during drought periods when water scarcity necessitates intermittent plant shut-downs (Howe & Clark, 2002). Additionally, the intermittent plant operation

was found to contribute to elevated iron (1 mg/L), aluminum (0.5 mg/L), and organic matter (3.8 mg/L DOC) concentrations in the settled water.

The organic matter, as measured by color, UV 254, and DOC, tended to be higher in the summer and early fall months and lower in the winter and spring months. The raw water color and DOC averages were 70 CU and 6.8 mg/L, respectively. Based on the relatively high UV 254 (0.31 1/cm) and SUVA (4.6 L/mg-m) values, the DOC was mainly comprised of hydrophobic, aromatic organic compounds. The hydrophobic character of the raw water DOC was further illustrated by fluorescence EEM results. The fluorescence intensity of the raw water was plotted in a three-dimensional contour plot (shown in Figure 4-15) as a function of excitation and emission wavelengths.
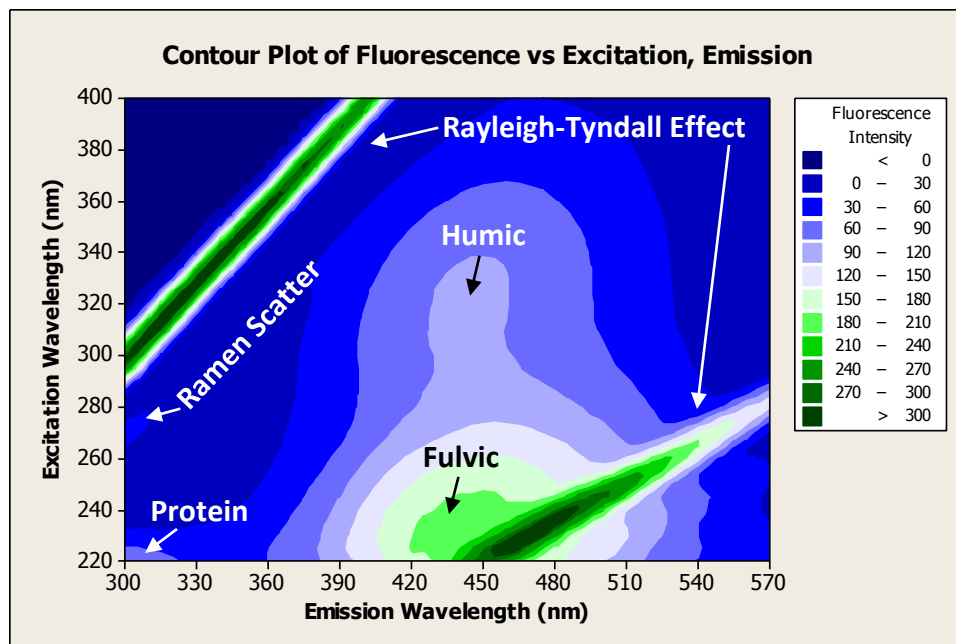
Figure 4–15 Raw Water EEM Diagram

In the EEM diagram, the peaks associated with specific DOM fractions were identified by comparing the experimental EEM to the general EEM template of Figure 3-6, which was developed in previous studies (Chen et al., 2003; Hudson et al., 2007; Bridgeman et al., 2011). The Rayleigh-Tyndall lines result from cuvette wall effects; and the Raman line results from the scattering properties of water's O-H covalent bonds. Based on the EEM diagram, the DOM of the raw water is mainly hydrophobic fulvic and humic organic acids. The slight fluoresce peak at excitation-emission wavelengths of 220 and 300 nm reveal that the DOC also contains a smaller fraction of hydrophobic neutral proteins (Tyrosine-like). The tyrosine-like proteins are amino acids with aromatic ring structures. However, debate remains among researchers whether tyrosine-like proteins originate from freely available amino acids or from viable cellular matter (Hudson et al., 2007).

Because of the hydrophobic nature of the raw water DOM, the coagulation process removed a significant portion of the organic acids as demonstrated by the reduction in color and DOC to 3 CU and 2.7 mg/L. The color and DOC reduction was accompanied by a reduction in the UV 254 and SUVA to 0.047 1/cm and 1.7 mg/L. The change in the organic character of the settled water DOC confirms that the hydrophilic organic fraction remains in the settled water after coagulation. The character of the DOM after coagulation was further defined using the fluorescence EEM diagram, displayed in Figure 4-16.
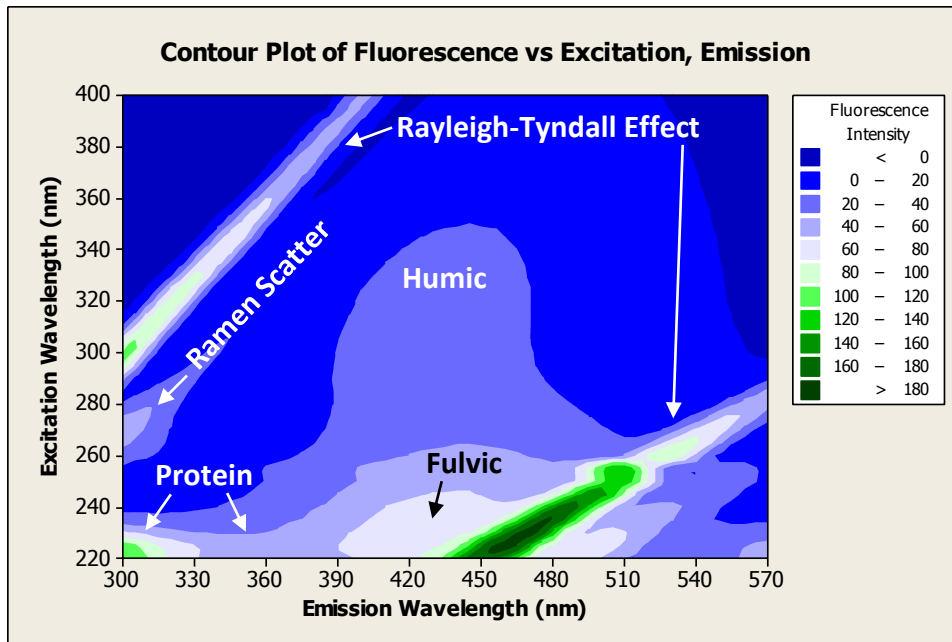
Figure 4–16 Settled Water EEM Diagram

The EEM for the coagulated-settled water is similar to the raw water EEM; however, the settled water EEM has lower fluorescence intensities due to the reduction in DOM concentration. Furthermore, the hydrophobic and hydrophilic protein peaks are more pronounced in the settled water EEM diagram. The fluoresce peak at excitation-emission wavelengths of 230 and 350 nm is characteristic of more tryptophan-like proteins. The presence of tryptophan-type proteins has been related to biological activity (Hudson et al., 2007). Consequently, the detection of the tyrosine and tryptophan protein-like DOM in the EMM uncovers the possibility of organic and biological fouling of the downstream UF membranes (Lozier et al., 2008; Nguyen et al., 2012).

After coagulation, the UF process effectively removed the remaining fine particulates, as demonstrated by the low (0.06 ntu) turbidity of the UF filtrate. In addition, UF membrane filtration further reduced the settled water iron and aluminum concentrations. The iron and aluminum species were likely bound or enmeshed in the settled water floc aggregates and precipitates (MWH,

91

2005). The organic concentration and character also changed across the UF membrane. The DOC decreased by about 15 percent to 1.7 mg/L and the SUVA value increased by about 12 percent to 1.9 L/mg-m. The decrease in DOC and increase in SUVA suggest that the UF membrane retains a portion of the larger hydrophilic DOC fraction. The larger hydrophilic DOC fraction has been shown to contribute to membrane specific flux decline (Huang et al., 2007). Based on the changes in water quality across the UF process, membrane fouling of the full-scale plant is most likely due to the deposition and accumulation of particulate matter (flocs), iron, aluminum, organic, and possibly biological matter. Hence, additional pretreatment is expected to reduce these foulants, especially the DOM that may contribute directly to organic fouling or indirectly to biological fouling (Nguyen et al., 2012).

To summarize the full-scale water treatment performance and compare the full to pilot scale UF processes, the average turbidity and DOC concentrations across the existing system are presented in column graphs (Figures 4-17 and 4-18). Additional water quality comparisons for color, UV 254, SUVA, iron, and aluminum are included in Figures E-9 through E-13 of Appendix E. The column graphs show average concentration, 95 percent confidence interval error bars, the percent removals, and hypothesis testing results for the full versus pilot scale UF comparison. On average, the conventional-UF process removes 98 percent of the raw turbidity, 96 percent of color, 66 percent of DOC, 98 percent of iron, and 97 percent of aluminum. The hypothesis testing for the pilot and full scale UF filtrate water quality revealed that the results were not statistically different. Therefore, the control-UF pilot provided an effective means of demonstrating the effect of additional pretreatment on water quality.
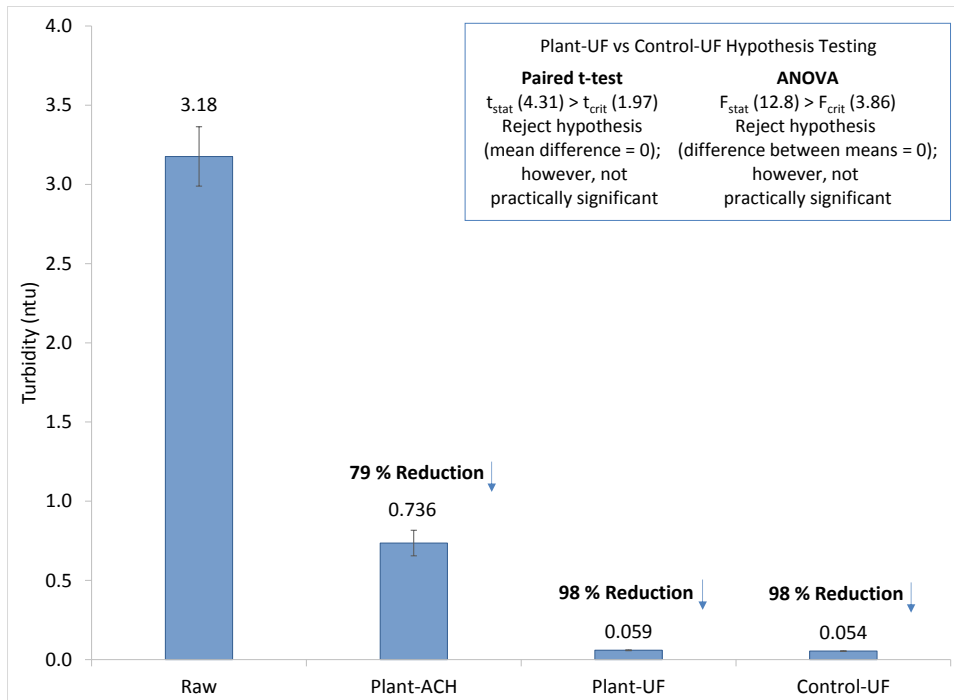
Figure 4–17 Olinda WTP Average Turbidity
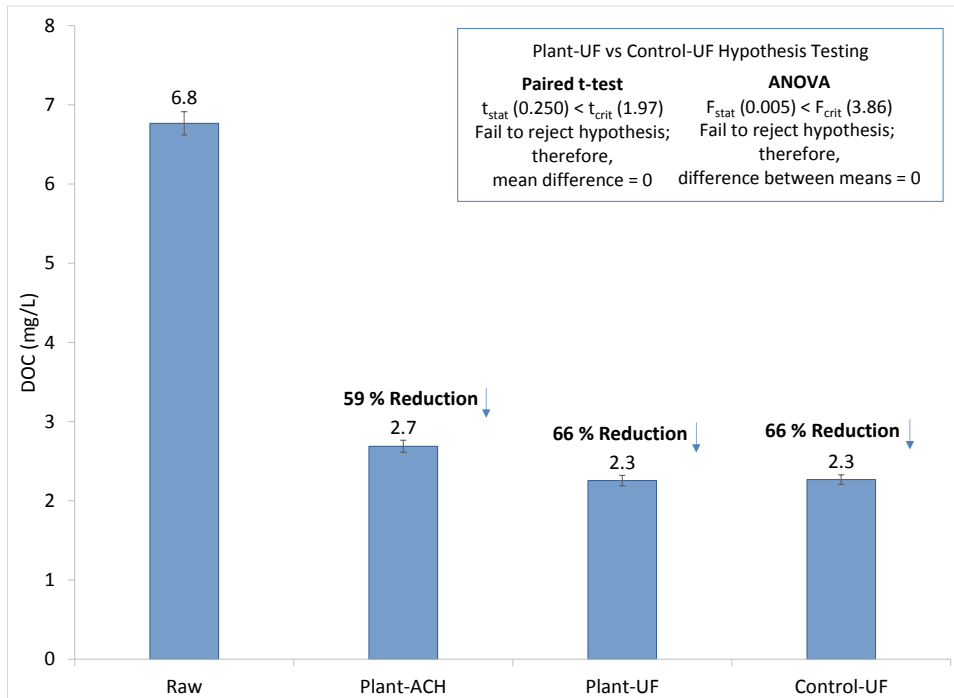
Figure 4–18 Olinda WTP Average DOC

In addition to monitoring the water quality across the existing Olinda WTP, the TTHM and HAA$_5$ formation potential was determined for the full and pilot scale UF finished waters. For the full versus pilot scale DBP analysis, the summaries of the four-day TTHM and HAA$_5$ formation concentrations are shown in Figures 4-19 and 4-20. Based on the TTHM results ranging from 120 to 250 µg/L, the TTHM formation potential with free chlorine disinfection exceeds the MCL of 80 µg/L. Similarly, the experimental HAA$_5$ levels (45 to 110 µg/L) revealed the possibility for exceedance of the 60 µg/L MCL with free chlorine disinfection. In December 2012, January 2013, and April 2013, the Standard Method 6251 B was used to measure the HAA$_5$ concentrations. Both the Standard Method 6251 B and EPA 552.3 Method were used to measure the HAA$_5$ levels in August, October, and December 2013. The results from the EPA 552.3 Method are reported herein because it produced more conservative results based on higher recoveries of spiked samples.

The high DBP formation potential results demonstrate that the DOM remaining after coagulation (combination of residual fulvic acids and proteins) is highly reactive with chlorine to form quantities of THMs and HAAs that exceed regulatory limits (Chowdhury et al., 2009). Therefore, additional organic removal pretreatment is needed to allow the conversion of the disinfectant from monochloramine to free chlorine. The hypothesis testing results show that the plant-UF and control-UF filtrates formed similar levels of DBPs. The similar DBP concentrations further confirms the adequacy of using the control-UF pilot unit as a means of evaluating pretreatment performance.
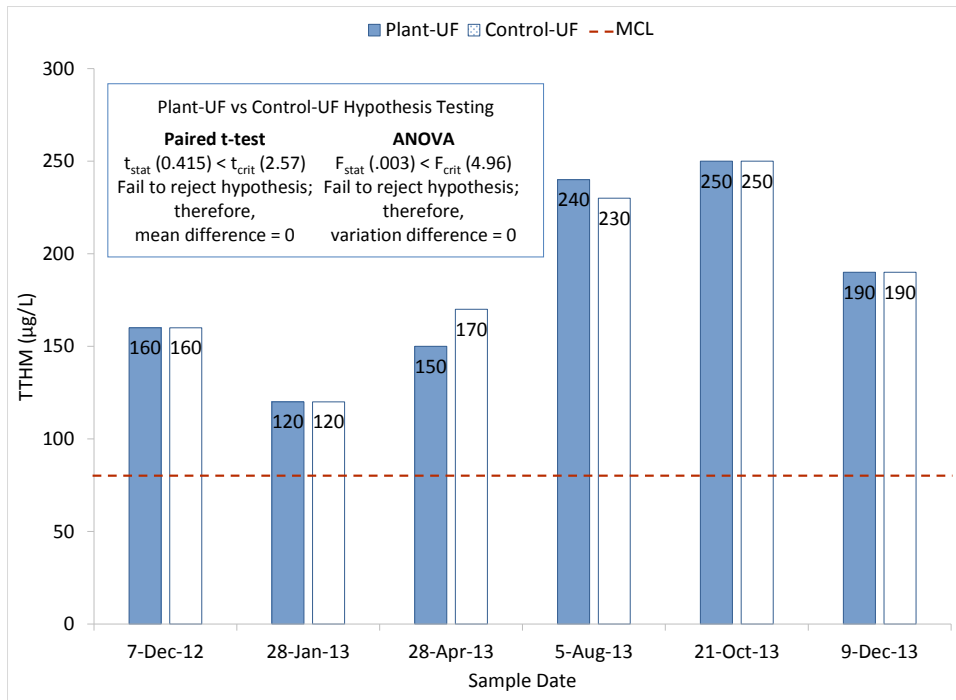
Figure 4–19 Four-Day TTHM Formation Potential of Full versus Pilot Scale UF
Note: Experimental parameters and speciation are included in Appendices E, F, and G.
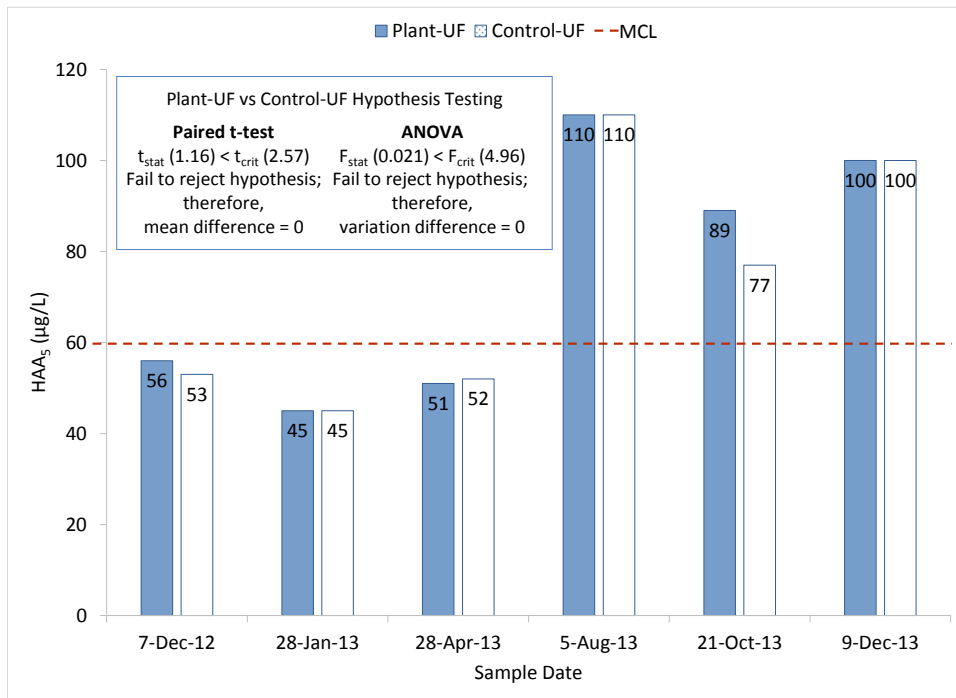
Figure 4–20 Four-Day HAA$_5$ Formation Potential of Full versus Pilot Scale UF
Note: Experimental parameters and speciation are included in Appendices E, F, and G.

95

Ultrafiltration Process Confirmation

From September 2012 to December 2013, operational parameters were monitored for the full-scale and pilot-scale UF processes. The full to pilot scale UF performance comparison excluded periods of intermittent plant or pilot operation, including September 2012 through February 2013 (MIEX® testing phase) and September through December 2013 (portion of BAC testing phase). The UF operating data from the third full-scale train (CMF3) was selected for the UF comparison because the membranes were cleaned with sodium hypochlorite and citric acid near the start-up date of the control-UF pilot. Hence, both the CMF3 and control-UF operating performance analysis commenced with clean UF membranes.

The average membrane percent recovery and operational parameters for the full-scale (plant-UF) and pilot-scale (control-UF) membranes are listed in Table 4-2. For the selected operating time frame, the full and pilot scale UF processes achieved similar membrane percent recoveries of 90 and 89 percent, respectfully. The percent recoveries were calculated from the total filtrate volume produced, and the filtrate volume used for backwashing and CIPs. Both the full and pilot UF membranes were backwashed every 20 minutes with water and air scour. The full-scale membranes were cleaned daily with sodium hypochlorite and cleaned 9 times with citric acid, while the pilot-scale membrane was cleaned on three occasions with sodium hypochlorite followed by citric acid. The volume of filtrate used during backwashing and CIPs were estimated from the membrane technical specifications.

Table 4–2 Full-Scale versus Pilot-Scale UF Membrane Performance Comparison

Operational Parameter	Plant-UF	Control-UF
Selected Time Frame	Apr 28, 2013 through Sep 4, 2013	
Membrane Recovery		
Backwash Frequency (minutes)	20	20
Backwash Volume (gal/module)	7.1	10.6
Number of Sodium Hypochlorite CIPs	125 (Daily)	3
Number of Citric Acid CIPs	9	3
CIP Volume (gal/module)	27	40
Percent Recovery	90	89
Average Membrane Process Data		
Flow per Module (gpm)	3.9	4.0
Membrane Area (ft^2)	252	300.3
Flux Rate (gal/ft^2-d)	22.1	19.1
TCTMP @ 20 ºC (psi)	3.7	13.9
Specific Flux @ 20 ºC (gal/ft^2-d-psi)	6.7	1.4

As emphasized in Table 4-2, the average temperature corrected TMP (TCTMP) and temperature corrected specific flux values of the full and pilot UF processes are not of similar magnitudes. The variation in TCTMPs and specific fluxes is likely due to the differences in membrane surface area, membrane age, and housing vessel configuration. Although the magnitudes of the TCTMP and specific flux cannot be directly compared, the pilot and full scale membrane fouling trends for temperature corrected TMP and specific flux provide a relative means of comparison.

In Figures 4-21 and 4-22 the TCTMP and specific flux time series trends are depicted for the full and pilot scale UF processes from late April 2013 to early September 2013. The plant citric acid CIPs and control-UF CIPs were designated by vertical lines. Since the sodium hypochlorite CIPs for the full-scale UF were performed daily, designation lines were not included in the time series graphs.
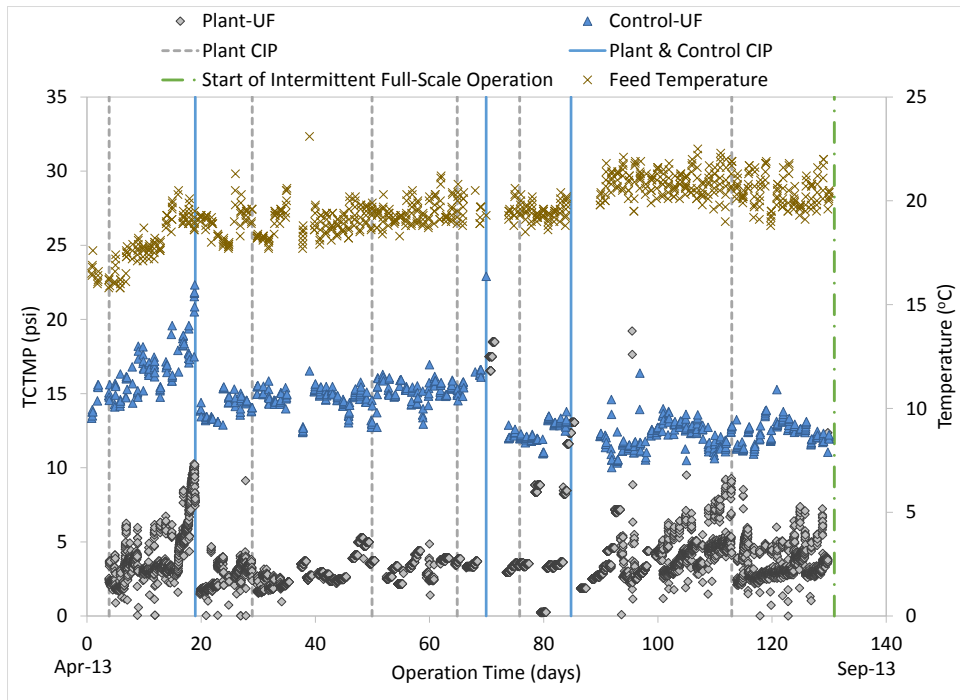
Figure 4–21 Full-Scale versus Pilot-Scale TCTMP Time-Series Trend
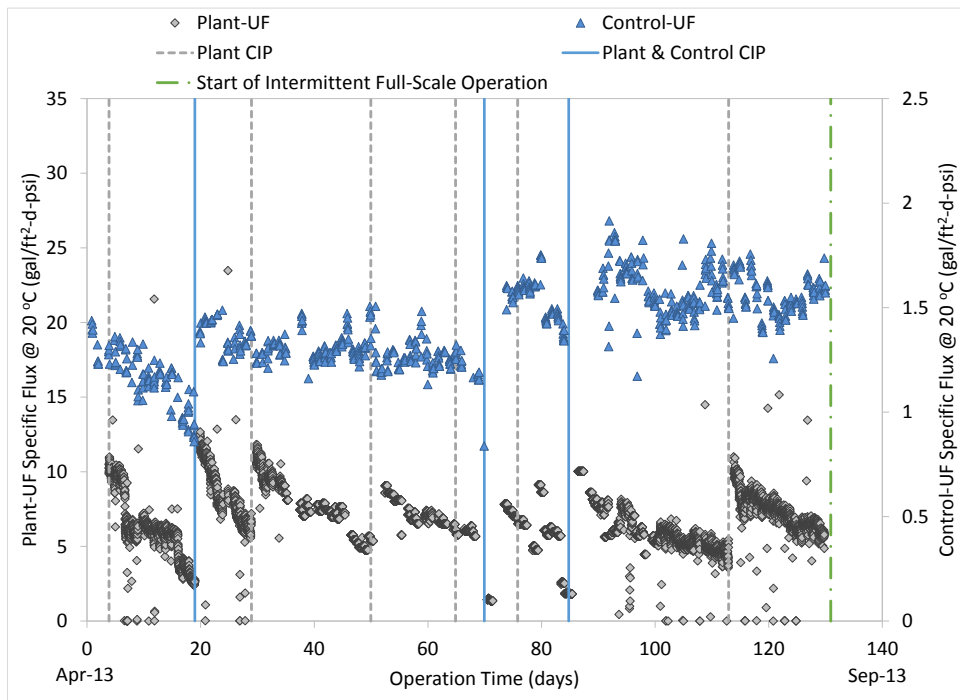
Figure 4–22 Full-Scale versus Pilot-Scale Specific Flux Time-Series Trend

Evaluation of the TCTMP and specific flux time series graphs reveals that the plant-UF and control-UF membrane fouling trends (TMP rise and specific flux decline) follow similar slopes. The comparable fouling trends are most evident during the first 20 days of operation, for which both the full and pilot scale TCTMP rise was about 0.5 TMP/day. After the 20 days of operation, both the plant-UF and pilot-UF membranes were chemically cleaned with sodium hypochlorite and citric acid to recover the TMP rise across the membranes. Additionally, the subsequent pilot CIPs coincided with plant citric acid CIPs.

The full-scale UF membranes were cleaned with sodium hypochlorite daily, and cleaned with citric acid when the TMP reached 10 psi. The pilot-scale UF membranes were cleaned with sodium hypochlorite followed by citric acid when the TMP reached three quarters of the maximum housing pressure (22 psi). The pilot was chemically cleaned less frequently to minimize chemical usage and observe longer fouling trends between cleanings. The minimal impact of the difference in the sodium hypochlorite CIP frequency is likely due in part to the lower operating flux rate of the pilot. The lower pilot flux rate, which in turn lowers the rate of foulant accumulation on the membrane, was necessitated by the confines of the piloting equipment (Huang et al., 2007). As supported by the feed water quality results, the gradual fouling trends of the full and pilot UF processes may be attributed to the daily accumulation of rejected organic and particulate matter not removed during the water and air scour backwashing (Howe & Clark, 2002; Huang et al., 2007). The occurrences of sharper specific flux decline and TMP rise, which coincided with full and pilot scale CIPs, was related to turbidity spikes in the settled water. The settled water turbidity spikes greater than 0.6 ntu occurred in early May 2013 and middle of July 2013.

Additional pretreatment that reduces both the inorganic particulate and organic loading to the UF membranes would be expected to reduce the specific flux decline and TMP rise. The reduction in operating specific flux would in turn reduce the use of CIP chemicals and decrease the operational economics of water production. Besides differences in full to pilot scale UF membrane operation, both UF processes achieved similar membrane productivities (recoveries) and demonstrated similar specific flux and TMP fouling trends. Therefore, the control-UF pilot skid provided an acceptable control condition for evaluating the impact of pretreatment on UF operating performance.

MIEX® Pretreatment Performance Assessment

MIEX® was evaluated as a UF pretreatment alternative ahead of coagulation and UF membrane processes. The impact of MIEX® pretreatment on the overall water treatment and production efficiency of the UF membrane process was assessed by determining and comparing the operational, water quality, and UF operation (specific flux, TMP, and membrane autopsy) considerations for the MIEX® pretreatment and control pilots.

MIEX® Operational and Water Quality Performance

Operational Analysis

The operation of the MIEX® system required daily monitoring and trouble shooting of malfunctioning alarms. The alarms were related to paint chips in the resin, irregularities with the software settings, interruption of the regeneration cycle, malfunctioning of conductivity probes, pump failure, and power outages. The operation of the MIEX® system was further complicated by

the need to accommodate full-scale UF membrane replacement activities and severe drought conditions. The combination of MIEX® alarms, maintenance activities, and drought conditions resulted in the intermittent operation of the MIEX®-UF and control-UF pilots. In an effort to offset the negative impacts of intermittent pilot operation, several process adjustments were implemented. The process adjustments included manually removing the paint chips from the resin, decreasing the MIEX® flow from 8 to about 6 gpm on October 27, 2012, and replacing the ACH feed pump to a low-dose digital peristaltic pump on November 22, 2012 (see Table 3-10).

The average MIEX® operational parameters (flow, resin concentration, and contact time) and ACH coagulant dose for each of the major MIEX® testing conditions (initially with an 8 gpm flow set-point, 6 gpm flow set-point, and ACH feed pump replacement, respectively) are shown in Figure 4-23. In the figure, the error bars represent confidence intervals at the 95 percent level.
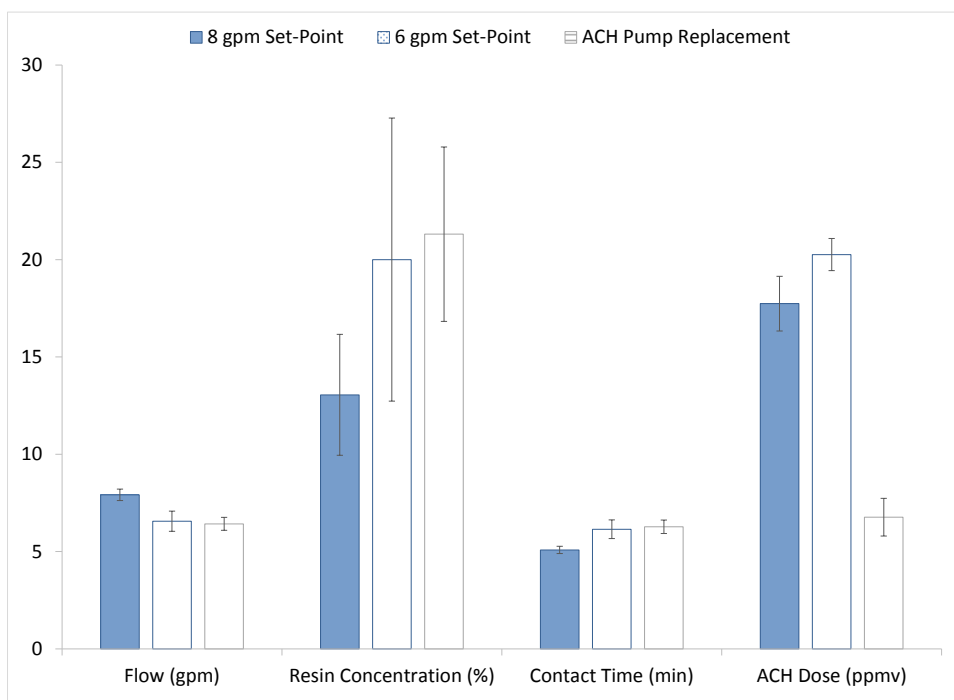
Figure 4–23 MIEX® Operational Performance Summary

The MIEX® resin concentration was the lowest during the initial 8-gpm set point because the paint chips interrupted the regeneration of the resin and caused resin loss from the system. Once the paint chips were removed, an improvement in the resin concentration was observed during the succeeding testing phases.

After MIEX® treatment, the pilot coagulation dosed ACH to destabilize particulate and remaining organic matter prior to removal by settling and UF membrane filtration. At pilot start-up, a positive displacement LMI pump injected the ACH at the lowest allowable rate (0.5 to 1 mL/min). At the lowest ACH feed rate, the coagulant dose ranged from 19 to 45 mg/L. The pilot-scale ACH dose range was greater than full-scale ACH dose range (20 to 33 mg/L). Therefore, it was deducted that the pilot coagulation process was overdosing the ACH coagulant.

The overdosing of the ACH coagulant was accompanied by the observation of pin floc formation. To improve the settling characteristics of the floc aggregates, the LMI pump was changed to a low-dose digital peristaltic pump. After the ACH pump was replaced, the pilot-scale ACH dose ranged between 5 and 17 mg/L. The lower ACH dose was necessary because the MIEX® pretreatment decreased the organic loading and in turn reduced the raw water coagulant demand. On average, the MIEX® pretreatment reduced the ACH dose by 57 percent. The 57 percent reduction in coagulant dose agrees with the findings of other researchers, who observed 50 to 70 percent reductions in coagulant dose (Boyer & Singer, 2006; Jarvis et al., 2008).

Water Quality Analysis

Water quality was measured for raw, MIEX®, MIEX®-ACH, MIEX®-UF, plant-ACH and control-UF water samples. The average water quality results were separated by major testing period (8 gpm flow set-point, 6 gpm flow set-point, and ACH pump replacement) and are summarized in Tables F-1 through F-3 of Appendix F. The pH, temperature, turbidity, color, UV 254, DOC, SUVA, iron, and aluminum time-series graphs are included in Figures F-1 through F-8 of Appendix F. The impact of operation on water quality treatment performance was assessed by determining the particulate and organic removals across the MIEX®, coagulation, and UF membrane processes. Turbidity, color, UV 254, and DOC removals for each MIEX® testing period are displayed in Figures 4-24 through 4-27. The column graphs present averages with 95 percent confidence interval error bars.

During pilot start-up, the MIEX® system increased turbidity by 29 percent and decreased the color, UV 254, and DOC by 28, 35, and 35 percent. After decreasing the MIEX® flow and replacing the ACH feed pump, the MIEX® process increased the turbidity by 17 percent, and decreased the color, UV 254, and DOC by 51, 57, and 46 percent. Although the MIEX® system is designed to have a negligible impact on turbidity, other researchers have noted an increase in turbidity through the carry-over of resin particles (Xu et al., 2013). Therefore, removing the paint chips from the resin reduced resin carry-over, as measured by the smaller increase in turbidity. In addition, retention of the resin in the contactor enhanced color, UV 254, and DOC removal efficiencies. The positive relationship between resin dose and organic removal was also demonstrated by Boyer and Singer (2005), who found that increasing the MIEX® resin dose resulted in a corresponding improvement in the DOC and UV 254 removal efficiencies.
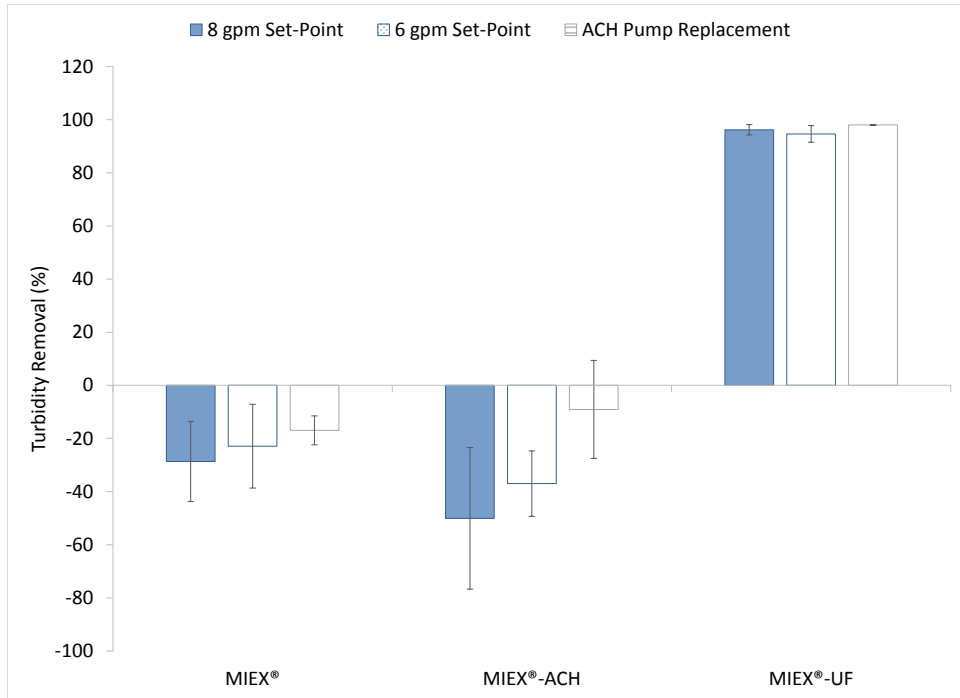
Figure 4–24 MIEX® Phase Turbidity Removal
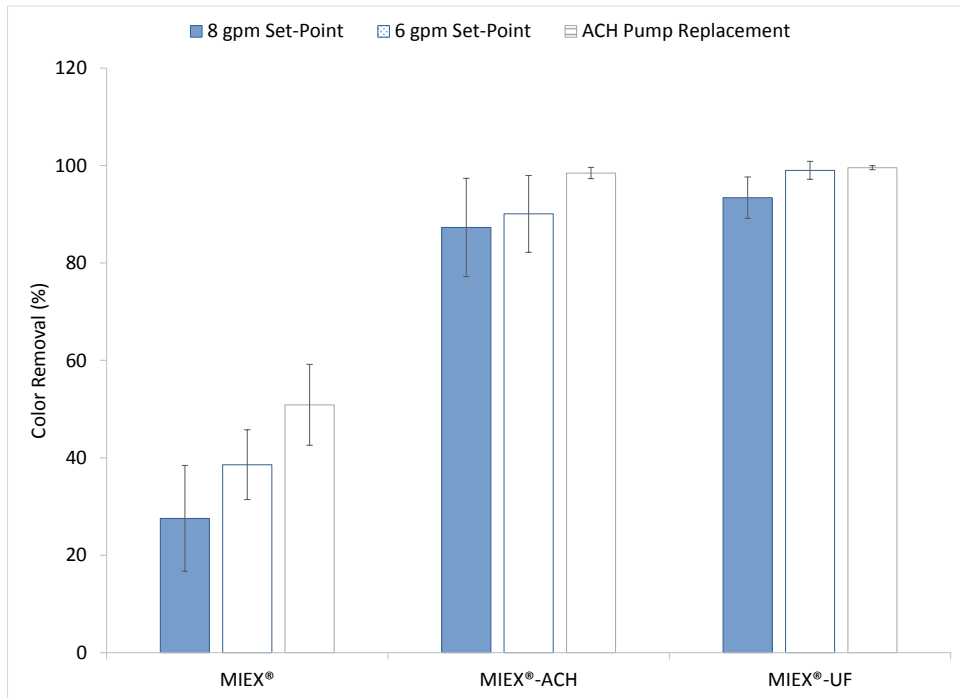
Figure 4–25 MIEX® Phase Color Removal
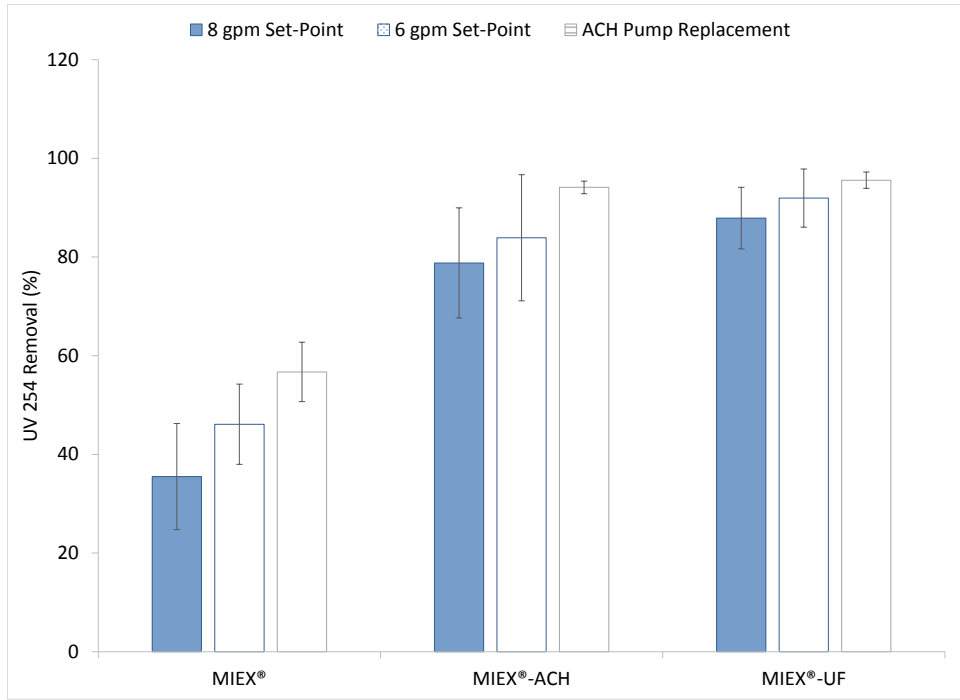
Figure 4–26 MIEX® Phase UV 254 Removal
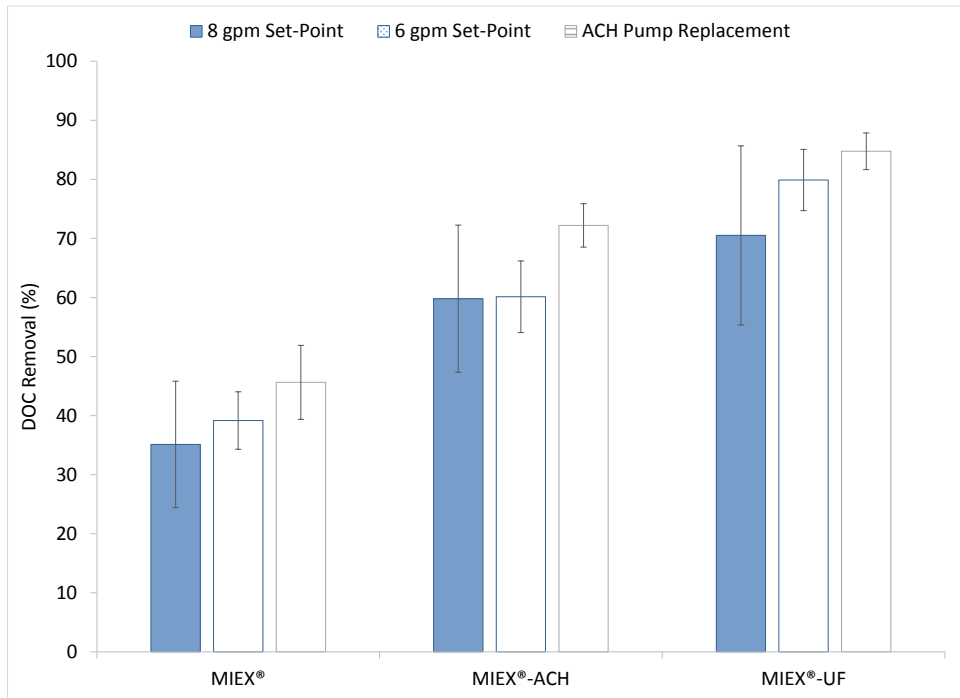
Figure 4–27 MIEX® Phase DOC Removal

The process improvements of the MIEX® system were also reflected in the turbidity and organic removals across the coagulation pilot. At pilot start-up, the pilot coagulation increased the raw water turbidity by 50 percent and decreased the color, UV 254, and DOC by 87, 79, and 60 percent. After the ACH pump replacement, the increase in turbidity was reduced to 9 percent and the color, UV 254, and DOC percent removals were increased to 98, 94, and 72 percent. Although the coagulation pilot did not achieve complete settling of the coagulated flocs, replacing the ACH feed pump allowed for more effective coagulant dosing. The adequate coagulant dosing resulted in improved formation of discrete flocs and higher removal of DOM.

Based on the turbidity and organic removal results, the most effective MIEX® pilot operation was achieved after the ACH feed pump replacement. After the pump replacement, UV 254 and DOC removal efficiencies (57 and 46 percent) for the MIEX® system were comparable to the results obtained by other researchers (Jarvis et al., 2008). In their study, Jarvis and colleagues (2008) found that the MIEX® system removed 49 and 47 percent of the UV 254 and DOC for a raw water source of similar DOC, UV 254, and turbidity levels (7.3 mg/L, 0.404 1/cm and 1.7 ntu). Therefore, additional water quality and DBP formation potential assessments were conducted for the time period after the ACH pump replacement (November 22, 2012 through February 3, 2013).

MIEX® Water Quality Performance after ACH Feed Pump Replacement

For the operating period after the ACH feed pump replacement, the impact of MIEX® pretreatment on the on turbidity, color, UV 254, DOC, and SUVA levels is demonstrated in the column graphs of Figures 4-28 through 4-32. In the column graphs, the average water quality of the MIEX® pretreatment unit operations (raw, MIEX®, MIEX®-ACH, and MIEX®-UF) is compared to the

106

control treatment train (plant-ACH and control-UF). For each water quality average, the error bars represent the confidence intervals at the 95 percent level.

Compared to the full-scale coagulation process, the pilot-scale MIEX®-coagulation produced settled water with a higher average turbidity of 2.7 ntu. The elevated settled water turbidity resulted from the carry-over of coagulated floc aggregates. The presence of un-settled flocs in the MIEX®-coagulated water is confirmed by the higher aluminum and iron concentrations of 1.1 and 0.26 mg/L as compared to the aluminum and iron levels of 0.07 and 0.06 mg/L for the full-scale coagulated and settled water. Due to minimum MIEX® flow and site-space constraints, the coagulation pilot was not able to reproduce the low settling rate (0.035 gpm/ft^2) of the full-scale coagulation process. Consequently, the pilot coagulation operated as a direct coagulation pretreatment to UF membrane filtration.
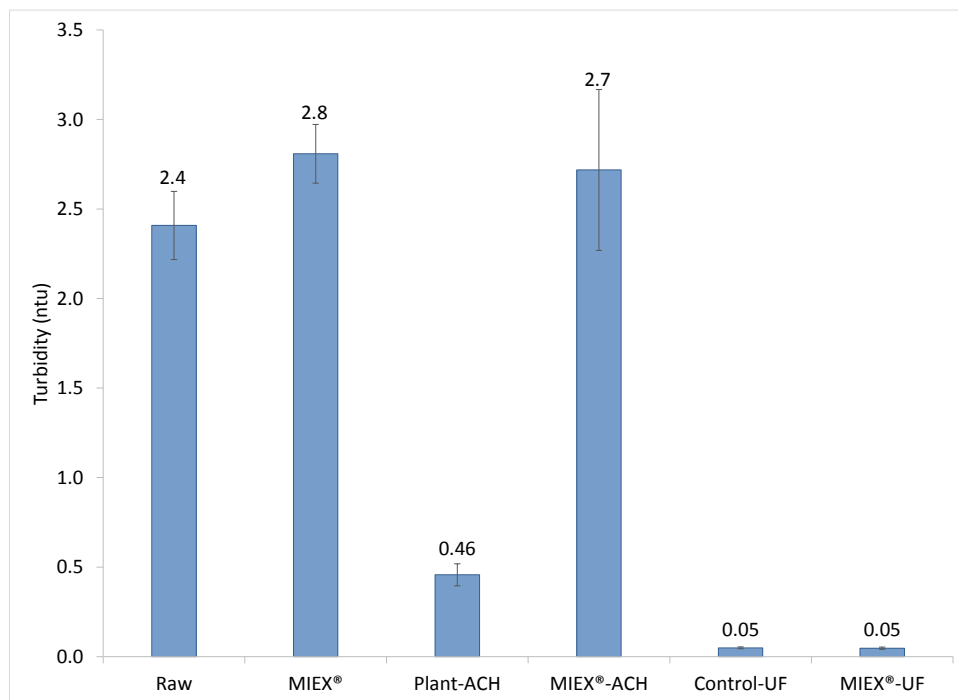
Figure 4–28 MIEX® Phase Average Turbidity
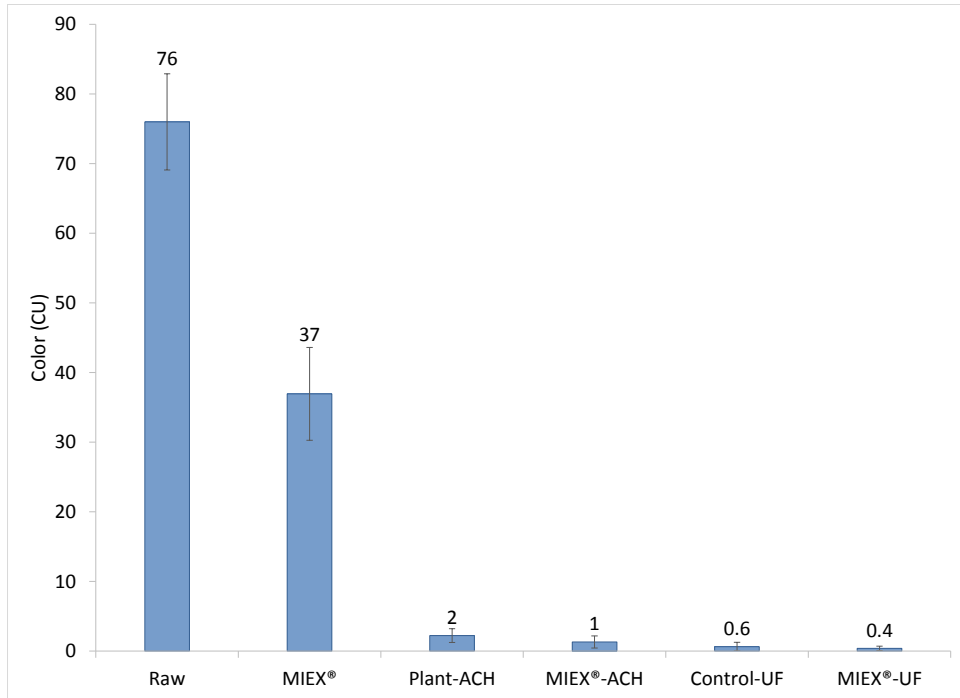
Figure 4–29 MIEX® Phase Average Color
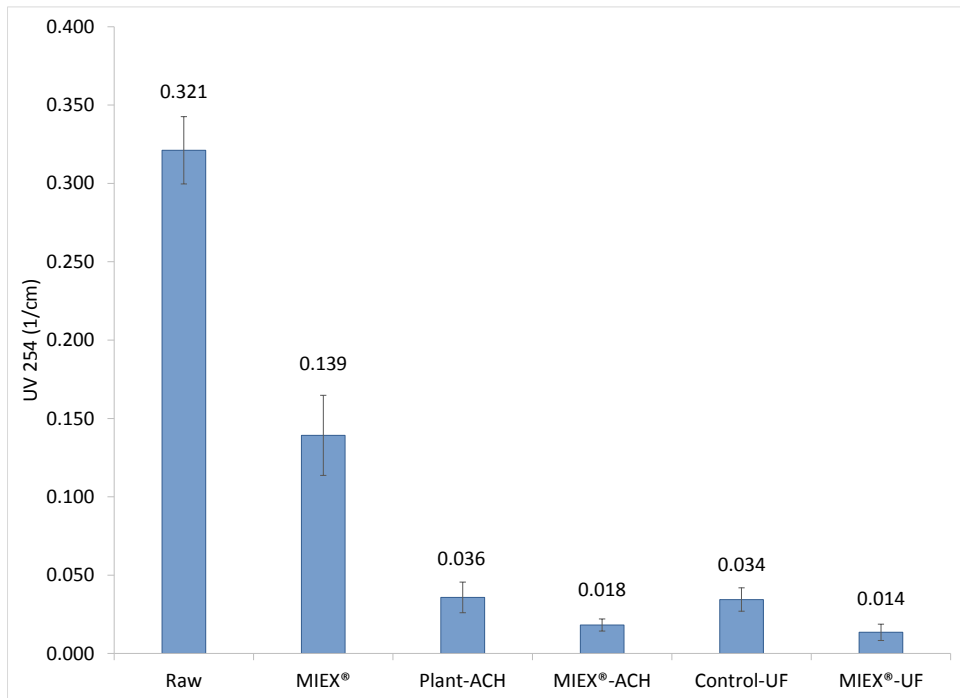
Figure 4–30 MIEX® Phase Average UV 254
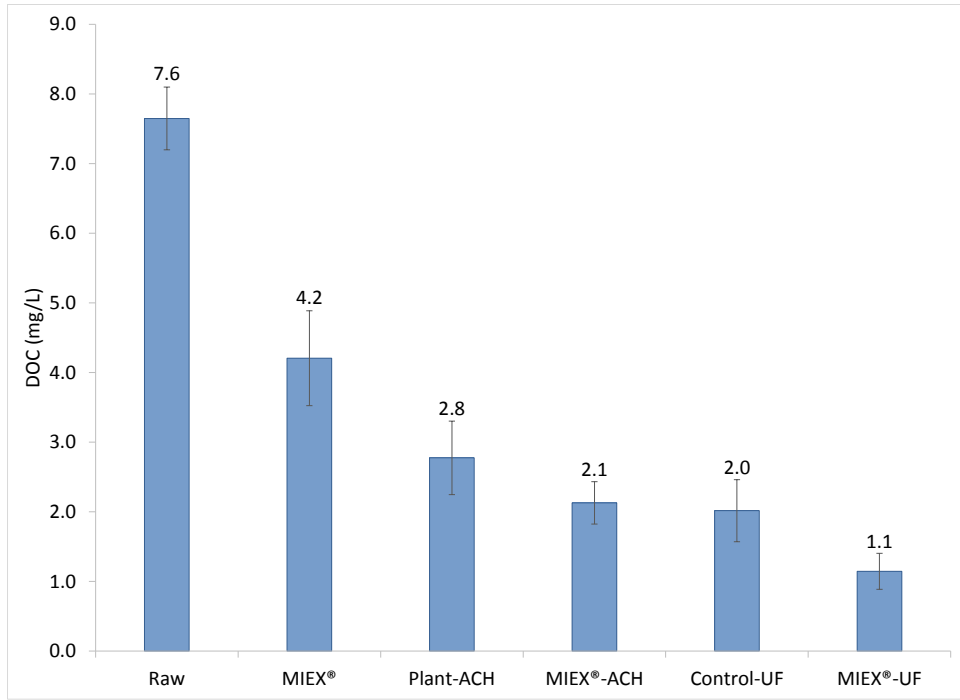
Figure 4–31 MIEX® Phase Average DOC
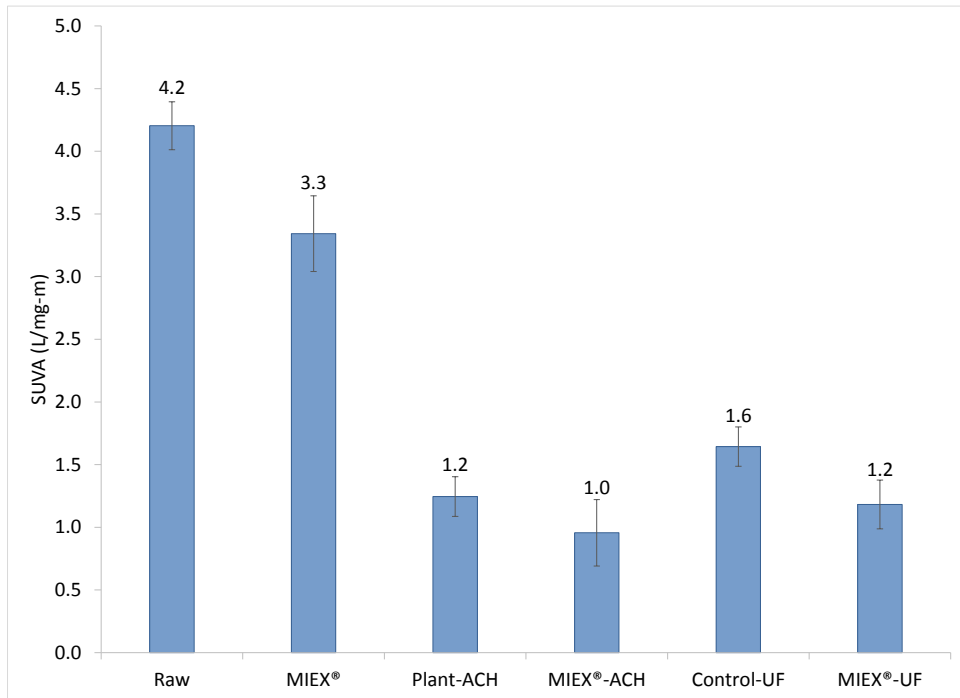
Figure 4–32 MIEX® Phase Average SUVA

Although both the control and MIEX® pretreatment scenarios reduced the color to less than 1 CU, the additional MIEX® pretreatment lowered the raw water color from 76 to 37 CU. The reduction in color prior to coagulation supports the lower ACH coagulant dose requirements for the MIEX®-coagulation operation as compared to the existing coagulation process. The full-scale coagulation reduced the UV 254 and DOC levels by 89 and 64 percent, respectively. These UV 254 and DOC removals were improved to 94 and 72 percent by the MIEX®-coagulation pretreatment.

After the coagulation step, additional UV 254 and DOC reductions were observed across the control-UF and MIEX®-UF membranes. The control-UF membrane removed 6 and 29 percent of the plant settled water UV 254 and DOC levels; and the MIEX®-UF membrane removed 22 and 48 percent of the pilot coagulated UV 254 and DOC concentrations. The organic removal results imply that organic matter was retained directly on the UF-control membrane and contributed to irreversible fouling. However, direct coagulation prior to the MIEX®-UF process provided a protective cake layer on the membrane that helped absorb organic matter and prevent direct deposition of organic foulants on the membrane surface (Dong et al., 2007; Wang et al., 2008). Overall, the UV 254 and DOC levels of the MIEX®-UF filtrate were 59 and 45 percent lower than the control-UF filtrate. The improvement in organic removal was also demonstrated by Jarvis and colleagues (2008), who found that MIEX® with coagulation reduced the DOC to 0.9 mg/L, while coagulation alone reduced the DOC to 1.2 mg/L.

The character of the organic matter throughout the pretreatment-UF and control-UF process trains changed from mainly hydrophobic organic acids to more hydrophilic organic acids and proteins as implied by the SUVA values of Figure 4-32. After MIEX® treatment the average SUVA value decreased from 4.2 L/mg-m to 3.3 L/mg-m. Since the average SUVA value of 3.3 L/mg-m

remained indicative of mostly hydrophobic organics, the corresponding 46 percent reduction in DOC suggest that the MIEX® system removed both hydrophobic and hydrophilic organic fractions. The ability of MIEX® to remove hydrophobic and hydrophilic organics has also been recognized by other researchers (Boyer & Singer, 2005; Zhang et al., 2006; Jarvis et al., 2008; Dixon et al., 2010; Xu et al., 2011; Xu et al., 2013). Through the interpretation of EEM data, Xu and colleagues (2013) found that MIEX® removed fulvic and humic organic acids along with aromatic proteins. By partly removing fulvic, humic, and aromatic protein-like DOM, the MIEX® system provided an advantage over coagulation alone, which partly removed the larger hydrophobic organic acids. The effective removal of organic acids via coagulation is emphasized by the decrease in SUVA to 1.2 and 1.0 L/mg-m for the coagulated plant-ACH and MIEX®-ACH samples. The low SUVA values confirm that mainly the hydrophilic organic fractions remained after coagulation.

Following coagulation, UF membrane filtration of the coagulated raw and MIEX® pretreated waters increased the SUVA values to 1.6 and 1.2 L/mg-m. The higher SUVA values indicate that the control-UF and to a lesser extent the pretreatment-UF processes removed more of the non-UV absorbing organic fraction. The non-UV absorbing organics are typically categorized as hydrophilic protein-like organic compounds and have been shown to contribute to membrane flux decline (Huang et al., 2007; Lozier et al., 2008). By achieving a greater reduction in hydrophilic and hydrophobic DOM, the MIEX®-coagulation pretreatment enhanced the UF feed water quality with respect to membrane foulants.

DBP Formation Potential

The impact of MIEX® pretreatment on finished water quality was evaluated by determining the TTHM and HAA5 formation potentials for the control-UF and MIEX®-UF filtrates. Two sets of DBP formation potential experiments were conducted on December 7, 2012 and January 28, 2013. The water quality and operational parameters for the DBP formation potential experiments are summarized in Table 4-3. The TTHM and HAA5 speciation and corresponding chlorine residual results are included Tables F-4 through F-7 of Appendix F.

The comparisons between the control-UF and MIEX®-UF four-day DBP formation potential are presented in the column graphs of Figures 4-33 and 4-34. The MIEX® pretreatment lowered the four-day TTHM and HAA5 levels by 56 and 34 percent in December 2012 and by 51 and 33 percent in January 2013. The reduction in DBPs corresponded to UV 254 and DOC reductions of 50 and 35 percent in December 2012 and of 76 and 55 percent in January 2013 (see Figures F-9 and F-12 of Appendix F). In both experiments, the MIEX® pretreatment also decreased the SUVA values by about 0.4 to 0.9 L/mg-m. Based on the organic and four-day DBP comparisons, MIEX® pretreatment effectively removed DBP precursors and lowered TTHM and HAA5 concentrations below the 80 and 60 µg/L MCLs with free chlorine disinfection.

Table 4–3 MIEX® Phase DBP Formation Potential Experimental Parameters

Experimental Parameters	12/7/2012		1/28/2013	
	Control-UF	MIEX®-UF	Control-UF	MIEX®-UF
pH	8.81	8.76	8.81	8.77
UV 254	0.046	0.023	0.034	0.008
DOC (mg/L)	2.37	1.54	1.76	0.787
SUVA (L/mg-m)	1.9	1.5	1.9	1.0
Chlorine Dose (mg/L Cl_2)	4	4	4	4
Incubation Temperature (°C)	15-22	15-22	12-21	12-21
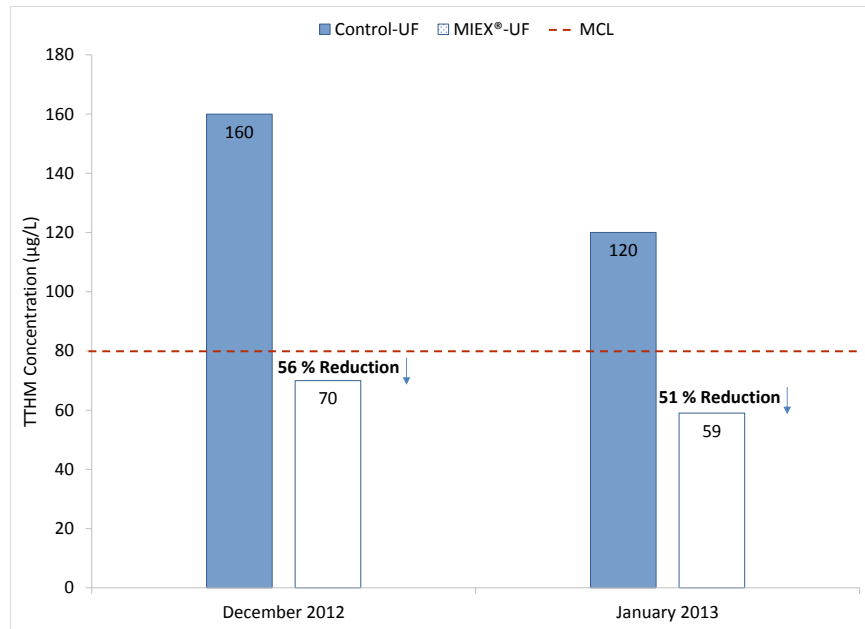
Figure 4–33 MIEX® Phase Four-Day TTHM Formation Potential
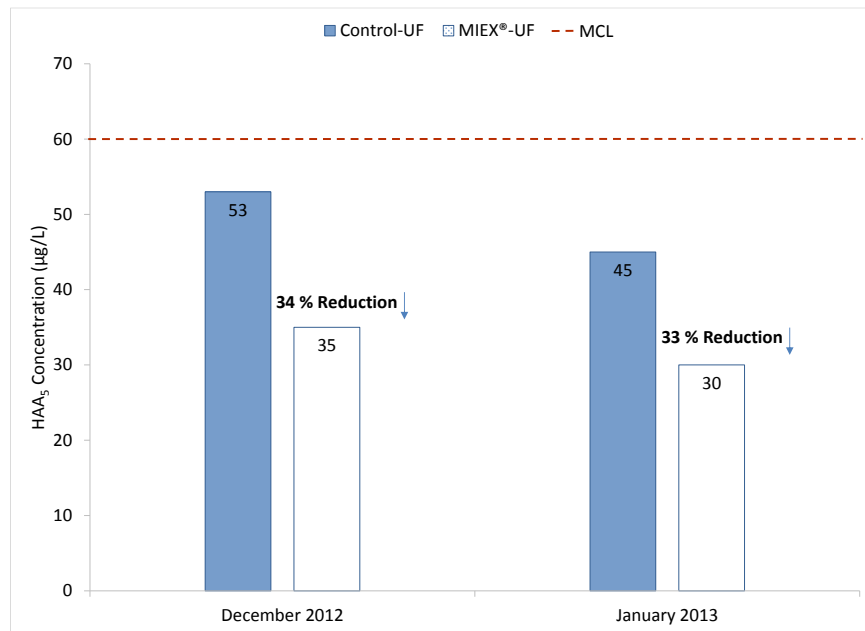
Figure 4–34 MIEX® Phase Four-Day HAA$_5$ Formation Potential

The corresponding TTHM formation potential and chlorine decay curves for the December 2012 and January 2013 experiments are included in Figures F-10, F-11, F-13, and F-14 of Appendix F. In the TTHM formation potential graphs, the increase in TTHM concentration with contact time followed a typical logarithmic shape (Reckhow & Singer, 2011). Initially, chlorine reacted rapidly with DOM to form DBPs, then the reaction kinetics slowed after about 24 hours of contact time. Similar reaction rates were observed in the chlorine decay curves, in which a greater consumption in demand occurred during the first 6 to 24 hours. After 24 hours, the chlorine consumption was more gradual. As shown in the TTHM formation and chlorine decay curves, the MIEX® pretreatment reduced the TTHM formation potential and chlorine demand of the finished water by an average of 75 µg/L and 0.3 mg/L. The lower reduction in the chlorine demand by the MIEX® pretreatment during the January 2013 experiment likely resulted from under-dosing the sodium hypochlorite. Nevertheless, the TTHM formation and chlorine decay results confirm the effectiveness of the MIEX® pretreatment in controlling disinfection byproducts.

MIEX® Pretreatment Impacts on UF Membrane Performance

The effect of MIEX® pretreatment on UF membrane operating performance was assessed by comparing the feed water quality, temperature corrected TMP and specific flux, fouling trends, membrane percent recovery, and membrane autopsy results for the MIEX®-UF and control-UF. The temperature corrected TMP and specific flux time-series graphs for the control-UF and MIEX®-UF are illustrated in Figures F-15 through F-18 of Appendix F. In the graphs, feed temperature, flow, TMP, and specific flux are plotted as functions of filtration run time. The process adjustments are designated by varying dashed lines, and CIPs are designated by solid lines.

Prior to the ACH feed pump replacement, the MIEX®-UF pilot experienced sharp specific flux decline, which required frequent CIPs to maintain a constant water production. The intermittent operation of the MIEX® pilot increased the settled water turbidity as compared to the control. Consequently, the pronounced fouling of the MIEX®-UF membrane as compared to the control-UF likely resulted from the carry-over of pin flocs. After the ACH feed pump replacement, more effective coagulant dosing produced larger discrete floc aggregates and a corresponding decrease in the MIEX®-UF fouling rate was observed. While additional shut-downs were encountered starting December 16, 2012, the MIEX®, coagulation, and UF membrane filtration pilot plants were operated continuously from November 22, 2012 to December 9, 2012. Therefore, the MIEX®-UF operation results from November 22nd to December 9th 2012 were analyzed to assess the pretreatment impacts on UF membrane performance.

The average operational parameters for the MIEX®-UF and control-UF membrane pilots are outlined in Table 4-4. The UF membrane performance was analyzed at the beginning of the filter run, following a hypochlorite and citric acid CIP. Because of the difference in CIP frequencies between the MIEX®-UF and control-UF pilots, the clean membrane filter run for the control-UF commenced earlier on October 20, 2012 and the MIEX®-UF filter run started on November 22, 2012. For the selected filter run times, the UF membranes were backwashed every 10 minutes to effectively remove the flocculant cake layer deposited from MIEX® with direct coagulation pretreatment. The increase in backwashing frequency reduced the membrane recovery from 89 (20 minute backwash frequency) to 82 percent, which falls below the typical target range 85 to 95 percent (Alspach et al., 2005).

Table 4–4 MIEX®-UF versus Control-UF Operational Parameter Summary

Operational Parameter	Control-UF	MIEX®-UF
Start of Filter Run	Oct 20, 2012 (Clean Membrane)	Nov 22, 2012 (Clean Membrane)
Filtration Run Time (days)	12	13
Membrane Recovery		
Backwash Frequency (min)	10	10
Backwash Volume (gal/module)	10.6	10.6
Number of Hypochlorite CIPs	1	2
Number of Citric Acid CIPs	1	2
CIP Volume (gal/module)	40	40
Percent Recovery	82	82
Average Membrane Process Data		
Flow (gpm)	4.2	4.2
Flux Rate (gal/ft^2-day)	20.2	20.3
TCTMP @ 20 ºC (psi)	14	12
Specific Flux @ 20 ºC (gal/ft^2-d-psi)	1.5	1.7

For full-scale application of MIEX® pretreatment ahead of coagulation and UF membrane processes, adequate settling of the coagulated flocs prior to UF membrane filtration could possibly achieve more effective membrane recovery. Nevertheless, adjusting the backwash frequency of both UF pilots allowed for the side by side comparison of the MIEX®-UF and control-UF membrane operational results. For the operational conditions tested, the MIEX®-UF process operated at a higher average specific flux of 1.7 gal/ft^2-d-psi and lower average TMP of 12 psi as compared to the control-UF process, which operated at 1.5 gal/ft^2-d-psi and 14 psi. The statistical spread of the TMP and specific flux results is shown in the box-and-whisker plots of Figures 4-35 and 4-36. Since the MIEX®-UF process had a smaller inner quartile range as compared to the control-UF, the MIEX®-UF operation was more stable and experienced fewer swings from minimum to maximum values.
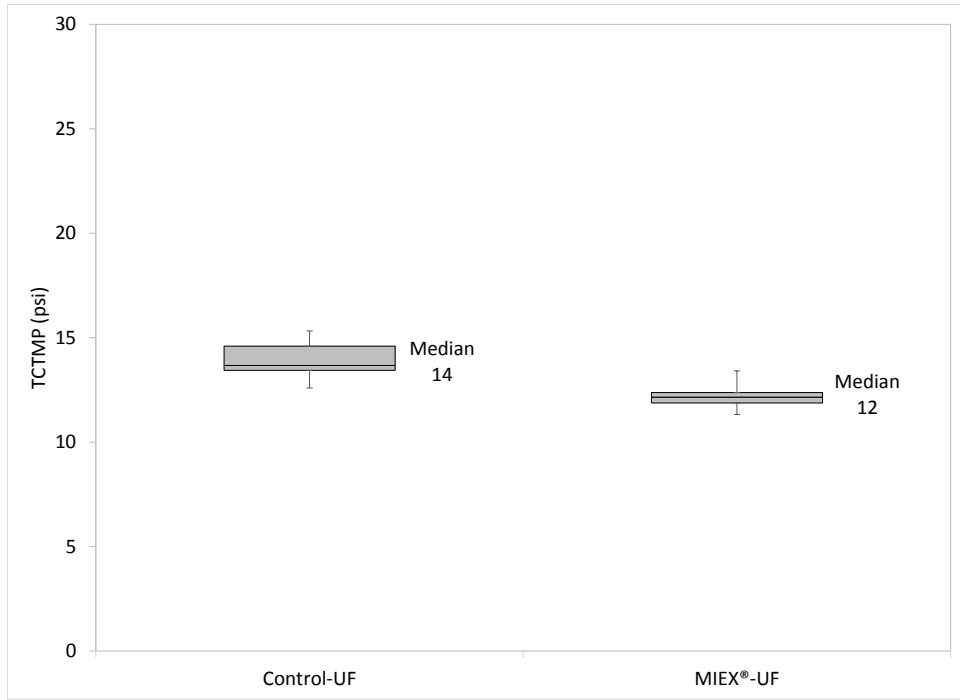
Figure 4–35 MIEX® Phase TCTMP Box-and-Whisker Plot
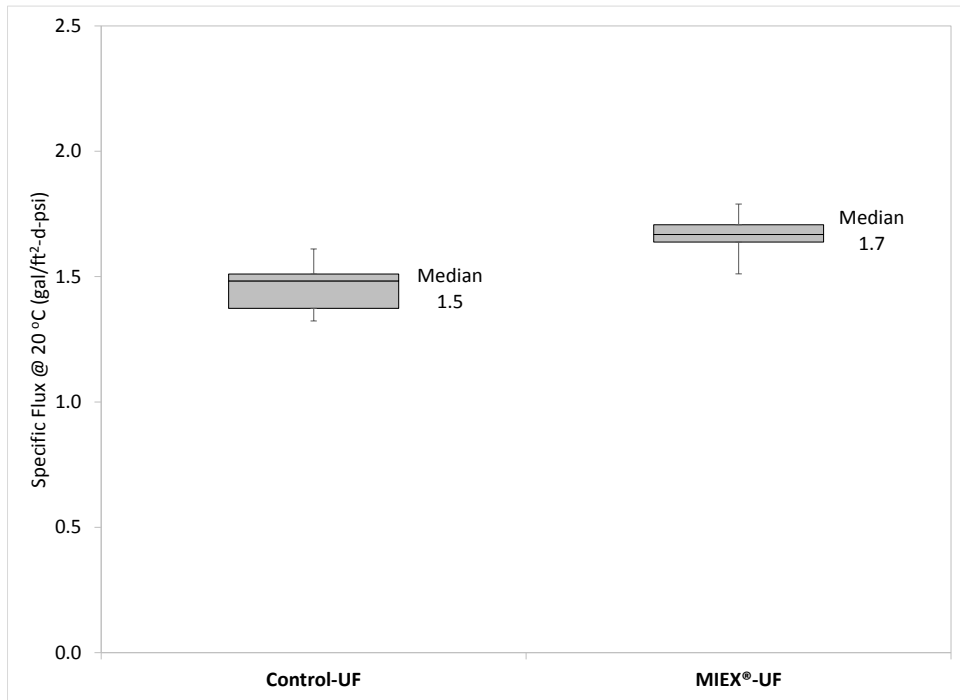
Figure 4–36 MIEX® Phase Specific Flux Box-and-Whisker Plot

The improvement in MIEX®-UF membrane performance is further emphasized by the TMP and specific flux time-series trends for the MIEX®-UF and control UF processes (shown in Figures 4-37 and 4-38). As compared to the control-UF, the additional MIEX® pretreatment improved the membrane productivity, as indicated by the higher specific flux and lower TMP values. The independent t-tests and ANOVAs confirm that changes in specific flux and TMP between the MIEX®-UF and control-UF treatments were statistically significant at 95 percent confidence. Therefore, the additional MIEX® pretreatment enhanced the membrane TMP and specific flux by 12 and 14 percent, respectively. The improvement in the downstream UF operating performance is supported by the work conducted by other researchers. Xu, Liu and other researchers have shown that MIEX® pretreatment reduced the membrane's operating TMP (Zhang et la., 2006; Dixon et al., 2010; Liu et al., 2011 Xu et al., 2011).
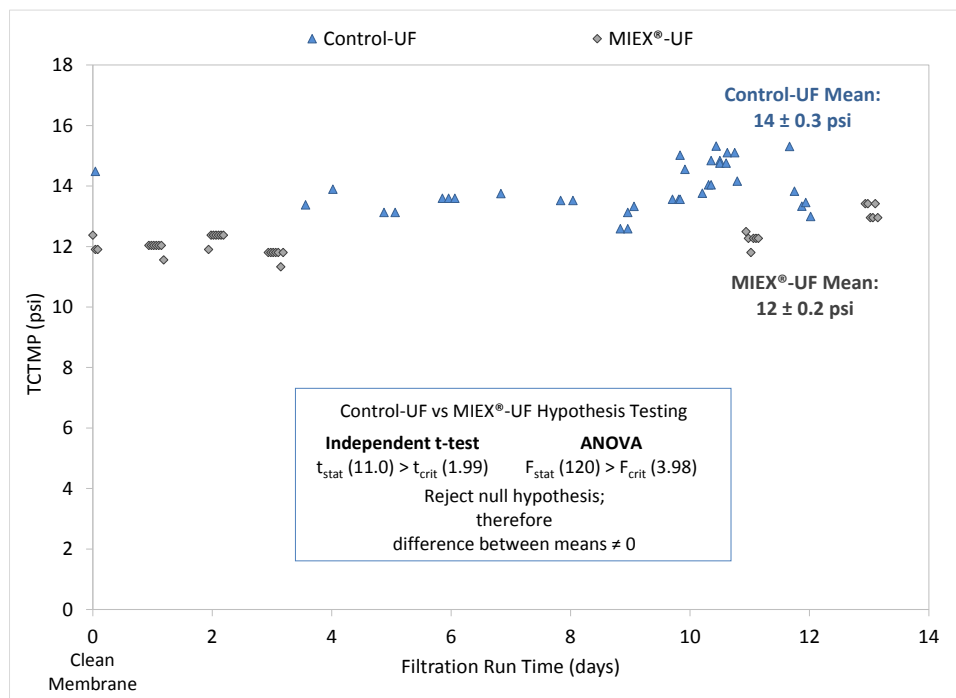
Figure 4–37 MIEX® Phase TMP Time-Series Trend
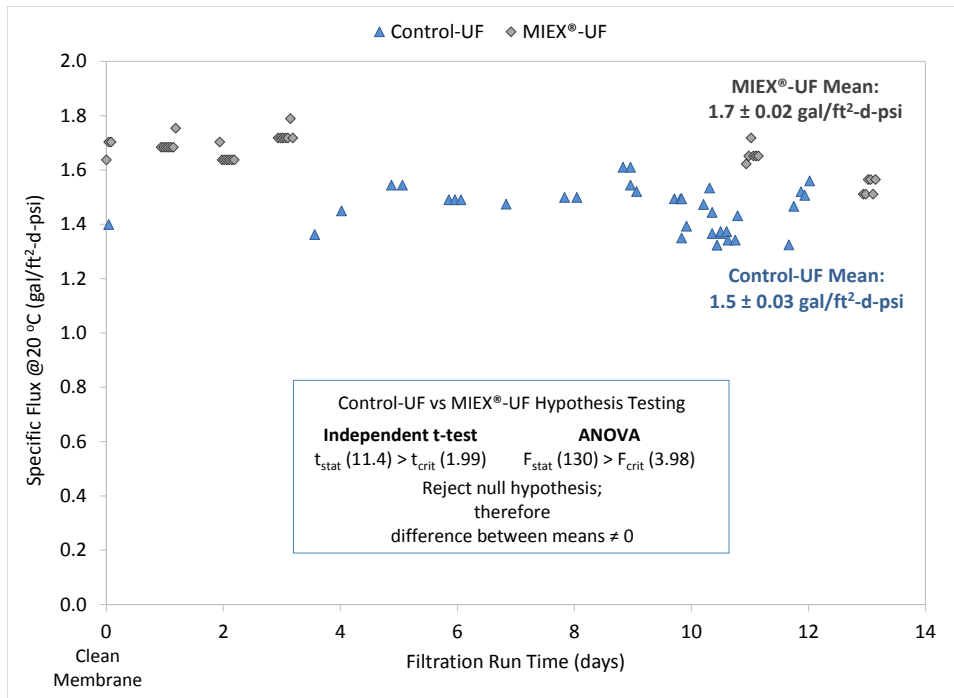
Figure 4–38 MIEX® Phase Specific Flux Time-Series Trend

Evaluation of the TMP and specific flux trends reveals that both the MIEX®-UF and control-UF membrane pilots exhibited a gradual TMP rise and specific flux decline. To identify possible explanations for the gradual fouling of the membranes, the impact of feed water quality on UF performance was established by plotting the difference in specific flux (control-UF minus MIEX®-UF) against the difference in feed water turbidity and DOC (plant-ACH minus MIEX®-ACH). The UF performance versus water quality scatterplot is presented in Figure 4-39. According to the scatterplot analysis, a lower increase in feed water turbidity and greater reduction in feed water DOC were proportional to the improvement in membrane specific flux. Consequently, the gradual fouling of the membranes was likely due to the accumulation of metal colloids and DOM that were not completely removed by the conventional or MIEX®-coagulation pretreatments (Dong et al., 2007; Wang et al., 2008).

119
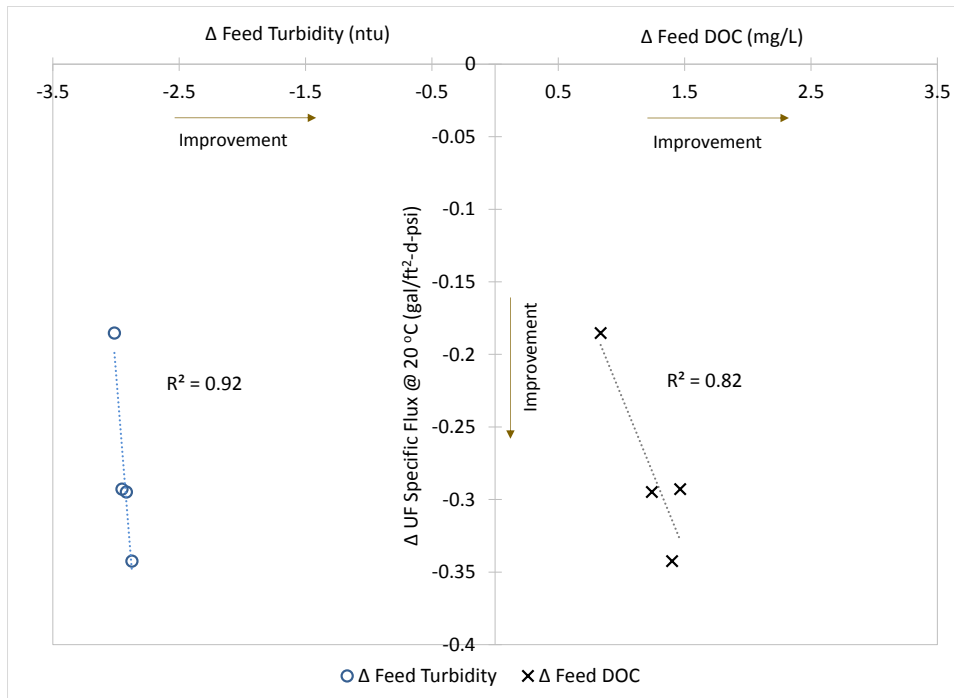
Figure 4–39 Scatterplot of Specific Flux versus Feed Water Turbidity and DOC

To confirm the impact of MIEX® pretreatment on the UF membrane performance, the comparison of turbidity, DOC, and specific flux differences before and after replacement of the ACH feed pump is shown in Figure 4-40. Prior to the ACH feed pump replacement, the MIEX®-coagulated feed water had higher turbidity and DOC levels as compared to the plant-coagulated feed water. The higher turbidity and DOC concentrations were accompanied by a decline in membrane specific flux. The loss of membrane productivity was most likely caused by the deposition and build-up of pin floc with high cake resistance and affinity to the membrane surface. The detrimental impact of overdosing coagulants prior to low pressure membrane filtration was documented by Wang and colleagues (2008). The researchers concluded that maintaining a lower optimum coagulant dose promoted the concomitant removal of organic acids and reduction in cake resistance (Wang et al., 2008).
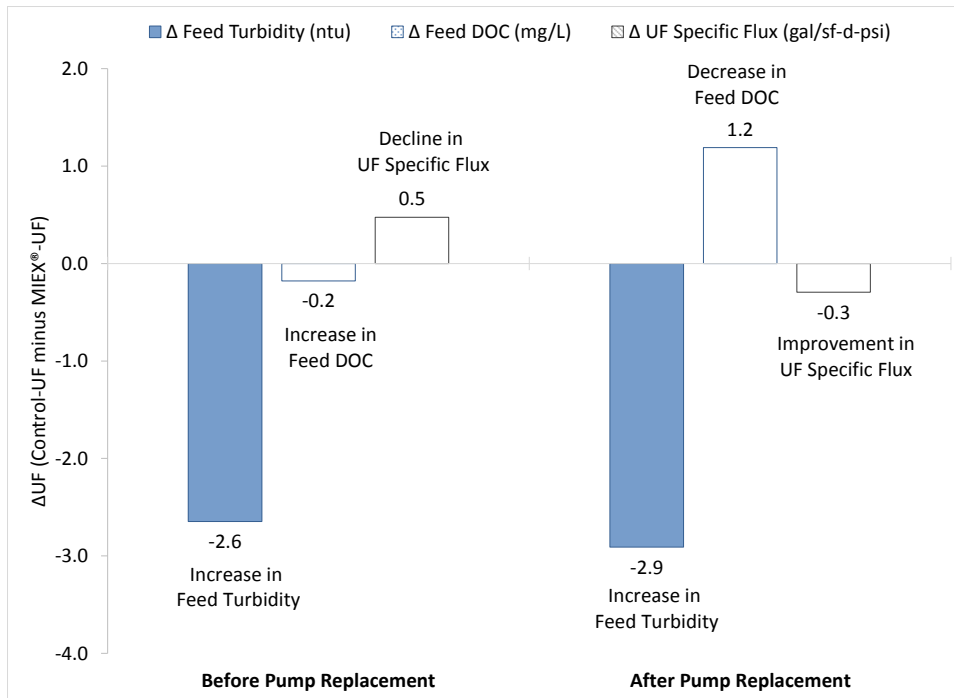
Figure 4–40 Feed Water Quality Before and After ACH Pump Replacement

After replacement of the ACH feed pump, the MIEX[®] pretreatment turbidity levels remained elevated, but the DOC concentration was lower and the corresponding membrane specific flux was improved. Since the increase in feed turbidity remained about the same, more effective dosing of the ACH coagulant possibly altered the character of the floc aggregates from pin floc to more discrete floc with higher water permeability. The change in floc formation is supported by the work conducted by Jarvis et al. (2008). In their study, the researchers observed that MIEX[®] pretreatment ahead of coagulation increased the size and strength of floc aggregates (Jarvis et al., 2008). The increase in floc resistance to shear stress possibly allowed for the formation of a more permeable cake layer that according to Dong and colleagues (2007) protects the membrane from smaller flocs and DOM and is more easily removed during backwashing.

In addition to improved floc characteristics, the lower DOC concentration in the feed water reduced the organic loading onto the MIEX®-UF membrane. In similar MIEX® pretreatment investigations, the researchers related the improvement in membrane performance to the removal of hydrophobic and hydrophilic organic fractions by the MIEX® treatment (Xu et al., 2011; Zhang et al., 2006; Liu et al., 2011; Dixon et al., 2010). Therefore, based on the improvement in coagulant dosing and corresponding DOC removal, the observed 14 percent increase in membrane specific flux derived from a combination of the reduction in DOM (34 percent of DOC) and formation of more discrete, permeable flocs that were more easily removed during backwashing.

MIEX® Phase Membrane Autopsy Analysis

At the conclusion of the MIEX® pilot testing, Evoqua performed membrane autopsies on the control-UF and MIEX®-UF membranes. Membrane CIPs were not performed prior to autopsy analysis. The autopsy analysis included physical examination of the membrane modules, scanning electron microscopy (SEM), and energy dispersive spectroscopy (EDS). Evoqua performed the SEM and EDS analysis on 3 membrane fibers from the top-outside, middle-outside, middle-inside, and bottom-outside of both membrane modules. In addition, Evoqua collected SEM and EDS data from four foulant layer samples extracted from the MIEX®-UF membrane.

The physical inspection results and comments are summarized in Table 4-5.The membrane weight increased for the control-UF and MIEX®-UF membranes by 2 and 3.5 pounds. The weight increase for the control-UF was attributed to solids accumulation; and for the MIEX®-UF was attributed to the accumulation of solids and MIEX® resin carried over into the membrane module.

Table 4–5 Physical Inspection of MIEX® Phase Membrane Modules by Evoqua

Consideration	MIEX®-UF	Control-UF
Module Weight (lbs)	18	16.5
Virgin Module Weight	14.5	14.5
Inspector Comments	• MIEX® resin suspected to have carried through into the membrane module • No CIP performed prior to pulling module from membrane housing • CIP likely would not have recovered to normal module weight	• Slight accumulation of solids (based on weight) • No CIP performed prior to pulling module from membrane housing • CIP likely would have recovered the module weight

Source: Information provided by Evoqua Water Technologies

Although the control-UF module was expected to return to the normal weight after the CIP, the presence of MIEX® particles would prevent the MIEX®-UF membrane from returning to the normal weight after cleaning. The increased MIEX®-UF weight was also likely caused by the higher turbidity loading that resulted from the direct coagulation operation.

The summary of the SEM and EDS results for one of the membrane fibers at each membrane location (top-outside, middle-outside, middle-inside, and bottom-outside) is presented in the Figures within Tables 4-6 through 4-9). The SEM and EDS results for the second and third membrane fibers and MIEX® foulant samples are included in Tables F-8 through F-16 of Appendix F. In the summary tables, the SEM images at 100 and 1000 times magnification are compared between the MIEX®-UF and control-UF membrane fibers located in the top-outside, middle-outside, middle-inside, and bottom-outside of the membrane fiber. The SEM images reveal that the MIEX®-UF had a larger visible amount of foulant accumulated on the fiber surfaces than the control-UF. The thicker foulant layer on the MIEX®-UF fibers resulted from the direct carry-over

of floc aggregates. Although direct coagulation may promote the development of a cake that acts as a protective layer against pin floc and other DOM foulants, the lack of continuous monitoring and control over the optimum coagulant dose may hinder UF membrane performance (Dong et al., 2007; Wang et al., 2008).

Because of the pilot shut-downs experienced after December 16, 2012, unstable operation and insufficient control over coagulant dose contributed to the accumulation of an irreversible cake layer. Furthermore, Evoqua found evidence of the carry-over of MIEX® resin fines that may have also contributed to membrane fouling. The fouling of bench-scale UF membrane downstream of a MIEX® process was also observed by Huang and colleagues (2012). The researchers identified the deposition of MIEX® resin as the major cause of the downstream membrane fouling (Huang et al., 2012). Comparing the different membrane fiber locations within the module reveals that the top and bottom fibers were more heavily fouled than the middle fibers in both the MIEX® pretreatment and control cases. The difference in foulant density throughout the membrane module is due to the module configuration, in which the feed water entered near the top of the pilot unit and filtrate exited near the bottom of the housing vessels.

In addition to the SEM images, EDS analyses were performed on the fouled fibers to uncover the elemental breakdown of the foulant material. The EDS results show the elemental peaks at varying x-ray emission spectrums. The height of the elemental peaks provides qualitative information on the relative quantities of each detected element. Comparing the heavily and lightly fouled fibers allows for the distinction between the elemental peaks associated with the membrane material and the peaks associated with the foulant material.

In the EDS results for the lightly fouled fibers, the dominant carbon and fluorine peaks are indicative of the PVDF membrane material. On the other hand, the EDS results for the heavily fouled fibers reveal the major presence of carbon, oxygen, aluminum, and iron. Since fluorine was not detected the elemental analysis of the heavily fouled fibers, the source of the carbon detected on the heavily fouled fibers is most likely the foulant material. Therefore, the EDS results confirm that the foulant material for both the MIEX®-UF and control-UF membranes consisted mainly of organic, aluminum, and iron compounds in the form of complexes or enmeshed in metal precipitates – $Al(OH)_3$ and $Fe(OH)_3$ (MWH, 2005). The accumulation of the foulant material on the membranes resulted from the presence of un-settled aluminum hydrolysis products and medium to large DOM in the feed water. Although MIEX® with direct coagulation pretreatment was shown to improve downstream membrane performance, the autopsy results show that including the clarification step would likely further enhance the UF membrane performance by minimizing particulate and organic loading to the membrane.

Table 4–6 Top-Outside Fiber 1 SEM and EDS Results

MIEX®-UF	Control-UF
SEM at 100 Times Magnification	
SEM at 1000 Times Magnification	
EDS	
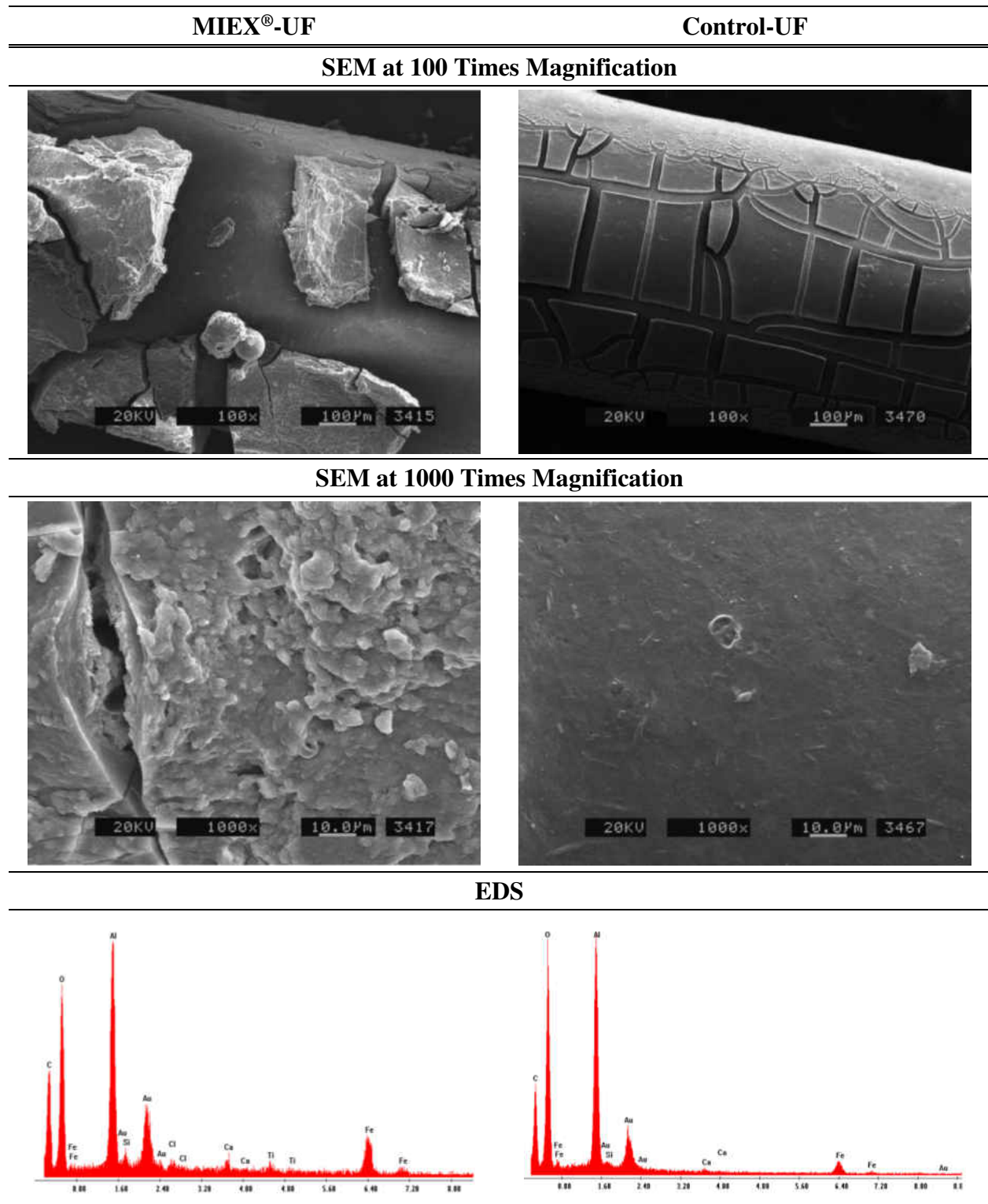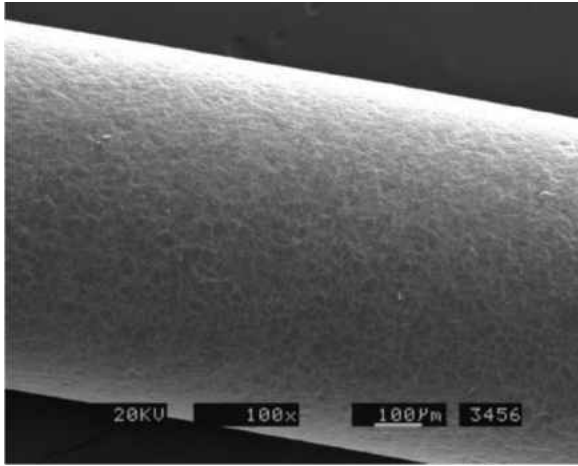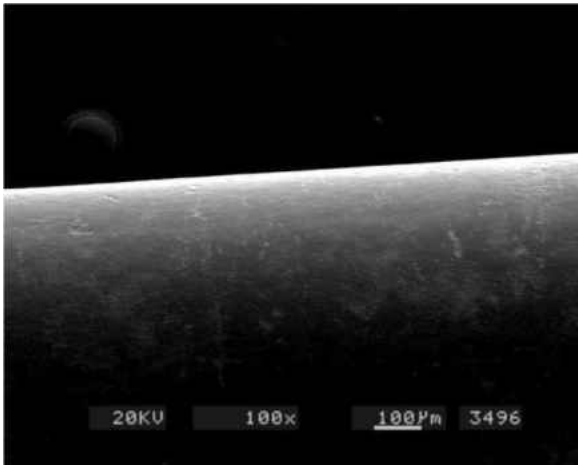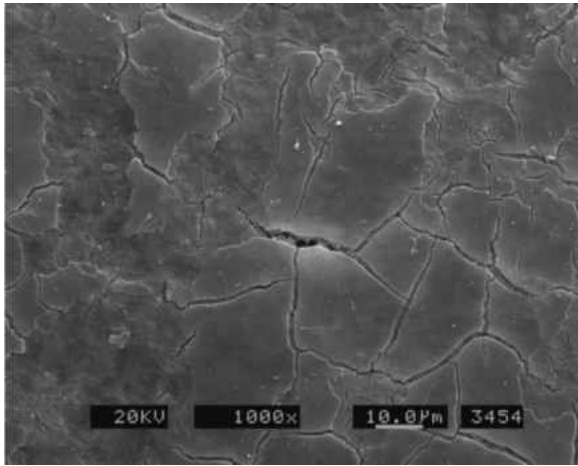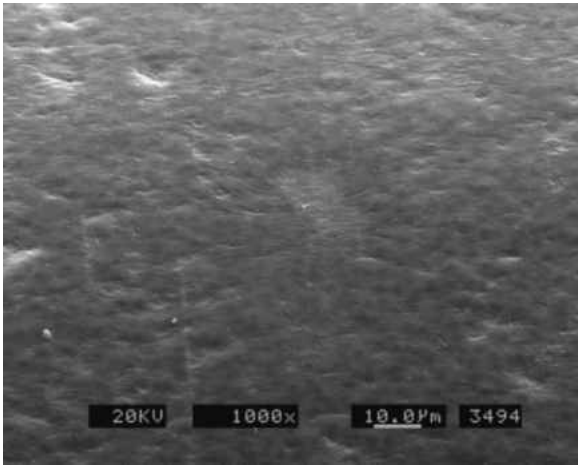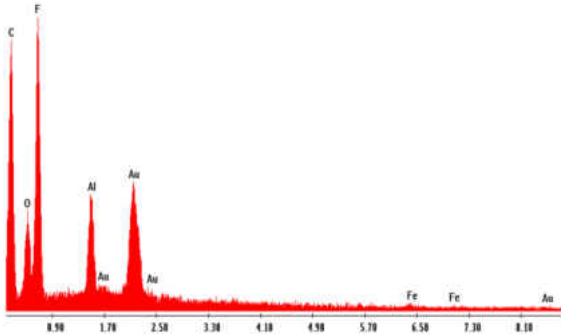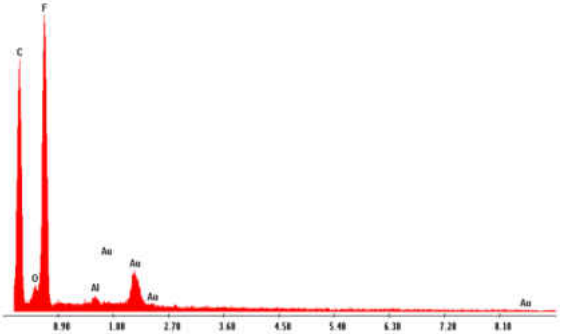
Source: Courtesy of Evoqua Water Technologies

Table 4–7 Middle-Outside Fiber 1 SEM and EDS Results

MIEX®-UF	Control-UF
SEM at 100 Times Magnification	

SEM at 1000 Times Magnification	

EDS	

Source: Courtesy of Evoqua Water Technologies

127
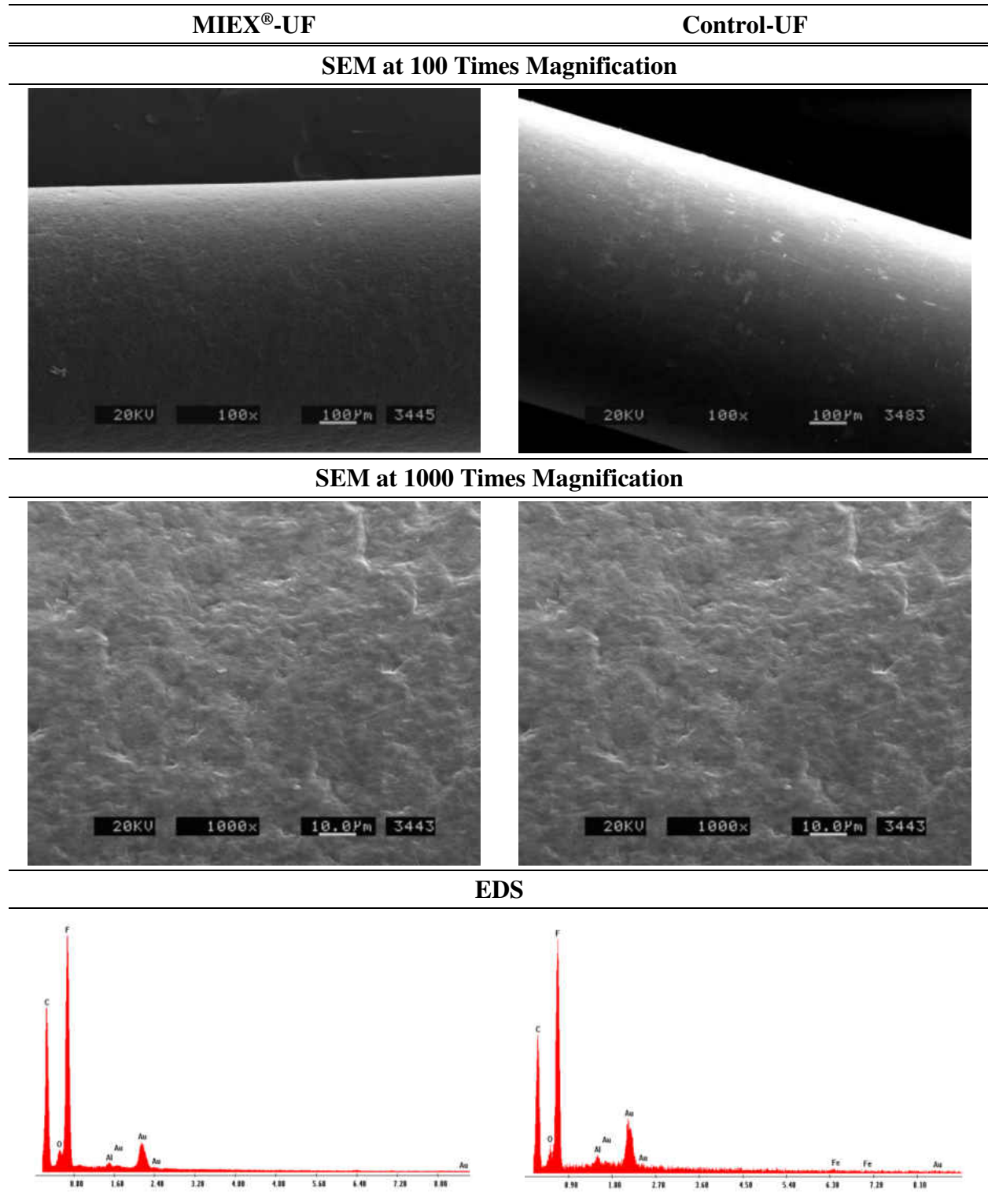
Table 4–8 Middle-Inside Fiber 1 SEM and EDS Results

MIEX®-UF	Control-UF
SEM at 100 Times Magnification	
SEM at 1000 Times Magnification	
EDS	

Source: Courtesy of Evoqua Water Technologies

128

Table 4–9 Bottom-Outside Fiber 1 SEM and EDS Results

MIEX®-UF	Control-UF
SEM at 100 Times Magnification	

SEM at 1000 Times Magnification	

EDS	
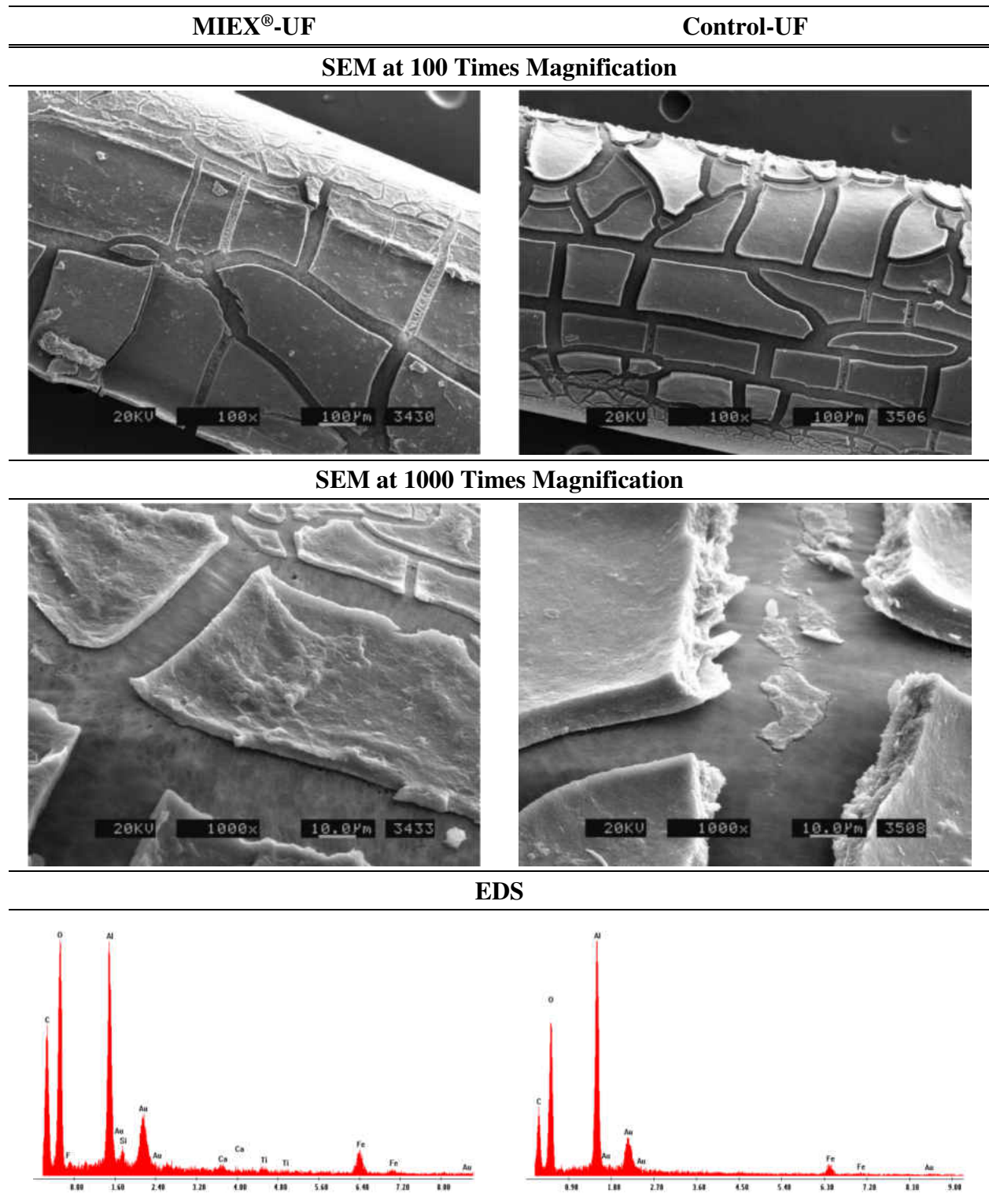
Source: Courtesy of Evoqua Water Technologies

GAC and BAC Pretreatment Performance Evaluation

The performance of GAC adsorption and BAC filtration as pretreatments to UF membrane processes was assessed according to pilot-scale determinations of operational parameters, water quality, and UF membrane TMP, specific flux, recovery, and autopsy results. To examine the effects of different GAC treatment mechanisms, the results were organized with respect to the sequential phases of GAC filtration: adsorption, transition, biological with orthophosphate adjustment, and biological with orthophosphate and pH adjustment.

GAC and BAC Operational and Water Quality Performance

Operation Analysis

As compared to MIEX® pretreatment, GAC filtration required fewer maintenance activities. Maintenance activities consisted of performing fluidized bed backwashes once the pressure drop across the filter exceeded either 5 psi during the initial adsorption mode or 10 psi during the subsequent biological mode. Major operational parameters included flow rate, EBCT, HLR, and filter run time. The minimum, average, and maximum operational parameters for each of the GAC testing phases (GAC adsorption, BAC transition, BAC with orthophosphate adjustment, and BAC with orthophosphate and pH adjustment) are listed in Table 4-10. During the adsorption period, the average flow was 9.3 gpm which corresponded to an EBCT of 14 minutes and HLR of 0.74 gpm/ft^2. In addition, the GAC filter experienced filter runs ranging from 216 to 744 hours of filtration. The longer filter runs indicate that the pressure drop across the filter increased gradually due to the lack of particulate and biological accumulation on the filter media.

Table 4–10 GAC and BAC Operational Parameter Summary

Testing Period	Flow (gpm)			EBCT (min)			HLR (gpm/ft^2)			Filter Run Time (hours)		
	Min	Avg	Max	Min	Avg	Max	Min	Avg	Max	Min	Avg	Max
GAC Adsorption	7.1	9.3	11.5	11	14	18	0.56	0.74	0.92	216	480	744
BAC Transition	7.7	10.5	12.9	10	12	16	0.61	0.84	1.0	72	168	288
BAC (Ortho-P Adjustment)	7.8	10.5	13.6	9	12	16	0.62	0.83	1.1	24	120	384
BAC (Ortho-P & pH Adjustment)	6.6	10.9	13.7	9	12	19	0.53	0.86	1.1	168	192	264

In the subsequent BAC evaluation phases, the BAC contactor was operated at a lower EBCT of 12 minutes to improve the economics of construction and GAC replacement. Furthermore, the 12 minute experimental EBCT fell within the 5 to 15 minute range employed in similar biological pretreatment studies (Halle et al., 2009; Peldszus et al., 2012). For the 12 minute EBCT, the corresponding average flow rate was about 10.5 gpm and the hydraulic loading rate was about 0.83 gpm/ft^2, which remained gradual to promote the growth of the biofilm. Evidence of the development of the biofilm was provided by shorter filter run times ranging from 24 to 384 hours of filtration. The increased frequency of backwashing signaled that particulate and bio-growth accumulation attributed to an increase in the pressure drop. Increased pressure drop as a result of increased bio-growth on the media has also been observed by Huck and colleagues (2000) in bench and pilot scale biofiltration studies. The observed filter run times between 24 and 384 hours are similar to filter run times reported in the literature, ranging from 24 to 224 hours (Goldgrabe et al., 1993; Lauderdale et al., 2014).

Water Quality Analysis

Water quality was monitored for raw, plant-ACH, GAC or BAC, pretreatment-UF, and control-UF water samples. The water quality averages were compiled for each of the activated carbon testing periods (adsorption, transition, BAC with orthophosphate adjustment, and BAC with orthophosphate and pH adjustment) and are recorded in Tables G-1 through G-5 of Appendix G. The accompanying time-series graphs for pH, temperature, turbidity, aluminum, iron, manganese, UV 254, DOC, SUVA, orthophosphate, free ATP, viable ATP, and HPC are illustrated in Figures G-1 through G-12 of Appendix G.

The performance of the activated carbon pretreatment was evaluated according to the reduction in the level of particulate matter, organic matter, and metals. In Figure 4-41, average turbidity, UV 254, and DOC removals with 95 percent confidence interval error bars are specified for each testing period. Similarly, average of differences between outlet and inlet aluminum, iron, and manganese concentrations is presented in Figure 4-42. Optimum pretreatment performance was achieved during the GAC adsorption phase. GAC adsorption removed on average 39 percent of turbidity, 48 percent of UV 254, 35 percent of DOC, and had a negligible impact on metals concentrations. The effectiveness of GAC in removing turbidity is attributed to the relatively low feed (plant-settled) water turbidity of 0.3 ntu. Additionally, the effective organic removal likely resulted from the strong affinity between the GAC active sites and dissolved organics (MWH, 2005). The GAC results are supported by a previous pilot-scale study, in which Yang and researchers (2010) showed that GAC treatment removed the majority of the inlet turbidity and reduced the UV 254 by nearly 60 percent.
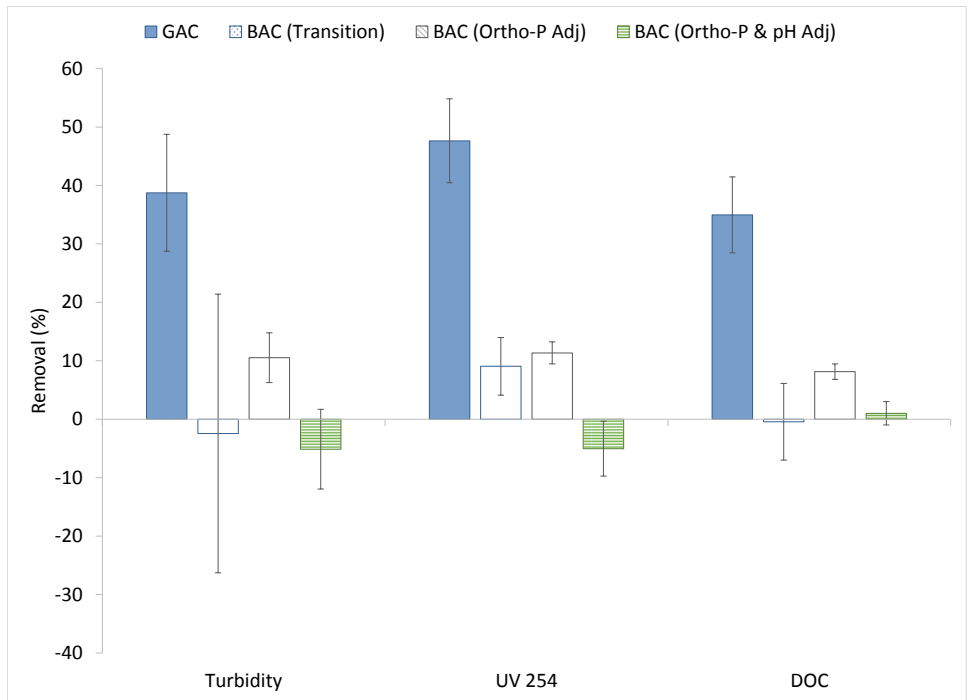
Figure 4–41 GAC/BAC Phase Average Particulate and Organic Removal
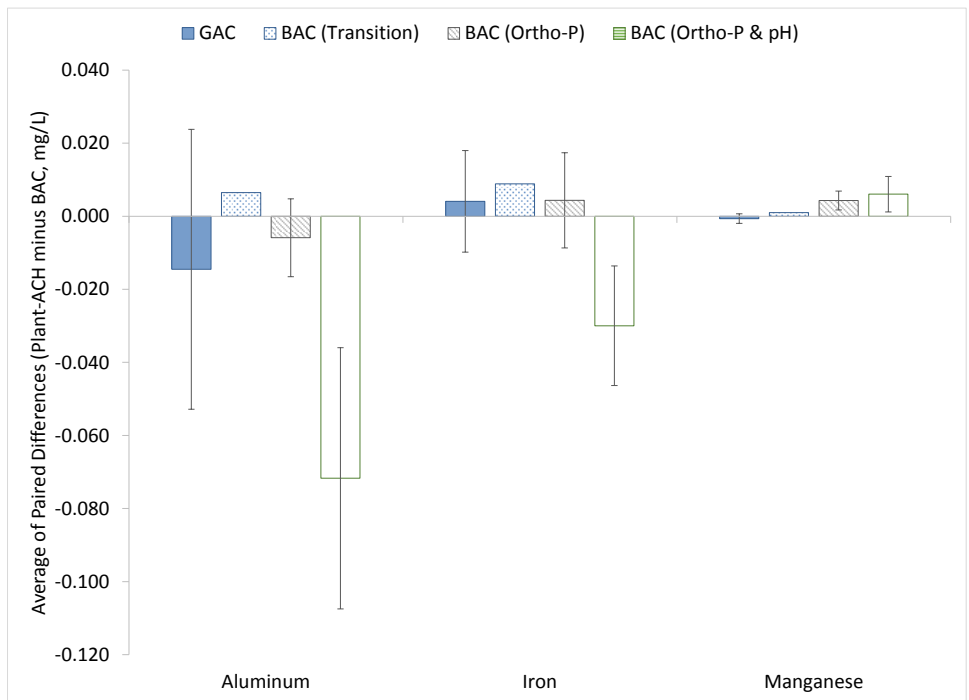
Figure 4–42 GAC/BAC Phase Average Difference in Aluminum, Iron, and Manganese

133

As the active carbon sites became saturated with DOC, GAC filtration operation entered the BAC transition mode, where remaining active sites were exhausted and bacteria began colonizing the media. Evidence of the start of biological activity was offered by a 16 pg/mL increase in total ATP across the biofilter. Due to the unsteady-state or acclimation nature of the transition mode, BAC in transition had negligible impacts on turbidity, DOC, and metals, but removed about 11 percent of UV absorbing constituents. The reduction in UV absorbing constituents likely resulted from adsorption to remaining active carbon sites.

Once orthophosphate addition began, the BAC transition was converted to BAC mode. BAC filtration removed on average about 11 percent of both turbidity and UV 254, and 8 percent of DOC. BAC filtration had no significant impact on the aluminum and iron levels, but reduced the manganese by about 20 percent. For BAC treatment, the 11 percent removal in turbidity was less than the 33 to 65 percent range reported by other researchers (Rittmann et al., 2002; Naidu et al., 2013; Wang, 2014). Similarly, manganese removal was lower than the 70 percent removal reported by Granger and colleagues (2014) in their biofiltration study that assessed direct biofiltration of surface water. The 11 percent UV 254 removal was comparable to the 10 percent UV 254 removal reported in a previous research study that investigated BAC treatment of ozonated surface water (Geismar et al., 2012). On the other hand, the observed 8 percent reduction in DOC falls within the low range of DOC removal results (3 to 65 percent) reported in other BAC evaluation studies (Shon et al., 2005; Brown and Lauderdale, 2006; Naidu et al., 2013; Wang, 2014).

A further decline in the BAC performance was observed during the subsequent orthophosphate and pH adjustment phase. While the reduction in manganese was maintained at 30 percent, BAC pretreatment failed to reduce the turbidity, UV 254, and DOC levels in the feed water. The lack of

particulate and organic removal was accompanied by an increase in the aluminum and iron levels across the BAC filter. The maintenance in the manganese removal suggest that the treatment conditions favored the proliferation of manganese oxidizing bacteria over iron oxidizing bacteria (Tekerlekopoulou et al., 2013). Therefore, biofilm detachment may have caused the breakthrough of metal precipitates and organic matter. The breakthrough of metals and organics from the BAC filter is suggested by the occurrence of BAC turbidity spikes reaching 3.5 ntu. In a published literature review on BAC treatment, Simpson supports that excess bio-growth can lead to the breakthrough of target contaminants, including turbidity and organics (2008).

In an effort to identify additional causes for the loss in BAC treatment efficiency, the BAC inlet and outlet water quality averages were analyzed and compared. A summary of the water quality averages are presented in Figures G-13 through G-20 of Appendix G. The time-series graph of the inlet turbidity with corresponding DOC concentrations across the BAC is displayed in Figure 4-43. Over time, the GAC adsorption capacity for DOC was exhausted and the GAC transitioned into biological degradation mode. While in biological mode, Figure 4-43 shows that feed water turbidity increased from 1 ntu to upwards of 3 ntu. The increase in feed water turbidity was likely caused by intermittent operation of the full-scale coagulation and sedimentation basin that began on September 7, 2013. Unsteady-state operation of the coagulation process lead to the observed formation of pin-floc that was carried over to the BAC pilot. Pin floc carry-over was accompanied by a loss in the DOC removal efficiency.
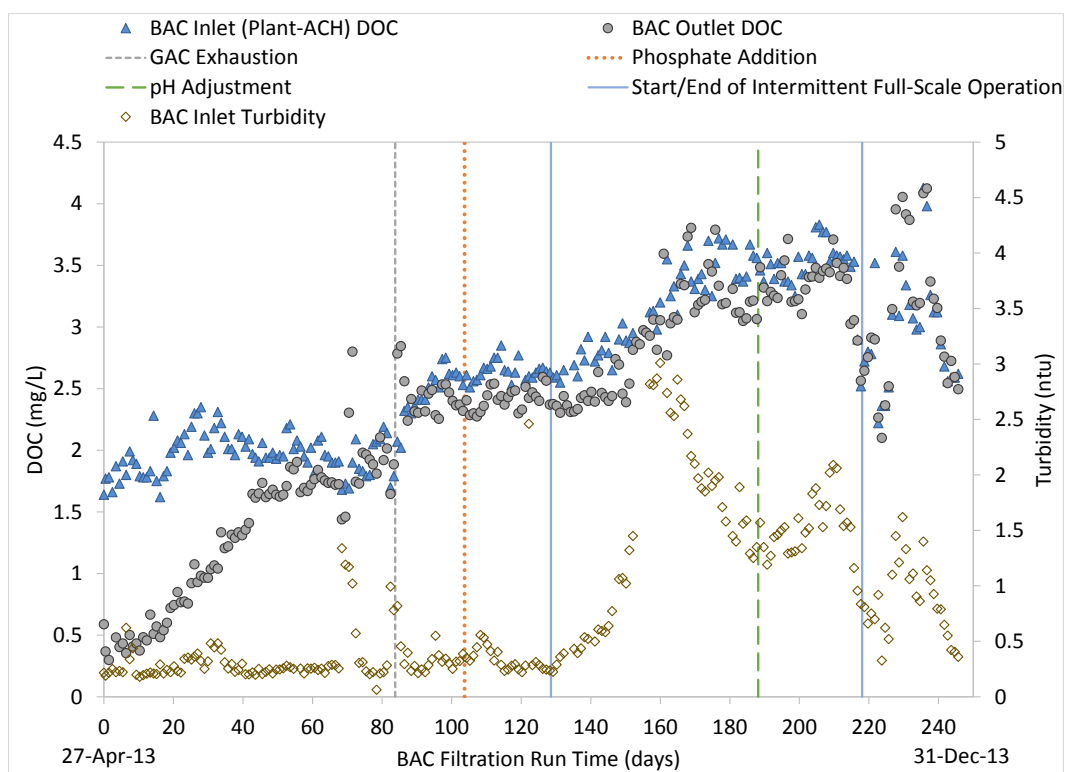
Figure 4–43 GAC/BAC Phase DOC and Feed Turbidity Time-Series Graph

Niquette et al. (1998) and Lauderdale et al. (2014) have observed similar detrimental impacts of floc carry-over on biodegradable contaminant removal. While Niquette et al. (1998) identified the interference of the diffusion barrier as a possible mechanism, Lauderdale et al. (2014) attributed detrimental impacts of floc carry-over to the consumption of essential orthophosphorus nutrient by the coagulant (2014). For this study, the latter explanation is unlikely as orthophosphorus in the BAC filtered water was maintained at about 0.3 mg/L as PO_4^{3-}, which corresponded to an acceptable C:N:P molar ratio of 100:10:1 (LeChevallier et al., 1991). While diffusion limitations and variable feed water quality likely contributed in part to diminishing DOC removal, an alternative explanation is offered related to a critical water quality factor not commonly emphasized in previous biofiltration studies—alkalinity.

136

The low alkalinity nature of the BAC feed water may have lacked sufficient cations to support a robust biofilm on the filter media. Instead the biofilm was susceptible to sloughing and detachment of the generated biomass. Susceptibility of the biofilm to detachment is supported by the biological monitoring results. While direct ATP measurements were not conducted on the filter media, an increase in the free and viable ATP levels across the BAC filter was observed and is shown in Figures 4-44 and 4-45. Increases in free and viable ATP were accompanied by increases in HPC across the BAC. The BAC filtration increased HPC levels by more than 1000 CFU/mL as emphasized in Figure 4-46. The scatterplot for the natural logarithm (ln) of HPC versus the natural logarithm of viable ATP (shown in Figure 4-47) reveals a weak but apparent positive exponential relationship between HPCs and viable ATP results. Additionally, the increase in biological activity across the BAC filter was accompanied by turbidity spikes in the BAC effluent. Although these pilot-scale results are insufficient to prove specific mechanisms, the ATP, HPC, and turbidity results offer motivation for future studies to uncover the mechanisms behind the effect of alkalinity on the biodegradable DOC removal by biofiltration.

The average UV 254, DOC, and SUVA levels for the control-UF and pretreatment-UF processes are presented in Figures 4-48 through 4-50. GAC adsorption pretreatment reduced UV 254, DOC, and SUVA levels by 49, 42, and 13 percent. During the subsequent BAC evaluation with orthophosphate addition, BAC filtration reduced the UV 254, DOC, and SUVA by 12, 10, and 3 percent. In the BAC with pH adjustment phase, the organic reduction fell to 4 and 5 percent of the UV 254 and DOC with a negligible impact on SUVA. Based on the organic removal results, the highest DOC removals were achieved during the adsorptive phase and reached a steady-state DOC removal of 10 percent during the BAC phase.
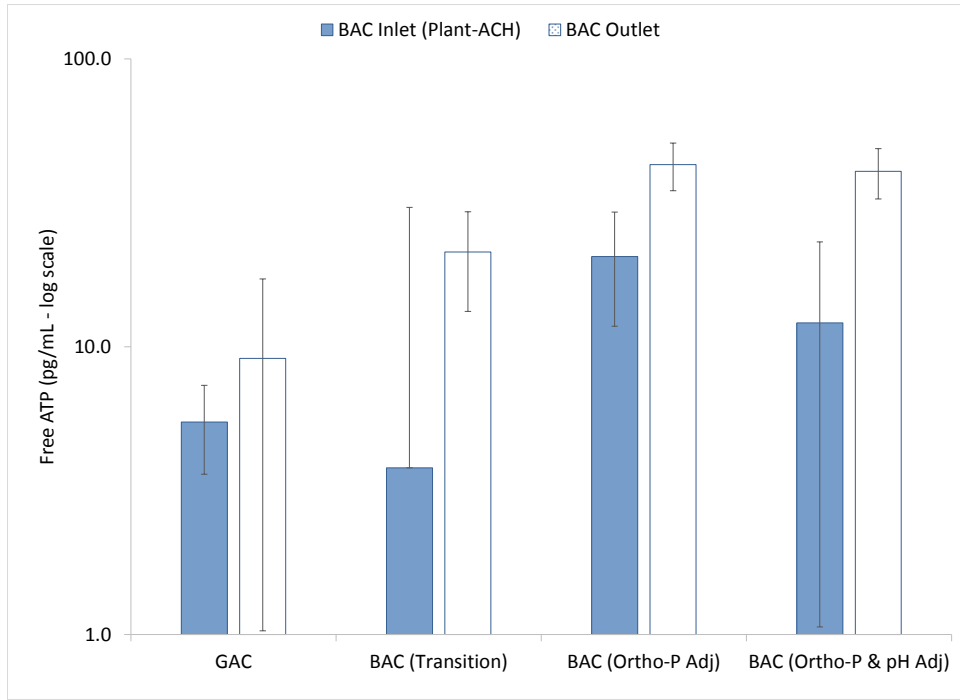
Figure 4–44 GAC/BAC Phase Average Free ATP
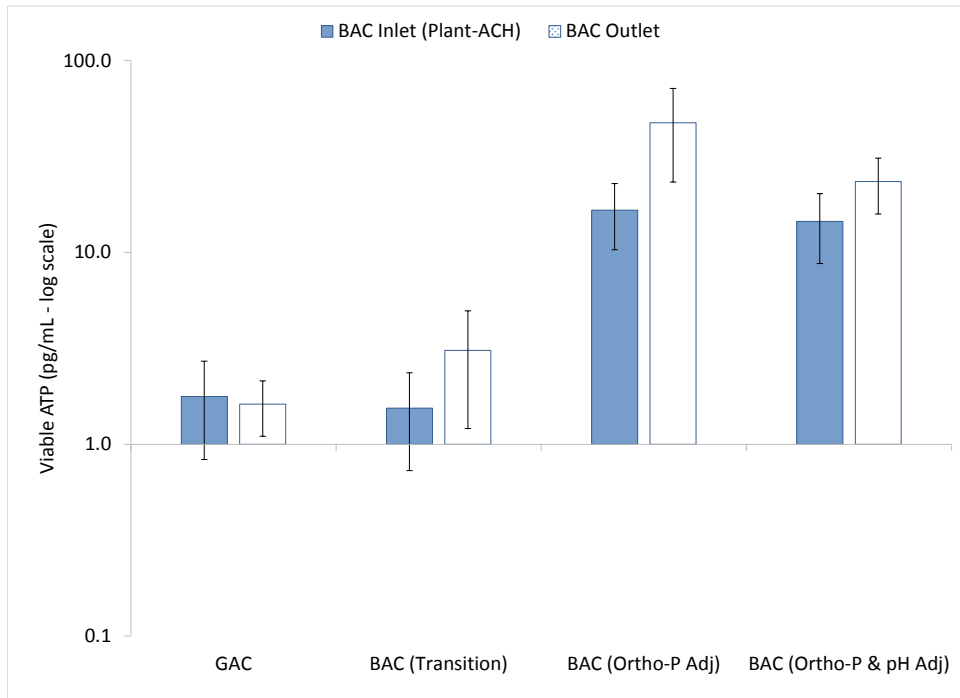
Figure 4–45 GAC/BAC Phase Average Viable ATP
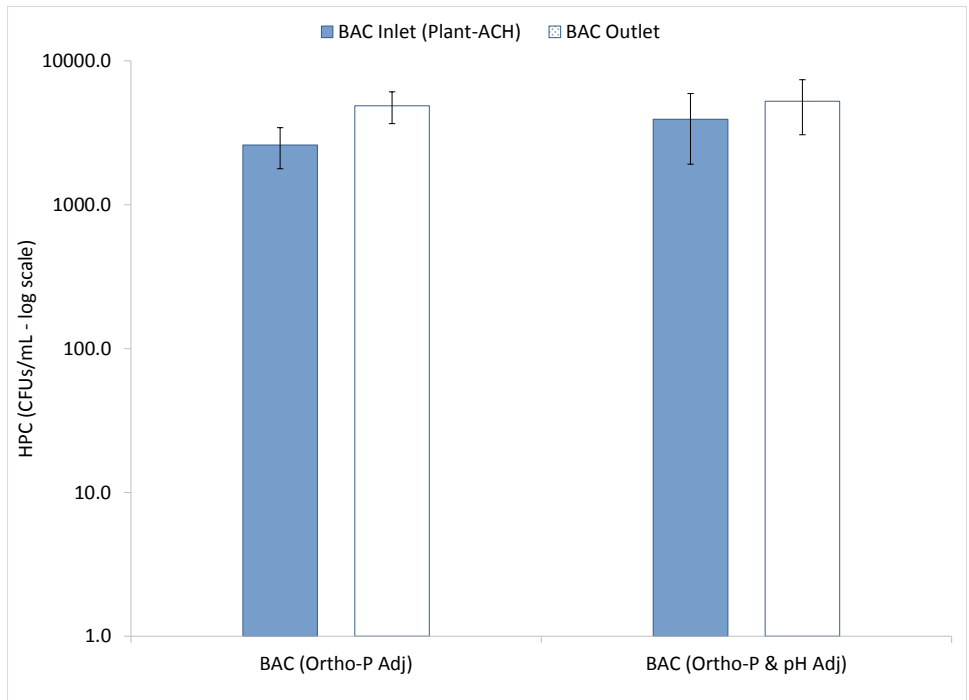
Figure 4–46 BAC Phase Average HPC
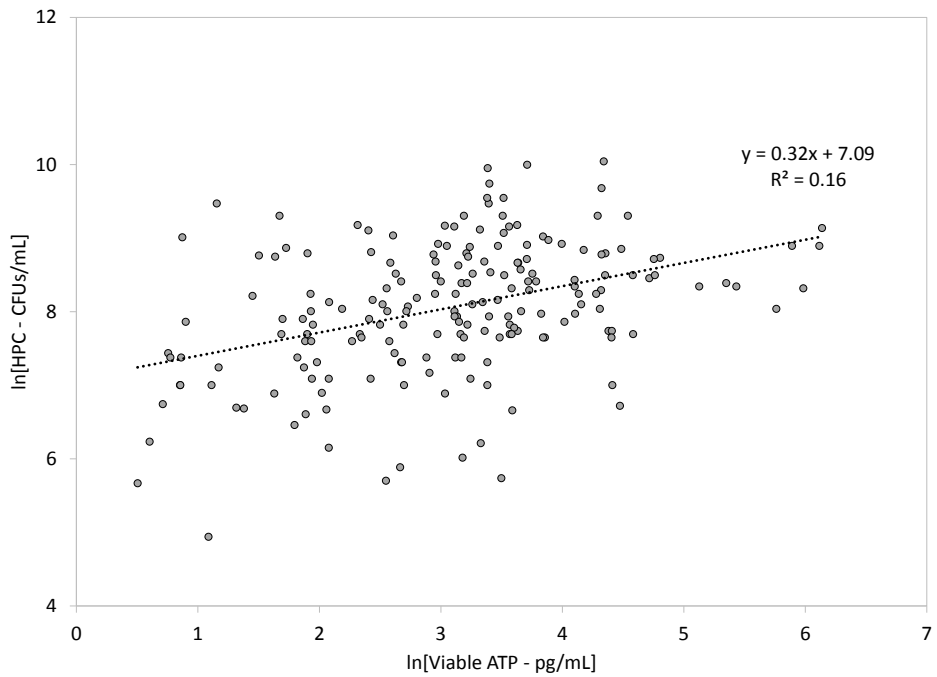
Figure 4–47 ln[HPC] versus ln[Viable ATP]

139
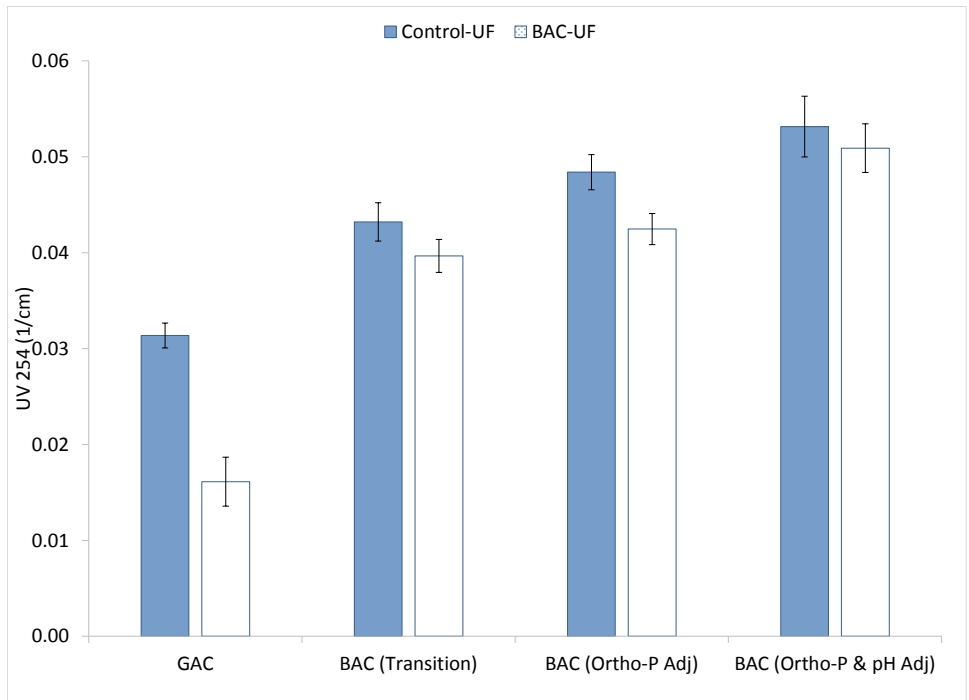
Figure 4–48 GAC/BAC Phase UF Average UV 254
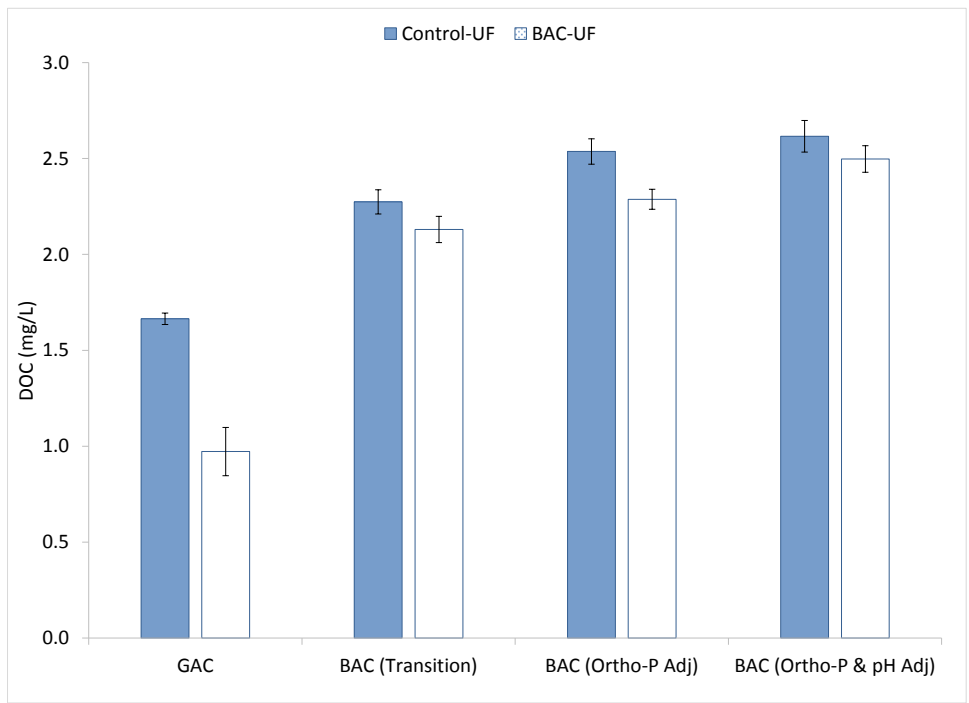
Figure 4–49 GAC/BAC Phase UF Average DOC
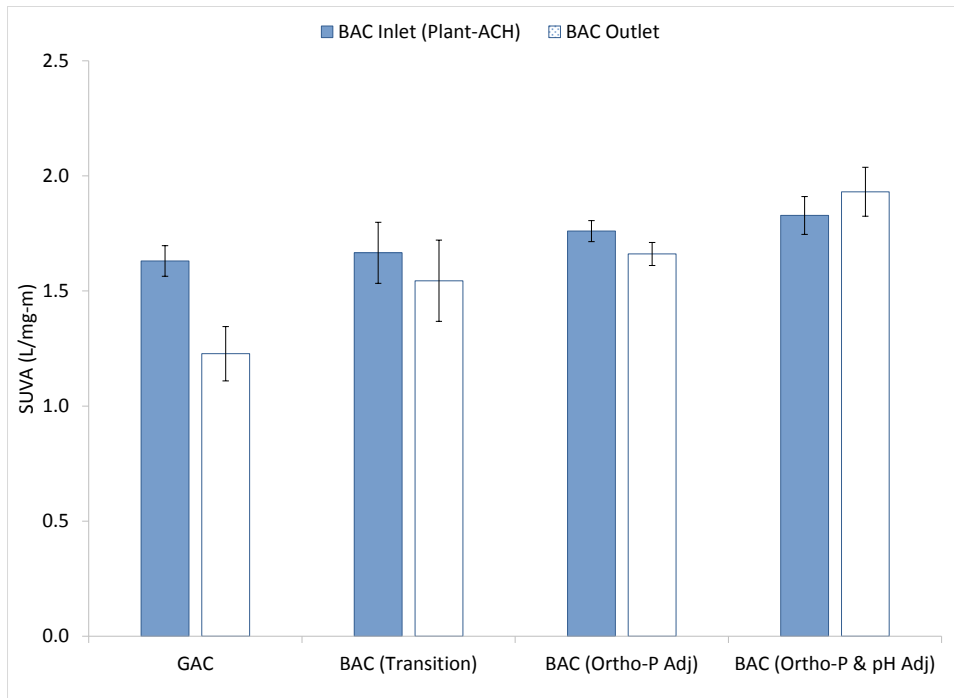
Figure 4–50 GAC/BAC Phase UF Average SUVA

DBP Formation Potential

The impact of GAC adsorption, transition, and biological pretreatment on the finished water quality was determined by comparing the TTHM and HAA_5 formation potential between the control-UF and pretreatment-UF filtrates. Four sets of DBP formation potential experiments were conducted on April 28, August 5, October 21, and December 9, 2013 to capture the sequential modes of GAC filtration: adsorption (start-up), transition, BAC (orthophosphate), and BAC (orthophosphate and pH). The water quality and operational parameters for the DBP formation potential experiments are summarized in Table 4-11. The TTHM and HAA_5 speciation and corresponding chlorine residual results for the control-UF and pretreatment-UF filtrates are included Tables G-6 through G-9 of Appendix G.

Table 4–11 GAC/BAC Phase DBP Formation Potential Experimental Parameters

Testing Parameters	GAC Adsorption		BAC Transition		BAC Ortho-P		BAC Ortho-P & pH	
	Control-UF	GAC-UF	Control-UF	BAC-UF	Control-UF	BAC-UF	Control-UF	BAC-UF
pH	8.80	8.85	8.79	8.75	8.76	8.83	8.79	8.8
UV 254[1] (1/cm)	0.03	0.003	0.05	0.042	0.054	0.051	0.056	0.053
TOC[1] (mg/L)	1.47	0.18	2.37	2.19	2.85	2.72	2.61	2.31
SUVA[1] (L/mg-m)	2.04	1.64	2.11	1.92	1.89	1.88	2.15	2.29
Chlorine Dose (mg/L Cl_2)	2.5	2	4	4	4	4	3.5	3.5
Incubation Temp. (ºC)	12-22	12-22	18-25	18-25	16-25	16-25	20-25	20-25

(1) Water quality comparison graphs are included in Figures G-21, G-24, G-27, and G-30 of Appendix G.

The comparisons between the control-UF and pretreatment-UF four-day chlorine demand and DBP formation potential are presented in the column graphs of Figures 4-51 through 4-53. At GAC pilot start-up, the GAC adsorption lowered the chlorine demand to less than 0.2 mg/L and reduced the TTHM and HAA_5 levels by 95 and 42 percent. The low DBP formation potential results indicate that GAC adsorption is effective in removing DBP precursors. Based on the DOC time-series trend, GAC adsorption is expected to maintain effective DBP precursor removal up to approximately 45 days of filtration time. The GAC pilot-breakthrough calculations are presented in Appendix I. After about 45 days of filtration time the DOC reduction would likely not be sufficient to control regulated DBP formation.

During the transition mode, the activated carbon filtration reduced the chlorine demand by 0.2 mg/L and both the TTHM and HAA_5 formation potential by 13 percent. The reduction in chlorine

demand and DBP formation potential was likely due to the combination of adsorption and biodegradation mechanisms. In the subsequent BAC with orthophosphate phase, BAC filtration reduced the chlorine demand by 0.5 mg/L and the TTHM formation potential by 8 percent, but did not reduce the HAA$_5$ formation potential. During the BAC pH adjustment phase, the BAC filter achieved a 0.3 mg/L reduction in chlorine demand that corresponded to 5 and 19 percent reductions in TTHM and HAA$_5$ formation potential. Although BAC filtration reduced chlorine demand and regulated DBP formation potential, biological pretreatment was not sufficient to lower TTHM and HAA$_5$ levels below the MCLs of 80 and 60 µg/L.
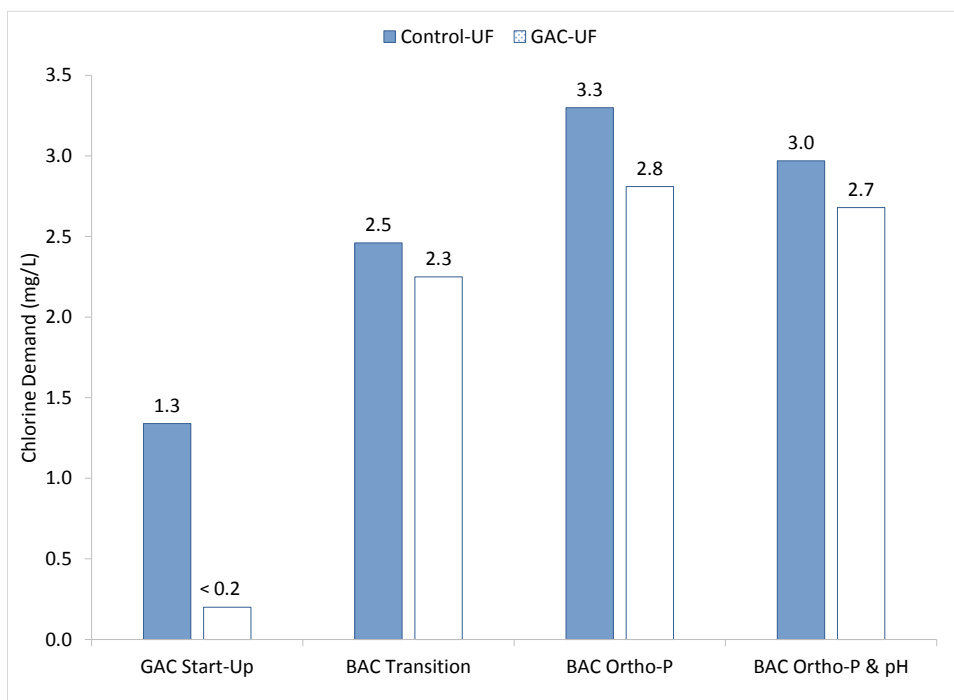
Figure 4–51 GAC/BAC Phase Four-Day Chlorine Demand
Note: Chlorine decay curves are illustrated in Figures G-22, G-25, G-28, and G-31.
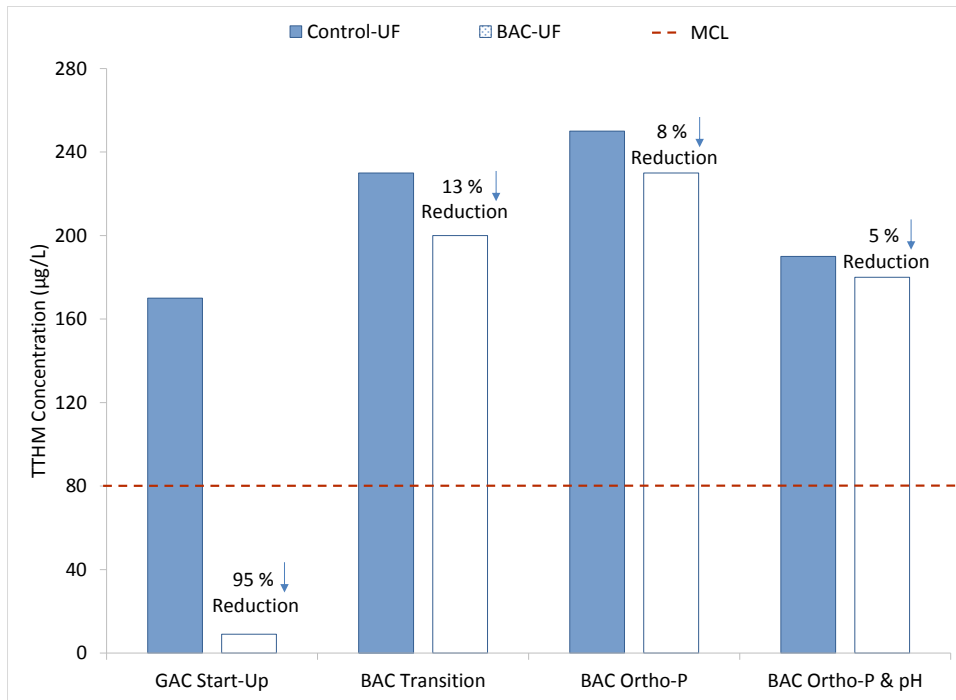
Figure 4–52 GAC/BAC Phase Four-day TTHM Formation Potential
Note: Formation potential curves are illustrated in Figures G-23, G-26, G-29, and G-32.
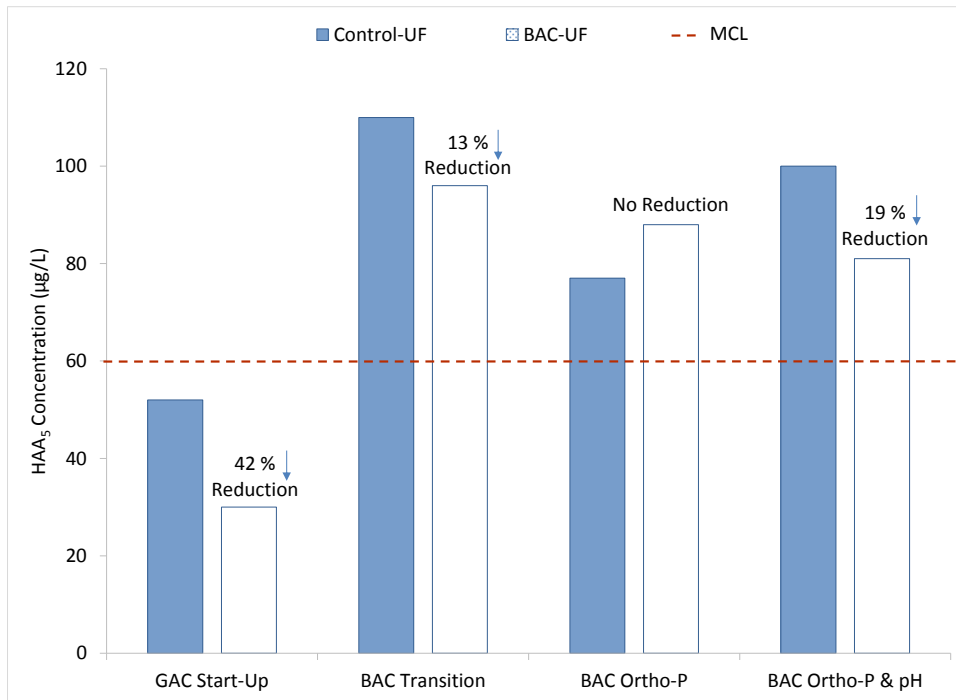
Figure 4–53 GAC/BAC Phase Four-Day HAA$_5$ Formation Potential

GAC and BAC Pretreatment Impacts on UF Membrane Performance

The effect of GAC and BAC pretreatments on UF operating performance was assessed by comparing the UF membrane feed water quality, operational parameters, and autopsy results for the control-UF and pretreatment-UF pilot plants. The pilot plants were operated continuously throughout the pilot testing. However, the intermittent operation of the full-scale plant between September 7 and December 4, 2013 altered the water quality of the excess settled water that was continuously supplied to the BAC filter and control-UF pilots. Consequently, UF operation was compiled into five periods: GAC adsorption (initial run), BAC transition, BAC with orthophosphate (continuous full-scale), BAC with orthophosphate (intermittent full-scale), and BAC with orthophosphate and pH adjustment. The continuous versus intermittent terminology refers to the full-scale plant operation not the BAC and UF pilot operation.

For each evaluation period, the average membrane recovery and process data is summarized in Table 4-12. Throughout the UF pilot testing, the membrane percent recovery remained around 89 percent for a backwashing frequency of 20 minutes. Overall, the pretreatment reduced the number of hypochlorite and citric acid CIPs by about half. GAC adsorption increased the average specific flux by 30 percent. Additionally, the BAC with orthophosphate (intermittent full-scale) increased the specific flux by 9 percent. Negligible impacts on specific flux were observed during the other BAC operating periods. To observe the effect of pretreatment on the statistical spread of the UF process data, TMP and specific flux box-and-whisker plots for the control-UF and pretreatment UF are compared in Figures 4-54 through 4-58. As indicated by the narrower quartile and whisker ranges, the pretreatment-UF exhibited more stable operation with fewer swings between extreme values.

145

Table 4–12 GAC/BAC Phase Pretreatment-UF versus Control-UF Operation

Operational Parameter	GAC Adsorption		BAC Transition		BAC with Ortho-P (Continuous Full-Scale Operation)		BAC with Ortho-P (Intermittent Full-Scale Operation)		BAC with Ortho-P & pH	
	Control	GAC	Control	BAC	Control	BAC	Control	BAC	Control	BAC
Selected Time Frame	4/27/13 to 5/16/13		7/26/2013 to 8/9/13		8/10/13 to 9/6/13		9/7/13 to 11/2/13		11/3/13 to 12/31/13	
Membrane Recovery										
Number of Hypochlorite CIPs	1	0	1	1	0	0	2	0	1	1
Number of Citric Acid CIPs	1	0	1	1	0	0	2	0	1	1
PERCENT RECOVERY	89	89	89	89	89	89	89	89	89	89
Average Membrane Process Data[1]										
Flow (gpm)	4	4	4	4	4	4	4	4	4	4
Flux Rate (gal/ft^2-day)	19.0	19.4	19.2	19.2	19.1	19.2	19.2	19.2	19.2	19.2
TCTMP @ 20 ºC (psi)	17	13	12	13	12	13	15	14	15	16
Specific Flux @ 20 ºC (gal/ft^2-d-psi)	1.2	1.5	1.6	1.5	1.6	1.5	1.3	1.4	1.3	1.2

(1) TMP and specific flux time-series graphs throughout the pilot testing are included in Figures G-33 and G-34 of Appendix G.
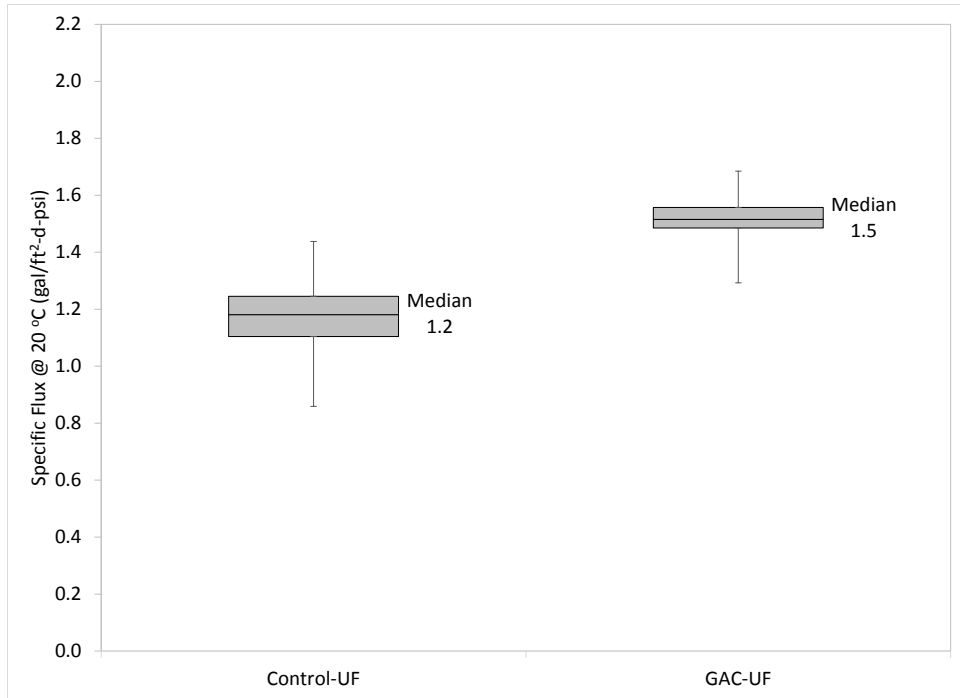
Figure 4–54 GAC Specific Flux
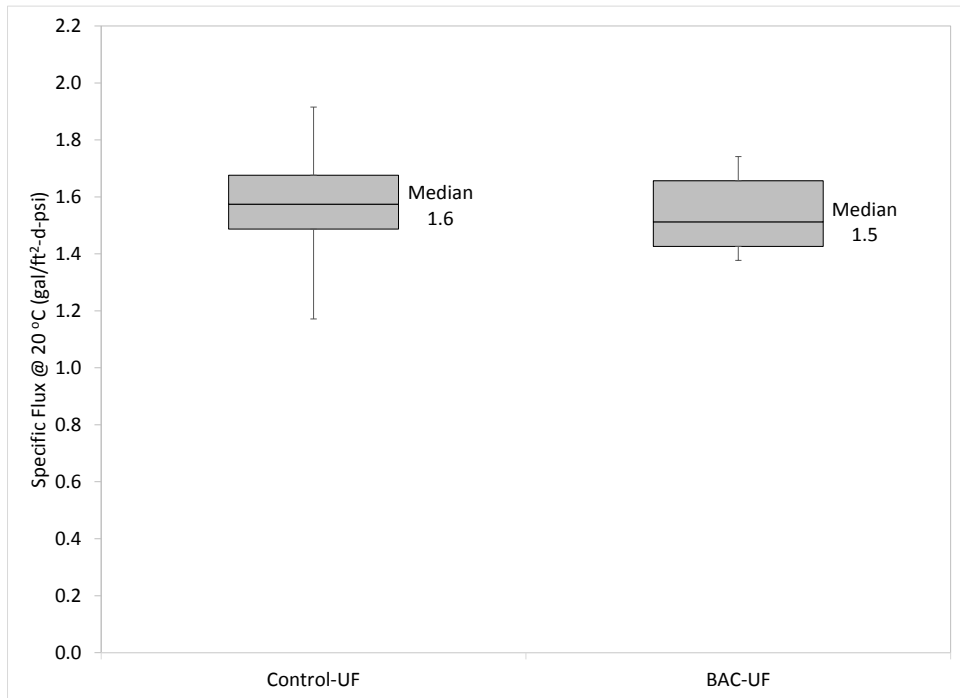
Figure 4–55 Transition Specific Flux
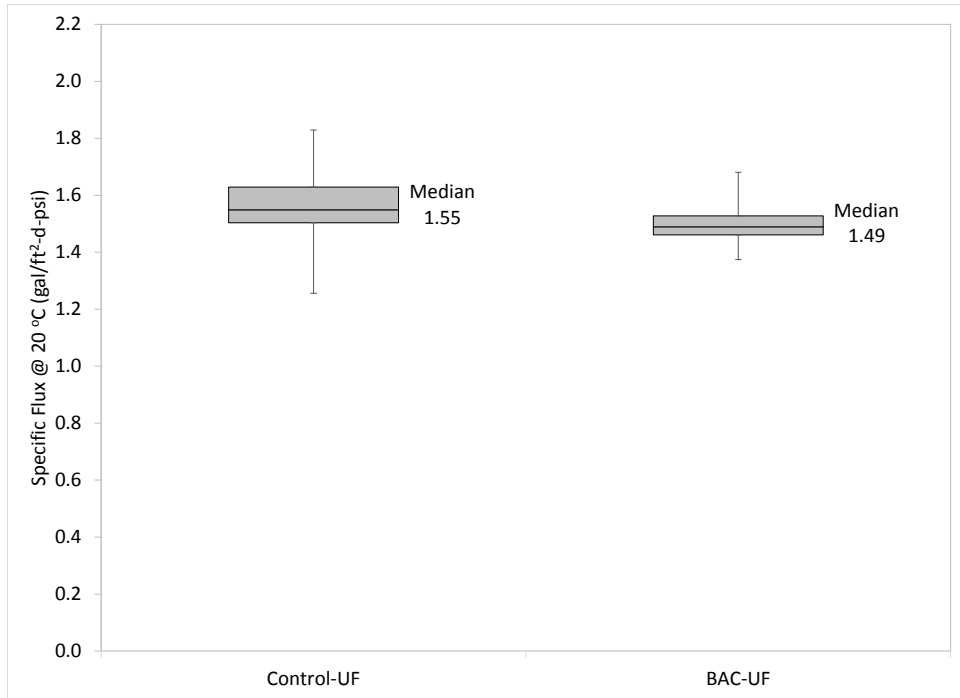
Figure 4–56 BAC with Orthophosphate (Continuous Full-Scale) Specific Flux
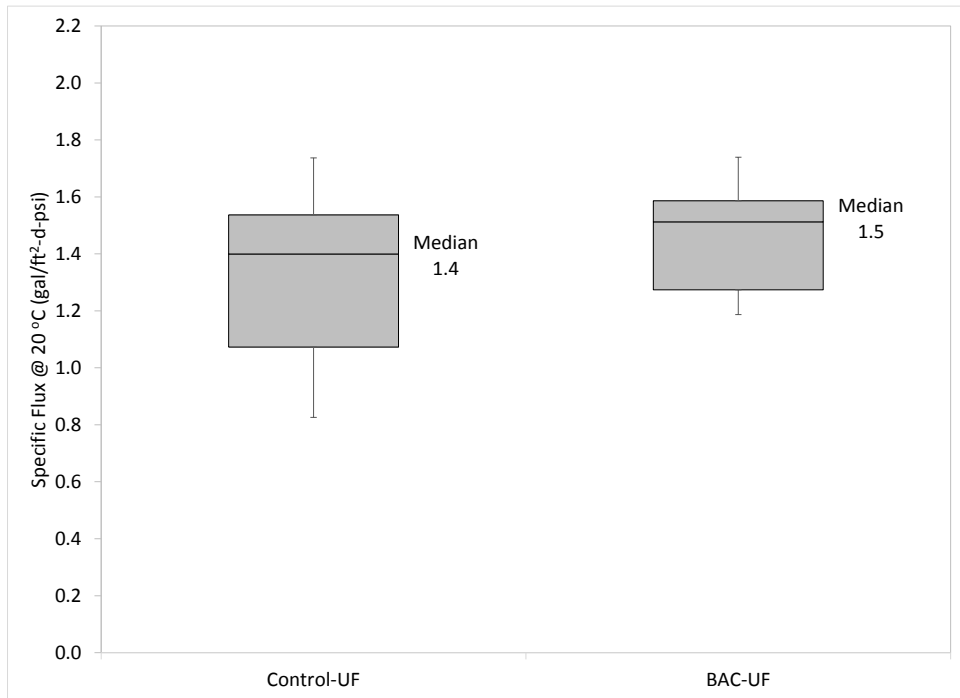
Figure 4–57 BAC with Orthophosphate (Intermittent Full-Scale) Specific Flux
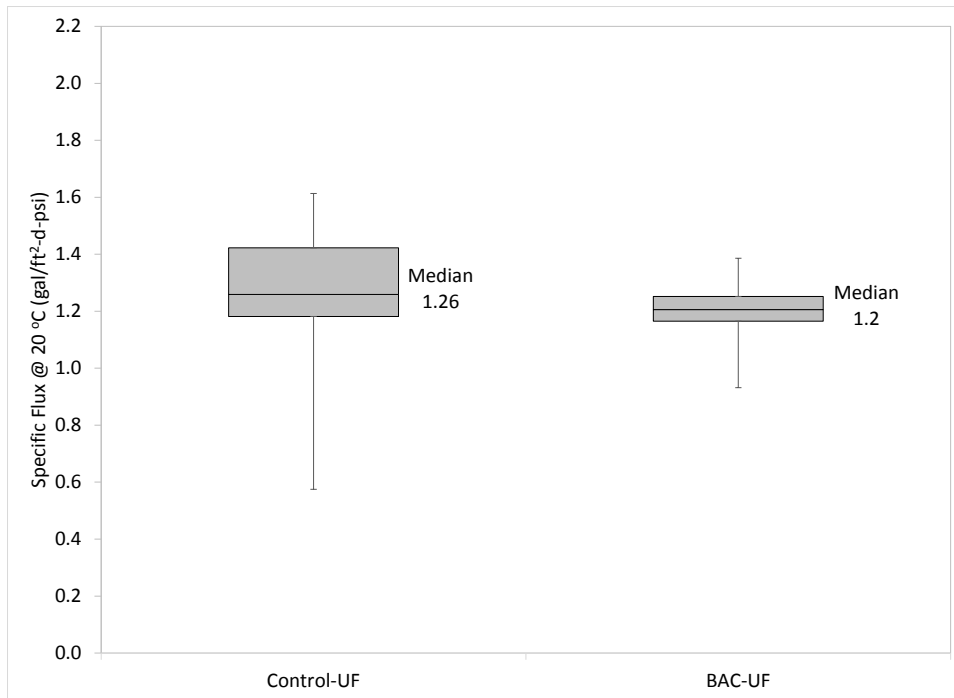
Figure 4–58 BAC with Orthophosphate and pH Adjustment Specific Flux

Membrane fouling trends were examined by plotting the control-UF and pretreatment-UF specific fluxes as functions of operation time during each of the evaluation periods. The specific flux time-series graphs are presented in Figures 4-59 through 4-63. As demonstrated in Figure 4-59, GAC adsorption pretreatment decreased the rate of specific flux decline; thus, reduced the fouling rate of the UF membrane as compared to the control. The control-UF membrane required a hypochlorite followed by citric acid CIP to recover the decline in specific flux. In the subsequent transition and BAC (continuous full-scale) evaluation periods, the pretreatment-UF specific flux trend mirrored the performance of the control-UF as shown in Figures 4-60 and 4-61.

Figure 4–59 GAC Specific Flux Time-Series Graph

Figure 4–60 Transition Specific Flux Time-Series Graph

150
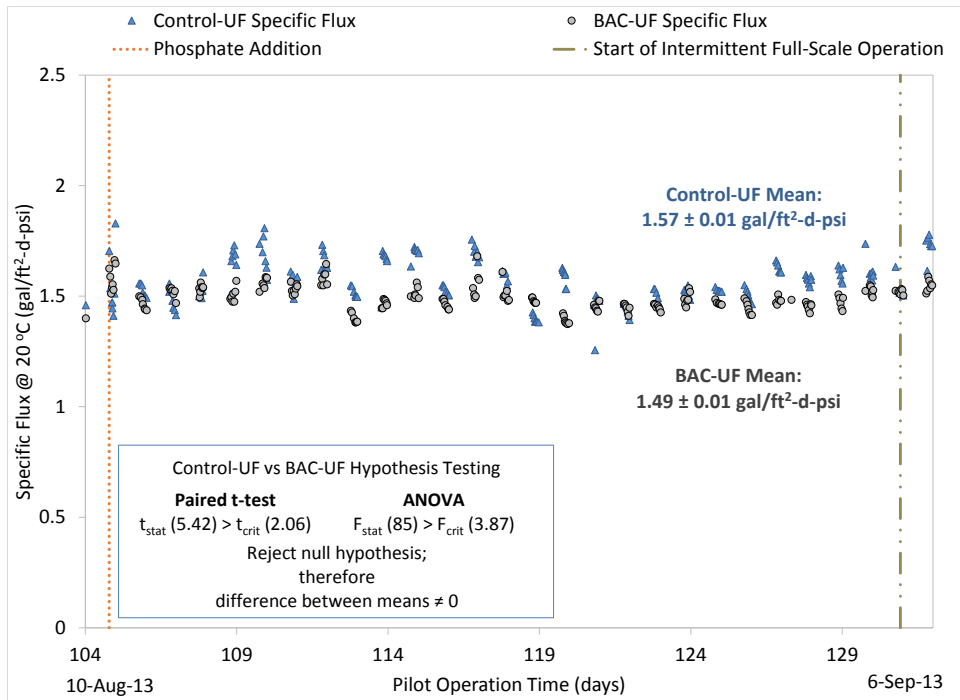
Figure 4–61 BAC with Orthophosphate (Continuous Full-Scale) Specific Flux Graph
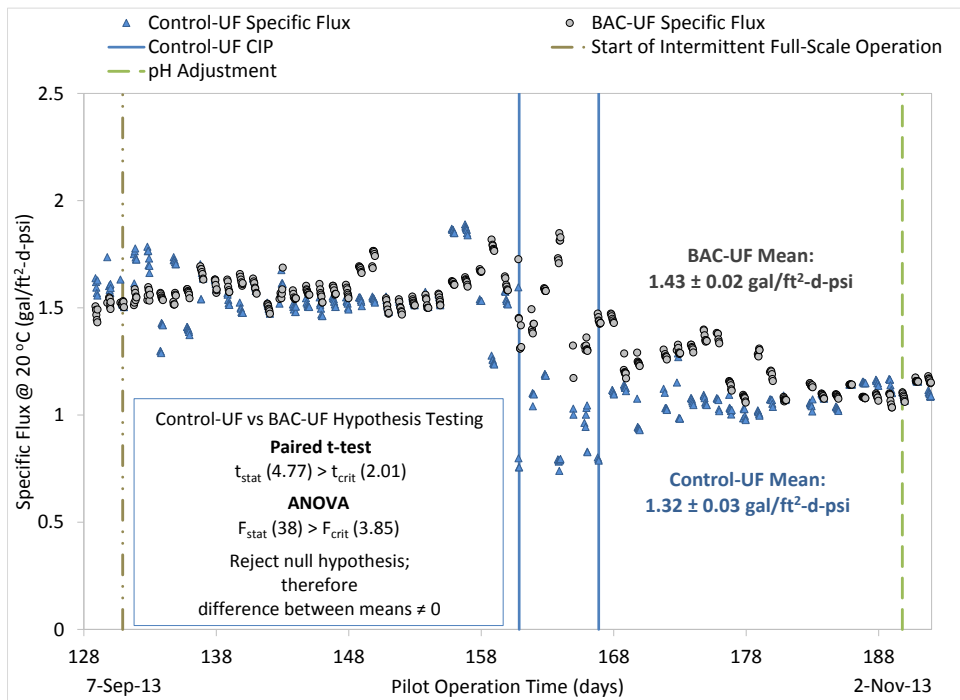
Figure 4–62 BAC with Orthophosphate (Intermittent Full-Scale) Specific Flux Graph

151
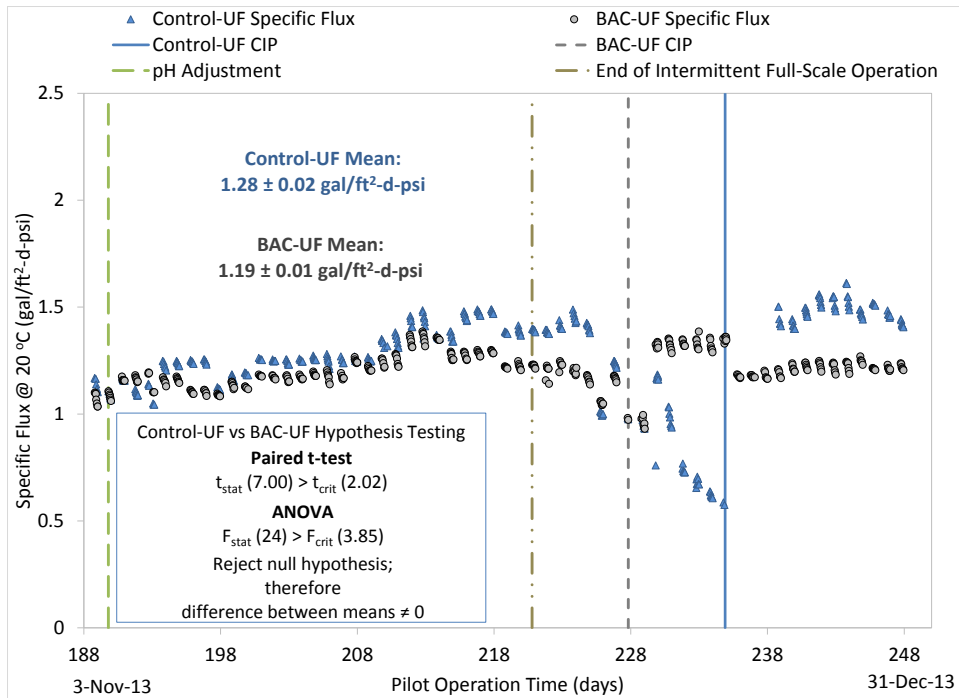
Figure 4–63 BAC with Orthophosphate and pH Adjustment Specific Flux Time-Series Graph

Deviation between the control-UF and pretreatment-UF specific-flux trends was observed following the start of the intermittent full-scale operation as emphasized in Figure 4-62. During the BAC (intermittent full-scale) evaluation, the BAC pretreatment attenuated the rapid rate of specific flux decline experienced by the control-UF membrane. The control-UF membrane required two CIPs with hypochlorite followed by citric acid to recover the specific flux to levels approaching the pretreatment-UF specific flux. After the start of the pH adjustment phase, the control-UF and pretreatment-UF membranes followed similar specific flux trends until the end of the intermittent full-scale operation. The change in full-scale operation appeared to cause a lag in the control-UF fouling trend, which corresponded with more frequent CIPs as compared to the pretreatment-UF membrane.

152

The specific flux fouling trends revealed that the impact of pretreatment on UF membrane performance varied throughout the sequential GAC operating phases. During the GAC adsorption and BAC (intermittent full-scale) testing phases, the pretreatment enhanced UF membrane performance by increasing the average specific flux and reducing the fouling rate and CIP frequency. On the other hand, BAC pretreatment failed to improve UF membrane performance during the transition, BAC (continuous full-scale), and BAC with pH adjustment phases. To identify reasons for the variation in UF membrane performance, the difference in specific flux (control-UF minus pretreatment-UF) was plotted against the difference in feed water turbidity and DOC (BAC inlet minus outlet). The specific flux versus turbidity and DOC scatterplots are presented in Figures 4-64 and 4-65.
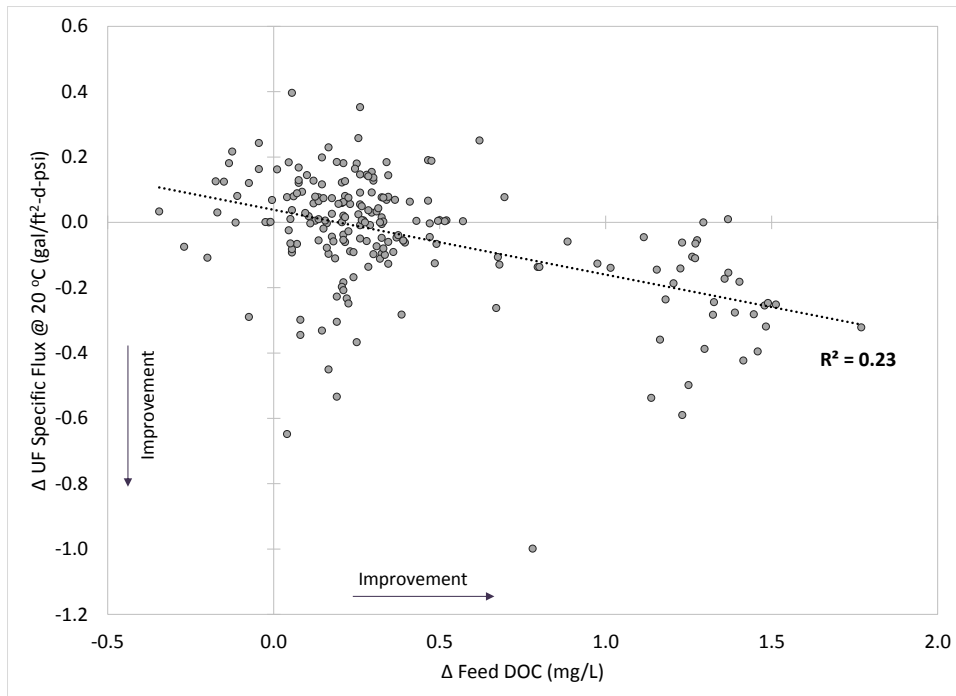
Figure 4–64 Scatterplot of Specific Flux versus Feed DOC
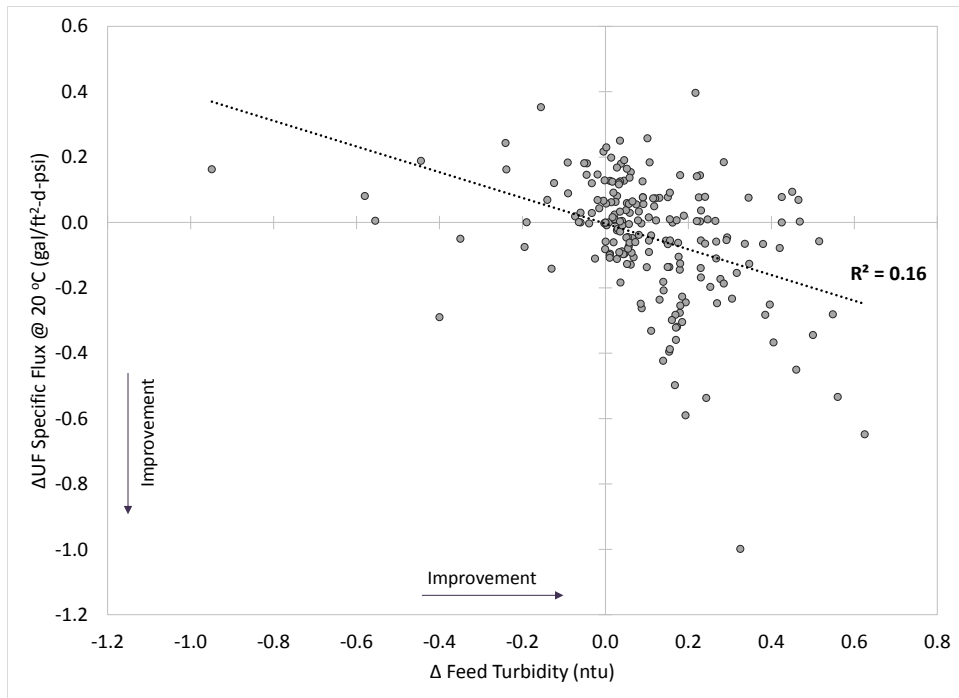
Figure 4–65 Scatterplot of Specific Flux versus Feed Turbidity

As also demonstrated in the MIEX® evaluation phase, the DOC and turbidity scatterplot results indicate that the specific flux improved with greater reduction in feed water DOC and turbidity. The influence of UF feed turbidity is also demonstrated by the time-series plot of specific flux along with feed turbidity, included in Figure G-34. Throughout UF pilot operation, the CIP events typically coincided with increases or spikes in the feed water turbidity to the membranes.

In addition to water quality scatter-plots, average of paired differences in UF specific flux and feed water turbidity, DOC, free ATP, and viable ATP were determined and compared. The average of paired differences throughout the GAC and BAC operational phases is illustrated in Figures 4-66 and 4-67. The comparison of the average of paired differences in specific flux and feed water turbidity and DOC supports the positive correlation between specific flux improvement and lower feed turbidity and DOC.
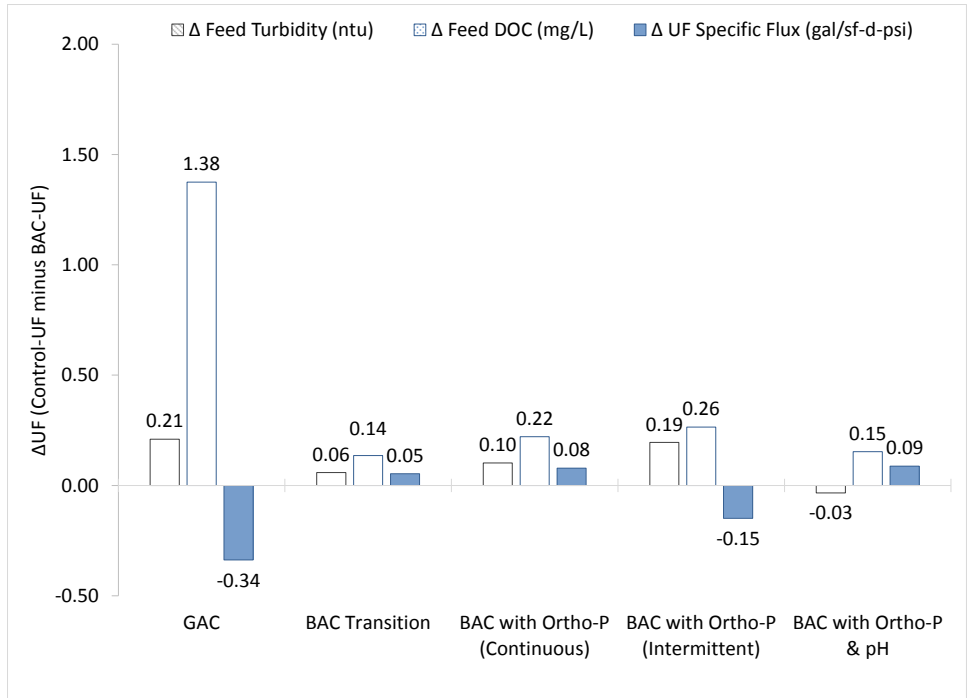
Figure 4–66 Average Difference in Specific Flux and Feed Water Turbidity and DOC
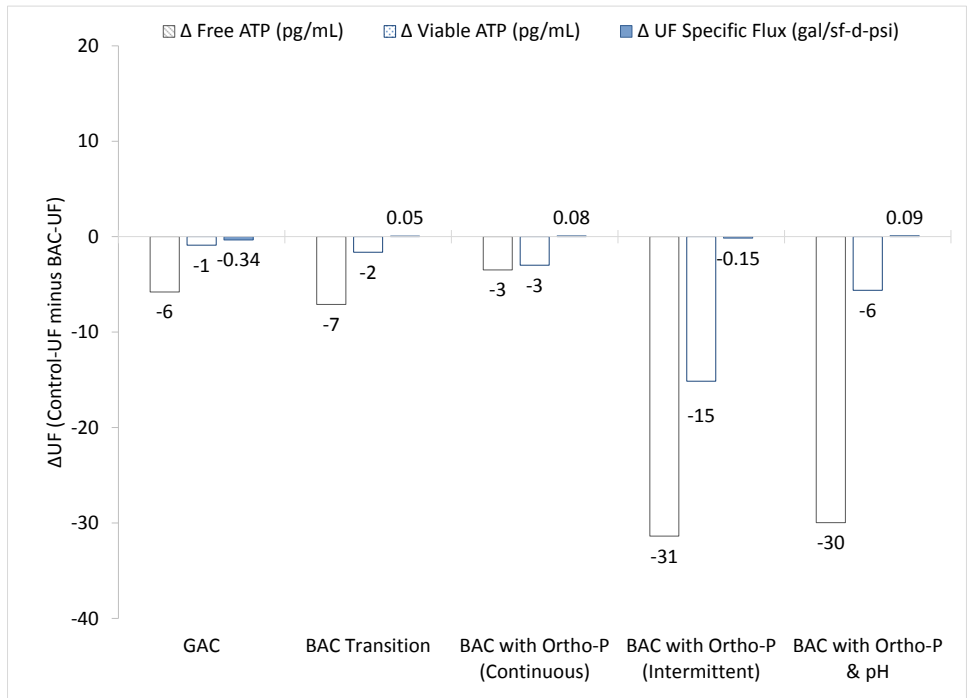
Figure 4–67 Average Difference in Specific Flux and Feed Water Free and Viable ATP

The GAC adsorption phase achieved the highest levels of DOC and turbidity removal, which coincided with the greatest improvement in UF specific flux. Of the BAC pretreatment modes, the BAC (intermittent full-scale) evaluation phase achieved the largest differences in feed water DOC and turbidity, and showed the most improvement in the membrane specific flux. Furthermore, the comparison of the differences in free and viable ATP between the UF feed waters reveals that the largest increase in biological activity occurred during the BAC (intermittent full-scale) evaluation phase.

The UF membrane operation results reveal that GAC adsorption pretreatment was effective in improving the water production efficiency of the UF membrane by increasing the specific flux and reducing the fouling rate and CIP frequency. The GAC results support the findings from Tsujimo and associates (1998), who demonstrated that GAC pretreatment allowed for the stable operation of the downstream membrane process. On the other hand, when applying BAC filtration downstream of sedimentation and ahead of UF membrane filtration, coagulation operation and control of settled water turbidity appeared to exert a stronger influence on the downstream UF membrane performance. Consequently, the benefits of BAC pretreatment, mainly the slight increase in the specific flux and decrease in the CIP frequency, would not outweigh the associated construction of operating costs of the additional pretreatment.

The relatively poor performance of BAC pretreatment for UF membrane processes contradicts the research findings presented by Huck, Wei, Duranceau and other researchers (Wend et al., 2003; Basu & Huck, 2004; Halle et al., 2009; Peldszus et al., 2012; Wei et al., 2011; Mosqueda-Jimenez & Huck, 2006; Dureanceau & Tharamapalan, 2013). A possible explanation for the poor BAC performance includes the unsteady feed water turbidity, organic, and biological composition.

However, LeChevallier and coworkers (1992) have demonstrated that a pre-ozonated BAC process, influenced by poor turbidity removal of the upstream pilot-scale coagulation, still achieved a 56 reduction in the TOC. Additionally, experiments conducted without pre-ozonation showed that BAC filtration without pre-ozonation produced similar effluent AOC levels (92 µg/L) as with pre-ozonation (100 µg/L) (LeChevallier et al., 1992). One major difference between the present study and previous research studies is the level of feed water alkalinity. Raw water alkalinity levels in previous studies have been greater than 30 mg/L $CaCO_3$ (see Table 2-1); however, the average alkalinity of Olinda raw water is about 2 mg/L as $CaCO_3$. Thus, the deficient BAC performance observed in the present study suggests that low alkalinity or "alkalinity limited" water supplies do not effectively support attached biological processes. The impact of alkalinity on biofilter performance relative to UF membrane processes was examined through the development of a new model framework.

GAC and BAC Phase Membrane Autopsy

At the conclusion of the BAC pilot testing, Avista performed membrane autopsies on the control-UF (also referred to as "UF A") and pretreatment-UF (also referred to as "UF B") membranes. Membrane CIPs were not performed prior to autopsy analysis. The autopsy analysis included physical examination of the membrane modules and stereoscope imaging of the fibers. A foulant analysis was also conducted which included the following tests: loss on ignition, acid testing, microscope analysis of foulant material, fourier transform infrared (FTIR) analysis, energy dispersive x-ray (EDX) analysis, scanning electron microscope (SEM), chromatic elemental imaging (CEI).

<u>Physical Inspection and Stereoscope imaging</u>

The physical inspection and stereoscope imaging results are summarized in Tables 4-13 and 4-14. In general, the BAC-UF visually appeared more discolored and fouled than the Control-UF. The orange colored foulant was observed to be denser and darker on the BAC-UF. Furthermore, comparing the different membrane fiber locations within the module for both the Control-UF and BAC-UF membranes reveals that the top and bottom fibers were more heavily fouled than the middle fibers. The difference in foulant density throughout the membrane module is due to the module configuration, in which the feed water entered near the top of the pilot unit and filtrate exited near the bottom of the housing vessels.

Table 4–13 Photographs of Physical Inspection of BAC Phase Membrane Modules by Avista

Module	Image of Module	Image of "product end"
Control-UF		
BAC-UF		

Source: Courtesy of Avista Technologies

Table 4–14 Description of Physical Condition of BAC Phase Membrane Modules by Avista

Consideration	Control-UF	BAC-UF
cage wrap	Good condition and free of foulant material	Good mechanical condition, but was coated with red-brown colored foulant material.
plastic cover	Good condition and free of foulant material	No obvious signs of plugging; however, the epoxy was orange in some areas and foulant debris was detected on the outer radius.
internal inspection	The fibers closest to the cage wrap in the center of the module were virtually free of foulant debris	The fibers closest to the outer cage wrap displayed a distinct pattern of fouling consistent with the cage wrap material.
Stereoscope imaging	foulant material varied in thickness and was unevenly distributed	foulant material varied in thickness and was unevenly distributed

Source: Information provided by Avista Technologies

Organic Content Analysis through Loss on Ignition Test

The "Loss on Ignition" test provided an estimate of the ratio of organic to inorganic material in the foulant. The percent organic content as detected by the loss on ignition testing is shown in Figure 4-68. The organic portion did not significantly differ between the control and the BAC foulant material and was roughly 60% organic and 40% inorganic.

Acid Testing for Carbonate Presence

Acid testing was conducted to detect the presence of carbonates in the foulant. Carbonate was not detected in the foulant collected from both the control-UF and BAC-UF.

UF-Control

41.70%

58.30%

UF-BAC

39.00%

61.00%

Organic Portion Inorganic Portion   Organic Portion Inorganic Portion
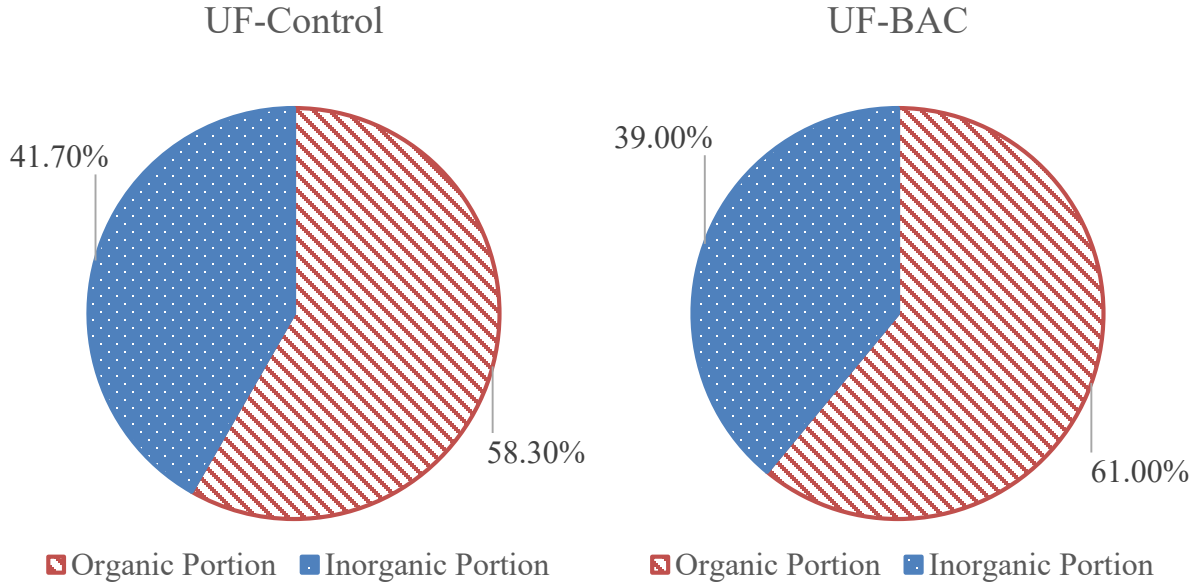
Figure 4–68 Comparison of BAC Phase Membrane Module Loss on Ignition (%)
Source: Data provided by Avista Technologies

Microscopic Evaluations

Microscopic evaluations were then conducted to test for the presence of microbiological organisms in the foulant material. Images from the foulant microscopic inspection (at 1000 times magnification) with stained microbiological organisms for the control and pretreatment membranes are shown in Table 4-15. In the microscopic tests, the results appeared similar for the both samples of foulant. Inorganic material, colloids, algae and Gram negative bacteria were detected for foulant collected from both the control-UF and BAC-UF.

Table 4–15 Comparison of Microscope Images for BAC Pretreatment Evaluation

Control-UF	BAC-UF
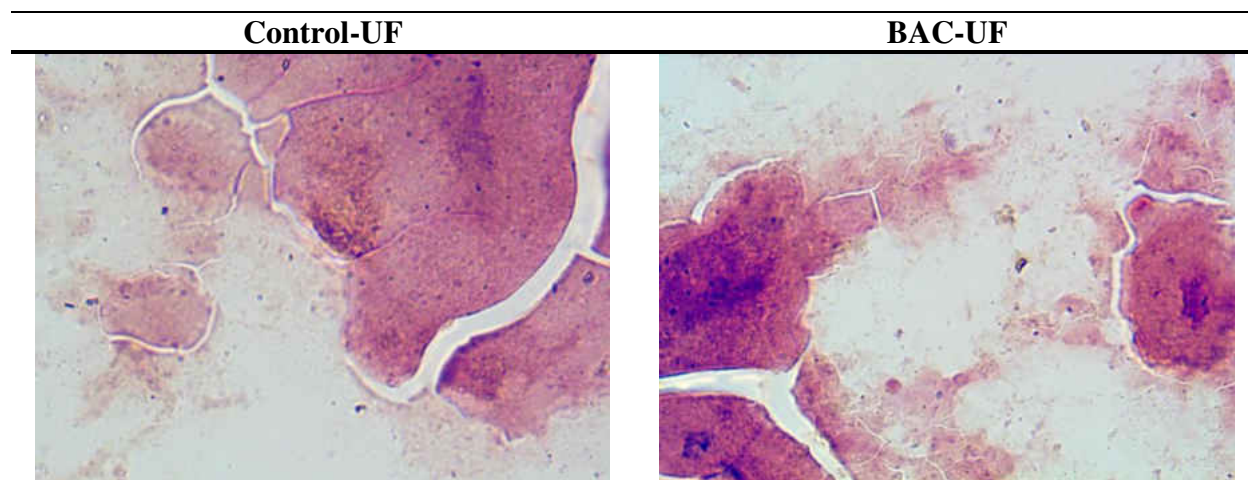
Source: Courtesy of Avista Technologies

Fourier Transform Infrared Spectroscopy

Fourier Transform Infrared Spectroscopy (FTIR) analysis detects the presence of functional groups of organic and inorganic foulant constituents. The results of the FTIR analysis revealed several differences between functional groups detected in the foulant collected from the heavily fouled fibers from the control-UF and the BAC-UF fibers. The comparison is shown below in Table 4-16. Only aldehyde and the C-H organic functional group was detected in the BAC-UF and was previously undetected in the foulant collected from the control-UF. Conversely, C-N, N-H, C-C, and C=C were detected in the control-UF foulant but was not present in the BAC-UF foulant. Additionally, the peak for N-C-O was stronger in the control-UF foulant. The results of the FTIR analysis indicate that the foulant collected from the BAC-UF contained fewer organic and inorganic functional groups.

Table 4–16 Comparison of FTIR Analysis Results for BAC Evaluation Phase

Functional Group	Control-UF	BAC-UF
C-H	Weak	Yes
C-N	Yes	No
N-H	Yes	No
C-C	Yes	No
C=C	Yes	No
H-C-OH	Weak	Weak
N-H-C=O	Weak	Weak
N-C-O	Yes	Weak
C-O-C	Weak	Weak
PVDF	Weak	Weak
Aldehyde	Not Reported	Yes

Source: Information provided by Avista Technologies

Energy Dispersive X-ray (EDX or EDS) Analysis

EDX analysis was conducted to identify inorganic foulant constituents. The results of this test are shown in Figure 4-69 and 4-70. Most notably, the iron content appeared to increase significantly in the foulant for the BAC-UF. Manganese content also increased but was a relatively small percentage of the foulant material. The manganese content was also detectable in the CEI results. Additional imagery was taken including SEM and CEI images, for which figures are presented in Table G-10 of Appendix G. The following observations were noted:

- The SEM images reveal that the BAC-UF had a larger visible amount of foulant accumulated on the fiber surfaces than the control-UF.

- CEI images revealed the presence of manganese on the BAC-UF membrane which was not present on the control-UF.
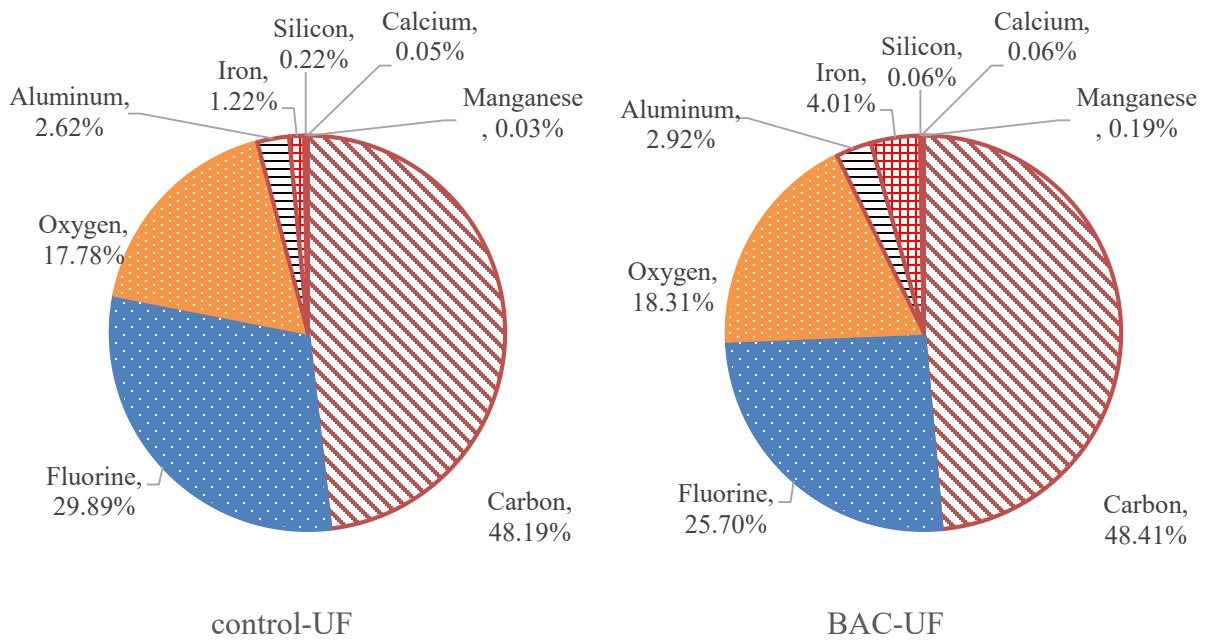
Figure 4–69 Comparison of EDX Analysis results from the control-UF and BAC-UF
Source: Data provided by Avista Technologies
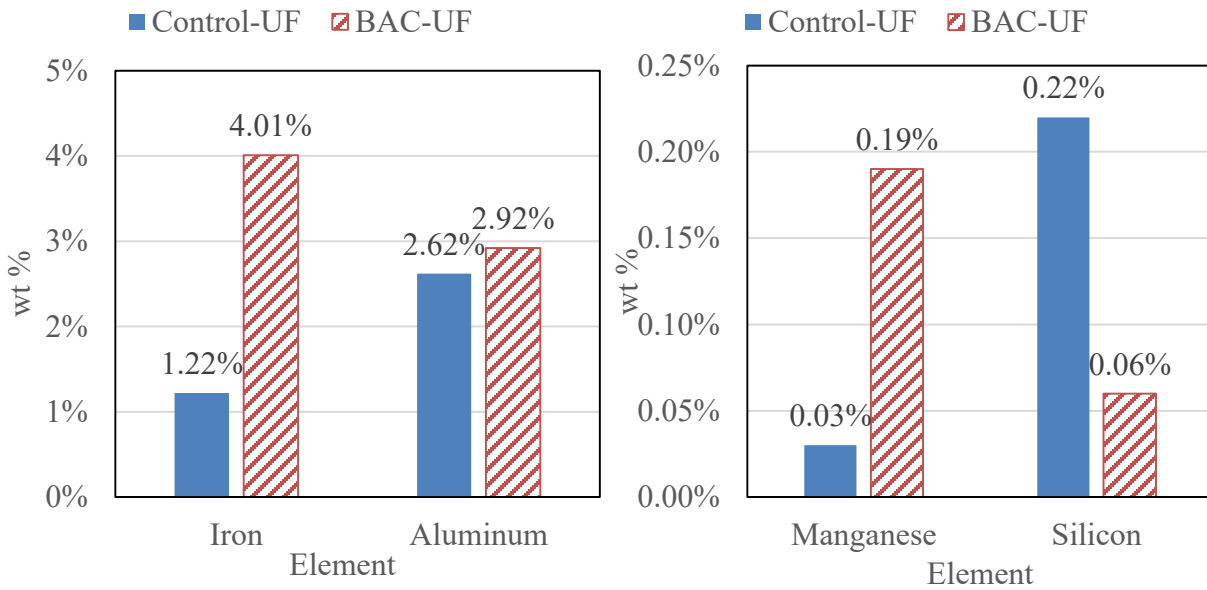
Figure 4–70 Select results of EDX analysis from the control-UF and BAC-UF
Source: Data provided by Avista Technologies

An Approach for Modeling Biofiltration Performance

In an effort to provide the water industry a simple yet practical model for predicting the performance of biofiltration pretreatment ahead of UF membrane processes, an innovative modeling approach for predicting biofiltration performance was developed. The modeling concept is based on the empirical relationship between the ratio of inorganic carbon (alkalinity) to organic carbon or substrate (DOC) and the corresponding improvement to the UF membrane's specific flux or mass transfer coefficient (MTC). Converting the alkalinity units from mg/L as $CaCO_3$ to mg/L as C, as shown in Equation 4-1, allowed for the development of a dimensionless alkalinity to substrate (ALK/DOC) ratio, which is calculated according to Equation 4-2. For the alkalinity unit conversion equation, it was assumed that the equivalent weights of carbon and calcium carbonate were 6 and 50 mg/mequivalent, respectively. The improvement to the UF membrane's MTC is calculated using the temperature corrected specific flux, previously defined in Equation 2-4, for the membrane with and without biofiltration pretreatment (see Equation 4-3).

$$Alkalinity\left(\frac{mg}{L}C\right) = Alkalinity\left(\frac{mg}{L}CaCO_3\right) \times \frac{EW_C}{EW_{CaCO_3}} \tag{4-1}$$

$$\frac{ALK}{DOC}(dimensionless) = \frac{Alkalinity(mg\ C/L)}{DOC(mg\ C/L)} \tag{4-2}$$

$$MTC\ Improvement(\%) = \frac{MTC_{biofiltration} - MTC_{control}}{MTC_{control}} \times 100 \tag{4-3}$$

Where:

$$EW_C(mg/mequivalent) = \frac{MW_C(mg/mmol)}{2(mequivalent/mmol)}$$

$$EW_{CaCO_3}(mg/mequivalent) = \frac{MW_{CaCO_3}(mg/mmol)}{2(mequivalent/mmol)}$$

MW_C = Molecular weight of carbon (12 mg/mmol)

MW_{CaCO3} = Molecular weight of calcium carbonate (100 mg/mmol)

DOC = Dissolved organic carbon concentration in the biofilter feed water (mg/L)

$MTC_{biofiltration}$ = Specific flux at 20 ^{o}C of UF with biofiltration pretreatment (gal/ft^2-day-psi at 20°C)

$MTC_{control}$ = Specific flux at 20 ^{o}C of UF without biofiltration pretreatment (gal/ft^2-day-psi at 20°C)

The empirical model was developed using experimental data retrieved from previous research studies and BAC pilot testing results from the present research. The ALK/DOC ratio of the BAC feed water and corresponding MTC improvement values for the Olinda pilot testing were averaged across the BAC evaluation phase (August 10, 2013 to December 31, 2013). Table 4-17 presents the alkalinity to substrate (ALK/DOC) ratio and MTC improvement data that was used to investigate the relationship between the ALK/DOC ratio and MTC improvement.

The relationship was examined by plotting MTC improvement versus ALK/DOC ratio. The scatter-plot analysis of the biofiltration data is illustrated in Figure 4-71. Figure 4-71 reveals that the relationship between MTC improvement and ALK/DOC ratio exhibits a parabolic shape. Thus, the biofiltration data may be fitted to a quadratic equation as defined in Equation 4-4 and displayed in Figure 4-72. For a quadratic model, boundary conditions would be defined by the range of input data, which includes ALK/DOC ratios between zero and approximately 24. Beyond an ALK/DOC ratio of 24, MTC improvement would approach a parabolic negative infinity.

Table 4–17 Biofiltration Data from Literature for Model Development

Reference[1]	Water Source	Feed Water Quality Alkalinity (mg/L CaCO$_3$)	Alkalinity (mg/L C)	DOC (mg/L)	ALK/DOC Ratio	MTC (gal/ft^2-day-psi) Control	Biofiltration	MTC Improvement
Cumming, 2015	Natural SW	3.68	0.44	3.14	0.14	-	-	4.5[2]
Wend et al., 2003	Synthetic SW	100[3]	12	4.0	3.0	0.54	0.59	8.7
Peldszus et al., 2012	Natural SW	213	26	5.8	4.4	7.6	10.4	36
Wang 2014	Natural SW	89	11	2.0	5.3	7.5	10.6	40
Duranceau & Tharamapalan, 2013	Surficial GW	166	20	2.0	10	13	20	54
Mosqueda-Jimenez & Huck, 2006	Synthetic SW	272[4]	33	2.1	16	58[5]	88[5]	52
Wei et al., 2011	Synthetic SW	200[6]	24	1.3	19	2.7	3.8	39
Basu & Huck, 2004	Synthetic SW	325	39	2.0	20	18	23	25
Lipp et al., 1998	Natural SW	250	30	1.3	23	5.2	5.7	10

(1) The data excludes studies that used water sources not directly impacted by surface water, used higher pressure NF or RO membranes, or lacked reported data to calculate either the ALK/DOC ratio or MTC improvement.

(2) The MTC improvement was calculated from the average of paired control and biofiltration MTC values not overall averages.

(3) Alkalinity level was retrieved form City of Bozeman WTP's Water Quality Report (City of Bozeman, 2014).

(4) Alkalinity level was estimated using the reported hardness concentration (283 mg/L as CaCO3) and alkalinity to hardness fraction of 0.96, which was retrieved from similar bench-scale studies performed by Basu & Huck, 2006 and Mosqueda-Jimenez & Huck, 2009.

(5) The MTC units are relative specific flux (%) as reported in research paper (Mosqueda-Jimenez & Huck, 2006).

(6) The researchers added domestic wastewater to the synthetic surface water source; therefore, the alkalinity was assumed to be approximately 200 mg/L as CaCO$_3$, which is the typical average alkalinity for domestic wastewater (Metcalf & Eddy, 2003).

Alternatively, it may be assumed that for ALK/DOC values greater than 24, the MTC improvement approaches a boundary level. This assumption may be modeled using a normal or Gaussian distribution. An example of a Gaussian distribution curve and mathematical equation is presented in Figure 4-73 and Equation 4-5.
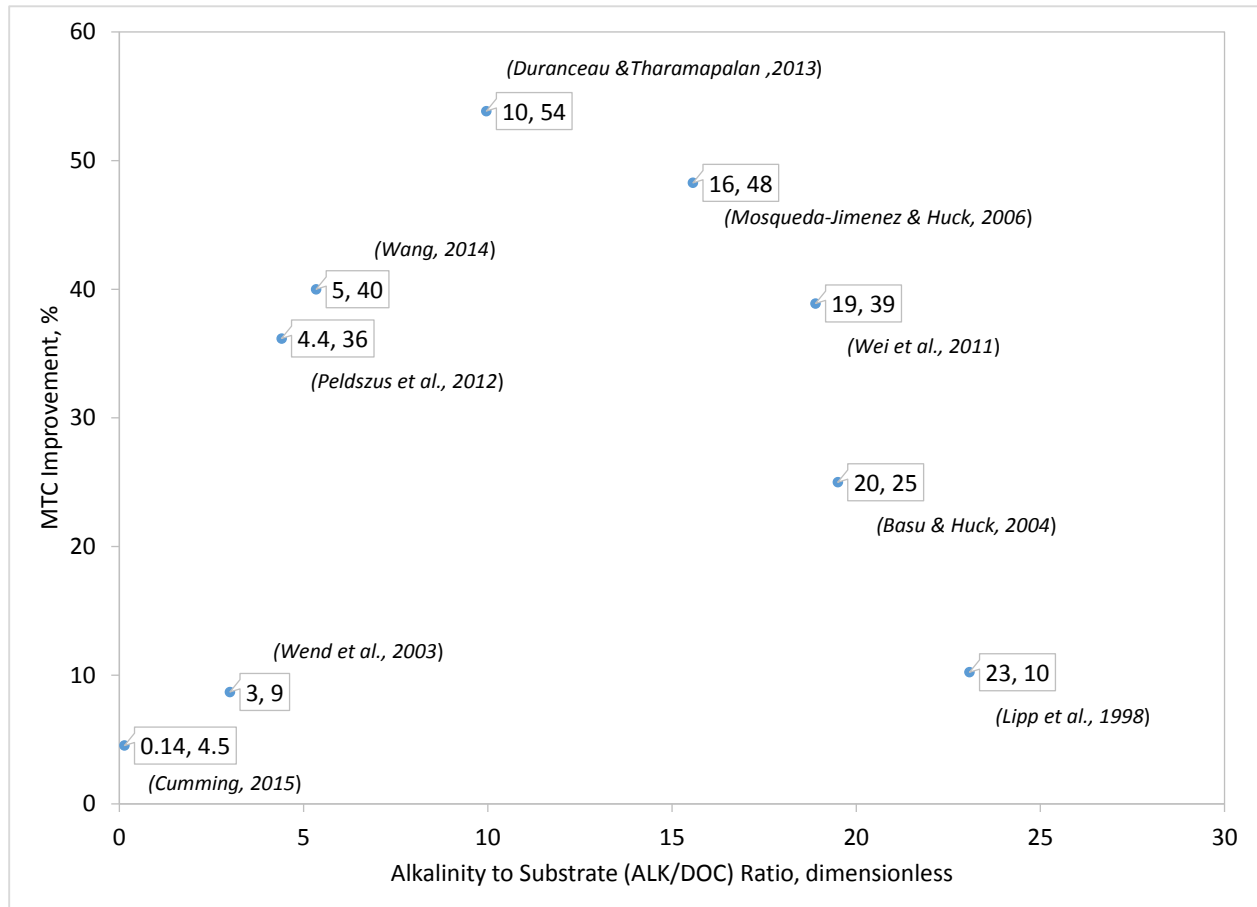
Figure 4–71 MTC Improvement versus ALK/DOC Ratio Scatter-Plot Analysis

$$MTC\ Improvement(\%) = a\left(\frac{ALK}{DOC} + b\right)^2 + c \quad \textbf{OR} \quad = c_1 + c_2\left(\frac{ALK}{DOC}\right) + c_3\left(\frac{ALK}{DOC}\right)^2$$

c

b

y-axis, dependent variable

x-axis, independent variable
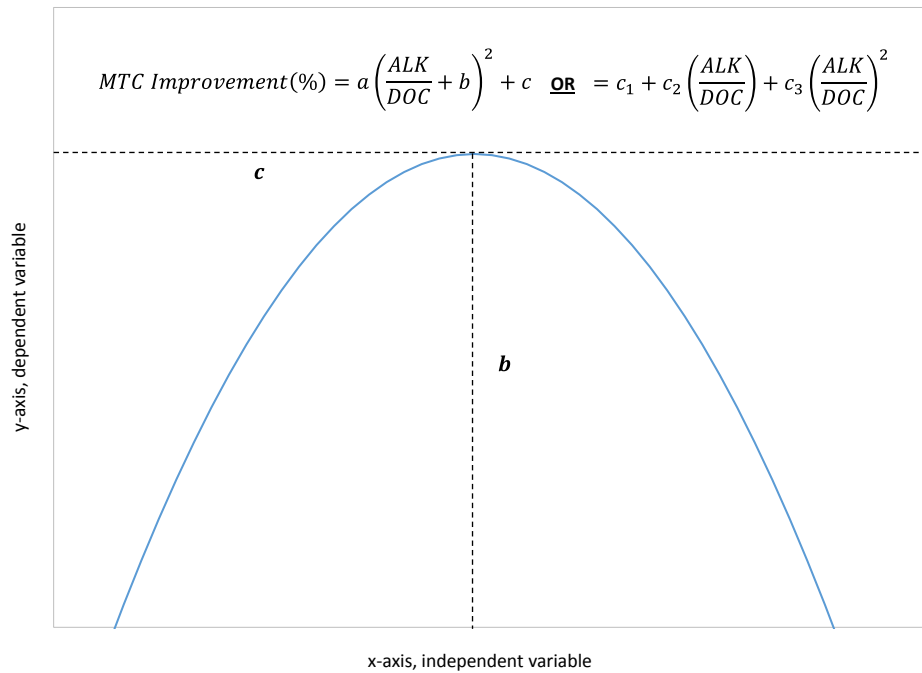
Figure 4–72 Example of Quadratic Equation

$$MTC\ Improvement(\%) = a\left(\frac{ALK}{DOC} + b\right)^2 + c = c_1 + c_2\left(\frac{ALK}{DOC}\right) + c_3\left(\frac{ALK}{DOC}\right)^2 \qquad (4\text{-}4)$$

Where:

a = Constant describing steepness of parabolic curve

b = Constant describing x-axis translation

c = Constant describing y-axis translation

c_1 = Model parameter, $c_1 = ab^2 + c$

c_2 = Model parameter, $c_2 = 2ab$

c_3 = Model parameter, $c_3 = a$
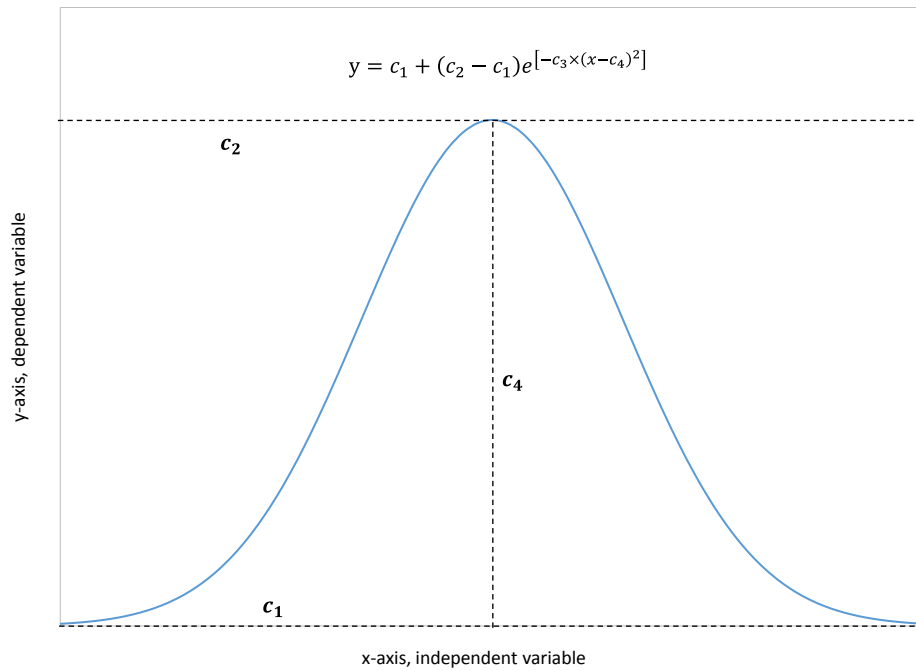
Figure 4–73 Example of Gaussian Distribution

$$MTC\ Improvement(\%) = c_1 + (c_2 - c_1)e^{\left[-c_3 \times \left(\frac{ALK}{DOC} - c_4\right)^2\right]} \tag{4-5}$$

Where:

c_1 = Model parameter describing y-axis translation

c_2 = Model parameter describing maximum y-value of curve peak

c_3 = Model parameter describing steepness of Gaussian distribution

c_4 = Model parameter describing x-axis translation

To determine whether a quadratic equation or Gaussian distribution could be used to develop a predictive model, Equations 4-4 and 4-5 were fitted against the biofiltration data using non-linear regression in Minitab®. The starting values for the model parameters (included in Table 4-18) were selected based on evaluation of Figure 4-71.

169

Table 4–18 Starting Values for Model Parameters in Minitab®

Parameter	Starting Value	
	Quadratic Equation	**Gaussian Distribution**
c_1	1	0
c_2	1	55
c_3	1	0
c_4	-	12

For the quadratic equation, starting model parameters were set to one. For the Gaussian distribution, y-axis peak, y-axis translation, x-axis translation, and curve steepness were approximated as 55, 0, and 12, and 0, respectively. After the starting parameters were selected, the Minitab® software executed the non-linear regression analysis for the quadratic equation and Gaussian distribution.

The Minitab® non-linear regression models with fitted constants are presented in Equations 4-6 and 4-7. The corresponding quadratic equation and Gaussian distribution fitted line plots for the MTC improvement versus ALK/DOC ratio is illustrated in Figure 4-74. The model statistics are summarized in Table 4-19. The complete Minitab® output summary is included in Appendix H.

$$\text{Quadratic: } MTC\ Imp. = -1.023 + 8.966 \left(\frac{ALK}{DOC}\right) - 0.3720 \left(\frac{ALK}{DOC}\right)^2 \qquad (4\text{-}6)$$

$$\text{Gaussian: } MTC\ Imp. = -36.46 + (57.26 + 36.46)e^{\left[-0.0061 \times \left(\frac{ALK}{DOC} - 12.03\right)^2\right]} \qquad (4\text{-}7)$$
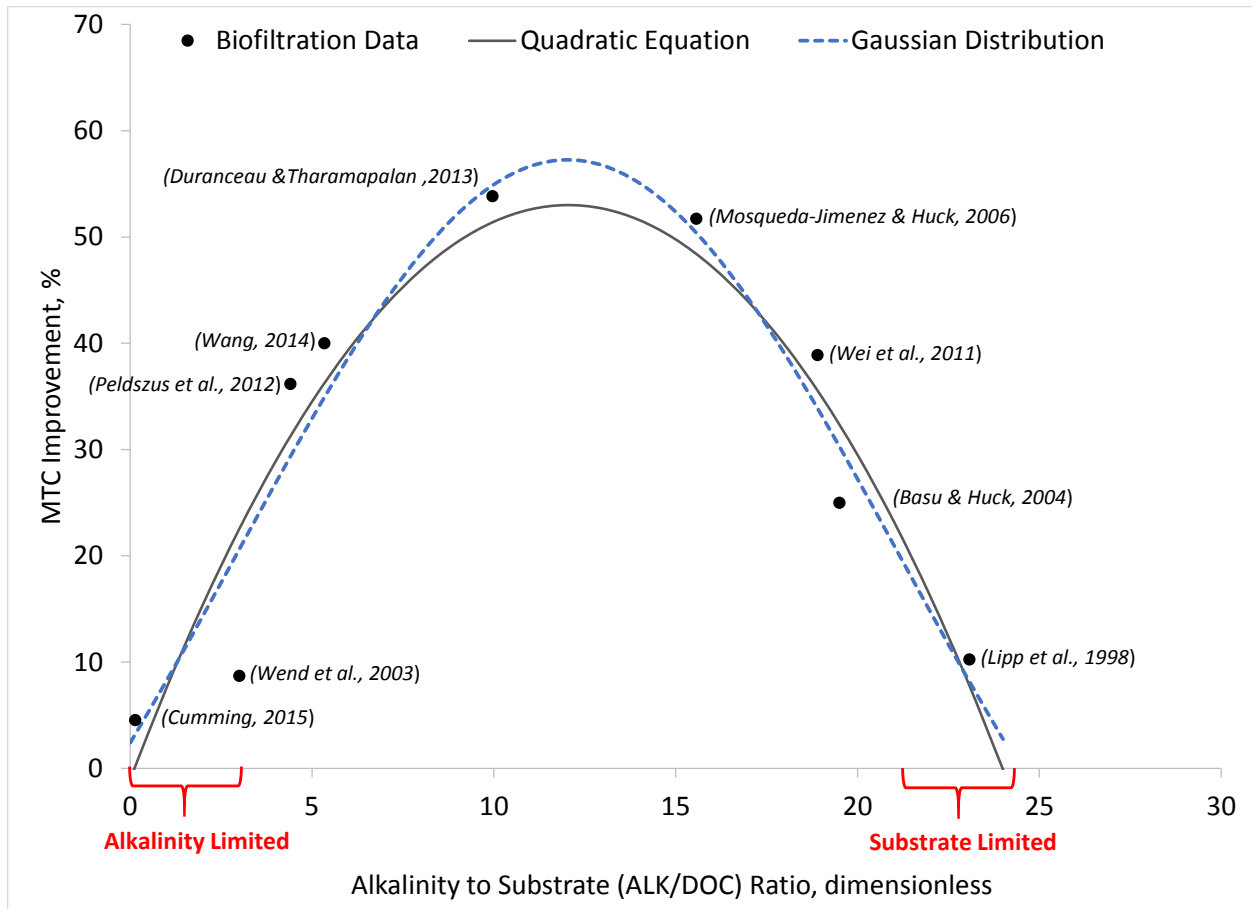
Figure 4–74 ALK/DOC versus MTC Improvement Empirical Model

Table 4–19 Minitab® Model Statistics Summary

Statistic	Value	
	Quadratic Equation	**Gaussian Distribution**
Iterations	2	11
Degrees of Freedom	6	5
Mean Square Error (MSE)	54.3	55.9
Standard Deviation (s)	7.37	7.47

As shown in Figure 4-74, both the quadratic equation and Gaussian distribution fitted models followed the data closely. The model statistics reveal that the quadratic equation had a lower MSE value of 54.3 as compared to the Gaussian distribution model, which had a MSE of 55.9. Nevertheless, the relatively low MSE values of both models confirm that the biofiltration performance correlates with the dimensionless alkalinity to substrate ratio. Hence, the empirical relationship between MTC improvement and ALK/DOC ratio can be modeled as a quadratic or Gaussian mathematical equation. For the quadratic equation, boundary conditions are defined as ALK/DOC ratios between zero and 24. For the Gaussian distribution, it appears that the MTC improvement boundary level approaches negative 36 percent for ALK/DOC ratios greater than 40.

According to both ALK/DOC models, biofiltration performance is optimized when the alkalinity to substrate ratio is between 10 and 14. Interestingly, for this data set, the ALK/DOC optimum ratio approximates twelve. Alkalinity to substrate ratios less than 10 or greater than 14 yield a diminished improvement on the membrane's MTC. MTC improvement drops below 20 percent for alkalinity to substrate ratios less than 3 or greater than 21. The water quality conditions where the alkalinity to substrate ratio is less than 3 or greater than 21 are newly defined as "alkalinity limited" or "substrate limited."

For alkalinity limited water supplies, the waters may contain adequate substrate levels, but are low in alkalinity. It is anticipated that low alkalinity water sources lack sufficient levels of polyvalent metal cations, mainly calcium and magnesium that aid in strengthening the EPS matrix necessary for the development of a robust biomass on the filter media (Lion et al., 1988; Novak et al., 1998; Zhu et al., 2010). Therefore, poor attachment and possible detachment of the biomass may increase the bioactivity in the biofilter effluent as measured by viable ATP or HPC.

LeChevallier and colleagues (1992) reported an increase in HPC bacterial counts across a biofilter treating surface water with relatively low ALK/DOC ratio of 1.2 and total hardness of 56 mg/L. It is expected that higher biological activity in the biofilter effluent would offer limited benefit to a downstream UF membrane process; however, the researchers did not evaluate a membrane process downstream of the biofilter (LeChevallier et al., 1992).

To investigate whether hardness could be used in place of alkalinity to model biofilter performance, an analogous evaluation of MTC improvement versus dimensionless hardness to DOC ratio was performed. The MTC improvement versus harness to DOC ratio scatter-plot (Figure 4-75) reveals a weak linear correlation with r-squared value of 0.46.
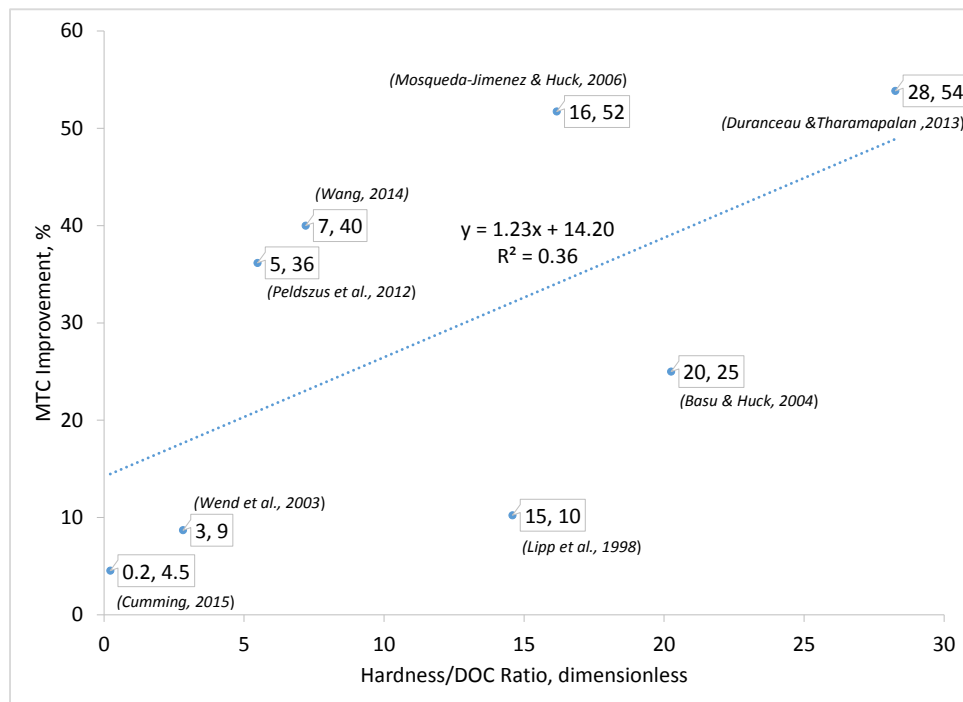
Figure 4–75 MTC Improvement versus Hardness to DOC Ratio Scatter-Plot
Note: Hardness data for Wang, 2014 reference was retrieved from Regional Municipality of Peel, 2014; hardness data was not found for Wei et al., 2011 source

The hardness to DOC ratio analysis implies that alkalinity is not simply a surrogate parameter but likely plays a direct role in chemical and biological processes within biofilters. Furthermore, the Olinda BAC pilot study incorporated pH adjustment to reach a neutral pH with caustic, yet the engineered biofiltration measure did not enhance biofilter performance. Hence, it is anticipated that both hardness (calcium and magnesium) and alkalinity (inorganic carbon) concentrations influence biofilter performance relative to UF membranes. Further research is needed to identify and understand the chemical and biological mechanisms occurring in alkalinity-limited bio-stabilization. Nevertheless, the results from the present BAC pilot study document for the first time the limitation of biofilters treating low alkalinity surface water sources ahead of UF membranes.

In addition to alkalinity limited constraints, biofiltration processes treating waters rich in alkalinity but poor in substrate would not provide sufficient benefit to downstream UF membranes. Under the substrate limited water quality condition there is not enough carbon or energy source ("food") for microorganisms to sustain their metabolic processes, as has been previously demonstrated by LeChevallier (1991) and Metcalf and Eddy (2003).

Based on the concept of alkalinity or substrate limited water supplies, the ALK/DOC model provides a method for optimizing biofilters by targeting the ALK/DOC ratio that maximizes improvement on the membrane's MTC. Generally, ALK/DOC ratios between 5 and 20 are expected to yield between 30 to 57 percent improvement on the membrane MTC. If the feed water quality falls out of the 5 to 20 ALK/DOC range, the feed water may be supplemented with either alkalinity (bicarbonate) or substrate (acetic acid) to achieve adequate biofilter performance.

While the models cannot be fully validated due to the absence of additional data, the relatively low MSE values indicate that the models are a good fit for the data. Additionally, predicted versus actual scatter-plots of the MTC improvement data for the quadratic and Gaussian models are presented in Figure 4-76. The scatter-plots reveal a linear fit with r-squared values of 0.88 and 0.89 for the quadratic and Gaussian models, respectively. The predicted versus actual analysis supports that the ALK/DOC empirical models provide a promising foundation for future researchers to validate and refine the models. Further research, particularly at low and high ALK/DOC ratios is needed to better define the MTC improvement behavior near the "tails" or boundaries of the models. Nevertheless, both ALK/DOC models are expected to provide a practical approach for identifying alkalinity or substrate limitations and optimizing biofilter performance.
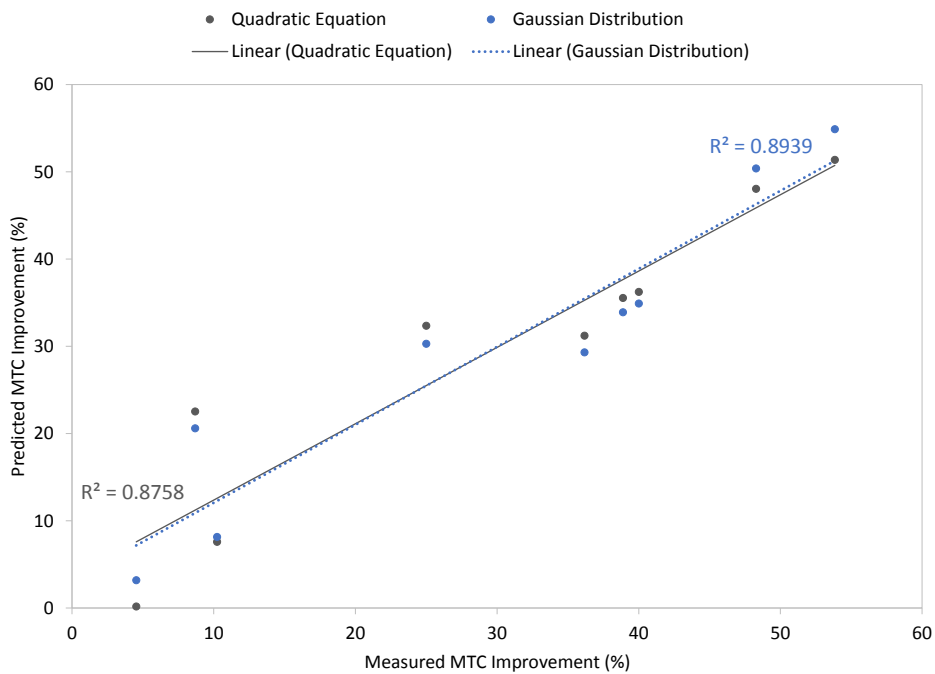
Figure 4–76 Predicted versus Actual MTC Improvement

Addressing the Notice of Retraction of Wei et al., 2011 Reference

After development of the biofiltration models defined in Equations 4-6 and 4-7, IEEE (2015) released a notice of retraction for the Wei et al. (2011) reference. The Minitab® non-linear regressions were re-evaluated without the Wei et al. (2011) data reference. The model parameters and statistical outputs for the quadratic equation and Gaussian distribution are included in Appendix H. The Minitab® regression results revealed that without the Wei et al. (2011) reference the fitted quadratic equation had a MSE of 62.4 and the fitted Gaussian distribution had a MSE of 59.8. While each model similarly predicts biofiltration performance as was previously defined in Equations 4-6 and 4-7 respectively, the Gaussian distribution model revealed a better statistical fit to the data without the Wei et al. (2011) reference.

Conceptual Economic Evaluation

The MIEX®, GAC adsorption, and BAC pretreatment alternatives were further evaluated based on qualitative non-cost considerations and conceptual opinions of probable construction and operating costs. The non-cost considerations provide a means of comparison based on water quality, regulation compliance, and operational performance. Additionally, the conceptual cost opinions provide a means of economical comparison based on vendor based estimates, experience with analogous systems, USEPA cost curves, and literature citations.

Non-Cost Evaluation

The purpose of analyzing the pretreatment alternatives based on non-cost considerations is to aid in identifying the process that best meets regulatory, water quality, and operating goals. The pretreatment options were compared to the status quo (existing system condition) according to the following conceptual evaluation strategies.

- Advantages and Disadvantages

- Water Treatment Performance

- Non-Cost Criteria Matrix

- Conceptual Risk Assessment Matrix

The non-cost evaluation was developed based on the understanding of the alternative technologies and the site-specific issues associated with the Upcountry water systems. The advantages and disadvantages of the alternatives and status quo are outlined in Table 4-20.

The water treatment performance evaluation consists of rating each alternative as either not effective, partially effective, or effective treatment against major microbial and organic contaminants. The treatment ratings for the alternatives and status quo are presented in Table 4-21. The water quality treatment performance evaluation revealed that the UF process of the status quo is the most effective with respect to microbial treatment, and the MIEX® and GAC pretreatments are the most effective for organic carbon and DBP control. For the Olinda water quality conditions, the BAC pretreatment offers partial treatment effectiveness for microbial and organic removal. Therefore, for effective microbial and organic treatment a combination of the existing system and MIEX® or GAC would be the preferred integrated treatment process.

177

Table 4–20 Advantages and Disadvantages of Treatment Strategies

Treatment Strategies	Advantages	Disadvantages
Status Quo – Existing System	• Maintain DBP compliance with chloramine disinfection • No additional water treatment costs	• Membrane fouling related to floc carry over • Nitrification events trigger distribution system flushing • Lower system cannot supplement Upper system during drought conditions
Install MIEX® High Rate system pretreatment of Olinda raw water ahead of coagulation	• Reduce dissolved organic precursors • Meet DBP regulations on free chlorine • Reduce ACH coagulant dose requirements and associated chemical costs	• Capital costs • Salt required for resin regeneration • Resin supplementation • Brine waste disposal • Complex operation and maintenance requirements • Possible 24 hour staffing requirement • Frequent transportation of salt, resin, and brine through narrow residential roadway (*City of St. Could, 2011*; *Palm Beach County, 2014*)
Install GAC contactor column post-coagulation/pre-filtration treatment of Olinda settled water	• Reduce dissolved organic precursors • Meet DBP regulations on free chlorine • Further reduce organic and particulate loading on the UF membranes, which may reduce UF backwashing and chemical cleaning frequencies, and increased productivity • Ease of operation and maintenance	• Capital costs • High GAC replacement frequency and costs due to rapid exhaustion of the GAC media • Pilot testing revealed a monthly GAC replacement frequency • Frequent transportation of spent and fresh GAC through narrow residential roadway
Install BGAC filtration post-coagulation/pre-filtration treatment of Olinda settled water	• Reduce DBP formation potential through natural bacterial degradation of dissolved organic carbon • Reduce particulate and organic fouling of UF membranes • Extend the GAC bed life and reduce change-out frequency by biological regeneration • Ease of operation and maintenance	• Capital cost • Pilot study demonstrated that BGAC filtration treatment did not significantly extend the GAC bed life nor reduce the DBP formation potential of the chlorinated Olinda finished water

Table 4–21 Conceptual Evaluation of Treatment Performance

Water Quality→ Treatment↓	**Microbial**				**Organic**			
	Bacteria	Virus	Turbidity	Giardia/ Crypto	HAA$_5$ Precursor	TTHM Precursor	TOC	Color
Status Quo								
Coagulation/ Flocculation/ Basin[1]	◑	○	◑	○	◑	◑	◑	●
UF	●	◑	●	●	○	○	○	○
Chloramines	●	●	○	○	◑	◑	○	○
Possible Pretreatments								
MIEX®	○	○	○	○	●	●	●	●
GAC	◑	○	◑	○	●	●	●	●
BGAC	◑	○	◑	○	○	○	○	◑

○ not effective treatment
◑ partially effective treatment
● effective treatment

(1) The basin is intended to serve as a clarifier; however, the basin is not designed to provide clarification as no sludge handling facility exists.

The descriptions and impact factors for the selected non-cost criteria are defined in Table 4-22. The non-cost criteria matrix evaluation assigns a numerical ranking system for each alternative with respect to how effective the treatment is the four major areas of consideration—sustainability, operability, reliability and constructability. Each criteria has an impact factor for the entire category and sub-categories for which each technology is assigned a score. The technology that achieves the highest score is considered to be the preferred process with respect to the specified non-cost criteria. The scores for each pretreatment alternative were selected based on the performance of each alternative and its applicability to the unique conditions of the Upcountry water system.

Table 4–22 Non-Cost Criteria Evaluation

Criteria	Sub-Criteria	Impact Factor Weight (%)	Description	Scale	
				Lowest= 1	Highest = 5
Sustainability	Public Perception Chemical Efficiency Energy Efficiency Production Efficiency	12.3%	✓ Public perception issues ✓ Chemical and energy usage ✓ Water loss	Lowest public acceptability and process efficiency	Highest public acceptability and process efficiency
Operability	Residuals Disposal	8.7%	✓ Residual type and quantity ✓ Ease of disposal	Highest residual quantity and disposal challenges	Lowest residual quantity and disposal challenges
	Staffing Requirements	9.8%	✓ Operator training and staffing	Highest training and staffing requirements	Lowest training and staffing requirements
	Operator Safely	18.8%	✓ Operational safety risks	Highest risk	Lowest risk
	Maintainability	11.9%	✓ Operation and maintenance requirements	Most challenging to operate and maintain	Easiest to operate and maintain
Reliability	Proven Technology	10.1%	✓ Effective performance proven with previous successful installations	Least references and installation	Most references and installations
	Flexibility/ Water Quality	20.2%	✓ Meeting current and future regulations ✓ Variation in water quality	Lowest probability of meeting regulations	Highest probability of meeting regulations
Constructability	Flexibility Footprint	8.2%	✓ Expandability ✓ Environmental impacts ✓ Footprint requirement	Lowest flexibility of construction and expandability and highest footprint	Highest flexibility of construction and expandability and lowest footprint

The non-cost consideration results, presented in Table 4-23, found that the highest ranked pretreatment alternative based on non-cost criteria was GAC followed by MIEX® and BAC. The GAC alternative achieved the highest non-cost criteria score because of the high DBP precursor removal efficiency and relatively easy operation and maintenance requirements. The MIEX® received a lower score due to the intensive operation and maintenance requirements and the need to dispose of a concentrated brine waste stream. The BAC received the lowest non-cost criteria score because of the low treatment efficiency relative to regulated DBP formation potential.

The conceptual risk assessment is displayed in Figure 4-77. For the conceptual risk analysis, the alternatives were assigned a grid (x,y) score based on the impact on Olinda WTP costs (x) and probability of success with DBP compliance (y). The status quo provides the baseline for comparison and was assigned a grid score of (5,5). The pretreatment alternatives were assigned a (x,y) score based on the treatment efficiency and relative impact on water treatment costs. The interpretation of the (x,y) score depends on the grid quadrant location. Alternatives that fall on the status quo lines have similar impacts as the status quo. The preferred alternative would be located in the fourth quadrant, in which effective DBP control is achieved at lower costs.

The risk assessment revealed that the MIEX® and GAC alternatives fell in the first quadrant, while the BAC alternative fell in the second quadrant. Based on the relative impacts on DBP control and treatment costs, the MIEX® alternative would achieve DBP compliance with free chlorine disinfection at the lowest impact on Olinda WTP costs. The GAC alternative offers a high probability of success relative to DBP compliance with free chlorine at the highest impact on Olinda WTP costs. On the other hand, the BAC would yield a low probability of success relative to DBP compliance with free chlorine at a high impact to Olinda WTP costs.

Table 4–23 Non-Cost Considerations Matrix

Consideration	Impact Weight Factor[1]	Alternative Score[3]					
		GAC		MIEX®		BAC	
		PS[2]	WS[3]	PS[2]	WS[3]	PS[2]	WS[3]
Sustainability[4]	12.3%	4	0.10	3.5	0.09	4.25	0.10
Public Perception		5		4		3	
Chemical Efficiency		1		1		4	
Energy Efficiency		5		5		5	
Production Efficiency		5		4		5	
Operability							
Residuals Disposal	8.7%	1	0.02	1	0.02	2	0.03
Staffing Requirements	9.8%	5	0.10	1	0.02	5	0.10
Operator Safety	18.8%	4	0.15	4	0.15	5	0.19
Maintainability	11.9%	1	0.02	2	0.05	5	0.12
Reliability							
Proven Technology	10.1%	5	0.10	5	0.10	2	0.04
Flexibility/Water Quality	20.2%	5	0.20	5	0.20	1	0.04
Constructability[4]	8.2%	3.5	0.06	4	0.07	3.5	0.06
Flexibility		4		5		4	
Footprint		3		3		3	
Total Score [3]			**0.75**		**0.69**		**0.68**

(1) Non-cost considerations are assigned an impact weight factor.

(2) Processes are ranked with a point score (PS) from 1 to 5 with 5 being the best.

(3) The normalized weighted score (WS) is the product of the impact weight factor (%) and the point score divided by 5 (IF x PS / 5).The preferred process is the one with the highest total score (closest to 1).

(4) The average PS of the respective sub-considerations is used to calculate the normalized WS.
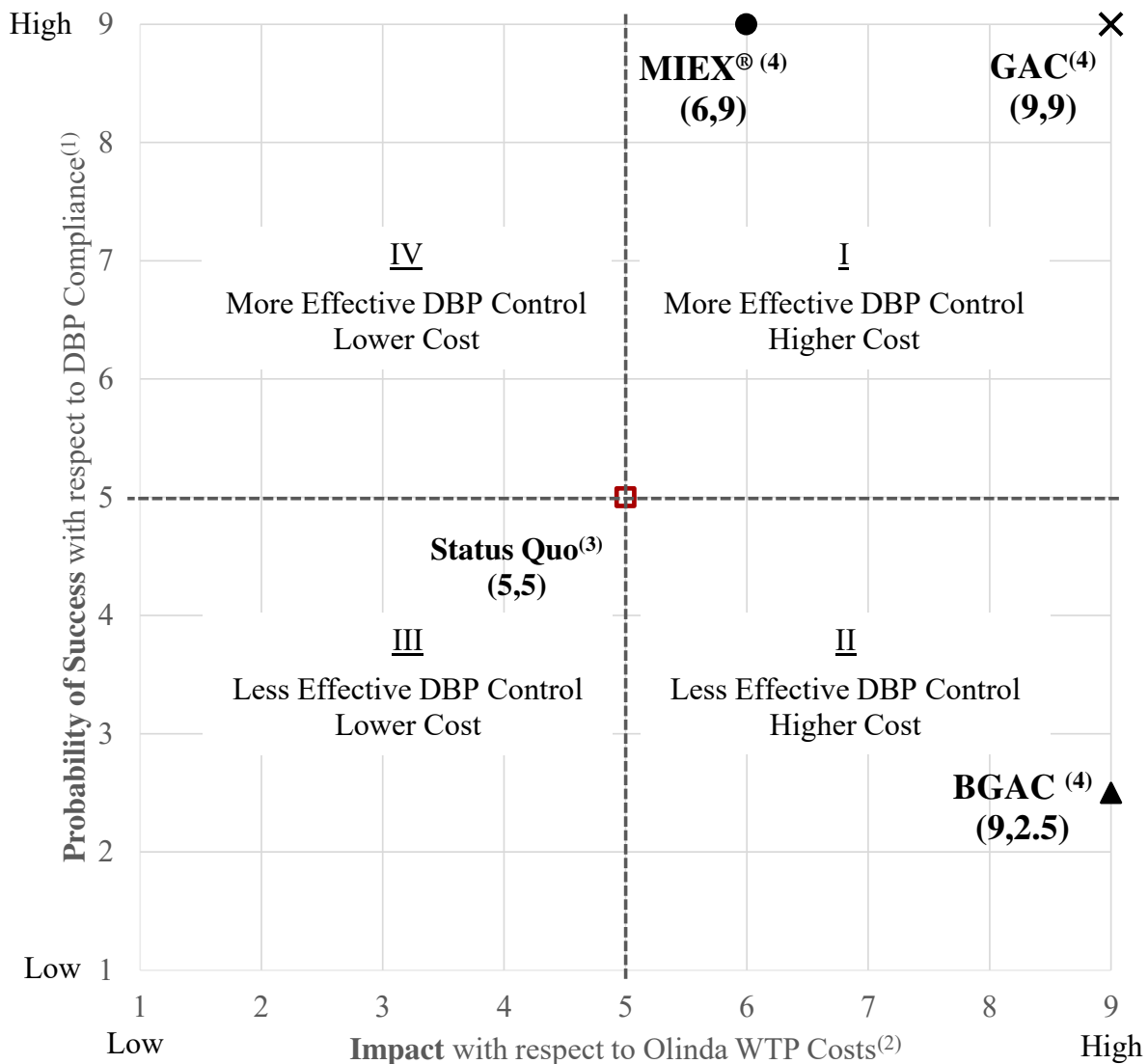
Figure 4–77 Conceptual Risk Assessment

(1) Probability of success ranked from lowest probability (1 is least favorable) to highest probability (9 is best) of DBP compliance in the Upper Kula distribution system.
(2) Impact on Olinda WTP operation & maintenance and water supply costs ranked from lowest cost impact (1 is best) to highest cost impact (9 is lease favorable). The scores are linearly correlated to the conceptual opinion of amortized total costs of Table 4-24.
(3) Ranked based on maintaining chloramines in Upper system and free chlorine in the Lower systems.
(4) Ranked based on uniform free chlorine disinfection throughout the Upcountry system.

Conceptual Opinion of Probable Construction and Operating Costs

The conceptual cost opinions for the MIEX®, GAC, and BAC pretreatment alternatives were developed based on a 2.7 million gallon per day (MGD) treated water capacity. USEPA cost curves, literature citations, vendor based estimates and experience with analogous systems were used to develop conceptual cost opinions (USEPA, 1979; 1979; MWH, 2005; Lekven, 2011; City of St. Cloud, 2011; Orica Watercare, 2011; Sharma et al., 2011; County of Maui, 2012; 2013; Palm Beach County, 2014). The conceptual cost opinions are intended to be used for comparison purposes only, as they do not represent design-based engineering estimates. In addition, conceptual operating cost opinions were based on process operation costs only. Labor, delivery charge, and debt service were not included in the operating cost calculations. Appendix J presents relevant assumptions and calculations utilized to determine the conceptual cost opinions.

The conceptual cost opinions with non-cost considerations are summarized in Table 4-24. Of the pretreatment alternatives (not considering the status quo), the more economically feasible pretreatment option would be installing a MIEX® high rate system for $1.86/1000 gallons. The GAC and BAC alternatives would require a significant financial expenditure of $4.45/1000 gallons because of the high cost of activated carbon replacement, which is required to maintain effective DBP control with free chlorine disinfection. While the MIEX® alternative offers a more economically favorable option over the GAC and BAC alternatives, the MIEX® system has limited applicability in the Upcountry water system because of the operational and brine waste disposal challenges. Because of the limited applicability of MIEX® and high cost of GAC and BAC, the conceptual economic evaluation revealed that the status quo is the preferred engineering alternative for the Olinda WTP and Upcountry water system.

Table 4–24 Conceptual Evaluation of Olinda Water Treatment and Management Options

Description of Alternatives	Conceptual Opinion of Probable Construction Cost[1] ($)	Conceptual Opinion of Probable Operating Cost[1] ($)	Conceptual Opinion of Amortized Total Cost[2] ($/1000 gal)	Non-Cost Consideration Normalized Weighted Score (Highest is preferred)	Conceptual Risk Score (x,y) (Lowest x and highest y value is preferred)	Subjective Advantages	Subjective Disadvantages
Status Quo	0	1,080,000	1.10	Baseline (N/A)	Baseline (5,5)	• No additional water treatment costs	• Does not address existing operational challenges
Install MIEX® High Rate System at Olinda WTP	4,890,000	1,460,000	1.86	0.690	(6,9)	• Meet DBP regulations with free chlorine disinfection	• Difficult to operate and maintain • Resin and salt costs • Brine generation and disposal costs
Install GAC at Olinda WTP	2,780,000	4,170,000	4.45	0.748	(9,9)	• Meet DBP regulations with free chlorine disinfection	• High GAC replacement cost due to short GAC bed-life
Install BAC at Olinda WTP	2,780,000	4,170,000	4.45	0.683	(9,2.5)	• Reduce UF membrane fouling • Ease of operation	• Not effective in controlling DBP formation potential

(1) The US EPA cost curves, literature citations, vendor based estimates and experience with analogous systems were used to develop conceptual opinions of probable costs (Lekven, 2011; City of Sanford, 2013, County of Maui, 2012, 2013 & 2014; MWH, 2005; Orica Watercare, 2011; Sharma et al., 2011; US EPA, 1979 & 1979).

(2) The conceptual opinions of probable costs calculations and relevant assumptions are included in the Appendix J.

CHAPTER 5. SUMMARY AND CONCLUSIONS

In 2012, the County partnered with the WRF and UCF in a tailored collaboration research project at the Olinda WTP to address water quality and operational challenges that are due in part to the difficulties of coagulating low alkalinity, organic-laden surface water prior to UF membrane filtration. To help identify an effective pretreatment strategy for the UF membrane process, MIEX®, GAC adsorption, and BAC filtration were evaluated. Of the pretreatment alternatives, biofiltration has been recently identified by researchers as an option for controlling UF membrane fouling. Consequently, the main objective of the research was to contribute to the body of knowledge with regards to biofiltration pretreatment for UF membrane processes. Specifically, three central research questions were addressed:

1. How is biofiltration performance impacted by low alkalinity water sources?
2. What are the treatment impacts and possible benefits of integrating biofiltration within conventional-UF processes?
3. Can a new modeling framework be developed to offer a practical approach for predicting biofilter performance ahead of UF membrane processes?

To propose answers to these questions, biofiltration pretreatment was evaluated holistically by examining source water chemistry and extending the analysis into the drinking water distribution system. Waikamoi watershed quality was profiled to understand the chemistry of the water as it travels from the flume to the Olinda WTP. Additionally, MIEX®, GAC adsorption, and BAC filtration were compared at the pilot-scale in terms of operational requirement, DOC removal, and improvement to downstream UF process operation. UF performance was determined by

186

calculating the percent MTC improvement relative to the existing conventional-UF process that served as the control. The pretreatment alternatives were further evaluated based on cost and non-cost considerations.

Compared to MIEX® and GAC, which achieved effective DOC removal (40 and 40 percent, respectively) and MTC improvement (14 and 30 percent, respectively), BAC achieved the lowest overall DOC removal (5 percent) and MTC improvement (4.5 percent). While MIEX® relies on anion exchange and GAC relies on adsorption to target DOC removal, biofiltration uses microorganisms attached on the filter media to remove biodegradable DOC. Based on the BAC results, two mathematical models were developed that allow for a predictive means to optimize operation of biofiltration prior to UF membrane processes treating surface water.

From the experimental data, one could conclude that optimized biological pre-stabilization prior to UF and chlorination will resolve biological fouling problems. Nevertheless, the total effect of pretreatment must be evaluated. Although biofiltration shows promise and appears to be a viable alternative, bio-stabilizing ahead of a UF process may not provide sufficient DBP precursor removal. Also, AOC was not evaluated in the study as chlorine was the target disinfectant. While monochloramine may be the disinfectant of economic choice to provide a disinfection residual for high TOC water supplies, it may not provide the desired disinfection effectiveness and its use may result in the formation of DBPs that may come into regulation in the future.

<u>Surface Overland Flow Water Quality Analysis</u>

The headwaters of the Waikamoi watershed contained upwards of 10 mg/L of DOC at a pH of approximately 4.0 pH units; however, the ATP levels were typically less than 250 pg/mL. These findings were unlike the reservoirs that contained the greatest biological ATP levels, upwards of 500 pg/mL at a pH of about 6.0 pH units and DOC level of approximating 6.5 mg/L. Furthermore, the rainy season was characterized by higher turbidity, higher DOC, and higher ATP content as compared to the drought condition.

The watershed quality results reveal that the inorganic, organic, and biological composition of the source water is most influenced by system elevation, reservoir storage condition, and weather condition. Generally, the highest watershed locations contained elevated DOC levels and low pH units; the reservoirs contained the highest biological ATP levels; and rainy weather conditions experienced higher turbidity, DOC, and ATP levels. Establishing the watershed quality trends offered useful insights for identifying watershed management strategies that would help facilitate treatment at the Olinda WTP.

<u>Confirmation of Existing Conventional-UF Process Operations</u>

Based on the findings from the pilot and full scale monitoring and jar testing results, the following conclusions are offered.

- On average, the full-scale Olinda WTP's coagulation process reduced the raw water turbidity, color, UV 254, and DOC by 79, 94, 83, and 59 percent, respectively.

- Jar testing results at varying ACH doses and pH units revealed that the average optimum turbidity, color, UV 254, and DOC removals were 64, 95, 87, and 62 percent, respectively.

- Comparisons between the full-scale and jar testing results revealed that Olinda's coagulation process is operating near optimum particulate and organic removals. Therefore, additional DOC removal treatment is necessary to achieve greater DBP precursor removal.

- The Olinda chlorinated TTHM and HAA_5 formation potential exceeded the regulatory MCLs. The DBP results further support the need for additional DBP precursor treatment to allow for conversion of the disinfectant from monochloramine to free chlorine.

- Olinda raw and coagulated water EEM matrix diagrams indicated that the dissolved organic matter (DOM) was primarily comprised of hydrophobic fulvic and humic organic acids and aromatic protein-like organics. Fulvic and humic acids are known precursors to DBP formation and contribute to UF membrane fouling. Protein-like organics also contribute to UF membrane fouling. Furthermore, DOM supplies the substrate for biological metabolic processes, which can also aggravate membrane fouling.

- Although the pilot and full UF membrane processes did not operate at similar TMP and specific flux magnitudes, they shared similar fouling trends and produced filtrates with comparable water quality. Therefore, the UF pilot provided an acceptable control condition for evaluating the impact of pretreatment on UF operating performance.

- Pilot testing and subsequent membrane autopsies confirmed that alum floc carryover impacted process operations and was found to be a more significant contributor to UF productivity decline than other identified foulants.

189

- Typically, source water turbidity averages about 3.2 ntu and settled water turbidity averages approximately 0.8 ntu. However, the Olinda WTP experienced settled water turbidity upwards of 3.0 ntu during drought condition when the full-scale plant was intermittently operated. Correspondingly, DOC removal effectiveness dropped to 45 percent during drought condition. Thus, intermittent full-scale plant operation during drought was found to be detrimental to treatment performance.

Ultrafiltration Pretreatment Assessment

A summary of the MIEX®, GAC adsorption, and BAC pretreatment performance is presented in Table 5-1. Of the pretreatment alternatives evaluated, GAC adsorption achieved the greatest overall improvement in specific flux. The MIEX® system was a close second with a 14 percent average improvement in the specific flux. Both GAC and MIEX® achieved similar DBP formation removal efficiency. BAC pretreatment achieved the lowest improvement in specific flux and reduction in regulated DBP formation.

Table 5–1 MIEX®, GAC Adsorption, and BAC Pretreatment Performance Summary

Pretreatment	Improvement		
	Specific Flux	TTHM	HAA5
MIEX®	14%	54%	36%
GAC Adsorption[1]	30%	54%	40%
BAC	4.5%	8%	9%

(1) DBP removals approximated based on the average between GAC start-up and transition.

Based on the pretreatment water quality, operation, economic, and UF membrane analysis, the following conclusions were formulated.

MIEX® High Rate System Pretreatment

- The MIEX® pilot required intensive operation and maintenance activities.
- The MIEX® pilot experienced frequent pilot shut-downs that were inadvertently caused by: drought impacting operation flexibility, paint chips in the resin, irregularities with the software settings, interruption of the regeneration cycle, conductivity probe malfunction, pump failure, and power outages.
- On-site space constraints limited the settling rate of the of the coagulation pilot. Therefore, the coagulation pilot was operated as a direct coagulation pretreatment process.
- Once continuous operation of the MIEX®, coagulation, and UF membrane pilots was established, MIEX® pretreatment was able to be assessed for treatment effectiveness.
- MIEX® pretreatment reduced the downstream ACH coagulant dose by 57 percent.
- The MIEX® and coagulation pretreatment increased the average operating specific flux by 14 percent as compared to coagulation and clarification pretreatment. The improvement in membrane productivity was attributed to reduction in DOC and pin floc loading to the UF membrane.
- The MIEX®-UF process reduced the average four-day TTHM and HAA$_5$ formation potential to 65 µg/L and 33 µg/L. Based on the simulated DBP results, the MIEX® pretreatment effectively lowered the chlorinated TTHM and HAA$_5$ formation potential below the 80 µg/L and 60 µg/L MCL.

- The carry-over of permeable floc aggregates from the MIEX® with direct coagulation pretreatment contributed to the formation of a protective cake layer on the membrane. To remove the cake layer before irreversible compaction, membrane operation required a 10 minute backwashing frequency. A 10 versus 20 minute backwashing frequency reduced the membrane recovery from 89 to 82 percent.

- The Evoqua membrane autopsy results confirmed that the major components of the membrane foulant material were aluminum, iron, and organic matter.

GAC Adsorption Pretreatment

- GAC pretreatment required few operation and maintenance activities, which mainly consisted of filter backwashing.

- On average, GAC removed 50 and 40 percent of the feed water turbidity and DOC.

- At pilot-start up, GAC adsorption reduced the four-day TTHM and HAA_5 formation potential below the regulatory 80 and 60 µg/L MCLs with free chlorine disinfection.

- GAC pretreatment improved UF specific flux rate by 30 percent. The increase in specific flux was accompanied by a reduction in the membrane fouling trend and chemical cleaning frequency. The observed enhancement in UF operating performance was most likely due to a reduction in feed water turbidity and DOC.

- GAC adsorption capacity was exhausted in about 60 days of filtration run time. Effective DBP precursor (DOC) removal is expected to continue through approximately 45 days of filtration, after which the reduction in DOC would likely not be sufficient.

BAC Pretreatment

- BAC operation and maintenance activities consisted of filter backwashing, orthophosphate injection for nutrient enhancement, and sodium hydroxide chemical feed injection for pH adjustment.

- Engineered BAC pretreatment demonstrated evidence of biological DOC degradation, manganese oxidation, and turbidity removal. On average, the BAC filter reduced the inlet DOC, turbidity, and manganese levels by 11, 8, and 20 percent.

- BAC pretreatment lowered the four-day TTHM and HAA$_5$ formation potential by approximately 8 and 9 percent. However, the reduction in chlorinated DBP levels was not sufficient to achieve regulatory compliance.

- By dampening the spikes in settled water turbidity and DOC concentration, BAC pretreatment reduced the membrane CIP frequency and increased the operating specific flux by about 4.5 percent, on average.

- Intermittent full-scale plant operation during drought was found to correspond to spikes in plant settled water turbidity upwards of 3 ntu. This change in plant settled water quality that supplied the BAC pilot contributed in part to a decrease in the BAC treatment effectiveness relative to turbidity and DOC removal.

- The Avista autopsy results confirmed that aluminum, iron, and organic matter contributed to membrane fouling.

An Approach for Modeling Biofilter Performance

By combining the BAC results with findings from previous studies, two empirical models were developed for predicting the performance of biofiltration pretreatment for UF membrane processes. The empirical models describe the relationship between the alkalinity to substrate (ALK/DOC) ratio and the corresponding improvement of the UF membrane's MTC. Based on the empirical modeling results, the following conclusions were developed.

- For surface water sources, MTC improvement can be modeled as a quadratic or Gaussian distribution function of the ALK/DOC ratio.

- While the models cannot be fully validated due to the absence of additional data, the relatively low MSE values of 54.3 and 55.9 for the quadratic and Gaussian distribution models, respectively, indicate that both models provide a good fit for the data.

- According to both the quadratic and Gaussian distribution ALK/DOC models, biofiltration performance is optimized when the alkalinity to substrate ratio is between 10 and 14. Alkalinity to substrate ratios less than 10 or greater than 14 yield a diminished improvement on the membrane's MTC.

- The surface water quality conditions where the alkalinity to substrate ratio is less than 3 or greater than 21 are newly defined as "alkalinity limited" or "substrate limited."

- For alkalinity limited water supplies, waters may contain adequate substrate levels, but are low in alkalinity. On the other hand, substrate limited water sources are rich in alkalinity but poor in substrate.

- Based on the concept of alkalinity or substrate limited water supplies, the ALK/DOC empirical models provide a practical method for optimizing biofilters by targeting the

ALK/DOC ratio that maximizes improvement on the membrane's MTC. Generally, ALK/DOC ratios between 5 and 20 are expected to yield between 30 to 57 percent improvement on the MTC.

Conceptual Economic Evaluation of Ultrafiltration Pretreatment Alternatives

Based on the conceptual economic analysis, the following conclusions were formulated.

- The MIEX® pretreatment alternative would provide effective DBP precursor treatment at a conceptual cost opinion of $1.86/1000 gallons. However, the applicability of installing the MIEX® system at the Olinda WTP and Upcountry water system is limited by intensive operation and maintenance activities and the absence of a feasible method for disposing of the aqueous brine waste stream.

- The GAC pretreatment option offers effective DBP precursor treatment with low operation and maintenance requirements. However, the GAC alternative would require an economic expenditure of $4.45/1000 gallons because of the high GAC replacement frequency.

- While the BAC pretreatment reduces UF membrane fouling, the BAC pretreatment would not be effective in controlling DBP formation potential. Controlling regulated DBPs would require the operation of the activated carbon in the adsorption mode, which translates to an estimated conceptual cost opinion of expenditure of $4.45/1000 gallons.

CHAPTER 6. RECOMMENDATIONS

To provide value to researchers and the professional water community, the following recommendations are offered.

With respect to source water quality monitoring:

- The County should consider placing high elevation source intakes temporarily offline during the elevated DOC seasons (rainy conditions) to help dampen the organic load to the Olinda WTP.

- The County operations staff can anticipate the use of higher ACH coagulant doses during and after rain events due to higher organic and turbidity levels in the source water.

- The biological activity and leaching of metals in surface water reservoirs may be reduced by implementing a sediment cleaning schedule.

- The County should consider providing a protective coating or lining for the Kahakapao reservoirs to prevent leaching of the concrete, which could lead to structural failure.

- The County should continue to monitor water quality within and throughout the Waikamoi watershed conveyance system that provides raw water to the Olinda WTP.

With respect to conventional-ultrafiltration process operation:

- Surface water treatment plants that employ an integrated conventional-UF process should optimize the coagulation and sedimentation processes to achieve less than 1 ntu settled water turbidity. Based on the results from this study, settled water turbidities greater than

1 ntu are expected to have detrimental impacts on the operating efficiency of downstream UF membrane processes.

- The County should continue to optimize its coagulation and sedimentation processes, particularly during times of drought when the plant is operated intermittently.

- Since the sedimentation basin does not have sludge handling capabilities, it is expected that the intermittent operation causes an upwelling of the sedimentation sludge layer.

- Since the Olinda facility can experience drought conditions for over 30 percent of the year, it is recommended that the County consider upgrading the Olinda settled water basin to a clarifier with sludge handling system.

With respect to ultrafiltration pretreatment alternatives

- Due to the operation, financial, or performance limitations of the evaluated pretreatment alternatives, the existing pretreatment system or status quo is considered to be the preferred engineering alternative.

- According to the BAC results, biofiltration pretreatment of low alkalinity surface water is not expected to significantly improve UF membrane operating performance. Nevertheless, the newly developed mathematical models revealed that biofilter performance may be optimized by targeting a feed water alkalinity to substrate (ALK/DOC) ratio between 10 and 14.

- Additional research with respect to biofiltration pretreatment is necessary to: validate the ALK/DOC models; further define the alkalinity and substrate limited tails of the ALK/DOC models; and elucidate the mechanisms for the impact of alkalinity on biofiltration performance.

APPENDIX A. WATER QUALITY METHODS

Table A–1 Water Quality Analysis Summary

Test	Method Reference Number (Standard Method-SM); Instrument	Method Reporting Level (MRL)	Method Detection Level goal (MDL)	Accuracy	Precision	Holding time (HT)	Sample Vol. (SV)	Cont. Type (CT)	Preservative
pH	SM 4500-H$^+$ B Electrometric; HACH HQ440d Meter and PHC281 pH Electrode; EUTECH Portable pH Meter (pHTestr 30)	0.0010 units	0.0010 units	± 0.1 pH	± 0.13 pH unit Control Chart	Analyze immediately	125 mL	Plastic	None Required
Temperature	SM 2550 B Mercury-filled Celsius thermometer; Digital thermometer	0.1 °C	0.1 °C	± 0.1 °C	NIST approved	Analyze immediately	125 mL	Plastic	None Required
Turbidity	EPA Method 180.1 Nephelometric; HACH Laboratory and Portable Turbidimeter	0.05 ntu	0.012 ntu	± 2 % of reading plus 0.01 ntu	Greater of: ± 1 % of reading or ± 0.01 ntu	48 hours	125 mL	Plastic	Cool, 4 °C
Alkalinity	SM 2320 B Potentiometric titration of low alkalinity to end-point pH (4.3 to 4.7 pH units)	2 mg/L as CaCO$_3$	2 mg/L as CaCO$_3$	80-120 % Recovery	< 20 % RPD	14 days	200 mL	Plastic	Cool, 4 °C
Color	SM 2120 B Visual Comparison; HACH Spectrophotometer (HACH Method 8025)	5 CU	1 CU	± 16 CU	< 20 % RPD	48-hrs	500 mL	Plastic	Cool, 4 °C
Ultraviolet Absorbing Organics (UV 254)	SM 5910 B Ultraviolet Adsorption; HACH Spectrophotometer (HACH Method 10054)	0.005 cm-1	0.001 cm-1	N/A	< 20 % RPD	48-hrs	125 mL	Amber borosilicate glass bottle; teflon lined cap	Cool, 4 °C

Test	Method Reference Number (Standard Method); Instrument	Method Reporting Level (MRL)	Method Detection Level goal (MDL)	Accuracy	Precision	Holding time (HT)	Sample Vol. (SV)	Cont. Type (CT)	Preservative
Total and Dissolved Organic Carbon	SM 5310 C Persulfate-Ultraviolet Oxidation; Sievers 5310 C Analyzer	0.5 mg/L	0.067 mg/L	80-120 % Recovery	< 20 % RPD	28-days	125 mL	Amber borosilicate glass bottle; 200eflon lined cap	Cool, 4°C; add H_2SO_4 to pH < 2
Dissolved Oxygen	SM 4500-O G Membrane Electrode; YSI 58 Dissolved Oxygen Metter with YSI 5905 Probe	0.1 mg DO/L	0.1 mg DO/L	±0.1 mg DO/L	±0.05 mg DO/L	Analyze immediately	300 mL	Plastic or glass	None required
Phosphorus – Reactive Phosphate	SM 4500-P E Ascorbic Acid Method; HACH Spectrophotometer (HACH Method 8048)	0.02 mg/L PO_4^{3-}	0.02 mg/L PO_4^{3-}	80-120 % Recovery	< 20 % RPD	28-days	100 mL	Plastic or Glass	Cool, 4 °C; add H_2SO_4 to pH < 2
Nitrogen – Nitrate	HACH Method 8039 Cadmium Reduction	0.30 mg/L	0.30 mg/L	80-120 % Recovery	< 20 % RPD	48 hours at 4 °C	125 mL	Plastic	Cool, 4°C
Heterotrophic Plate Count (HPC)	SM 9215 B Pour Plate Method with R2A Agar	1-cfu/mL	1-cfu/mL	N/A	N/A	24-hrs	250 mL	Sterile Plastic or glass Bottle	Cool, 4°C; add 0.2 mL of 3% $Na_2S_2O_3$ to chlorinated samples
Free and Total Adenosine Triphosphate (ATP)	Based on SM 9211C.1 Bioluminescence Test; 3M Clean-Trace Luminometer with 3M Clean-Trace Free and Total ATP test kits	N/A	N/A	N/A	N/A	Analyze immediately	100 mL	Sterile Plastic Bottle	None required

Test	Method Reference Number (Standard Method); Instrument	Method Reporting Level (MRL)	Method Detection Level goal (MDL)	Accuracy	Precision	Holding time (HT)	Sample Vol. (SV)	Cont. Type (CT)	Preservative
Total Dissolved Solids	SM 2540 C Total Dissolved Solids Dried at 180 °C; Oven	10 mg/L	7.661 mg/L	N/A	< 20 % RPD	7 days	200 mL	Plastic	Cool, 4°C
Total Suspended Solids	SM 2540 D Total Suspended Solids Dried at 103-105 °C; Oven	1 mg/L	1 mg/L	N/A	<20 % RPD	7 days	100 mL	Plastic	Cool, 4°C
Iron	SM 3120 B Inductively Coupled Plasma (ICP)	0.005 mg/L	0.001 mg/L	80-120 % Recovery	< 20 % RPD	6-months	125 mL	Plastic	Cool, 4°C; 2 % HNO_3
Manganese	SM 3120 B Inductively Coupled Plasma (ICP)	0.005 mg/L	0.001 mg/L	80-120 % Recovery	< 20 % RPD	6-months	125 mL	Plastic	Cool, 4°C; 2 % HNO_3
Aluminum	SM 3120 B Inductively Coupled Plasma (ICP)	0.05 mg/L	0.005 mg/L	80-120 % Recovery	< 20 % RPD	6-months	125 mL	Plastic	Cool, 4°C; 2 % HNO_3
Calcium	SM 3120 B Inductively Coupled Plasma (ICP)	0.1 mg/L	0.1 mg/L	80-120 % Recovery	< 20 % RPD	6-months	125 mL	Plastic	Cool, 4°C; 2 % HNO_3
Magnesium	SM 3120 B Inductively Coupled Plasma (ICP)	0.1 mg/L	0.03 mg/L	80-120 % Recovery	< 20 % RPD	6-months	125 mL	Plastic	Cool, 4°C; 2 % HNO_3
Silica	SM 3120 B Inductively Coupled Plasma (ICP)	0.1 mg/L	0.05 mg/L	80-120 % Recovery	< 20 % RPD	28-days	125 mL	Plastic	Cool, 4°C; 2 % HNO_3
Chloride	SM 4110 B Ion Chromatography (IC) with Chemical Suppresion of Eluent Conductivity	0.5 mg/L	0.004 mg/L	80-120 % Recovery	< 20 % RPD	28-days	125 mL	Plastic	None
Sulfate	SM 4110 B Ion Chromatography (IC) with Chemical Suppresion of Eluent Conductivity	0.5 mg/L	0.018 mg/L	80-120 % Recovery	< 20 % RPD	28-days	125 mL	Plastic	Cool, 4°C

Test	Method Reference Number (Standard Method); Instrument	Method Reporting Level (MRL)	Method Detection Level goal (MDL)	Accuracy	Precision	Holding time (HT)	Sample Vol. (SV)	Cont. Type (CT)	Preservative
Bromide	SM 4110 B Ion Chromatography (IC) with Chemical Suppresion of Eluent Conductivity	0.20 mg/L	0.014 mg/L	80-120 % Recovery	< 20 % RPD	28-days	125 mL	Plastic	Cool, 4°C
DBP Formation Potential	SM 5110 A through D Formation of THMs and other DBPs	N/A	N/A	N/A	N/A	N/A	2 – 12 L	Amber borosilicate glass; TFE lined cap	Cool, 4°C
Chlorine – free and total	SM 4500-Cl G DPD Colorimetric; HACH Spectrophotometer and Pocket Colorimeter II (HACH Method 8021)	0.02 mg/L	0.01 mg/L	80-120 % Recovery	< 20 % RPD	Analyze Immediately	250 mL	Amber borosilicate glass; TFE lined cap	None Required
THMs	SM 6232 B Liquid-Liquid Extraction Gas Chromatographic; Gas chromatograph with electron-capture detector	8 µg/L	1 µg/L	80-120 % Recovery	< 20 % RPD	14 days	1 L	Amber borosilicate glass; TFE lined cap	Cool, 4°C; add 1 mL of 100 g/L Na_2SO_3 quenching reagent
HAAs	SM 6251 B Micro Liquid-Liquid Extraction or EPA Method 552.3 Liquid-Liquid Micro-extraction; Gas chromatograph with electron-capture detector	SM – 25 µg/L EPA – 10 µg/L	SM – 0.4 µg/L EPA – 0.5 µg/L	70-130 % Recovery	< 30 % RPD	14 days	1 L	Amber borosilicate glass; TFE lined cap	Cool, 4°C; add 1 mL of 50 g/L NH_4Cl quenching reagent

APPENDIX B. QUALITY ASSURANCE AND QUALITY CONTROL

Quality assurance and quality control (QA/QC) was an integral part of the research. The goal of the QA/QC program was to ensure that the design and testing activities are carried out in a controlled and traceable manner. General laboratory practices included the use of suitable grades of reagents, gases, glassware, and standard materials. Reagents were of at least reagent grade for the inorganic analyses. ACS or HPLC (or higher) grade solvents were used for organic analyses. Gases and standards were of the highest purity obtainable; with the exact purity of the primary standard materials being known. Primary standards were purchased fresh at least every six months with working standard solutions being replaced in accordance with the particular analytical methods. Volumetric glassware was Class A grade. Periodic checks on performance of the laboratory equipment were performed regularly as part of the quality control program. Likewise the performance of the analytical balances was be monitored on a semi-annual basis by weighing a series of Class S weights and making any necessary adjustments.

Laboratory quality control procedures according to the <u>Handbook of Analytical Quality Control in Water and Wastewater Laboratories</u> and the <u>Standard Methods for the Examination of Water and Wastewater</u> were followed to monitor and evaluate the reliability of the data collection process (APHA, AWWA & WEF, 2005; USEPA, 1979). These quality control procedures include proper sample collection, storage, cleaning of glassware, and maintenance of equipment. The reliability of the data with respect to precision and accuracy was evaluated by analyzing duplicate and spike samples. During sample collection and analysis about 1 out of every 5 samples was duplicated. The precision of the analyses was assessed by calculating the relative standard deviation (RSD) at 95% confidence for each duplicate pair according to Equation B-1, where A and B represent the concentrations of the duplicate pairs. The accuracy of the analyses was assessed by calculating the

percent recoveries on the spiked samples according to Equation B-2, where $C_{sample+spike}$, C_{sample}, and C_{spike} represent the concentrations of the spiked sample, original sample, and spike respectively.

$$\%RSD_{95} = \frac{|A-B|}{A+B} \times 0.89 \times 100 \tag{B-1}$$

$$\%Recovery = \frac{C_{sample+spike}-C_{sample}}{C_{spike}} \times 100 \tag{B-2}$$

Laboratory quality control compliance was assessed by developing control charts for precision (percent RSD) and accuracy (percent recovery). To develop the control chart for precision, the expected value (average) of approximately 20 RSD duplicate pairs was utilized to construct the upper warning limit (UWL) and upper control limit (UCL) according to Equations B-3 and B-4. The control chart for precision was constructed using the expected value and standard deviation (s) of about 20 determinations of percent recovery. Equations B-5 through B-8 were applied to calculate the upper (UWL) and lower warning limits (LWL) and upper (UCL) and lower control limits (LCL). The duplicate sample pairs are in compliance if the RSD determinations are within 20% and remain within the warning and control limits. Similarly, the spiked samples are in compliance if the percent recovery falls between 70 and 130% and remain within the warning and control limits. Furthermore, if two consecutive determinations fall outside the warning limit or one determination falls outside the control limit, corrective action is taken to maintain the determinations within the warning and control limits.

$$Precision \; UWL = 2.512 \times RSD_{AVG} \tag{B-3}$$

$$Precision \; UCL = 3.267 \times RSD_{AVG} \tag{B-4}$$

$$Accuracy\ UWL = \%Recovery_{AVG} + 2s \qquad\qquad\qquad\qquad (B\text{-}5)$$

$$Accuracy\ LWL = \%Recovery_{AVG} - 2s \qquad\qquad\qquad\qquad (B\text{-}6)$$

$$Accuracy\ UCL = \%Recovery_{AVG} + 3s \qquad\qquad\qquad\qquad (B\text{-}7)$$

$$Accuracy\ LCL = \%Recovery_{AVG} - 3s \qquad\qquad\qquad\qquad (B\text{-}8)$$

The laboratory quality control charts for the DBP (TTHMs and HAA$_5$s), metals (iron, manganese, calcium, magnesium, silica, and aluminum), anions (chloride and sulfate), and total solids (sum of total suspended and dissolved solids) analyses are presented in Figures B-1 through B-21. As demonstrated in Figures B-1 through B-21, the percent RSD and recovery determinations exhibited variation from the corresponding expected values. The variation in percent RSD and recovery determinations may be attributed to the heterogeneous nature of surface water samples, experimental errors associated with sample dilutions, preparation of analyte standards and spikes, equipment operation, and equipment maintenance. Nevertheless, the variation in the percent RSD and recovery within 30 percent is acceptable for assessing differences between experimental treatments.

The TTHM analyses were in compliance with the QA/QC plan for precision and accuracy. The HAA$_5$ analyses were in compliance with the QA/QC plan for precision; however, about two HAA$_5$ percent recovery determinations fell below 70 percent. The lower HAA$_5$ percent recoveries may be attributed to the different procedure used for extracting standards versus samples in both the Standard 6251 and EPA 552.3 methods.

Of the metal analyses, the manganese, calcium, magnesium, silica, and aluminum results were in compliance with the QA/QC plan for precision and accuracy, while one iron percent recovery determination exceeded the UCL. Corrective action was taken by remaking standards and spike samples and reanalyzing the corresponding sample set to obtain adherence to the QA/QC program. For the total suspended and dissolved solids, analyte spike samples and recoveries were not measured and the RSD determinations varied about the 22 percent expected value. The variation in the total solids analysis may have resulted from the heterogeneous characteristics of surface water samples, absorption of moisture onto solids, and experimental errors associated with filtering, drying, and weighing procedures.
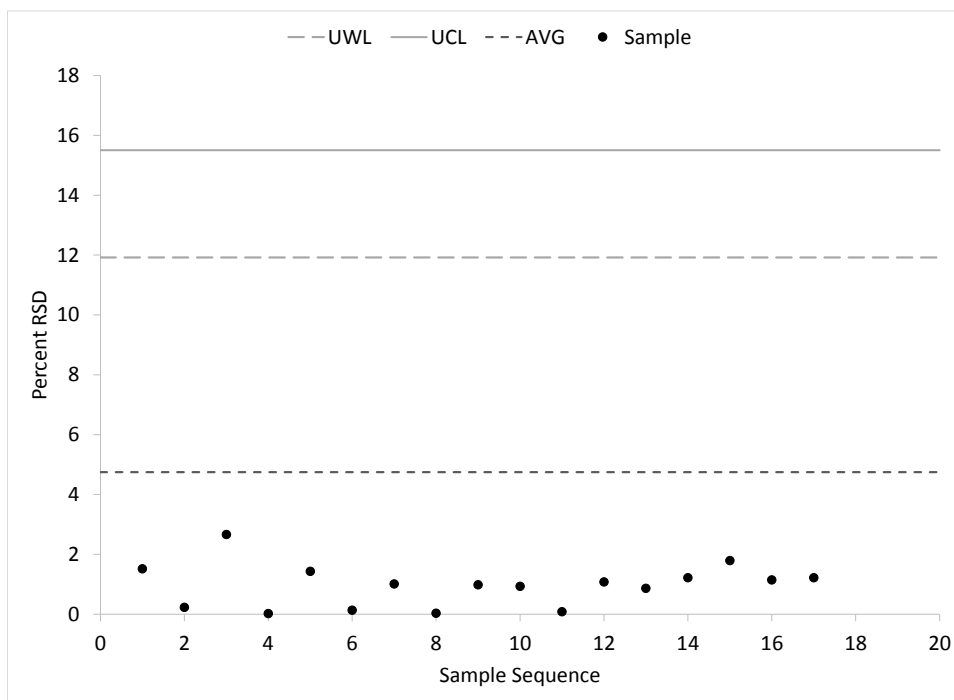
Figure B–1: TTHM Quality Control Chart for Precision
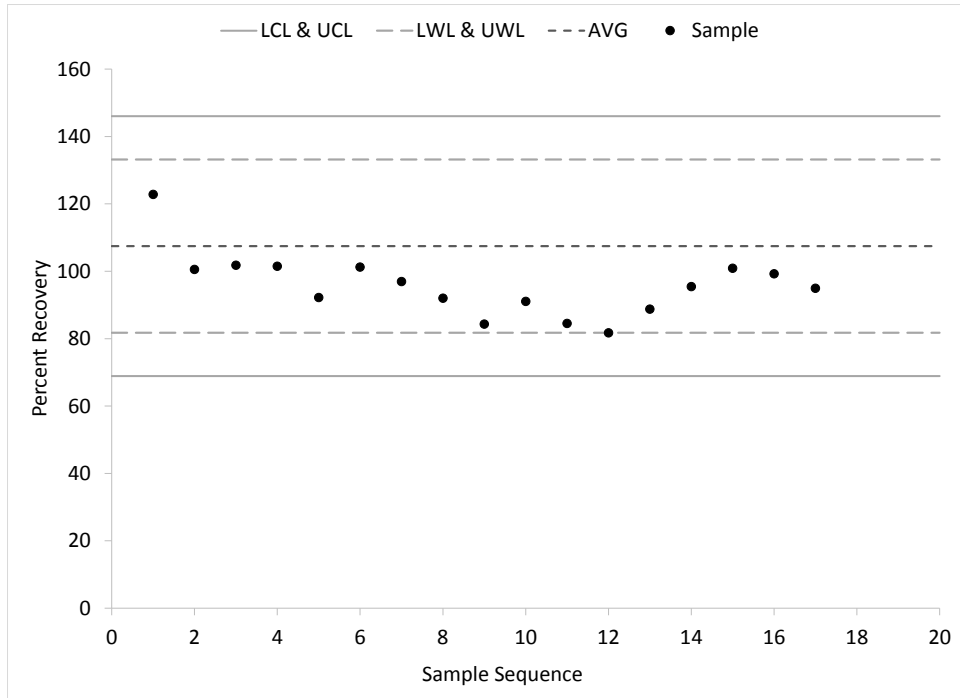
Figure B–2: TTHM Quality Control Chart for Accuracy
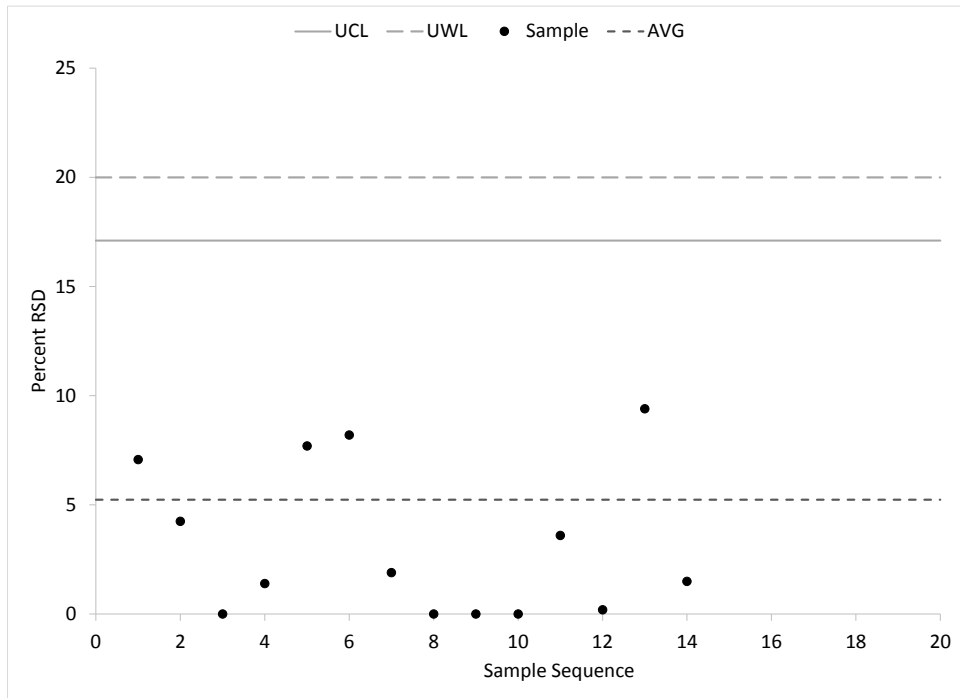
Figure B–3: HAA$_5$ Quality Control Chart for Precision
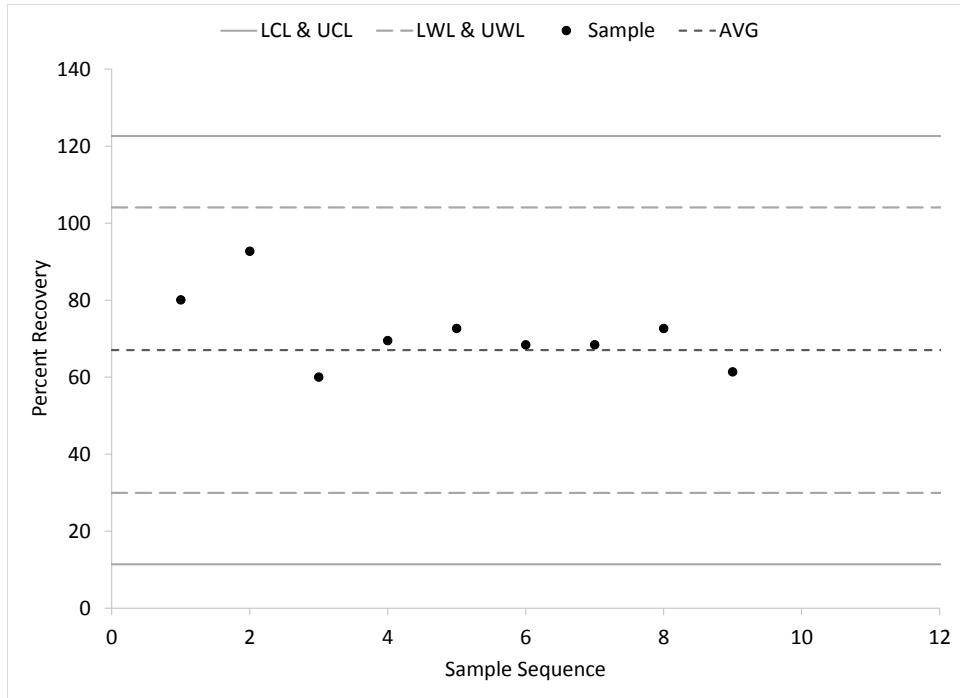
Figure B–4: HAA$_5$ Quality Control Chart for Accuracy
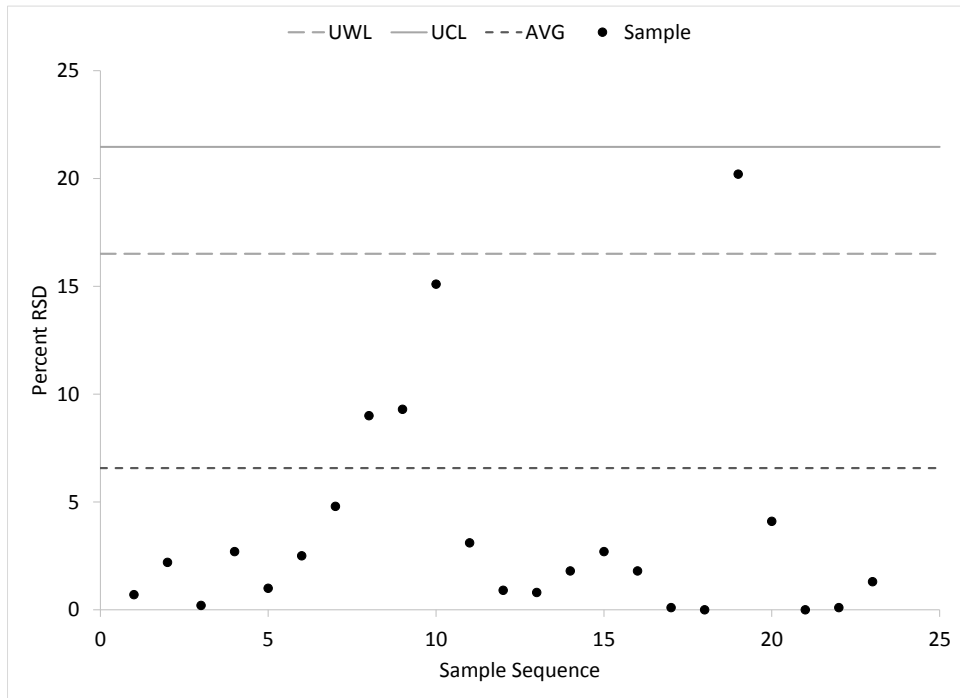
Figure B–5: Iron Quality Control Chart for Precision

209
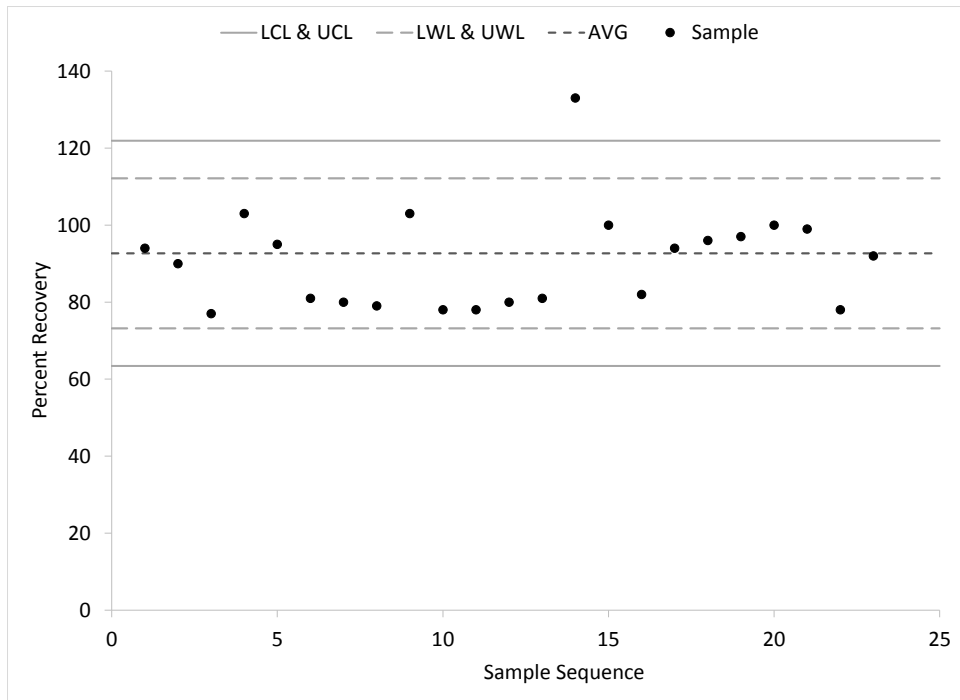
Figure B–6: Iron Quality Control Chart for Accuracy
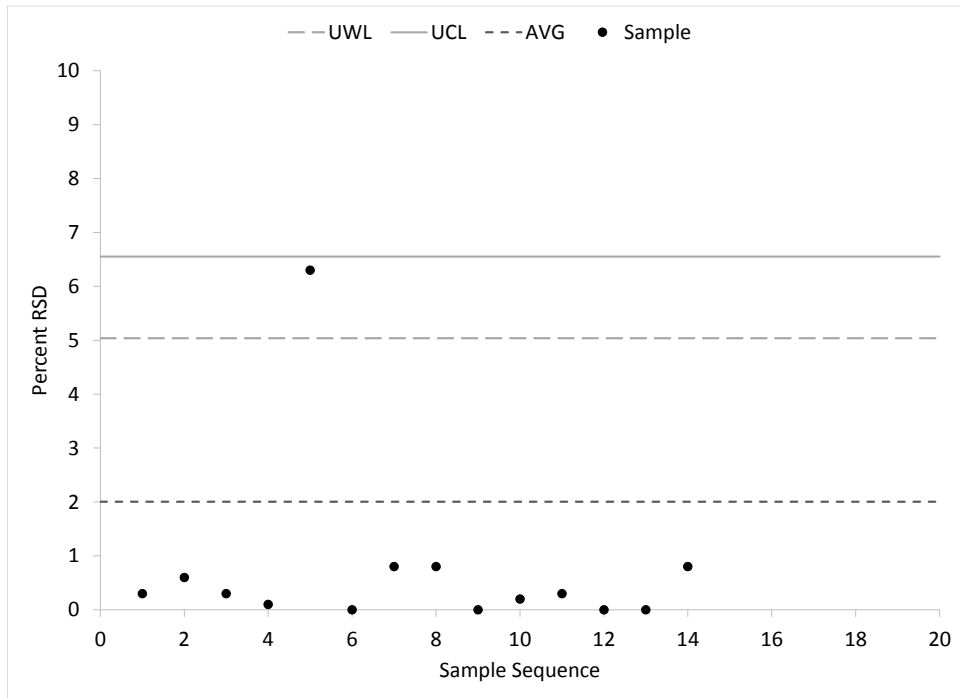
Figure B–7: Manganese Quality Control Chart for Precision
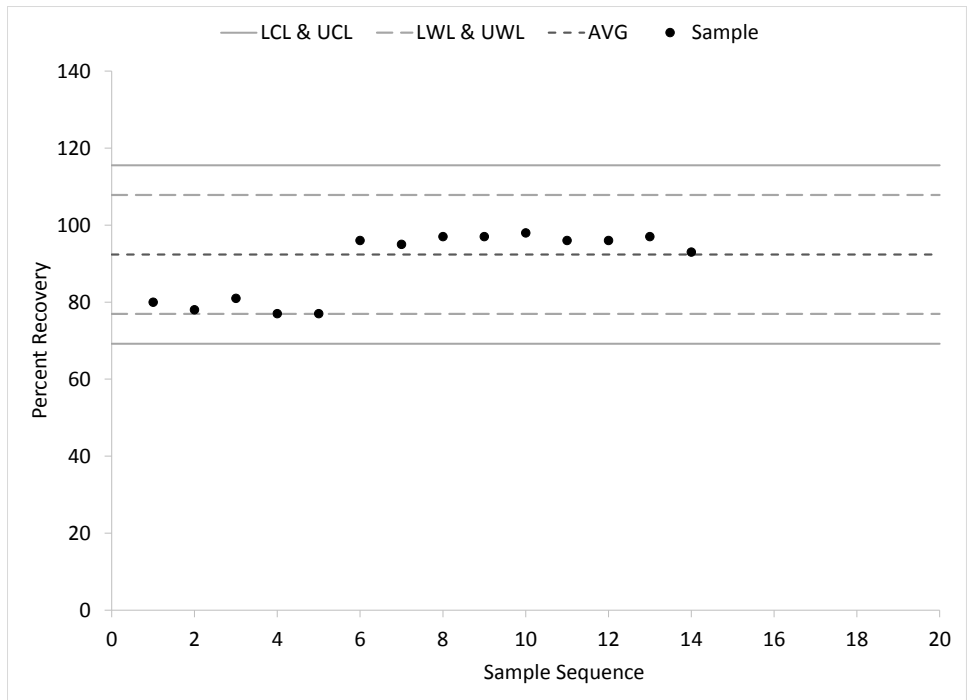
Figure B–8: Manganese Quality Control Chart for Accuracy
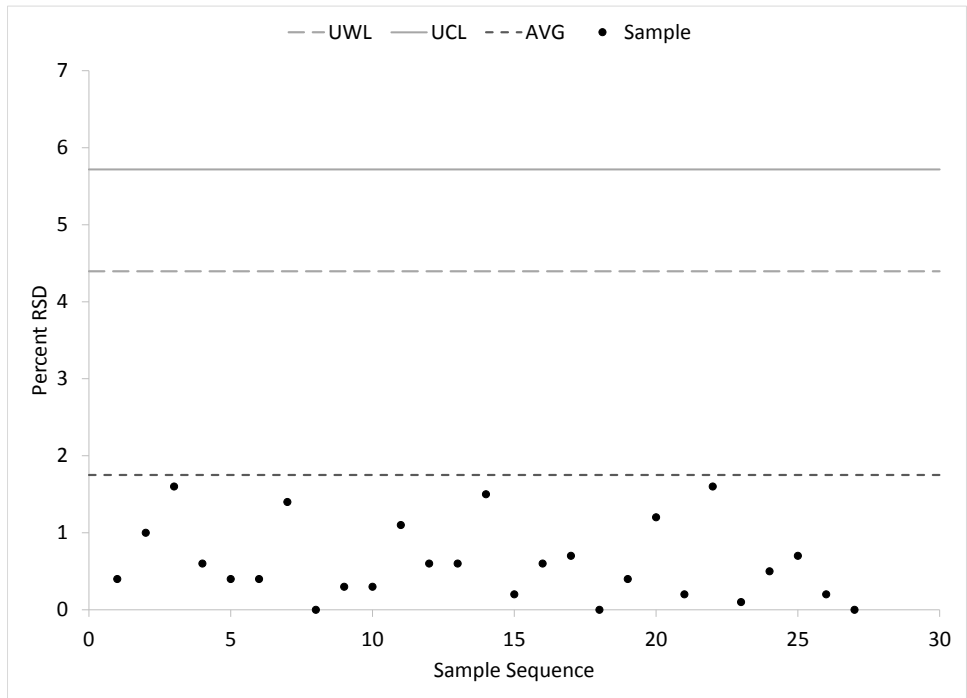
Figure B–9: Calcium Quality Control Chart for Precision

211
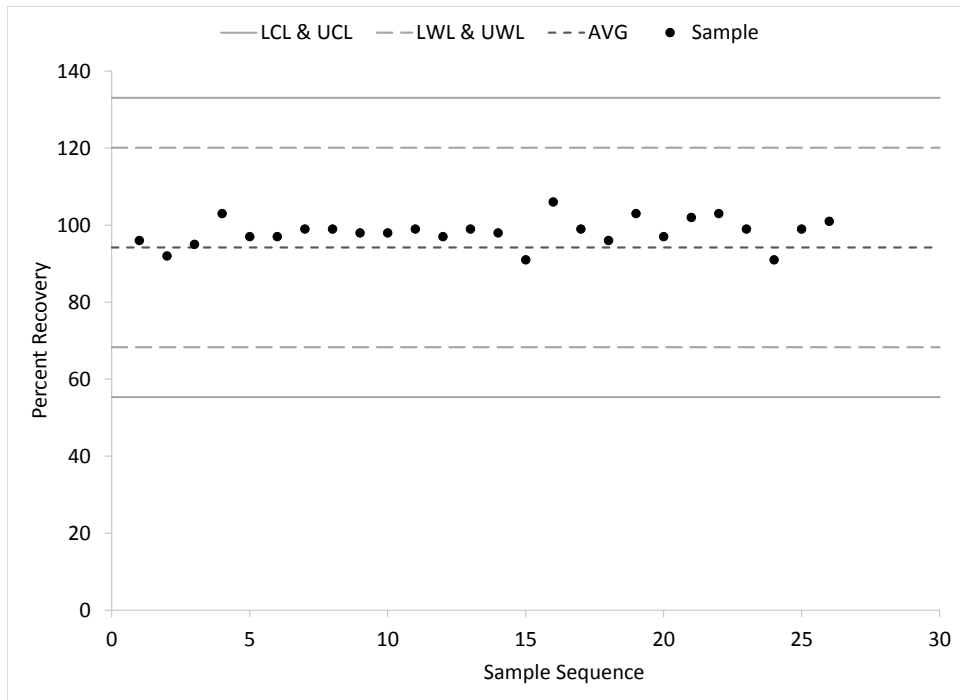
Figure B–10: Calcium Quality Control Chart for Accuracy
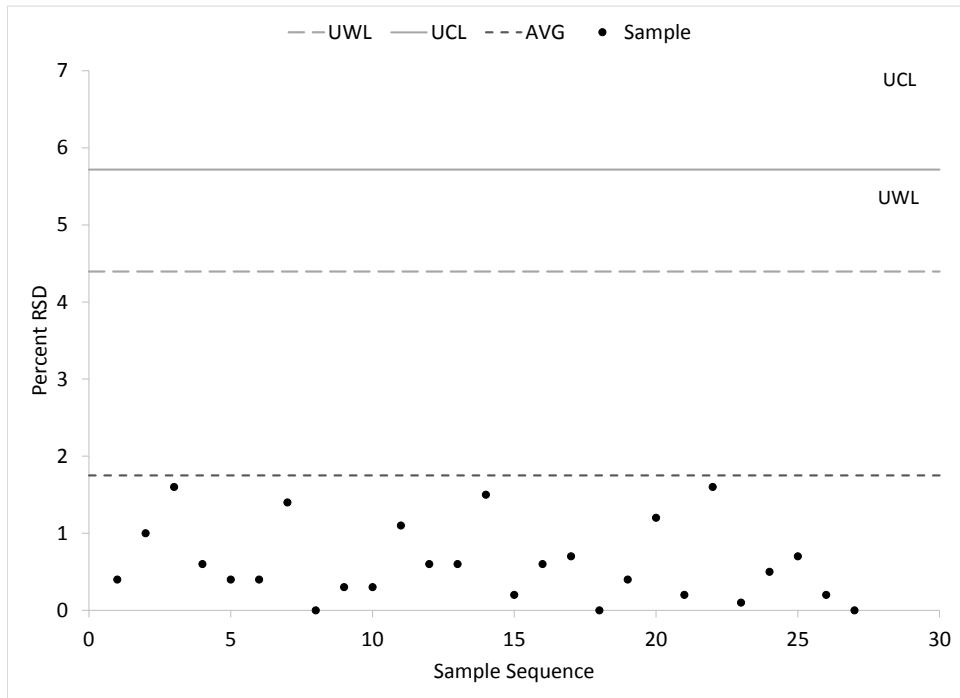
Figure B–11: Magnesium Quality Control Chart for Precision

212
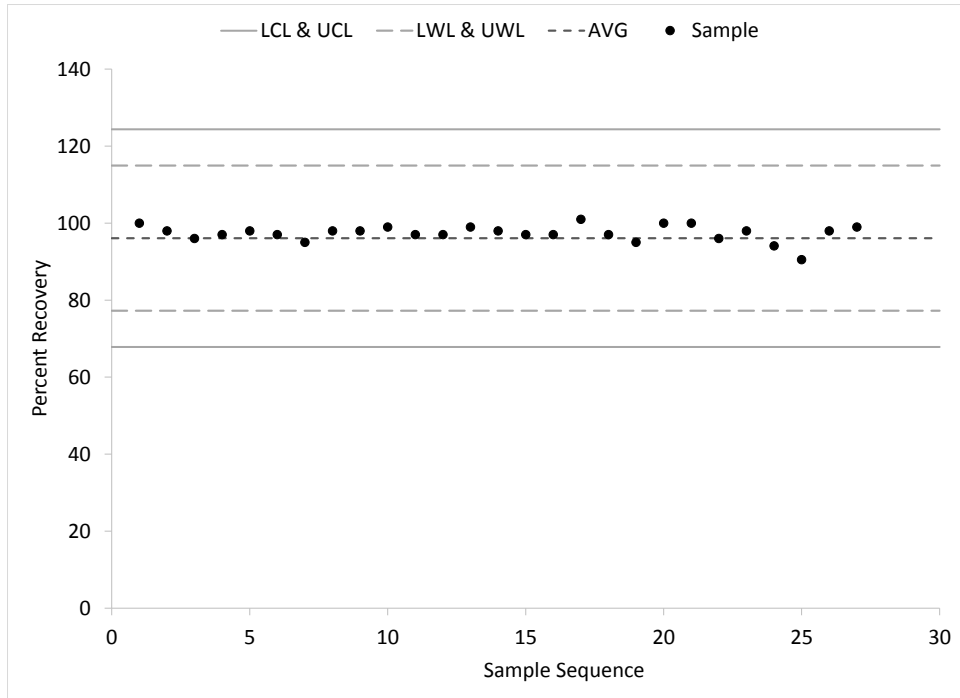
Figure B–12: Magnesium Quality Control Chart for Accuracy
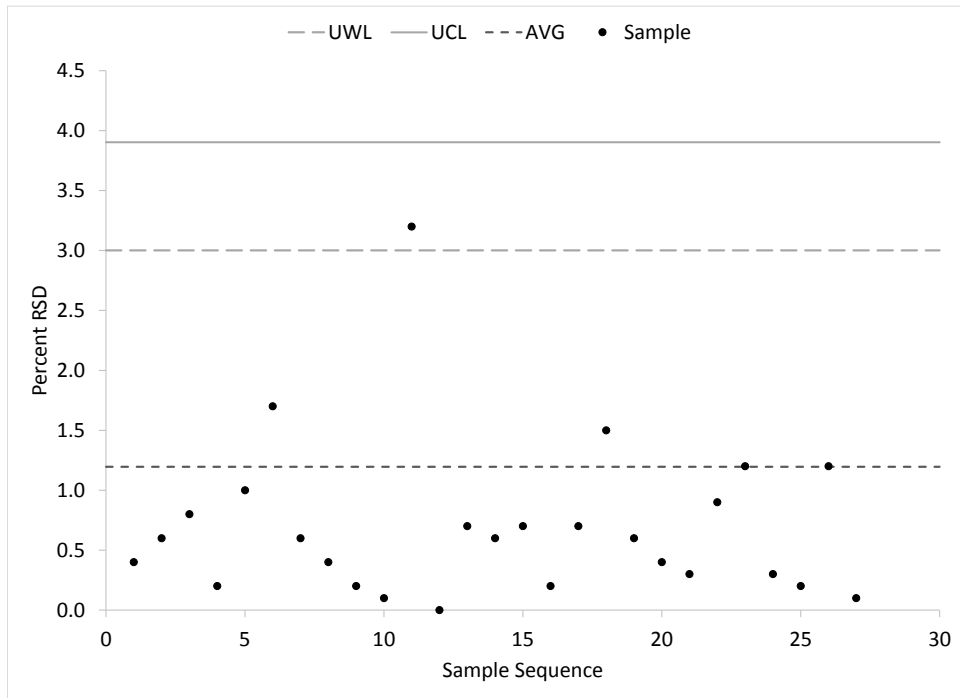
Figure B–13: Silica Quality Control Chart for Precision
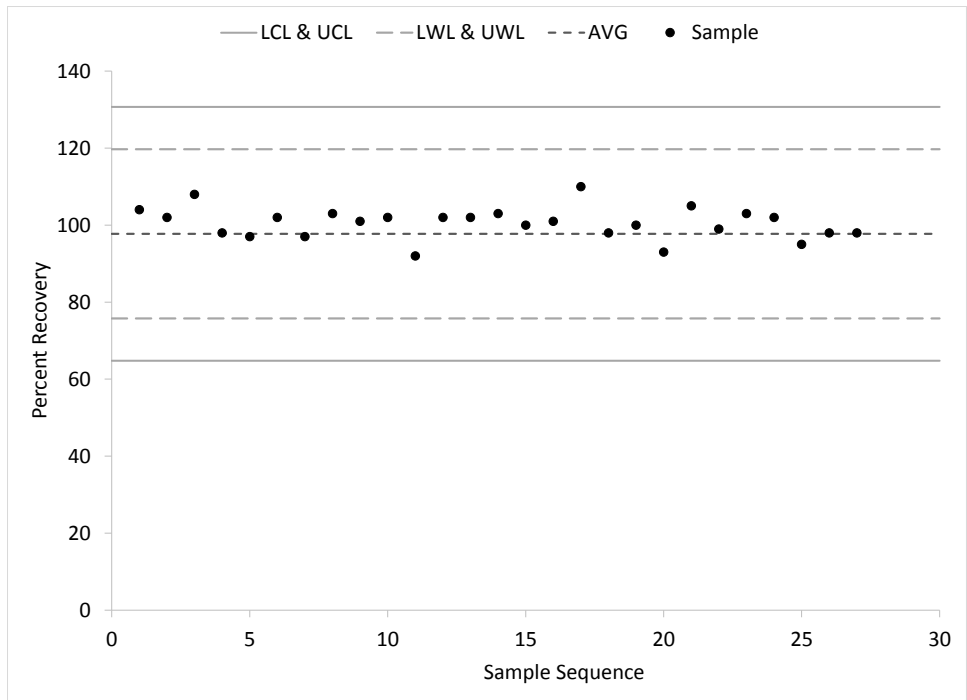
Figure B–14: Silica Quality Control Chart for Accuracy
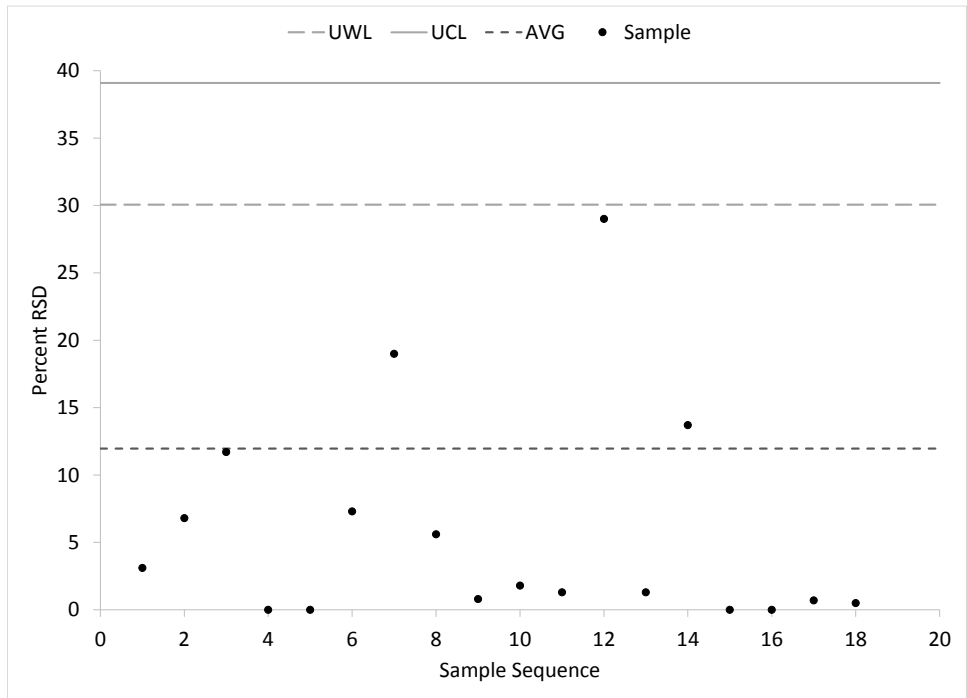
Figure B–15: Aluminum Quality Control Chart for Precision
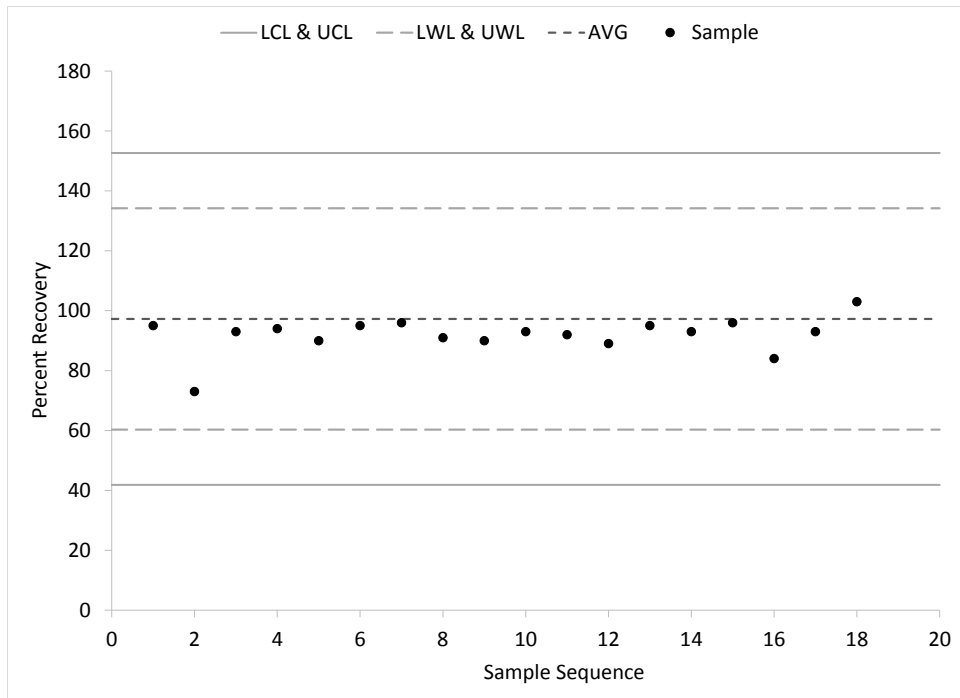
Figure B–16: Aluminum Quality Control Chart for Accuracy
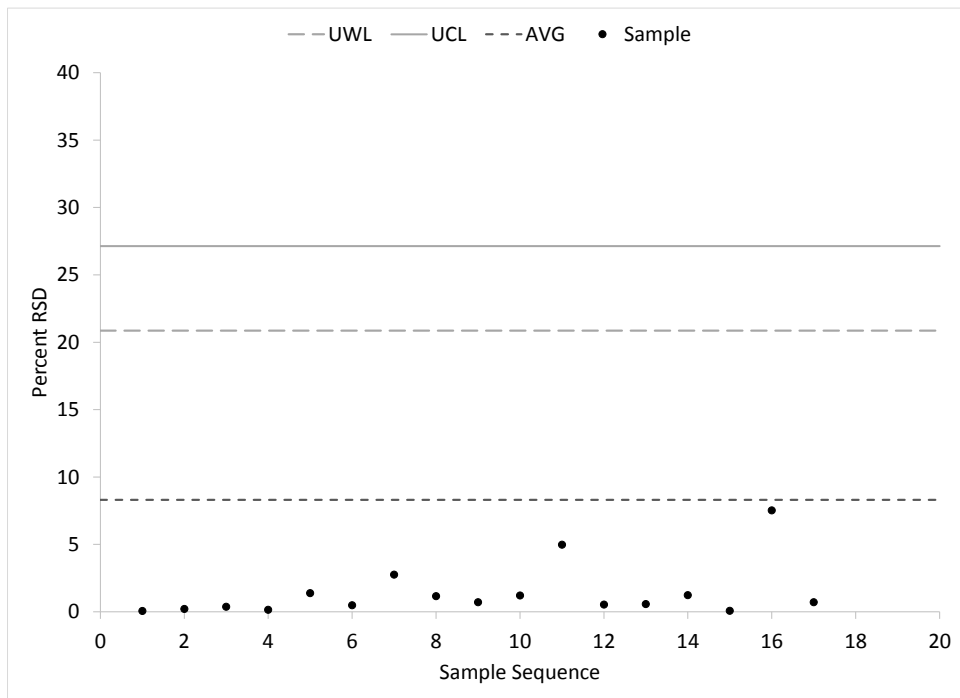
Figure B–17: Chloride Quality Control Chart for Precision
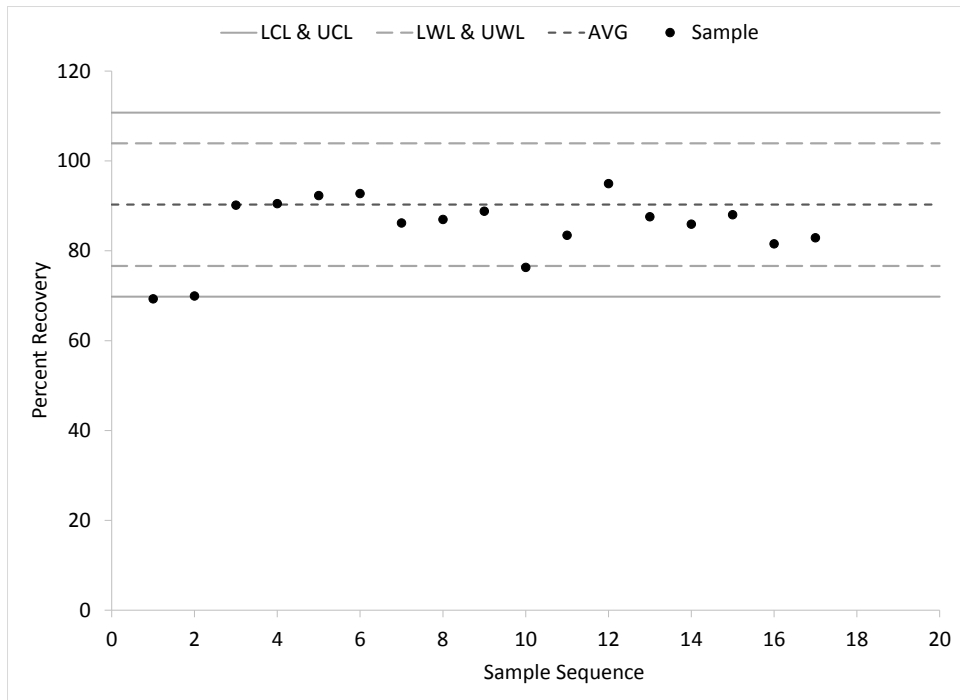
Figure B–18: Chloride Quality Control Chart for Accuracy
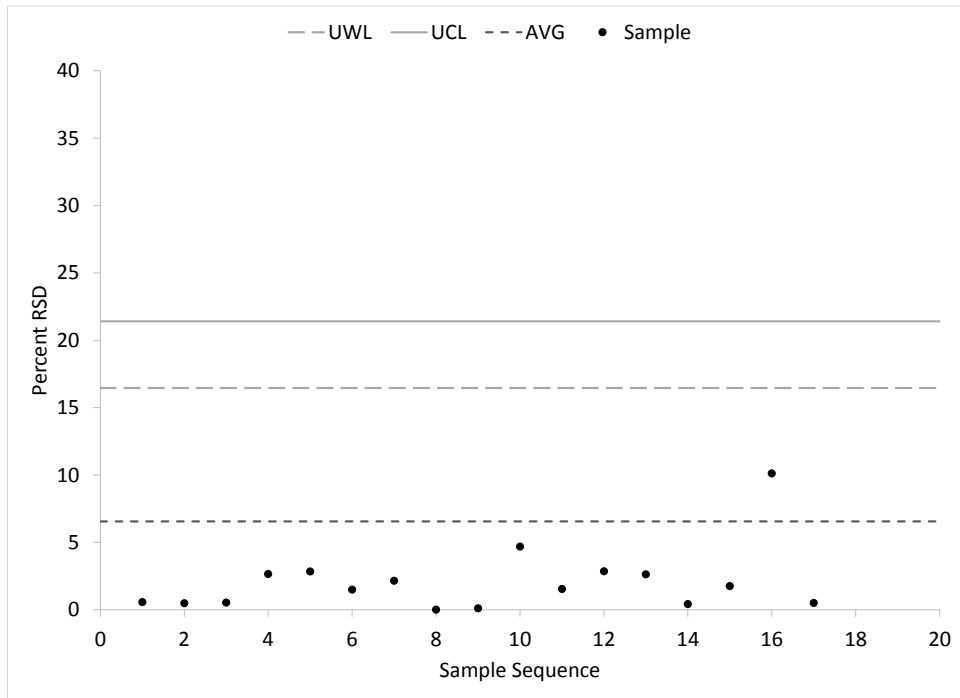
Figure B–19: Sulfate Quality Control Chart for Precision
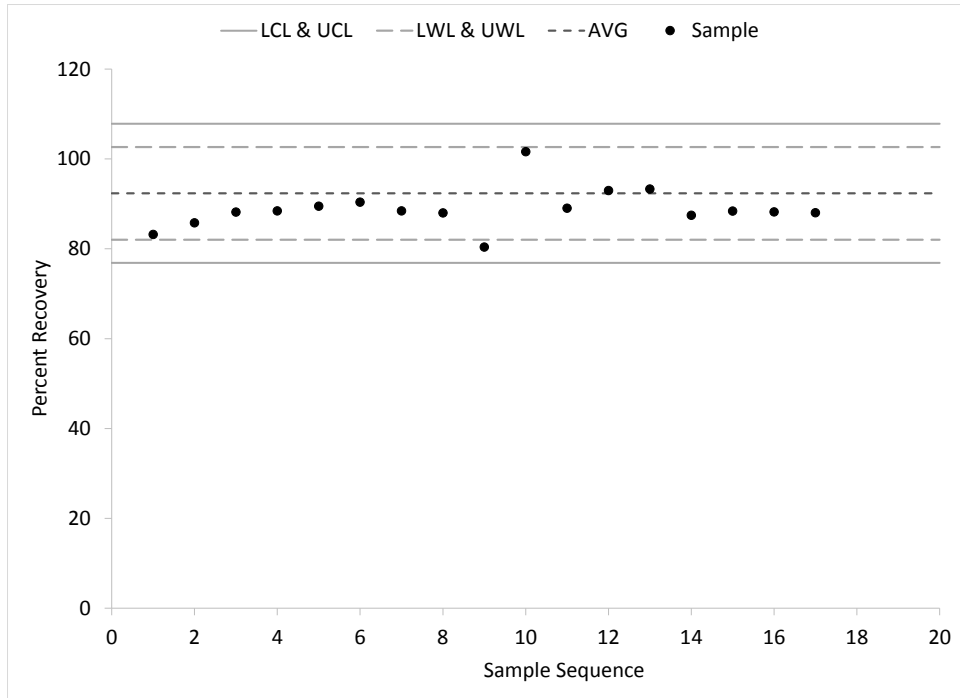
Figure B–20: Sulfate Quality Control Chart for Accuracy
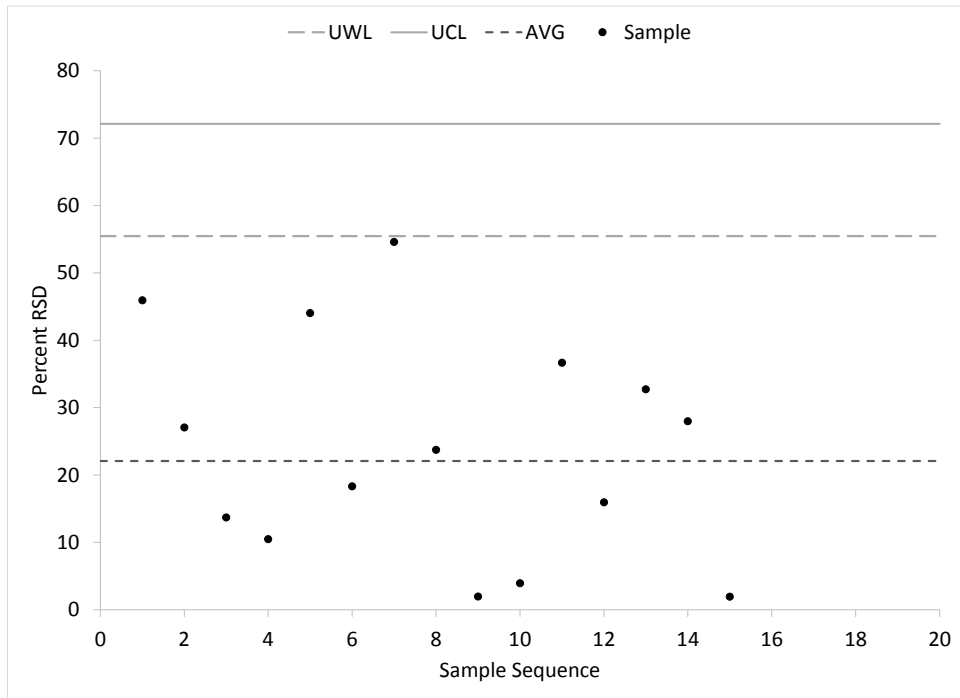
Figure B–21: Total Solids Quality Control Chart for Precision

Free and Total Adenosine Triphosphate Analysis

The free and total ATP calibration curves are illustrated in Figures B-22 and B-23, The calibration curves exhibited a good linear correlation for their respective linear mathematical regressions.

$$Free\ ATP\ RLUs = 6.1897 \left(Free\ ATP\ \frac{pg}{mL}\right) \tag{B-9}$$

$$Total\ ATP\ RLUs = 6.1582 \left(Total\ ATP\ \frac{pg}{mL}\right) \tag{B-10}$$

The laboratory quality control analysis for precision and accuracy was performed on four duplicate and spike sample pairs. The expected value of the percent relative standard deviation (RSD) and recovery for the free ATP were 29 ±17 % and 92 ± 64 %. The expected value of the percent RSD and recovery for the total ATP were 13 ± 13 % and 107 ± 67 %. Additional experiments with 20 + determinations of duplicate pairs and percent recoveries would be necessary in future work to establish a quality control chart for accuracy and precision for the free and total ATP. Nevertheless, the rapid ATP luminometer detection method is expected to be a useful tool for monitoring biological activity by allowing the relative comparison of ATP content in source water samples.
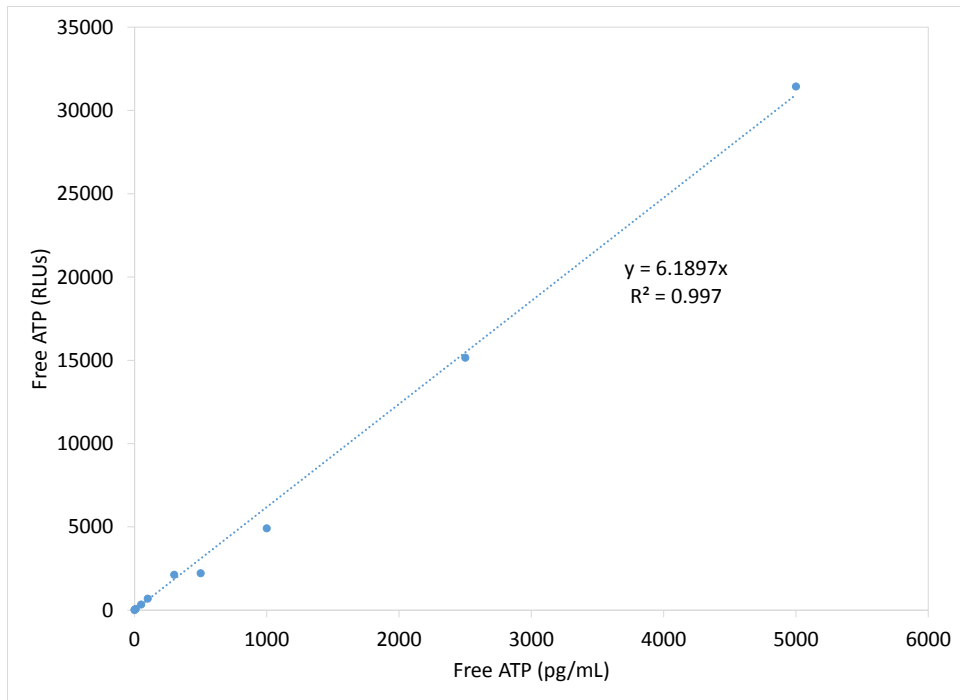
Figure B–22: Free ATP Calibration Curve
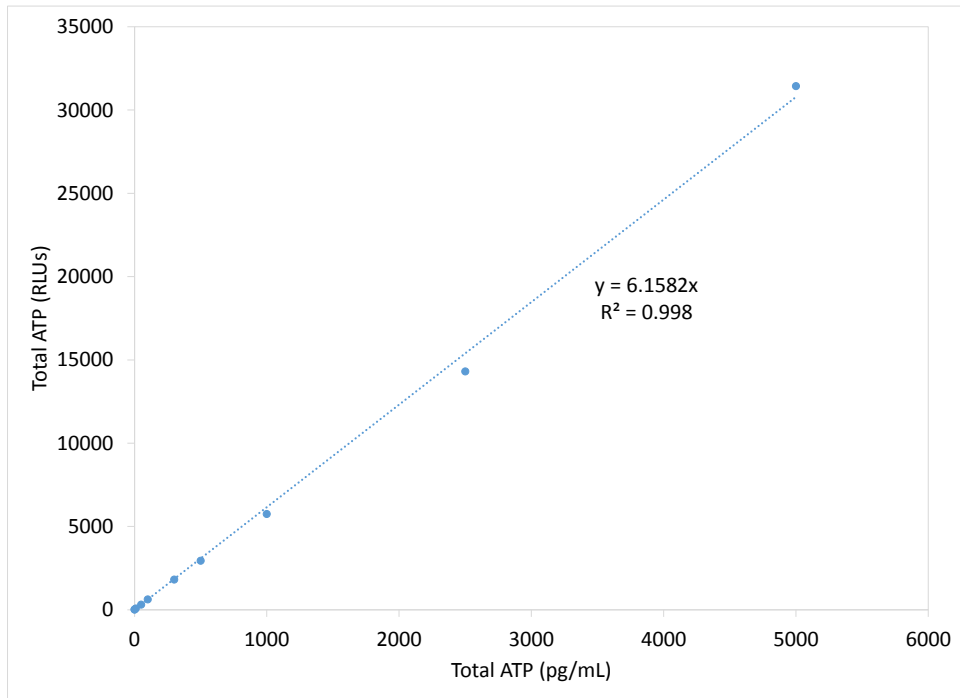
Figure B–23: Total ATP Calibration Curve

APPENDIX C. CHEMICAL USE INFORMATION

Table C–1 Chemical Information Summary

Name	Purpose	CAS No.	Strength	Source
Aluminum chlorohydrate (ACH)	Coagulant	12042-91-0	50% liquid; Specific gravity = 1.34	California Aluminum Chemicals (Modesto, CA)
Citric Acid	Membrane clean in place (CIP)	77-92-9	50% liquid	Brenntag Pacific, Inc.
Sodium hypochlorite solution (with 1% sodium hydroxide)	Membrane CIP	7681-52-9	12.5% liquid	BEI Hawaii (Honolulu, HI)
Sodium hydroxide (caustic)	pH adjustment	1310-73-2	50% liquid	BEI Hawaii (Honolulu, HI)
Monophotassium phosphate (food grade)	Nutrient enhancement	7778-77-0	98% powder	Tianjin Ronghong Chemical Col, LTD (Tianjin,China)
Food grade lime (calcium oxide)	pH adjustment	1305-78-8	99% powder	Fisher Scientific
Sodium hypochlorite	Simulated disinfection	7681-52-9	4-6% liquid	Fisher Scientific
Adenosine triphosphate (ATP)	Calibration standard	987-65-5	100 mM	Thermo Scientific

APPENDIX D. WAIKAMOI WATERSHED CHARACTERIZATION

Figure D–1 Kahakapao Reservoirs

Figure D–2 First Caisson Pipeline

Figure D–3 Second Caisson Pipeline

Figure D–4 Waikamoi Reservoirs
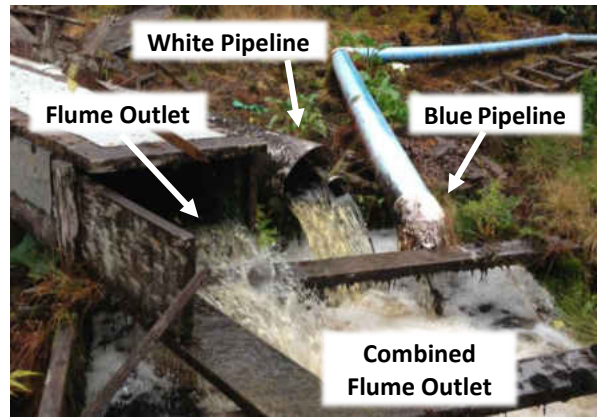
Figure D–5 Waikamoi Flume Outlet

Figure D–6 Aluminum vs Redwood Flume

Figure D–7 Flume Intake 2 (Middle)

Figure D–8 Flume Intake 1 (Beginning)

Table D–1 Waikamoi Watershed Preliminary DOC vs TOC Comparison

Location[1]	DOC (mg/L)	TOC (mg/L)	DOC/TOC Fraction
Kahakapao Reservoir 1	8.58	8.24	1.0
Kahakapao Reservoir 2	8.14	8.61	0.9
1st Caisson Pipeline	8.78	8.6	1.0
2nd Caisson Pipeline	8.15	7.9	1.0
Waikamoi Reservoir	9.78	10.1	1.0
Flume Outlet	10	10.5	1.0
Flume Intake 2	10	11.7	0.9
Flume Intake 1	9.2	10.1	0.9
Blue Pipeline	11.3	11.6	1.0

(1) Data collected on November 15, 2012
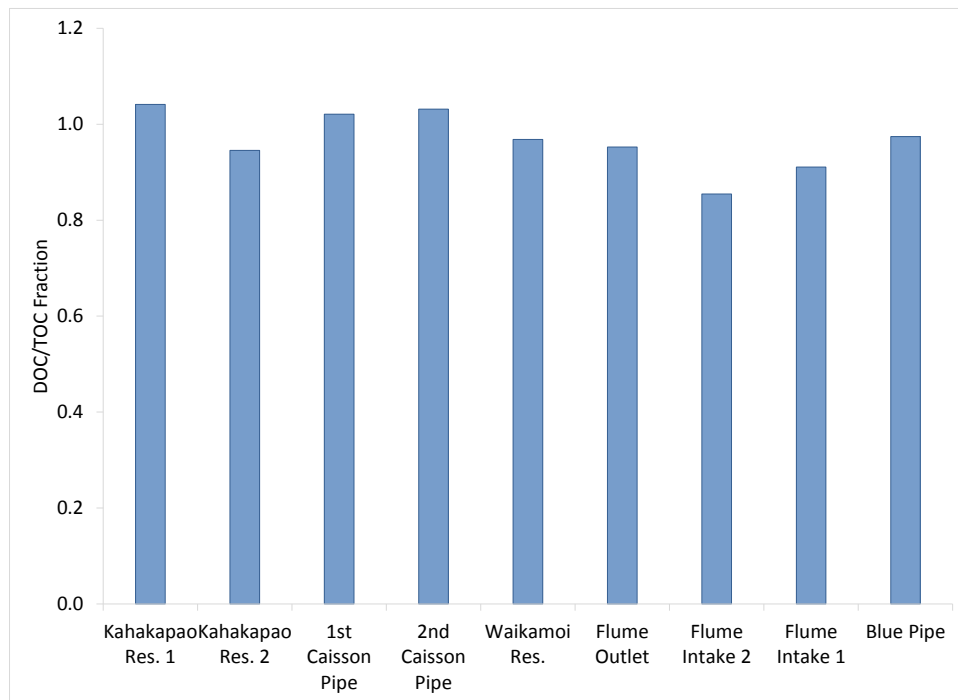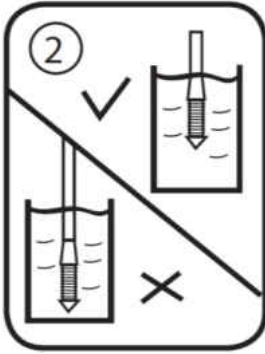
Figure D–9 Waikamoi Watershed Preliminary DOC/TOC Fraction Comparison

Table D–2 3M Clean-Trace™ Free and Total ATP Product Instructions

Procedure[1]	Diagram[1]
Step 1 • Place the free or total ATP test devices at room temperature for at least 10 minutes before use. • Collect water samples from the test sites.	
Step 2 • Swirl to mix the sample. • Remove a Free or Total ATP test device from the foil pouch. • Remove the sampling stick from the 3M device and immerse the sample collection rings into the water sample, tapping the handle gently if bubbles form.	
Step 3 • Immediately remove the sampling stick from the water sample and carefully return it to the test device such that the handle is at its starting position. • To process the sample, push down firmly on the top of the free or total ATP sample stick handle. The handle will slide into the test device tube and the top of the handle should be level with the top of the device tube when fully depressed.	

(1) Product instructions reproduced with permission from 3M (2012 & 2013).

	Procedure	Diagram
Step 4	• Grip the top of the test device and shake rapidly side-to-side for at least five seconds to mix the sample and reagent.	
Step 5	• Immediately open the sample chamber of the 3M Clean-Trace NG Luminometer and insert the free or total ATP test device. • Close the chamber cap and press the measure button. The light emitted by the 3M Clean-Trace test device will be measured and the result (in RLU) will appear on the display.	
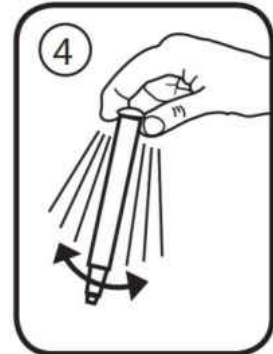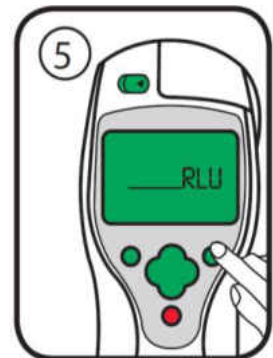
Table D–3 Dry vs Rainy Watershed Quality Averages

Water Quality		Kahakapao Res. 1	Kahakapao Res. 2	1st Caisson Pipeline	2nd Caisson Pipeline	Waikamoi Res.	Combined Flume Outlet	White Pipeline	Flume Outlet	Flume Intake 2	Flume Intake 1	Blue Pipeline
pH	Dry	6.5	6.3	5.5	5.7	5.7	5.0	4.8	4.8	4.9	4.8	4.4
	Rainy	6.3	6.5	5.3	5.1	4.7	4.6	4.7	4.3	4.3	4.1	4.3
Temp. (ºC)	Dry	21.3	21.5	17.4	18.7	22.2	19.3	22.4	18.2	19.0	19.0	17.9
	Rainy	17.5	17.5	15.2	15.4	16.1	17.3	18.0	16.0	16.2	15.0	15.6
Turb. (ntu)	Dry	2.58	3.48	0.97	3.30	6.15	1.93	3.18	1.15	1.34	0.51	0.75
	Rainy	2.73	3.10	2.25	3.95	6.63	5.25	5.47	5.02	3.02	4.42	4.05
Alk. (mg/L CaCO$_3$)	Dry	4.8	4.5	3.3	4.4	5.5	2.0	4.0	0.9	4.0	3.5	0.3
	Rainy	4.6	4.0	2.5	2.4	1.6	1.0	0.5	0.8	0.8	0.3	0.7
DO (mg/L)	Dry	6.8	6.7	6.2	5.4	6.5	7.0	7.2	6.7	6.8	7.0	6.4
	Rainy	8.5	8.3	9.2	8.1	8.5	7.7	7.5	9.1	10.0	9.7	8.7
Color (CU)	Dry	66	72	27	15	50	83	64	86	29	11	88
	Rainy	67	67	38	43	94	117	110	113	109	118	133
UV254 (1/cm)	Dry	0.315	0.330	0.162	0.092	0.283	0.378	0.298	0.392	0.167	0.085	0.428
	Rainy	0.301	0.295	0.228	0.252	0.426	0.541	0.498	0.537	0.508	0.568	0.626
DOC (mg/L)	Dry	6.5	6.6	4.7	3.3	6.5	7.0	5.0	7.8	4.2	3.1	7.9
	Rainy	7.2	7.0	7.1	7.2	8.4	9.6	7.9	10	9.5	10	11
SUVA (L/g-m)	Dry	4.8	5.0	3.5	2.8	4.5	5.3	6.0	5.0	4.0	2.8	5.2
	Rainy	4.1	4.2	3.2	3.4	5.1	5.6	6.3	5.2	5.4	5.4	5.7
F ATP (pg/mL)	Dry	115	150	35	36	166	58	55	45	53	23	55
	Rainy	54	58	67	69	125	69	57	89	60	62	45
T ATP (pg/mL)	Dry	316	305	58	86	571	73	68	70	61	24	65
	Rainy	106	183	104	179	214	242	221	126	117	50	85
Cellular ATP (pg/mL)	Dry	201	155	23	50	405	15	13	26	8	0	10
	Rainy	52	116	41	150	154	173	164	67	95	4	59
F/T ATP	Dry	0.40	0.58	0.67	0.40	0.47	0.78	0.81	0.64	0.88	0.99	0.87
	Rainy	0.63	0.37	0.81	0.64	0.47	0.29	0.26	0.70	0.44	0.94	0.48

Water Quality		Kahakapao Res. 1	Kahakapao Res. 2	1st Caisson Pipeline	2nd Caisson Pipeline	Waikamoi Res.	Combined Flume Outlet	White Pipeline	Flume Outlet	Flume Intake 2	Flume Intake 1	Blue Pipeline
TSS	Dry	2.3	3.2	4.7	2.2	3.3	1.1	3.2	0.4	3.0	0	0
(mg/L)	Rainy	1.7	3.0	2.3	2.8	3.2	2.5	1.5	3.7	2.9	2.0	0.8
TDS	Dry	27	29	16	16	25	25	26	13	22	12	20
(mg/L)	Rainy	39	27	14	20	37	27	36	63	40	23	58
Fe	Dry	0.412	0.522	0.636	0.883	1.237	0.557	0.999	0.602	0.688	0.050	0.359
(mg/L)	Rainy	0.442	0.499	0.434	0.413	0.702	0.410	0.211	0.428	0.523	0.313	0.497
Mn	Dry	0.016	0.024	0.037	0.038	0.054	0.021	0.030	0.020	0.030	0.004	0.021
(mg/L)	Rainy	0.010	0.014	0.018	0.013	0.014	0.016	0.010	0.014	0.015	0.012	0.023
Ca	Dry	1.55	1.45	0.72	1.22	1.11	0.63	0.59	0.52	0.46	0.45	0.39
(mg/L)	Rainy	1.43	1.42	0.63	0.60	0.55	0.22	0.14	0.47	0.35	0.50	0.50
Mg	Dry	0.38	0.41	0.51	0.52	0.75	0.33	0.33	0.33	0.38	0.31	0.29
(mg/L)	Rainy	0.32	0.31	0.48	0.46	0.32	0.20	0.16	0.28	0.27	0.31	0.28
Si	Dry	1.48	1.60	1.28	1.48	1.81	3.30	3.78	2.18	4.22	5.10	2.13
(mg/L)	Rainy	1.39	1.37	1.42	1.28	1.07	0.59	0.42	0.85	0.78	1.09	0.82
Al	Dry	0.21	0.21	0.17	0.11	0.22	0.22	0.20	0.29	0.11	0.06	0.28
(mg/L)	Rainy	0.16	0.15	0.14	0.21	0.24	0.36	0.20	0.26	0.33	0.35	0.25
Cl^-	Dry	3.9	3.9	4.2	4.5	4.0	4.0	5.2	3.4	5.6	4.8	3.5
(mg/L)	Rainy	3.5	3.4	3.8	3.6	3.3	1.9	1.7	3.2	3.3	3.8	2.9
SO_4^{2-}	Dry	1.6	1.6	1.5	1.6	1.2	1.4	1.6	1.2	1.9	1.9	1.3
(mg/L)	Rainy	1.6	1.5	1.6	1.7	1.5	0.8	0.8	1.7	1.7	1.9	1.1
Br^-	Dry	<0.2	<0.2	<0.2	<0.2	<0.2	<0.2	<0.2	<0.2	<0.2	<0.2	<0.2
(mg/L)	Rainy	<0.2	<0.2	<0.2	<0.3	<0.2	<0.2	<0.2	<0.2	<0.2	<0.2	<0.2
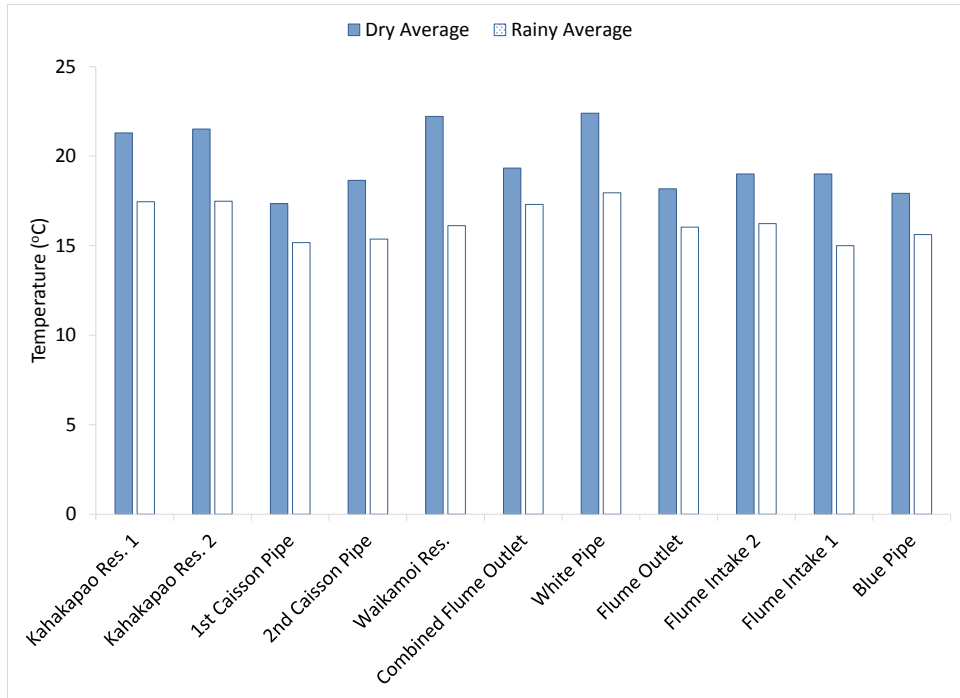
Figure D–10 Dry vs Rainy Temperature
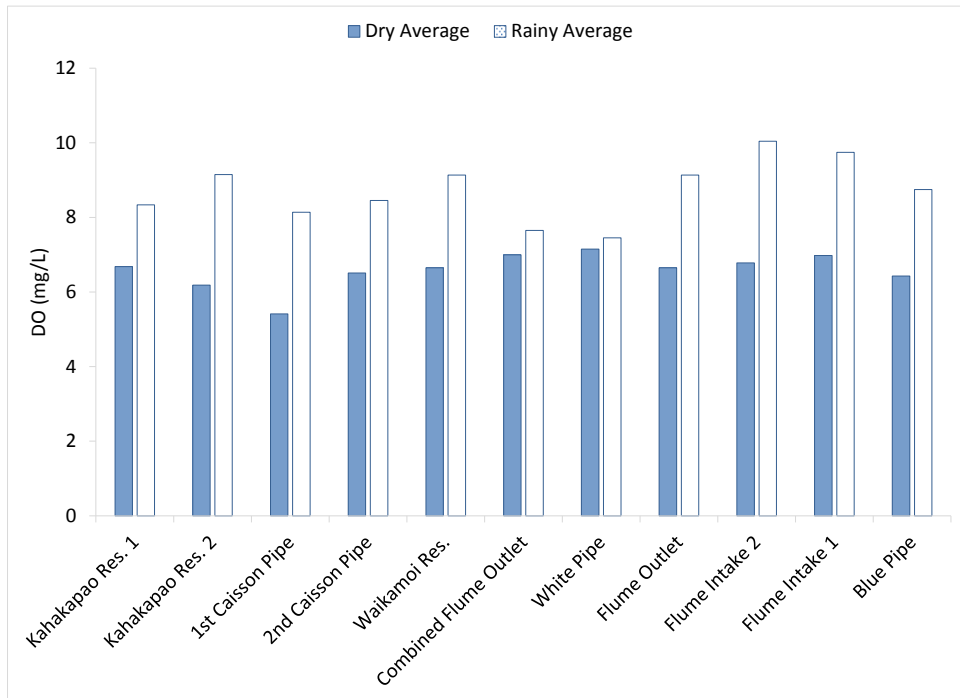
Figure D–11 Dry vs Rainy Dissolved Oxygen
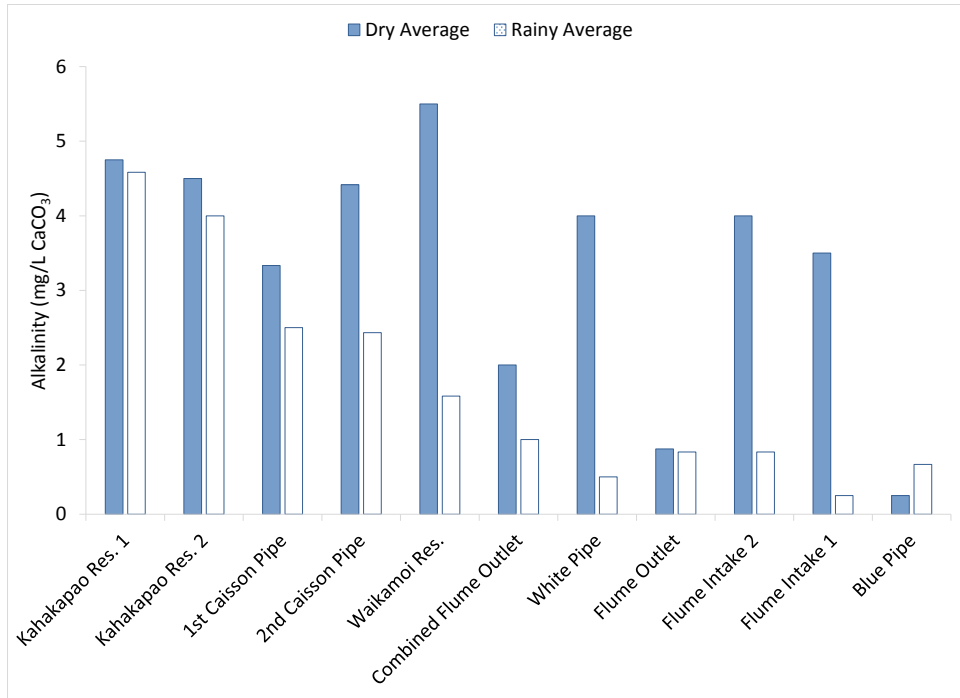
Figure D–12 Dry vs Rainy Alkalinity
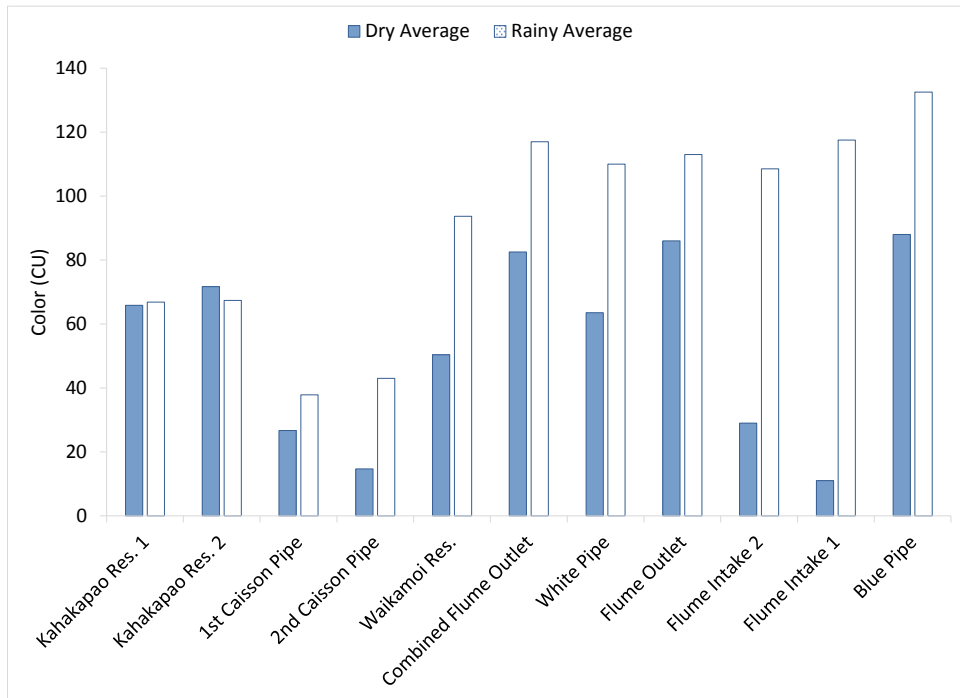
Figure D–13 Dry vs Rainy Color

232
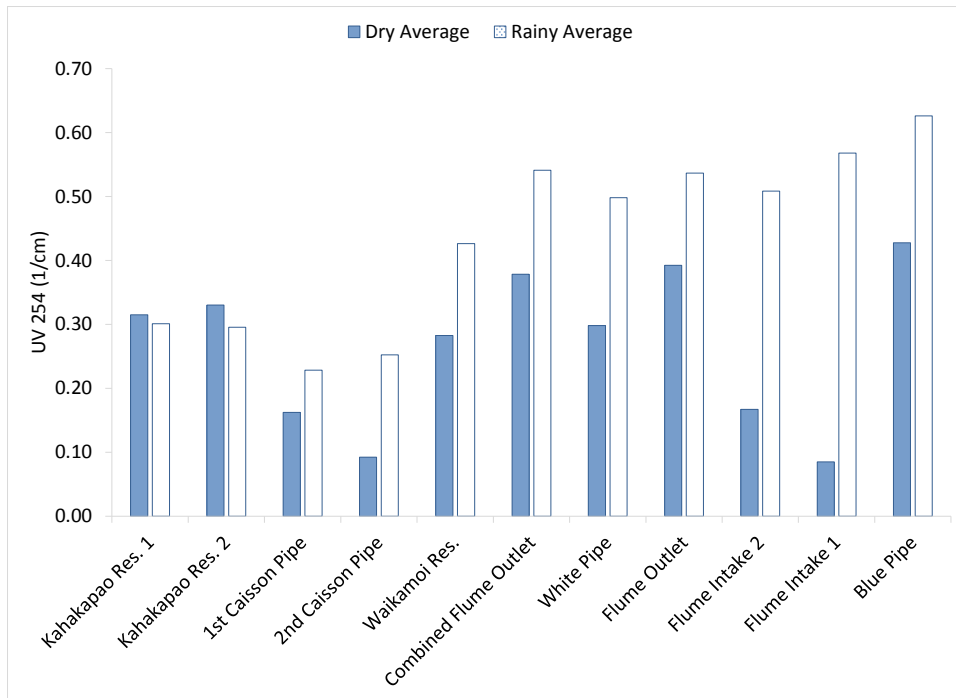
Figure D–14 Dry vs Rainy UV 254
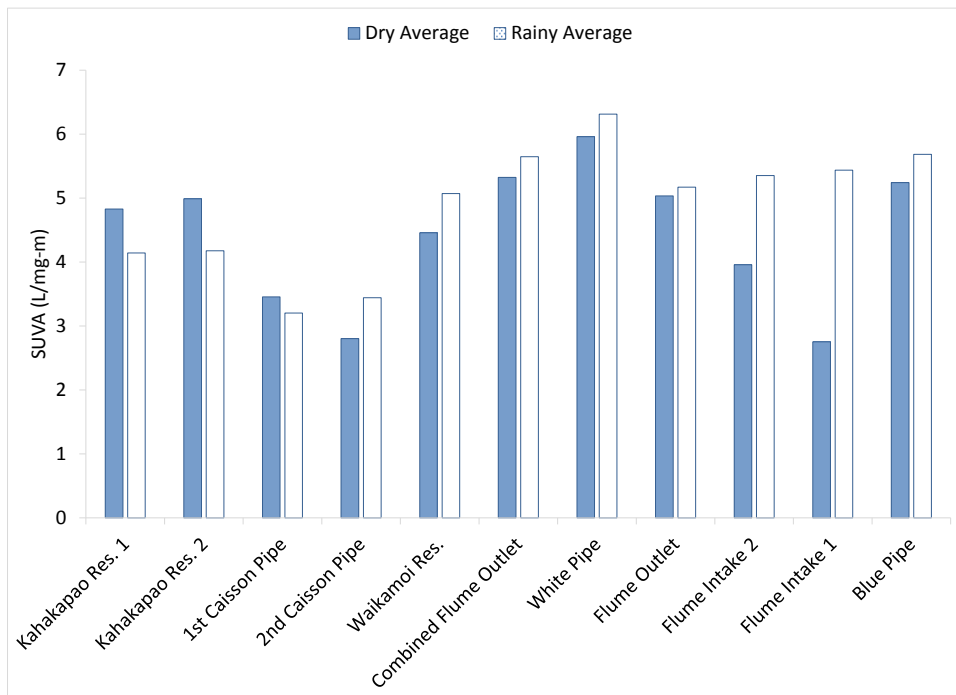
Figure D–15 Dry vs Rainy SUVA
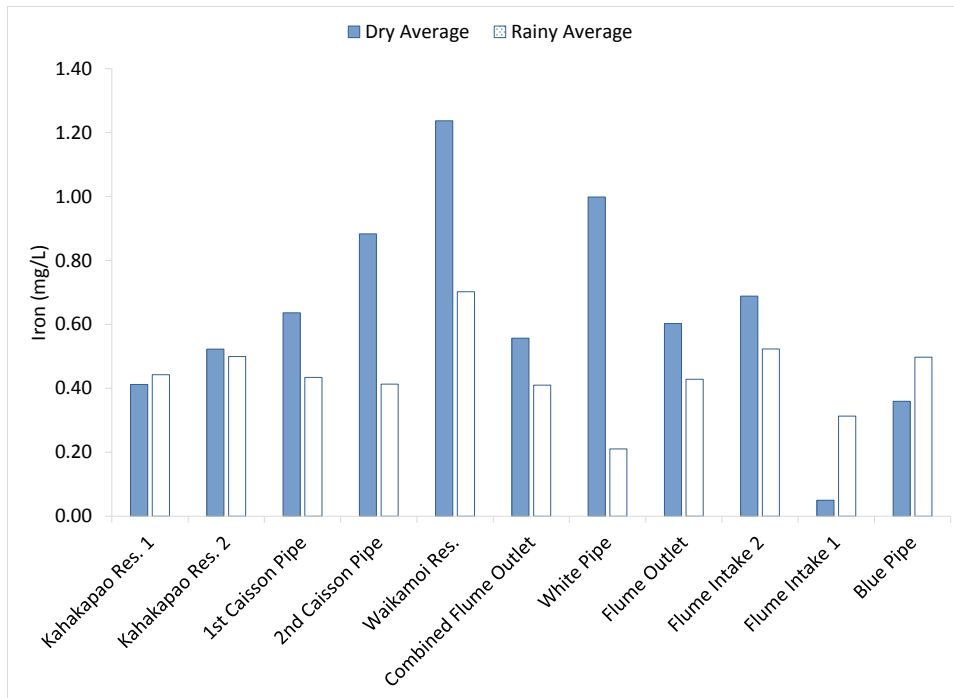
Figure D–16 Dry vs Rainy Iron
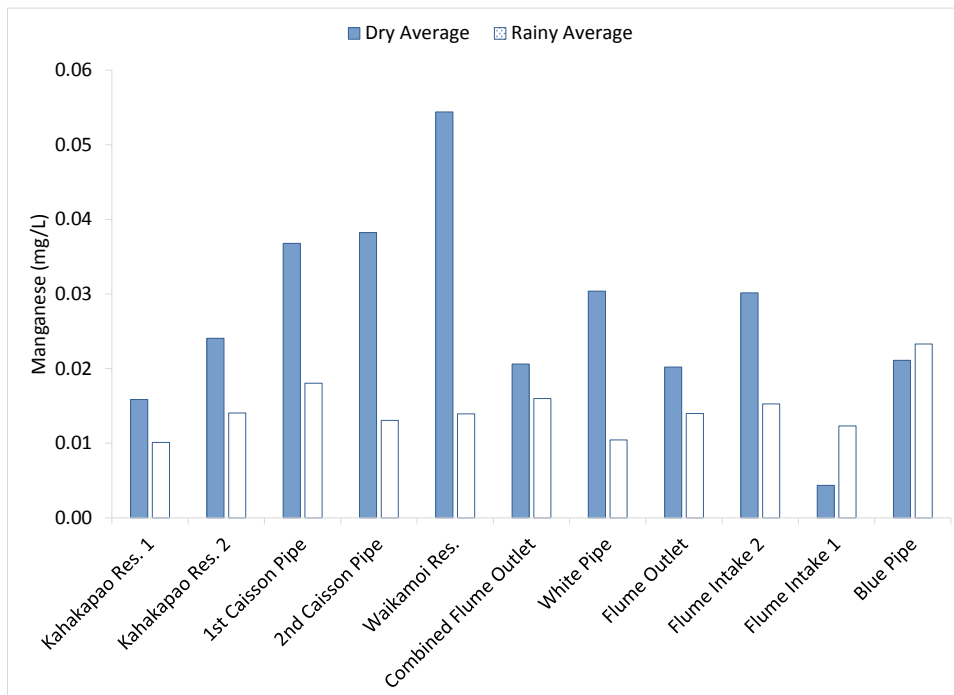
Figure D–17 Dry vs Rainy Manganese
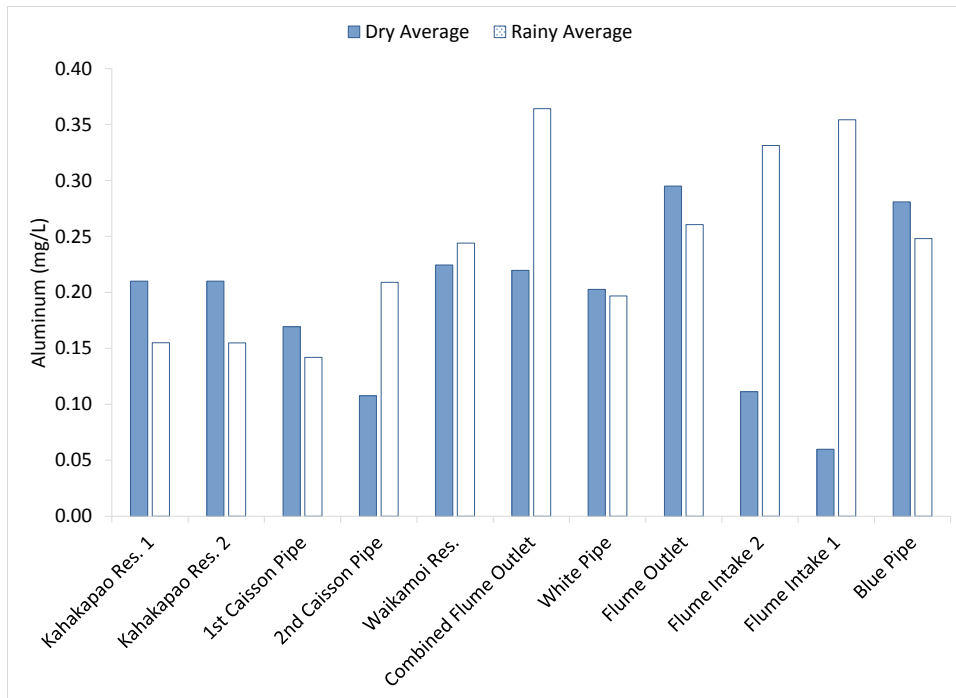
Figure D–18 Dry vs Rainy Aluminum
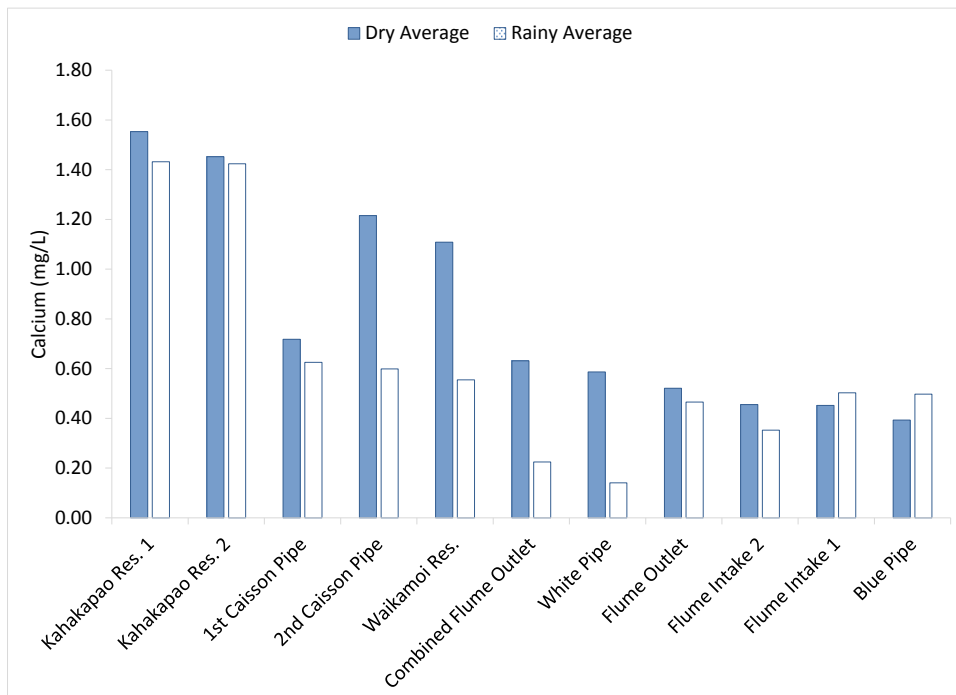
Figure D–19 Dry vs Rainy Calcium
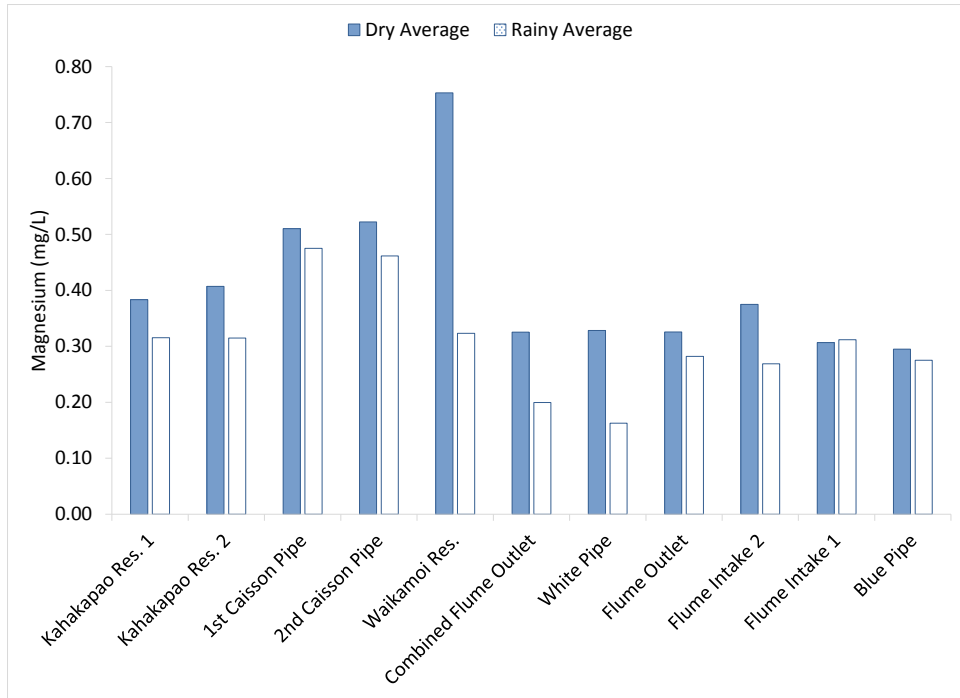
Figure D–20 Dry vs Rainy Magnesium
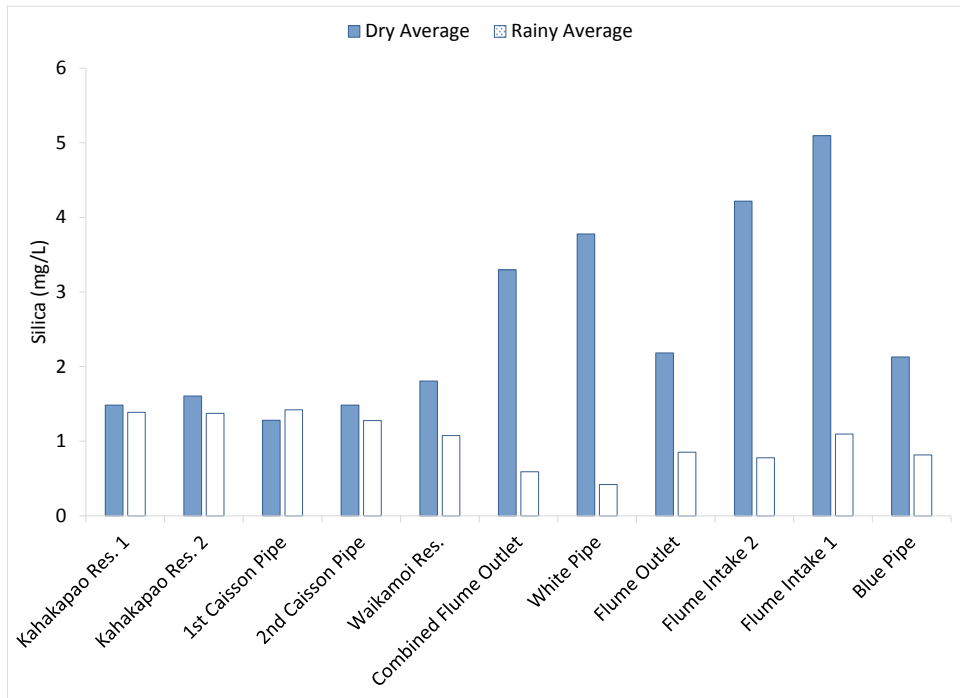
Figure D–21 Dry vs Rainy Silica

Table D–4 Waikamoi Watershed Quality Summary

Date	Kahakapao Res. 1	Kahakapao Res. 2	1st Caisson Pipeline	2nd Caisson Pipeline	Waikamoi Res.	Combined Flume Outlet	White Pipeline	Flume Outlet	Flume Intake 2	Flume Intake 1	Blue Pipeline
pH											
11/15/2012	5.88	5.97	5.09	4.87	4.30	-	-	4.03	3.84	4.12	3.99
1/31/2013	6.29	6.99	5.13	5.18	4.92	-	-	4.31	4.47	4.17	4.24
4/30/2013	6.77	6.53	5.66	5.84	6.09	5.07	4.85	-	4.89	4.78	-
8/6/2013	6.59	6.30	5.29	5.16	4.58	4.38	-	4.67	-	-	4.07
10/22/2013	6.24	6.00	5.68	6.00	6.48	5.43	-	5.00	-	-	4.64
5/12/2014	6.61	6.40	5.62	5.15	4.74	4.56	4.72	4.51	4.57	-	4.56
Temperature (ºC)											
11/15/2012	17.6	17.4	15.1	15.6	15.2	-	-	15.0	16.9	15.5	15.1
1/31/2013	15.7	16.7	14.1	14.4	16.1	-	-	15.9	14.3	14.5	14.4
4/30/2013	21.8	21.5	17.3	17.6	25.2	22.7	22.4	-	19.0	19.0	-
8/6/2013	22.1	22.6	18.2	18.9	19.6	18.6	-	19.5	-	-	18.7
10/22/2013	20.0	20.6	16.6	19.5	21.9	16.7	-	16.9	-	-	17.2
5/12/2014	19.1	18.4	16.4	16.2	17.1	17.3	18.0	17.3	17.5	-	17.4
Turbidity (ntu)											
11/15/2012	3.56	4.60	2.21	2.74	6.46	-	-	2.77	1.91	1.60	2.63
1/31/2013	2.72	2.69	2.35	1.32	3.39	-	-	7.48	2.55	7.24	4.60
4/30/2013	1.80	2.20	0.84	3.05	6.36	2.94	3.18	-	1.34	0.51	-
8/6/2013	3.40	4.37	1.39	3.87	7.41	2.09	-	1.33	-	-	1.07
10/22/2013	2.54	3.86	0.69	2.99	4.69	0.75	-	0.98	-	-	0.43
5/12/2014	1.92	2.01	2.21	7.79	10.1	5.25	5.47	4.81	4.62	-	4.93

Date	Kahakapao Res. 1	Kahakapao Res. 2	1st Caisson Pipeline	2nd Caisson Pipeline	Waikamoi Res.	Combined Flume Outlet	White Pipeline	Flume Outlet	Flume Intake 2	Flume Intake 1	Blue Pipeline
Alkalinity (mg/L as CaCO3)											
11/15/2012	3.75	5	2	1.5	0.75	-	-	0	0	0	0
1/31/2013	5.5	3.5	2.5	3.3	2	-	-	1.5	2	0.5	1
4/30/2013	6	5.5	5.5	5	9	4	4	-	4	3.5	-
8/6/2013	5	5	3.5	3.5	2.25	1.5	-	1.75	-	-	0.5
10/22/2013	3.25	3	1	4.75	5.25	0.5	-	0	-	-	0
5/12/2014	4.5	3.5	3	2.5	2	1	0.5	1	0.5	-	1
DO (mg/L)											
11/15/2012	7.4	7.2	8.4	7.4	8.4	-	-	8.7	9.1	8.7	8.1
1/31/2013	11.3	10.8	12.2	9.9	10.2	-	-	10.9	11.0	10.8	10.7
4/30/2013	7.6	7.0	7.0	6.4	7.2	7.1	7.2	-	6.8	7.0	-
8/6/2013	6.3	6.2	5.3	4.5	5.8	6.7		6.4	-	-	6.8
10/22/2013	6.4	6.9	6.3	5.3		7.2		6.9	-	-	6.1
5/12/2014	7.0	7.0	7.0	7.1	6.8	7.7	7.5	7.9	-	-	7.5
Color (CU)											
11/15/2012	84	84	44	42	99	-	-	97	112	81	122
1/31/2013	65	66	45	26	81	-	-	123	108	154	139
4/30/2013	43	44	22	6	45	59	64	-	29	11	-
8/6/2013	78	83	36	22	67	128	-	96	-	-	122
10/22/2013	77	88	22	16	39	61	-	76	-	-	54
5/12/2014	52	52	25	61	101	117	110	120	106	-	137

Date	Kahakapao Res. 1	Kahakapao Res. 2	1st Caisson Pipeline	2nd Caisson Pipeline	Waikamoi Res.	Combined Flume Outlet	White Pipeline	Flume Outlet	Flume Intake 2	Flume Intake 1	Blue Pipeline
UV 254 (1/cm)											
11/15/2012	0.365	0.363	0.260	0.247	0.479	-	-	0.484	0.534	0.432	0.586
1/31/2013	0.296	0.306	0.258	0.151	0.343	-	-	0.578	0.511	0.704	0.677
4/30/2013	0.223	0.224	0.146	0.061	0.290	0.270	0.298	-	0.167	0.085	-
8/6/2013	0.352	0.370	0.195	0.124	0.328	0.562	-	0.440	-	-	0.566
10/22/2013	0.370	0.397	0.146	0.092	0.230	0.303	-	0.345	-	-	0.289
5/12/2014	0.242	0.217	0.167	0.359	0.457	0.541	0.498	0.549	0.480	-	0.616
DOC (mg/L)											
11/15/2012	8.58	8.14	8.78	8.15	9.78	-	-	10.00	10.00	9.20	11.30
1/31/2013	7.21	6.96	7.04	4.92	7.66	-	-	11.20	9.66	11.40	12.30
4/30/2013	4.62	4.46	4.15	2.97	5.12	4.80	5.00	-	4.22	3.09	-
8/6/2013	7.52	7.75	5.47	3.81	7.45	9.44	-	8.59	-	-	9.21
10/22/2013	7.44	7.68	4.45	2.97	6.95	6.91	-	6.97	-	-	6.66
5/12/2014	5.95	5.91	5.61	8.50	7.82	9.58	7.89	9.94	8.85	-	9.68
SUVA (L/mg-m)											
11/15/2012	4.25	4.46	2.96	3.03	4.90	-	-	4.84	5.34	4.70	5.18
1/31/2013	4.11	4.40	3.66	3.07	4.47	-	-	5.16	5.29	6.18	5.50
4/30/2013	4.83	5.02	3.52	2.05	5.66	5.63	5.96	-	3.96	2.75	-
8/6/2013	4.68	4.77	3.56	3.25	4.40	5.95	-	5.12	-	-	6.15
10/22/2013	4.98	5.17	3.28	3.10	3.31	4.38	-	4.95	-	-	4.34
5/12/2014	4.07	3.67	2.98	4.22	5.84	5.65	6.31	5.52	5.42	-	6.36

Date	Kahakapao Res. 1	Kahakapao Res. 2	1st Caisson Pipeline	2nd Caisson Pipeline	Waikamoi Res.	Combined Flume Outlet	White Pipeline	Flume Outlet	Flume Intake 2	Flume Intake 1	Blue Pipeline
Free ATP (pg/mL)											
11/15/2012	-	-	-	-	-	-	-	-	-	-	-
1/31/2013	57	53	75	41	158	-	-	80	31	62	39
4/30/2013	89	140	45	19	136	49	55		53	23	-
8/6/2013	146	213	47	62	149	90	-	41	-	-	81
10/22/2013	109	98	13	25	213	35	-	48	-	-	30
5/12/2014	52	62	59	98	92	69	57	98	89	-	51
Total ATP (pg/mL)											
11/15/2012	104	201	98	100	86	-	-	63	41	34	46
1/31/2013	63	115	60	40	243	-	-	82	59	66	65
4/30/2013	185	149	47	58	889	57	68	-	61	24	-
8/6/2013	516	461	106	135	161	103	-	64	-	-	98
10/22/2013	247	307	22	65	664	59	-	77	-	-	33
5/12/2014	151	233	155	399	313	242	221	231	250	-	143
Cellular ATP (pg/mL)											
11/15/2012	-	-	-	-	-	-	-	-	-	-	-
1/31/2013	6	62	<0.5	<0.5	86	-	-	2	28	4	27
4/30/2013	96	9	2	39	753	8	13	-	8	0	-
8/6/2013	370	247	59	73	12	12	-	23	-	-	17
10/22/2013	138	208	9	39	451	24	-	29	-	-	3
5/12/2014	99	170	96	301	222	173	164	133	162	-	92

Date	Kahakapao Res. 1	Kahakapao Res. 2	1st Caisson Pipeline	2nd Caisson Pipeline	Waikamoi Res.	Combined Flume Outlet	White Pipeline	Flume Outlet	Flume Intake 2	Flume Intake 1	Blue Pipeline
					Free/Total ATP Fraction						
11/15/2012	-	-	-	-	-	-	-	-	-	-	-
1/31/2013	0.91	0.46	1.24	1.04	0.65	-	-	0.98	0.53	0.94	0.59
4/30/2013	0.48	0.95	0.97	0.33	0.15	0.86	0.81	-	0.88	0.99	-
8/6/2013	0.28	0.47	0.45	0.46	0.93	0.89	-	0.65	-	-	0.83
10/22/2013	0.44	0.32	0.61	0.39	0.32	0.60	-	0.63	-	-	0.90
5/12/2014	0.35	0.27	0.38	0.25	0.29	0.29	0.26	0.43	0.36	-	0.36
					TSS (mg/L)						
11/15/2012	0.7	4.0	2.0	0.2	1.2	-	-	0.5	0.7	-	0.0
1/31/2013	2.5	3.0	3.0	1.5	2.5	-	-	7.3	4.0	2.0	2.0
4/30/2013	3.0	3.0	2.5	3.0	6.5	3.2	3.2	-	3.0	0.0	-
8/6/2013	2.5	3.5	11.5	3.7	1.0	0.0	-	0.4	-	-	0.0
10/22/2013	1.2	3.0	0.0	0.0	2.5	0.0	-	0.4	-	-	0.0
5/12/2014	1.7	2.0	2.0	6.5	6.0	2.5	1.5	3.3	4.0	-	0.5
					TDS (mg/L)						
11/15/2012	62	36	12	5	50	-	-	101	35	-	87
1/31/2013	28	19	8	29	15	-	-	36	38	23	38
4/30/2013	33	43	23	33	53	23	26	-	22	12	-
8/6/2013	14	13	8	9	12	19	-	18	-	-	18
10/22/2013	33	31	19	6	10	32	-	9	-	-	22
5/12/2014	27	26	22	28	45	27	36	53	45	-	48

Date	Kahakapao Res. 1	Kahakapao Res. 2	1st Caisson Pipeline	2nd Caisson Pipeline	Waikamoi Res.	Combined Flume Outlet	White Pipeline	Flume Outlet	Flume Intake 2	Flume Intake 1	Blue Pipeline
					Iron (mg/L)						
11/15/2012	0.656	0.796	0.493	0.293	0.647	-	-	0.361	0.439	0.278	0.455
1/31/2013	0.362	0.337	0.292	0.180	0.662	-	-	0.549	0.665	0.348	0.610
4/30/2013	0.215	0.234	0.350	1.384	2.304	0.855	0.999	-	0.688	0.050	-
8/6/2013	0.554	0.623	1.136	0.665	0.674	0.381	-	0.512	-	-	0.438
10/22/2013	0.468	0.710	0.423	0.601	0.733	0.435	-	0.693	-	-	0.280
5/12/2014	0.308	0.365	0.516	0.767	0.796	0.410	0.211	0.374	0.464	-	0.426
					Manganese (mg/L)						
11/15/2012	0.010	0.020	0.030	0.012	0.015	-	-	0.015	0.014	0.014	0.015
1/31/2013	0.010	0.011	0.008	0.009	0.011	-	-	0.013	0.018	0.011	0.014
4/30/2013	0.006	0.010	0.009	0.066	0.102	0.027	0.030	-	0.030	0.004	-
8/6/2013	0.018	0.023	0.086	0.023	0.015	0.013	-	0.019	-	-	0.021
10/22/2013	0.023	0.039	0.015	0.025	0.046	0.021	-	0.022	-	-	0.021
5/12/2014	0.011	0.011	0.016	0.018	0.016	0.016	0.010	0.014	0.013	-	0.041
					Calcium (mg/L)						
11/15/2012	1.52	1.74	0.721	0.680	0.717	-	-	0.579	0.357	0.474	0.728
1/31/2013	1.58	1.41	0.713	0.725	0.579	-	-	0.595	0.456	0.531	0.525
4/30/2013	1.70	1.32	0.813	1.33	1.46	0.714	0.587	-	0.455	0.452	-
8/6/2013	1.47	1.48	0.616	0.630	0.490	0.473	-	0.507	-	-	0.411
10/22/2013	1.49	1.56	0.725	1.69	1.38	0.708	-	0.535	-	-	0.376
5/12/2014	1.19	1.12	0.441	0.391	0.369	0.224	0.140	0.221	0.243	-	0.238

Date	Kahakapao Res. 1	Kahakapao Res. 2	1st Caisson Pipeline	2nd Caisson Pipeline	Waikamoi Res.	Combined Flume Outlet	White Pipeline	Flume Outlet	Flume Intake 2	Flume Intake 1	Blue Pipeline
Magnesium (mg/L)											
11/15/2012	0.306	0.315	0.568	0.550	0.430	-	-	0.323	0.279	0.318	0.310
1/31/2013	0.351	0.343	0.453	0.444	0.259	-	-	0.328	0.307	0.306	0.304
4/30/2013	0.325	0.340	0.515	0.586	1.017	0.333	0.328	-	0.375	0.307	-
8/6/2013	0.394	0.406	0.467	0.440	0.371	0.328	-	0.327	-	-	0.304
10/22/2013	0.431	0.475	0.549	0.541	0.871	0.315	-	0.324	-	-	0.286
5/12/2014	0.289	0.288	0.405	0.391	0.281	0.200	0.163	0.194	0.221	-	0.211
Silica (mg/L)											
11/15/2012	1.52	1.56	1.51	1.46	1.14	-	-	0.943	0.853	1.13	0.991
1/31/2013	1.36	1.23	1.48	1.14	1.12	-	-	1.07	0.810	1.06	0.882
4/30/2013	1.20	1.40	1.10	1.33	2.55	3.92	3.78	-	4.22	5.10	-
8/6/2013	1.47	1.49	1.41	1.46	1.46	3.08	-	1.90	-	-	1.57
10/22/2013	1.78	1.92	1.32	1.66	1.41	2.90	-	2.47	-	-	2.68
5/12/2014	1.29	1.33	1.27	1.23	0.960	0.591	0.418	0.549	0.668	-	0.574
Aluminum (mg/L)											
11/15/2012	0.079	0.058	0.005	0.005	0.103	-	-	0.083	0.115	-	0.005
1/31/2013	0.221	0.226	0.228	0.170	0.262	-	-	0.362	0.438	0.354	0.399
4/30/2013	0.154	0.150	0.109	0.076	0.136	0.183	0.203	-	0.111	0.060	-
8/6/2013	0.211	0.237	0.304	0.177	0.406	0.270	-	0.363	-	-	0.370
10/22/2013	0.266	0.243	0.096	0.069	0.131	0.205	-	0.227	-	-	0.192
5/12/2014	0.165	0.181	0.193	0.452	0.367	0.364	0.197	0.337	0.441	-	0.340

Date	Kahakapao Res. 1	Kahakapao Res. 2	1st Caisson Pipeline	2nd Caisson Pipeline	Waikamoi Res.	Combined Flume Outlet	White Pipeline	Flume Outlet	Flume Intake 2	Flume Intake 1	Blue Pipeline
Chloride (mg/L)											
11/15/2012	3.81	3.62	4.68	4.50	4.38	-	-	4.43	4.45	3.95	4.40
1/31/2013	4.27	4.45	4.28	4.09	3.55	-	-	3.00	3.74	3.64	2.32
4/30/2013	4.99	4.80	5.29	5.91	5.20	4.98	5.19	-	5.58	4.77	-
8/6/2013	4.11	3.99	4.30	4.37	4.26	4.16	-	3.99	-	-	4.19
10/22/2013	2.73	2.97	3.16	3.21	2.68	2.82	-	2.86	-	-	2.82
5/12/2014	2.34	2.16	2.57	2.25	2.00	1.92	1.74	2.08	1.75	-	1.91
Sulfate (mg/L)											
11/15/2012	1.77	1.62	1.76	1.73	1.68	-	-	1.53	1.58	1.51	1.53
1/31/2013	2.09	2.04	2.25	2.39	1.93	-	-	2.74	2.86	2.38	1.00
4/30/2013	2.05	1.90	1.77	1.99	1.00	1.63	1.64	-	1.86	1.92	-
8/6/2013	1.87	1.86	1.84	1.89	1.81	1.83	-	1.78	-	-	1.77
10/22/2013	0.82	0.90	0.80	0.86	0.77	0.77	-	0.70	-	-	0.81
5/12/2014	0.86	0.85	0.92	0.92	0.79	0.80	0.78	0.83	0.78	-	0.78
Bromide (mg/L)											
11/15/2012	<0.2	<0.2	<0.2	<0.2	<0.2	-	-	<0.2	<0.2	<0.2	<0.2
1/31/2013	<0.2	<0.2	<0.2	<0.2	<0.2	-	-	<0.2	<0.2	<0.2	<0.2
4/30/2013	<0.2	<0.2	<0.2	<0.2	<0.2	<0.2	<0.2	-	<0.2	<0.2	-
8/6/2013	<0.2	<0.2	<0.2	<0.2	<0.2	<0.2	-	<0.2	-	-	<0.2
10/22/2013	<0.2	<0.2	<0.2	<0.2	<0.2	<0.2	-	<0.2	-	-	<0.2
5/12/2014	<0.2	<0.2	<0.2	<0.2	<0.2	<0.2	<0.2	<0.2	<0.2	-	<0.2

APPENDIX E. CONFIRM EXISTING PROCESS OPERATION

Table E–1 Preliminary and Experimental Jar Testing Results

ACH Dose (mg/L)	pH	Temperature, ºC	Alkalinity, mg/L CaCO$_3$	Turbidity, ntu (Removal, %)	Color, CU (Removal, %)	UV254, 1/cm (Removal, %)	DOC, mg/L (Removal, %)	SUVA, L/mg-m (Removal, %)
		Date: 9/18/12	Plant ACH Dose: 29.5 mg/L	pH Adjustment: None				
0 (Raw)	5.6	17	2.25	1.42	83	0.362	7.05	5.13
21.4	-	-	-	3.19 (0)	-	-	-	-
24.1	-	-	-	1.35 (5)	-	-	-	-
25.5	-	-	-	1.09 (23)	-	-	-	-
29.5	-	-	-	1.09 (23)	-	-	-	-
29.5	-	-	-	1.49 (0)	-	-	-	-
32.2	-	-	-	3.24 (0)	-	-	-	-
		Date: 4/23/13	Plant ACH Dose: 21 mg/L	pH Adjustment: None				
0 (Raw)	6.09	15.8	5	2.1	48	0.217	4.66	4.66
18.8	6.08	20.5	3.5	0.819 (61)	2 (96)	0.03 (86)	-	-
20.1	5.85	20.5	3.5	0.888 (58)	0.5 (99)	0.026 (88)	2.2 (53)	1.18 (75)
21.4	5.88	19.7	3.5	0.753 (64)	0.5 (99)	0.028 (87)	2.19 (53)	1.28 (73)
21.4	5.88	20	3.5	0.763 (64)	1 (98)	0.029 (87)	2.15 (54)	1.35 (71)
22.8	5.88	20	3.5	1.01 (52)	3 (94)	0.028 (87)	-	-
24.1	5.86	20.3	3.5	3.06 (0)	0.5 (99)	0.024 (89)	-	-
		Date: 4/24/13	Plant ACH Dose: 21.7 mg/L	pH Adjustment: None				
0 (Raw)	6.09	16	5.5	2.02	44	0.218	4.58	4.76
18.8	5.94	21.7	3.5	0.5 (75)	3 (93)	0.038 (83)	-	-
20.1	5.9	21.4	3.25	0.597 (70)	3 (93)	0.03 (86)	-	-
21.4	5.86	21.1	3.5	0.433 (79)	3 (93)	0.039 (82)	-	-
21.4	5.86	21.4	3.5	0.49 (76)	3 (93)	0.037 (83)	-	-
22.8	5.84	21.6	3.5	0.594 (71)	3 (93)	0.033 (85)	-	-
24.1	5.77	21.9	3.5	1.46 (28)	2 (95)	0.027 (88)	-	-

ACH Dose (mg/L)	pH	Temperature, ºC	Alkalinity, mg/L CaCO$_3$	Turbidity, ntu (Removal, %)	Color, CU (Removal, %)	UV254, 1/cm (Removal, %)	DOC, mg/L (Removal, %)	SUVA, L/mg-m (Removal, %)
— Date: 5/17/14 Plant ACH Dose: 21 mg/L pH Adjustment: None								
0 (Raw)	5.38	17.9	4	2.61	64	0.246	6.15	4.00
14.7	-	-	-	1.38 (47)	7 (89)	0.062 (75)	3.09 (50)	2.01 (50)
17.4	-	-	-	0.845 (68)	3 (95)	0.048 (80)	2.41 (61)	1.99 (50)
20.1	-	-	-	1.58 (39)	4 (94)	0.027 (89)	1.96 (68)	1.38 (66)
22.8	-	-	-	3.27 (0)	3 (95)	0.024 (90)	1.85 (70)	1.30 (68)
25.5	-	-	-	4.39 (0)	1 (98)	0.024 (90)	2.13 (65)	1.13 (72)
28.1	-	-	-	4.34 (0)	1 (98)	0.032 (87)	2.55 (59)	1.25 (69)
Date: 5/18/14 Plant ACH Dose: 21 mg/L pH Adjustment: 8.00								
0 (Raw)	5.8	18.6	2	3.67	62	0.246	6.27	3.92
25.5	-	-	-	3.08 (16)	8 (87)	0.045 (82)	3 (52)	1.50 (62)
28.1	-	-	-	1.17 (68)	5 (92)	0.038 (85)	2.57 (59)	1.48 (62)
30.8	-	-	-	0.571 (84)	2 (97)	0.025 (90)	2.22 (65)	1.13 (71)
33.5	-	-	-	0.53 (86)	2 (97)	0.025 (90)	2.13 (66)	1.17 (70)
36.2	-	-	-	0.8 (78)	7 (89)	0.042 (83)	2.39 (62)	1.76 (55)
Date: 5/21/14 Plant ACH Dose: 21.2 mg/L pH Adjustment: 7.00								
0 (Raw)	5.4	18.3	3	3.54	67	0.309	6.5	4.75
17.4	-	-	-	2.74 (23)	8 (88)	0.065 (79)	3.12 (52)	2.08 (56)
20.1	-	-	-	1.56 (56)	6 (91)	0.045 (85)	2.82 (57)	1.60 (66)
22.8	-	-	-	0.81 (77)	2 (97)	0.034 (89)	2.4 (63)	1.42 (70)
25.5	-	-	-	0.62 (82)	2 (97)	0.027 (91)	2.23 (66)	1.21 (75)
28.1	-	-	-	0.74 (79)	3 (96)	0.028 (91)	2.32 (64)	1.21 (75)
30.8	-	-	-	0.9 (75)	8 (88)	0.043 (86)	2.48 (62)	1.73 (64)
Date: 5/22/14 Plant ACH Dose: 23.6 mg/L pH Adjustment: 7.50								
0 (Raw)	5.4	18.1	3	3.18	63	0.274	6.33	4.33
17.4	-	-	-	2.51 (21)	7 (89)	0.061 (78)	3.02 (52)	2.02 (53)
20.1	-	-	-	1.42 (55)	5 (92)	0.044 (84)	2.64 (58)	1.67 (61)
22.8	-	-	-	0.73 (77)	2 (97)	0.032 (88)	2.33 (63)	1.37 (68)
25.5	-	-	-	0.54 (83)	2 (97)	0.024 (91)	2.18 (66)	1.10 (75)
28.1	-	-	-	0.8 (75)	1 (98)	0.027 (90)	2.26 (64)	1.19 (72)
30.8	-	-	-	0.89 (72)	4 (94)	0.038 (86)	2.47 (61)	1.54 (64)

ACH Dose (mg/L)	pH	Temperature, ºC	Alkalinity, mg/L CaCO$_3$	Turbidity, ntu (Removal, %)	Color, CU (Removal, %)	UV254, 1/cm (Removal, %)	DOC, mg/L (Removal, %)	SUVA, L/mg-m (Removal, %)
			Date: 5/23/14	Plant ACH Dose: 22.1 mg/L	pH Adjustment: 6.5			
0 (Raw)	5.43	18	3	3.14	65	0.268	6.1	4.39
14.7	-	-	-	1.25 (60)	9 (86)	0.065 (76)	2.92 (52)	2.23 (49)
17.4	-	-	-	0.92 (71)	9 (86)	0.052 (81)	2.53 (59)	2.06 (53)
20.1	-	-	-	0.78 (75)	3 (95)	0.025 (91)	2.07 (66)	1.21 (73)
22.8	-	-	-	1.13 (64)	3 (95)	0.054 (80)	2.39 (61)	2.26 (49)
25.5	-	-	-	2.58 (18)	8 (88)	0.059 (78)	2.64 (57)	2.23 (49)
28.1	-	-	-	3.15 (0)	11 (83)	0.067 (75)	3.02 (50)	2.22 (50)
			Date: 5/29/14	Plant ACH Dose: 21.3 mg/L	pH Adjustment: 8.70			
0 (Raw)	5.43	18	3	3.14	65	0.268	6.1	4.39
34.8	-	-	-	0.98 (69)	2 (97)	0.034 (87)	2.25 (63)	1.51 (66)
37.5	-	-	-	0.52 (83)	1 (98)	0.024 (91)	1.94 (68)	1.24 (72)
40.2	-	-	-	0.47 (85)	2 (97)	0.026 (90)	1.98 (68)	1.31 (70)
			Date: 5/31/14	Plant ACH Dose: 19.8 mg/L	pH Adjustment: 8.50			
0 (Raw)	5.41	18.9	3	3.34	63	0.327	6.51	5.02
32.2	-	-	-	1.1 (67)	3 (95)	0.048 (85)	2.62 (60)	1.83 (64)
34.8	-	-	-	0.84 (75)	2 (97)	0.031 (91)	2.3 (65)	1.35 (73)
37.5	-	-	-	0.57 (83)	2 (97)	0.025 (92)	1.91 (71)	1.31 (74)
40.2	-	-	-	0.53 (84)	2 (97)	0.028 (91)	2.15 (67)	1.30 (74)
			Date: 6/1/14	Plant ACH Dose: 22.4 mg/L	pH Adjustment: 7.50			
0 (Raw)	5.18	18.6	3	2.58	69	0.303	6.29	4.82
20.1	-	-	-	1.61 (38)	7 (90)	0.053 (83)	2.79 (56)	1.90 (61)
22.8	-	-	-	1.23 (52)	5 (93)	0.043 (86)	2.57 (59)	1.67 (65)
25.5	-	-	-	0.74 (71)	3 (96)	0.039 (87)	2.4 (62)	1.63 (66)
28.1	-	-	-	0.47 (82)	1 (99)	0.026 (91)	1.99 (68)	1.31 (73)
30.8	-	-	-	0.6 (77)	2 (97)	0.033 (89)	2.2 (65)	1.50 (69)
33.5	-	-	-	0.69 (73)	3 (96)	0.035 (88)	2.28 (64)	1.54 (68)

Table E–2 Water Quality Averages for Olinda Process Train and Control-UF

Water Quality	Raw			Plant-ACH			Plant-UF			Control-UF		
	Min	Avg	Max	Min	Avg	Max	Min	Avg	Max	Min	Avg	Max
pH	4.6	5.9	7.3	4.7	5.7	7.2	4.7	5.7	7.3	4.7	5.6	6.7
Temp. ($^\circ$C)	13.8	18.7	22.1	15.2	19.1	22.2	15.1	19.3	22.7	15.8	19.4	22.7
Turb. (ntu)	0.71	3.2	12	0.06	0.74	3.01	0.04	0.06	0.31	0.03	0.05	0.12
Alk. (mg/L $CaCO_3$)	0.75	4.5	13	0.75	3.5	11	0.75	3.5	10	0.75	3.3	9.8
Color (CU)	2	70	108	0	3	16	0	2	9	0	2	12
UV254 (1/cm)	0.039	0.309	0.441	0.012	0.047	0.350	0.013	0.043	0.085	0.010	0.043	0.104
DOC (mg/L)	3.0	6.8	10.4	1.6	2.7	4.8	1.3	2.3	5.7	1.3	2.3	3.6
SUVA (L/mg-m)	1.2	4.6	8.6	0.64	1.7	10.6	0.76	1.9	2.9	0.41	1.9	3.1
TSS (mg/L)	0.5	3	6	0	1	4	0	0	0.5	0	0	0.5
TDS (mg/L)	9	41	100	7	32	90	4	31	98	3	26	62
Fe (mg/L)	0.282	0.612	0.968	0.003	0.053	0.150	0.002	0.012	0.043	0.002	0.010	0.029
Mn (mg/L)	0.007	0.017	0.041	0.012	0.018	0.025	0.010	0.018	0.026	0.010	0.018	0.025
Al (mg/L)	0.005	0.256	0.444	0.005	0.042	0.251	0.005	0.008	0.043	0.005	0.007	0.037
Ca (mg/L)	0.96	1.50	2.49	1.20	1.84	2.97	1.09	1.44	1.93	1.02	1.42	1.92
Mg (mg/L)	0.30	0.38	0.47	0.33	0.39	0.45	0.30	0.37	0.44	0.30	0.37	0.45
Si (mg/L)	1.35	1.51	1.81	1.29	1.56	1.91	1.30	1.45	1.70	1.29	1.44	1.69
Cl^- (mg/L)	2.6	4.6	8.3	4.5	6.4	10.1	4.4	6.0	7.9	4.4	6.0	7.1
SO_4^{2-} (mg/L)	0.73	1.5	2.0	0.69	1.4	2.2	0.69	1.4	2.1	0.70	1.4	1.9
Br^- (mg/L)	<0.2	0.2	0.6	-	<0.2	-	-	<0.2	-	-	<0.2	-
TTHM (μg/L)	-	-	-	-	-	-	120	185	250	120	187	250
HAA_5 (μg/L)	-	-	-	-	-	-	45	75	110	45	73	110
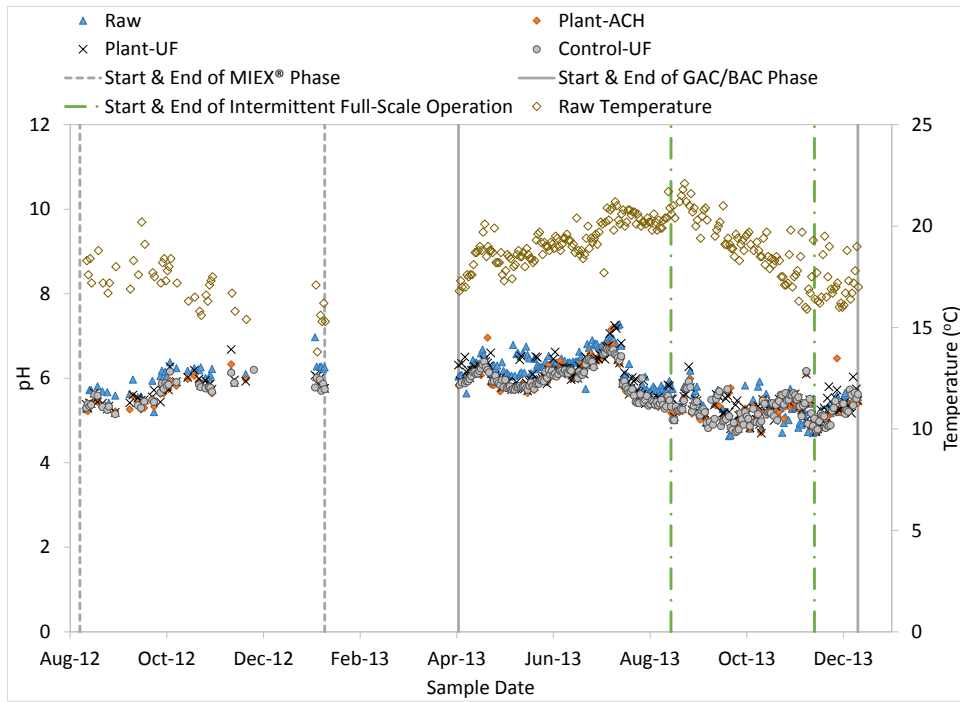
Figure E–1 Olinda WTP Temperature and pH Time-Series Graph
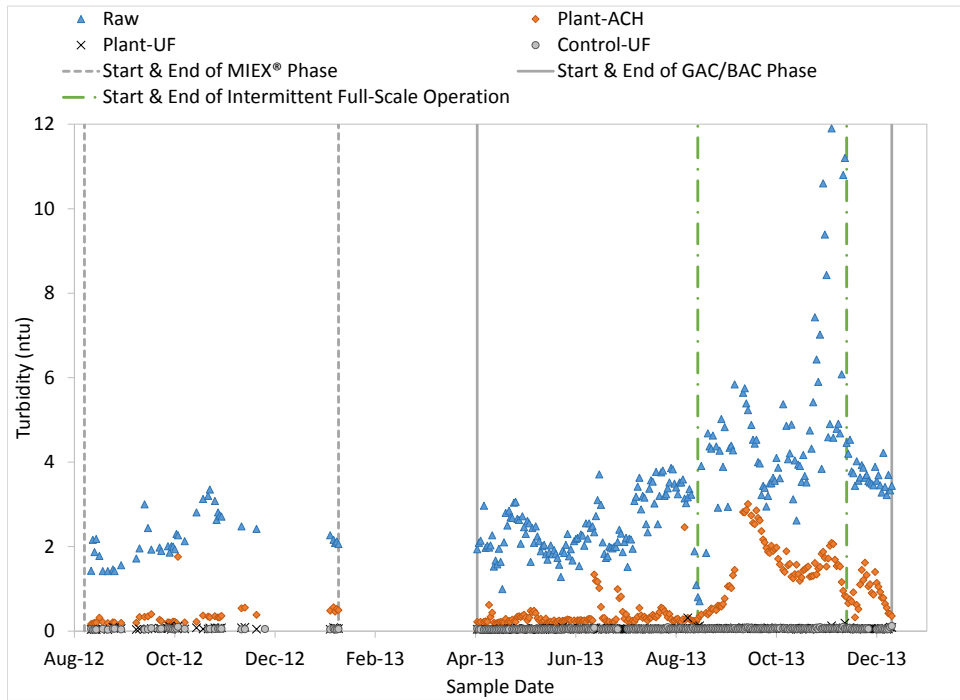
Figure E–2 Olinda WTP Turbidity Time-Series Graph

250
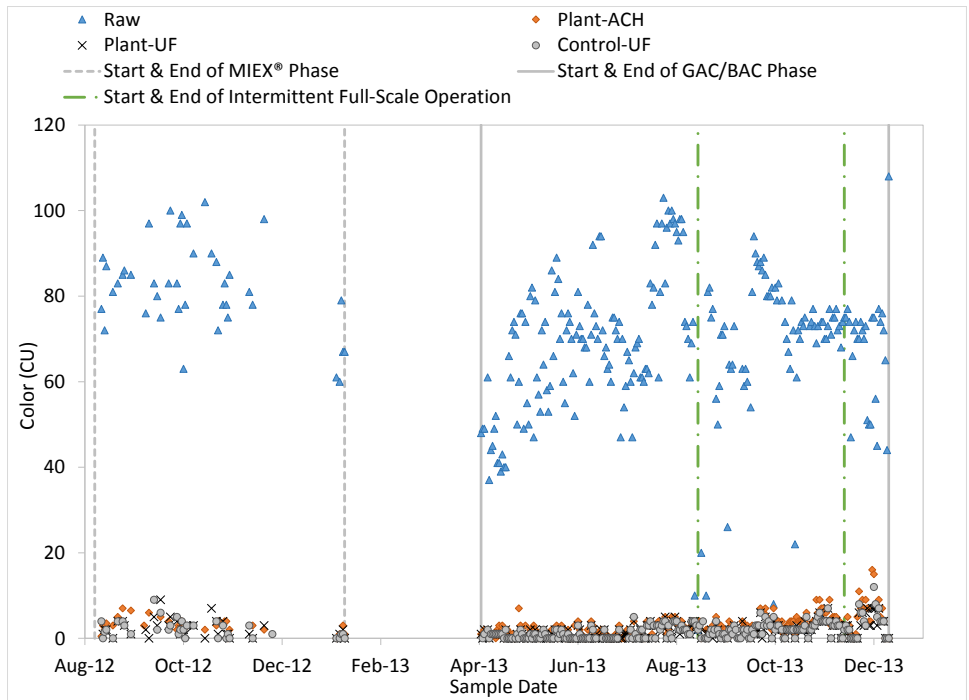
Figure E–3 Olinda WTP Color Time-Series Graph
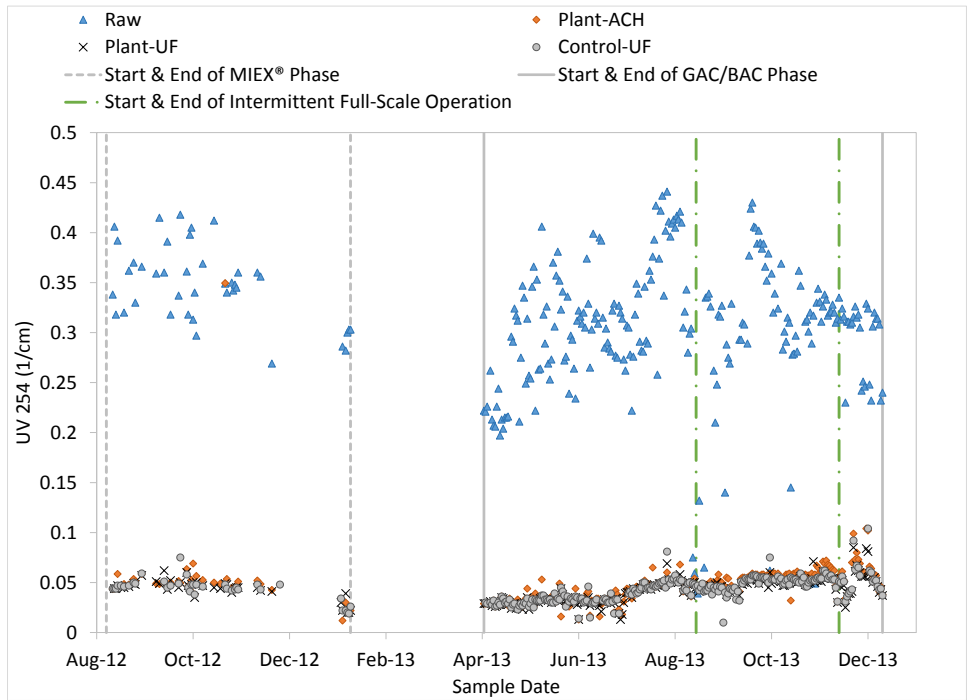
Figure E–4 Olinda WTP UV 254 Time-Series Graph

251
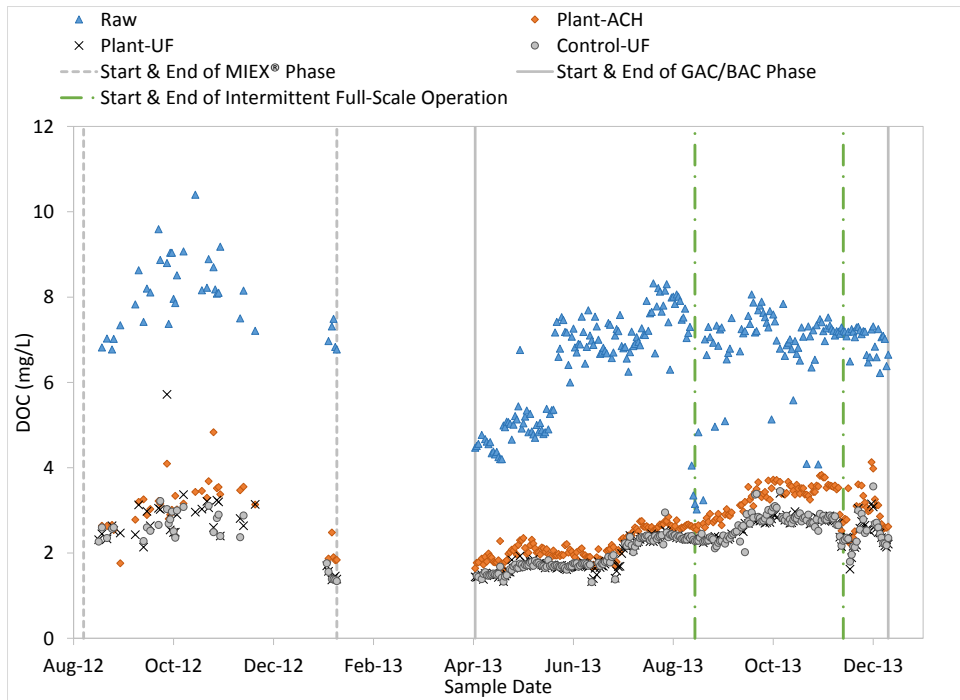
Figure E–5 Olinda WTP DOC Time-Series Graph
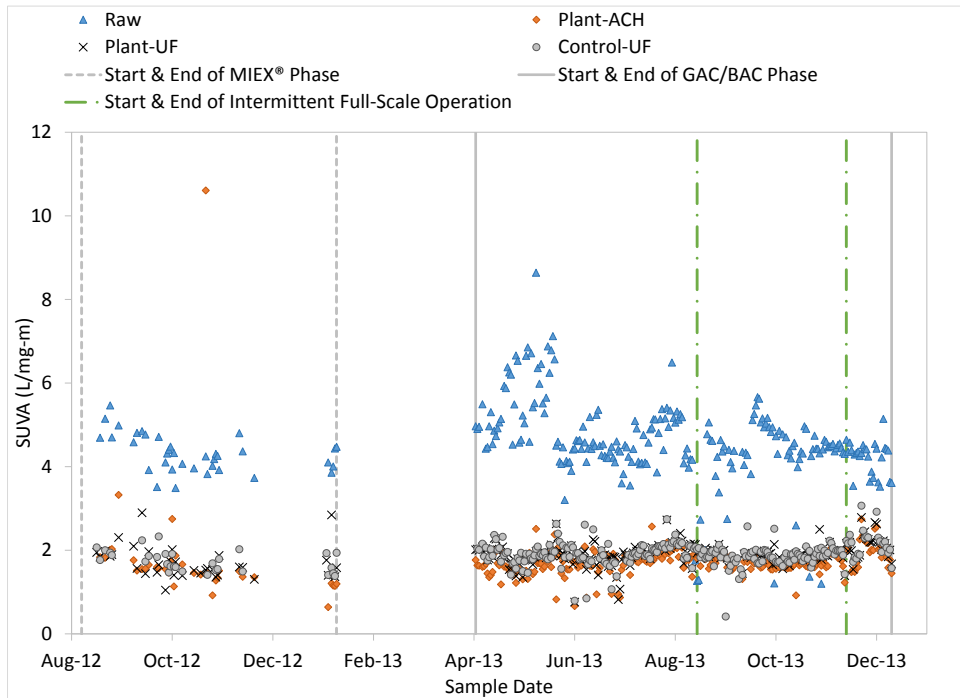
Figure E–6 Olinda WTP SUVA Time-Series Graph

252
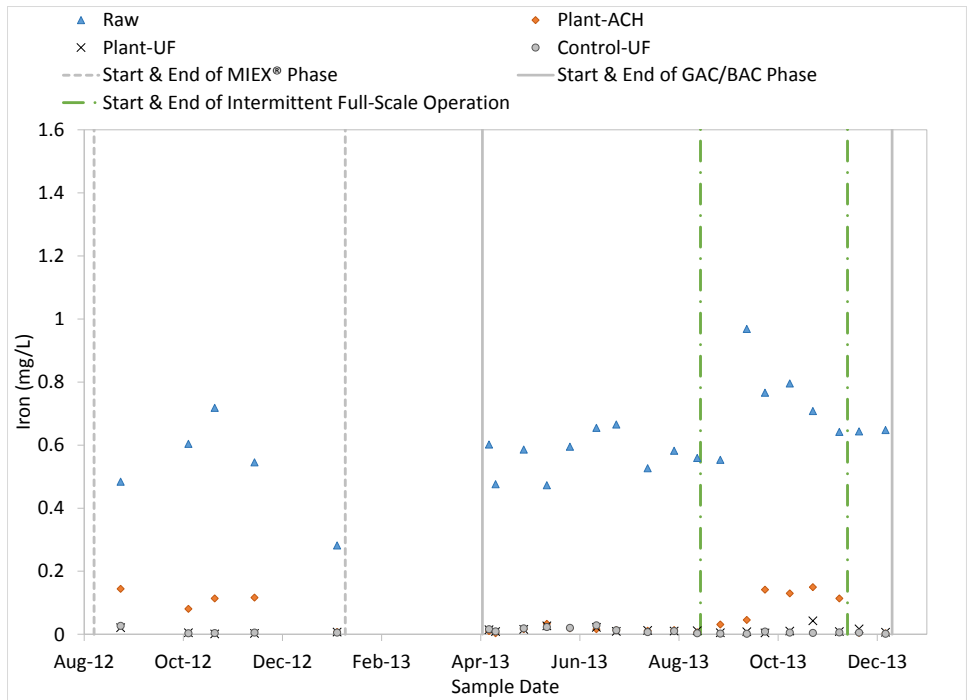
Figure E–7 Olinda WTP Iron Time-Series Graph
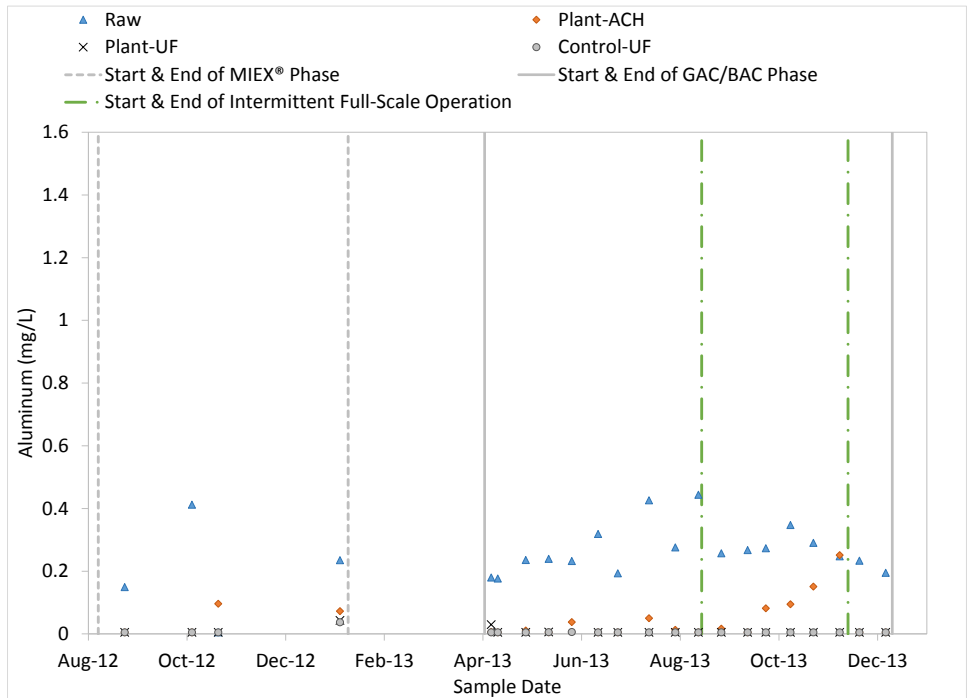
Figure E–8 Olinda WTP Aluminum Time-Series Graph

253
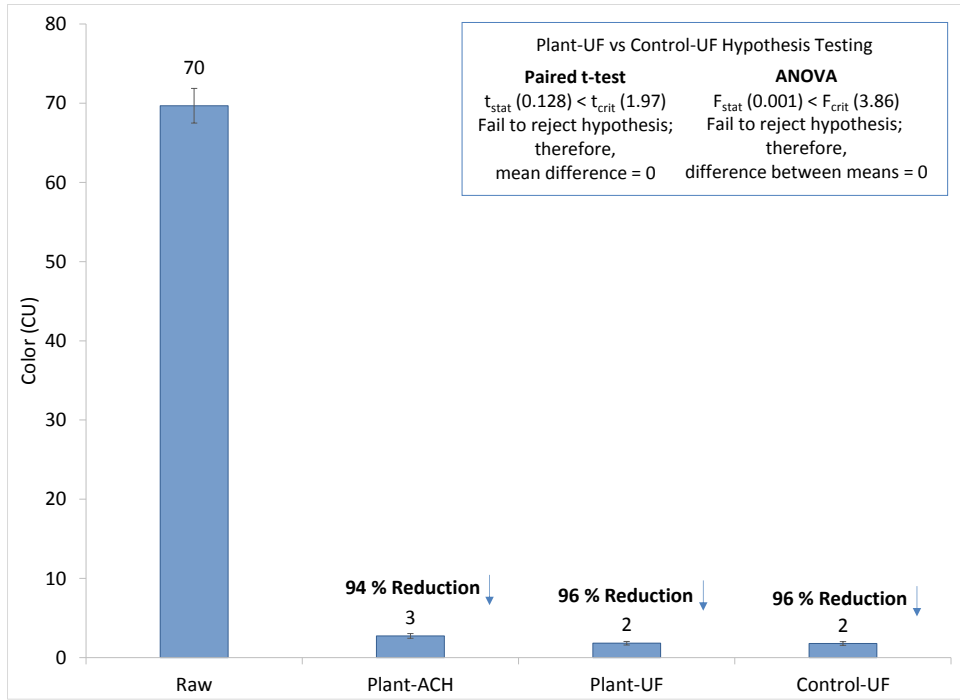
Figure E–9 Olinda WTP Average Color
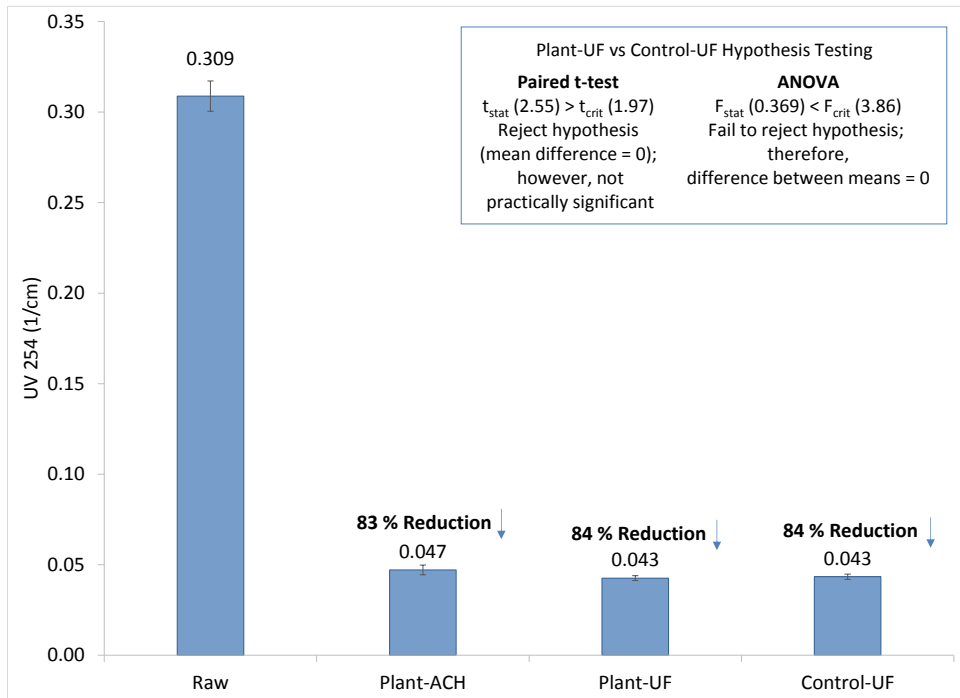
Figure E–10 Olinda WTP Average UV 254
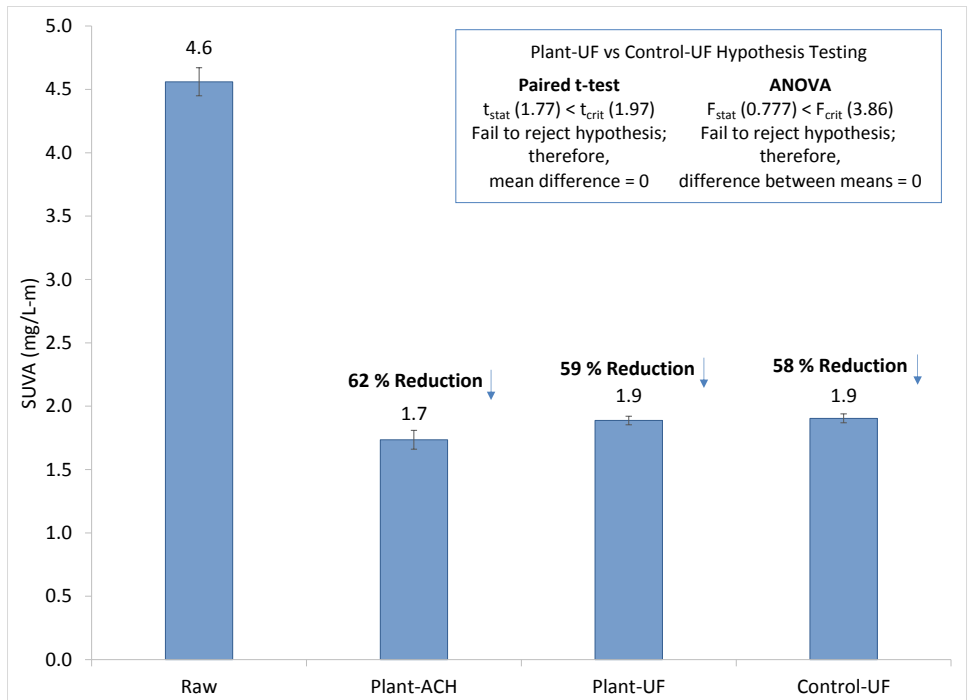
Figure E–11 Olinda WTP Average SUVA
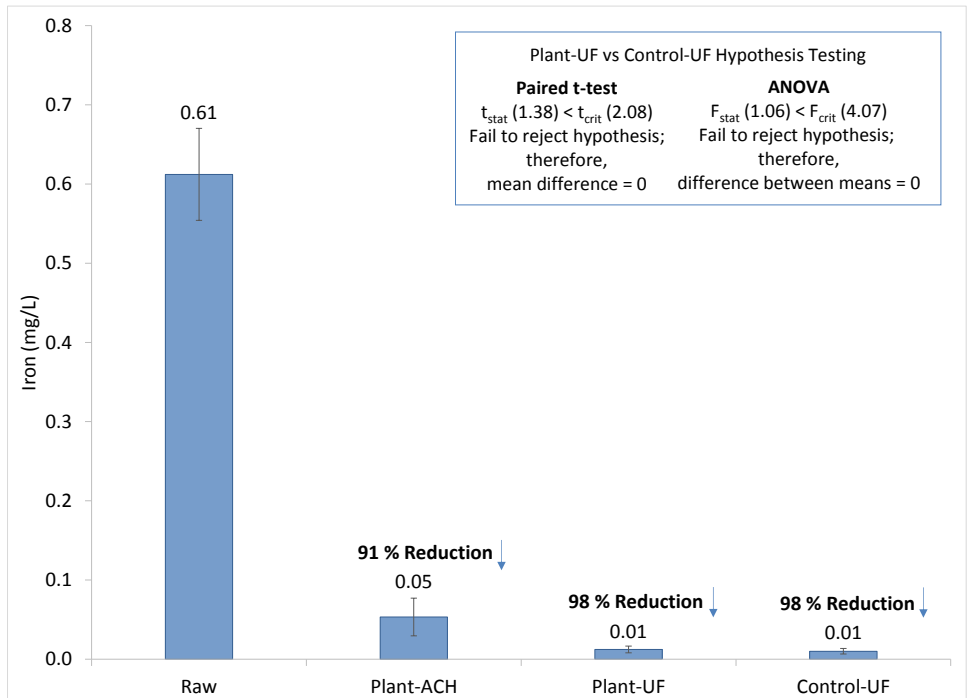
Figure E–12 Olinda WTP Average Iron
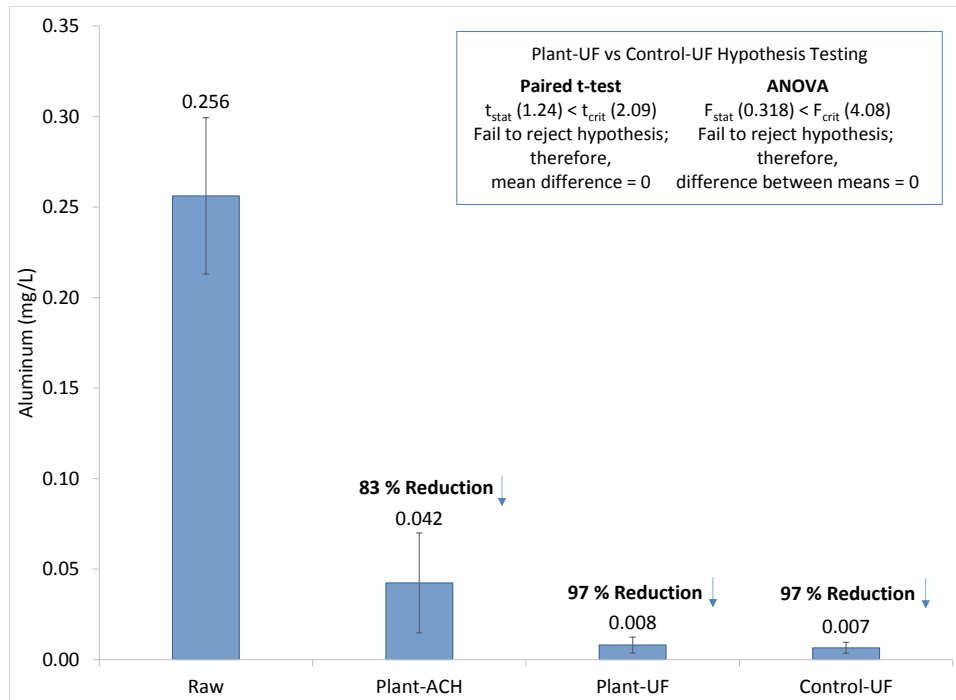
Figure E–13 Olinda WTP Average Aluminum

Table E–3 Full-Scale DBP Formation Potential Experimental Parameters

Experimental Parameters	7-Dec-12	28-Jan-13	28-Apr-13	5-Aug-13	21-Oct-13	9-Dec-13
pH	8.81	8.7	8.75	8.7	8.78	8.81
UV 254	0.045	0.03	0.029	0.048	0.054	0.052
TOC (mg/L)	2.51	1.7	1.43	2.38	2.79	2.34
SUVA (L/mg-m)	1.8	1.8	2.03	2.02	1.94	2.22
Chlorine Dose (mg/L Cl_2)	4	4	2.5	4	4	3.5
Incubation Temperature (°C)	15-22	12-21	12-22	18-25	16-25	20-25

Table E–4 Full-Scale TTHM Speciation

Contact Time (hrs)	Cl₂ Residual (mg/L)	THM Concentration (µg/L)				
		Chloroform	Bromo-dichloromethane	Dibromo-chloromethane	Bromoform	TTHMs
7-Dec-12						
9	3	89	5	1	1	96
24	2	105	6	1	1	113
47	2	120	7	1	1	128
92	2	150	8	1	1	160
185	1	157	8	1	1	168
28-Jan-13						
7	3	64	5	1	1	71
24	2	81	6	1	1	89
48	2	87	6	1	1	95
92	2	112	8	1	1	122
168	2	127	9	1	1	138
28-Apr-13						
6	2	110	2	1	1	115
24	2	132	3	1	1	138
54	1	155	4	1	1	148
96	1	149	4	1	1	154
168	1	176	5	1	1	183
5-Aug-13						
8	1	185	2	1	1	189
25	2	191	2	1	1	195
48	2	213	3	1	1	218
93	2	237	4	1	1	243
188	1	242	4	1	1	248
21-Oct-13						
6	2	135	7	2	1	144
26	2	178	9	2	1	190
48	1	224	11	2	1	238
94	1	240	12	2	1	255
165	1	259	12	2	1	274
9-Dec-13						
6	2	112	3	1	1	117
24	1	143	4	1	1	149
48	1	165	4	1	1	172
96	1	181	4	1	1	187
168	0	209	5	1	1	216

Table E–5 Full-Scale HAA$_5$ Speciation

| Date | HAA Concentration (µg/L) | | | | | |
	Chloroacetic Acid	Bromoacetic Acid	Dichloro-acetic Acid	Trichloro-acetic Acid	Dibromo-acetic Acid	HAA$_5$
7-Dec-12	5	5	21	20	5	56
28-Jan-13	5	5	14	17	5	45
28-Apr-13	10	5	16	15	5	51
5-Aug-13	9	1	51	46	1	108
21-Oct-13	7	1	48	29	3	89
9-Dec-13	18	1	53	25	6	103

APPENDIX F. MIEX® PRETREATMENT PERFORMANCE EVALUATION

Table F–1 8 gpm Set-Point: MIEX® Phase Average Water Quality

Water Quality	Raw	MIEX®	Plant-ACH	MIEX®-ACH	Control-UF	MIEX®-UF
pH	5.7	5.6	5.4	5.5	5.4	5.4
Temp. (°C)	18.0	18.6	18.1	19.5	19.0	19.0
Turb. (ntu)	1.84	2.4	0.24	2.86	0.06	0.07
Alk. (mg/L CaCO$_3$)	3.07	2.4	2	1.94	1.9	1.9
Color (CU)	84	60	4	11	3	6
UV254 (1/cm)	0.358	0.231	0.061	0.076	0.048	0.041
DOC (mg/L)	7.9	5.1	2.9	3.1	2.6	2.1
SUVA (L/g-m)	4.3	4.3	1.8	2.39	1.9	1.4
TSS (mg/L)	1.5	1	0	3	0	0
TDS (mg/L)	77	46	64	50	35	43
Fe (mg/L)	0.484	0.455	0.144	0.427	0.027	0.036
Mn (mg/L)	0.008	0.009	0.012	0.008	0.010	0.009
Al (mg/L)	0.149	0.148	0.005	1.552	0.005	0.005
Ca (mg/L)	1.08	1.09	2.96	3.58	1.08	1.01
Mg (mg/L)	0.30	0.31	0.39	0.39	0.30	0.30
Si (mg/L)	1.41	1.42	1.70	2.03	1.31	1.30
Cl$^-$ (mg/L)	4.2	4.5	5.9	5.4	5.7	5.3
SO$_4^{2-}$ (mg/L)	1.39	1.3	1.3	<1.0	1.3	<1.0
Br$^-$ (mg/L)	<0.2	<0.2	<0.2	<0.2	<0.2	<0.2

Table F–2 6 gpm Set-Point: MIEX® Phase Average Water Quality

Water Quality	Raw	MIEX®	Plant-ACH	MIEX®-ACH	Control-UF	MIEX®-UF
pH	6.2	5.8	5.9	5.6	5.9	5.6
Temp. (ºC)	17.0	18.1	17.6	18.8	18.2	19.0
Turb. (ntu)	2.62	3.1	0.42	3.29	0.06	0.11
Alk. (mg/L CaCO$_3$)	4.35	2.3	2	1.79	2.3	1.5
Color (CU)	86	50	4	9	2	1
UV254 (1/cm)	0.353	0.185	0.082	0.053	0.045	0.027
DOC (mg/L)	8.7	5.2	3.4	3.4	2.8	1.7
SUVA (L/g-m)	4.0	3.6	2.5	1.58	1.6	1.6
TSS (mg/L)	1.5	1	1	9	0	0
TDS (mg/L)	53	34	95	54	80	41
Fe (mg/L)	0.661	0.694	0.097	0.613	0.004	0.002
Mn (mg/L)	0.010	0.011	0.009	0.011	0.011	0.009
Al (mg/L)	0.209	0.117	0.051	3.064	0.005	0.029
Ca (mg/L)	1.57	1.59	2.25	1.87	1.47	1.58
Mg (mg/L)	0.31	0.31	0.35	0.34	0.31	0.31
Si (mg/L)	1.49	1.47	1.73	1.97	1.38	1.43
Cl$^-$ (mg/L)	3.8	8.7	7.9	12.0	5.8	8.9
SO$_4^{2-}$ (mg/L)	1.48	1.4	1.4	<1	1.4	<1
Br$^-$ (mg/L)	<0.2	<0.2	<0.2	<0.2	<0.2	<0.2

Table F–3 ACH Pump Replacement: MIEX® Phase Average Water Quality

Water Quality	Raw	MIEX®	Plant-ACH	MIEX®-ACH	Control-UF	MIEX®-UF
pH	6.2	5.7	5.9	5.7	5.9	5.7
Temp. (ºC)	16.1	16.2	16.8	16.9	16.7	16.9
Turb. (ntu)	2.41	2.8	0.46	2.72	0.05	0.05
Alk. (mg/L $CaCO_3$)	4.52	2.6	3	2.44	2.6	2.4
Color (CU)	76	37	2	1	1	0
UV254 (1/cm)	0.321	0.139	0.036	0.018	0.034	0.014
DOC (mg/L)	7.6	4.2	2.8	2.1	2.0	1.1
SUVA (L/g-m)	4.2	3.3	1.2	0.96	1.6	1.2
TSS (mg/L)	2.1	3	1	4	0	0
TDS (mg/L)	49	34	34	23	17	29
Fe (mg/L)	0.414	0.322	0.062	0.258	0.005	0.078
Mn (mg/L)	0.008	0.011	0.013	0.014	0.013	0.012
Al (mg/L)	0.235	0.118	0.073	1.133	0.037	0.191
Ca (mg/L)	2.04	2.57	2.19	2.91	1.54	2.63
Mg (mg/L)	0.34	0.37	0.38	0.39	0.33	0.36
Si (mg/L)	1.42	1.46	1.71	1.68	1.36	1.43
Cl^- (mg/L)	5.9	10.2	6.9	12.9	6.4	12.8
SO_4^{2-} (mg/L)	2.02	<1	2.1	<1	1.9	<1
Br^- (mg/L)	0.39335	<0.2	<0.2	<0.2	<0.2	<0.2

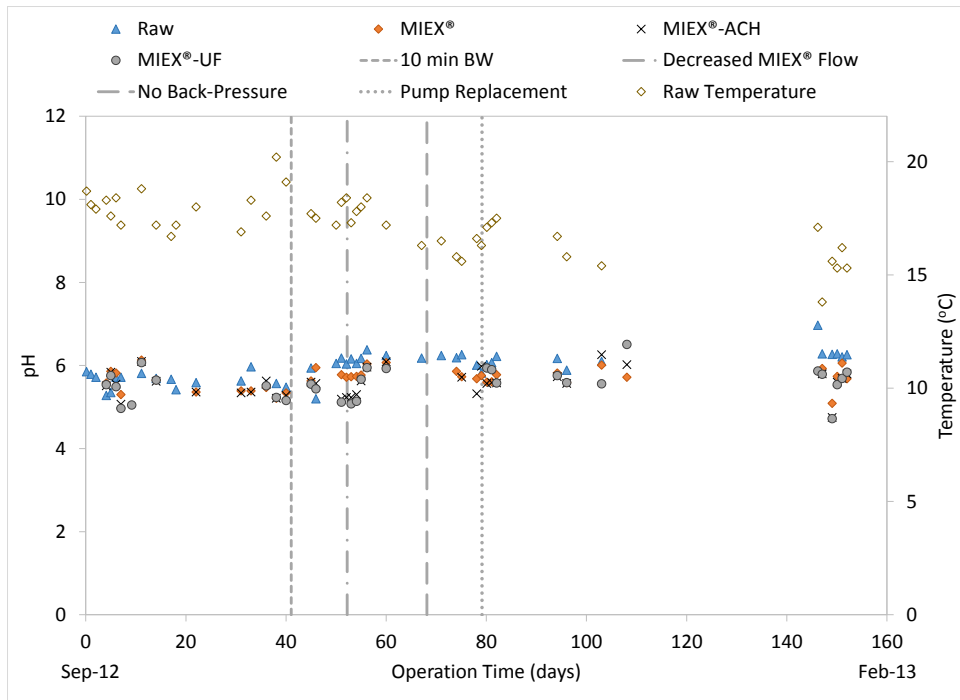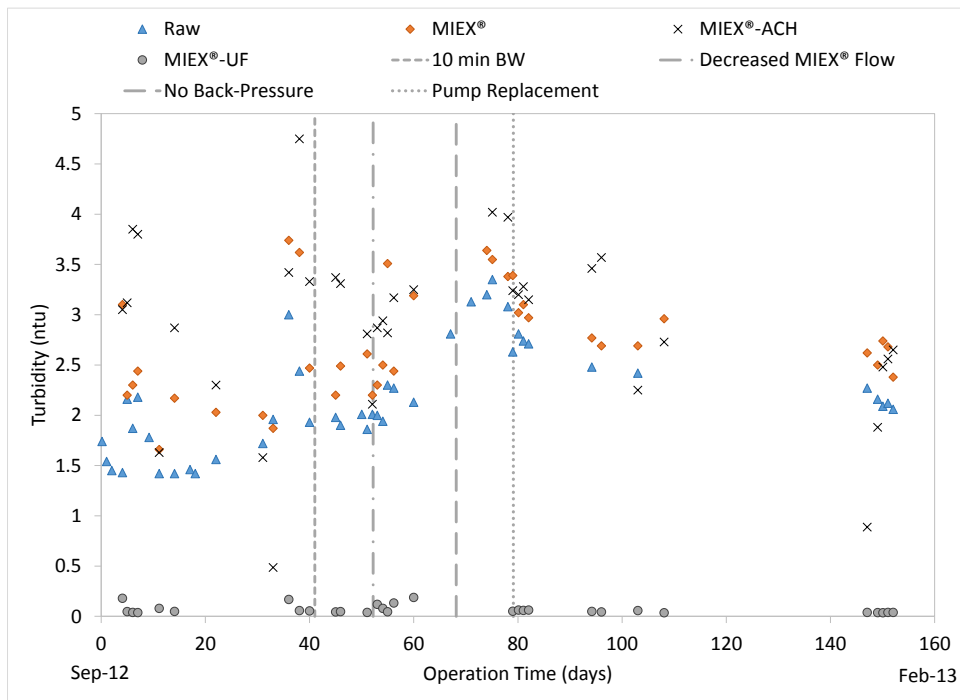Figure F–1 MIEX® Phase Temperature and pH Time-Series Graph

Figure F–2 MIEX® Phase Turbidity Time-Series Graph

263
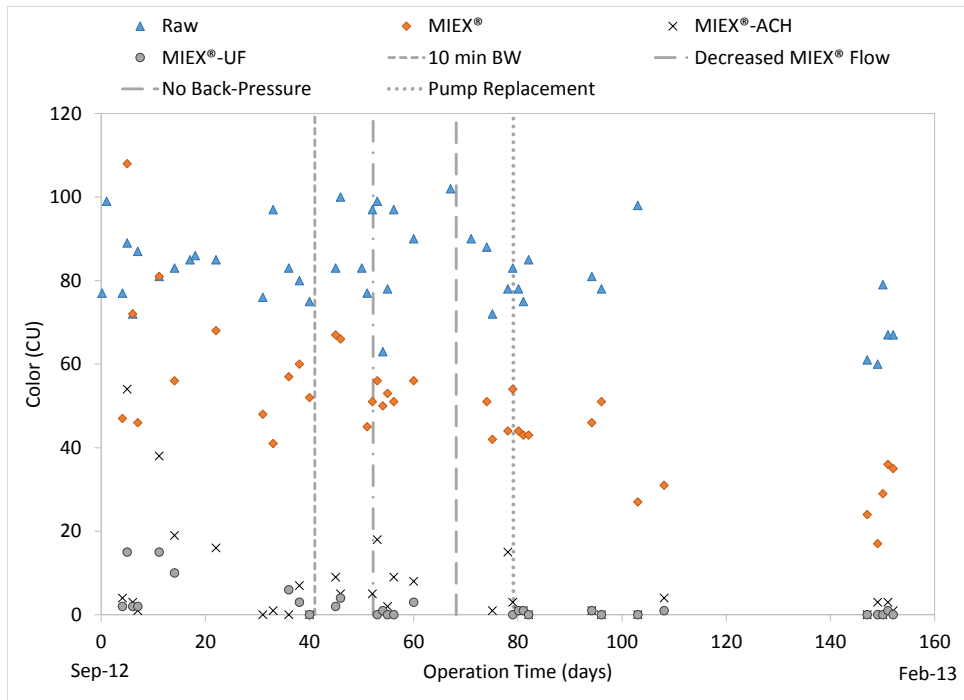
Figure F–3 MIEX® Phase Color Time-Series Graph
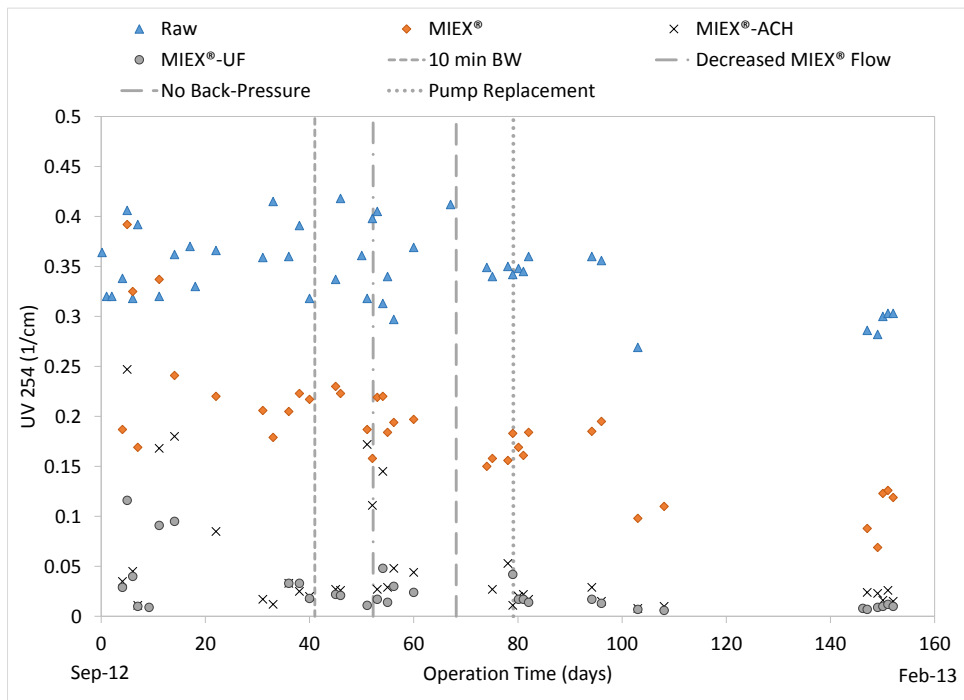
Figure F–4 MIEX® Phase UV 254 Time-Series Graph
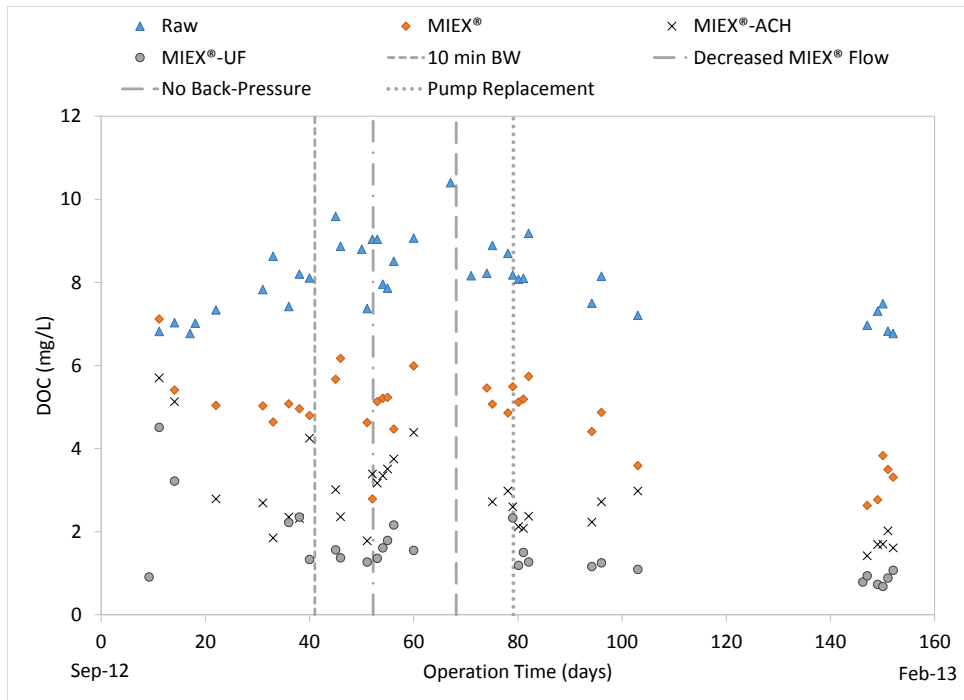
Figure F–5 MIEX® Phase DOC Time-Series Graph
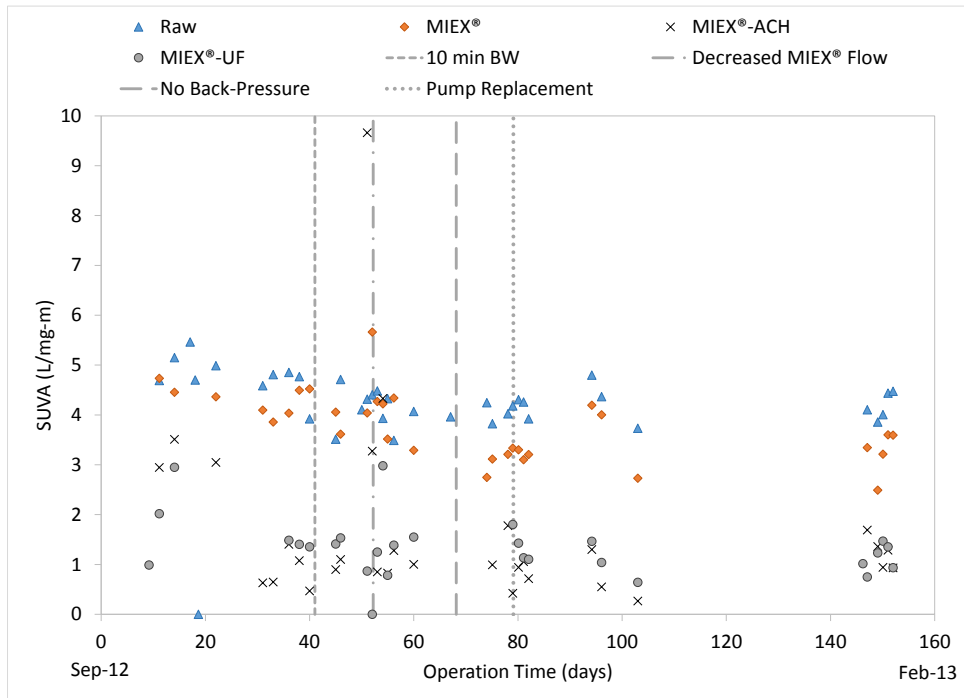
Figure F–6 MIEX® Phase SUVA Time-Series Graph

265
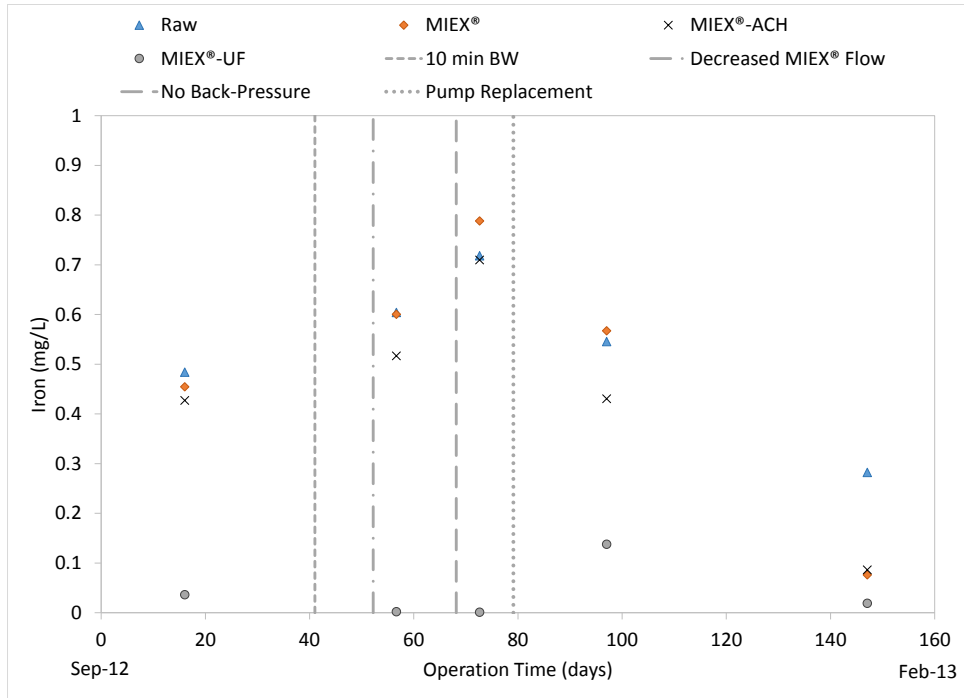
Figure F–7 MIEX® Phase Iron Time-Series Graph
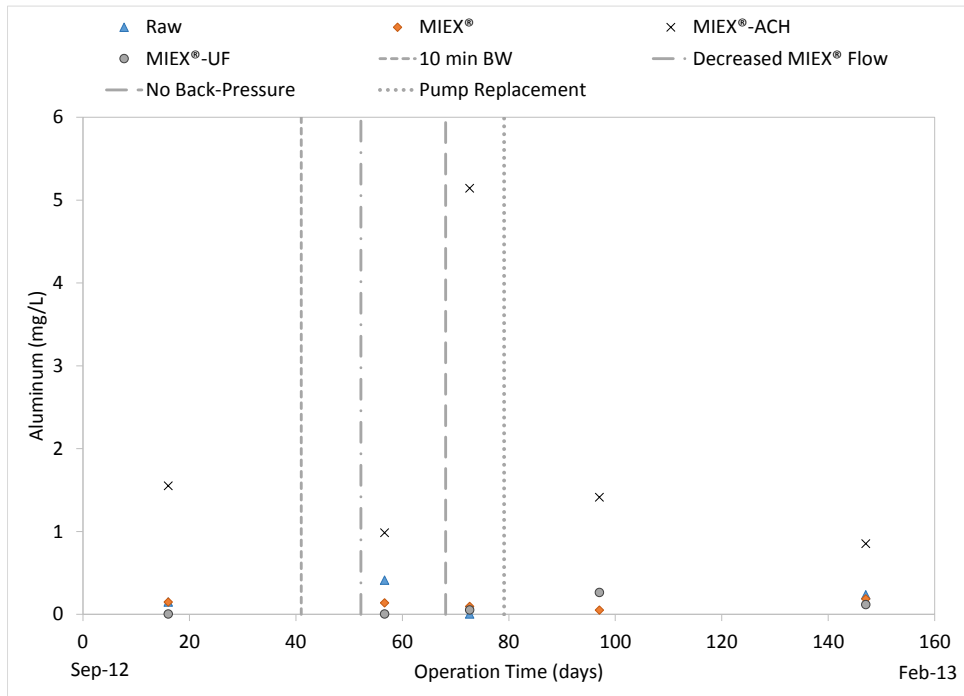
Figure F–8 MIEX® Phase Aluminum Time-Series Graph

266

Table F–4 MIEX® Phase Control-UF TTHM speciation

Contact Time (hrs)	Cl₂ Residual (mg/L)	THM Concentration (µg/L)				
		Chloroform	Bromo-dichloromethane	Dibromo-chloromethane	Bromoform	TTHMs
		7-Dec-12				
11	2	82	4	1	1	88
25	2	101	6	1	1	109
49	2	133	7	1	1	142
93	2	145	8	1	1	155
186	1	179	9	1	1	190
		28-Jan-13				
6	3	60	5	1	1	67
24	3	76	6	1	1	84
48	2	85	7	1	1	94
91	2	107	8	1	1	117
168	2	128	10	1	1	140

Table F–5 MIEX® Phase Control-UF HAA₅ Speciation

Date	HAA Concentration (µg/L)					
	Chloroacetic Acid	Bromoacetic Acid	Dichloro-acetic Acid	Trichloro-acetic Acid	Dibromo-acetic Acid	HAA₅
7-Dec-12	5	5	22	16	5	53
28-Jan-13	5	5	14	17	5	45

Table F–6 MIEX®-UF TTHM Speciation

| Contact Time (hrs) | Cl₂ Residual (mg/L) | THM Concentration (µg/L) | | | | |
		Chloroform	Bromo-dichloromethane	Dibromo-chloromethane	Bromoform	TTHMs
7-Dec-12						
10	3	39	1	1	1	42
24	3	46	1	1	1	49
48	1	57	1	1	1	60
92	2	67	1	1	1	70
185	2	78	1	1	1	82
28-Jan-13						
6	3	46	2	1	1	49
24	2	53	2	1	1	57
48	2	59	3	1	1	64
91	2	55	2	1	1	59
168	2	64	3	1	1	69

Table F–7 MIEX®-UF HAA₅ Speciation

| Date | HAA Concentration (µg/L) | | | | | |
	Chloroacetic Acid	Bromoacetic Acid	Dichloro-acetic Acid	Trichloro-acetic Acid	Dibromo-acetic Acid	HAA₅
7-Dec-12	5	5	9	11	5	35
28-Jan-13	5	5	9	6	5	30
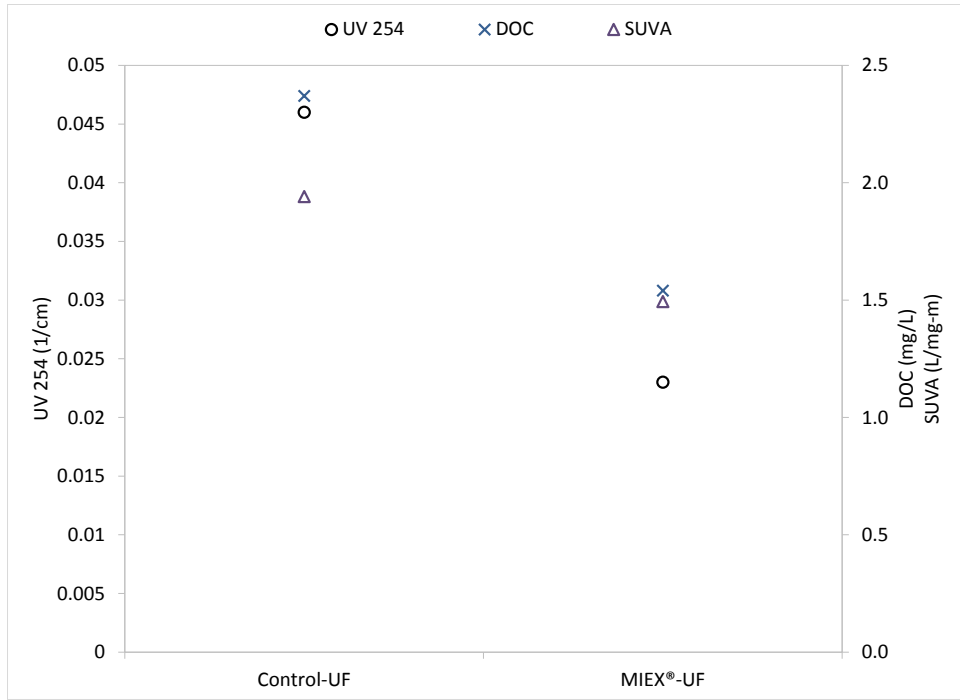
Figure F–9 Control vs MIEX® Organic Water Quality for 7-Dec-12
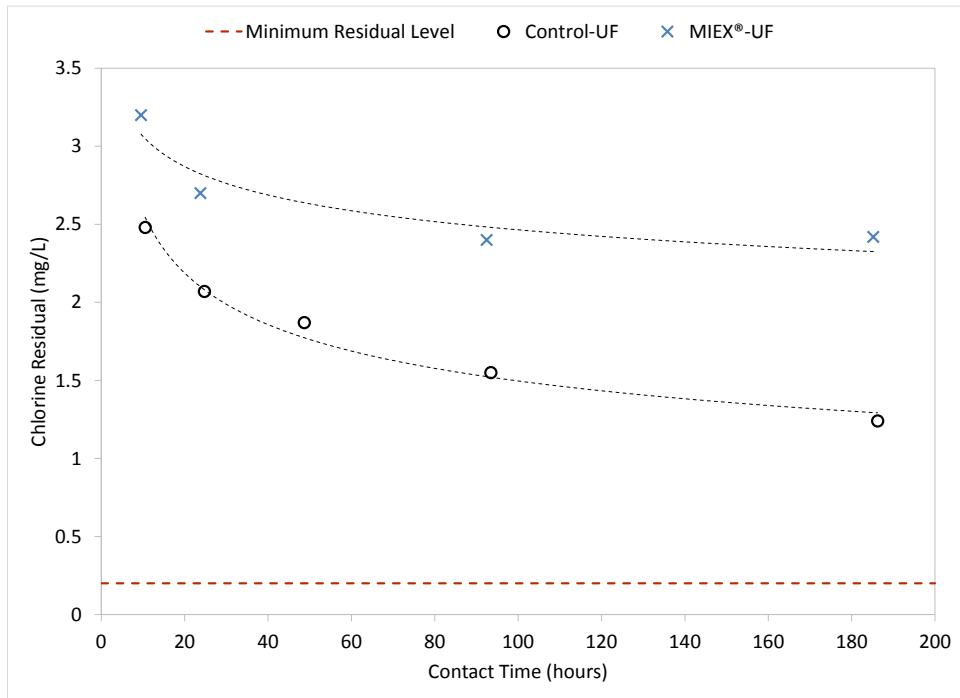
Figure F–10 Control vs MIEX® Chlorine Residual Decay for 7-Dec-12
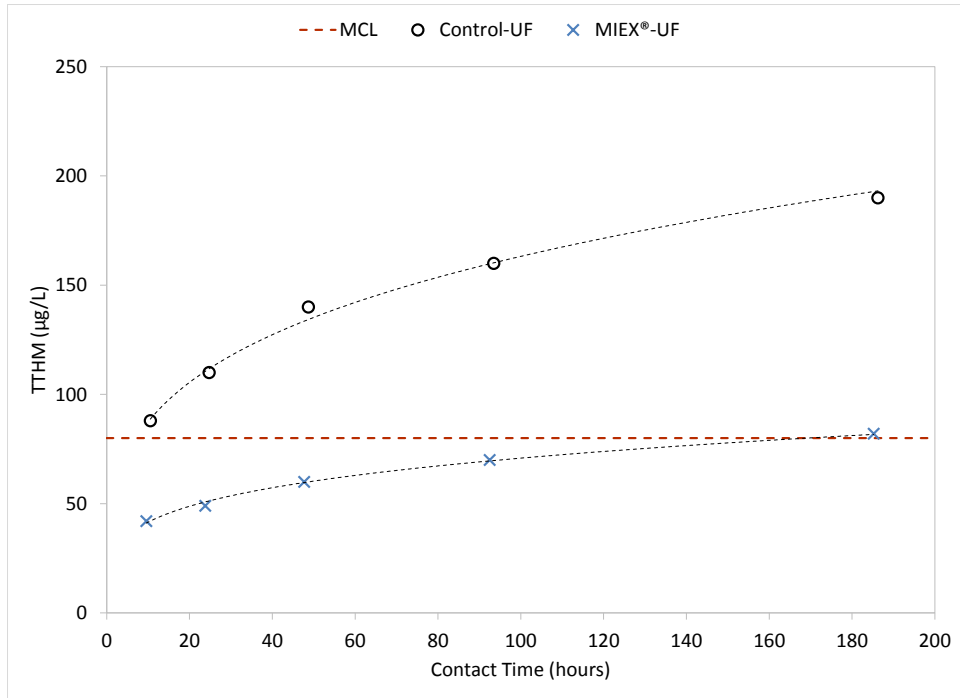
Figure F–11 Control vs MIEX® TTHM Formation Potential for 7-Dec-12
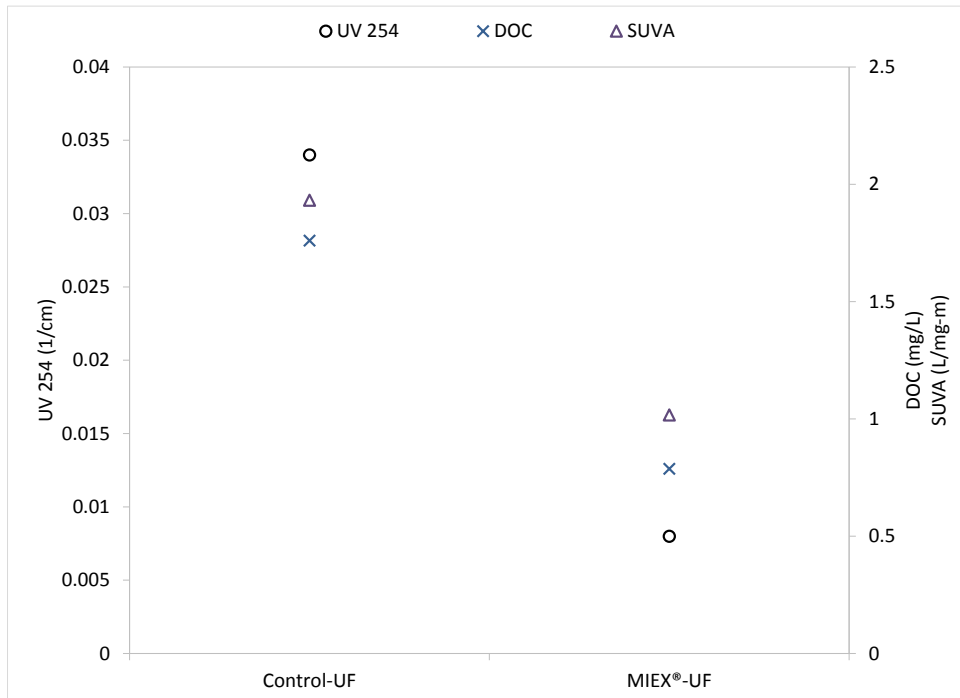
Figure F–12 Control vs MIEX® Organic Water Quality for 28-Jan-13

270
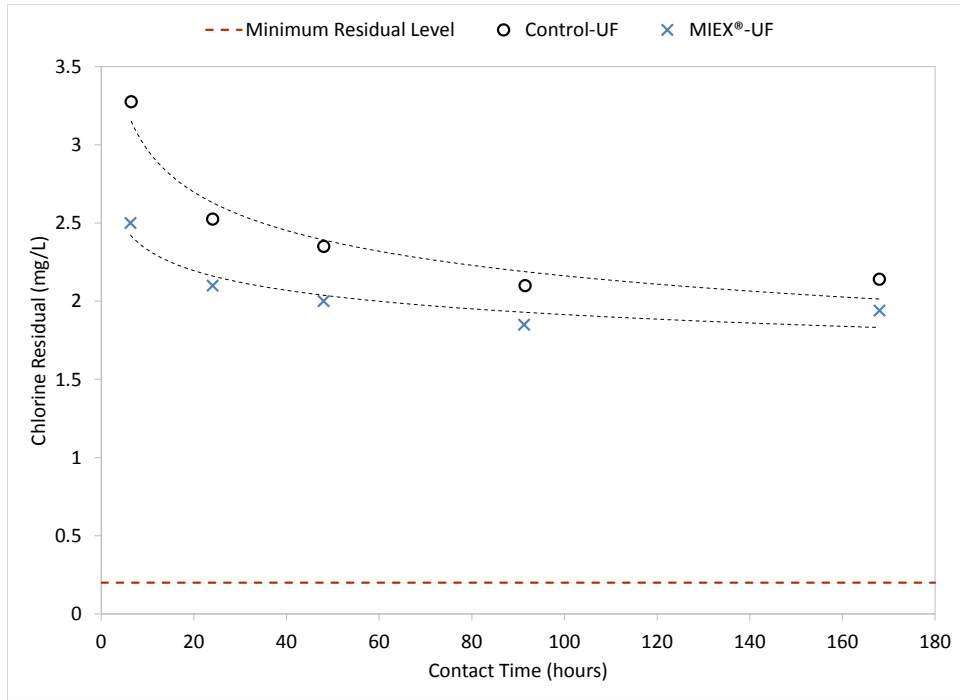
Figure F–13 Control vs MIEX® Chlorine Residual Decay for 28-Jan-13
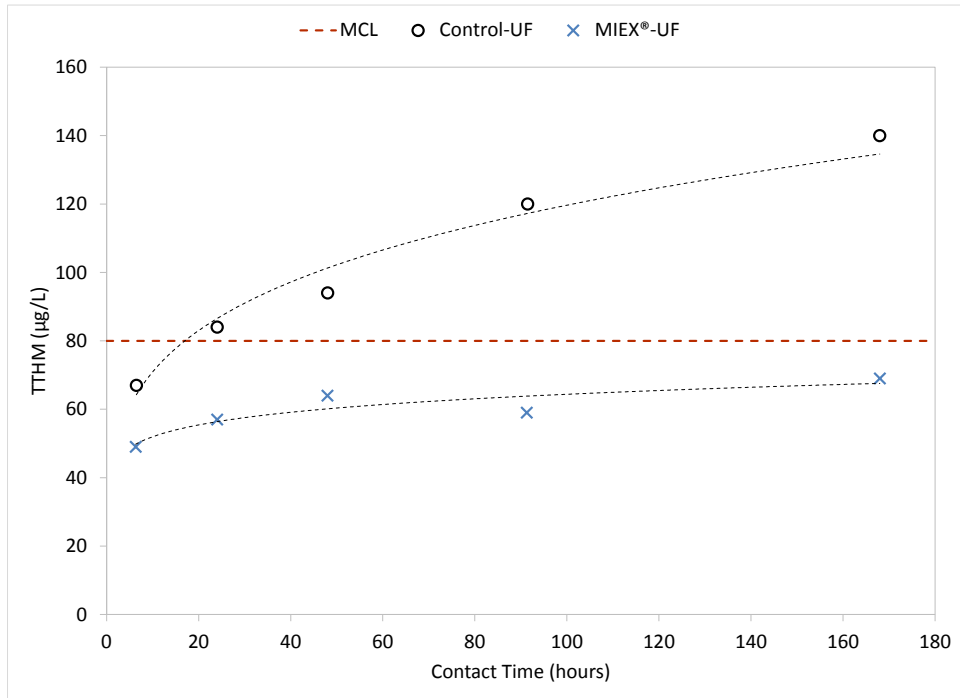
Figure F–14 Control vs MIEX® TTHM Formation Potential for 28-Jan-13

271
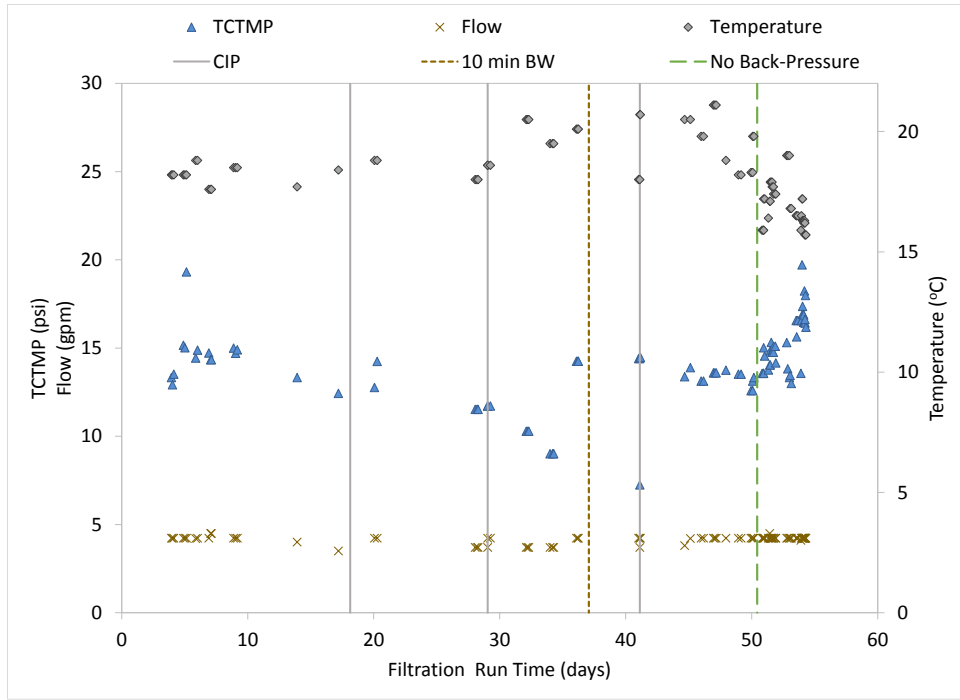
Figure F–15 Control-UF Feed Temperature, Flow, and TMP
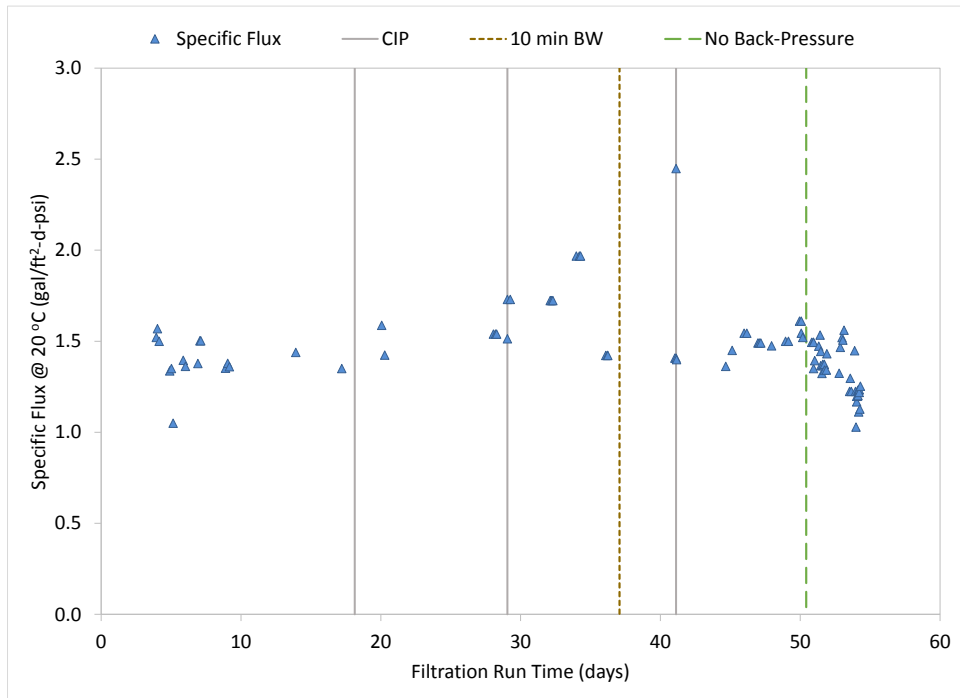
Figure F–16 Control-UF Specific Flux
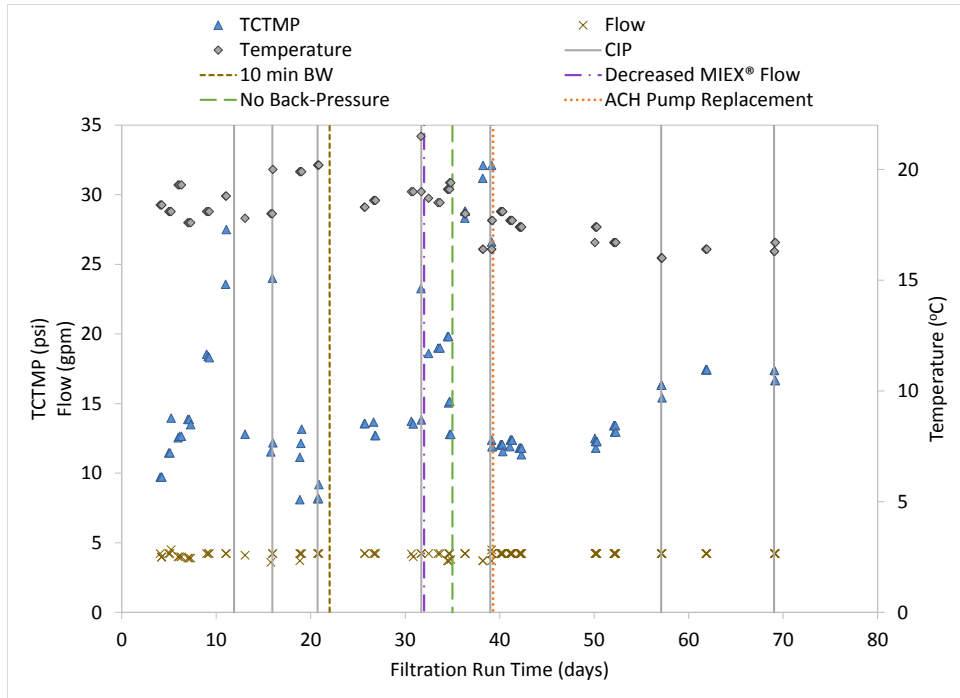
Figure F–17 MIEX®-UF Feed Temperature, Flow, and TMP
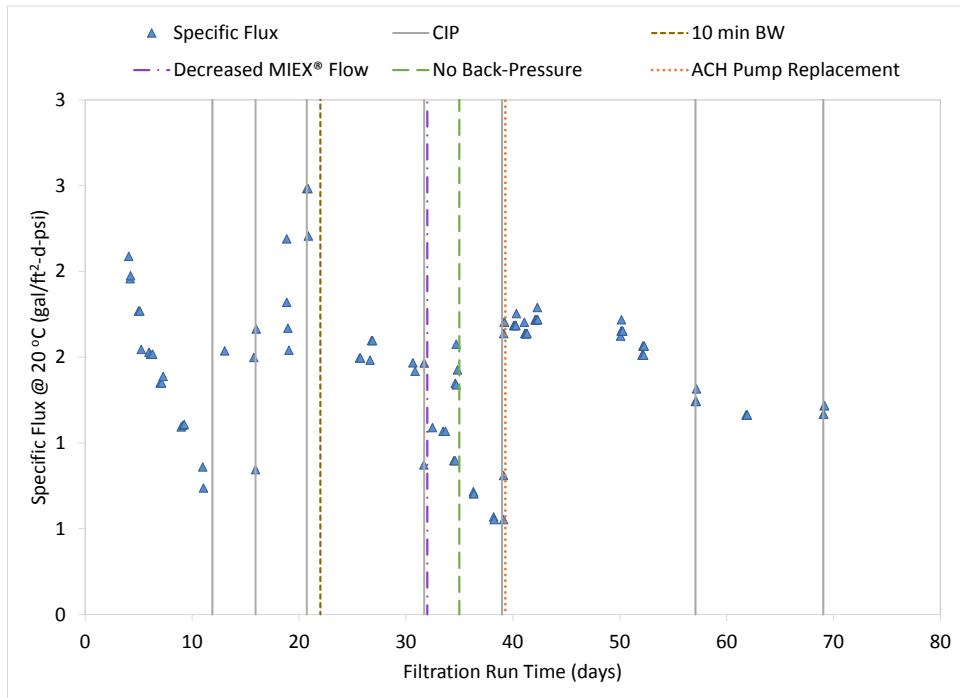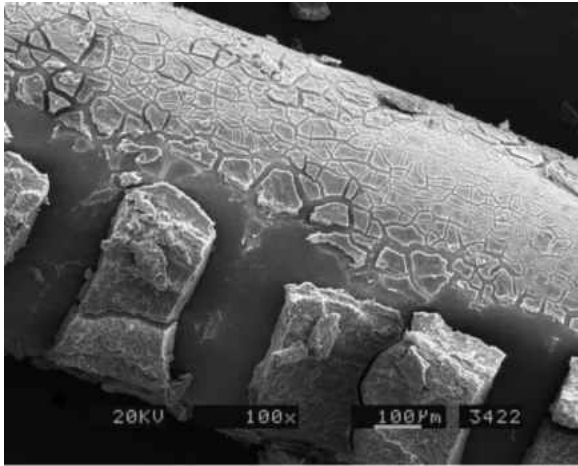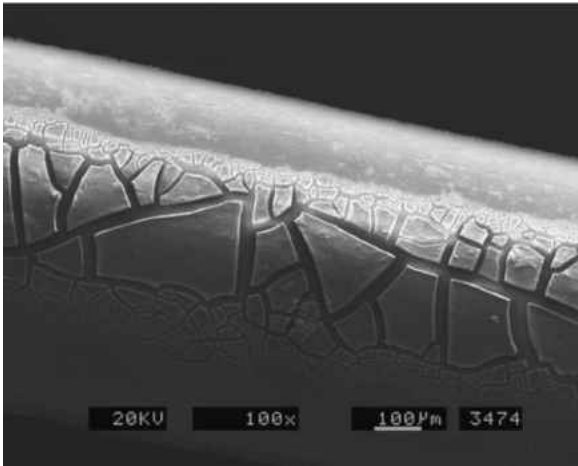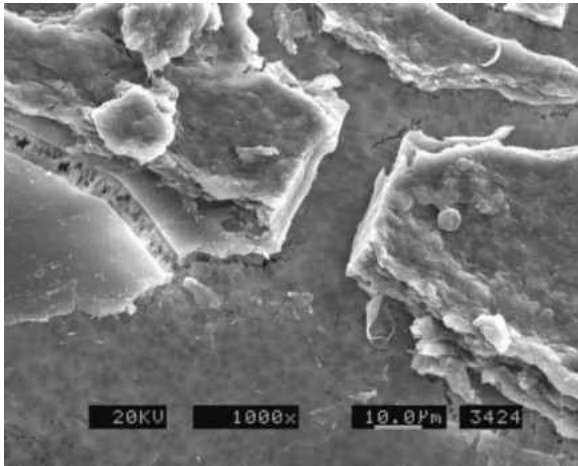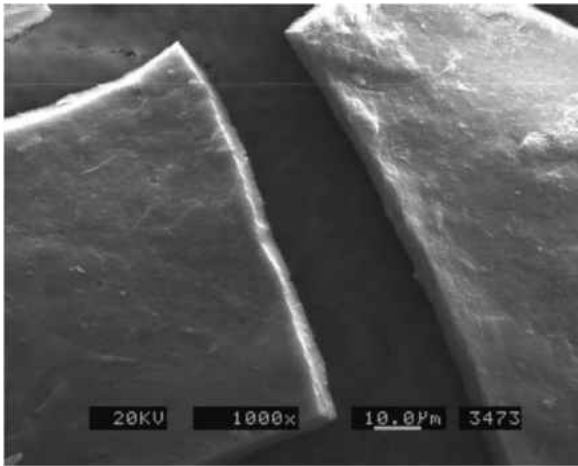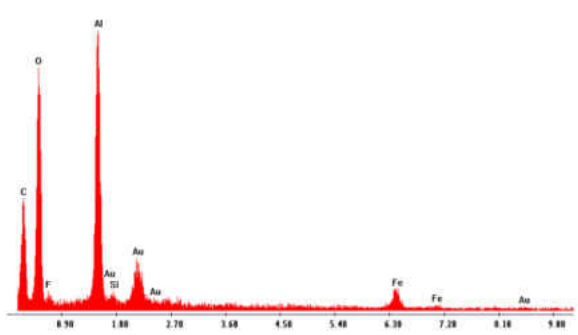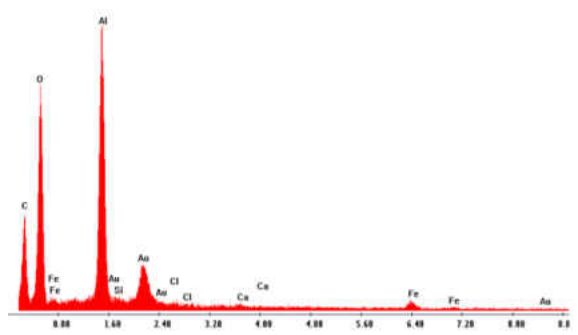
Figure F–18 MIEX®-UF Specific Flux

273

Table F–8 Top-Outside Fiber 2 SEM and EDS Results

MIEX®-UF	Control-UF
SEM at 100 Times Magnification	
SEM at 1000 Times Magnification	
EDS	

Source: Courtesy of Evoqua Water Technologies

274

Table F–9 Top-Outside Fiber 3 SEM and EDS Results

MIEX®-UF	Control-UF
SEM at 100 Times Magnification	

SEM at 2500 Times Magnification	**SEM at 1000 Times Magnification**

EDS	
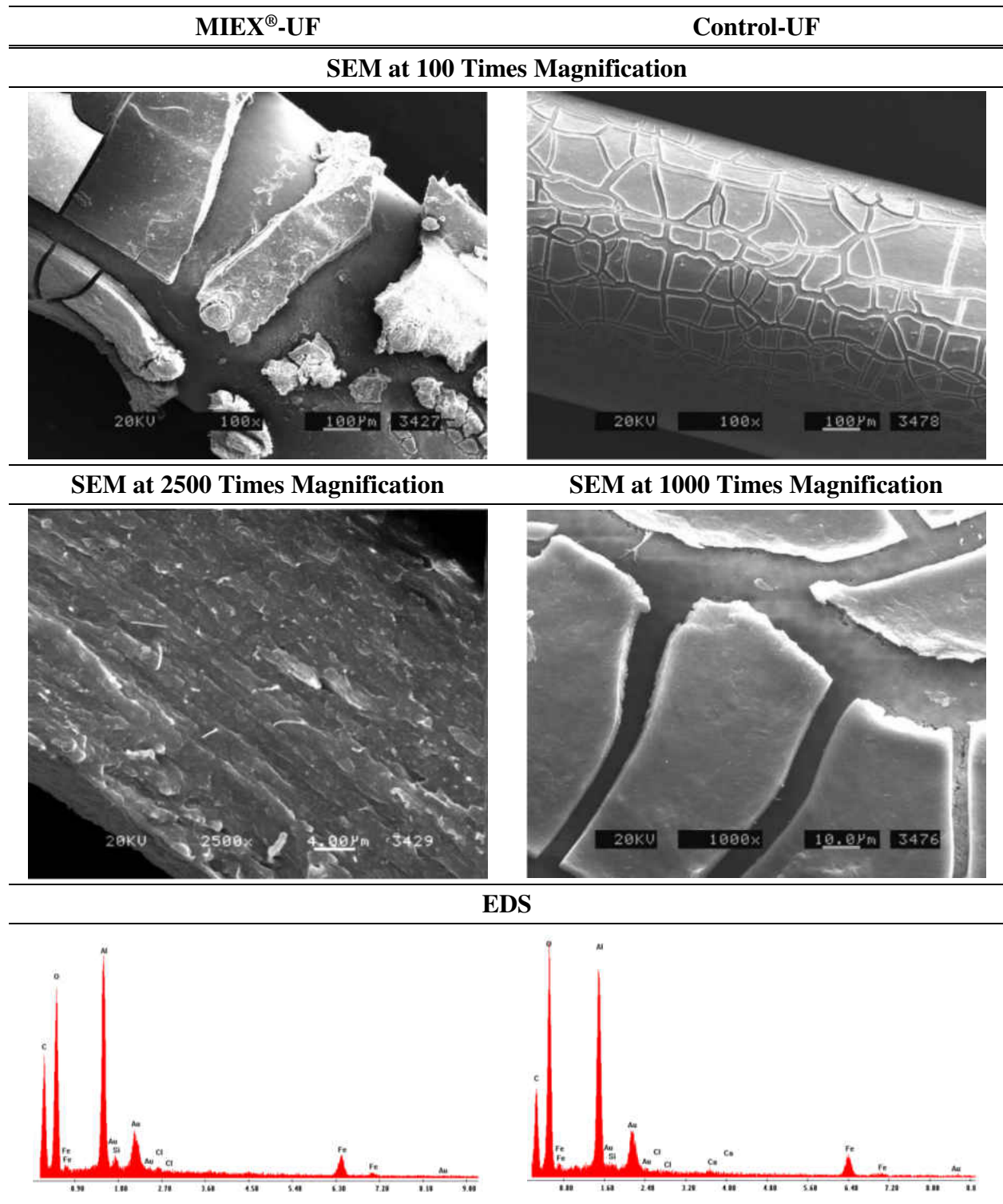
Source: Courtesy of Evoqua Water Technologies

Table F–10 Middle-Outside Fiber 2 SEM and EDS Results

MIEX®-UF	Control-UF
SEM at 100 times magnification	

| SEM at 1000 times magnification | |

| EDS | |

Source: Courtesy of Evoqua Water Technologies

276
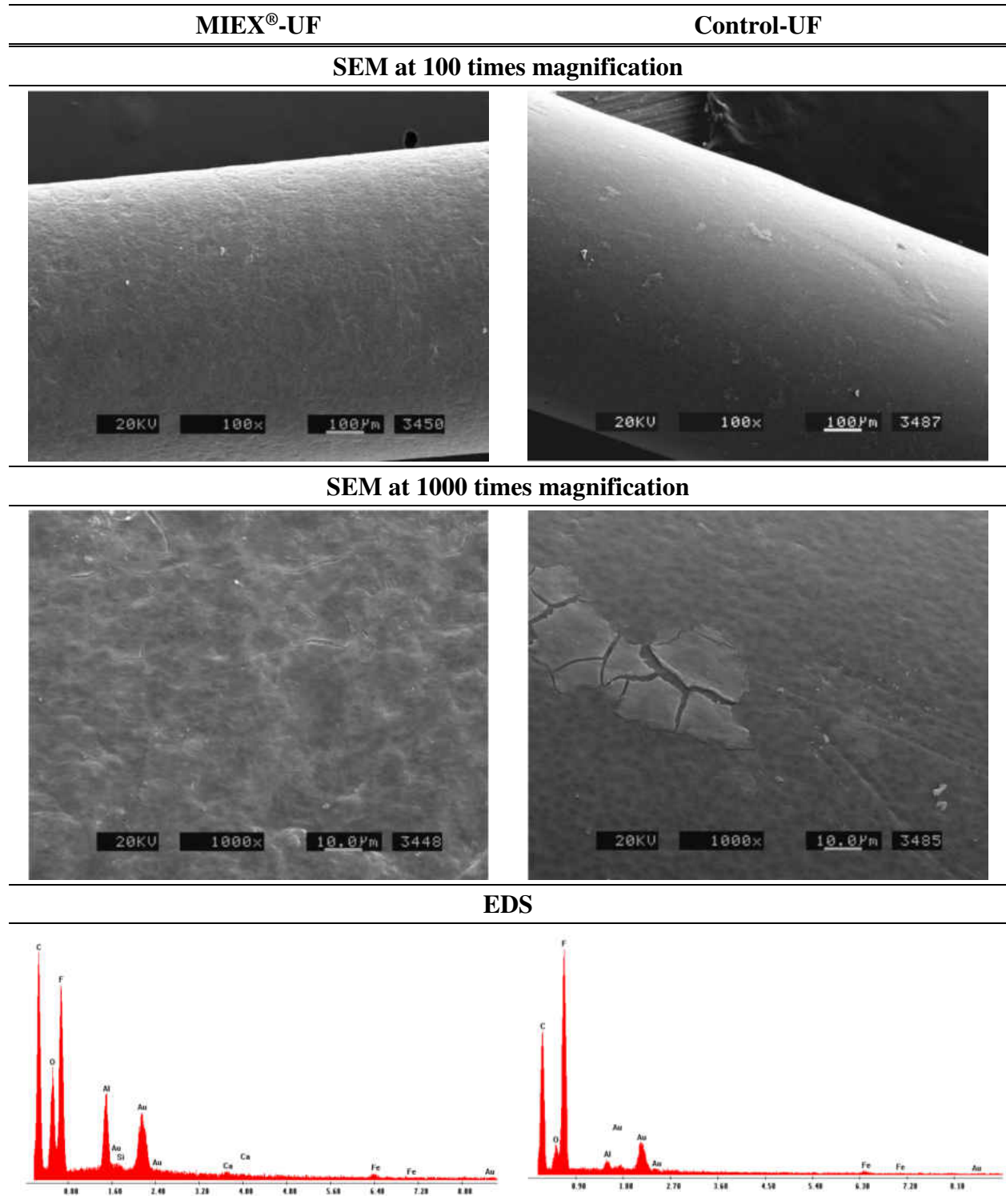
Table F–11 Middle-Outside Fiber 3 SEM and EDS Results

MIEX®-UF	Control-UF
SEM at 250 times magnification	**SEM at 500 times magnification**
SEM at 1000 times magnification	**SEM at 2000 times magnification**

EDS
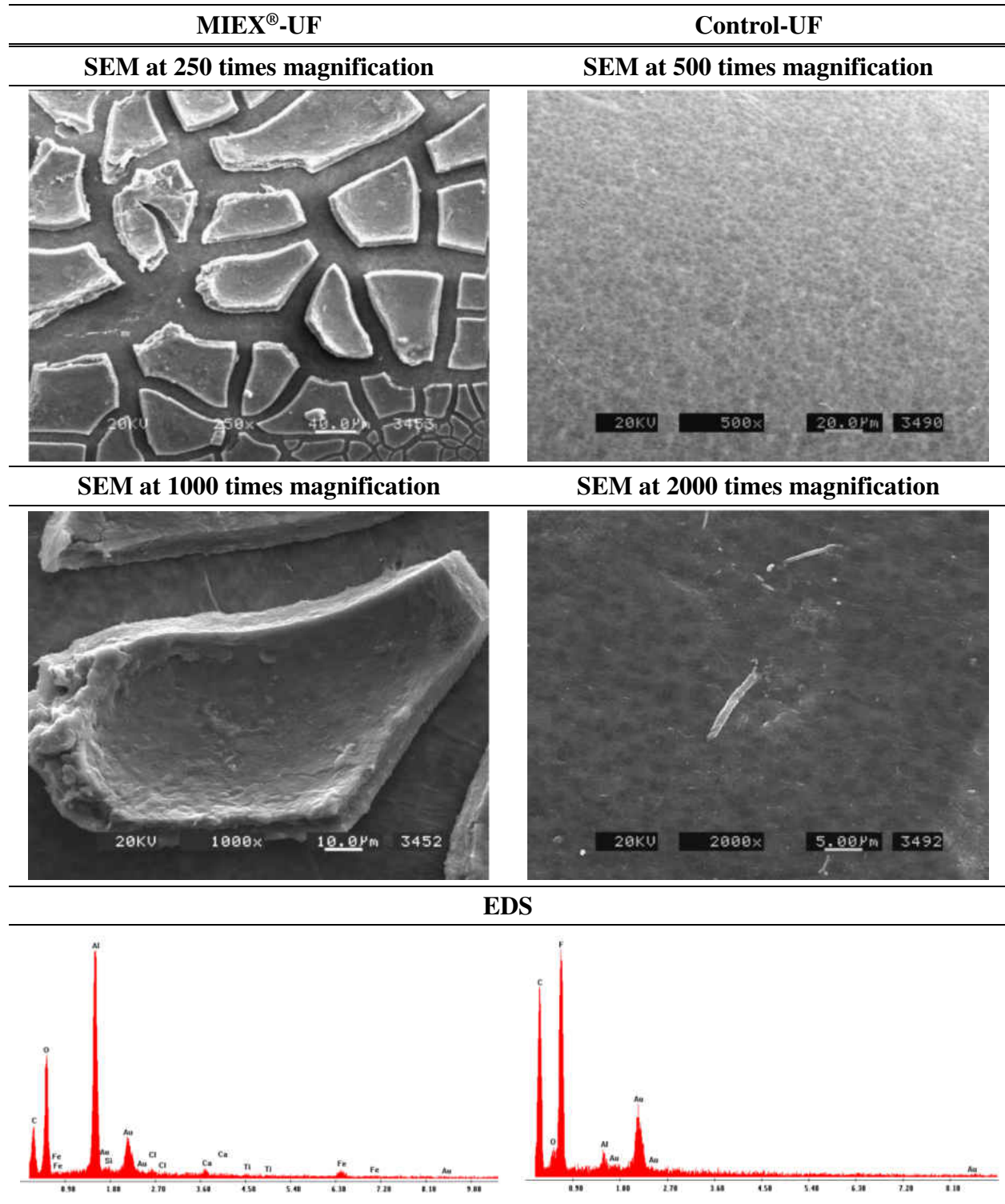
Source: Courtesy of Evoqua Water Technologies

Table F–12 Middle-Middle Fiber 2 SEM and EDS Results

MIEX®-UF	Control-UF
SEM at 100 times magnification	

SEM at 1000 times magnification	**SEM at 2500 times magnification**

EDS

Source: Courtesy of Evoqua Water Technologies

278
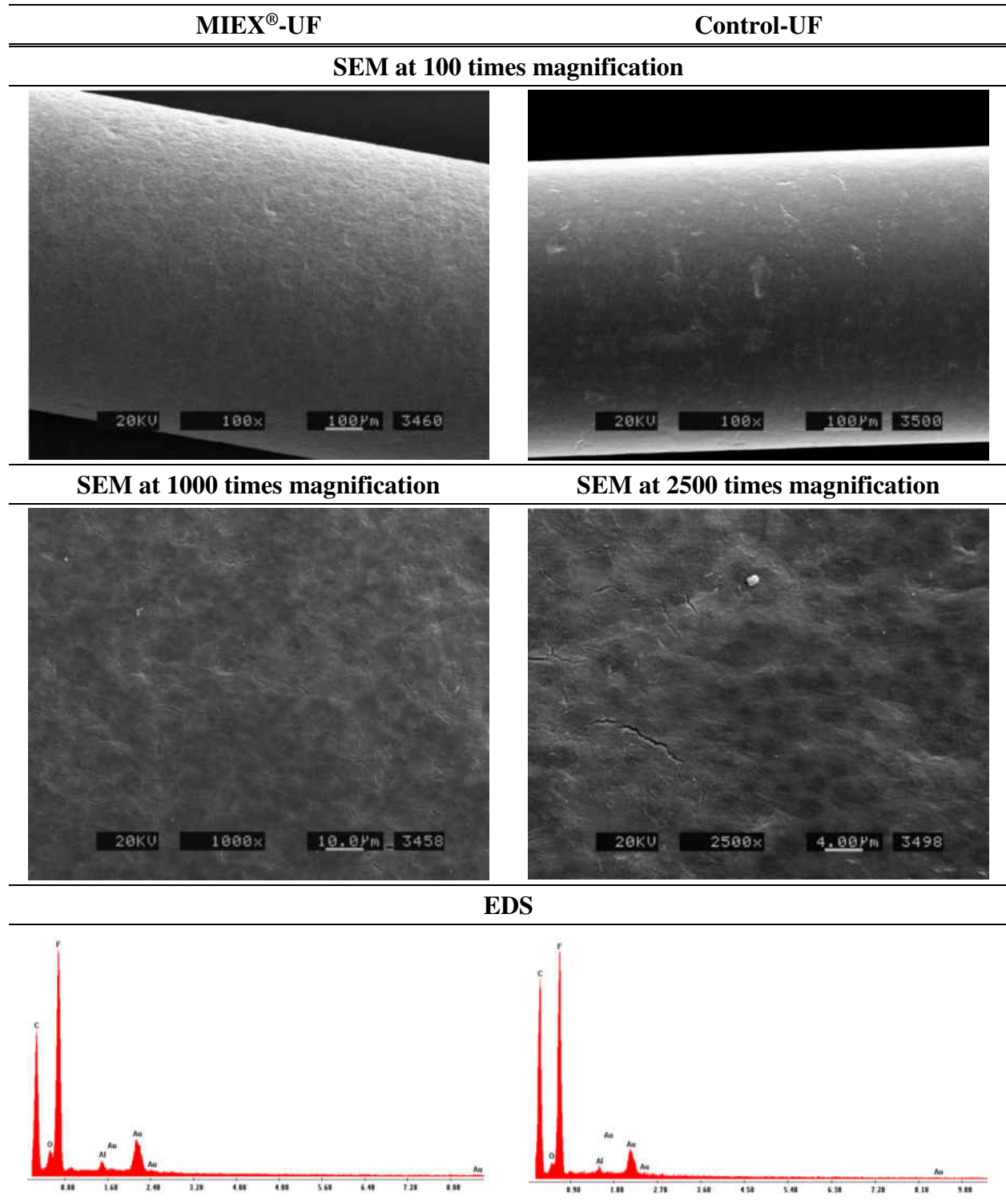
Table F–13 Middle-Middle Fiber 3 SEM and EDS Results

MIEX®-UF	Control-UF
SEM at 100 times magnification	

SEM at 1000 times magnification	

EDS	
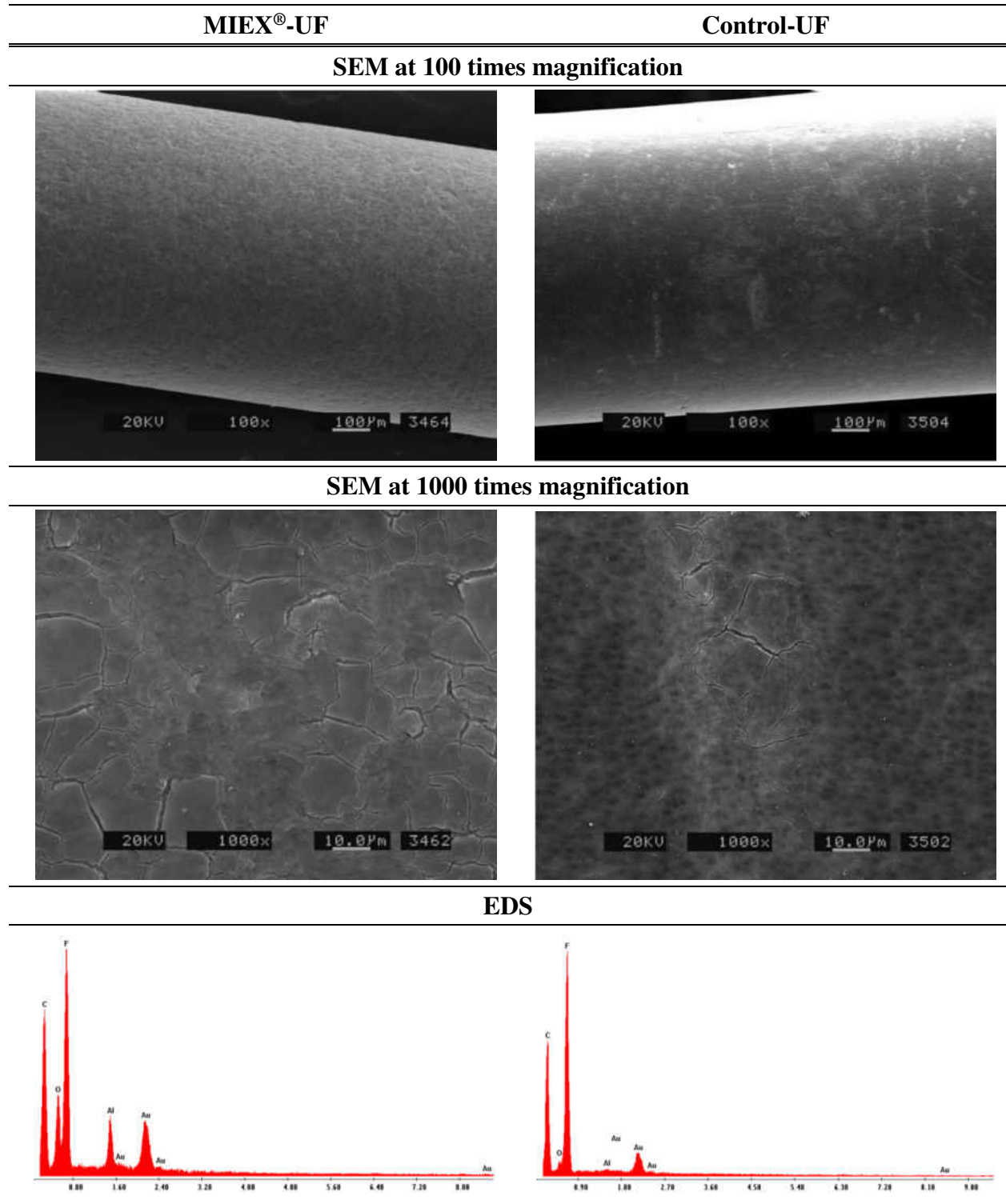
Source: Courtesy of Evoqua Water Technologies

Table F–14 Bottom-Outside Fiber 2 SEM and EDS Results

MIEX®-UF	Control-UF
SEM at 100 times magnification	

| **SEM at 1000 times magnification** | |

| **EDS** | |

Source: Courtesy of Evoqua Water Technologies

280
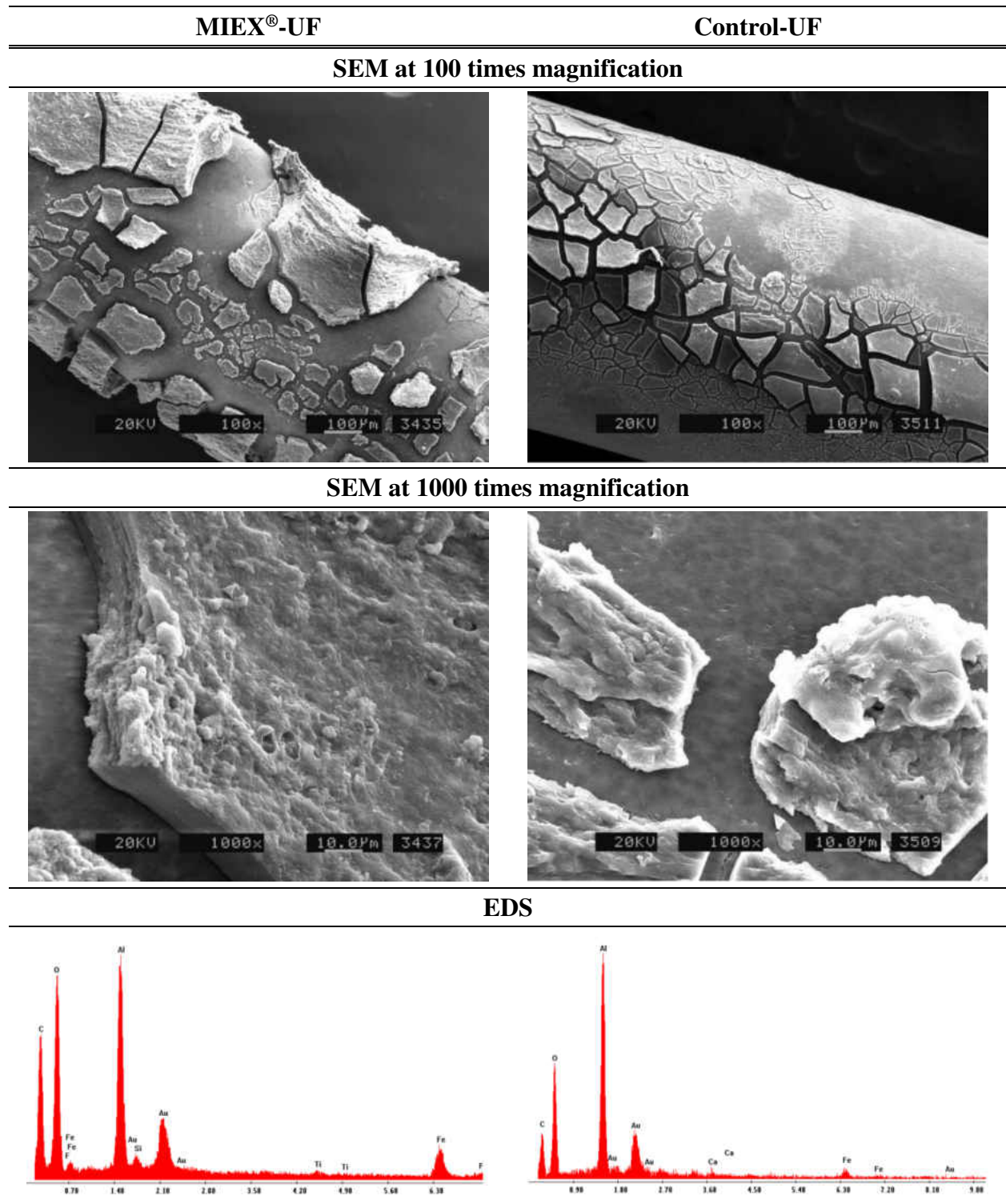
Table F–15 Bottom-Outside Fiber 3 SEM and EDS Results

MIEX®-UF	Control-UF
SEM at 100 times magnification	

SEM at 1000 times magnification	

EDS	
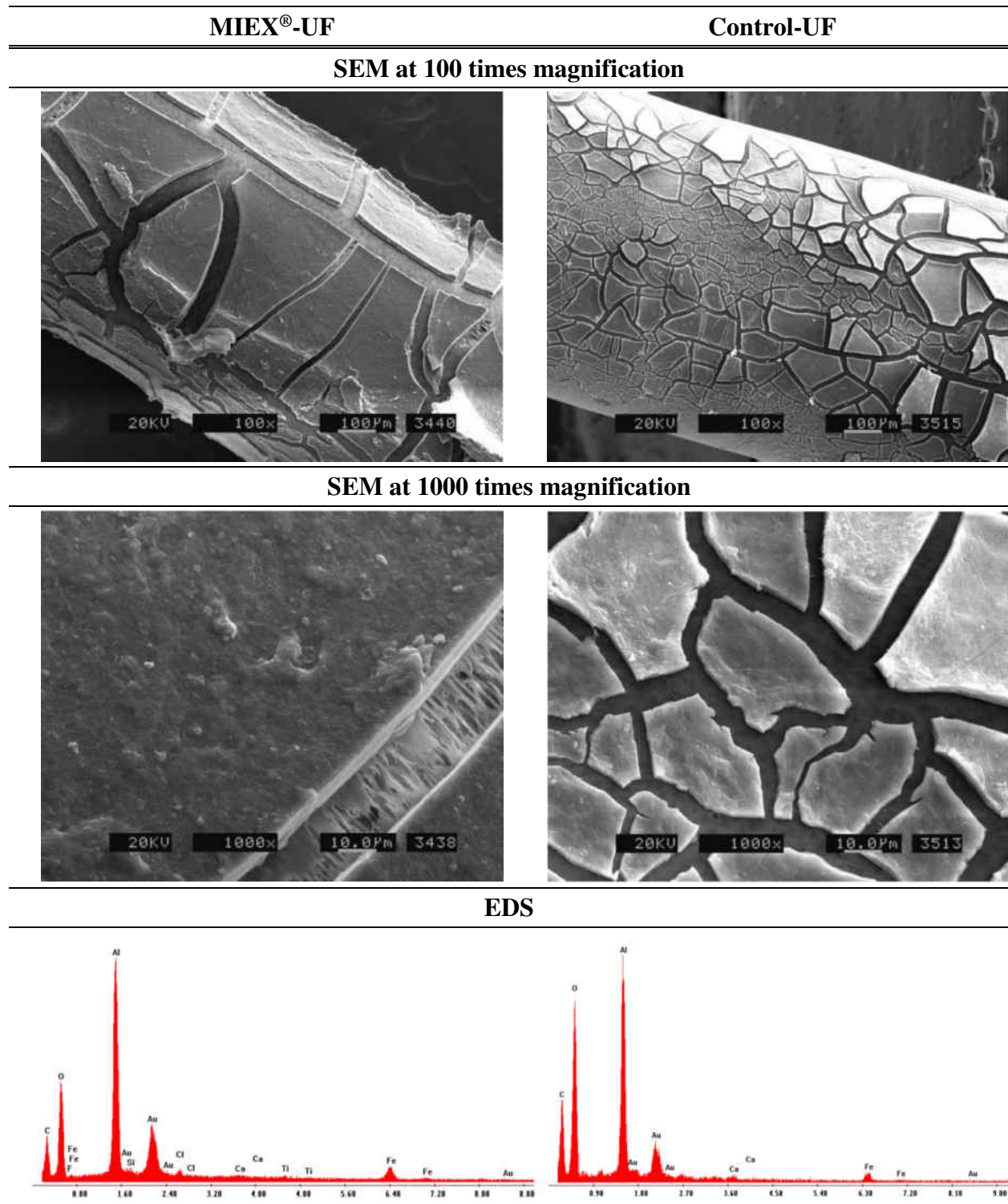
Source: Courtesy of Evoqua Water Technologies

Table F–16 MIEX® Foulant SEM and EDS Results

SEM	EDS
60 times magnification	**Foulant 1**
1000 times magnification	**Foulant 2**
2500 times magnification	**Foulant 3 & 4 Sphere**

Source: Courtesy of Evoqua Water Technologies

APPENDIX G. GAC AND BAC PRETREATMENT EVALUATION

Table G–1 GAC Adsorption Phase Average Water Quality

Water Quality	Raw	Plant-ACH	GAC	GAC-UF	Control-UF
pH	6.3	6.0	6.1	6.1	6.0
Temp. (°C)	18.7	19.1	19.5	19.6	19.1
Turb. (ntu)	2.18	0.3	0.20	0.05	0.05
Alk. (mg/L $CaCO_3$)	6.45	5.0	5	5.14	4.9
Color (CU)	65	1	0.3	0.3	1
UV254 (1/cm)	0.292	0.032	0.017	0.016	0.031
DOC (mg/L)	5.8	2.0	1.3	1.0	1.7
SUVA (L/g-m)	5.1	1.6	1.2	1.6	1.9
DO (mg/L)	-	7.0	6.0	-	-
Ortho-P (mg/L PO_4^{3-})	-	0.04	0.02	-	-
Nitrate (mg/L N)	-	<0.1	<0.1	-	-
Fe (mg/L)	0.58	0.016	0.012	0.008	0.019
Mn (mg/L)	0.015	0.016	0.017	0.016	0.016
Al (mg/L)	0.23	0.011	0.025	0.005	0.005
Ca (mg/L)	1.26	1.80	1.26	1.25	1.23
Mg (mg/L)	0.38	0.39	0.38	0.38	0.38
Si (mg/L)	1.49	1.48	1.47	1.47	1.44
Cl^- (mg/L)	5.0	6.8	6.5	6.6	6.6
SO_4^{2-} (mg/L)	1.88	1.8	1.8	1.45	1.5
Br^- (mg/L)	<0.2	<0.2	<0.2	<0.2	<0.2
TSS (mg/L)	2.4	1	0	0.3	0
TDS (mg/L)	27	20	17	16	16

Table G–2 BAC Transition Phase Average Water Quality

Water Quality	Raw	Plant-ACH	BAC	BAC-UF	Control-UF
pH	6.8	6.5	6.4	6.4	6.4
Temp. (ºC)	20.2	20.4	20.6	21.2	20.8
Turb. (ntu)	2.65	0.4	0.40	0.05	0.05
Alk. (mg/L $CaCO_3$)	9.5	8.1	7.9	8.1	8.0
Color (CU)	63	1.5	1.2	1.4	1.5
UV254 (1/cm)	0.303	0.041	0.037	0.040	0.043
DOC (mg/L)	7.0	2.4	2.4	2.1	2.3
SUVA (L/g-m)	4.3	1.7	1.5	1.9	1.9
DO (mg/L)	-	7.6	6.7	-	-
Ortho-P (mg/L PO_4^{3-})	-	0.04	0.06	-	-
Nitrate (mg/L N)	-	<0.1	<0.1	-	-
Fe (mg/L)	0.53	0.011	0.003	0.005	0.007
Mn (mg/L)	0.017	0.018	0.017	0.017	0.018
Al (mg/L)	0.43	0.050	0.005	0.005	0.005
Ca (mg/L)	1.50	1.54	1.50	1.49	1.47
Mg (mg/L)	0.40	0.42	0.40	0.40	0.41
Si (mg/L)	1.53	1.91	1.54	1.47	1.47
Cl^- (mg/L)	5.5	6.3	6.3	6.1	6.1
SO_4^{2-} (mg/L)	1.86	1.8	1.8	1.81	1.8
Br^- (mg/L)	<0.2	<0.2	<0.2	<0.2	<0.2
TSS (mg/L)	3.5	0	0	0.2	0
TDS (mg/L)	9	12	12	5	4

Table G–3 BAC with Ortho-P Adjustment Phase Average Water Quality

Water Quality	Raw	Plant-ACH	BAC	BAC-UF	Control-UF
pH	5.5	5.3	5.2	5.3	5.3
Temp. (°C)	20.1	20.6	21.0	21.0	20.6
Turb. (ntu)	3.75	1.1	1.05	0.07	0.06
Alk. (mg/L $CaCO_3$)	2.9	2.1	1.9	2.0	2.0
Color (CU)	72	3.0	2.3	1.8	2.0
UV254 (1/cm)	0.320	0.052	0.045	0.042	0.048
DOC (mg/L)	7.0	3.0	2.7	2.3	2.5
SUVA (L/g-m)	4.4	1.8	1.7	1.9	1.9
DO (mg/L)	-	7.3	6.3	-	-
Ortho-P (mg/L PO_4^{3-})	-	0.36	0.26	-	-
Nitrate (mg/L N)	-	<0.1	<0.1	-	-
Fe (mg/L)	0.70	0.061	0.057	0.002	0.005
Mn (mg/L)	0.025	0.023	0.018	0.019	0.022
Al (mg/L)	0.31	0.036	0.005	0.042	0.005
Ca (mg/L)	1.74	1.58	1.59	1.51	1.50
Mg (mg/L)	0.40	0.39	0.39	0.38	0.38
Si (mg/L)	1.59	1.50	1.52	1.48	1.48
Cl^- (mg/L)	5.0	5.9	5.9	5.8	5.6
SO_4^{2-} (mg/L)	1.16	1.1	1.1	1.14	1.1
Br^- (mg/L)	<0.2	<0.2	<0.2	<0.2	<0.2
TSS (mg/L)	4.1	2	2	0.0	0
TDS (mg/L)	37	24	26	25	25

Table G–4 BAC with Ortho-P & pH Adjustment Phase Average Water Quality

Water Quality	Raw	Plant-ACH	BAC	BAC-UF	Control-UF
pH	5.2	5.3	5.3	5.9	5.9
Temp. (ºC)	17.5	17.9	18.7	18.8	18.4
Turb. (ntu)	4.83	1.2	1.24	0.06	0.06
Alk. (mg/L CaCO$_3$)	2.5	2.3	5.2	5.3	2.4
Color (CU)	67	4.9	5.7	3.3	3.1
UV254 (1/cm)	0.294	0.060	0.063	0.051	0.053
DOC (mg/L)	6.9	3.2	3.2	2.5	2.6
SUVA (L/g-m)	4.2	1.8	1.9	2.0	2.0
DO (mg/L)	-	7.3	6.6	-	-
Ortho-P (mg/L PO$_4^{3-}$)	-	0.42	0.39	-	-
Nitrate (mg/L N)	-	<0.1	<0.1	-	-
Fe (mg/L)	0.66	0.068	0.098	0.001	0.004
Mn (mg/L)	0.023	0.019	0.013	0.012	0.020
Al (mg/L)	0.24	0.103	0.175	0.005	0.005
Ca (mg/L)	1.36	1.75	1.74	1.61	1.62
Mg (mg/L)	0.40	0.42	0.42	0.41	0.42
Si (mg/L)	1.49	1.52	1.53	1.50	1.49
Cl$^-$ (mg/L)	2.7	5.4	5.5	5.4	5.4
SO$_4^{2-}$ (mg/L)	0.78	0.9	0.8	0.83	0.7
Br$^-$ (mg/L)	<0.2	<0.2	<0.2	<0.2	<0.2
TSS (mg/L)	4.0	2	2	0.1	0
TDS (mg/L)	46	43	44	43	39

Table G–5 GAC and BAC Phase Biological Activity Results Summary

Testing Period	Free ATP (pg/mL)		Total ATP (pg/mL)		Free/Total ATP Fraction		Viable ATP (Total - Free, pg/mL)		HPC (CFU/mL)	
	Plant-ACH	BAC	Plant-ACH	BAC	Plant-ACH	BAC	Plant-ACH	BAC	Plant-ACH	BAC
GAC Adsorption	5	9	6	10	0.83	0.86	1.8	1.6	-	-
BAC Transition	4	21	5	21	0.75	0.78	1.5	3.1	-	-
BAC (Ortho-P Adjustment)	21	43	36	90	0.54	0.59	17	47	2600	4900
BAC (Ortho-P & pH Adjustment)	12	41	26	59	0.60	0.68	14	23	3900	5200
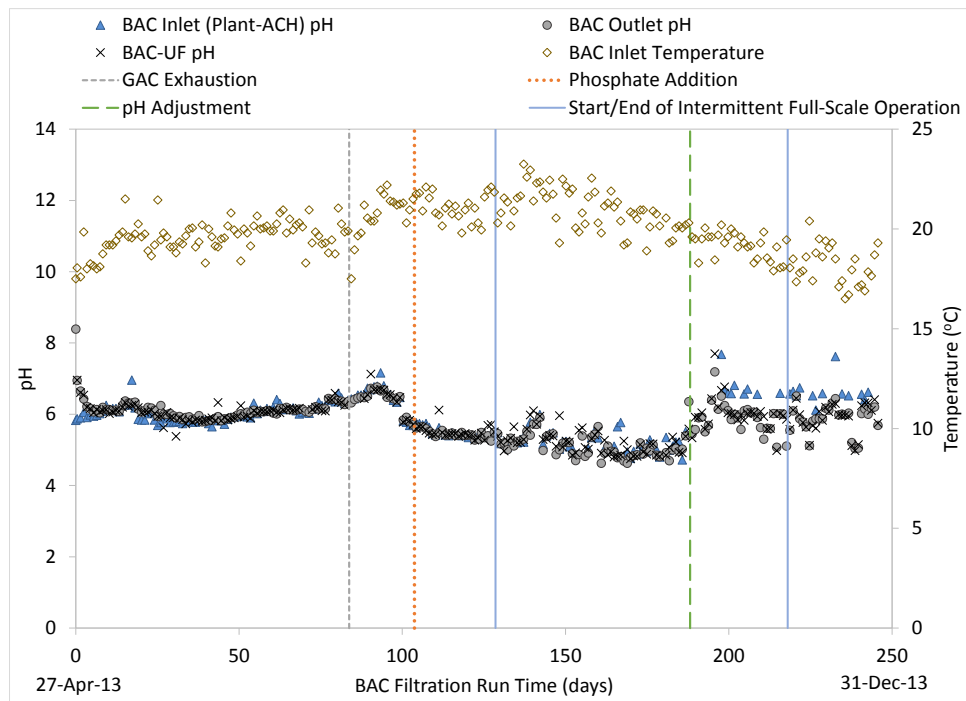
Figure G–1 GAC/BAC Phase Temperature and pH Time-Series Graph

288
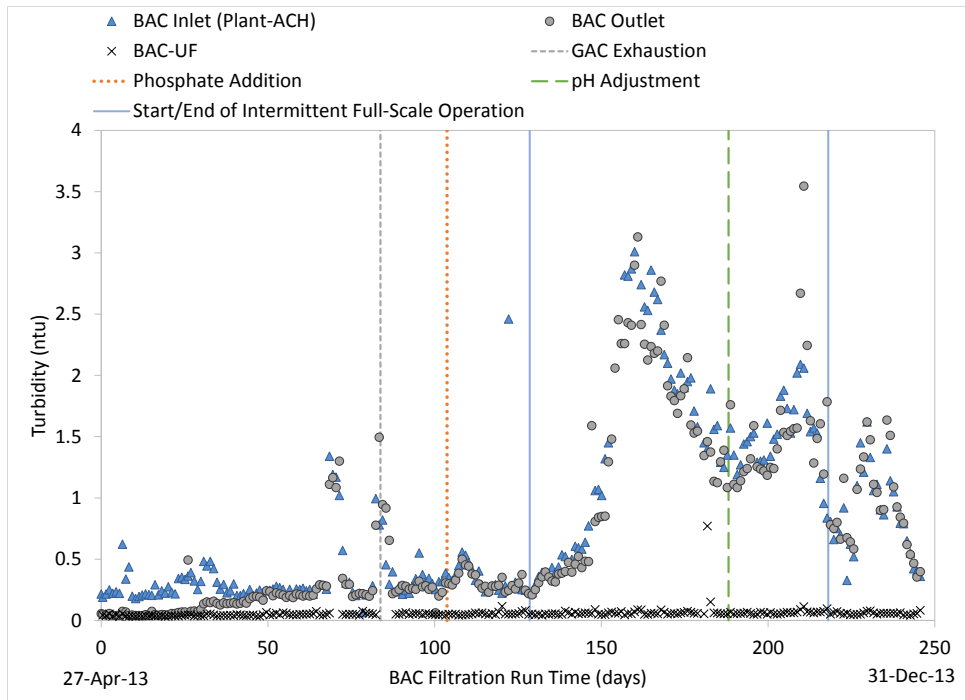
Figure G–2 GAC/BAC Phase Turbidity Time-Series Graph
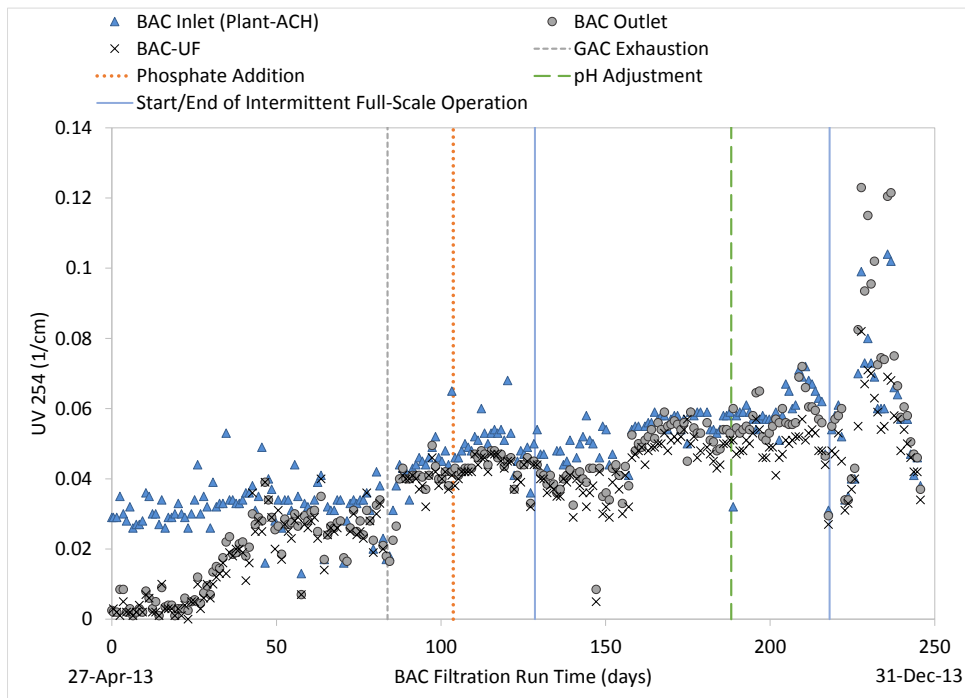
Figure G–3 GAC/BAC Phase UV 254 Time-Series Graph
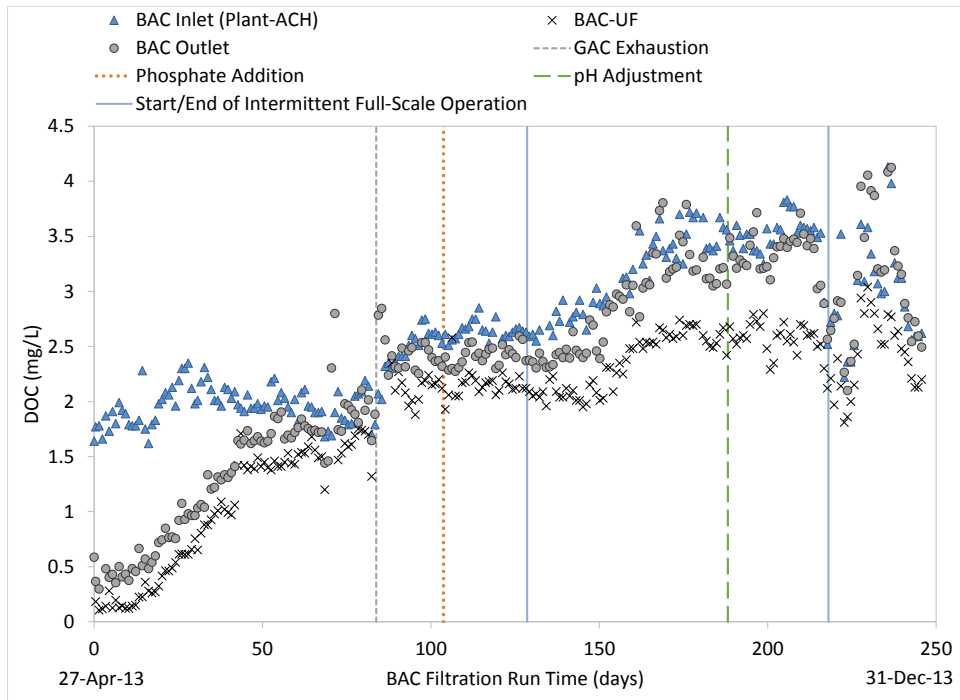
Figure G–4 GAC/BAC Phase DOC Time-Series Graph
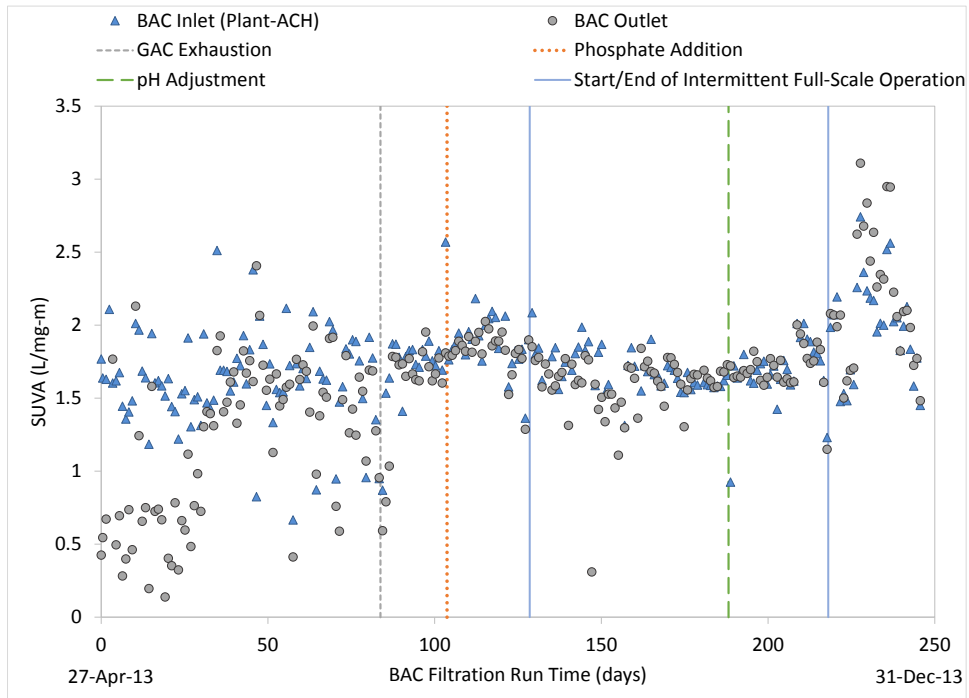
Figure G–5 GAC/BAC Phase SUVA Time-Series Graph
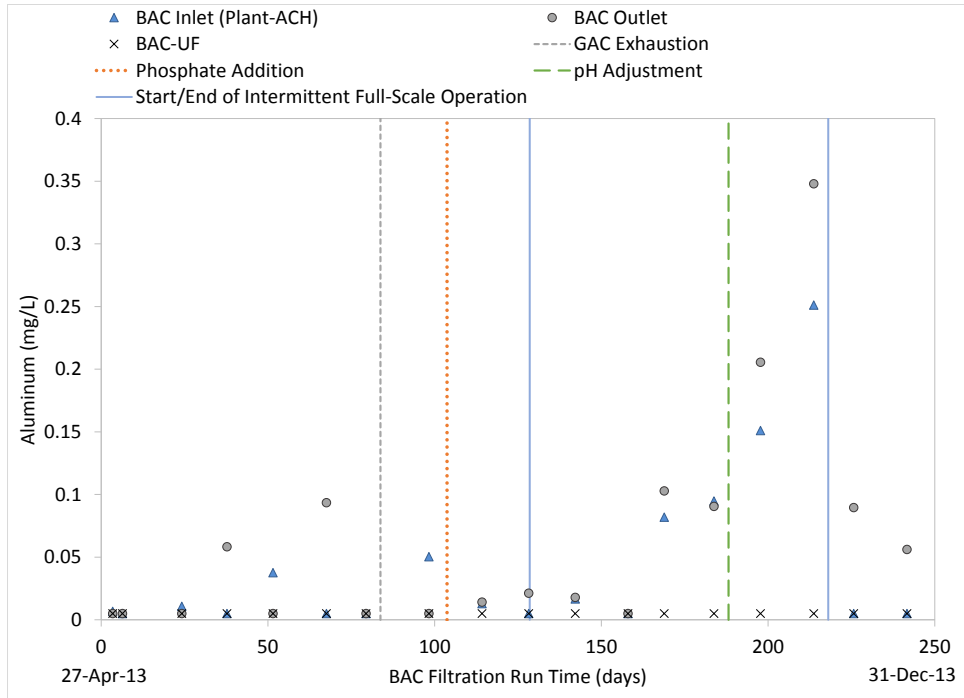
Figure G–6 GAC/BAC Phase Aluminum Time-Series Graph
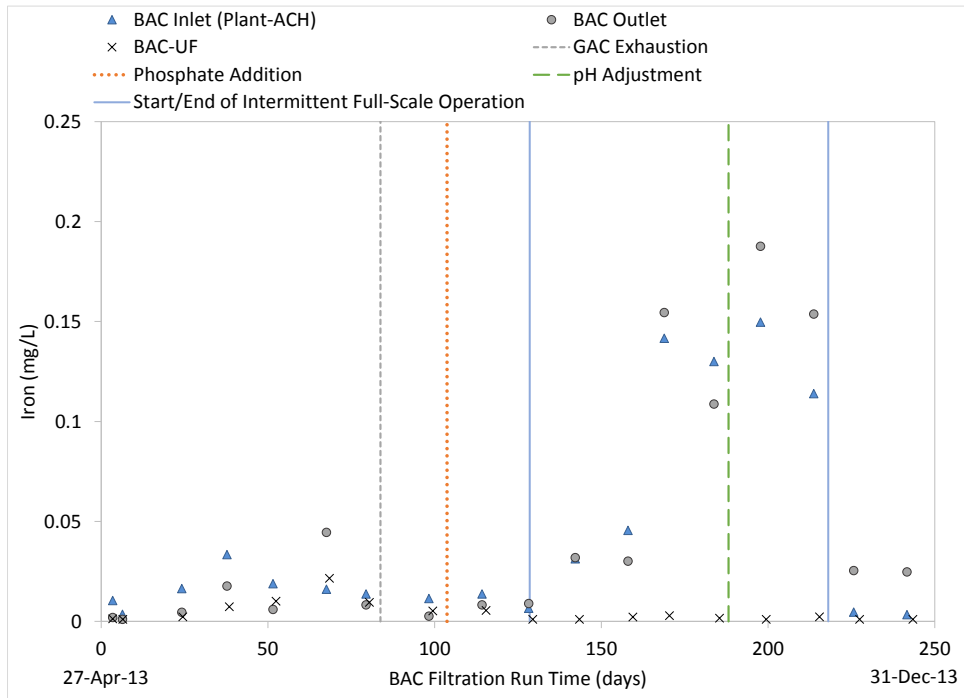
Figure G–7 GAC/BAC Phase Iron Time-Series Graph

291
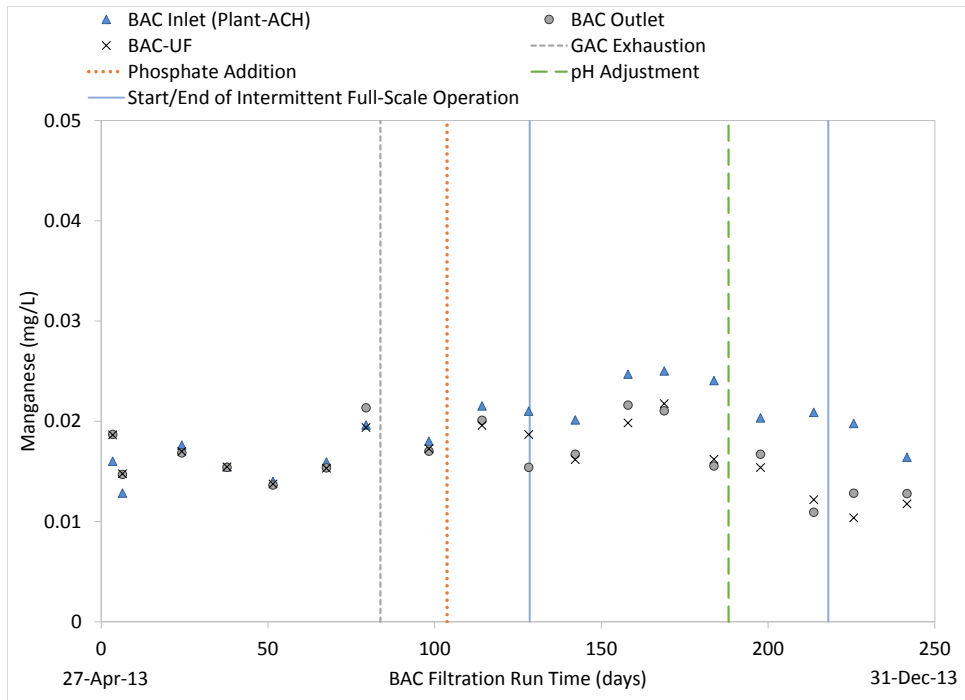
Figure G–8 GAC/BAC Phase Manganese Time-Series Graph
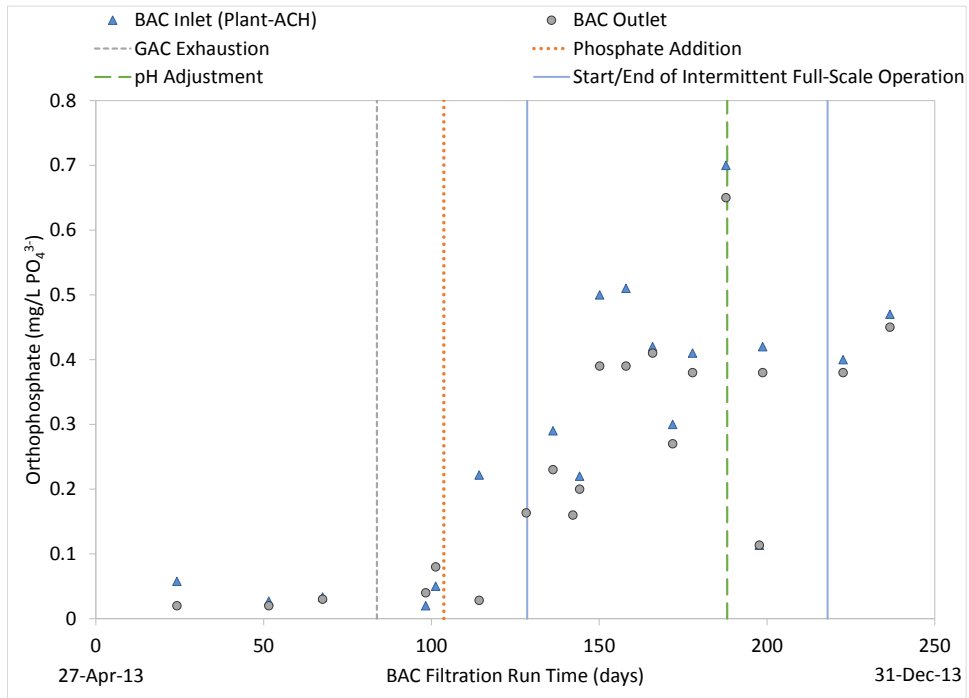
Figure G–9 GAC/BAC Phase Orthophosphate Time-Series Graph

292
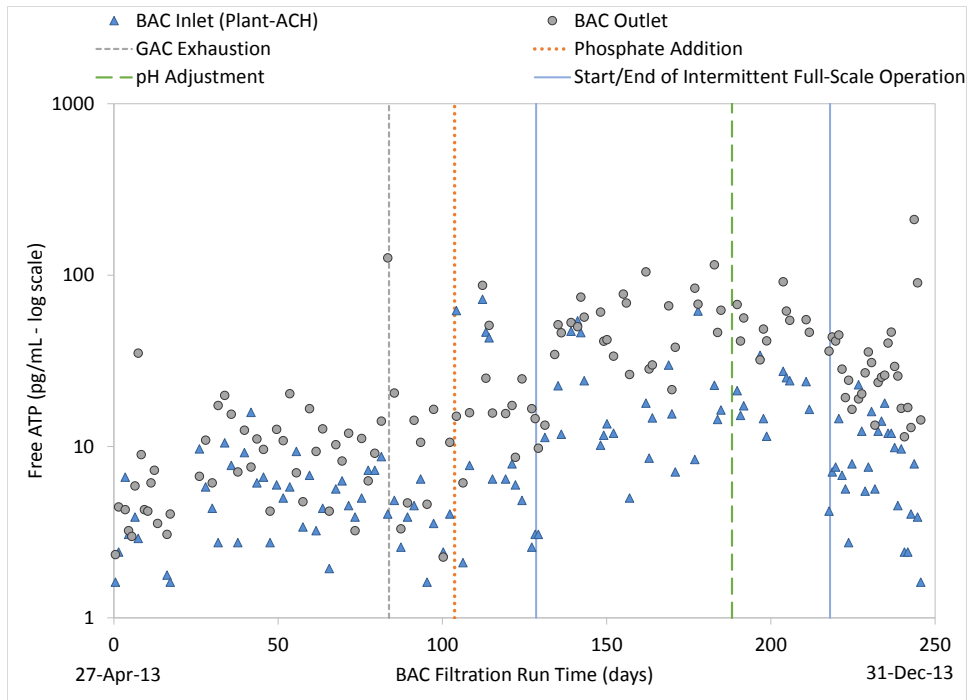
Figure G–10 GAC/BAC Phase Free ATP Time-Series Graph
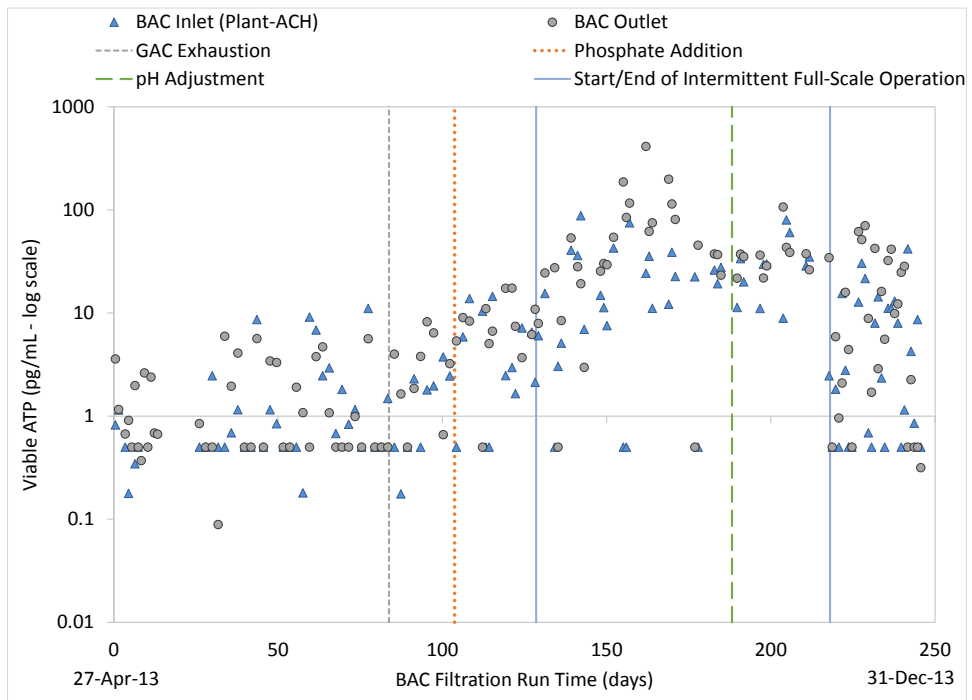
Figure G–11 GAC/BAC Phase Viable ATP Time-Series Graph

293
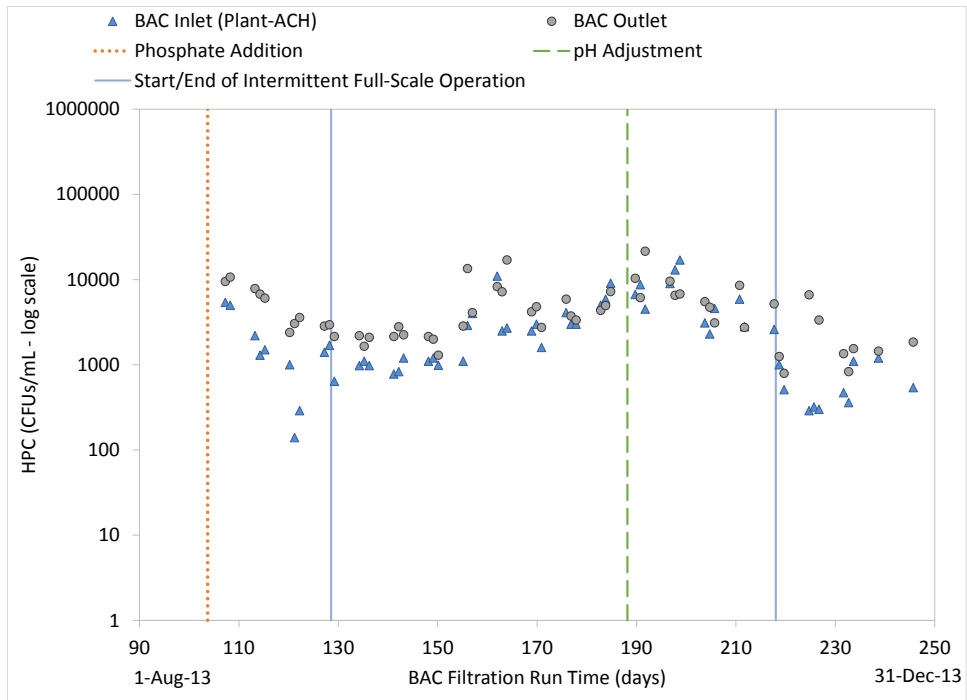
Figure G–12 GAC/BAC Phase HPC Time-Series Graph
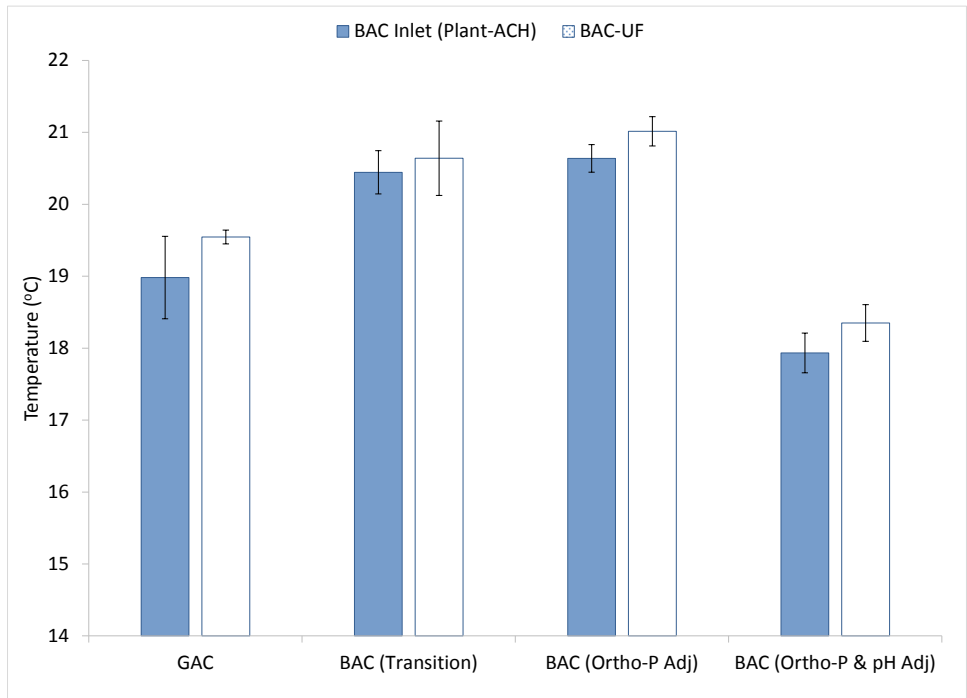
Figure G–13 GAC/BAC Phase Average Temperature

294
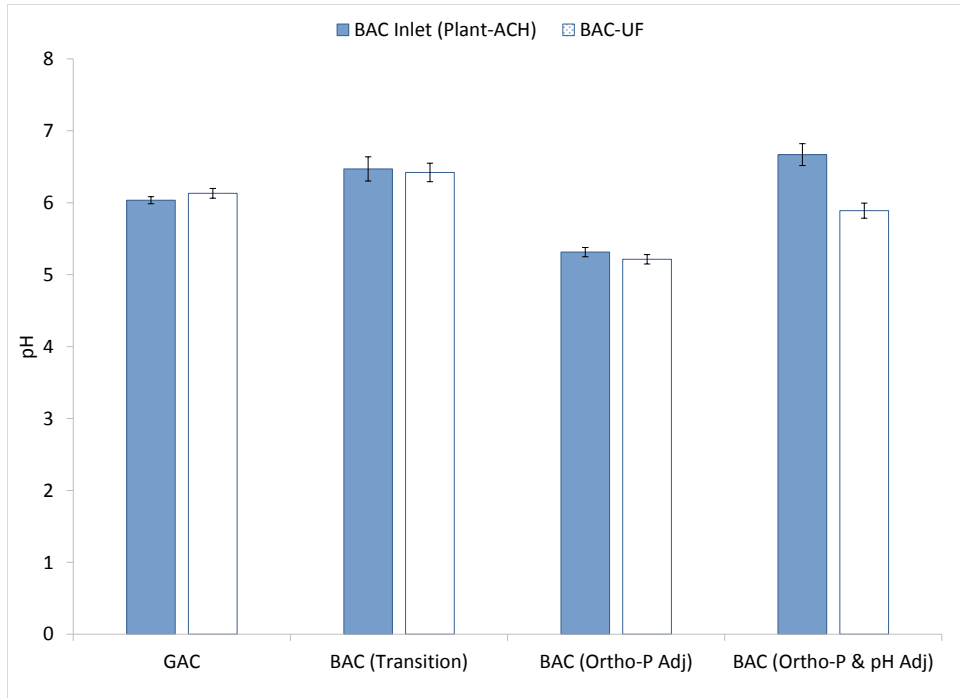
Figure G–14 GAC/BAC Phase Average pH
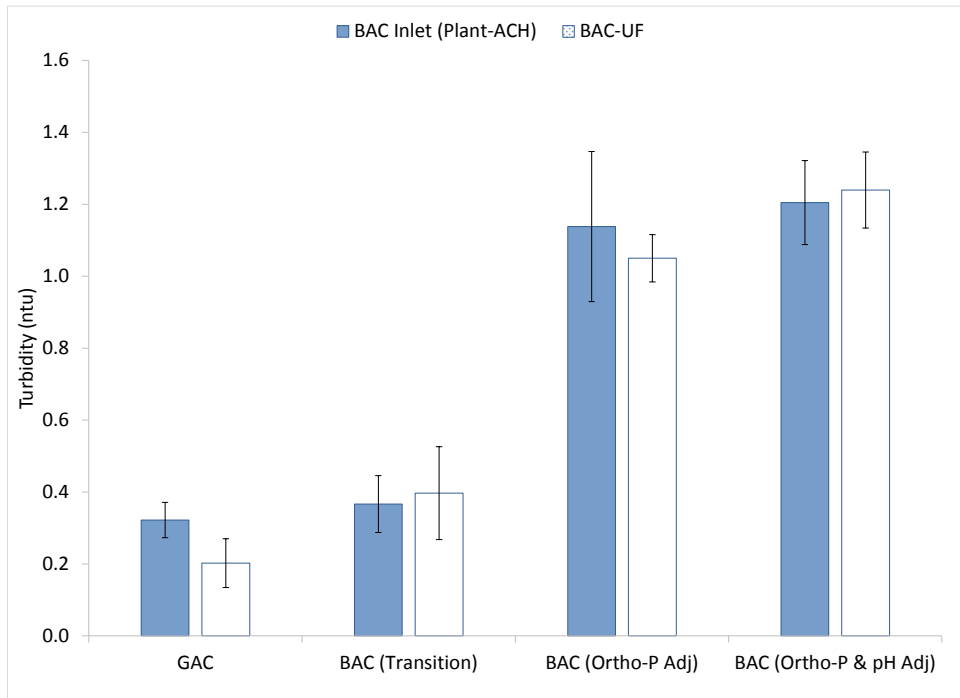
Figure G–15 GAC/BAC Phase Average Turbidity
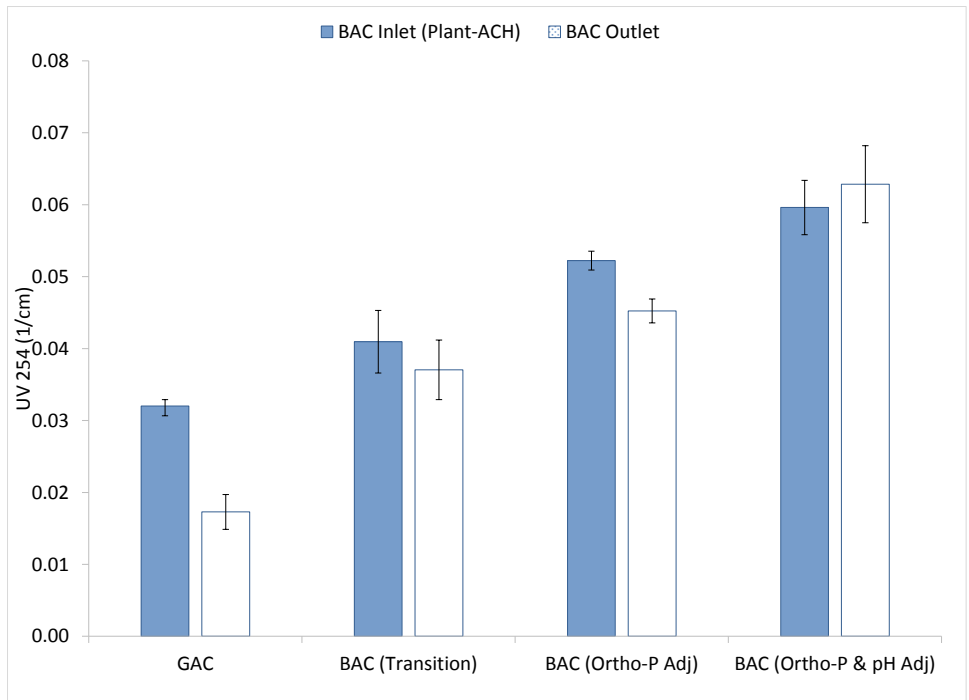
Figure G–16 GAC/BAC Phase Average UV 254
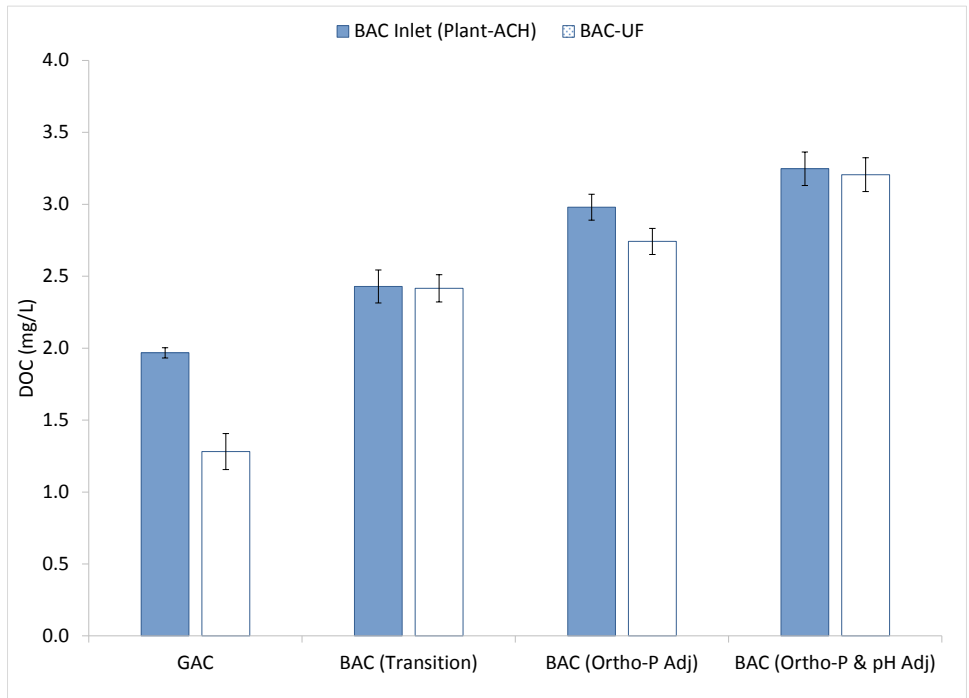
Figure G–17 GAC/BAC Phase Average DOC
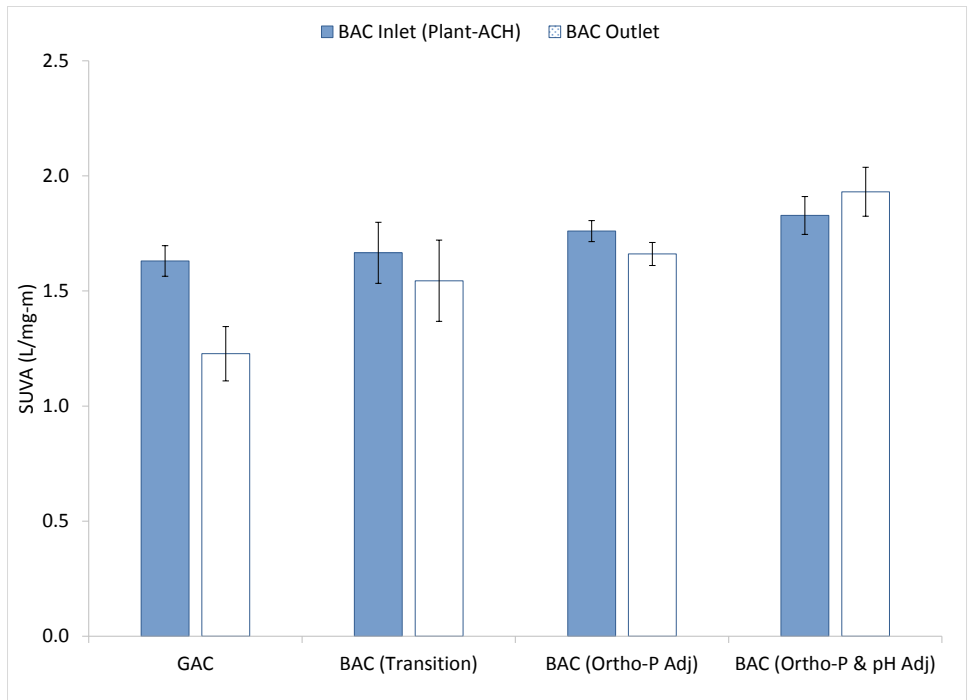
Figure G–18 GAC/BAC Phase Average SUVA
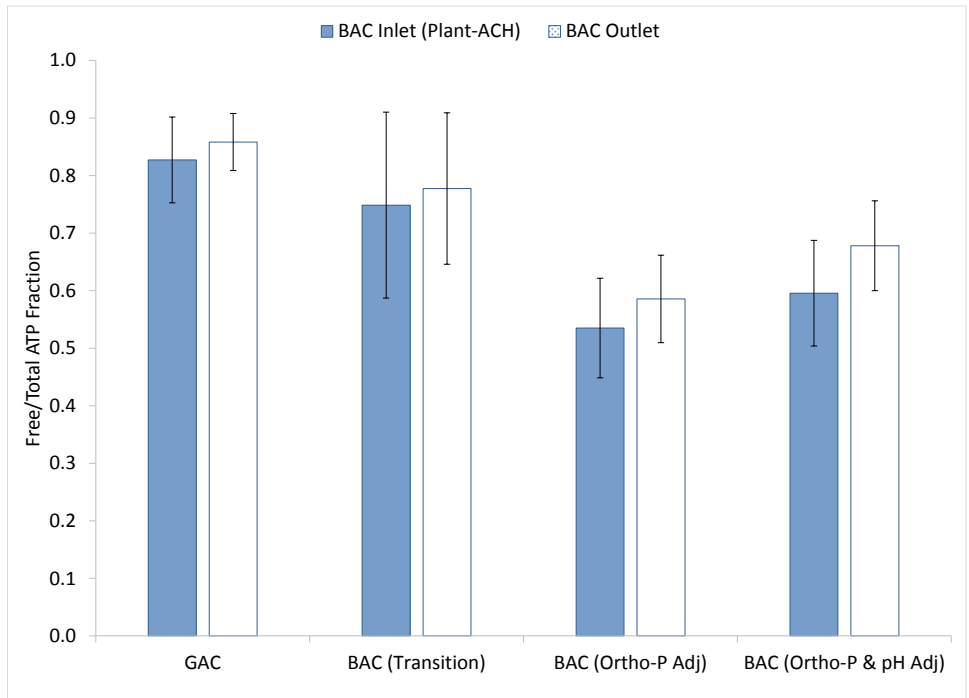
Figure G–19 GAC/BAC Phase Average Free/Total ATP Fraction

297
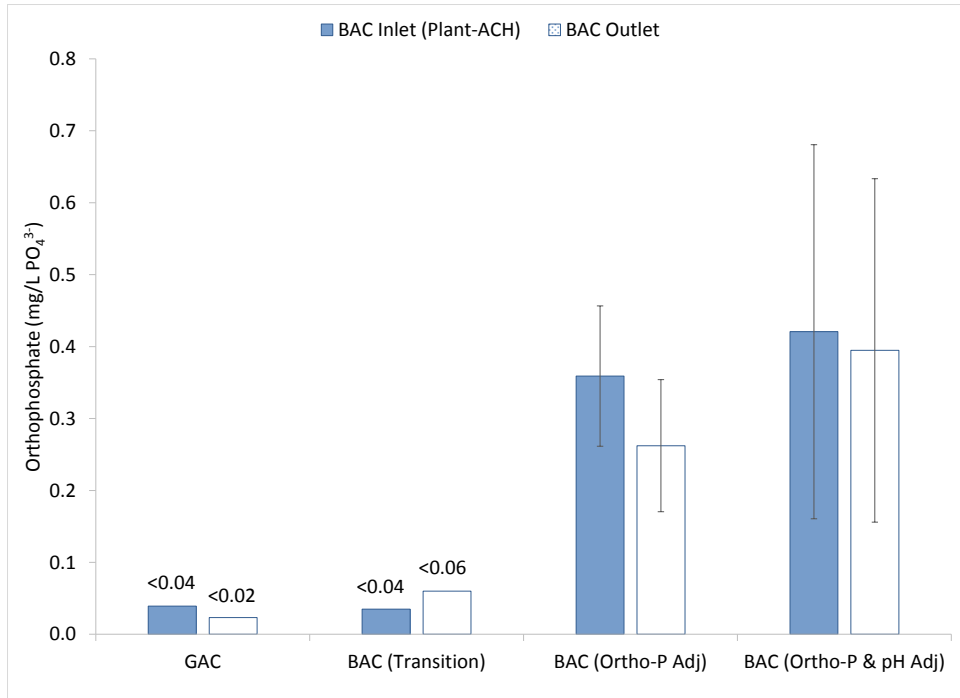
Figure G–20 GAC/BAC Phase Average Orthophosphate

Table G–6 GAC/BAC Phase Control-UF TTHM Speciation

Contact Time (hrs)	Cl₂ Residual (mg/L)	THM Concentration (µg/L)				
		Chloroform	Bromo-dichloromethane	Dibromo-chloromethane	Bromoform	TTHMs
28-Apr-13						
6	2.4	120	3	1	1	124
24	2.5	143	3	1	1	149
54	1.6	159	4	1	1	165
96	1.4	166	4	1	1	172
168	1.2	158	4	1	1	164
5-Aug-13						
7.1	1.2	199	2	1	1	203
24	2.3	219	3	1	1	223
48	1.9	205	3	1	1	209
92	1.5	220	3	1	1	225
187	1.0	263	4	1	1	270
21-Oct-13						
6	2.2	139	7	2	1	149
25	1.6	190	10	2	1	203
59	1.1	223	11	2	1	237
94	0.7	231	11	2	1	245
164	0.5	259	12	2	1	273
9-Dec-13						
6	1.7	106	2	1	1	110
24	1.2	143	4	1	1	148
48	0.8	163	4	1	1	169
96	0.5	185	5	1	1	192
168	0.3	190	4	1	1	197

Table G–7 GAC/BAC Phase Control-UF HAA$_5$ Speciation

Date	Chloroacetic Acid	Bromoacetic Acid	Dichloro-acetic Acid	Trichloro-acetic Acid	Dibromo-acetic Acid	HAA$_5$
	HAA Concentration (µg/L)					
28-Apr-13	10	5	17	16	5	52
5-Aug-13	10	1	55	41	1	108
21-Oct-13	7	1	43	23	2	77
9-Dec-13	18	1	52	26	6	103

Table G–8 GAC/BAC-UF TTHM Speciation

Contact Time (hrs)	Cl$_2$ Residual (mg/L)	Chloroform	Bromo-dichloromethane	Dibromo-chloromethane	Bromoform	TTHMs
		THM Concentration (µg/L)				
			28-Apr-13			
6	2.3	5	1	1	1	8
24	2.4	5	1	1	1	8
55	2.3	5	1	1	1	8
96	2.4	6	1	1	1	9
168	2.3	8	1	1	1	11
			5-Aug-13			
1	1.2	106	1	1	1	109
24	2.5	178	3	1	1	183
48	2.1	203	3	1	1	208
92	1.8	193	3	1	1	198
187	1.2	274	5	1	1	281
			21-Oct-13			
6	2.5	113	8	2	1	124
25	2.0	138	9	2	1	150
59	1.5	164	10	2	1	177
93	1.2	213	12	2	1	227
164	1.0	246	13	2	1	262
			9-Dec-13			
6	2.0	89	4	1	1	95
24	1.4	130	3	1	1	136
48	1.1	158	4	1	1	164
96	0.8	173	4	1	1	179
168	0.6	185	4	1	1	191

Table G–9 GAC/BAC-UF HAA$_5$ Speciation

| Date | HAA Concentration (µg/L) | | | | | |
	Chloroacetic Acid	Bromoacetic Acid	Dichloro-acetic Acid	Trichloro-acetic Acid	Dibromo-acetic Acid	HAA$_5$
28-Apr-13	10	5	5	5	5	30
5-Aug-13	9	1	50	35	1	96
21-Oct-13	6	1	49	30	2	88
9-Dec-13	5	1	48	21	6	81
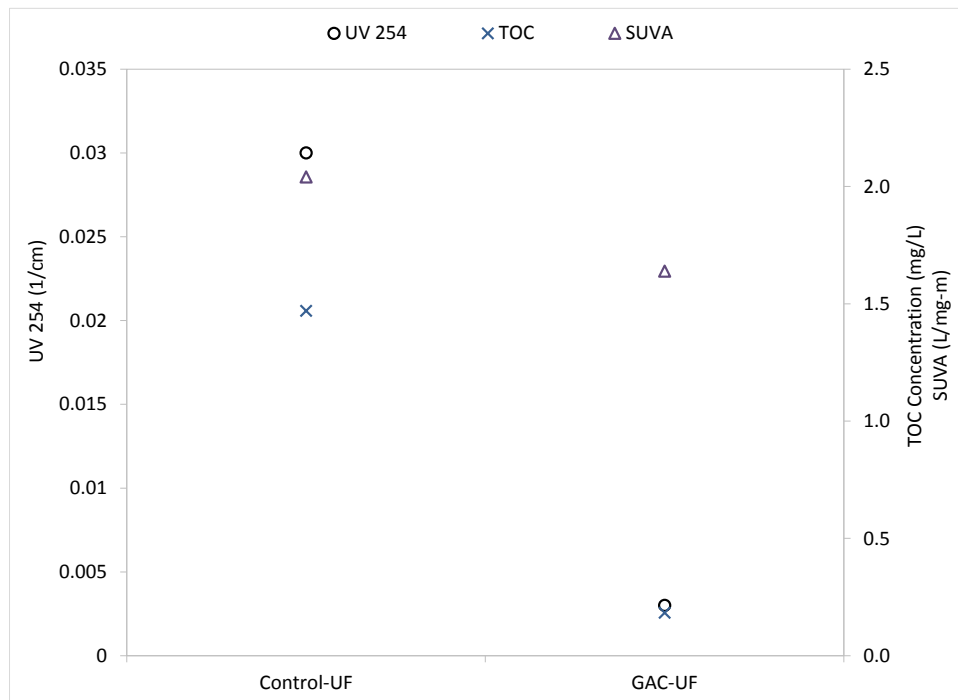
Figure G–21 GAC Start-Up Organic Water Quality
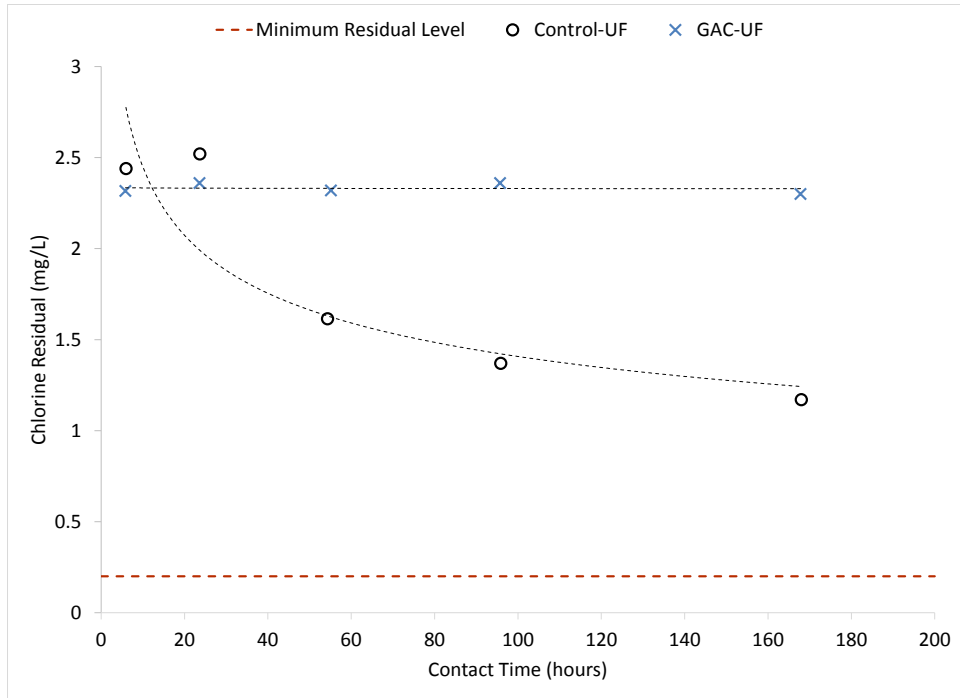
Figure G–22 GAC Start-Up Chlorine Decay
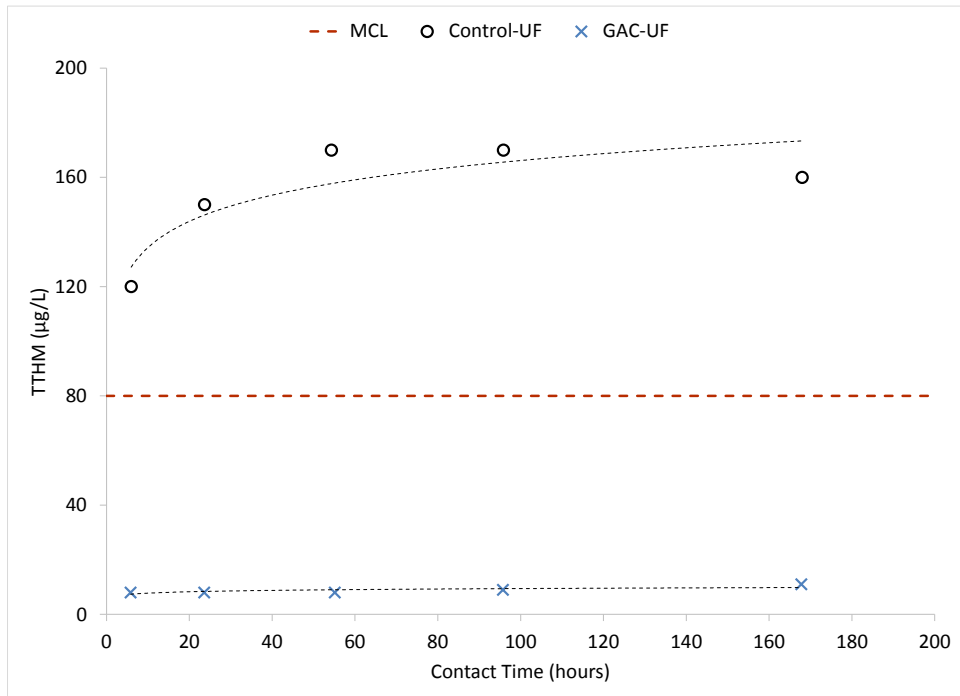
Figure G–23 GAC Start-Up TTHM Formation Potential

302
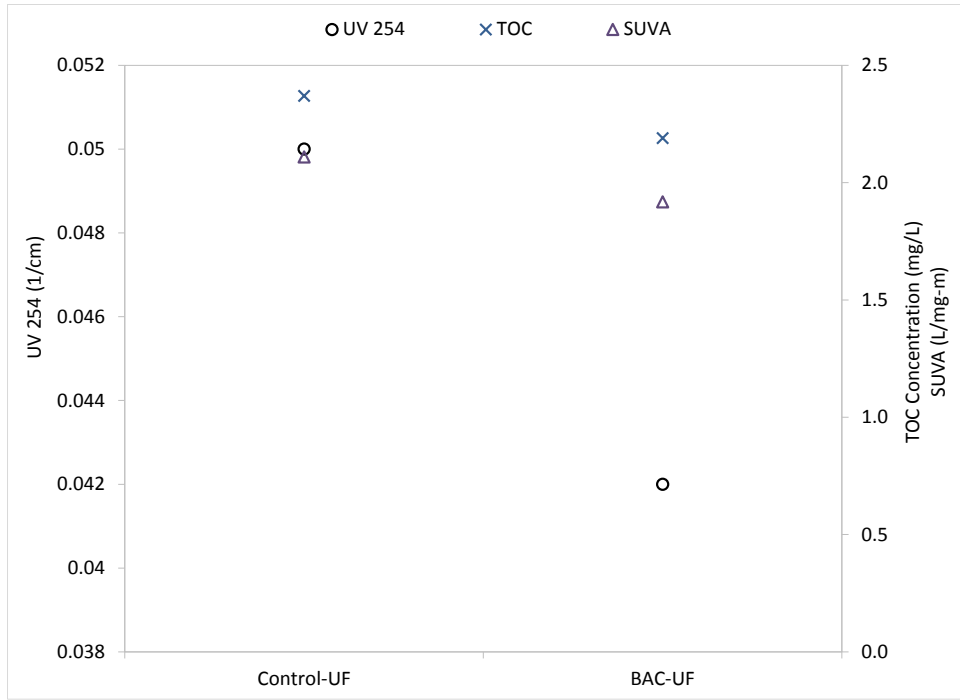
Figure G–24 BAC Transition Organic Water Quality
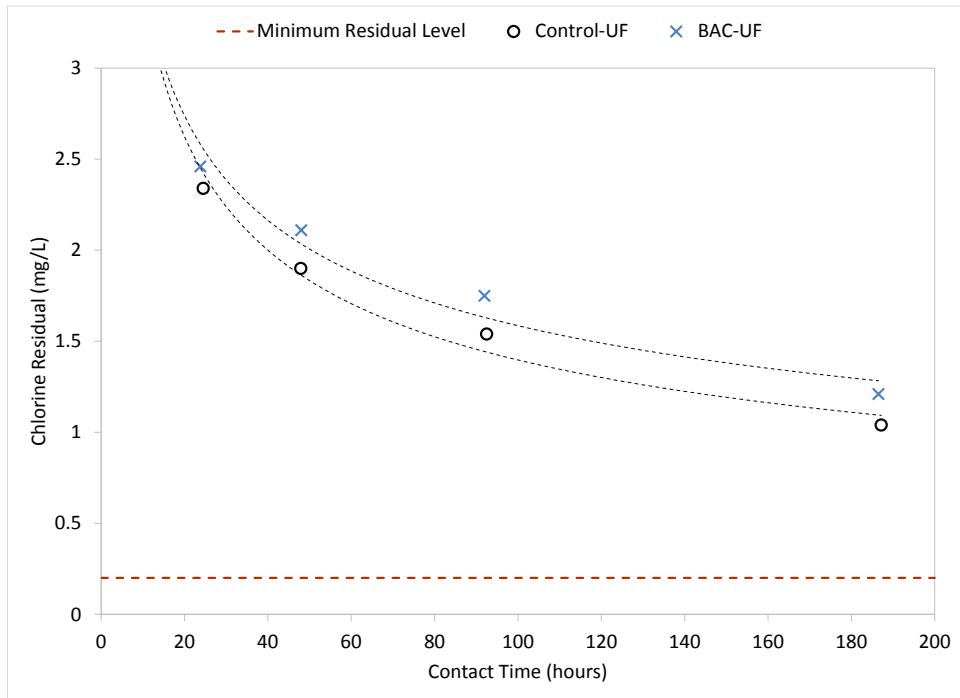
Figure G–25 BAC Transition Chlorine Decay
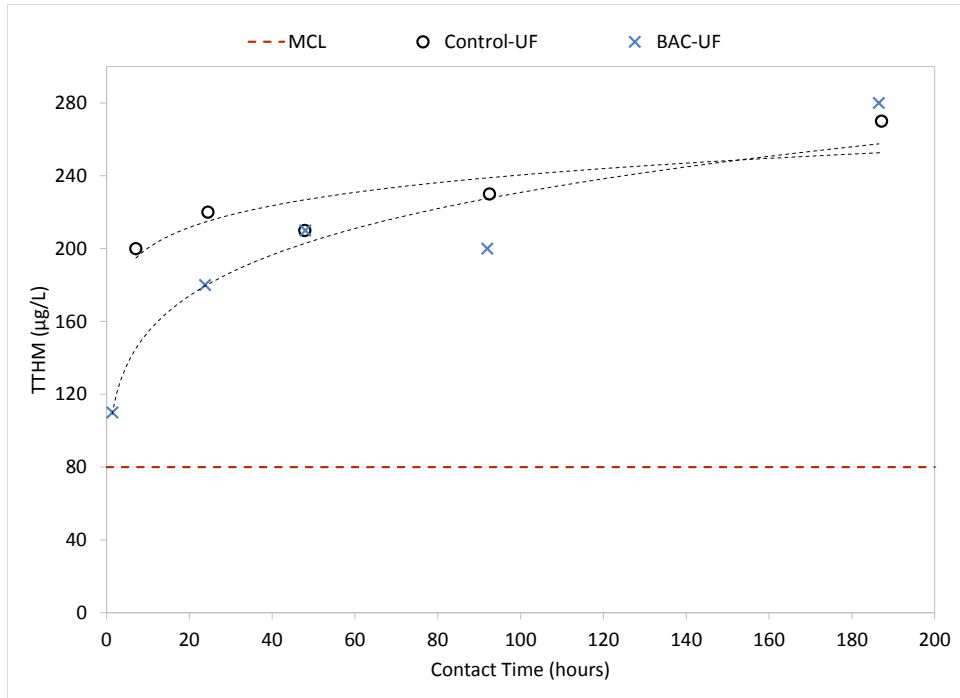
Figure G–26 BAC Transition TTHM Formation Potential
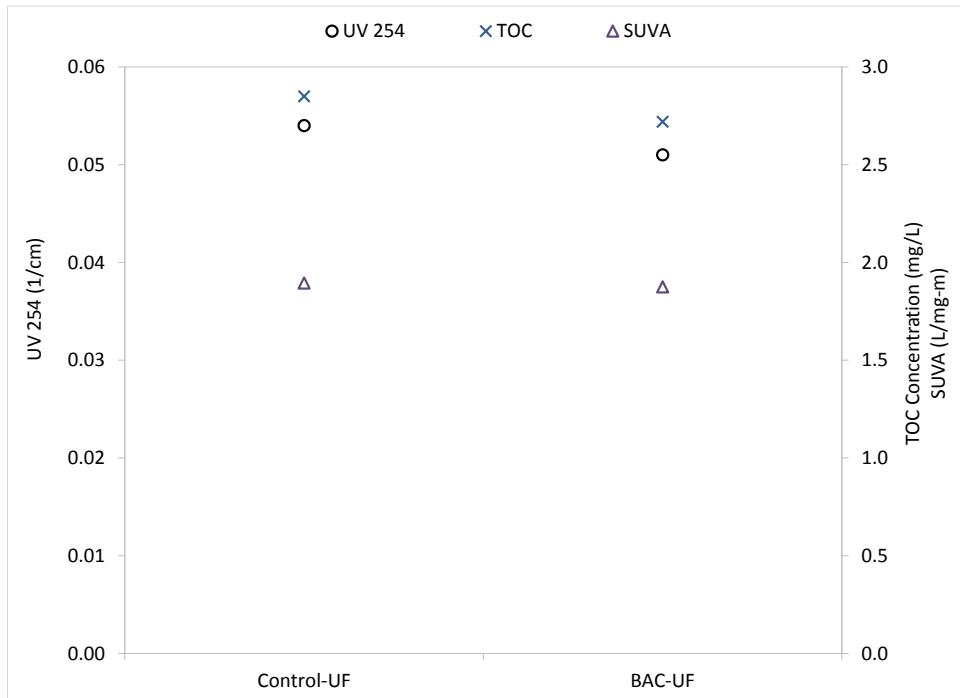
Figure G–27 BAC Ortho-P Organic Water Quality
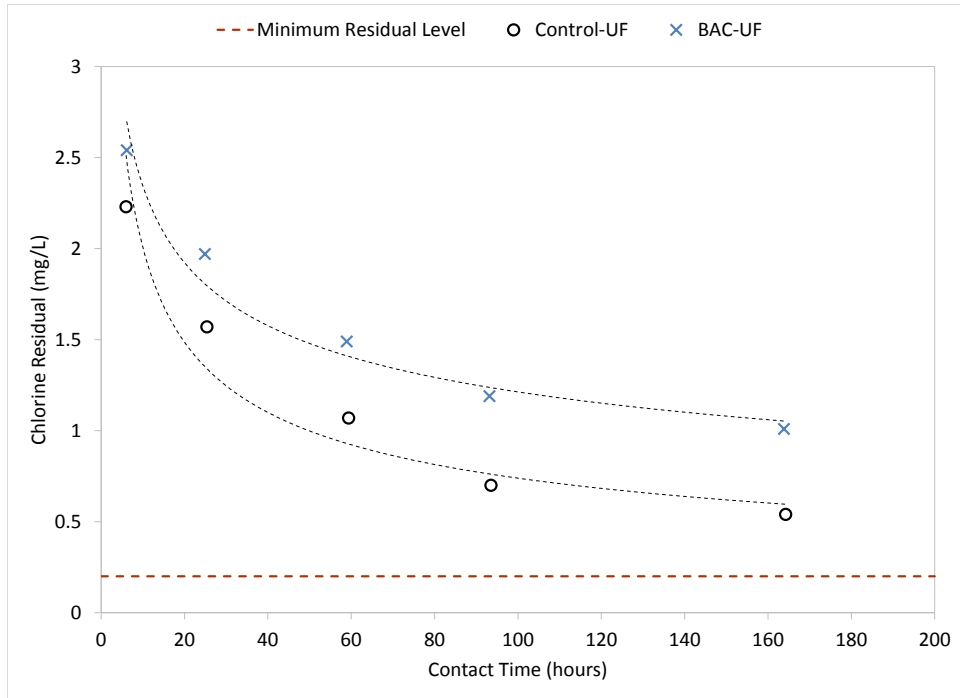
Figure G–28 BAC Ortho-P Chlorine Decay
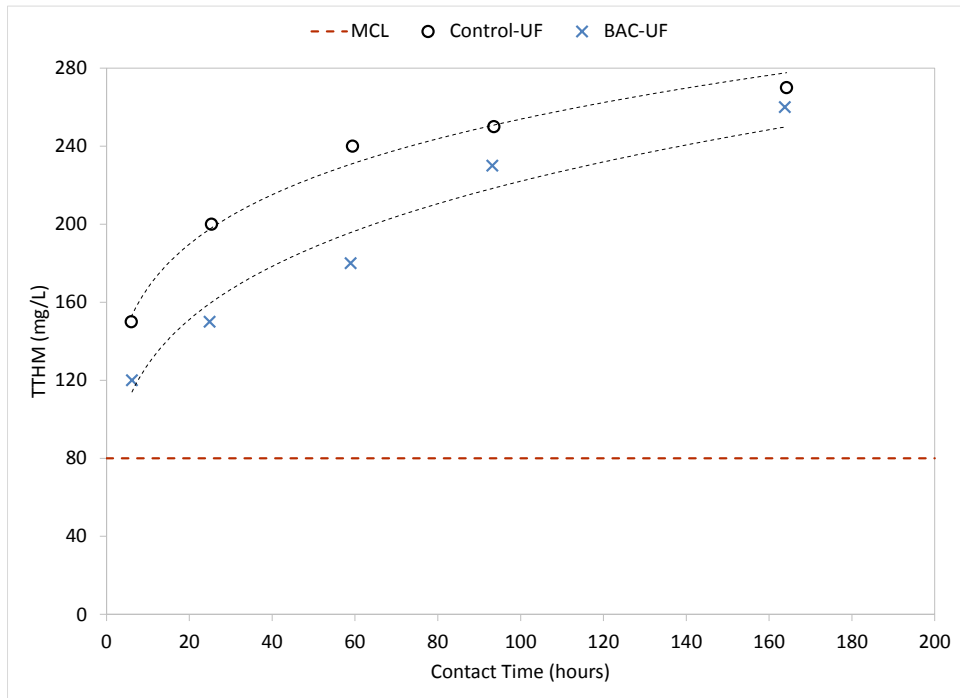
Figure G–29 BAC Ortho-P TTHM Formation Potential

305

Figure G–30 BAC Ortho-P & pH Organic Water Quality
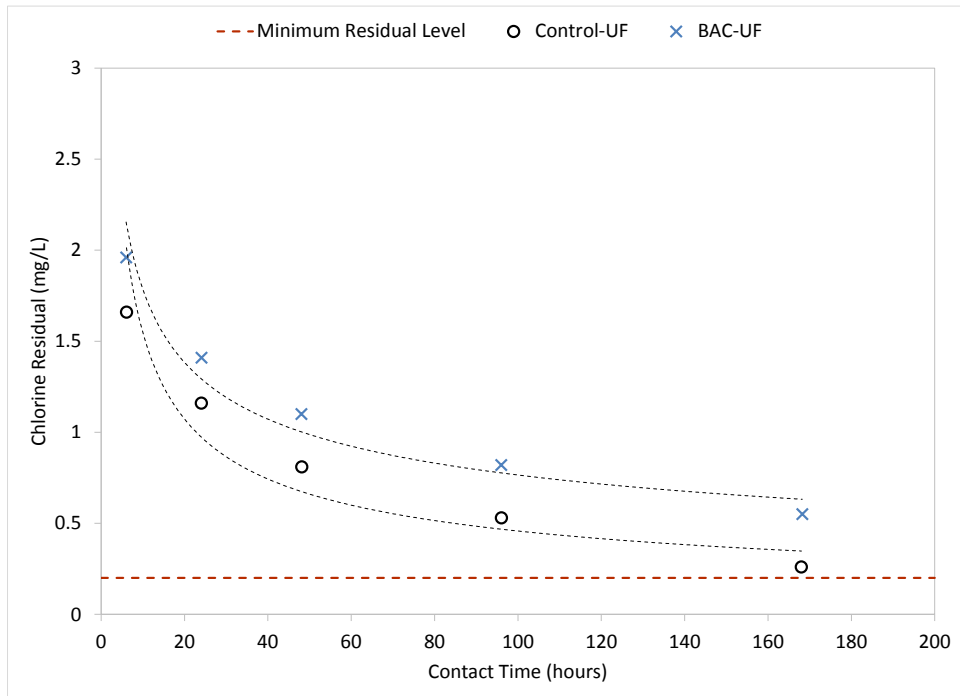
Figure G–31 BAC Ortho-P & pH Chlorine Decay

306
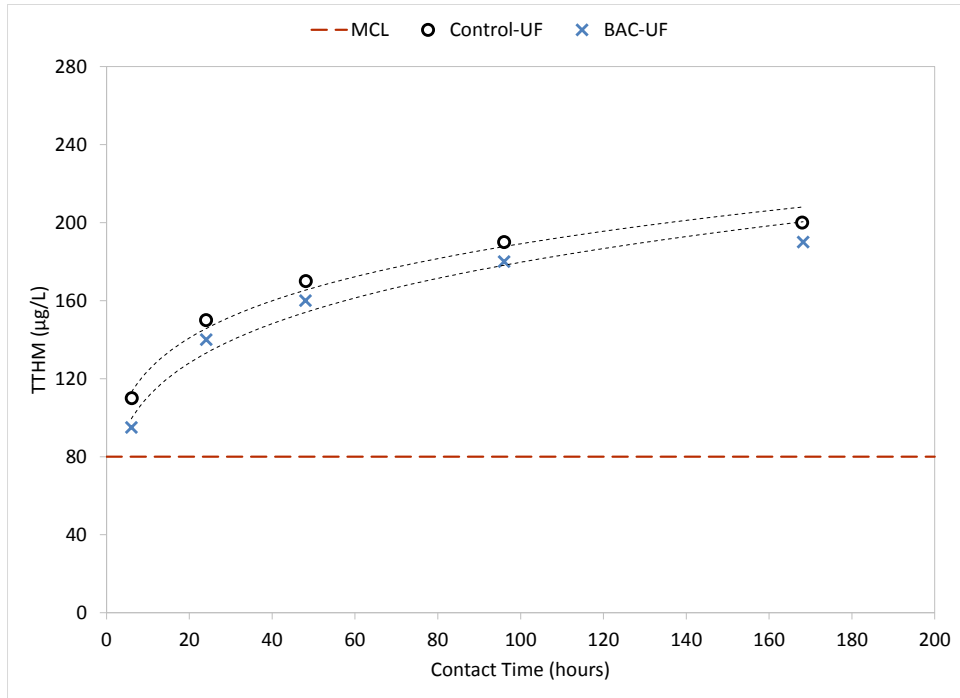
Figure G–32 BAC Ortho-P & pH TTHM Formation Potential
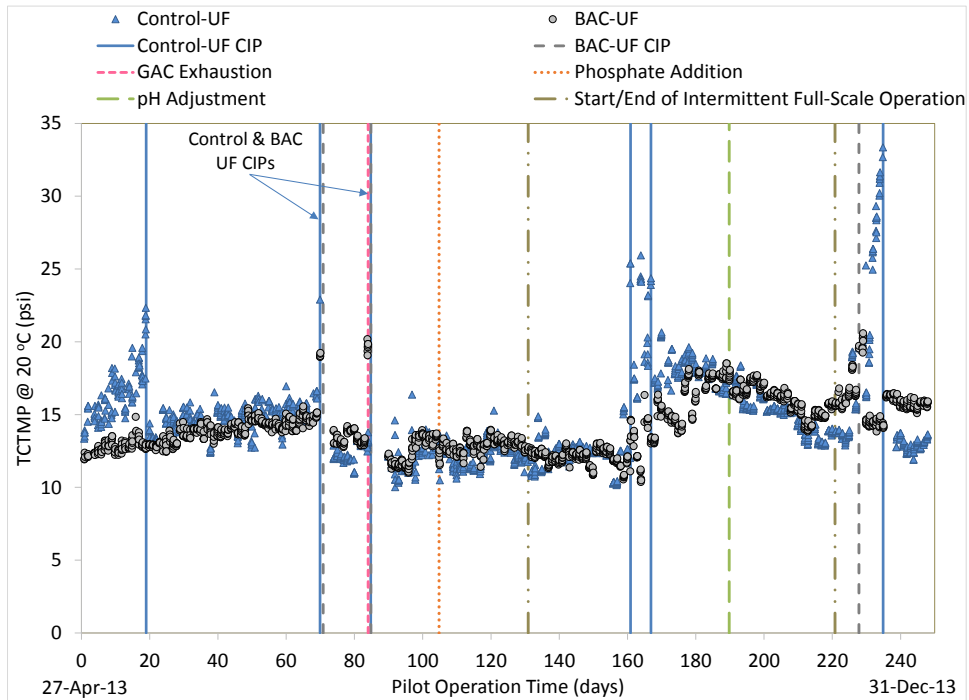
Figure G–33 GAC/BAC Thase TCTMP Time-Series Graph

307
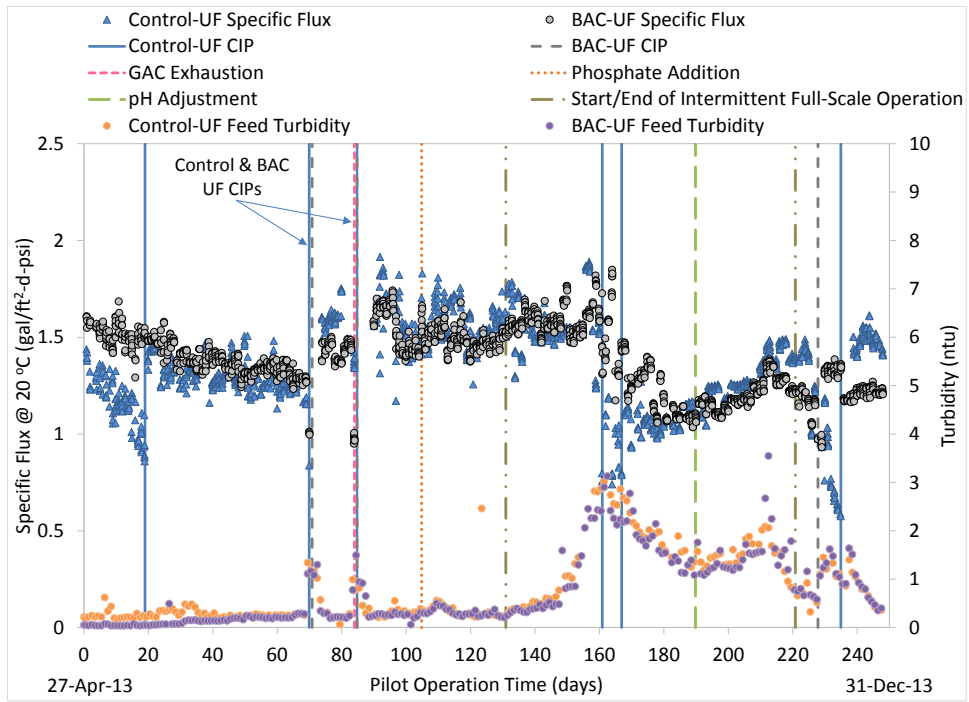
Figure G–34 GAC/BAC Phase Specific Flux Time-Series Graph

Table G–10 Additional Results and Figures from Avista Autopsy Results

Control-UF	BAC-UF
FTIR results for lightly fouled fiber	

| **FTIR results for heavily fouled fiber** | |

SEM at 200 times magnification of lightly fouled feed size (exterior)
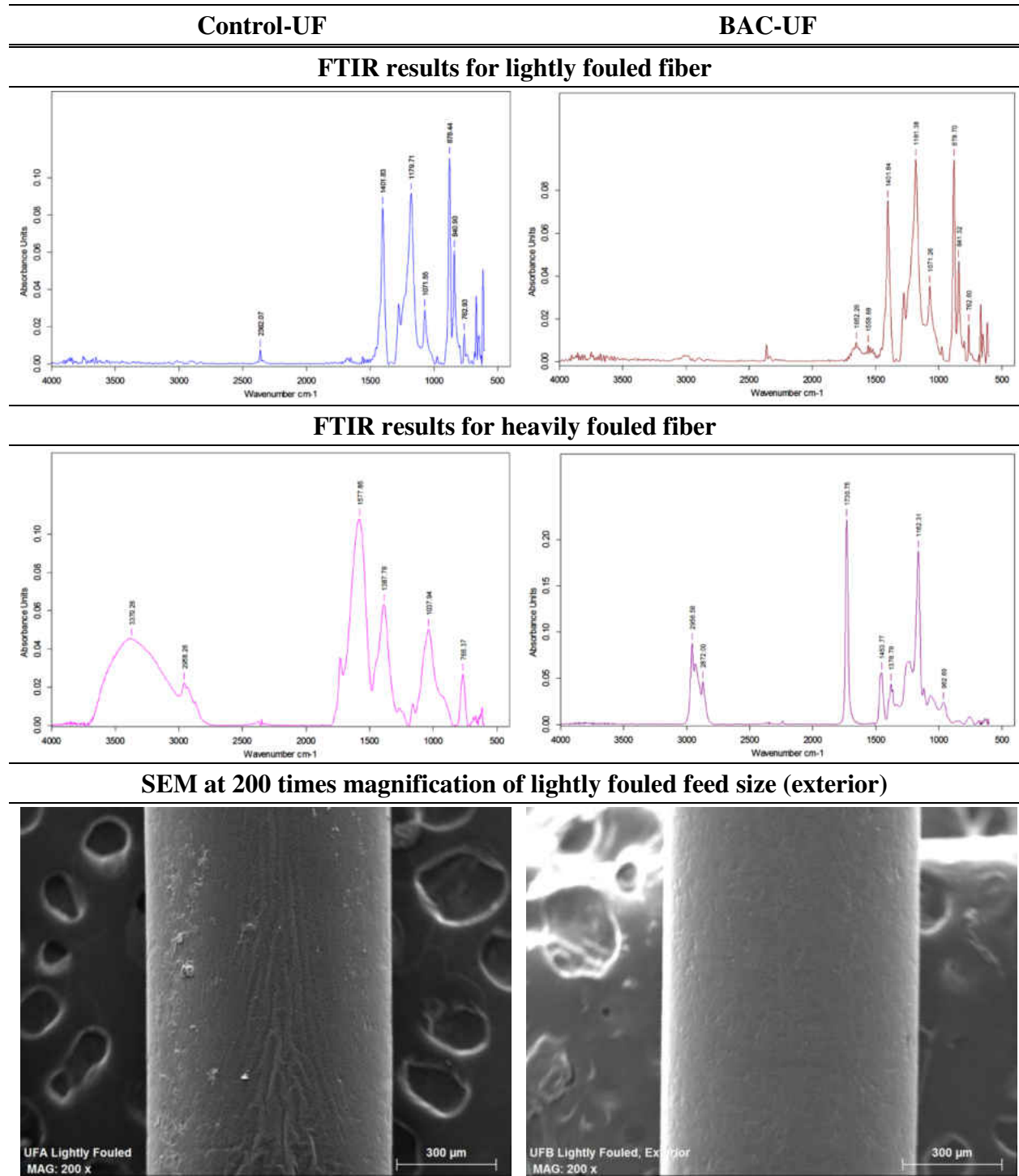
Source: Courtesy of Avista Technologies

Control-UF	BAC-UF

SEM at 200 times magnification of heavily fouled fiber (exterior feed side)
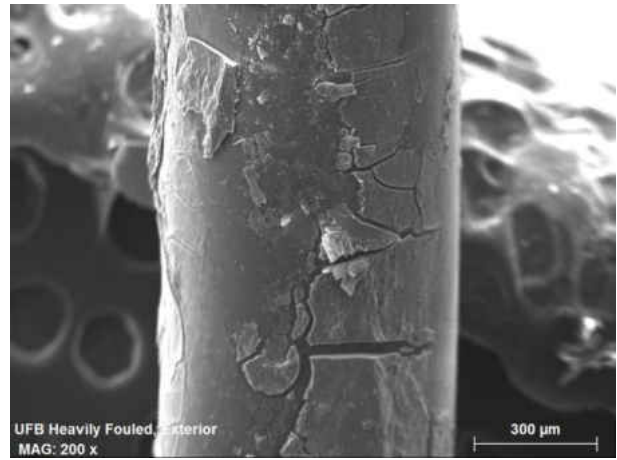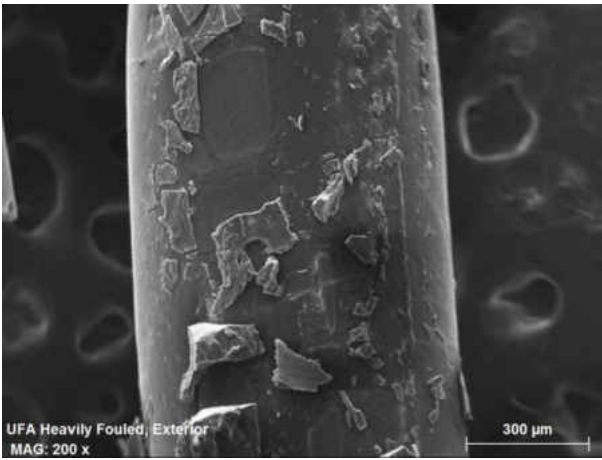
CEI image at 500 times magnification of lightly fouled fiber (exterior feed side)

Source: Courtesy of Avista Technologies

Control-UF	BAC-UF

CEI image at 500 times magnification of heavily fouled fiber (cross section)
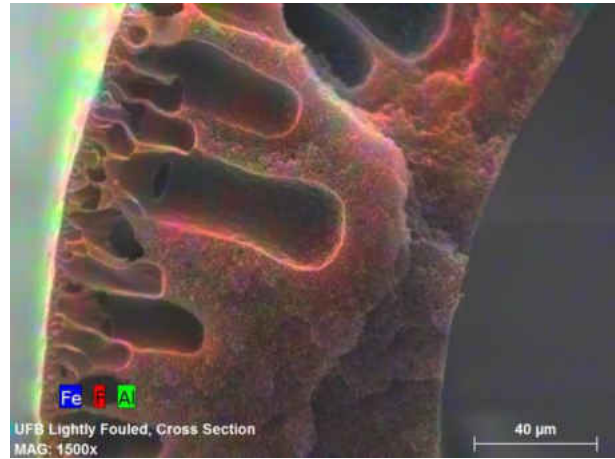
CEI image at 500 times magnification of heavily fouled fiber (exterior feed side)
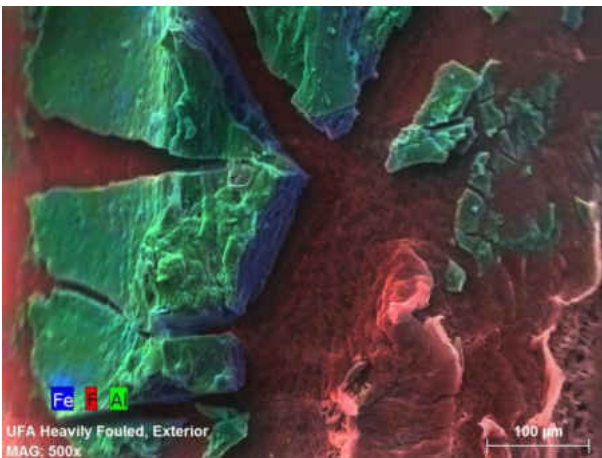
Source: Courtesy of Avista Technologies

APPENDIX H. MINITAB® SOFTWARE OUTPUT

<p style="text-align: center;">Minitab® Output Summary</p>

Table H–1 Minitab® Model Parameter Estimates

Parameter	Quadratic Equation		Gaussian Distribution	
	Estimate	95% Confidence Interval	Estimate	95% Confidence Interval
c_1	-1.023	(-15.54, 13.49)	-36.46	(- , 52.1058)
c_2	8.966	(5.596, 12.34)	57.26	(41.30, 75.22)
c_3	-0.3720	(-0.5138, -0.2302)	0.0061	(-0.0131, 0.0266)
c_4	-	-	12.03	(10.78, 13.37)

Table H–2 Confidence and Prediction Intervals for MTC Improvement Model Output

ALK/DOC Ratio Observation	Quadratic Equation		Gaussian Distribution	
	Predicted MTC Improvement	95% Confidence Interval	Predicted MTC Improvement	95% Confidence Interval
0.135	0.1807	(-13.97, 14.33)	3.18	(-13.12, 19.48)
3.00	22.53	(13.77, 31.29)	20.6	(9.592, 31.65)
4.40	31.24	(23.20, 39.28)	29.3	(18.19, 40.48)
5.34	36.25	(28.09, 44.41)	34.9	(24.24, 45.63)
9.96	51.37	(40.94, 61.81)	54.9	(39.41, 70.30)
15.7	48.40	(38.85, 57.95)	50.4	(38.15, 62.65)
18.9	35.56	(27.01, 44.11)	33.9	(22.76, 45.01)
19.5	32.35	(23.57, 41.14)	30.3	(18.66, 41.91)
23.1	7.770	(-6.982, 22.52)	8.15	(-6.089, 22.40)

Minitab® Output for Quadratic Equation Curve Fit
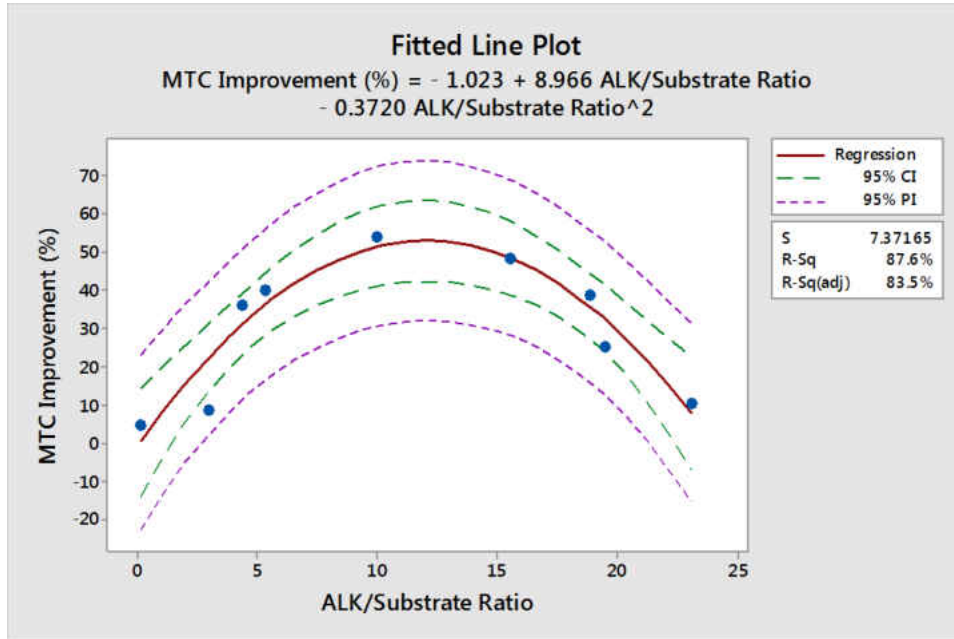
Figure H–1 Fitted Line Plot with Confidence and Prediction Intervals for Quadratic Model
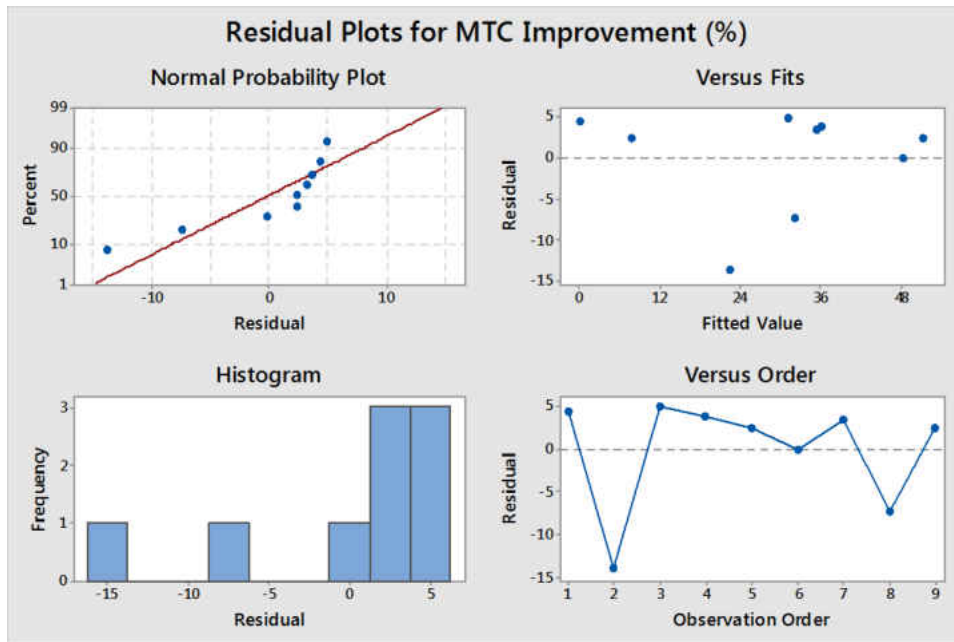
Figure H–2 Residual Plots for Model

314

Nonlinear Regression: MTC Improvement (%) = theta1 + ...

```
Method

Algorithm         Gauss-Newton
Max iterations            200
Tolerance            0.00001


Starting Values for Parameters

Parameter  Value
theta1         1
theta2         1
theta3         1


Estimates at Each Iteration

Iteration     SSE    theta1    theta2    theta3
        0  601761   1.00000   1.00000   1.00000
        1     326  -1.02290   8.96575  -0.37201
        2     326  -1.02290   8.96575  -0.37201


Equation

MTC  Improvement  (%)  =  -1.0229  +  8.96575  *  'ALK/Substrate  Ratio'  -  0.372005  *
'ALK/Substrate
    Ratio' ^ 2


Parameter Estimates

Parameter  Estimate  SE Estimate          95% CI
theta1     -1.02290      5.93137  (-15.5364, 13.4906)
theta2      8.96575      1.37724  (  5.5958, 12.3357)
theta3     -0.37201      0.05795  ( -0.5138, -0.2302)

MTC Improvement (%) = theta1 + theta2 * 'ALK/Substrate Ratio' + theta3 * 'ALK/Substrate
    Ratio' ^ 2


Correlation Matrix for Parameter Estimates

          theta1      theta2
theta2  -0.812753
theta3   0.699026  -0.974081


Lack of Fit

There are no replicates.
Minitab cannot do the lack of fit test based on pure error.


Summary
```

```
Iterations          2
Final SSE    326.048
DFE               6
MSE          54.3413
S            7.37165


Prediction

New   ALK/Substrate
Obs           Ratio       Fit   SE Fit          95% CI                95% PI
  1          0.1350    0.1807  5.78199   (-13.9673, 14.3287)   (-22.7437, 23.1051)
  2          3.0000   22.5263  3.57983   ( 13.7668, 31.2858)   (  2.4741, 42.5785)
  3          4.4028   31.2401  3.28536   ( 23.2011, 39.2791)   ( 11.4920, 50.9882)
  4          5.3400   36.2463  3.33452   ( 28.0870, 44.4055)   ( 16.4489, 56.0436)
  5          9.9600   51.3724  4.26432   ( 40.9380, 61.8069)   ( 30.5341, 72.2108)
  6         15.5659   48.4011  3.90413   ( 38.8481, 57.9542)   ( 27.9898, 68.8125)
  7         18.8976   35.5578  3.49347   ( 27.0095, 44.1060)   ( 15.5970, 55.5186)
  8         19.5000   32.3542  3.59029   ( 23.5691, 41.1393)   ( 12.2908, 52.4176)
  9         23.0769    7.7696  6.02853   ( -6.9817, 22.5209)   (-15.5319, 31.0712)
```

Minitab® Output for Gaussian Distribution Curve Fit
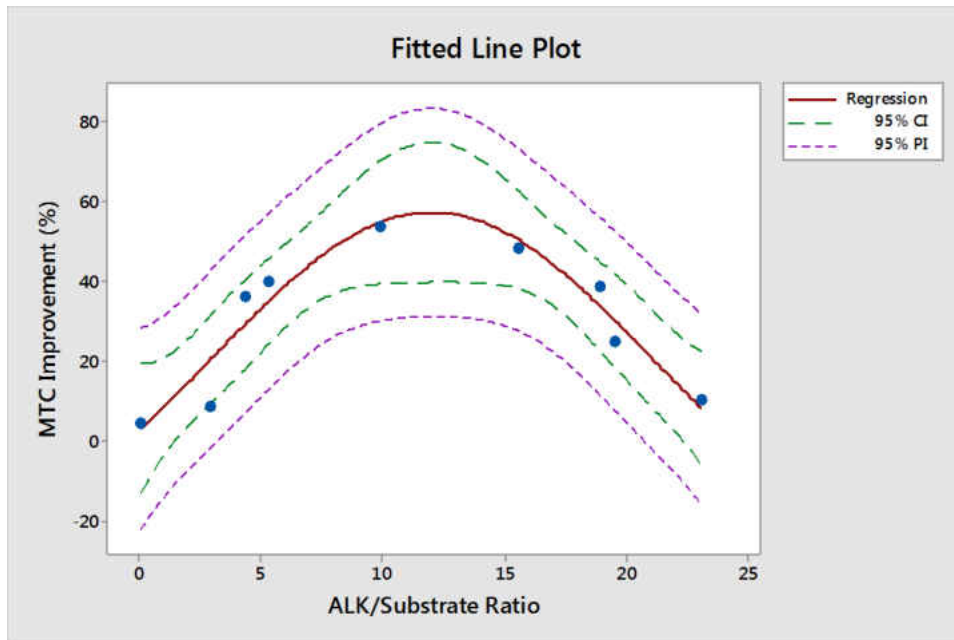
Figure H–3 Fitted Line Plot with Confidence and Prediction Intervals for Gaussian Model
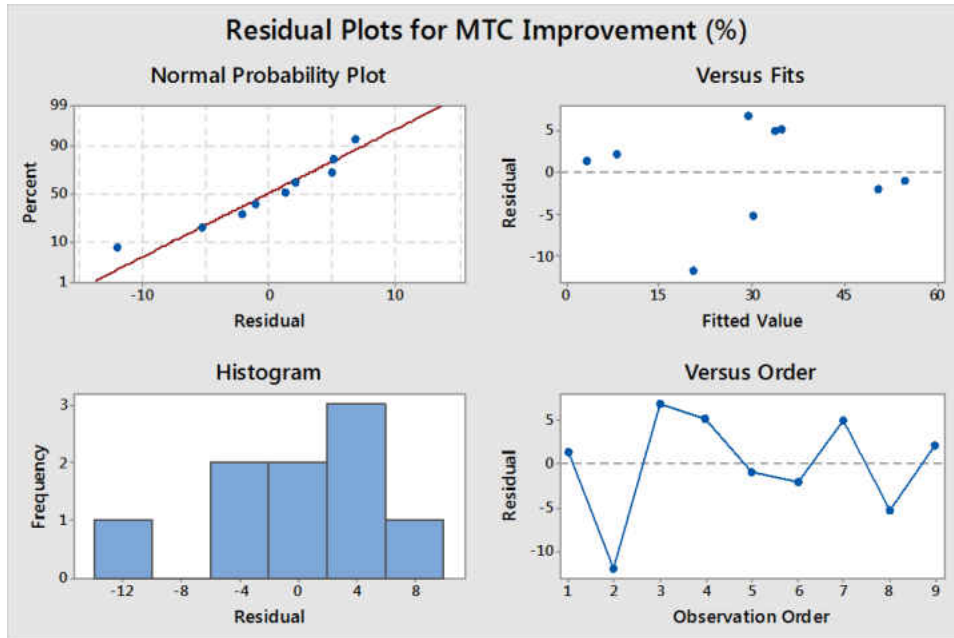
Figure H–4 Residual Plots for Gaussian Model

Nonlinear Regression: MTC Improvement (%) = Theta1 + (Theta2 - ...

```
* WARNING * Singular or nearly singular gradient matrix detected at iteration: 0.

Method

Algorithm        Gauss-Newton
Max iterations          200
Tolerance           0.00001

Starting Values for Parameters

Parameter  Value
Theta1         0
Theta2        55
Theta3         0
Theta4        12

Estimates at Each Iteration

Iteration      SSE     Theta1    Theta2      Theta3    Theta4
        0  8480.22     0.0000   55.0000   0.0000000   12.0000
        1   980.28     0.0000   55.0000   0.0073233   12.0000
        2   399.56   -35.6362   57.1759   0.0052219   12.0287
        3   280.51   -32.9267   57.3414   0.0063262   12.0381
        4   279.30   -36.8847   57.2293   0.0060238   12.0272
        5   279.25   -36.3116   57.2727   0.0060960   12.0301
        6   279.25   -36.4934   57.2620   0.0060790   12.0294
        7   279.25   -36.4535   57.2645   0.0060829   12.0296
        8   279.25   -36.4629   57.2639   0.0060820   12.0296
```

317

```
         9   279.25  -36.4607  57.2641  0.0060822  12.0296
        10   279.25  -36.4612  57.2640  0.0060822  12.0296
        11   279.25  -36.4611  57.2640  0.0060822  12.0296
```

Equation

MTC Improvement (%) = -36.4611 + (57.264 + 36.4611) * exp(-0.0060822 * ('ALK/Substrate
Ratio'
    - 12.0296) ^ 2)

Parameter Estimates

```
Parameter  Estimate  SE Estimate       95% CI
Theta1     -36.4611      72.7092  (       *, 52.1058)
Theta2      57.2640       6.8018  (41.2980, 75.2149)
Theta3       0.0061       0.0071  (-0.0131,  0.0266)
Theta4      12.0296       0.4607  (10.7780, 13.3702)
```

MTC Improvement (%) = Theta1 + (Theta2 - Theta1) * exp(-Theta3 * ('ALK/Substrate
Ratio' -
    Theta4) ^ 2)

Correlation Matrix for Parameter Estimates

```
          Theta1      Theta2      Theta3
Theta2  0.601767
Theta3  0.989384    0.685153
Theta4  0.043688   -0.028455   0.0232639
```

Lack of Fit

There are no replicates.
Minitab cannot do the lack of fit test based on pure error.

Summary

```
Iterations       11
Final SSE   279.253
DFE               5
MSE         55.8505
S           7.47332
```

Prediction

```
New  ALK/Substrate
Obs          Ratio      Fit   SE Fit           95% CI                 95% PI
  1         0.1350   3.1794  6.33974  (-13.1174, 19.4762)  (-22.0127, 28.3715)
  2         3.0000  20.6195  4.28999  (  9.5918, 31.6473)  ( -1.5314, 42.7705)
  3         4.4028  29.3360  4.33671  ( 18.1881, 40.4838)  (  7.1249, 51.5470)
  4         5.3400  34.9309  4.16049  ( 24.2360, 45.6258)  ( 12.9437, 56.9180)
  5         9.9600  54.8540  6.00782  ( 39.4104, 70.2975)  ( 30.2053, 79.5027)
  6        15.5659  50.3995  4.76589  ( 38.1483, 62.6506)  ( 27.6147, 73.1842)
  7        18.8976  33.8878  4.32800  ( 22.7623, 45.0133)  ( 11.6880, 56.0876)
  8        19.5000  30.2876  4.52207  ( 18.6633, 41.9120)  (  7.8337, 52.7416)
  9        23.0769   8.1539  5.54082  ( -6.0892, 22.3970)  (-15.7610, 32.0688)
```

Minitab® Output for Quadratic Equation Curve Fit
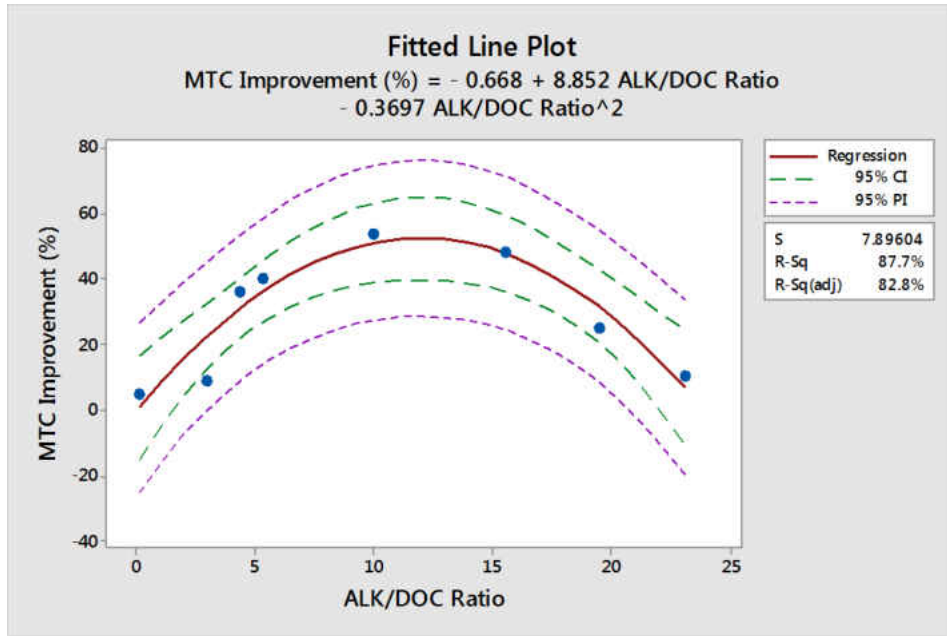
Figure H–5 Minitab® Quadratic Fitted Line Plot Excluding Wei et al., 2011 Reference
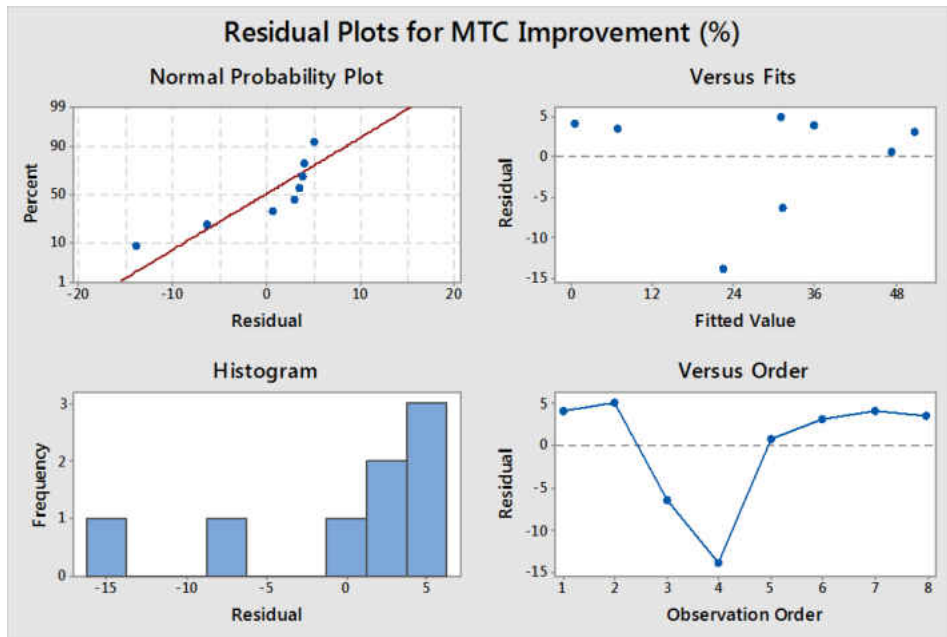
Figure H–6 Residual Plots for Quadratic Model Excluding Wei et al., 2011 Reference

Nonlinear Regression: MTC Improvement (%) = theta1 + ...

```
Method

Algorithm        Gauss-Newton
Max iterations          200
Tolerance           0.00001


Starting Values for Parameters

Parameter   Value
theta1          1
theta2          1
theta3          1


Estimates at Each Iteration

Iteration     SSE     theta1    theta2     theta3
        0  487429   1.00000   1.00000    1.00000
        1     312  -0.66839   8.85164   -0.36966
        2     312  -0.66839   8.85164   -0.36966


Equation

MTC Improvement (%) = -0.668392 + 8.85164 * 'ALK/DOC Ratio' - 0.369662 * 'ALK/DOC Ratio'
^ 2


Parameter Estimates

Parameter  Estimate  SE Estimate         95% CI
theta1     -0.66839      6.39625  (-17.1105, 15.7737)
theta2      8.85164      1.49431  (  5.0104, 12.6929)
theta3     -0.36966      0.06226  ( -0.5297, -0.2096)

MTC Improvement (%) = theta1 + theta2 * 'ALK/DOC Ratio' + theta3 * 'ALK/DOC Ratio' ^ 2


Correlation Matrix for Parameter Estimates

          theta1      theta2
theta2  -0.815414
theta3   0.701276  -0.971179


Lack of Fit

There are no replicates.
Minitab cannot do the lack of fit test based on pure error.


Summary

Iterations        2
Final SSE   311.737
```

```
DFE               5
MSE         62.3475
S           7.89604


Prediction

New  ALK/DOC
Obs    Ratio      Fit   SE Fit         95% CI                95% PI
  1   0.1350   0.5199  6.23363  (-15.5042, 16.5439)  (-25.3404, 26.3802)
  2   4.4028  31.1376  3.52556  ( 22.0749, 40.2004)  (  8.9089, 53.3664)
  3  19.5000  31.3748  4.35522  ( 20.1794, 42.5703)  (  8.1946, 54.5551)
  4   3.0000  22.5596  3.83511  ( 12.7011, 32.4181)  ( -0.0053, 45.1245)
  5  15.5659  47.5474  4.54573  ( 35.8622, 59.2326)  ( 24.1267, 70.9681)
  6   9.9600  50.8230  4.70947  ( 38.7169, 62.9290)  ( 27.1895, 74.4565)
  7   5.3400  36.0583  3.59322  ( 26.8216, 45.2949)  ( 13.7580, 58.3585)
  8  23.0769   6.7391  6.80622  (-10.7569, 24.2351)  (-20.0582, 33.5364)
```

Minitab® Output for Gaussian Distribution Curve Fit
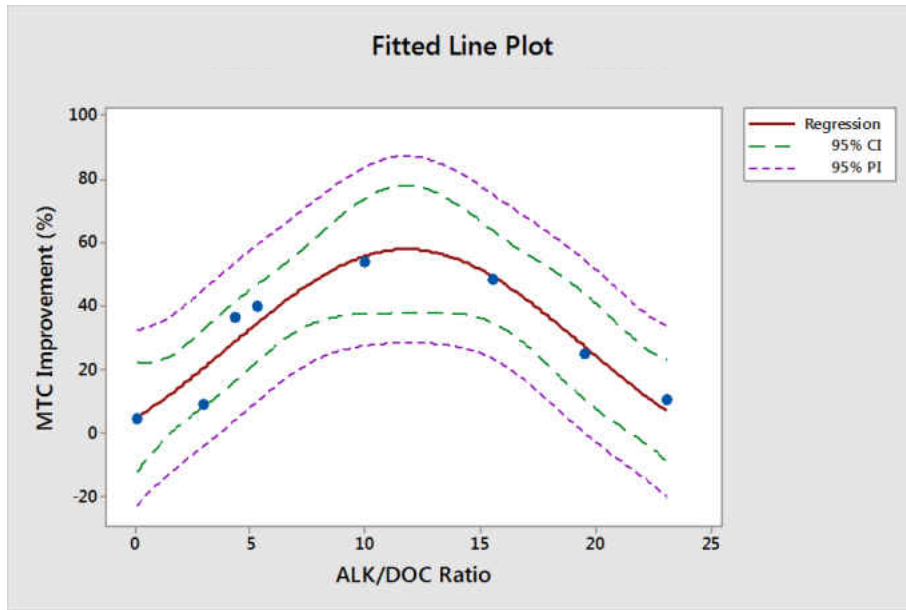
Figure H–7 Minitab® Gaussian Fitted Line Plot Excluding Wei et al., 2011 Reference
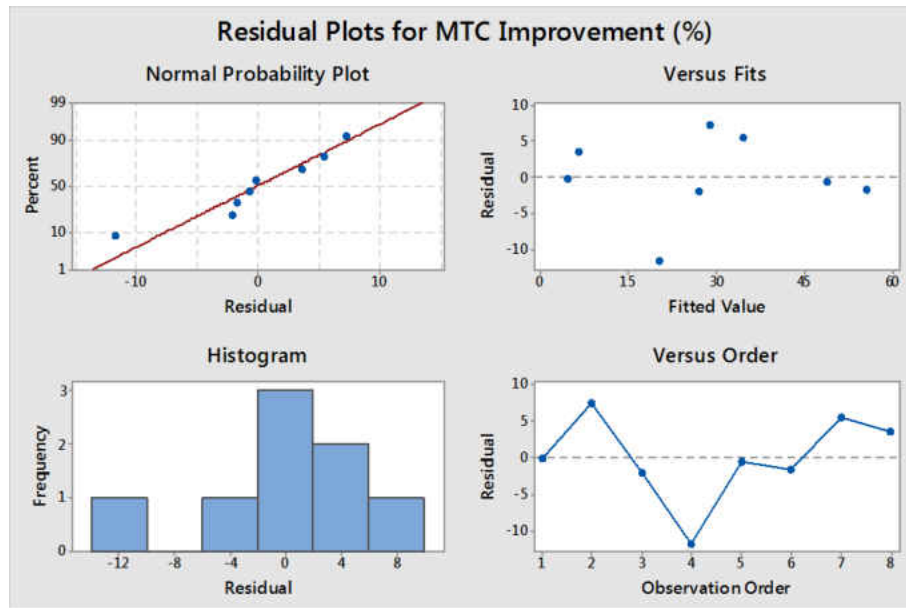
Figure H–8 Residual Plots for Gaussian Model Excluding Wei et al., 2011 Reference

Nonlinear Regression: MTC Improvement (%) = Theta1 + (Theta2 - ...

```
* WARNING * Singular or nearly singular gradient matrix detected at iteration: 0.


Method

Algorithm          Gauss-Newton
Max iterations            200
Tolerance             0.00001


Starting Values for Parameters

Parameter  Value
Theta1         0
Theta2        55
Theta3         0
Theta4        12


Estimates at Each Iteration

Iteration      SSE     Theta1    Theta2      Theta3     Theta4
        0  8220.66     0.0000   55.0000   0.0000000   12.0000
        1   999.93     0.0000   55.0000   0.0072594   12.0000
        2   244.61   -21.7323   57.4164   0.0084077   11.7437
        3   239.38   -17.9545   57.8878   0.0088073   11.8022
        4   239.30   -19.2989   57.7362   0.0085578   11.8003
        5   239.29   -19.1442   57.7605   0.0085943   11.8038
        6   239.29   -19.2297   57.7504   0.0085777   11.8034
```

322

```
 7    239.29   -19.2129   57.7525   0.0085809   11.8036
 8    239.29   -19.2189   57.7518   0.0085798   11.8036
 9    239.29   -19.2175   57.7520   0.0085800   11.8036
10    239.29   -19.2179   57.7519   0.0085800   11.8036
11    239.29   -19.2178   57.7519   0.0085800   11.8036
```

Equation

MTC Improvement (%) = -19.2178 + (57.7519 + 19.2178) * exp(-0.00857998 * ('ALK/DOC Ratio'
-
    11.8036) ^ 2)

Parameter Estimates

```
Parameter  Estimate  SE Estimate        95% CI
Theta1     -19.2178      41.8079  (        *, 47.6929)
Theta2      57.7519       7.2381  (39.2758, 78.6417)
Theta3       0.0086       0.0081  (-0.0151,  0.0374)
Theta4      11.8036       0.5462  (10.0065, 13.4888)
```

MTC Improvement (%) = Theta1 + (Theta2 - Theta1) * exp(-Theta3 * ('ALK/DOC Ratio' -
Theta4) ^
    2)

Correlation Matrix for Parameter Estimates

```
           Theta1      Theta2      Theta3
Theta2   0.544095
Theta3   0.980540    0.650960
Theta4  -0.148798   -0.054324   -0.175574
```

Lack of Fit

There are no replicates.
Minitab cannot do the lack of fit test based on pure error.

Summary

```
Iterations       11
Final SSE   239.292
DFE               4
MSE         59.8230
S           7.73453
```

Prediction

```
New   ALK/DOC
Obs    Ratio      Fit    SE Fit        95% CI                95% PI
  1   0.1350    4.7138   6.27447  (-12.7069, 22.1345)   (-22.9383, 32.3658)
  2   4.4028   28.8912   4.51828  ( 16.3464, 41.4359)   (  4.0210, 53.7613)
  3  19.5000   27.0838   6.02764  ( 10.3484, 43.8192)   ( -0.1417, 54.3093)
  4   3.0000   20.3667   4.38194  (  8.2005, 32.5329)   ( -4.3147, 45.0481)
  5  15.5659   48.9492   5.21149  ( 34.4798, 63.4186)   ( 23.0548, 74.8435)
  6   9.9600   55.5398   6.54138  ( 37.3780, 73.7016)   ( 27.4150, 83.6646)
  7   5.3400   34.5653   4.38213  ( 22.3986, 46.7320)   (  9.8836, 59.2469)
  8  23.0769    6.6499   5.90101  ( -9.7339, 23.0337)   (-20.3609, 33.6607)
```

APPENDIX I. GAC PILOT BREAKTHROUGH EVALUATION

This Appendix section presents the calculations and relevant assumptions utilized to estimate the GAC change-out frequency for a full-scale GAC contactor system. The full-scale GAC projections are based on the pilot-scale performance data. The pilot-scale data was utilized to determine the absorptive capacity of GAC media for the removal of DOC from the Olinda settled water.

<u>Determining the GAC Bed Life and Change-out Frequency</u>

The pilot and full scale GAC design parameters are summarized in Table I-1. The average inlet DOC concentration of 2.75 mg/L represents the average DOC level of the Olinda settled water. The GAC treatment objective was estimated at 1.4 mg/L DOC based on the pilot-scale observation that the downstream UF membrane process removes an additional 15 percent of the DOC. With the additional DOC removal, the Olinda filtered water DOC concentration at GAC breakthrough is estimated to be about 1.2 mg/L. This DOC level is expected to meet the DBP regulation requirements.

The GAC bed life and change-out frequency were estimated using the pilot information from Table I-1 and Equations 2-7 through 2-10. The procedure for projecting the GAC bed life and change-out frequency is enumerated in the following sample calculations.

Table I–1 Pilot and Full Scale GAC Design Parameters

Parameter	Pilot	Full-Scale per Vessel
Average inlet DOC (mg/L)	2.75	2.75
Treatment objective - TOC (mg/L)	1.4	1.4
Carbon Type	Evoqua's UltraCarb® 1240	Evoqua's UltraCarb® 1240
Carbon Density (g/L)[1]	495	495
Contactor Volume (cf)	16.76	1020[2]
Carbon Mass (g)	234881	14300000
Flow Rate (L/m)	33.0	Scenario 1: 1752[3] Scenario 2: 2366[4]
Carbon Usage Rate (g GAC/L treated)	0.118	0.118
Time to breakthrough t_{bk} (days)	42	Scenario 1: 48 Scenario 2: 36
Change-out frequency (times/year)	9	Scenario 1: 7 Scenario 2: 10

(1) The carbon density was estimated by averaging the 450 to 540 g/L density range provided by Evoqua Water Technologies.
(2) The contactor volume was selected based on the contactor size utilized for the conceptual opinion of probable capital cost calculations.
(3) Scenario 1 represents the average daily flow (2 MGD) condition.
(4) Scenario 2 represents the peak daily flow (2.6 MGD) condition.

1. The time-series plot of treated water DOC versus filtration run time (Figure I-1) reveals that

   the GAC pilot's time to breakthrough was 42 days.
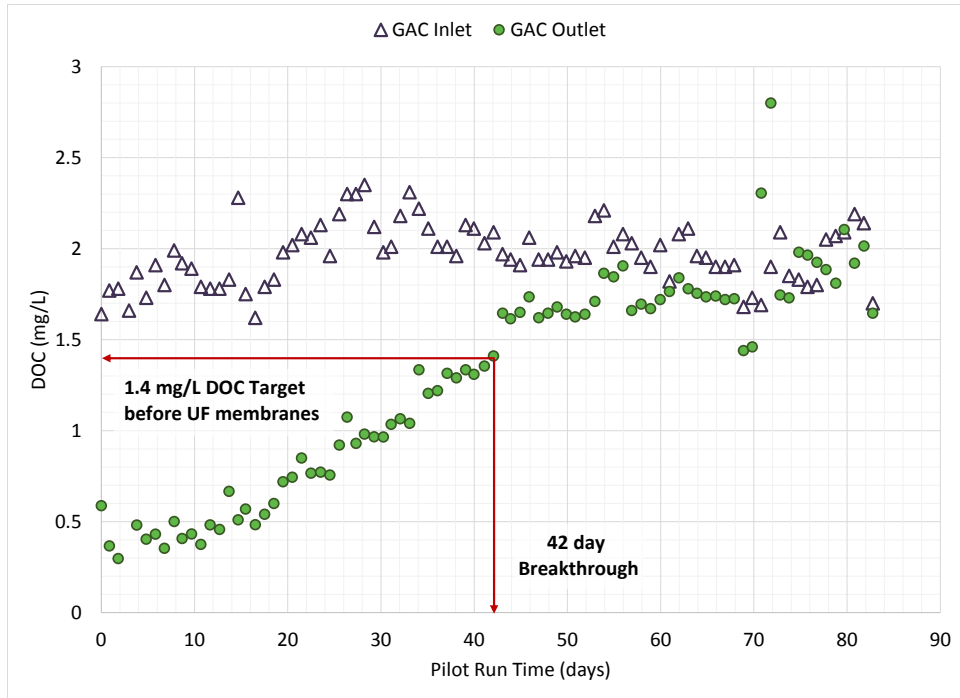
Figure I–1 Pilot-Scale Time to Breakthrough Graphical Analysis

2. Based on the pilot's time to breakthrough of 42 days, GAC mass of 234881 g, and treatment flow rate of 33.0 L/min; the carbon usage rate (CUR) is calculated according to:

$$CUR = \frac{M_{GAC}}{Q \times t_{bk}} = \frac{234881\ g}{33.0\frac{L}{min} \times 42\ day\ \times \frac{1440\ min}{day}} = 0.118\frac{g\ GAC}{L\ treated}$$

3. Using the full-scale design criteria (contactor volume) and estimated carbon density (495 g/L), the estimated mass of GAC for the full-scale plant is calculated as follows:

$$Estimated\ Full\ Scale\ M_{GAC} = 1020ft^3 \times 28.32\frac{L}{ft^3} \times 495\frac{g}{L} = 14.3 \times 10^6 g\ GAC$$

4. Applying the full-scale GAC mass, CUR, and alternative operating flow rates, the full-scale time to breakthrough is estimated according to:

(a) Scenario 1: $t_{bk} = \dfrac{M_{GAC}}{Q \times CUR} = \dfrac{14.3 \times 10^6 \, g \, GAC}{463 \frac{gal}{min} \times 3.785 \frac{L}{gal} \times \frac{1440 \, min}{day} \times 0.118 \frac{g \, GAC}{L}} = 48 \, days$

(b) Scenario 2: $t_{bk} = \dfrac{M_{GAC}}{Q \times CUR} = \dfrac{14.3 \times 10^6 \, g \, GAC}{625 \frac{gal}{min} \times 3.785 \frac{L}{gal} \times \frac{1440 \, min}{day} \times 0.118 \frac{g \, GAC}{L}} = 36 \, days$

5. Assuming there are 30 days in a month and 12 months in a year, the GAC change-out frequency is projected as:

(a) Scenario 1: $Change \, out \, frequency = \dfrac{30 \frac{days}{month} \times 12 \frac{months}{year}}{48 \, days} = 7 \, \dfrac{times}{year}$

(b) Scenario 2: $Change \, out \, frequency = \dfrac{30 \frac{days}{month} \times 12 \frac{months}{year}}{36 \, days} = 10 \, \dfrac{times}{year}$

APPENDIX J. ECONOMIC EVALUATION

This Appendix presents the calculations and assumptions utilized to determine the conceptual opinions of probable construction and operating cost for the Olinda water treatment alternatives. The conceptual opinions of probable construction and operational cost are intended to be used for comparison purposes only, as they do not represent design-based engineering estimates.

Common Economic Assumptions

Table J–1 Common Capital Cost Assumptions

Description	Value
Mobilization and Bonding	1.5%
Contractor Overhead	10%
Contingency	25%
Planning Period (n)	20 years
Interest Rate (i)	4.5%
Olinda Water Treatment Capacity (Peak)	2.7 MGD

Table J–2 Common Operating Cost Assumptions

Description	Value[1]
Contingency	25%
Olinda Water Treatment Capacity (Peak)	2.7 MDG
Electrical Cost	$0.40/kwh
Equipment Maintenance Materials[2]	2% of equipment cost per year
Trucking[2]	$22.5/ton
Tipping[2]	$96/ton
Caustic[2]	$5.32/gal
Aluminum Chlorohydrate (ACH)[3]	$6.45/gal
Chlorine[3]	$1.09/lb
Anhydrous Ammonia [3]	$3.49/lb
Citric Acid[3]	$17.83/gal
Sodium Hypochlorite[3]	$3.75/gal
Lime[3]	$0.70/lb

(1) Conceptual opinions of probable operating cost does not include the cost of labor.
(2) Data retrieved from Lekven, 2011.
(3) Costs provided by the County based on actual 2013 Olinda chemical costs.

Amortized Present Cost Calculation:

$$Amortized\ Capital\ (Cap.)\ Cost = Present\ Construction\ Cost \times \frac{(1+i)^n - 1}{i(1+i)^n}$$

$$Amortized\ Total\ Cost\ \frac{\$}{1000gal} = \frac{Operating\ Cost\ \frac{\$}{yr} + Amortized\ Cap.Cost\ \frac{\$}{yr}}{\frac{2700000 \times 365}{1000}\ \frac{gal}{yr}}$$

Update of Construction Costs:

$$CC_{current} = CC_{past} \times \frac{Current\ ENR\ Cost\ Index}{Past\ ENR\ Cost\ Index}$$

Status Quo

Table J–3 Status Quo Conceptual Opinions of Construction and Operating Costs

Estimated Capital Cost	
Total Estimated Capital	$0
Amortized Capital $/yr	$0
Estimated Operating Cost[1]	
Olinda Process Power	$191,000
Phase 6 Pumping Process Power[2]	$564,000
ACH	$49,000
Citric	$19,000
Bleach	$8,500
Lime	$12,000
Anhydrous Ammonia	$7,300
Chlorine	$9,200
Operation Subtotal	$860,000
Contingency (25%)	$215,000
Total Operating Costs	$1,080,000
Amortized Total Cost $/1000gal	**$1.10**

(1) The County provided UCF the Olinda process power and chemical costs incurred in 2013.
(2) Phase 6 pumping refers to a distribution system management condition, in which water is pumped from Lower Kula to Upper Kula. It was assumed that Upper Kula operates under Phase 6 pumping approximately 36 percent of the year. The sample cost calculation is presented in the following equation.

Phase 6 Pumping Process Power Cost:

$$Phase\ 6\ Cost\left(\frac{\$}{yr}\right) = 4pumps\ \frac{150hp}{pump}\ \frac{kw}{1.34102hp}\ \frac{8,760hr \times 0.36}{yr}\ \frac{\$0.40}{kwh} = \$564,000/yr$$

<u>MIEX® High Rate System</u>

Table J–4 MIEX® Economic Assumptions

Description	Value
MIEX® Equipment Cost Estimate[1]	$1,759,583
MIEX® Resin Cost[1]	$16.50/L
MIEX® Resin Use[1]	2.0 L/MG
Sodium Chloride Cost[2]	$0.17/lb
Salt Regeneration Use[1]	350 lb/MG
Salt Brine Residual Production[1]	400 gal/MG
Process Power Factor[1]	45 kwh/MG
Electrical Cost[3]	$0.40/kwh
Discharge of Brine to WWTF[4]	$0.081
Olinda WTP Operating Cost[5]	Cost savings related to discontinuing the ammonia feed, and reduction in ACH usage

(1) Cost estimate adjusted to 2.7 MGD design flow from Orica Watercare's County's 6.0 MGD MIEX® Treatment System Budgetary Proposal for the Pi'iholo WTP.
(2) Data retrieved from Lekven 2011.
(3) Conservative estimate; Rounded Lekven's $0.35/kwh estimate to $0.40/kwh
(4) Brine disposal costs were evaluated by assuming trucking and discharge to waste water treatment facility (WWTP) through a receiving tank with pump metering system.
(5) Assumed conversion to free chlorine. Assumed MIEX® pretreatment prior to coagulation reduces the ACH usage by half of current usage.

Table J–5 MIEX® Design Assumptions

Description	Value
MIEX® System	Atmospheric (gravity flow) configuration
Treatment Capacity	2.7 MGD
Regeneration Rate	1000 Bed Volumes
Resin Contactor Concentration	200 to 250 mL/L
Contact Time	4 – 8 minutes
Regenerant	Sodium chloride

Table J–6 MIEX® Conceptual Opinions of Construction and Operating Costs

Estimated Capital Cost	
MIEX® Equipment	$1,759,583
Replacement of frame and structural members with 316 SS	$126,894
Spare parts	$29,608
Concrete Basins	$200,000
Jib Crane & Hoist for MIEX® Loading	$31,000
Aluminum Cover	$90,000
Stairs	$8,000
Handrail	$4,050
Misc. Metals (weirs, wall pipes, etc.)	$8,333
TOC/DOC/Color Analyzer	$35,000
Furnishings	$60,000
MIEX® Chemical Feed Building	$150,000
Electrical	$145,000
Process Piping & Valves	$700,000
Instrumentation & SCADA System	$125,000
Brine Receiving Tank (Two-4,000 gal capacity Fiberglass tanks)	$32,600
Brine Metering Pumps	$2,600
Capital Subtotal	$3,510,000
Mobilization and Bonding	$52,650
Contractor Overhead and Profit	$351,000
Contingency (25%)	$980,000
Total Estimated Capital	$4,890,000
Amortized Capital $/yr	$375,924
Estimated Operating Cost	
Process Power – Olinda WTP[1]	$187,000
Process Power – Phase 6 Pumping[1]	$564,000
Chemical – Olinda WTP[1]	$73,000
Process Power – MIEX®	$20,000
Maintenance Materials	$70,000
Resin Replacement	$120,000
Salt	$60,000
Brine Trucking	$40,000
Brine Discharge to WWTF	$30,000
Operation Subtotal	$1,164,000
Contingency (25%)	$291,000
Total Operating Costs	$1,460,000
Amortized Total Cost $/1000gal	**$1.86**

(1) Olinda process power and chemical costs were estimated by subtracting the ammonia feed system costs from the provided 2013 Olinda cost data, and dividing the 2013 Olinda ACH cost by two.

GAC Contactor Columns

Table J–7 GAC Economic Assumptions

Description	Value
GAC Construction Cost Estimate[1]	$2,070,225
Initial GAC Cost[2]	$1.60/lb
GAC Process Power Factor[2]	78 kwh/MG
GAC Replacement[2]	$2.60/lb
Electrical Cost[3]	$0.40/kwh
Olinda WTP Operating Cost[4]	Cost savings related to discontinuing the ammonia feed

(1) Cost estimate retrieved from the County's 2013 Pi'iholo WTP GAC Bid Summary. No additional costs associated with mobilization, bonding, overhead, or profit were added to the construction cost estimate.
(2) Data retrieved from Lekven 2011.
(3) Conservative estimate; Rounded Lekven's $0.35/kwh estimate to $0.40/kwh
(4) Assumed conversion to free chlorine.

Table J–8 GAC Design Assumptions

Description	Value
Average Influent TOC	2.75 mg/L
TOC Treatment Objective	1.4 mg/L
Carbon Type	Evoqua's UltraCarb 1240®
Carbon Density	495 g/L
Carbon Usage Rate[1]	0.118 g GAC/L treated
Number of GAC Vessels	3
Mass of Carbon per Vessel	31,500 lbs
Design Flow Rate per Vessel	2366 L/min
EBCT per Vessel	12.25 min
GAC Change-out Frequency[1]	10 times/yr

(1) The carbon usage rate and GAC change-out frequency were determined according to pilot-scale DOC breakthrough evaluation, which is presented in Appendix I.

Table J–9: GAC Conceptual Opinions of Construction and Operating Costs

Estimated Capital Cost	
GAC Contactors (3-1020 ft^3 vessels)	$2,070,225
Initial GAC	$151,200
Capital Subtotal	$2,221,000
Contingency (25%)	$560,000
Total Estimated Capital	$2,780,000
Amortized Capital $/yr	$213,716
Estimated Operating Cost	
Process Power – Olinda WTP[1]	$187,000
Process Power – Phase 6 Pumping[1]	$564,000
Chemical – Olinda WTP[1]	$98,000
Process Power – GAC	$30,000
Carbon Replacement	$2,460,000
Operation Subtotal	$3,339,000
Contingency (25%)	$834,750
Total Operating Costs	$4,170,000
Amortized Total Cost $/1000gal	**$4.45**

(1) Olinda process power and chemical costs were estimated by subtracting the ammonia feed system costs from the provided 2013 Olinda cost data.

BAC Contactor Columns

The BAC pilot scale evaluation revealed that operating the GAC in biological mode was not effective in controlling the regulated DBP formation potential. Consequently, in order to effectively remove the DBP precursors, the BAC must be operated in the GAC adsorption mode. Based on the necessity of operating the BAC in adsorption mode, the conceptual opinions of probable capital and operating costs for the BAC are the same as for the GAC. The conceptual opinions of construction and operating costs are presented in Table J-9.

APPENDIX K. PERMISSION TO REPRODUCE MATERIALS

Permission to Use 3M Free and Total ATP Product Instructions

andreajc10

From:	tedewey@mmm.com
Sent:	Thursday, August 28, 2014 10:44 AM
To:	andreajc10
Cc:	cmschweitzer@mmm.com; mastump@mmm.com; vjkasanezky@mmm.com
Subject:	RE: Request for Use of Product Instructions

Andrea,

Great talking to you regarding the tailored collaboration project with the University of Central Florida and the county of Maui Department of Water Supply and the Water Research Foundation.

Thanks for reaching out to 3M for the approval of use for our instructions to be included in your research. We are aligned and approve the use of the 3M materials for your work.

We are updating the current agreement to align with this project. We will forward the updated agreement ASAP. Please review, sign and return at your earliest convenience

Best regards,
Tom Dewey

3M

Tom Dewey | Global Marketing Manager
3M Food Safety Department
3M Center, 275-5W-05 | St. Paul, MN 55144
Office: 651 733 3485 | Mobile: 612 730 9962 | Fax: 651 737 1994
tedewey@3M.com | www.3M.com | www.3M.com/Foodsafety

April 14, 2014

Andrea Cumming
Graduate Research Assistant
Department of Civil, Environmental and Construction Engineering
College of Engineering and Computer Science
University of Central Florida
Orlando, Florida
andreajc10@knights.ucf.edu

Permission to utilize Evoqua Water Technologies autopsy results from the Olinda WTP

Andrea:

This letter is to confirm permission to use the Evoqua Water Technologies autopsy results from the Maui DWS' Olinda WTP in your dissertation "Assessing Biofiltration Pretreatment For Ultrafiltration Membrane Processes" to be published by University of Central Florida along with the Tailored Collaboration (#4477) Research Report to be published by the Water Research Foundation.

Thank you for all of your contributions to assist Evoqua Water Technologies and our client, the County of Maui Department of Water Supply.

Congratulations on completing your dissertation and all your work towards the degree of Doctor of Philosophy!

Regards,

John Kutilek
Technical Sales Manager, MEMCOR Products
john.kutilek@evoqua.com

CC: Dr. Steven Duranceau, University of Central Florida
      Don Moore
      Aaron Balczewski

558 Clark Road
Tewksbury, MA 01876 USA

www.evoqua.com

andreajc10

From:	Dave Walker <dwalker@avistatech.com>
Sent:	Tuesday, April 14, 2015 12:47 PM
To:	andreajc10
Cc:	'Doug Eisberg'; 'Sara Pietsch'; 'Karen Lindsey'; Steven.Duranceau@ucf.edu
Subject:	RE: Request for Use of Avista Autopsy Results from the Maui-UCF Study

Andrea,

Thank you for making the effort to acknowledge Avista in your dissertation. We are pleased to give you permission to use the images in your dissertation from our work order WO#010914-14.

I realize that the copy you sent over for our review is a draft but I wanted to take this opportunity to point out that on a few of the pages under the images the acknowledgement to Avista was missing. I am sure you would have caught this in your final edit.

Good luck with the completion of your dissertation and I look forward to the possibility of you one day working full time in the water treatment industry. If there is anything more we can do personally or professionally please let us know.

Best Regards,

Dave Walker
President
_____

Avista Technologies, Inc.
140 Bosstick Boulevard
San Marcos, California 92069
_____

Tel. | +1.760.744.0536
Fax. | +1.760.744.0619
dwalker@avistatech.com
www.avistatech.com

Avista
TECHNOLOGIES   *Creative Chemistry, Smart Solutions.*

A trusted expert in membrane system chemistry and global process support.
• REVERSE OSMOSIS • MICRO/ULTRA FILTRATION • MULTIMEDIA FILTRATION

The contents of this email and/or its attachments may contain confidential or proprietary information of Avista Technologies, Inc., and are intended solely for the use of the individual to whom it is addressed. Any views or opinions expressed herein are solely those of the author and do not necessarily represent those of Avista. AVISTA is a registered trademark of Avista Technologies, Inc. Information regarding additional trademarks and intellectual property held by the corporation can be found at: http://www.avistatech.com/disclaimer.htm.

From: Sara Pietsch [mailto:spietsch@avistatech.com]
Sent: Tuesday, April 14, 2015 8:36 AM
To: 'Doug Eisberg'; 'Karen Lindsey'; 'Dave Walker'
Subject: FW: Request for Use of Avista Autopsy Results from the Maui-UCF Study
Importance: High

Doug,

Steven Duranceau called me yesterday and asked if we could give them permission to use the images from the autopsy we did for them in his student's dissertation. They need an email or some sort of document stating that we give them permission to use the images. Please look over the request below and let me know how you would like me to respond.

Sara

From: andreajc10 [mailto:andreajc10@knights.ucf.edu]
Sent: Tuesday, April 14, 2015 5:48 AM
To: Sara Pietsch
Cc: deisberg@avistatech.com; klindsey@avistatech.com; Steven Duranceau
Subject: Request for Use of Avista Autopsy Results from the Maui-UCF Study

Good Morning Sara,

Thank you for taking the time to speak with Dr. Duranceau and I yesterday about obtaining permission to use the Avista autopsy results from the Maui-UCF Study (WO#010914-14).

As discussed, the purpose of this email is to request permission for use of the Avista autopsy results in my dissertation to be published by UCF and our Tailored Collaboration (#4477) research report to be published by the Water Research Foundation. I have attached the information that will be included in the dissertation and Tailored Collaboration reports. Please let me know if you require additional information. Your time and assistance are greatly appreciated.

Thank you,

Andrea Cumming, E.I.
Graduate Research Assistant
University of Central Florida

REFERENCES

3M. (2012). *AQT200 water plus-total ATP product instructions.* (No. 34-8710-6650-1). St. Paul, MN: 3M.

3M. (2013). *AQF100 water-free ATP product instructions.* (No. 34-8710-2415-3). St. Paul, MN: 3M.

Alspach, B., Adham, S., Cooke, T., Delphos, P., Garcia-Aleman, J., Jacangelo, J., . . . Sethi, S. (2005). *Microfiltration and ultrafiltration membranes for drinking water (M53)*. Denver, CO: American Water Works Association.

Alspach, B., Adham, S., Cooke, T., Delphos, P., Garcia-Aleman, J., Jacangelo, J., . . . Sethi, S. (2008). Microfiltration and ultrafiltration membranes for drinking water. *Journal / American Water Works Association, 100*(12), 84-97.

Amirtharajah, A. (1991). *Optimum backwash of dual media filters and GAC filter-adsorbers with air scour*. Denver, CO: AWWA Research Foundation.

APHA, AWWA, & WEF. (2005). *Standard methods for the examination of water & wastewater*. Washington D.C.: American Public Health Association.

Archer, A. D., & Singer, P. C. (2006). Effect of SUVA and enhanced coagulation on removal of TOX precursors. *Journal / American Water Works Association, 98*(8), 97-107.

Avista Technologies. (2015). A new approach to membrane separations. Retrieved from http://www.avistatech.com/cei.htm

Badawy, M. I., Gad-Allah, T., Ali, M. E. M., & Yoon, Y. (2012). Minimization of the formation of disinfection by-products. *Chemosphere, 89*(3), 235-240. doi:10.1016/j.chemosphere.2012.04.025

Basu, O., & Huck, P. (2004). Integrated biofilter-immersed membrane system for the treatment of humic waters. *Water Research, 38*(3), 655-662.

Basu, O., & Huck, P. (2005). Impact of support media in an integrated biofilter–submerged membrane system. *Water Research, 39*(17), 4220-4228.

Bouwer, E. J., & Crowe, P. B. (1988). Biological processes in drinking water treatment. *Journal / American Water Works Association, 80*(9), 82-93.

Boyd, C. C., Duranceau, S. J., & Tharamapalan, J. (2012). Impact of carboxylic acid ultrafiltration recycle streams on coagulation. *Journal of Water Supply: Research and Technology— AQUA, 61*(5), 306-318.

Boyd, C. C. (2013). *Assessment, optimization, and enhancement of ultrafiltration (UF) membrane processes in potable water treatment. [electronic resource]* Orlando, Fla. : University of Central Florida, 2013. Retrieved from https://login.ezproxy.net.ucf.edu/login?auth=shibb&url=http://search.ebscohost.com/login.aspx?direct=true&db=cat00846a&AN=ucfl.032665518&site=eds-live&scope=site; http://purl.fcla.edu/fcla/etd/CFE0005088

Boyer, T. H., & Singer, P. C. (2006). A pilot-scale evaluation of magnetic ion exchange treatment for removal of natural organic material and inorganic anions. *Water Research, 40*(15), 2865-2876.

Boyer, T. H., & Singer, P. C. (2005). Bench-scale testing of a magnetic ion exchange resin for removal of disinfection by-product precursors. *Water Research, 39*(7), 1265-1276. doi:10.1016/j.watres.2005.01.002

Bridgeman, J., Bieroza, M., & Baker, A. (2011). The application of fluorescence spectroscopy to organic matter characterisation in drinking water treatment. *Reviews in Environmental Science and Bio/Technology, 10*(3), 277-290.

Brown, J. C., & Lauderdale, C. V. (2006). Efficient, simultaneous destruction of multiple drinking water contaminants using biological filtration. *Florida Water Resources Journal, November*, 28-30.

Budd, G. C., Hess, A. F., Shorney-Darby, H., Neemann, J. J., Spencer, C. M., Bellamy, J. D., & Hargette, P. H. (2004). Coagulation applications for new treatment goals. *Journal / American Water Works Association, 96*(2), 102-113.

Chaudhary, D. S., Vigneswaran, S., Ngo, H., Shim, W. G., & Moon, H. (2003). Biofilter in water and wastewater treatment. *Korean Journal of Chemical Engineering, 20*(6), 1054-1065.

Chen, W., Westerhoff, P., Leenheer, J. A., & Booksh, K. (2003). Fluorescence excitation-emission matrix regional integration to quantify spectra for dissolved organic matter. *Environmental Science & Technology, 37*(24), 5701-5710.

Chen, Y., Dong, B., Gao, N., & Fan, J. (2007). Effect of coagulation pretreatment on fouling of an ultrafiltration membrane. *Desalination, 204*(1), 181-188.

Chowdhury, S., Champagne, P., & McLellan, P. J. (2009). Models for predicting disinfection byproduct (DBP) formation in drinking waters: A chronological review. *Science of the Total Environment, 407*(14), 4189-4206.

City of St. Cloud Environmental Utilities Department. (September 16, 2011). *9.0 MGD MIEX plant site visit*

County of Maui Department of Water Supply. (2012). *Bid summary for Pi'iholo Water Treatment Plant organic carbon reduction project.* (No. DWS JOB NO. 08-02). Wailuku: County of Maui.

County of Maui Department of Water Supply. (2013). *2013 Olinda WTP electrical and chemical cost data*. Wailuku: County of Maui.

Davis, W., Macler, B., Pollock, B., & Waite, A. (2008). *Upcountry Maui drinking water treatment and distribution system optimization study.* (Final). Maui, HI: US Environmental Protection Agency.

Dixon, M., Morran, J., & Drikas, M. (2010). Extending membrane longevity by using MIEX as a pre-treatment. *Journal of Water Supply: Research and Technology—AQUA, 59*(2-3), 92-99.

Dong, B., Chen, Y., Gao, N., & Fan, J. (2007). Effect of coagulation pretreatment on the fouling of ultrafiltration membrane. *Journal of Environmental Sciences, 19*(3), 278-283.

Duranceau, S. J., & Taylor, J. S. (2011). Chapter 11: Membranes. In J. K. Edzwald (Ed.), *Water quality and treatment: A handbook on drinking water* (Sixth ed., pp. 11.1) McGraw-Hill.

Duranceau, S. J., & Tharamapalan, J. (2013). Optimizing a Community's fresh and brackish water supplies with an aeration, ion-exchange, and reverse osmosis treatment portfolio. *Florida Water Resources Journal, September*, 24.

Emelko, M. B., Huck, P. M., Coffey, B. M., & Smith, E. F. (2006). Effects of media, backwash, and temperature on full-scale biological filtration. *Journal / American Water Works Association, 98*(12), 61-73.

Evans, P. J., Smith, J. L., LeChevallier, M. W., Schneider, O. D., Weinrich, L. A., & Jjemba, P. K. (2013). *Biological filtration monitoring and control toolbox: Guidance manual*. Denver, CO: Water Research Foundation.

Farley, C. G., Gentzler, R., & Flythe, C. W. (2012). What happens when chloramines and chlorine meet? *Opflow, 38*(3), 22-26.

Gao, W., Liang, H., Ma, J., Han, M., Chen, Z., Han, Z., & Li, G. (2011). Membrane fouling control in ultrafiltration technology for drinking water production: A review. *Desalination, 272*(1), 1-8.

Garrett, R. G. (2000). Natural sources of metals to the environment. *Human and Ecological Risk Assessment, 6*(6), 945-963.

Geesey, G. G., Wigglesworth-Cooksey, B., & Cooksey, K. (2000). Influence of calcium and other cations on surface adhesion of bacteria and diatoms: A review. *Biofouling, 15*(1-3), 195-205.

Geismar, N., Bérubé, P. R., & Barbeau, B. (2012). Variability and limits of the unified membrane fouling index: Application to the reduction of low-pressure membrane fouling by ozonation and biofiltration. *Desalination and Water Treatment, 43*(1-3), 91-101.

Goldgrabe, J. C., Summers, R. S., & Miltner, R. J. (1993). Particle removal and head loss development in biological filters. *Journal / American Water Works Association, 85*(12), 94-106.

Graham, N. J. (1999). Removal of humic substances by oxidation/biofiltration processes—a review. *Water Science and Technology, 40*(9), 141-148.

Granger, H. C., Stoddart, A. K., & Gagnon, G. A. (2014). Direct biofiltration for manganese removal from surface water. *Journal of Environmental Engineering, 140*(4) doi:http://dx.doi.org/10.1061/(ASCE)EE.1943-7870.0000819

Halle, C., Huck, P. M., Peldszus, S., Haberkamp, J., & Jekel, M. (2009). Assessing the performance of biological filtration as pretreatment to low pressure membranes for drinking water. *Environmental Science & Technology, 43*(10), 3878-3884.

Hammes, F., Goldschmidt, F., Vital, M., Wang, Y., & Egli, T. (2010). Measurement and interpretation of microbial adenosine tri-phosphate (ATP) in aquatic environments. *Water Research, 44*(13), 3915-3923.

Howe, K. J., & Clark, M. M. (2002). Fouling of microfiltration and ultrafiltration membranes by natural waters. *Environmental Science & Technology, 36*(16), 3571-3576.

Hozalski, R. M., Goel, S., & Bouwer, E. J. (1995). TOC removal in biological filters. *Journal / American Water Works Association, 87*(12), 40-54.

Hu, J., Song, L., Ong, S., Phua, E., & Ng, W. (2005). Biofiltration pretreatment for reverse osmosis (RO) membrane in a water reclamation system. *Chemosphere, 59*(1), 127-133.

Huang, G., Meng, F., Zheng, X., Wang, Y., Wang, Z., Liu, H., & Jekel, M. (2011). Biodegradation behavior of natural organic matter (NOM) in a biological aerated filter (BAF) as a pretreatment for ultrafiltration (UF) of river water. *Applied Microbiology and Biotechnology, 90*(5), 1795-1803.

Huang, H., Cho, H., Schwab, K. J., & Jacangelo, J. G. (2012). Effects of magnetic ion exchange pretreatment on low pressure membrane filtration of natural surface water. *Water Research, 46*(17), 5483-5490.

Huang, H., Lee, N., Young, T., Gary, A., Lozier, J. C., & Jacangelo, J. G. (2007). Natural organic matter fouling of low-pressure, hollow-fiber membranes: Effects of NOM source and hydrodynamic conditions. *Water Research, 41*(17), 3823-3832.

Huang, H., Schwab, K., & Jacangelo, J. G. (2009). Pretreatment for low pressure membranes in water treatment: A review. *Environmental Science & Technology, 43*(9), 3011-3019.

Huber, S. A., Balz, A., Abert, M., & Pronk, W. (2011). Characterisation of aquatic humic and non-humic matter with size-exclusion chromatography–organic carbon detection–organic nitrogen detection (LC-OCD-OND). *Water Research, 45*(2), 879-885.

Huck, P., & Sozanski, M. (2008). Biological filtration for membrane pre-treatment and other applications: Towards the development of a practically-oriented performance parameter. *Journal of Water Supply: Research and Technology—AQUA, 57*(4), 203-224.

Huck, P. M., Coffey, B. M., Amirtharajah, A., & Bouwer, E. J. (2000). *Optimizing filtration in biological filters*. Denver, CO: AWWA Research Foundation and American Water Works Association.

Huck, P., Peldszus, S., Halle, C., Ruiz, H., Jin, X., Van Dyke, M., . . . Mosqueda-Jimenez, D. (2011). Pilot scale evaluation of biofiltration as an innovative pre-treatment for ultrafiltration membranes for drinking water treatment. *Water Science & Technology: Water Supply, 11*(1), 23-29.

Hudson, N., Baker, A., & Reynolds, D. (2007). Fluorescence analysis of dissolved organic matter in natural, waste and polluted waters—a review. *River Research and Applications, 23*(6), 631-649.

Humbert, H., Gallard, H., Jacquemet, V., & Croué, J. (2007). Combination of coagulation and ion exchange for the reduction of UF fouling properties of a high DOC content surface water. *Water Research, 41*(17), 3803-3811.

IEEE. (2015). Notice of retraction: Pilot study on hybrid biological filter-coagulation-submerged ultrafiltration membrane for drinking water treatment. Retrieved from http://ieeexplore.ieee.org/xpls/abs_all.jsp?arnumber=5780966

Jarvis, P., Mergen, M., Banks, J., McIntosh, B., Parsons, S. A., & Jefferson, B. (2008). Pilot scale comparison of enhanced coagulation with magnetic resin plus coagulation systems. *Environmental Science & Technology, 42*(4), 1276-1282.

Jensen, J. N. (2003). *A problem-solving approach to aquatic chemistry*. Hoboken, NJ: John Wiley & Sons, Inc.

Jiang, T., Kennedy, M. D., De Schepper, V., Nam, S., Nopens, I., Vanrolleghem, P. A., & Amy, G. (2010). Characterization of soluble microbial products and their fouling impacts in membrane bioreactors. *Environmental Science and Technology, 44*(17), 6642-6648.

Kristiana, I., Joll, C., & Heitz, A. (2011). Powdered activated carbon coupled with enhanced coagulation for natural organic matter removal and disinfection by-product control: Application in a western australian water treatment plant. *Chemosphere, 83*(5), 661-667.

Lattner, D., Flemming, H., & Mayer, C. (2003). 13 C-NMR study of the interaction of bacterial alginate with bivalent cations. *International Journal of Biological Macromolecules, 33*(1), 81-88.

Lauderdale, C. V., Brown, J. C., Chadik, P., & Kirisits, M. J. (2011). *Engineered biofiltration for enhanced hydraulic and water treatment performance.* (Final Report No. TC #4215). Denver, CO: Water Research Foundation.

Lauderdale, C. V., Scheitlin, K., Nyfennegger, J., Upadhyaya, G., Brown, J. C., Raskin, L., . . . Pinto, A. (2014). *Optimizing engineered biofiltration.* (Final Report No. TC #4346). Denver, CO: Water Research Foundation.

Lauderdale, C., Chadik, P., Kirisits, M. J., & Brown, J. (2012). Engineered biofiltration: Enhanced biofilter performance through nutrient and peroxide addition. *Journal / American Water Works Association, 104*(5), E298-E309. doi:http://dx.doi.org/10.5942/jawwa.2012.104.0073

Laurent, P., Prévost, M., Cigana, J., Niquette, P., & Servais, P. (1999). Biodegradable organic matter removal in biological filters: Evaluation of the CHABROL model. *Water Research, 33*(6), 1387-1398.

LeChevallier, M. W., Becker, W., Schorr, P., & Lee, R. (1992). AOC reduction by biologically active filtration. *Revue Des Sciences De l'Eau/Journal of Water Science, 5*, 113-142.

LeChevallier, M. W., Schulz, W., & Lee, R. G. (1991). Bacterial nutrients in drinking water. *Applied and Environmental Microbiology, 57*(3), 857-862.

Lekven, C. C. (2011). *Organic carbon reduction study for the County of Maui Department of Water Supply.* (No. Final). Maui, HI: Brown and Caldwell.

Letterman, R. D., & Yiacoumi, S. (2011). Chapter 8 coagulation and flocculation. In J. K. Edzwald (Ed.), *Water quality & treatment: A handbook on drinking water* (Sixth ed., pp. 8.1). New York: McGraw Hill.

Liang, L., & Singer, P. C. (2003). Factors influencing the formation and relative distribution of haloacetic acids and trihalomethanes in drinking water. *Environmental Science and Technology, 37*(13), 2920-2928.

Lion, L. W., Shuler, M. L., Hsieh, K. M., Ghiorse, W. C., & Corpe, W. A. (1988). Trace metal interactions with microbial biofilms in natural and engineered systems. *Critical Reviews in Environmental Science and Technology, 17*(4), 273-306.

Lipp, P., Baldauf, G., Schick, R., Elsenhans, K., & Stabel, H. (1998). Integration of ultrafiltration to conventional drinking water treatment for a better particle removal—efficiency and costs? *Desalination, 119*(1), 133-142.

Liu, C., Chen, W., Robert, V., & Han, Z. (2011). Removal of algogenic organic matter by magnetic ion exchange resin pre-treatment and its effect on fouling in ultrafiltration. *Water Science & Technology: Water Supply, 11*(1), 15-22.

Liu, X., Huck, P. M., & Slawson, R. M. (2001). Factors affecting drinking water biofiltration. *Journal / American Water Works Association, 93*(12), 16-90. Retrieved from http://search.proquest.com/docview/221603227?accountid=10003

Lovins III, W. A., Duranceau, S. J., Gonzalez, R. M., & Taylor, J. S. (2003). Optimized coagulation assessment for a highly organic surface water supply. *Journal / American Water Works Association, 95*(10), 94-108.

Lozier, J., Cappucci, L., Amy, G., Lee, N., Jacangelo, J., Huang, H., . . . Heijmann, B. (2008). *Natural organic matter fouling of low-pressure membrane systems*. Denver, CO: AWWA Research Foundation.

Mac Berthouex, P., & Brown, L. C. (2002). *Statistics for environmental engineers* (2nd ed.). Boca Raton, FL: CRC Press LLC.

Markarian, A., Carriere, A., Dallaire, P., Servais, P., & Barbeau, B. (2010). Hybrid membrane process: Performance evaluation of biological PAC. *Journal of Water Supply: Research and Technology—AQUA, 59*(4), 209.

Matilainen, A., Vepsalainen, M., & Sillanpaa, M. (2010). Natural organic matter removal by coagulation during drinking water treatment: A review. *Advances in Colloid and Interface Science, 159*(2), 189-197. doi:10.1016/j.cis.2010.06.007

Metcalf & Eddy. (2003). *Wastewater engineering : Treatment and reuse* (4th ed; revised by George Tchobanoglous, Franklin L. Burton, H. David Stensel). Boston, MA: McGraw-Hill.

Miltner, R. J., Summers, R. S., & Wang, J. Z. (1995). Biofiltration performance: Part 2, effect of backwashing. *Journal / American Water Works Association, 87*(12), 64-70.

Miltner, R. J., Shukairy, H. M., & Summers, R. S. (1992). Disinfection by-product formation and control by ozonation and biotreatment. *Journal / American Water Works Association, 84*(11), 53-62.

Minitab. (2010). *Minitab 17 statistical software*. State College, PA: Minitab, Inc.

Moll, D. M., & Summers, R. S. (1999). Assessment of drinking water filter microbial communities using taxonomic and metabolic profiles. *Water Science and Technology, 39*(7), 83-89.

Mosqueda-Jimenez, D. B., & Huck, P. M. (2009). Effect of biofiltration as pretreatment on the fouling of nanofiltration membranes. *Desalination, 245*(1), 60-72.

Mosqueda-Jimenez, D., & Huck, P. (2006). Fouling analysis of ultrafiltration and nanofiltration membranes. *Water Practice & Technology, 1*(04)

MWH. (2005). *Water treatment : Principles and design* (2nd ed. ed.). Hoboken, N.J: J. Wiley.

Naidu, G., Jeong, S., Vigneswaran, S., & Rice, S. A. (2013). Microbial activity in biofilter used as a pretreatment for seawater desalination. *Desalination, 309,* 254-260.

Nguyen, T., Roddick, F. A., & Fan, L. (2012). Biofouling of water treatment membranes: A review of the underlying causes, monitoring techniques and control measures. *Membranes, 2*(4), 804-840.

Niquette, P., Prevost, M., Maclean, R. G., Thibault, D., Coallier, J., Desjardins, R., & Lafrance, P. (1998). Backwashing first-stage sand-BAC filters. *Journal / American Water Works Association, 90*(1), 86-97.

Novak, J. T., Love, N. G., Smith, M. L., & Wheeler, E. R. (1998). The effect of cationic salt addition on the settling and dewatering properties of an industrial activated sludge. *Water Environment Research, 70*(5), 984-996.

Orica Watercare Inc. (2011). *Pi'iholo water treatment plant 6.0 MGD MIEX® Treatment system budgetary proposal.* (No. MR-2010-015).Orica Watecare, Inc.

Ostrowski, S. (2011). *Protocol to evaluate the MIEX process for DOC removal at the Lower Kula (Pi'iholo) Water Treatment Plant.* (No. TP-2011-06).Orica Watercare, Inc.

Palm Beach County Water Utilities Department. (March 27, 2014). *Water treatment plant 2 MIEX facility (16.4 MGD) site visit*

Peiris, R. H., Budman, H., Moresoli, C., & Legge, R. L. (2010). Understanding fouling behaviour of ultrafiltration membrane processes and natural water using principal component analysis of fluorescence excitation-emission matrices. *Journal of Membrane Science, 357*(1), 62-72.

Peldszus, S., Benecke, J., Jekel, M., & Huck, P. M. (2012). Direct biofiltration pretreatment for fouling control of ultrafiltration membranes. *Journal / American Water Works Association, 104*(7), 45.

Pernitsky, D., & Edzwald, J. (2003). Solubility of polyaluminium coagulants. *Journal of Water Supply: Research and Technology—AQUA, 52,* 395-406.

Persson, F., Heinicke, G., Uhl, W., Hedberg, T., & Hermansson, M. (2006). Performance of direct biofiltration of surface water for reduction of biodegradable organic matter and biofilm formation potential. *Environmental Technology, 27*(9), 1037-1045.

Reckhow, D. A., & Singer, P. C. (2011). Chapter 19: Formation and control of disinfection by-products. In J. K. Edzwald (Ed.), *Water quality and treatment: A handbook on drinking water* (Sixth ed., pp. 19.1) McGraw-Hill.

Regional Municipality of Peel. (2014). *Water quality report: Brampton, Mississauga and South Caledon.* (No. Final). Brampton, ON: Region of Peel.

Reiling, S. J., Roberson, J. A., & Cromwell, J. E. (2009). Drinking water regulations: Estimated cumulative energy use and costs. *Journal / American Water Works Association, 101*(3), 42-53.

Ren, X., Shon, H., Jang, N., Lee, Y. G., Bae, M., Lee, J., . . . Kim, I. S. (2010). Novel membrane bioreactor (MBR) coupled with a nonwoven fabric filter for household wastewater treatment. *Water Research, 44*(3), 751-760.

Rittmann, B. E., & McCarty, P. L. (2001). *Environmental biotechnology: Principles and applications*. New York, NY: McGraw-Hill.

Rittmann, B. E., & Snoeyink, V. L. (1984). Achieving biologically stable drinking water. *Journal / American Water Works Association, 76*(10), 106-114.

Rittmann, B. E., & McCarty, P. L. (1980). Model of steady-state-biofilm kinetics. *Biotechnology and Bioengineering, 22*(11), 2343-2357.

Rittmann, B. E., Stilwell, D., Garside, J. C., Amy, G. L., Spangenberg, C., Kalinsky, A., & Akiyoshi, E. (2002). Treatment of a colored groundwater by ozone-biofiltration: Pilot studies and modeling interpretation. *Water Research, 36*(13), 3387-3397.

Saez, P. B., & Rittmann, B. E. (1992). Accurate pseudoanalytical solution for steady-state biofilms. *Biotechnology and Bioengineering, 39*(7), 790-793.

Sáez, P. B., & Rittmann, B. E. (1988). Improved pseudoanalytical solution for steady-state biofilm kinetics. *Biotechnology and Bioengineering, 32*(3), 379-385.

Sawyer, C. N., McCarty, P. L., & Parkin, G. F. (2003). *Chemistry for environmental engineering and science* (Fifth ed.). New York: McGraw-Hill.

Sharma, J. R., Najafi, M., & Qasim, S. R. (2013). Preliminary cost estimation models for construction, operation, and maintenance of water treatment plants. *Journal of Infrastructure Systems, 19*(4), 451-464.

Shimadzu Corporation. (1994). *Instruction manual for RF-1501 shimadzu spectrofluorophotometer.* (No. P/N 206-62901). Columbia, MD: Shimadzu Corporation.

Shon, H., Vigneswaran, S., Aim, R. B., Ngo, H., Kim, I. S., & Cho, J. (2005). Influence of flocculation and adsorption as pretreatment on the fouling of ultrafiltration and nanofiltration membranes: Application with biologically treated sewage effluent. *Environmental Science & Technology, 39*(10), 3864-3871.

Simpson, D. R. (2008). Biofilm processes in biologically active carbon water purification. *Water Research, 42*(12), 2839-2848.

Singer, P. C., & Bilyk, K. (2002). Enhanced coagulation using a magnetic ion exchange resin. *Water Research, 36*(16), 4009-4022. doi:10.1016/S0043-1354(02)00115-X

Singer, P. C., Boyer, T., Holmquist, A., Morran, J., & Bourke, M. (2009). Integrated analysis of NOM removal by magnetic ion exchange. *Journal / American Water Works Association, 101*(1), 65-73.

Song, B., & Leff, L. G. (2006). Influence of magnesium ions on biofilm formation by pseudomonas fluorescens. *Microbiological Research, 161*(4), 355-361.

State of Hawaii. (2009). *Instream flow standard assessment report for Island of Maui hydrologic unit 6047 Waikamoi.* (No. PR-2009-1). Oahu: State of Hawaii.

Stoquart, C., Servais, P., Bérubé, P. R., & Barbeau, B. (2012). Hybrid membrane processes using activated carbon treatment for drinking water: A review. *Journal of Membrane Science, 411-412*, 1-12.

Summers, R. S., Knappe, D. R. U., & Snoeyink, V. L. (2011). Chapter 14: Adsorption of organic compounds by activated carbon. In J. K. Edzwald (Ed.), *Water quality and treatment: A handbook on drinking water* (Sixth ed., pp. 14.1) McGraw-Hill.

Sun, C., Fiksdal, L., Hanssen-Bauer, A., Rye, M. B., & Leiknes, T. (2011). Characterization of membrane biofouling at different operating conditions (flux) in drinking water treatment using confocal laser scanning microscopy (CLSM) and image analysis. *Journal of Membrane Science, 382*(1), 194-201.

Tang, F., Shi, Z., Li, S., & Su, C. (2010). Effects of bio-sand filter on improving the bio-stability and health security of drinking water. Paper presented at the *2010 International Conference on Mechanic Automation and Control Engineering (MACE),* Wuhan. 1878-1881.

Tekerlekopoulou, A. G., Pavlou, S., & Vayenas, D. V. (2013). Removal of ammonium, iron and manganese from potable water in biofiltration units: A review. *Journal of Chemical Technology and Biotechnology, 88*(5), 751-773.

Tharamapalan, J. (2012). *Application and optimization of membrane processes treating brackish and surficial groundwater for potable water production. [electronic resource]* Orlando, Fla. : University of Central Florida, 2012. Retrieved from https://login.ezproxy.net.ucf.edu/login?auth=shibb&url=http://search.ebscohost.com/login.aspx?direct=true&db=cat00846a&AN=ucfl.031987988&site=eds-live&scope=site; http://purl.fcla.edu/fcla/etd/CFE0004609

Tsujimoto, W., Kimura, H., Izu, T., & Irie, T. (1998). Membrane filtration and pre-treatment by GAC. *Desalination, 119*(1), 323-326.

Urfer, D., Huck, M., Booth, S. D., & Coffey, B. M. (1997). Biological filtration for BOM and particle removal: A critical review. *Journal / American Water Works Association, 89*(12), 83-98.

USEPA. (1979). *Estimating water treatment costs: Volume 2 cost curves applicable to 1 to 200 mgd treatment plants.* (No. Contract No. 68-03-2516). Springfield: National Technical Information Service.

USEPA. (1979). *Process design manual for sludge treatment and disposal.* (No. EPA 625/1-79-011).U.S. Environmental Protection Agency.

National primary drinking water regulations: stage 2 disinfectants and disinfection byproducts rule, final rule, Federal Register Vol. 71, No. 2, Pg 387 (2006).

van Loosdrecht, M. C., Lyklema, J., Norde, W., & Zehnder, A. J. (1989). Bacterial adhesion: A physicochemical approach. *Microbial Ecology, 17*(1), 1-15.

Velten, S., Boller, M., Köster, O., Helbing, J., Weilenmann, H., & Hammes, F. (2011). Development of biomass in a drinking water granular active carbon (GAC) filter. *Water Research, 45*(19), 6347-6354.

Wang, J., Guan, J., Santiwong, S., & Waite, T. D. (2008). Characterization of floc size and structure under different monomer and polymer coagulants on microfiltration membrane fouling. *Journal of Membrane Science, 321*(2), 132-138.

Wang, S., Liu, C., & Li, Q. (2011). Fouling of microfiltration membranes by organic polymer coagulants and flocculants: Controlling factors and mechanisms. *Water Research, 45*(1), 357-365.

Wang, Y. (2014). *Assessment of ozonation and biofiltration as a membrane pre-treatment at a full-scale drinking water treatment plant* (Thesis).

Wei, Z., Xiaojian, Z., Chao, C., Jun, W., & Yuanyuan, L. (2011). Pilot study on hybrid biological filter-coagulation-submerged ultrafiltration membrane for drinking water treatment. Paper

presented at the *2011 5th International Conference on Bioinformatics and Biomedical Engineering (iCBBE),* Wuhan. 1-5.

Wend, C. F., Stewart, P. S., Jones, W., & Camper, A. K. (2003). Pretreatment for membrane water treatment systems: A laboratory study. *Water Research, 37*(14), 3367-3378.

Xiao, F., Zhang, X., Zhai, H., Yang, M., & Lo, I. M. C. (2010). Effects of enhanced coagulation on polar halogenated disinfection byproducts in drinking water. *Separation and Purification Technology, 76*(1), 26-32. doi:10.1016/j.seppur.2010.09.016

Xu, H., Chen, W., Sun, J., & Yuan, Z. (2011). Impact of magnetic ion exchange resin pretreatment on alleviating UF membrane fouling. *Water Science & Technology: Water Supply, 11*(1), 7-14.

Xu, Z., Jiao, R., Liu, H., Wang, D., Chow, C. W. K., & Drikas, M. (2013). Hybrid treatment process of using MIEX and high performance composite coagulant for DOM and bromide removal. *Journal of Environmental Engineering (United States), 139*(1), 79-85. doi:10.1061/(ASCE)EE.1943-7870.0000622

Yan, M., Wang, D., Ni, J., Qu, J., Chow, C. W., & Liu, H. (2008). Mechanism of natural organic matter removal by polyaluminum chloride: Effect of coagulant particle size and hydrolysis kinetics. *Water Research, 42*(13), 3361-3370.

Yan, M., Wang, D., Qu, J., He, W., & Chow, C. W. (2007). Relative importance of hydrolyzed al(III) species (al(a), al(b), and al(c)) during coagulation with polyaluminum chloride: A case study with the typical micro-polluted source waters. *Journal of Colloid and Interface Science, 316*(2), 482-489. doi:S0021-9797(07)01196-4 [pii]

Yang, J., Yuan, D., & Weng, T. (2010). Pilot study of drinking water treatment with GAC, O 3/BAC and membrane processes in kinmen island, taiwan. *Desalination, 263*(1), 271-278.

Yu, J., Wang, D., Yan, M., Ye, C., Yang, M., & Ge, X. (2007). Optimized coagulation of high alkalinity, low temperature and particle water: PH adjustment and polyelectrolytes as coagulant aids. *Environmental Monitoring and Assessment, 131*(1-3), 377-386.

Zhang, R., Vigneswaran, S., Ngo, H. H., & Nguyen, H. (2006). Magnetic ion exchange (MIEX®) resin as a pre-treatment to a submerged membrane system in the treatment of biologically treated wastewater. *Desalination, 192*(1), 296-302.

Zhang, S., & Huck, P. M. (1996). Removal of AOC in biological water treatment processes: A kinetic modeling approach. *Water Research, 30*(5), 1195-1207.

Zhang, Z., Wang, L., & Shao, L. (2010). Study on relationship between characteristics of DOC and removal performance by BAC filter. Paper presented at the *2010 4th International Conference on Bioinformatics and Biomedical Engineering (iCBBE),* Chengdu. 1-4.

Zhang, Y., Love, N., & Edwards, M. (2009). Nitrification in drinking water systems. *Critical Reviews in Environmental Science and Technology, 39*(3), 153-208. doi:10.1080/10643380701631739

Zheng, X., Mehrez, R., Jekel, M., & Ernst, M. (2009). Effect of slow sand filtration of treated wastewater as pre-treatment to UF. *Desalination, 249*(2), 591-595.

Zheng, X., Ernst, M., & Jekel, M. (2009). Identification and quantification of major organic foulants in treated domestic wastewater affecting filterability in dead-end ultrafiltration. *Water Research, 43*(1), 238-244.

Zheng, X., Ernst, M., & Jekel, M. (2010). Pilot-scale investigation on the removal of organic foulants in secondary effluent by slow sand filtration prior to ultrafiltration. *Water Research, 44*(10), 3203-3213.

Zhu, I. X., Getting, T., & Bruce, D. (2010). Review of biologically active filters in drinking water applications. *Journal / American Water Works Association, 102*(12), 67-77.